Linking through Biomechanics

CSB 2010 SCB

Joindre par la Biomécanique

The Proceedings of the 16th Biannual Conference of The Canadian Society for Biomechanics

Queen's University, Kingston, Ontario, Canada
June 9-12, 2010

The 16th Biannual Conference of The Canadian Society for Biomechanics

Queen's University, Kingston, Ontario, Canada
June 9-12, 2010

Organizing Committee:

Chair: Joan Stevenson, School of Kinesiology and Health Studies
Co-chairs: Patrick Costigan, School of Kinesiology and Health Studies
Elsie Culham, School of Rehabilitation Therapy
Genevieve Dumas, Department of Mechanical and Materials Engineering
Samantha Reid, School of Kinesiology and Health Studies

Members: Alice Aiken, School of Rehabilitation Therapy
Scott Brandon, Department of Mechanical and Materials Engineering
Brenda Brouwer, School of Rehabilitation Therapy
Tim Bryant, Department of Mechanical and Materials Engineering
Kevin Deluzio, Department of Mechanical and Materials Engineering
Kari Hurst, Human Mobility Research Centre
Qinggio Li, Department of Mechanical and Materials Engineering
Linda McLean, School of Rehabilitation Therapy
Alison Novak, School of Rehabilitation Therapy
Lucie Pelland, School of Rehabilitation Therapy
Sandra Olney, School of Rehabilitation Therapy
Leone Ploeg, Human Mobility Research Centre

Program Committee:
Elsie Culham, School of Rehabilitation Therapy
Genevieve Dumas, Department of Mechanical and Materials Engineering
Patrick Costigan, of Kinesiology and Health Studies

Awards Committee:
Kevin Deluzio, Queen's University
David Pearsall, McGill University
Andrea Clark, University of Calgary
Graham Caldwell, University of Massachusetts Amherst
Tammy Egar, Laurentian University
David Andrews, University of Windsor

Reviewers: Alice Aiken, Queen's University
David Andrews, Univerity of Windsor
Janie Astephen Wilson, Dalhousie University
Trevor Birmingham, University of Western Ontario
Steven Boyd, University of Calgary
Brenda Brouwer, Queen's University
Tim Bryant, Queen's University
Jack Callaghan, University of Waterloo
Peter Cripton, University of British Columbia
Elsie Culham, Queen's University
Kevin Deluzio, Queen's University
Nandini Deshpande, Queen's University
Clark Dickerson, University of Waterloo
Jim Dickey, University of Western Ontario
Jon Doan, University of Lethbridge
Genevieve Dumas, Queen's University
Mansour Eslami, University of Mazanderan
Dany Gagnon, University of Montreal
Paul Ivancic, Yale University
Joel Lanovaz, University of Saskatchewan
Qingguo Li, Queen's University
Monica Maly, McMaster University
Linda McLean, Queen's University
Sylvie M. Nadeau, University of Montreal
Kathleen Norman, Queen's University
David Pearsall, McGill University
Lucie Pelland, Queen's University
André Plamondon, Institut de recherche Robert-Sauvé en santé et en sécurité du travail
Aliaa Rehan Youssef, University of Calgary
Gordon Robertson, University of Ottawa
Cécile Smeesters, Université de Sherbrooke
Les Sudak, University of Calgary
James Tung, University of Toronto
Stephen Waldman, Queen's University
R. Wells, University of Waterloo
Karl Zabjek, University of Toronto

Student Volunteers:

Stacey Acker
Erica Beaucage-Gaureau
Pamela Christie
Kamary Coriolano DaSilva
Kathleen Denbeigh
Pete Galbraith
Samantha Reid
Stephen Sebastyan
Shuozhi Yang
Jun-tian Zhang
Sivan Almosino
Scott Brandon
Allison Clouthier
Caroline Damecour
Steve Fung
Ryan Graham
Carol Murphy
Alison Novak
Erin Sadler
Steffani Vivani

Dear Colleagues,

Welcome to Queen's University and Kingston. We want you to enjoy the16th biannual conference of the Canadian Society for Biomechanics/Société Canadienne de Biomécanique. We have stimulating scientific sessions, comfortable conference facilities, and various social opportunities in a relaxed academic setting. We hope this conference is memorable, not only for the quality of the posters and papers but also for your time with old friends and colleagues and new contacts and partnerships.

Kingston, Canada's first capital city, is steeped with heritage from Fort Henry to the Rideau Canal to Sir John A. MacDonald memorabilia. Queen's too is steeped in history. Queen's University was established on 16 October 1841 by a royal charter issued by Queen Victoria and began with two professors and 13 students. Today, Queen's has ~14,500 undergraduates and ~3000 grad students. We have a full service university with Arts, Sciences, Engineering, Business, Medicine, Law and many more talented departments, schools and research centres. Although modest in size, we attract students from across Canada and the globe. Our spirited student body can boost of running more aspects of university life than any other university in Canada (non-academic discipline, residence life, book store, pubs, and eateries, sports clubs etc). Our graduate students have a greater opportunity to engage in multi-disciplinary research and education than on most Canadian campuses. Come soak in the spirit of Queen's and enjoy your stay.

The CSB/SCB-2010 Organizing Committee

Dear students,

Welcome to CBS/SCB 2010!

Over the course of the meeting, we are confident the outstanding scientific program that has been put together will encourage and inspire students and young investigators alike. CSB/SCB 2010 presents an exceptional opportunity for students to network, exchange ideas, and learn about advances and innovative research in the world of biomechanics.

Kingston is a majestic waterfront community steeped in Canadian history. Towering limestone buildings evoke the voices of our first parliamentarians, while the many harbours recall the founding of ice hockey and the glory of past Olympics. We have organized several exciting student events, including the student workshops and the student pub crawl, in addition to the welcome reception and banquet. Please take advantage of all these opportunities to interact with friends and colleagues. We are certain you will have an unforgettable experience in Kingston throughout this conference.

Have a great CSB/SCB 2010 meeting and enjoy Kingston!

The CSB Student Executive CSB 2010 Organizing Committee

Samantha M. Reid	Alison C. Novak	Scott Brandon
PhD Candidate	PhD Candidate	PhD Candidate
samantha.reid@queensu.ca	alison.novak@queensu.ca	brandon@me.queensu.ca
(SKHS)	(RHBS)	(Mech Eng)

Invited Speaker: Dr. Nikolaus F. Troje

Department of Psychology and School of Computing
Queen's University, Kingston, ON

Invited Talk: Gait analysis in the brain: What the visual system knows about biomechanics.

Bio: Niko Troje received his PhD in Biology from the Albert Ludwigs University in Freiburg, Germany, in 1994. Subsequently, he taught at the Max Planck Institute for Biological Cybernetics in Tübingen and later at Ruhr University in Bochum, Germany. In 2003, he joined Queen's University as a Canada Research Chair in Vision and Behavioural Sciences. He is a Full Professor in the Department of Psychology with a cross-appointment in the School of Computing at Queen's and an Adjunct Professor at the Centre for Vision Research at York University, at the School of Computing at Queen's and an Adjunct Professor at the Centre for Vision Research at York University. At Queen's he is the director of the BioMotion Lab. Dr. Troje has received several prestigious awards, both in Germany and in Canada and is currently holding a NSERC Steacie Fellowship. His main research interest is focused on questions concerning the Biology and Psychology of visual perception in social relevant contexts. He has been working for many years on human face recognition. Currently, most of the projects in his lab are concerned with visual information processing involved in the recognition of biological motion, particularly the recognition of human gait.

Invited Speaker: Dr. Idsart Kingma

Faculty of Human Movement Sciences
VU University Amsterdam, The Netherlands

Invited Talk: Recent Advances in Lifting Biomechanics

Bio: Idsart Kingma received his PhD in Human Movement Sciences in 1998 from the VU University, Amsterdam, the Netherlands. Currently he is associate professor at the faculty of Human Movement Sciences of the VU University, where he serves as a member of the faculty board, and he teaches courses on mechanics of human movement, measurement techniques, and pathology of human movement. His main research interest is occupational biomechanics, with a specific focus on the low back. He has (co) authored over 75 papers in international journals. About half of these papers concern spine loading and lifting. Furthermore, he is supervisor of four PhD students. Some of his current research targets are to bring lab-quality lifting biomechanics to the field and to unravel the complex interaction effects on low back loading between lifting task and lifting behavior.

Wednesday
June 9

4:00pm	Registration Biosciences Atrium
5:30pm	Welcome Reception Biosciences Atrium

Thursday
June 10

8:30-9:30 Keynote Address
Biosciences 1101

Dr. Nikolas Troje
Queen's University
Gait analysis in the brain: What the visual system knows about biomechanics.

	Biosciences 1101	Biosciences 1102
9:30	**Session: ISEK Award Finalists** Chair: Linda McLean	**Session: Tissue 1** Chairs: Salvatore Federico & Steve Waldman
10:30	Break	
10:45	**Session: NDI Award Finalists** Chairs: Kevin Deluzio & Graham Caldwell	
12:15	Box Lunch	
12:45 – 2:15	Poster Presentation	
1:00 – 2:00	Lab tours	
2:15	**Session: Gait 1** Chairs: Janie Astephen & Dany Gagnon	**Session: Occupational Biomechanics 1** Chairs: Mohamed Abdoli & Stuart McGill
3:45	Break	
4:00	**Session: Orthopaedics 1** Chairs: Joel Lanovaz & Monica Maly	**Session: Modelling** Chairs: Michele Oliver & Yvan Petit

Friday
June 11

8:30-9:30 Keynote Address
Biosciences 1101

Dr. Idsart Kingma
University of Amsterdam
Recent Advances in Lifting Biomechanics

	Biosciences 1101	Biosciences 1102	Biosciences 1103
9:30	**Session: Gait 2** Chairs: Elsie Culham & Cheryl Kozey	**Session: Sports 1** Chairs: David Pearsall & Lucie Pelland	**Session: Muscle 1** Chairs: Brenda Brouwer & Walter Herzog
10:30	Break		
10:45	**Session: Occupational Biomechanics 2** Chairs: David Andrews & Tammy Eger	**Session: Tissue 2** Chairs: Karen Gordon & Ron Zernicke	
12:15	Box Lunch		
12:45	Poster Presentation		
2:15	**Session: Motor Control** Chairs: Erika Nelson-Wong & Steve Prentice	**Session: Spine** Chairs: Jim Dickey & Paul Ivancic	
3:45	Break		
4:00	**Session: Gait 3** Chairs: Qingguo Li & Sylvie Nadeau	**Session: Muscle 2** Chairs: Pat Costigan & Nandini Despande	

8:30-9:00 NDI Promising Young Investigator
Biosciences 1101

Dr. Clark Dickerson
University of Waterloo
Is the Genesis of Rotator Cuff Disease (RCD) Linked to Muscle Fatigue?

	Biosciences 1101	Biosciences 1102
9:00	**Session: Gait 4** Chairs: Michael Cinelli & Cyril Duclos	**Session: Sports 2** Chairs: Gord Robertson & Cecile Smeesters
10:30	Break	
10:45	**Session: Orthopaedics 2** Chairs: Tim Bryant & Joseph Langenderfer	**Session: Methods** Chairs: Jack Callaghan & Heidi-Lynn Ploeg
12:15	Box Lunch	
12:45	CSB Annual General Meeting	
1:45	**Closing Ceremony**	

Table of Contents

Table of Contents i

ISEK Award Finalists

PREOPERATIVE EMG PATTERNS PREDICT TOTAL KNEE IMPLANT MIGRATION 1
David Wilson, Janie Astephen Wilson, Cheryl Hubley-Kozey, Michael Dunbar

BIOMECHANICAL IMPLICATIONS OF POLICE CRUISER REAR RESTRAINT CAGE CONFIGURATIONS AND MOBILE DATA TERMINAL LOCATION: HALF VERSUS FULL CAGE DESIGNS 2
Samantha Molenaar, Clark Dickerson

MUSCLE ACTIVATION DURING HAND DEXTERITY TASKS IN INDIVIDUALS WITH HAND OSTEOARTHRITIS 3
Kristina Calder, Victoria Galea, Jean Wessel, Joy MacDermid, Norma MacIntyre

PERFORMING SITTING PIVOT TRANSFERS REQUIRES GREATER UPPER LIMB MUSCULAR DEMAND THAN WEIGHT-LIFTS IN INDIVIDUALS WITH A SPINAL CORD INJURY 4
Dany Gagnon, Ariane Desharnais, Sylvie Nadeau

Tissue 1

BIOMECHANICAL PROPERTIES OF POSTEROMEDIAL KNEE JOINT CAPSULE IN CHRONIC OSTEOARTHRITIS 5
Justin Steeds, Mark Hurtig, Karen Gordon

TRANSVERSE CARPAL LIGAMENT STIFFNESS AND CARPAL BONE KINEMATICS DURING INDENTATION TESTING 6
Michael Holmes, Samuel Howarth, Jack Callaghan, Peter Keir

LOCALIZED STRAIN MEASUREMENTS OF THE INTERVERTEBRAL DISC ANNULUS 7
Thomas Karakolis, Diane Gregory, Jack Callaghan

THE EFFECT OF CHANGING CROSS-SECTIONAL AREA MEASUREMENTS ALONG SOFT TISSUE LENGTH FOR PREDICTION OF MECHANICAL PROPERTIES 8
Joanna Weber, Karen Gordon, Michele Oliver

NDI Award Finalists

BIOMECHANICS OF THE VERTEBRAL ARTERY DURING NECK MANIPULATIVE TREATMENTS 9
Conrad Tang

ANALYSIS OF THE EFFECT OF ROTATOR CUFF IMPINGEMENTS ON UPPER LIMB KINEMATICS IN AN ELDERLY POPULATION DURING ACTIVITIES OF DAILY LIVING . 10
Laurie Hall, Erin Middlebrook, Clark Dickerson

MALES, FEMALES AND LIFTING TECHNIQUE: A PRINCIPAL COMPONENT ANANLYSIS 11
Erin M Sadler, Ryan B Graham, Joan Stevenson

QUANTIFYING THE COCONTRACTION RELATIONSHIP BETWEEN ELBOW FLEXORS AND EXTENSORS DURING SUBMAXIMAL ISOMETRIC EXERTIONS 12
Rebecca Brookham, Erin Middlebrook, Tej-jaskirat Grewal, Clark Dickerson

LOCAL STABILITY OF DYNAMIC TRUNK MOVEMENTS DURING THE REPETITIVE LIFTING OF LOADS 13
Ryan B Graham, Erin M Sadler, Joan Stevenson

GROUND REACTION FORCES DIMINISH IN MICE AFTER BOTULINUM TOXIN INJECTION 14
Sarah L Manske, Steven K Boyd, Ronald F Zernicke

Poster- Occupational Biomechanics 1

WALKING TRUNK POSTURE DURING HEAD LOAD CARRIAGE FOR PREGNANT WOMEN IN WEST AFRICA 15
Erica Beaucage-Gauvreau, Geneviève Dumas, Mohamed Lawani

DEVELOPMENT AND EVALUATION OF AN OFFICE ERGONOMIC CHECKLIST: THE RAPID OFFICE STRAIN ASSESSMENT (ROSA) 16
Michael Sonne, David Andrews, Dino Villalta

BIOMECHANICS OF LEANING FORWARD AGAINST AN EXTERNAL SUPPORT WITH MILD FORWARD FLEXED TRUNK IN STANDING 17
Mohammad abdoli-Eramaki, Caroline Damecour, Ahmad Ghasempoor, Joan Stevenson

SPATIAL DEPENDENCYOF SHOULDER MUSCLE DEMANDS IN HORIZONTAL PUSHING AND PULLING 18
Alison McDonald, Bryan Picco, Amy Chow, Alicia Belbeck, Clark Dickerson

COMPARISON OF TWO FORWARD-PLACED TRUNK SUPPORTS FOR STANDING WITH REACHING TO A FIXED, EXTREME DISTANCE IN A DIAGONAL DIRECTION 19
Caroline Damecour, Mohammad abdoli-Eramaki, Ahmad Ghasempoor, Joan Stevenson

A BIOMECHANICAL ANALYSIS OF COKEOVEN STANDPIPE CLEANING LEADING TO DESIGN OF TARGETED ENGINEERING INTERVENTIONS 20
Micha Wallace, Michele Oliver, Mark Munro, James Sexsmith

A BIOMECHANICAL ANALYSIS OF COKEOVEN STANDPIPE CLEANING ASSESSING EFFECTIVENESS OF TARGETED ENGINEERING INTERVENTIONS 21
Micha Wallace, Michele Oliver, Mark Munro, James Sexsmith

Poster Gait 1

KINEMATICS AND KINETICS OF THE LOWER LIMB DURING STAIR AMBULATION IN OLDER ADULTS 22
Samantha Reid, Patrick Costigan

TRANSVERSE PLANE KINEMATICS AND UNDER-CORRECTION IN HIGH TIBIAL OSTEOTOMY 23
Rebecca Moyer, Trevor Birmingham, Ian Jones, J. Robert Giffin

EVALUATION OF GAIT SYMMETRY AFTER STROKE: A COMPARISON OF ANKLE-FOOT ORTHOTIC USERS AND NON-USERS. 24
Amanda Kay, Stephen Perry, William McIlroy

DYNAMIC STABILITY DURING GAIT AND SIT-TO-WALK ASSESSED WITH STABILIZING AND DESTABILIZING FORCES 25
Cyril Duclos, Pierre Desjardins, Hélène Corriveau, Brenda Brouwer, Sylvie Nadeau

STRATEGIES AND ADAPTATIONS DURING LEVEL GROUND WALKING AND OBSTACLE CLEARANCE TASKS WITH LIMB MASS 26
Marc DeRochie, Jonathan Singer, Jeremy Noble, Stephen Prentice

THE ASSESSMENT OF GAIT DISORDERS IN CHILDREN WITH AUTISM 27
Matthew Calhoun, Vicky Chester

THE EFFECTS OF AGING ON ACTION AND VISUAL STRATEGIES WHEN WALKING THROUGH APERTURES 28
Amy Hackney, Michael Cinelli

DYNAMICS OF UNEXPECTED SLIP PERTURBATIONS DURING BAREFOOT WALKING 29
Jessica Berrigan, Stephen Perry

EFFECT OF FOOT ORTHOSES AND NANICULAR DROP MEASURES ON FOOT SEGMENT COUPLING PATTERNS 30
Mansour Eslami, Reed Ferber, Mohsen Damavandi

Poster Methods

ATTITUDE INTERPOLATION USING CRAWFORD AND CARDAN ANGLES ON PELVIC MOTIONS AFTER REMOVING THE "GIMBAL LOCK" CONDITION 31
Pierre Desjardins, Sylvie Nadeau, André Plamondon

OPTIMAL MARKER PLACEMENT FOR LANDING ANALYSIS 32
Arsène Thouzé, Tony Monnet, Mickaël Begon, Matt Pain

IMPLICATIONS OF MARKER SIZES DURING GAIT ANALYSIS 33
Arsène Thouzé, Marine Gaihlard, Rachel Cotton, Mickaël Begon

SHOULDER MAXIMUM VOLUNTARY ELECTRICAL ACTIVITY: EFFECT OF BILATERAL VERSUS UNILATERAL EXERTIONS ON SIGNAL AMPLITUDE AND INTRAPARTICIPANT REPRODUCIBILITY 34
Tej-jaskirat Grewal, Steven Fischer, Richard Wells, Clark Dickerson

MRI DATA REGISTRATION USED IN INTRASUBJECT COMPARISON OF PELVIC CONFIGURATION 35
Pavel Ruzicka, Petra Bendova

THE INCLUSION OF A 30 HZ HIGH-PASS FILTER AS A UNIVERSAL EMG DATA PROCESSING COMPONENT 36
Chad Gooyers, Jack Callaghan

OVERGROUND WALKING STEP LENGTH ESTIMATION WITH INERTIA MEASUREMENT UNIT 37
Shuozhi Yang, Qingguo Li

TRANSMISSION OF ACCELERATION FROM VIBRATING EXERCISE PLATFORMS TO THE LUMBAR SPINE AND HEAD 38
Robert Caryn, James Dickey, Alan Salmoni, Peter Lemon, Tom Hazell

TRI-AXIAL ACCELEROMETERS FOR THE MEASUREMENT OF LUMBAR SPINE AND PELVIC ANGLES 39
Diana De Carvalho, Jack Callaghan

DEVELOPMENT OF A SYSTEM FOR MOBILE 3D RECONSTRUCTION 40
Emílio Cipolli, Tamotsu Hirata

Poster Modelling 1

A MODEL OF THE EXTRA-CELLULAR MATRIX OF ARTICULAR CARTILAGE 41
Malika Bongué Boma, Marcelo Epstein, Salvatore Federico

NON-LINEAR MODEL FOR COMPRESSION TESTS ON ARTICULAR CARTILAGE 42
Salvatore Federico, Alfio Grillo, Amr Guaily

INVESTIGATION OF THE COMPLIANCE MISMATCH AND WALL SHEAR STRESS DISTRIBUTION EFFECTS ON GRAFT FAILURE INITIATION IN A DISTAL END-TO-SIDE FEMORAL BYPASS GRAFT ANASTOMOSIS 43
Mostafa Toloui

DEFORMATION AND FLUID PRESSURE ANALYSIS OF KNEE CARTILAGES IN-SITU ... 44
Ke Gu, Leping Li

THEORETICAL SIMULATION OF SPONGY BONE REMODELING UNDER OVERLOAD USING A SEMI-MECHANISTIC BONE REMODELING THEORY 45
Xianjie Li, Gholamreza Rouhi

Poster Spine

NECK MOTION DUE TO THE HALO-VEST IN PRONE AND SUPINE POSITIONS 46
Paul Ivancic, Connor Telles

AGE EFFECTS ON TRUNK MUSCLE ACTIVATION RESOPNSES TO A SYMMETRICAL LIFT AND REPLACE TAKS IN HEALTHY ADULTS 47
Ruth Pelleg-Kallevag, Heather Butler, Edwin Hanada, Cheryl Hubley-Kozey

A NEW SURROGATE BONE MODEL FOR TESTING INTERVERTEBRAL DEVICES 48
Anthony Au, Ameet Aiyangar, Paul Anderson, Heidi-Lynn Ploeg

RELATIONSHIP BETWEEN LUMBAR REGION KINEMATICS DURING A CLINICAL TEST AND A FUNCTIONAL ACTIVITY IN PEOPLE WITH AND WITHOUT LOW BACK PAIN - A PILOT STUDY 49
Sara Gombatto, Mark Kroll, Kara McCallum, Melissa Shiffer

EFFECT OF COUPLED POSTURES ON LUMBAR MUSCLE ACTIVIY: DOES THE FLEXION RELAXATION PHENOMENON PERSIST? 50
Tara Diesbourg, Janessa Drake, Nadia Azar

Poster Sports 1

DAY TO DAY RELIABILITY OF KICKING ACCURACY IN SOCCER 51
Katharina Althoff, Ewald Hennig, Simon Batz, David Bürgel

ACUTE EFFECTS OF WHOLE BODY VIBRATION ON ACCURACY OF MOTOR PERFORMANCE 52
Nina Völkel, Ewald Hennig

SLAP AND WRIST SHOTS: THE EFFECT OF PLAYER CALIBRE ON STICK STRAIN GAUGE RESPONSE 53
Ashley Hannon, Yannick Michaud-Paquette, David Pearsall, Rene Turcotte

ANGULAR IMPULSE DURING BALLET TURNS 54
April Karlinsky, François D.Beaulieu, Gordon Robertson

MUSCLE ACTIVATION/RELAXATION CYCLES AND THE SPEED/STRENGTH PARADOX 55
Stuart McGill, David Frost, Tom Hubrecht

EFFECTS OF THE LOCATION OF INSTABILITY ON MOTION PATTERNS AND ELECTROMYOGRAPHICAL ACTIVITY IN BENCH PRESS EXERCISES 56
Brian Nairn, Chad Sutherland, Janessa Drake

Poster Muscle

LOWER EXTREMITY TISSUE MASS RATIO DIFFERENCES IN ATHLETES OF SPORTS INVOLVING REPETITIVE IMPACTS 57
Alison Schinkel-Ivy, Timothy Burkhart, David Andrews

THE EFFECT OF PERSPIRATION VOLUME ON THE AMPLITUDE AND FREQUENCY SPECTRUM 58
Mohammad abdoli-Eramaki, John Christenson, Caroline Damecour, Joan Stevenson

PASSIVE STRESSES GENERATED BY MYOFIBRILS FROM DILATED CARDIOMYOPATHIC HAMSTERS 59
Audree McKenzie, Appaji Panchangam, Walter Herzog

EFFECT OF EXTRINSIC FINGER FLEXOR AND EXTENSOR INTERCONNECTION ON FORCE AND MUSCLE ACTIVITY 60
Kia Sanei, Peter Keir

ELECTROMYOGRAPHIC ACTIVITY FOR TWO PARTS OF GLUTEUS MAXIMUS DURING SQUAT 61
Bhupinder Singh, John H Yack, Aaron Hefferman, Sarah Nolte, Nicole Helle, John Callaghan

MUSCLE ACTIVATION PATTERNS OF TRANSRADIAL AMPUTEES USING HIGH DENSITY EMG 62
Heather Daley, Usha Kuruganti, Kevin Englehart

Occupational Biomechanics 1

INVERSE DYNAMICS ANALYSIS OF TWO SNOW SHOVEL DESIGNS UNDER NO-FATIGUE CONDITIONS 63
Ryan Lewinson, Gordon Robertson, Gholamreza Rouhi

THE IMPACT OF A SLOPED SURFACE ON LOW BACK PAIN AND MUSCLE ACTIVATION PATTERNS DURING STANDING WORK 64
Erika Nelson-Wong, Jack Callaghan

POSTURE CATEGORY SALIENCE POSITIVELY AFFECTS ANALYST DECISION TIME AND ERROR RATE 65
Krysia Fiedler, David Andrews, Patricia Weir, Jack Callaghan

DIFFERENCES IN VERBALLY ESTIMATED HAND FORCES AFFECT PEAK AND CUMULATIVE LOW BACK AND SHOULDER LOADS OF NURSES IN AN ACUTE CARE HOSPITAL SETTING 66
Jennifer Lembke, Krysia Fiedler, Patricia Weir, David Andrews

IS A LINKED, UPPER BODY MODEL APPROPRIATE FOR ESTIMATING KINEMATIC AND KINETIC PARAMETERS FOR FIELD APPLICATIONS OF INERTIAL MOTION SENSORS 67
Alison Godwin, Joan Stevenson, Susan Reid

PRELIMINARY ASSESSMENT OF LIFTING TECHNIQUE CHANGES IN A PROLONGED LIFTING TASK 68
Wayne Albert, Robin Hampton, Matt Cochran, Usha Kuruganti

Gait 1

EARLY-STANCE DIFFERENCES BETWEEN TOTAL ANKLE ARTHROPLASTY AND ARTHRODESIS 69
Jason Fong, Janie Astephen Wilson, Kory Arsenault, Patricia Francis, Mark Glazebrook

TOWARDS THE REDUCTION OF FALL-RELATED INJURY RISK: NOVEL COMPLIANT FLOORS DO NOT INFLUENCE RATE OF BALANCE CONTROL RESPONSES IN OLDER WOMEN 70
Alexander Wright, Andrew Laing

HEEL COMPLIANCE AND WALKING MECHANICS USING THE NIAGARA FOOT PROSTHESIS 71
Valérie Wellens, Joel Lanovaz, Tim Bryant

BIOMECHANICAL CHANGES DUE TO TOTAL KNEE ARTHROPLASTY WITH TWO IMPLANT DESIGNS 72
Allison Clouthier, Scott Brandon, Kevin Deluzio, John Rudan

SHEAR AND VERTICAL FORCE CONTRIBUTIONS TO FRONTAL PLANE BALANCE WITH A ROLLATOR 73
James Tung, Brian Maki, William McIlroy

CHARACTERIZING FOOT PLACEMENT PATTERNS DURING REAL-WORLD ROLLATOR USE: INITIAL DEVELOPMENT AND VALIDATION 74
Justin Chee, James Tung, William Gage, William McIlroy, Karl Zabjek

Orthopaedics 1

EFFECT OF TOTAL KNEE ARTHROPLASTY ON THE TOTAL SUPPORT MOMENT DURING GAIT 75
Gillian Hatfield, Cheryl Hubley-Kozey, Michael Dunbar

TIBIAL BONE DENSITY IS ASSOCIATED WITH TOTAL KNEE IMPLANT MIGRATION .. 76
David Konadu, Janie Astephen Wilson, Michael Dunbar, Elise Laende, Allan Hennigar, Michael Gross

PASSIVE KNEE JOINT KINEMATIC PATTERNS DURING COMPUTER-ASSISTED TKA SURGERY DEPEND ON CHOICE OF KINEMATIC MODEL 77
Richard Roda, Janie Astephen Wilson, Michael Dunbar, Glen Richardson

THE PRE-OPERATIVE KNEE ADDUCTION MOMENT DURING GAIT IS ASSOCIATED WITH THE DYNAMIC VARUS/VALGUS ANGLE OF THE KNEE DURING COMPUTER-ASSISTED TKA SURGERY 78
Richard Roda, Janie Astephen Wilson, Michael Dunbar, Glen Richardson

KNEE JOINT MECHANICS IMPROVE TWO YEARS AFTER TOTAL KNEE REPLACEMENT SURGERY 79
Janie Astephen Wilson, Cheryl Hubley-Kozey, Michael Dunbar

OSTEOARTHRITIS KNEE PAIN DURING ISOKINETIC TESTING AT DIFFERENT VELOCITIES 80
Scott Brandon, Sivan Almosnino, Alison Chalmers, Elizabeth Sled

Modelling

UNDERSTANDING WOLFF'S LAW VIA MICRO-LEVEL TOPOLOGY OPTIMIZATION 81
Chris Boyle, Il Yong Kim

A NEW BIOMIMETIC COMPOSITE MATERIAL STEM IN SURFACE REPLACEMENT OF THE HIP 82
Christiane Caouette, Martin N. Bureau, Pascal-André Vendittoli, Martin Lavigne, Natalia Nuño

GREATER TROCHANTERIC PLATE DESIGN REFINEMENT USING FINITE ELEMENTS METHOD 83
Yan Bourgeois, Yvan Petit, Yves Laflamme

RADIUS MOVEMENT SIMULATION AND EVALUATION BASED ON ARTICULAR SURFACES 84
Julien Leboucher, Mathieu Lempereur, Valérie Burdin, Olivier Rémy-Néris

KINEMATIC MODEL OF A SHOULDER FITTED WITH AN ORTHOSIS 85
Maryline Doyon, Rachel Cotton, Mickaël Begon, Jacinte Bleau, Paul Allard

IN SILICO NANOMECHANICS OF COLLAGEN PEPTIDE BENDING AND MICROUNFOLDING 86
Jonathan W. Bourne, Peter A. Torzilli

Sports 1

CHANGES IN FOOTWEAR PROPERTIES AFTER 50, 200, 500, AND 1000 KM OF RUNNING 87
Ewald Hennig, Stephan Fischer

IMPACT FORCES IN MARTIAL ARTS BRICK BREAKING 88
Joel Lanovaz, Blair Healy, David Kobylak, Mike Smith

QUANTIFICATION OF LOAD DISTRIBUTION IN HELMET PADDING MATERIALS 89
Ryan Ouckama, David Pearsall

OPTIMAL GATE IMPACT HEIGHT FOR SIT-SKIER PERFORMANCE AND SAFETY - A TOP SECRET 2010 PROJECT 90
Marc Denninger, Eve Langelier, Cécile Smeesters, Cynthia Doré, Denis Rancourt

Gait 2

GROUND REACTION FORCE ADAPTATIONS DURING CROSS-SLOPE WALKING AND RUNNING 91
Mohsen Damavandi, Philippe Dixon, David Pearsall

INVESTIGATION OF DYNAMIC STABILITY DURING THE TRANSITION FROM LEVEL GROUND WALKING TO A CHANGE IN SURFACE HEIGHT IN HEALTHY YOUNG ADULTS 92
Kathleen O'Reilly, Rachel Campbell, Kristen MacDonell, Katherine Norrish, Kristen Whitney, Karl F Zabjek

STATIC AND DYNAMIC KNEE KINEMATICS IN HEALTHY WOMEN WITH KNEE HYPEREXTENSION 93
Patricia Teran-Yengle, Rebecca Birkhofer, Megan Sinnott, Kimberly Patton, Bhupinder Singh, John H Yack

NONLINEAR TIME SERIES ANALYSIS OF HUMAN GAIT UNDER COGNITIVE INTERFERENCE CONDITIONS 94
Karelia E. Tecante G., Peter Federolf, Benno Nigg

Muscle 1

EFFECT OF SENSORY FEEDBACK ON WALKING PATTERNS OF A NEUROMECHANICAL MODEL 95
Jeremy Noble

A MODEL FOR FORWARD DYNAMIC SIMULATION OF RAPID TAPPING MOTION OF INDEX FINGER 96
Mohammad Sharif Shourijeh, John J McPhee, Richard Wells

MUSCLE AND FASCICLE EXCURSIONS IN CHILDREN WITH CEREBRAL PALSY 97
Marlee Hahn, Megan Yaraskavitch, Walter Herzog

THE EFFECT OF ANTAGONISM ON THE CALCULATION OF MUSCLE MODEL PARAMETERS 98
Ross Miller, Graham Caldwell

Occupational Biomechanics 2

A COMPARISON OF PLATFORM MOTION WAVEFORMS DURING CONSTRAINED AND UNCONSTRAINED STANDING IN A MOVING ENVIRONMENTS 99
Carolyn Duncan, Scott MacKinnon, Wayne Albert

POSTURAL AND BALANCE CONSTRAINTS INFLUENCE BOTH HAND FORCE CAPABILITY AND MUSCLE ACTIVITY IN THE SHOULDER 100
Bryan Picco, Steven Fischer, Clark Dickerson, Richard Wells

COMPARISON BETWEEN ISO 2631-1 PREDICTED COMFORT AND SELF-REPORTED COMFORT VALUES DURING OCCUPATIONAL EXPOSURE TO WHOLE-BODY VEHICULAR VIBRATION 101
Katherine Plewa, James Dickey, Tammy Eger, Michele Oliver

A MODEL TO PREDICT CARPAL TUNNEL SYNDROME RISK 102
Justin Weresch, Peter Keir

BIOMECHANICAL AND ERGONOMIC ASSESSMENT OF URBAN TRANSIT OPERATORS 103
Wayne Albert, Donald Everson, Michelle Rae, Usha Kuruganti, Jack Callaghan

COORDINATION OF SHOULDER MUSCLES IN RESPONSE TO GRIPPING AND BICEPS ACTIVITY DURING STATIC AND DYNAMIC SHOULDER EXERTIONS 104
Joanne Hodder, Peter Keir

Tissue 2

NUMERICAL IMPLEMENTATION OF A NON-LINEAR MICROSTRUCTURAL MODEL OF CARTILAGE 105
Jan Pajerski, Amr Guaily, Christian Gasser, Salvatore Federico

IMPROVED PREDICTION OF STRESS RELAXATION INDENTATION RESPONSE OF CARTILAGE USING A NONLINEAR BIPHASIC POROVISCOELASTIC MODEL 106
Alireza Seifzadeh, Donatus Oguamanam, Marcello Papini

QUANTIFICATION OF CHANGE IN THICKNESS AND SHEAR MODULUS OF ARTICULAR CARTILAGE AFTER FREEZING 107
Nikolas Trutiak, Mark Lowerison, Manuela Kunz, Karen Gordon, Mark Hurtig

EFFECT OF SAMPLE PREPARATION ON THE MODULUS OF BOVINE LUMBAR CANCELLOUS TISSUE 108
Andrew Engbretson, Geneviève Dumas

WHICH YOUNG MODULUS SHOULD BE CHOSEN TO ADEQUATLY REPRESENT THE STRESS DISTRIBUTION WITHIN THE FEMUR 109
Michael Reimeringer, Natalia Nuño

AN INVESTIGATION INTO THE REMODELING PROCESS IN AN ARTIFICIALLY-MADE BONE TISSUE 110
Nima Jamilpour, Abdolhosein Fereidoon, Gholamreza Rouhi

Poster Occupational Biomechanics 2

QUANTIFICATION OF MUSCULAR, POSTURAL, AND UPPER LIMB MOVEMENT DEMANDS DURING CRANE OPERATION IN AN INTEGRATED STEEL MANUFACTURING PLANT 111
Mark Munro, Michele Oliver, Micha Wallace, James Sexsmith

COUPLING DOES NOT INFLUENCE LIFTING AFFORDANCES 112
Jon Doan, Stephen Gausman, Jason Flindall

ON THE USE OF A SCALING FACTOR TO ESTIMATE CUMULATIVE SPINAL LOADING 113
Kaitlin M. Gallagher, Steven Fischer, Samuel Howarth, Wayne Albert, Jack Callaghan

STEPPING RESPONSE DURING CONSTRAINED AND UNCONSTRAINED STANDING IN MOVING ENVIRONMENTS 114
Carolyn Duncan, Wayne Albert, Scott MacKinnon

POSTURAL ASSESSMENT OF CITY TRANSIT BUS DRIVERS 115
Wayne Albert, Michelle Rae, Donald Everson

SEAT EFFECTIVE AMPLITUDE TRANSMISSIBILITY BASED SEAT SELECTION TO MINIMIZE 6 DOF WHOLE-BODY VIBRATION IN INTEGRATED STEEL MANUFACTURING MOBILE MACHINERY 116
Leanne Conrad, Michele Oliver, Robert J. Jack, James Dickey, Tammy Eger

OCCUPATIONAL VIBRATION EXPOSURE AT THE FEET: CHARACTERISTICS AND HEALTH IMPLICATIONS 117
Tammy Eger, Ron House, Aaron Thompson, Mallorie Leduc, Alison Godwin

DIFFERING NECK POSTURES FOR OPERATING NORMAL AND LOW-PROFILE MACHINES 118
Alison Godwin, Tammy Eger, Sylvain Grenier

Poster Gait 2

PRINCIPLE COMPONENT DECOMPOSITION OF POSTURAL CONTROL MOVEMENTS 119
Peter Federolf

BIOMECHANICAL GAIT ANALYSIS USING HIGH-HEELED SHOES IN HORIZONTAL AND INCLINED WALKWAY 120
Glauce Silva, João Oliveira

GROUND REACTION FORCES IN ASSYMETRICAL GAIT USING SPLIT-BELT TREADMILL 121
Rachid Aissaoui, Philippe Gourdou, Sylvie Nadeau

IMPLEMENTATION AND VALIDATION OF A NOVEL INERTIAL MEASUREMENT SYSTEM FOR KINEMATIC GAIT ANALYSIS 122
Martin Brummund, Doan Jon , Block Ed, Brown Lesley, Hu Bin

GAIT MODE RECOGNITION FROM ABLE-BODIED LOWER LIMB EMG 123
Dan Rogers, Kevin Englehart, Ann Simon, Levi Hargrove

EFFECT OF ASYMMETRICAL LOAD CARRIAGE ON LOWER EXTREMITY JOINT KINEMATICS DURING NORMAL AND HIGH-HEELED GAIT IN FEMALES 124
Soul Lee, Jing Xian Li

MECHANISMS OF ANGULAR MOMENTUM TRANSFER DURING THE FOUETTÉ 125
Coren Walters-Stewart, Gholamreza Rouhi, Gordon Robertson

DIFFERENCES IN ANGULAR VELOCITIES, MOMENTS AND POWERS CAUSED BY USING DIFFERENT GAIT MARKER SETS 126
Li Zhang, Gordon Robertson

Poster Modelling 2

LUMBER SPINAL COMPRESSION FORCE MODEL FOR LIFTING TASK 127
Tamotsu Hirata, Danielle Oliveira, João Oliveira

DEVELOPMENT AND VALIDATION OF A FOUR BAR LINKAGE KINEMATIC MODEL OF THE UPPER LIMB AND JOYSTICK FOR USE IN VIRTUAL PROTOTYPING 128
Lauren Bailey, Michele Oliver

DEVELOPMENT AND VALIDATION OF A FOUR BAR LINKAGE KINETIC MODEL OF THE UPPER LIMB AND JOYSTICK FOR USE IN VIRTUAL PROTOTYPING 129
Lauren Bailey, Michele Oliver

TOWARDS AUTOMATED 3-D SCOLIOTIC SPINE RECONSTRUCTION BY USING BIPLANAR RADIOGRAPHIC IMAGES AND STATISTICAL MODLS 130
Behnam Heidari, Forough Madeh Khaksar, David FitzPatrick

KNEE MUSCLE CONTRIBUTIONS TO JOINT ROTATIONAL STIFFNESS 131
Joshua Cashaback, James Potvin

Poster Motor Control

REPEATABILITY OF MOTOR CONTROL PATTERNS DURING PROLONGED STANDING IN PEOPLE WITH AND WITHOUT STANDING-INDUCED LOW BACK PAIN 132
Erika Nelson-Wong, Jack Callaghan

SHOULD A MOVEMENT SCREEN BE USED TO GUIDE EXERCISE PRESCRIPTION? ... 133
David Frost, Tyson Beach, Jack Callaghan, Stuart McGill

MOTOR IMAGERY USE DURING SIMPLE KNEE FLEXION-EXTENSION EXERCISES MAY ENHANCE KNEE EXTENSOR MUSCLE RECRUITMENT AMPLITUDES 134
Phillip McKeen, Krista Munroe-Chandler, Nadia Azar

EXHAUSTIVE EXERCISE IMBALANCES NEUROMUSUCLAR ACTIVATION PATTERNS OF KNEE EXTENSORS AND FLEXORS IN YOUNG AND MIDDLE-AGED WOMEN 135
Monica Maly, Joanne Hodder, Heather Linley, Michael Pierrynowski, Tova Plashkes

QUANTIFYING DYNAMIC POSTURAL STABILITY DURING SITTING PIVOT TRANSFERS USING A NEW EQUILIBRIUM MODEL IN INDIVIDUALS WITH A SPINAL CORD INJURY: A CASE STUDY 136
Dany Gagnon, Cyril Duclos, Pierre Desjardins, Michel Danakas, Sylvie Nadeau

UPPER BODY ACCELERATIONS DURING BALANCE RECOVERY IN RESPONSE TO LEAN AND RELEASE PERTURBATION WITH AND WITHOUT GALVANIC VESTIBULAR STIMULATION 137
Dmitry Verniba, William Gage

Poster Orthopaedics

TENSILE TESTING OF MEDICAL GRADE UHMWPE TO RUPTURE WITH UTILIZATION OF 3D OPTICAL CORRELATION SYSTEM 138
Tomas Bouda, Radek Sedlacek, Pavel Ruzicka, Svatava Konvickova

A BIOMECHANICAL INVESTIGATION OF ANTERIOR AND POSTERIOR FEMORAL NECK NOTCHING 139
Zachary Morison, Gordon Higgins, Michael Olsen, Emil Schemitsch

WEAR TESTING OF A NOVEL TEMPOROMANDIBULAR JOINT IMPLANT 140
Ryan Frayne, James Dickey, Marvin Schwartz, Gary Morphy

QUANTIFYING THE TRADE-OFF BETWEEN WEAR AND KINEMATICS PERFORMANCE OF TOTAL KNEE REPLACEMENTS USING MULTIOBJECTIVE OPTMIZATION 141
Ryan Willing, Il Yong Kim

FINITE ELEMENT MODELING OF CAM IMPINGEMENT USING PATIENT-SPECIFIC DATA 142
K.C. Geoffrey Ng, Gholamreza Rouhi, Mario Lamontagne, Matthew Kennedy, Paul E. Beaule

EFFECTS OF HIND LIMB MUSCLE WEAKNESS ON TIBIAL CARTILAGE DEGENERATION IN RABBITS 143
Aliaa Rehan Youssef, Tim Leonard, Walter Herzog

DETERMINING THE EFFECTS OF WALKING POLES ON THE KNEE ADDUCTION MOMENT USING AN INSTRUMENTED NORDIC WALKING POLE: A PILOT STUDY 144
Daniel Bechard, Thomas Jenkyn, Ian Jones, Trevor Birmingham

INFLUENCE OF MATERIAL PROPERTIES OF HIP PROSTHESIS FEMORAL COMPONENT ON STRESS SHIELDING 145
Ashkan Lakzadeh, Tina Khazaei, Ali Ataei

Poster Sports 2

NEUROMUSCULAR APPROACH IN SPORT SPECIFICITY: ABILITY OF TWO OFF-ICE TRAINING DEVICES TO REPRODUCE FORWARD ICE SKATING 146
Jacob Smith, Scott Landry

MUSCLE ACTIVITY PATTERNS OF THE UPPER LIMB AND TRUNK DURING ACCELERATED AND CONSTANT VELOCITY SLEDGE HOCKEY PROPULSION 147
Lisa Chisholm, Rebecca Wightman, Roxanne Seaman, Scott Landry

CLUB POSITION RELATIVE TO THE SWING PLANE SIGNIFICANTLY AFFECTS SWING DYNAMICS 148
Sasho MacKenzie

KINEMATIC COMPARISON OF THE UNDERWATER DOLPHIN KICK BETWEEN SWIMMERS WITH DIFFERENT LEVELS OF COMPETITIVE ABILITY 149
Ryan Atkison, Volker Nolte

THE EFFECT OF DRAG SUIT TRAINING ON 50-M FREESTYLE PERFORMANCE 150
Andrew Dragunas, Volker Nolte, James Dickey

BIOMECHANICS OF THE CROSS-COUNTRY SIT-SKIER AND IMPACT ON SIT-SKI DESIGN - A TOP SECRET 2010 PROJECT 151
Marie-Pierre Leblanc-Lebeau, Denis Rancourt, Eve Langelier, Marc-André Cyr, Jean-Luc Lessard, Cécile Smeesters

CENTER OF MASS CONTROL IN PARALYMPIC ALPINE SKIING - A TOP SECRET 2010 PROJECT 152
Stéphane Martel, Eve Langelier, Cécile Smeesters, Jean-Luc Lessard, Nicolas Huppé, Denis Rancourt

Spine

MECHANISMS OF WHIPLASH INJURY PREVENTION ATTRIBUTABLE TO ENERGY-ABSORBING SEAT 153
Paul Ivancic, Ming Xiao

TEMPORAL ACTIVATION LAGS OF ADJACENT FIBRE COMPARTMENTS SUGGEST SEPARATE BIOMECHANICAL FUNCTION AND CONTROL IN IPSILATERAL LUMBAR ERECTOR SPINAE 154
Marilee Nugent, Theodore Milner

THE EFFECTS OF ACTIVE RELEASE TECHNIQUE® ON TIGHT HIP FLEXOR GROUPS WITH AND WITHOUT LOW BACK PAIN 155
Daniel Avrahami, James Potvin

LUMBAR MOTION AND MUSCLE ACTIVITY ON THE ELLIPTICAL TRAINER DIFFERS FROM WALKING 156
Janice Moreside, Stuart McGill

PREDICTING VERTEBRAL SHEAR FAILURE TOLERANCES FROM MORPHOLOGY AND BONE DENSITY 157
Samuel Howarth, Jack Callaghan

EFFECT OF THE RUPTURE OF THE TRANSVERSE LIGAMENT ON THE BIOMECHANICS OF THE CERVICAL SPINE IN COMPRESSION 158
Wissal Mesfar, Kodjo Moglo

Motor Control

HIP ABDUCTOR ACTIVATION AND COORDINATION WITH ABDOMINAL MUSCLES DURING WALKING IN CHRONIC LOW BACK PAIN AND ASYMPTOMATIC INDIVIDUALS 159
Fahad Algarni, Edwin Hanada , Cheryl Hubley-Kozey

TEMPORAL RECRUITMENT PATTERNS REMAIN ALTERED IN INDIVIDUALS WITH A LOW BACK INJURY THAT RETURN TO WORK 160
Heather Butler, Cheryl Hubley-Kozey, John Kozey

MONITORING UPPER LIMB ACTIVITY DURING STROKE REHABILITATION WITH ACCELEROMETERS 161
Jeremy Noble, Janice Eng, Debbie Rand

EVALUATION OF THE STEPPING LIMB CENTRE OF PRESSURE ON FOOT CONTACT DURING VOLITIONAL AND PERTURBATION-EVOKED STEPPING 162
Jonathan Singer, Stephen Prentice, William McIlroy

POSTURAL RESPONSE TO MULTIDIRECTIONAL PERTURBATIONS TO THE ARM DURING STANCE 163
Ali Forghani, Sheida Rabipour, Theodore Milner, Paul Stapley

ASSESSMENT OF THE POSTURAL CONTROL STRATEGIES USED TO PLAY TWO WII FITTM VIDEO GAMES 164
Anna Michalski, Cheryl Glazebrook, Alyson Martin, William Wong, Andrew Kim, Nancy Salbach, Bryan Steinnagel, Jan Andrysek, Ricardo Torres-Moreno, Karl Zabjek

Muscle 2

RESIDUAL FORCE ENHANCEMENT FOLLOWING STRETCH OCCURS IN A SINGLE SARCOMERE 165
Tim Leonard, Walter Herzog

NOVEL PROPERTIES OF TITIN IMMUNOGLOBULIN DOMAIN FROM HUMAN CARDIAC MUSCLE 166
Mike DuVall, Matthias Amrein, Jessica Gifford, Walter Herzog

SARCOMERE POPPING LIMITS FORCE LOSS IN STRETCH-INDUCED INJURY 167
Appaji Panchangam, Walter Herzog

MORPHOLOGICAL CHANGES IN CONTTRACTILE PROPERTIES OF MUSCLES SUBJECTED TO REPEAT INJECTIONS OF BOTULINUM TOXIN TYPE A (BOTOX) 168
Rafael Fortuna, Marco Aurelio Vaz, Aliaa Rehan Youssef, David Longino, Walter Herzog

AGING EFFECTS ON GRIP FORCE CONTROL: AN fMRI STUDY 169
Jeremy Noble, Janice Eng, Kristen Kokotilo, Lara Boyd

MUSCLE ACTIVATION AT THE KNEE JOINT DURING CLOSED KINETIC CHAIN LOADING 170
Teresa Flaxman, Andrew Speirs, Daniel Benoit

Gait 3

OBESITY AFFECTS GAIT PATTERN CHANGES IN MODERATE KNEE OSTEOARTHRITIS 171
Graeme Harding, Janie Astephen Wilson, Cheryl Hubley-Kozey

OBESITY DOES NOT ALTER CONTACT FORCES IN TIBIOFEMORAL JOINT WITH MODERATE OA 172
Graeme Harding, Janie Astephen Wilson, Cheryl Hubley-Kozey

SAGITTAL AND FRONTAL PLANE JOINT MOMENT PROFILES ASSOCIATED WITH STAIR ASCENT AND DESCENT IN YOUNG AND OLDER ADULTS 173
Alison Novak, Brenda Brouwer

IMPROVING GAIT CHARACTERISTICS IN OLDER ADULTS: THE EFFECT OF BIODEX BALANCE SYSTEM SDTM VERSUS WOBBLE BOARD BALANCE TRAINING 174
Brittney Muir, Shirley Rietdyk, Jeffery Haddad, Jessica Seaman

ARE HEAD ROTATIONS SUFFICIENT TO CAUSE A CHANGE IN TRAVEL PATH IN YOUNG AND OLDER ADULTS? 175
Michael Cinelli, William Warren

USE OF PROGRESSIVE GLASSES WHEN GOING DOWNSTAIRS MODIFIES POSTURAL AND MOTOR STRATEGIES IN ELDERLY PEOPLE 176
Julie Lecours, Sylvie Nadeau, Benoît Frenette, Jacques Gresset, Guillaume Giraudet

NDI New Investigator

IS THE GENESIS OF ROTATOR CUFF DISEASE (RCD) LINKED TO MUSCLE FATIGUE? 177
Clark Dickerson

Sports 2

BETWEEN-DAY RELIABILITY IN MEASUREMENT OF SHORT-LATENCY MUSCLE ACTIVATION AND FORCE-TIME VARIABLES OF THE NECK 178
Lucie Pelland, Sivan Almosnino, Joan Stevenson

THE INFLUENCE OF FATIGUE ON TISSUE VIBRATION IN PROLONGED RUNNING ... 179
Bernd Friesenbichler, Lisa Stirling, Peter Federolf, Benno Nigg

THE IMPACT OF MINI-BAND ON FRONTAL PLANE KNEE KINEMATICS DURING SQUAT TRAINING 180
Chad Gooyers, Tyson Beach, David Frost, Jack Callaghan

PREDICTORS OF LOWER EXTREMITY INJURIES IN VARSITY ATHLETES 181
Timothy Burkhart, Alison Schinkel-Ivy, David Andrews

DYNAMIC TRACKING OF MYOTENDINOUS JUNCTION: EFFECT OF IMMEDIATE EXERCISE ON TENDON PROPERTY USING ULTRASOUND IMAGING 182
mahta karimpoor, Richard Twycross-Lewis, Hazel Screen, Dylan Morrissey

3 DIMENSIONAL KINETIC ANALYSIS OF OLYMPIC WEIGHTLIFTING SNATCH LIFT .. 183
David John Saxby, Gordon Robertson

Gait 4

THE INFLUENCE OF SHOE CONSTRUCTION ON WALKING AND BALANCE PERFORMANCE 184
Ann-Kathrin Hömme, Ewald Hennig, Seungbum Park

QUANTIFICATION OF INERTIAL SENSOR-BASED 3D KNEE JOINT ANGLE MEASUREMENT ACCURACY USING AN INSTRUMENTED GIMBAL 185
Andrew Brennan, Kevin Deluzio, Qingguo Li

A NEW APPROACH TO POSTURAL STABILITY RESEARCH USING THE INVERTED PENDULUM MODEL 186
Nicholas Ali, Gordon Robertson, Gholamreza Rouhi

RUNNING SPEED ESTIMATION USING A LEG-MOUNTED INERTIAL MEASUREMENT UNIT 187
Chris Mohr, Shuozhi Yang, Qingguo Li

REORGANIZATION OF FRONTAL PLANE BIOMECHANICS AT THE HIP WHEN WALKING WITH A LOAD ON THE AFFECTED OR NON-AFFECTED LEG IN INDIVIDUALS WITH HEMIPARESIS 188
Carole Miéville, Cyril Duclos, Sylvie Nadeau

CUMULATIVE LOADING IS SUPERIOR TO THE PEAK KNEE ADDUCTION MOMENT WHEN DISTINGUISHING BETWEEN HEALTHY ADULTS AND ADULTS WITH KNEE OSTEOARTHRITIS 189
Monica Maly, Shawn Robbins

Orthopaedics 2

QUADRICEPS IMPAIRMENT AFFECTS LOWER EXTREMITY JOINT MOMENTS DURING GAIT IN YOUNG ADULTS 190
Gillian Hatfield, Cheryl Hubley-Kozey, William Stanish

MODEL-BASED RADIOSTEREOMETRIC ANALYSIS OF AN UNCEMENTED MOBILE-BEARING TOTAL ANKLE ARTHROPLASTY (TAA) SYSTEM 191
Jason Fong, David Wilson, Allan Hennigar, Michael Dunbar, Mark Glazebrook

UNCEMENTED FEMORAL STEM LENGTH EFFECT ON ITS PRIMARY STABILITY 192
Michael Reimeringer, Natalia Nuño, Christian Desmarais-Trépanier, Martin Lavigne, Pascal-André Vendittoli

PROBABILISTIC COMPARISION OF SHOULDER KINEMATIC DESCRIPTIONS FOR ROTATOR CUFF TEAR PATIENTS PRE- AND POST-SUBACROMIAL INJECTION 193
Joseph Langenderfer, Jason Scibek

FEA OF MECHANICAL STIMULI TRANSFER BETWEEN ORTHOPAEDIC SCREWS AND SURROUNDING BONE: A POSSIBLE METHOD FOR PREDICTING STRESS SHIELDING 194
Kristina Haase, Rouhi Gholamreza

Methods

FORCE VARIABILITY DURING FATIGUING MAXIMAL ISOMETRIC ELBOW FLEXION EXERTIONS 195
Tara Kajaks, Erik Paerels, James Potvin

COMPREHENSIVE ANALYTICAL DESCRIPTION OF KINEMATIC CROSSTALK 196
Andrew Brennan, Qingguo Li, Kevin Deluzio

SINGLE-PLANE FLUOROSCOPY ACCURACY FOR DETERMINING THE RELATIVE POSE BETWEEN TOTAL KNEE REPLACEMENT COMPONENTS 197
Stacey Acker, Heather Murray, Paul St. John, Scott Banks, Shang Mu, Urs Wyss, Kevin Deluzio

THE BIOMECHANICS OF ARTICULAR CARTILAGE CHONDROCYTES IN VIVO 198
Ziad Abusara, Walter Herzog

BILATERAL FREQUENCY CONTENT DIFFERENCES IN ISOKINETIC KNEE EXTENSION CURVES OF OSTEOARTHRITIS PATIENTS 199
Patrick Costigan, Sivan Almosnino, Elizabeth Sled, Alison Chalmers , Joan Stevenson

VERTICAL JUMP FORCE PREDICTS UNILATERAL PLANTAR FLEXOR DEFICITS IN ARTHRITIC CHILDREN 200
Matthew Kennedy, Mario Lamontagne, Johannes Roth

Author Index 201

Reviewers List 206

PREOPERATIVE EMG PATTERNS PREDICT TOTAL KNEE IMPLANT MIGRATION

David AJ Wilson[1,2], Janie L Astephen Wilson[1], Cheryl L Hubley-Kozey[1,3], Michael J Dunbar[1,2]
[1]School of Biomedical Engineering, Dalhousie University, Halifax, NS, Canada, wilsondaj@gmail.com
[2]Division of Orthopaedics, Department of Surgery, Dalhousie University, Halifax, NS, Canada
[3]School of Physiotherapy, Dalhousie University, Halifax, NS, Canada

INTRODUCTION

Postoperative total knee replacement (TKR) implant migration measured with radiostereometric analysis (RSA) has been shown to be predictive of early implant failure [1]. It has also previously been shown that high preoperative flexion moments during gait can predispose patients with TKR to early aseptic loosening [2]. The objective of this study was to determine whether preoperative patient neuromuscular activation patterns measured with electromyography (EMG) are associated with the post-TKR migration of total knee replacements.

METHODS

37 TKR patients were recruited to this study. Study participants had been randomized to receive the Nexgen LPS Trabecular Metal tibial monoblock component (n = 19) or the cemented NexGen Option Stemmed tibial component (n = 18) (Zimmer, Warsaw IN). RSA analysis was performed with MB-RSA (MEDIS, Leiden), and results were reported as 6 degrees of freedom translations and rotations at 6 months. All patients underwent 3D gait analysis in the week prior to their surgery. A synchronized motion capture (Optotrak, NDI) and electromyography (Bortec) system was used to capture neuromuscular control patterns of 7 major muscle sites surrounding the knee [3]. The EMG data were full wave rectified and normalized to maximums obtained at the same visit. Major patterns of variability in subject EMG patterns were captured with principal component analysis [4], and a set of discrete PC scores that represented weightings on these patterns were calculated. Associations between PC scores from each muscle were compared to post-TKR tibial implant migration using correlation analysis (p 0.001 with Bonferroni correction for multiple tests). The results of the correlations were used in conjunction with the authors` expertise to identify variables entered into a linear regression model.

RESULTS

A correlation was found between the PC3 of the lateral gastroc muscle (representing normal high gastroc activation in late stance) and the anterior migration of the component (R^2=0.247, p=0.002) but was not significant after correction**.** A significant correlation was found between the vastus medialis PC3 (representing normal high vastus medialis activation in early stance) and the anterior migration of the component (R^2= 0.338, p<0.001**).** A regression model was developed for the anterior migration of the tibial component. The two EMG variables that were most strongly correlated with anterior migration and that had a mechanistic reason to affect migration (PC3 of the lateral gastrocnemius and vastus medialis) were included in the model.

Anterior-Posterior Migration = 0.01 +0.12*Vastus Medialis PC3 + 0.074*Lateral Gastrocnemius PC3
(R^2=0.487, p<0.0001)

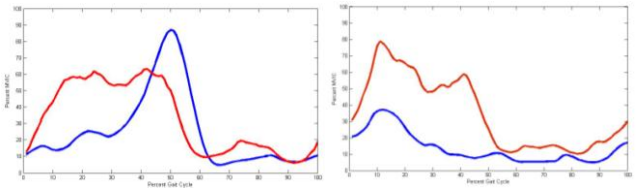

Figure 1. The average of the highest and lowest five scored waveforms (blue, red respectively) for the lateral gastrocnemius PC3 (left) and vastus medialis PC3 (right). Low scores (red) were associated with posterior implant migration; high score (blue) with anterior migration.

DISCUSSION AND CONCLUSIONS

In previous work using a force trasnducer instrumented total knee replacement, D'Lima et al. [5] found that during gait there is a net anterior shear force acting on the tibial component of a total knee replacement. In our study, we found patients with 'normal' EMG waveforms in the vastus and gastrocnemius muscle groups migrate anteriorly postoperatively. This is consistent with the result of D'Lima. However, patients with a pathological continuous co-contraction of the vastus and gastrocnemius muscle tended to migrate posteriorly. As both the vastus and gastrocnemius apply a posterior shear to the tibia, it is logical that in patients who are continuously contracting these muscles, there would be a net posterior shear acting on the tibia leading to posterior migration over time. Our results suggest that patient specific variables need to be taken into consideration in total knee replacement surgery to optimize outcomes.

REFERENCES

[1] Ryd L, Albrektsson et al. Radiostereometric analysis as a predictor of loosening of knee prostheses. J Bone Joint Surg Br 1995 May;77(3):377-83.
[2] Hilding MB et al. Knee joint loading and tibial component loosening. J Bone Joint Surg Br 1996 Jan;78(1):66-73.
[3] Hubley-Kozey CL et al. . Neuromuscular alterations during walking in persons with moderate knee osteoarthritis. J Electromyogr Kinesiol 2006 Aug;16(4):365-78.
[4] Deluzio KJ et al. Biomechanical features of gait waveform data - An application of principal component analysis. Gait & Posture 2007 Jan;25(1):86-93.
[5] D'Lima DD et al. In vivo knee moments and shear after total knee arthroplasty. J Biomech 2007;40 Suppl 1:S11-S17.

BIOMECHANICAL IMPLICATIONS OF POLICE CRUISER REAR RESTRAINT CAGE CONFIGURATIONS AND MOBILE DATA TERMINAL LOCATION: HALF VERSUS FULL CAGE DESIGNS

Samantha A. Molenaar, Clark R. Dickerson
Department of Kinesiology, University of Waterloo, Waterloo, ON

INTRODUCTION

Musculoskeletal disorders (MSDs) amongst mobile police are likely partly attributable to prolonged occupational driving and the performance of administrative tasks in the police cruiser[1,2], including Mobile Data Terminal (MDT) use. Due to the confined space of the mobile work environment, officers are often forced to reach and twist[2] to complete required tasks, which potentially puts their backs and shoulders at risk of injury. The purpose of this study was to quantify how modifications of the interior layout of the vehicle, achieved by modifying the restraint cage design, influence discomfort, task (typing and data entry) performance, and muscle activation while in a mobile environment.

METHODS

10 university aged subjects completed a single two hour session that included three sessions of typing trials at two different MDT locations, representing a standard cruiser and a cage modified cruiser, separated by a simulated driving task. All tasks were performed using a driving simulator. Outcome variables included 10 channels of normalized bilateral surface electromyography, ratings of perceived discomfort (RPD) for both shoulders, typing speed and typing accuracy. Participants wore an armoured vest and duty belt. A 2-factor ANOVA analysis was used to assess the influences of task order and MDT location (original – full cage; or modified – half cage) on the outcome variables.

RESULTS

While task order did not affect any outcome measure, MDT location influenced many significantly (Figure 1), including RPD and several specific muscle activity levels, and often bilaterally. The largest differences were seen in the RPD data (RPD was reduced by 69% on the left and 58% for the right side in the modified configuration). It is difficult to ascertain the physical importance of the muscular demand differences (Table 1), however, as the magnitudes of the exposures are relatively low compared to traditional endurance criteria. The largest demand existed in anterior deltoid and infraspinatus, likely due to the arm elevation needed to perform the typing tasks. More pronounced changes persistently existed for the left side over both metrics. Typing speed and accuracy were not influenced by the modified design (Table 1).

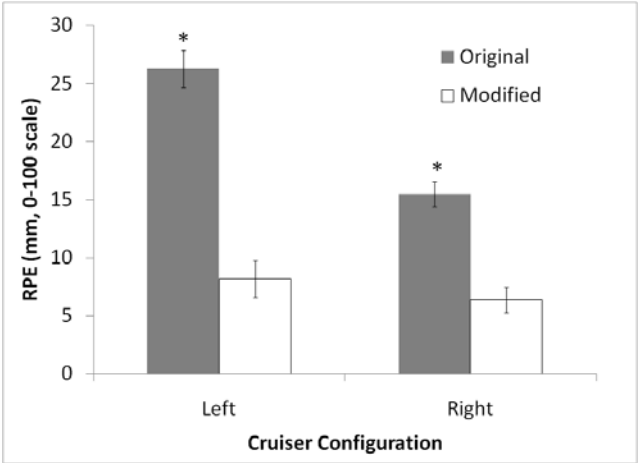

Figure 1: RPD ratings for original and modified cruiser configurations. * indicates a significant difference within side with a modification in configuration

DISCUSSION AND CONCLUSIONS

A modified single-occupant cage design appears to lower both muscle demands and discomfort in simulated police tasks. This may have implications for future police car designs. The most remarkable differences were in the RPD results. As RPD is a complex, integrative quantity – including sensation through multiple pathways - it punctuates that important differences exist between the conditions, even if they did not emerge readily from large magnitude differences in either the muscle activity or typing performance metrics. However, even the modest differences seen in individual muscles may result in higher cumulative exposures over shifts, workweeks, and a career in police work. These may lead to long term disability.

REFERENCES

[1] Gyi DE, Porter JM (1998). Musculoskeletal Problems and Driving in Police Officers. *Occ.l Med.* 48:153-160.
[2] McKinnon CD. (2009). Quantification and Evaluation of Physical Shoulder Exposures in Police Mobile Data Terminal. MSc. Dissertation, University of Waterloo, Waterloo, ON.

ACKNOWLEDGEMENTS

I would like to thank Steven Fisher and Colin McKinnon for their assistance in data processing.

Table 1: Outcome measures stratified by side and cruiser configuration. Significant differences (by side) are indicated in bold on the table. Muscle data is expressed as a percentage of maximum activation.

Side/ Configuration	RPD (0-100)	Anterior Deltoid	Middle Deltoid	Infra-spinatus	Supra-spinatus	Trapezius	Typing Speed	Typing Accuracy
Left Original	**26.3**	**6.8**	**2.7**	5.9	2.7	**2.5**	48.0	91.5
Left Modified	**8.2**	**3.7**	**1.6**	5.7	2.7	**2.8**	48.4	91.9
Right Original	**15.5**	**3.0**	**2.5**	**5.4**	**4.0**	**4.3**	N/A	N/A
Right Modified	**6.4**	**2.5**	**2.0**	**4.9**	**3.0**	**3.5**	N/A	N/A

MUSCLE ACTIVATION DURING HAND DEXTERITY TASKS IN INDIVIDUALS WITH HAND OSTEOARTHRITIS

Kristina Calder[1], Vicki Galea[1], Jean Wessel[1], Joy MacDermid[1], Norma MacIntyre[1]
[1]School of Rehabilitation Science, McMaster University, Hamilton, ON Canada, kcalder@mcmaster.ca

INTRODUCTION

Hand osteoarthritis (OA) is the most frequent condition leading to hand pain and disability [1]. It is unknown how common impairments (pain, strength deficits, and reduced flexibility) affect functional hand movements, particularly those requiring considerable dexterity. Electromyography (EMG) provides information on both neural drive (amplitude) and temporal/phasic (shape) activation characteristics of the musculature.

The primary purpose of this study was compare muscle activation patterns in women with and without hand osteoarthritis (OA). The secondary purpose was to investigate whether relationships exist between muscle activity and measures of impairment and function in persons with OA of the hand.

METHODS

Community-dwelling women over the age of 50 years without hand problems and those who met the American College of Rheumatology (ACR) clinical criteria for OA of the dominant hand were included in this study [2]. Three maximum voluntary grip and tripod grip strength of the dominant hand were each assessed and averaged using the NK Digits-Grip device of the NK Hand Assessment System (NK Biotechnical Corporation, Minneapolis, MN, USA). Dexterity was measured using the dexterity board of the NK Hand Assessment System. Two questionnaires: patient-rated wrist/hand evaluation (PRWHE); and the Arthritis Impact Measurement Scale (AIMS2) were completed by all subjects.

Dominant hand muscle activity was recorded using surface EMG from the thenar, first dorsal interossei (FDI), hypothenar, and extensor digitorum communis (EDC) muscles during a dexterity task. The first two digits of the hand were used to screw (assembly) and unscrew (disassembly) a small bolt from a thread. Average integrated EMG (IEMG) values were computed and cross-correlation analysis between six muscle pairs was performed. Pearson correlation coefficients were transformed to Fisher Z scores prior to statistical analyses. Independent *t*-tests were used to compare subject characteristics. To control for the effect of age, one-way analysis of covariance (ANCOVA) were used to compare groups with respect to strength (grip and pinch) and dexterity (small and large objects). The Group differences in IEMG of each muscle and the cross-correlations of six muscle pairs were compared using two-way repeated measures ANCOVAs. Pearson correlations were used to determine the relationship of the IEMG variables with PRWHE-pain, PRWHE-specific activity; AIMS2-hand and finger function scale, and dexterity for large and small objects in the hand OA group. Alpha level was set at 0.05 for all tests.

RESULTS

Seventeen women with hand OA (69.59 ±10.36 years) and nine healthy control subjects (58.33 ± 3.54 years) participated in the study. Women with hand OA were significantly older ($p < 0.05$). After controlling for age, women with hand OA had reduced strength (grip: F=11.610, p=0.002; tripod pinch: F=16.805, p=0.000) and took longer to manipulate large objects (F=5.636, p=0.026) when compared to the control group. Taking into account the effect due to age, women with hand OA had significantly larger IEMG during disassembly (F=4.542, p=0.04) whereas IEMG during assembly did not differ compared with the control group (p>0.05). No significant group differences were found when comparing correlations between muscle pairs during assembly or disassembly (p>0.05). Associations between IEMG and measures of dexterity, pain and self-reported disability in the women with hand OA revealed muscle activity during assembly was positively related to dexterity (thenar and EDC) and pain (FDI). During disassembly, only FDI muscle activity was associated with dexterity (large objects) and disability (AIMS-2).

DISCUSSION AND CONCLUSIONS

Individuals with hand OA appear to have altered motor function when compared to healthy control subjects. Given the cross-sectional nature of the study, it is unclear whether these represent adaptive muscle changes or were predisposing risk factors. Future studies should examine muscle activity across a variety of functional activities, over time in a larger sample of men and women with hand OA and consider the relationships between sensory and motor function. Additionally both alternative methods for obtaining and analyzing EMG activity may be needed to obtain more definitive information on muscle control and performance.

REFERENCES

[1] Bagis et al. (2003). The effect of hand osteoarthritis on grip and pinch strength and hand function in postmenopausal women. *Clin Rheumatol* Vol 22(6); p. 420-424.

[2] Bellamy et al. (1999). Perceptual variation in categorizing individuals according to American College of Rheumatology classification criteria for hand, knee, and hip osteoarthritis (OA): observations based on an Australian Twin Registry study of OA. *J Rheumatol* Vol 26(12); p. 2654-2658.

ACKNOWLEDGEMENTS

This work was supported in part by NSERC and ASHT Evelyn Mackin Grant for Research in Hand Therapy.

PERFORMING SITTING PIVOT TRANSFERS REQUIRES GREATER UPPER LIMB MUSCULAR DEMAND THAN WEIGHT-LIFTS IN INDIVIDUALS WITH A SPINAL CORD INJURY

Dany Gagnon[1,2], Ariane Desharnais[1,2], Sylvie Nadeau[1,2]
[1]School of Rehabilitation, University of Montreal, Montreal, Canada, dany.gagnon.2@umontreal.ca
[2]Center for Interdisciplinary Research in Rehabilitation (CRIR), Montreal, Canada [www.pathokin.ca]

INTRODUCTION

Individuals with a spinal cord injury (SCI) rely heavily on their upper limbs (U/Ls) when performing sitting pivot transfers (SPTs) and pressure-relieving weight-lift manoeuvres (WLMs). The substantial muscular demand repeatedly placed on the U/Ls while performing these tasks may increases the risk of developing secondary U/L impairments. Until now, no study has compared U/L muscular demand during SPTs and WLMs in a single sample of individuals with SCI. This study aimed to compare muscular demand of the dominant U/L when used in three distinct roles: leading U/L during SPTs; trailing U/L during SPTs; and lifting U/L during WRLs with symmetrical hand position in individuals with SCI. The hypotheses were that SPTs would generate greater muscular demand than WRLs, and that muscular demand during SPTs would be greater at the trailing U/L than at the leading U/L.

METHODS

Thirteen right-handed males (age = 42.50 ± 9.17 yrs; height = 1.76 ± 0.08 m; weight = 84.01 ± 18.30 kg) with complete motor thoracic spinal cord injury (T4-T11), who performed SPTs and WRLs independently, participated in this study. During a laboratory assessment [1], subjects performed three SPTs toward a target seat (leading role), three SPTs toward an initial seat (trailing role) and three WRLs with their hands positioned symmetrically on resting surfaces set 10 cm higher (lifting role) [2]. Surface electromyography (EMG) of the biceps, triceps, anterior deltoid, pectoralis major was recorded (600Hz) at the right U/L. To quantify the electromyographic muscular utilization ratio (MUR_{EMG}), EMG data recorded during the SPTs and WRLs were amplitude-normalized against values obtained during dynamic maximum voluntary contraction (isokinetic mode; 30°/s) completed on an instrumented dynamometer; this ratio was then multiplied by 100 to obtain a percentage ($\%MUR_{EMG}$). All EMG data were bandpass filtered (30-500 Hz), full-wave rectified and low-pass filtered at 3Hz to generate linear envelopes. The SPTs and WRLs were divided into pre-lift, lift and post-lift phases (time-normalized to 100 data points) for a total of 300 data points for the entire duration of the tasks [1, 2]. Averaged overall peak $\%MUR_{EMG}$ and the averaged mean $\%MUR_{EMG}$ measured during the lift phase were the main outcome measures.

RESULTS

The peak and mean $\%MUR_{EMG}$ values of the biceps, anterior deltoid and pectoralis major were significantly higher during SPTs than WRLs. During SPTs, the peak $\%MUR_{EMG}$ of the anterior deltoid was more elevated at the trailing U/L than at the leading U/L, whereas the mean $\%MUR_{EMG}$ of the pectoralis major reached its highest value when the dominant shoulder played a trailing role as opposed to a leading role.

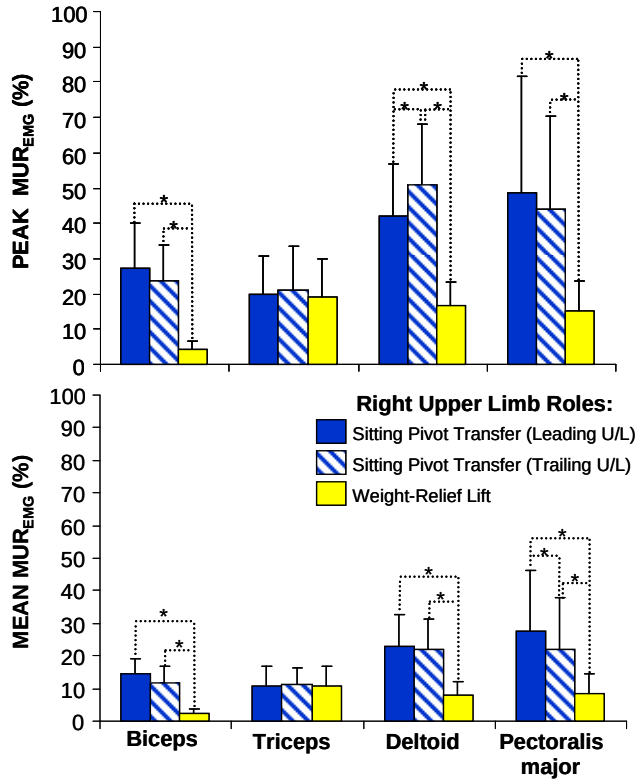

Figure 1: Averaged peak (top) and mean (bottom) muscular utilization ratio during SPTs and WRLs at the right U/L.

DISCUSSION AND CONCLUSIONS

This study confirms that the performance of SPTs imposes greater muscular demand than WRLs at the biceps, anterior deltoid and pectoralis major of the dominant U/L. This study also highlights that muscular demand is influenced by the role played by the U/L (leading vs. trailing role) during SPTs, especially for the anterior deltoid and pectoralis major during SPTs. These two muscles should be strengthened in clinical practice to reduce relative muscular demand and minimize the likelihood of developing secondary U/L impairments.

REFERENCES

[1] Gagnon, D et al. (2008) Biomechanical assessment of sitting pivot transfer tasks using a newly-developed instrumented transfer system. J Biomech, **41**: 1104-10.
[2] Gagnon, D et al. (2008) Comparison of peak shoulder and elbow mechanical loads during weight-relief lifts and sitting pivot transfers among manual wheelchair users with spinal cord injury. J Rehabil Res Dev, **45**:.863–73.

ACKNOWLEDGEMENTS

Funded by the Lindsay Rehabilitation Hospital Foundation and the Quebec Rehabilitation Research Network (REPAR). S. Nadeau is a senior researcher supported by the FRSQ.

BIOMECHANICAL PROPERTIES OF POSTEROMEDIAL KNEE JOINT CAPSULE IN CHRONIC OSTEOARTHRITIS

Justin Steeds[1], Mark Hurtig[2], Karen Gordon[1]
[1]School of Engineering, University of Guelph, Guelph, Canada, jsteeds@uoguelph.ca
[2]Dept. of Clinical Studies, University of Guelph, Guelph, Canada

INTRODUCTION

The contribution of joint capsule as a functionally significant restraining structure has been minimally investigated on the posteromedial aspect of the knee joint [1, 2]. Previous studies on human posteromedial joint capsule (PMC) have reported load-displacement behavior [1], and the role of capsular restraint on anterior-posterior drawer, internal-external, flexion and valgus rotation [2]. This work has indicated that the PMC has comparable biomechanical properties to the superficial and deep medial collateral ligaments [1], and plays a role in controlling tibiofemoral laxity in the extended knee [2]. The objective of this study was to determine the changes in the biomechanical properties of posteromedial stifle joint capsule due to osteoarthritis (OA) development using an ovine model.

METHODS

The use of animals in this study was approved by the University of Guelph Animal Care Committee and was in accordance with the Canadian Council on Animal Care. Five sheep underwent unilateral ACL transection and creation of a bucket handle medial meniscal tear (n=4) or a meniscal tear (n=1) alone. These and the contralateral joints were used for mechanical testing 1 year post surgery. Joints were dissected of all soft tissue and muscle except for the PMC, and then the tibia and femur were potted in a custom jig for mounting on an Instron 8872 servohydraulic testing machine (Instron Corp, MA, USA). Joint distraction tests at varying flexion angles of approximately 30°, 60° and 90° were conducted at strain rates of 10mm/min, 100mm/min and 1000mm/min. A test to failure was performed at 1000mm/min at approximately 30° of flexion. All specimens were preconditioned with 10 cycles at a strain rate of 10mm/min and a peak-to-peak displacement of 3mm prior to each test. An in-situ joint coordinate system [3] was established for each joint through digitizing the 3-D position of lead markers placed on bony landmarks on the femur and tibia using a Microscribe (Immersion Corp., CA, Canada). Lead markers fixed along the loading axis on the posterior aspect of the PMC were used to track uniaxial tissue strain. A single Grasshopper® GRAS-20S4M/C camera (Point Grey Research Inc., BC, Canada) with Correlated Solutions VIC-Snap (Correlated Solutions, Inc., SC, USA) image acquisition software was used to collect images during mechanical tests. Marker centroids were calculated by using custom written thresholding and segmenting code written in MATLAB® 7.1 (The MathWorks, Inc., MA, USA). Specimen thicknesses and widths were measured using calipers at a proximal and distal site with five replicates. Load-displacement graphs were constructed for all tests in Microsoft Excel (2007). Stiffness and Young's modulus were determined using linear regression from the largest linear portion of the load-displacement and stress-strain curves respectively having a coefficient of determination (R^2) greater than 0.95. Statistical evaluation used a linear model where stiffness was a function of treatment, flexion angle, and strain rate using R statistical software (v2.8.1, 2009).

RESULTS

The effect of flexion angle on PMC stiffness was determined to be statistically significant ($p < 0.0005$) with a decrease in stiffness of 0.67 N/mm with each one degree increment in flexion after accounting for strain rate and treatment (Figure 1). Stiffness was greater (25.6 N/mm) in the osteoarthritic versus contralateral PMC ($p < 0.02$), after accounting for flexion angle and strain rate (Figure 1).

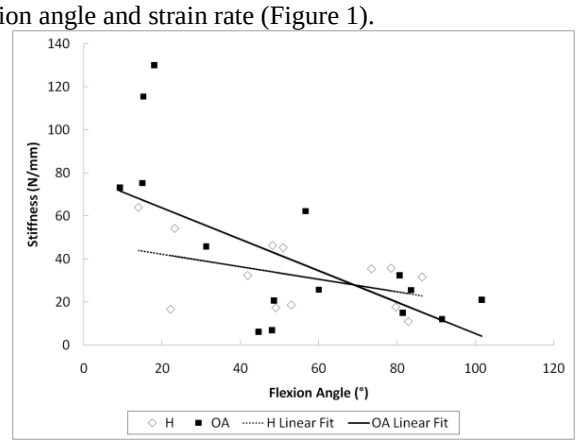

Figure 1: Stiffness of healthy contralateral (H) (n=5) and osteoarthritic (OA) (n=5) ovine stifle PMC uniaxially tested at 10mm/min at varying flexion angles.

DISCUSSION AND CONCLUSIONS

The results of this study validate the use of an ovine PMC model since the stiffness and Young's modulus values were comparable to human PMC [1]. These results also verify that the PMC plays a functional role in knee stability. Furthermore, a statistical difference between stiffness of the healthy contralateral and OA PMC were observed suggesting a change in biomechanical properties accompanies onset of OA.

REFERENCES

[1] Robinson et al. (2005). Structural properties of the medial collateral ligament complex of the human knee. J Biomech. Vol **38**(5); p. 1067-74.
[2] Robinson et al. (2006). The role of the medial collateral ligament and posteromedial capsule in controlling knee laxity. Am J Sports Med. Vol **34**(11); p. 1815-23.
[3] Grood et al. (1983). A joint coordinate system for the clinical description of three-dimensional motions: application to the knee. J Biomech Eng. Vol **105**(2); p. 136-144.

TRANSVERSE CARPAL LIGAMENT STIFFNESS AND CARPAL BONE KINEMATICS DURING INDENTATION TESTING

Michael W. Holmes[1], Samuel J. Howarth[2], Jack P. Callaghan[2] and Peter J. Keir[1]
[1]Department of Kinesiology, McMaster University, Hamilton, Canada, holmesmw@mcmaster.ca
[2]Department of Kinesiology, University of Waterloo, Waterloo, Canada

INTRODUCTION

Carpal tunnel syndrome (CTS) is linked to the mechanical properties of the carpal tunnel (CT). Hydrostatic pressure change within the CT is influenced by its contents and surrounding structures. The fibrous transverse carpal ligament (TCL) encloses the CT, influences tendon and nerve movement, and thus contributes to CT mechanics and stability. However, investigation of the material properties of the TCL has been limited to *in vivo* [1] studies or by CT expansion via palmarly directed forces to the TCL [2]. The exact role the TCL plays in CT stability remains unclear and only neutral or slightly extended wrist postures have been tested. The purpose of this study was to investigate the effects of loading and posture on carpal kinematics and material properties of the cadaveric TCL.

METHODS

Ten fresh-frozen cadaver arms, harvested at mid-humerus were used to test the properties of the TCL (3 male, 2 female pairs; 79.8 ± 7.0 yrs). Specimens were thawed overnight prior to removal of skin and subcutaneous tissue to expose the TCL and its attachment sites. Infrared-emitting diodes were attached to rigid markers inserted into the pisiform and scaphoid. Three-dimensional motion was measured during trials (Optotrak Certus, Northern Digital Inc., Waterloo, Canada). Each specimen was positioned below the actuator of a servo-hydraulic testing machine (8872, Instron Canada, Toronto, Canada) (Figure 1). The actuator was equipped with a load cell to which a cylinder shaped indenter was affixed. Four indenter sizes (5 mm, 10 mm, 20 mm, and 35 mm diameters) applied loads to the TCL in three wrist postures (30° extension, neutral and 30° flexion). A peak force of 50 N was generated at a rate of 5 N/second for each test. Ten pre-conditioning cycles (20mm indenter, neutral posture) were followed by 3 loading cycles for each posture and indenter combination. Force, actuator displacement and carpal kinematics were sampled at 100 Hz. For each loading phase, stiffness was calculated as the slope of the force-displacement relationship using custom software. A repeated measures ANOVA determined the effects of posture and indenter size on TCL stiffness.

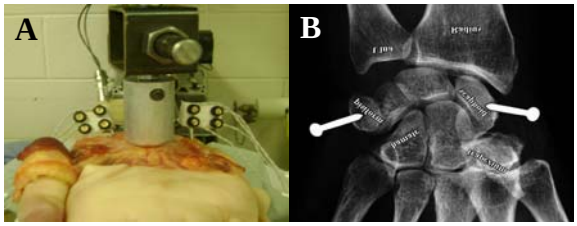

Figure 1: A) Markers inserted into pisiform and scaphoid; Neutral posture and 20 mm indenter shown. **B)** X-ray confirming placement of rigid body markers in each bone.

RESULTS

A significant main effect of posture was found for TCL stiffness. The flexed wrist posture demonstrated greater stiffness (40.0 ± 3.3 N/mm) than the neutral (35.9 ± 3.5 N/mm) and extended postures (34.9 ± 2.8 N/mm). A significant main effect of indenter size was also found for TCL stiffness. Stiffness from the 10 and 20 mm indenter was significantly larger than the 5 mm indenter. Mean TCL stiffness for each indenter across all postures was 40.9 ± 1.0 N/mm (20 mm), 37.9 ± 1.8 N/mm (10 mm), 35.2 ± 1.7 N/mm (35 mm) and 33.8 ± 0.7 N/mm (5 mm).

For actuator displacement, the 5 mm indenter was significantly different than all other indenter sizes. During loading, the largest displacement occurred with the 5 mm indenter (mean of all postures, 2.1 ± 0.2 mm). Additionally, marker transformations at each bone were used to calculate carpal tunnel arch width. Small differences were found in arch width during resting (29.3± 0.5 mm) and peak loading (28.7 ± 0.4 mm). At rest, the neutral posture had the smallest arch width (28.8 ± 0.7 mm) while width was the same for flexed and extended postures (29.4 ± 0.7 mm).

DISCUSSION AND CONCLUSIONS

In each posture, stiffness was greatest with the 20 mm indenter, which should only be acting on the TCL. Surprisingly low stiffness was found for the 35 mm indenter, which often covered the carpal bones. The 35 mm indenter may represent stiffness for the CT complex, which could provide reason for gender differences found in previous work [1]. In the flexed posture, the flexor tendons exert force against the TCL and this could explain the increased stiffness found in this posture.

It has been suggested that changes in carpal arch width is due to bone movement [2] or TCL elongation [3]. The small changes in carpal arch width during our indentations may suggest the TCL is lengthening. Greater TCL thickness at the radial and ulnar borders [4] will limit elongation at that location. As a result, greater strain is likely occurring around the indentation site. TCL stiffness from indentation appears dependent on the dimensions and shape of the indenter as well as CT width. Further analysis of carpal arch width and indentation depth will provide insight into TCL length and CT area during loading.

REFERENCES

[1] Li ZM. (2005). *J Musculoskeletal Res*, **9**; p.153-159.
[2] Li ZM et al. (2009). *J Biomech Eng*, ***131***; p.*1-6.*
[3] Sucher BM. (1998*). J Am Osteopath Assoc*, **98**; p.679-686
[4] Pacek CA et al. (2009). *Hand*, DOI 10.1007/s11552-009

ACKNOWLEDGEMENTS

Funded by CRE-MSD and NSERC Discovery grant #217382. Special thanks to Glenn Oomen, McMaster Anatomy.

LOCALIZED STRAIN MEASUREMENTS OF THE INTERVERTEBRAL DISC ANNULUS

Thomas Karakolis[1], Diane E. Gregory[2], Jack P. Callaghan[1]
[1]Department of Kinesiology, University of Waterloo, Waterloo, Canada , tkarakol@uwaterloo.ca
[2]Department of Orthopaedic Surgery, University of California, San Diego, San Diego, California

INTRODUCTION

Herniation of the intervertebral disc involves the nucleus pulposus breaching the surrounding composite laminate structure - the annulus fibrosus. Delamination of the annulus has been described as one of the initial stages of disc herniation [1]. Attempts to characterize initial lamellar failure of the annulus have involved tensile testing of small tissue samples in order to quantify some of the material properties of the annulus for numerical modeling [2,3]. The purpose of this study was to develop a method of measuring local strain through image analysis of a tensile test conducted on a small sample of annular tissue.

METHODS

Mechanical testing

Tensile testing was performed using a testing system specifically designed for testing thin biological tissues, BioTester 5000 (Waterloo Instruments Inc, ON, Canada). The tissue sample, consisting of two layers, was obtained from the superficial layers of the anterior annulus at the c3/c4 level of the porcine spine. Five-prong tungsten rakes secured the tissue during testing. Image resolution was 1280x690 pixels and captured at a rate of 1 Hz. Three tensile tests were performed at a constant strain rate of 2%/sec: (1) uniaxial tension test to 20% strain in the x-direction, (2) constrained tension test to 20% strain in the x-direction and no strain in the y-direction, (3) biaxial tension test to 20% strain in both x and y-directions. Force and displacement were sampled at 10 Hz throughout all mechanical testing.

Image Analysis

Images captured during mechanical testing were processed using the software package LabJoy 5.80 (Waterloo Instruments Inc, ON, Canada). A source image was defined as the image of the tissue sample constrained by the tungsten rakes prior to tensile testing. Virtual source points were distributed over a user defined region of interest on the source image, creating a grid of square elements (Figure 1a). The movement of each source point was then tracked on all successive images captured during a tensile test using a template matching algorithm. Based on the movement of the points, local strain was mapped over each image (Figure 2b).

The matching algorithm was able to track the movement of the source points by defining a template of pixels around each point on the source image. Subsequently, the optimal locations for the templates were determined on the target image. Parametric variations to the tracking technique were tested in order to determine the optimal parameters for tracking. These variations included: changing element size by varying the resolution of the grid in the user defined region (25, 100, 400 points); changing size of template surrounding source points (121, 225, 441 pixels); and switching between batch and sequential tracking techniques.

RESULTS

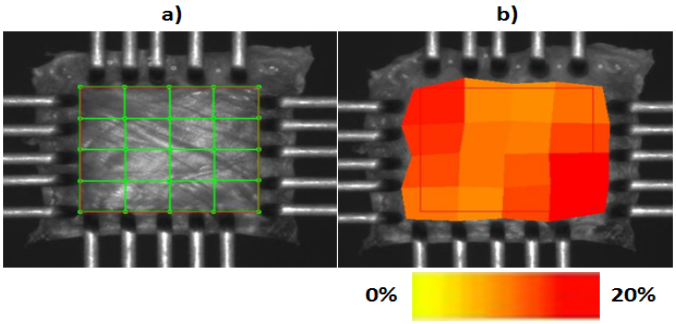

Figure 1: a) tissue sample prior to tensile loading with 25 virtual source points overlaid. b) tissue sample during tensile testing with local strain map overlaid

Average local strain measured did not vary notably when changing the size of the template surrounding each source point (SD= 0.005 strain). Average standard deviation (ASD) in local strain within a sample also was not affected by changes to template size (SD = 0.005). The resolution of the grid of source points did not cause considerable variation in the average local strain measured (SD = 0.004), however, did cause a relatively large variation in the ASD in local strain within a given sample (SD = 0.044).

During the batch matching technique, a large number of source points were found to be "sliding" past one another. This same problem was not found in the sequential matching technique.

DISCUSSION AND CONCLUSIONS

ASD was used as a measure of local strain distribution. Changing the size of the template surrounding each source point did not result in a dramatic change in the distribution of strains measured, however, changing the size of the elements did have a considerable effect on the distribution of strains. There is error associated with tracking each point. This error is the limiting factor for element size. The goal of future work will be to determine an optimal element size for mapping local strain distribution. The ability to quantify local strain during mechanical testing of annular tissue samples may one day lead to a better understanding of the onset of annular delamination.

REFERENCES

[1] Adams, M.A. et al. (1985). Gradual disc prolapse. *Spine* **10**(6); p. 524-531.

[2] Holzapfel, G.A. et al. (2005). Single lamellar mechanics of the human lumbar anulus fibrosus. *Biomechanics and Modeling Mechanobiology* **3**(3); p. 125-140

[3] Gregory, D.E. et al. (2009). Examining the mechanical properties of the intervertebral disc's inter-lamellar matrix and the effect of vibration exposure *J Biomechanics* (in review)

THE EFFECT OF CHANGING CROSS-SECTIONAL AREA MEASUREMENTS ALONG SOFT TISSUE LENGTH FOR PREDICTION OF MECHANICAL PROPERTIES

Joanna F. Weber (joanna@uoguelph.ca), Karen D. Gordon, Michele L. Oliver
School of Engineering, University of Guelph, Guelph, ON, Canada

INTRODUCTION

The accurate measurement of cross-sectional area (CSA) is essential for the determination of material properties of soft tissues such as tendons and ligaments. A new laser reflectance system (LRS) was developed in our lab which is capable of measuring the complex cross-sectional areas of soft tissue while mounted for testing[1]. Since most CSA measurements are taken at one location on a specimen, the purpose of this work was to determine how the CSA changes along the specimen length.

METHODS

The system is comprised of a Micro-Epsilon ILD 1700-50 CCD laser transducer (Micro-Epsilon, Ortenburg, Germany) fastened to a height adjustable linear motion guide, attached to a turntable bearing (Kaydon Corp., Muskegon, MI), which is rotated by a stepper motor (Automatic Direct, Cumming, GA), and mounted on an Instron 8872 servo-hydraulic testing machine (Instron Corp., Canton, MA).

Bovine digital extensor tendons (n = 10) and porcine digital flexor tendons (n = 5) were harvested. Each sample was approximately 8 cm in length. The tendons were mounted in the same orientation, proximal side up using serrated tissue clamps. An initial preload of 10N was applied to eliminate slack in the specimen.

CSA measurements were taken with the LRS using an angle increment of 0.255° which takes about 20s for one rotation around the sample. For each specimen, the CSA measurements started about 2 cm from the top clamp and moved down the specimen in regular intervals of 3 mm for a total of 10 measurements per specimen. Throughout preparation and testing, the tissue was kept well hydrated with 0.9% saline.

RESULTS

The average CSA measurement and standard deviation for bovine specimens is presented in Table 1. In general, standard deviations were low except for samples 1 and 8. The results for the porcine specimens are summarized in Table 2.

Two-way ANOVA revealed that there were no significant differences (p=0.99) between measurements across the length of the bovine specimens. As expected, there were significant (p=0.000) differences between bovine samples.

Table 2: Average CSA results and standard deviations for porcine soft tissue sample. CSA measured in mm^2.

Sample	1	2	3	4	5
Average CSA	27.16	30.77	33.68	29.46	25.86
SD	2.00	4.74	5.23	2.97	1.63

Similarly, two-way ANOVA results for the porcine specimens showed significant (p=0.000) differences between samples. Interestingly, a significant difference between means was found in the porcine samples for measurements across the length of the specimen. Subsequent Bonferroni post-hoc analyses revealed that for measurements along the length, CSA 1 was greater than CSAs 3 to 10, CSA 2 was greater than CSAs 7 to 10, and CSA 3 was greater than CSA 10.

DISCUSSION AND CONCLUSIONS

The bovine extensor tendons CSA did not differ significantly along the length. This suggests that further studies using this tendon only need to measure the CSA at one point along the specimen for those with laser reflectance systems. If a laser reflectance system is unavailable, these results suggest that the volumetric displacement technique for CSA estimation is also a valid approach. While based upon a small number of samples, the porcine flexor tendon results strongly suggest that CSA measurements for other tissues may not be as regular along the specimen length. This finding has substantial implications for mechanical property predictions for stress and modulus of elasticity.

REFERENCES

[1] Pokhai G, et al. (2009). A New Laser Reflectance System Capable of Measuring Changing Cross-Sectional Area of Soft Tissues During Tensile Testing. *Journal of Biomechanical Engineering* Vol **131** (9): 0945054

Table 1: Average CSA results and standard deviations for bovine soft tissue samples. CSA measurements in mm^2.

Sample	1	2	3	4	5	6	7	8	9	10
Average CSA	25.94	28.63	29.86	24.47	29.81	23.08	25.99	25.17	24.66	21.62
SD	4.05	1.61	0.47	0.41	0.75	0.64	1.57	4.23	0.77	0.33

Biomechanics of the Vertebral Artery during Neck Manipulative Treatments

Conrad Tang[1,] Bruce Symons[2], Sarah Wuest[3], Walter Herzog[4],
[1,4]Faculty of Kinesiology, University of Calgary, Calgary, Canada, ctang@kin.ucalgary.ca, walter@kin.ucalgary.ca
[2]Private practice, Sundance Chiropractic and Wellness, Calgary, Canada, drbpsymons@shaw.ca
[3]Private practice, Elite Sports Performance, Calgary, Canada, dr.swuest@gmail.com

INTRODUCTION

The risk of cerebro-vascular accidents (primarily strokes originating from the vertebral artery, VA) following neck manipulative treatments has been estimated to be between 1 in 5000 and 1 in 10 million[1,2,3,4,5]. However, whether neck manipulative treatments are the cause of such accidents remains a matter of scientific debate and there are no data on the relationship between the forces exerted during neck manipulative treatments and the stresses and strains acting on the VA in the region between cervical vertebrae C1-C6, the region most implicated in stroke. Therefore, the purpose of this study was to quantify the stresses and strains of VA during neck manipulative treatments.

METHODS

Eight piezoelectric crystals of 0.5mm diameter (Sonometrics Corporation, London, Ontario, Canada), were sutured into the lumen of 5 vertebral arteries of 3 fresh unembalmed post-rigor cadaveric specimens, from just above C1 to just below C6 at each vertebral level (n=8). 400ns ultrasound pulses were then sent between crystals to measure the instantaneous lengths of vertebral artery segments at a frequency of 200Hz. Vertebral artery engineering strains (zero strain was defined as the length of each segment with the head and neck in a neutral position) were calculated from the instantaneous lengths during (i) cervical spine range of motion testing, (ii) neck manipulative treatments, and (iii) vertebrobasilar insufficiency testing performed by two Chiropractors. The forces applied during the chiropractic treatments were measured using a thin, flexible pressure pad (Pedar, Novel Inc, München, Germany). The vertebral artery was then clamped into a materials testing machine (MTS, Eden Prairie, USA) in a vertical orientation at its neutral length with the sonomicrometry crystals still attached, and subsequently stretched at a speed of 60% strain/sec until mechanical failure while continuously measuring segment strains and forces.

RESULTS

The most significant findings of this study were that adjacent vertebral artery segments often experienced strains of opposite direction during range of motion and spinal manipulation testing (Fig 1), and that maximal strains during neck manipulative treatments were always significantly smaller than strains obtained during range of motion and VA insufficiency testing. The peak VA strains for the diagnostic and passive range of motion procedures were 8.5% (left rotation, segment C2-C3) and 13.0% (left rotation, segment C4-C5) for clinicians 1 and 2, respectively. The corresponding peak VA strains for the manipulative procedures were 2.2% (C2/C3 adjustment, segment C3-C4) and 3.1% (Lateral adjustment C4/C5, segment C4-C5) for clinicians 1 and 2, respectively.

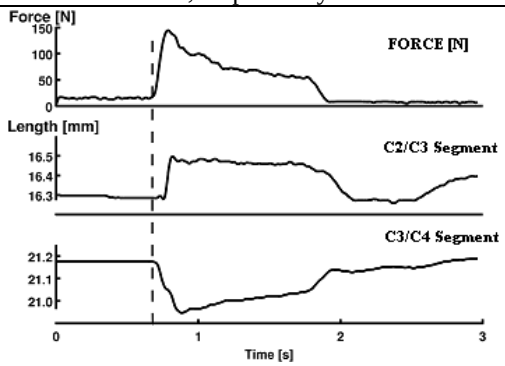

Figure 1. Force [N] time [s] and length [mm] time [s] histories for the right VA segments of a spinal manipulative treatment. The dashed vertical line indicates the start of the treatment thrust in which the C2/C3 segment elongates while the C3/C4 segment shortens.

DISCUSSION

Neck manipulative treatments have been implicated with serious injury to the VA and stroke. Injury and stroke have typically been thought to occur because of stretch-induced dissection of the VA. In the only previous work published on the relationship between neck manipulative treatments and the associated stresses and strains, we showed that for the segments distal to C1 and proximal to C6, stresses and strains were always much smaller than the strains observed during movement of the head and neck to the end range of passive motion[6]. Here, we demonstrate that in agreement with our previous results of VA segments outside C1-C6, stresses and strains of the VA are much smaller than what can be achieved by merely turning one's head to the side. However, and in contrast to our previous results, we found that one segment could undergo stretch while an adjacent segment was shortened during the same range of motion or treatment procedure. This result was reliable across three repeat measurements and consistent across both clinicians.

CONCLUSIONS

VA segments C1-C6 are strained significantly less during neck manipulative treatments than when turning one's head, as one does for example while backing a car out of a driveway.

REFERENCES

[1] Cote P et al. 1996. JMPT; 19: 159-164. [2] Frisoni GB et al. 1991. Spine; 24: 785-794. [3] Haldeman, S. 1999. Spine: 24:8 - pp 785-794. [4] Hurwitz EL. 1996. Spine; 21: 1746-1760. [5] Lee KP. 1996. Neurology; 45: 1213-1215. [6] Symons et al. 2002. JMPT; 25: 8: 504-510

ANALYSIS OF THE EFFECT OF ROTATOR CUFF IMPINGEMENTS ON UPPER LIMB KINEMATICS IN AN ELDERLY POPULATION DURING ACTIVITIES OF DAILY LIVING

Laurie C. Hall, Erin Middlebrook, Clark R.Dickerson
Department of Kinesiology, University of Waterloo, Waterloo, Canada, lchall@uwaterloo.ca

INTRODUCTION

Despite a large prevalence of rotator cuff impingements or tears in the elderly population, little research has focused on understanding how this population adapts to perform tasks of daily living [1,2]. The purpose of this thesis was to identify kinematic and shoulder loading differences between elderly mobile individuals and elderly individuals with rotator cuff impingements during specific activities of daily living.

METHODS

Thirteen mobile elderly and ten elderly with rotator cuff impingements participated in the study. Each completed five range of motion tasks (ROM) and six activities of daily living (ADL). ADLs included 2 reaching tasks, eating with a spoon, perineal care, washing the axilla and hair-combing. Vicon MX20+ system was used to capture motion of the right upper limb and trunk. The Shoulder Loading Analysis Modules [3] to estimate thoracohumeral kinematics. Custom software was used to express humeral angles in terms of 3 Euler rotations; plane of elevation, angle of elevation and humeral rotation.

RESULTS

Two-tailed t-tests with injury status as the factor determined that impingement populations showed decreased ranges of flexion/extension, abduction and internal and external rotation when compared to the mobile population. Repeated measures ANOVAs with injury status and task performed as factors were used on each of the outcome measure of the ADLs The Results this analysis showed that the mobile population had a 44% larger range of angle of elevation than the impinged population. Task was found to be a main effect for most variables examined including angle of elevation (figure 1). Participants with impingements had significantly lower ranges of humeral rotations during the tasks than the healthy population with ranges of 40 +/- 40º and 51 +/- 36º respectively. Perineal care, hair-combing and reaching tasks were the most demanding in terms of range of motion necessary to complete the task. The reaching tasks resulted in the highest shoulder moment.

DISCUSSION AND CONCLUSIONS

Shoulder range of motion is decreased in elderly populations with rotator cuff impingements when compared with a mobile elderly population in abduction, flexion and external rotation. Activities that required large ranges of motion were identified as reaching above shoulder height, a scaled reach, perineal care and hair-combing tasks. This investigation showed that developing adaptations for perineal care, hair-combing and reaching tasks should be prioritized when working with patients with impingements, as these tasks demanded the largest ranges of motion as well as high shoulder moments. The quantification of the active range of motion of elderly with rotator cuff impingements can be applied to the design of living environments that are more conducive to the reduced ranges of motion seen in this investigation.

REFERENCES

[1] Murray, I.A. & Johnson, G.R. (2004) A study of external forces and moments at the shoulder and elbow while performing every day tasks. *Clinical Biomech.*, 19:586-594.
[2] Magermans, D.J., Chadwick, E.K., Veeger, H.E. & van der Helm, F.C. (2005) Requirements for upper extremity motions during activities of daily living. *Clinical Biomechanics,* 20:591-599.
[3] Dickerson, C.R., Chaffin, D.B. & Hughes, R.E. (2007) A mathematical musculoskeletal shoulder model of proactive ergonomic analysis. *Computer Methods in Biomechanics and Biomedical Engineering*, 10: 389-400.

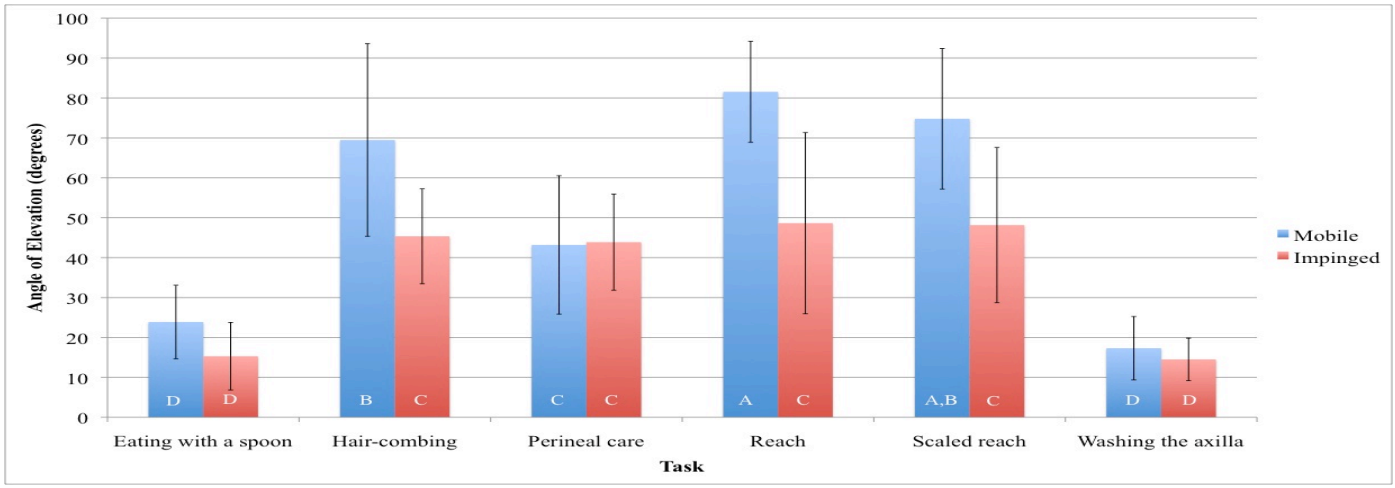

Figure 1: Mean range of angle of elevation interaction between injury status and task during ADL performance. Levels not sharing the same letter are significantly different between injury statuses.

MALES, FEMALES AND LIFTING TECHNIQUE: A PRINCIPAL COMPONENT ANALYSIS

Erin Sadler[1], Ryan Graham[1], Joan Stevenson[1]
[1]School of Kinesiology and Health Studies, Queen's University, Kingston, ON, Canada

INTRODUCTION

The majority of the research that exists regarding lifting has been completed using male subjects. Due to the pronounced differences between males' and females' anthropometry and strength profiles, it is difficult to extrapolate findings from this male-dominated research to a female population [1]. Previous researchers reported significant differences in lifting technique between males and females; however, several limitations to the protocol were also outlined [1]. The purpose of this work was to address these limitations through analysis of lifting kinematics of males and females using principal component analysis (PCA).

METHODS

Joint kinematic data of 30 healthy subjects (Table 1) were collected during a freestyle, symmetrical-lifting protocol. A two-camera Optotrak 3020 system (NDI, Waterloo, ON) was used to collect five marker triads at the shank, thigh, pelvis, T_{12} and C_7; capturing joint angles of the knee, hip, lumbar and thoracic spine on three axes. Subjects lifted a handled-box under two randomized load conditions (zero and 10% of their maximum back strength) from a target on a table (positioned at 50% of subject's height) to a target on the floor; completing 30 continuous lift cycles at a rate of 10 lifts per minute. Sufficient rest was given between trials. Lifting style and foot position was self-selected with foot position remaining constant for all trials.

Table 1: Subject pool characteristics.

	Age (yrs)		Height (cm)		Weight (kg)	
Females (n=15)	23.0	(±2.6)	170.1	(±6.1)	66.3	(±11.7)
Males (n=15)	24.2	(±2.9)	184.9	(±7.6)	85.4	(±10.7)

A principal component analysis model was employed and repeated measures ANOVA's were used to test for significance (α=0.05/23 comparisons =0.002).

RESULTS

Using a 90% trace criterion, 23 PCs were retained from all four joints in three axes (Table 2). None of the PC scores were significantly different between sexes and there were no significant interactions between sex and load. At this alpha level, the only significant differences were found between load conditions in PC2 of lumbar spine flexion (p<0.001) and PC2 of hip rotation (p<0.001). PC2 of lumbar spine flexion was interpreted to be a timing of lift operator, and PC2 of hip rotation was a peak difference operator.

Table 2: Retained principal components and *p* values of male and female PC score differences.

	Angle	PC	Variance explained (%)	*p* Value
Knee	Flexion	1	72.2	0.421
		2	14.2	0.088
		3	6.9	0.575
	Abduction	1	91.9	0.841
	Rotation	1	79.8	0.093
		2	15.2	0.463
Hip	Flexion	1	68.1	0.273
		2	15.3	0.596
		3	9.2	0.781
	Abduction	1	92.2	0.210
	Rotation	1	83.2	0.097
		2	9.1	0.765
Lumbar Spine	Flexion	1	85.7	0.823
		2	7.1	0.972
	Abduction	1	90.1	0.256
	Rotation	1	90.4	0.885
Thoracic Spine	Flexion	1	89.0	0.594
		2	5.9	0.483
	Abduction	1	71.5	0.025
		2	17.5	0.895
		3	3.7	0.496
	Rotation	1	79.3	0.022
		2	13.7	0.641

DISCUSSION AND CONCLUSIONS

The results of the current study indicate that male and females do not demonstrate significant differences in flexion, abduction, and rotation of the knee, hip, lumbar or thoracic spine during a freestyle lift. The only differences observed were between the zero and 10% of back strength load conditions for lumbar flexion and hip rotation, indicating that load has an effect on timing of lumbar flexion and peak differences in hip rotation independent of sex. These findings are important because previous research found significant sex differences for trunk and knee angular motion under constrained leg and back lifts using different loads for males and females [1]. Thus, by standardizing the load lifted to personal strength characteristics it is believed these differences are less pronounced. Future research should be conducted on constrained and freestyle lifts using PCA to further understand sex differences in lifting technique.

REFERENCES

[1] Lindbeck L and Kjellberg K (2001). Ergonomics **44**(2); p. 202-214.

ACKNOWLEDGEMENTS

The authors would like to thank NSERC, OGS and WSIB.

QUANTIFYING THE COCONTRACTION RELATIONSHIP BETWEEN ELBOW FLEXORS AND EXTENSORS DURING SUBMAXIMAL ISOMETRIC EXERTIONS

Rebecca Brookham, Erin Middlebrook, Tej-jaskirat Grewal & Clark Dickerson
Kinesiology Department, University of Waterloo, Waterloo, Canada, cdickers@uwaterloo.ca

INTRODUCTION

Biomechanical optimization models that apply efficiency-based objective functions (such as minimal physiological cost) often underestimate or negate antagonist cocontraction[1]. In the mathematical formulation of these objective functions, antagonistic contraction is counterproductive, as they produce moments that do not contribute to producing the required net joint moments. Cocontraction, however, is a well-known phenomenon used in control, stability and stiffness and should be carefully incorporated into existing models, with the expectation that more realistic model predictions of muscle force will result. The purpose of this study was to mathematically describe cocontraction relationships between elbow flexors and extensors during isometric exertions at varying intensity levels and postures. It was hypothesized that cocontraction levels will increase as the elbow moves towards full extension, as shown previously for a reduced task set in the elbow[2] and knee[3].

METHODS

8 male and 8 female healthy, right-handed individuals (aged 21 – 29 years) performed 72 isometric exertions (Eq'n 1) of 6 s duration while holding a load in their right hand.

Exertions = [4 elbow angles] · [2 exertion types] · [3 loads] · [3 shoulder angles]

0°, 45 °, 90 °, 135°	flex, extend	1, 2, 3 Kg	0° Flex, 0° Abduct 0° Flex, 45° Abduct 45° Flex, 0° Abduct

[1]

During the exertions, surface electromyography (EMG) was sampled at 3000 Hz from the biceps brachii, brachioradialis, and triceps brachii (long and lateral heads). Initial elbow flexion and extension maximal voluntary contractions (MVCs) were performed against a hand-held digital dynamometer (ergoFET300™, Utah, USA) and were used for normalization procedures. Maximal voluntary force produced during these MVCs indicated participant strength. Linear enveloped normalized EMG (processed in MATLAB™ 7.6.0, Mathworks, USA) was integrated between 2 – 4 s and used in the calculation of the cocontraction index (CI) (Eq'n 2).

$$CI = \frac{\int_{t1}^{t3} [EMG_{bi} + EMG_{brd}](t)dt}{\int_{t1}^{t3} [EMG_{bi} + EMG_{brd} + EMG_{trilat} + EMG_{trilong}](t)dt} \cdot 100 \qquad [2]$$

[Note: trilat = triceps (lateral head), trilong (triceps long head), bi = biceps, brd = brachioradialis]

The CI provides a relative measure of flexor contribution to total activation about the elbow. A CI of 0% indicates no cocontraction (flexors are not activated); a CI of 50% indicates full cocontraction (both flexors and extensors are activated in equal amounts); and a CI of 100% indicates no cocontraction (the extensors are not activated). Statistical analyses were performed in JMP 8® (SAS Institute Inc., Cary, NC). Potential predictor variables (arm posture, load and subject anthropometric factors) were analyzed for correlations and redundant variables were removed. A preliminary stepwise multiple linear regression analysis determined which predictor variables should be included in each of the cocontraction prediction models. These models (one for each of extension and flexion type exertions) were then developed using a repeated measures analysis of variance. Interaction effects were not significant and were thus excluded from the models.

RESULTS

The most parsimonious models for cocontraction during elbow flexion (CI_{flex}) and extension exertions (CI_{ext}) were (Eq'n 3-4):

$$CI_{flex} = 75.32 + [0.02 \cdot A_e] + [-0.15 \cdot A_{sf}] + [-0.20 \cdot A_{sa}] + [2.17 \cdot L]$$
($r^2 = 0.46$; $p < 0.0001$) [3]

$$CI_{ext} = 11.46 + [0.12 \cdot A_e] + [0.09 \cdot A_{sf}] + [-1.48 \cdot L]$$
($r^2 = 0.31$; $p < 0.0001$) [4]

[note: Ae = elbow angle; Asf = shoulder flexion angle; Asa = shoulder abduction angle; L = load]

F ratio values produced by these models appeared in the descending order of: shoulder abduction, shoulder flexion, load and elbow angle, respectively, for flexion exertions; and in the order of elbow angle, shoulder flexion and load, respectively, for extension exertions. Tukey post hoc analyses indicated more cocontraction (CIs closer to 50%) occurred at lesser degrees of flexion (0°, 45°) in flexion exertions, but less cocontraction occurred at greater degrees of flexion (90°, 135°) for extension exertions.

DISCUSSION AND CONCLUSIONS

Elbow cocontraction does occur during submaximal elbow exertions in both flexion and extension, and is sensitive to changes in posture and load. Cocontraction must be considered in biomechanical models if physiological realism is to be attained. Future efforts will include extrapolation of these relationships to different exertions, and inclusion of these relationships into a biomechanical model to determine if the inclusion of cocontraction constraints helps to generate predicted muscle force outputs that more realistically represent empirically gathered muscle activity data. If this inclusion is successful, the concept is extendible to other body joints.

REFERENCES

[1] Dickerson, CR (2008). Modeling and Simulation of Tissue Load. In Hong, Y & Bartlett, R (Eds.), *Routledge Handbook of Biomechanics and Human Movement Science* (pp 18-34). New York, NY: Routledge.

[2] Doheny EP et al. (2008). Effect of elbow joint angle on force-EMG relationships in human elbow flexor and extensor muscles. *JEK*, **18**; p.760-770.

[3] Kingma I et al. (2004). Are hamstrings activated to counteract shear forces during isometric knee extension efforts in healthy subjects? *JEK*, **14**; p. 307-315.

LOCAL STABILITY OF DYNAMIC TRUNK MOVEMENTS DURING THE REPETITIVE LIFTING OF LOADS

Ryan B. Graham[1], Erin M. Sadler[1], Joan M. Stevenson[1]
[1]School of Kinesiology and Health Studies, Queen's University, Kingston, ON, Canada, ryan.graham@queensu.ca

INTRODUCTION

Spinal stability is very important for preventing injury by maintaining intervertebral and global torso equilibrium under the influence of biomechanical or neuromuscular perturbations [1]. Although several researchers have quantified the control of spinal stability during static tasks, few have done the same during dynamic trunk movements. Dynamic stability can be estimated using nonlinear Lyapunov analyses to quantify time-dependent variance in kinematic data. To date, movement pace and direction [1] as well as fatigue [2] have been found to influence the control of dynamic spinal stability during a constrained trunk flexion task without any load. However, due to the fact that many workers are injured when lifting loads in occupational settings, it is important to characterize dynamic trunk stability under similar repetitive lifting and loaded conditions. This was the purpose of this body of work.

METHODS

Thirty healthy volunteers (15 males, 15 females) performed a trial of 30 continuous freestyle box lifts from a target on the floor to one on a table positioned at half of their height, under two randomized load conditions. Box placement on the target was synchronous to a metronome establishing a rate of 10 lifts per minute. The load conditions were zero load and 10% of each subject's maximum back strength [3].

Kinematic data were recorded at 100Hz from marker triads located on fins over the vertebral processes at T_{12} and S_1 using an Optotrak 3020 active movement registration system with two cameras (Northern Digital Inc., Waterloo, ON, CA). These data were used to calculate 3-D trunk angles using Euler rotations (Figure 1a), which were then low-pass filtered at 10Hz. Stability analyses occurred on the Euclidean norm of the three trunk angles at each time (Figure 1b) [1]. The first five lifts were ignored to ensure steady state movement.

Local dynamic stability of the trunk was assessed from the maximum finite-time Lyapunov exponent, λ_{max}, quantifying responses to an infinitesimally small perturbation. To create an n-dimensional state-space from the 1-D Euclidean norm of the trunk angles, the method of delays was used (Figure 1c). A constant time delay of 10% of the average lift and a dimension of 5 were used for embedding [1]. Using the constructed state space, the average logarithmic rate of divergence of nearest neighbours was then calculated (Figure 1d), and the slope of the line during two time intervals (0-0.5 and 4-10 lift cycles) was found to estimate short and long term λ_{max} values [4].

RESULTS

Using a mixed-design repeated-measures ANOVA, it was found that increasing the load lifted significantly reduced the short term, but not long term, λ_{max} value (Table 1). There were no between-subject effects of sex, or significant interactions.

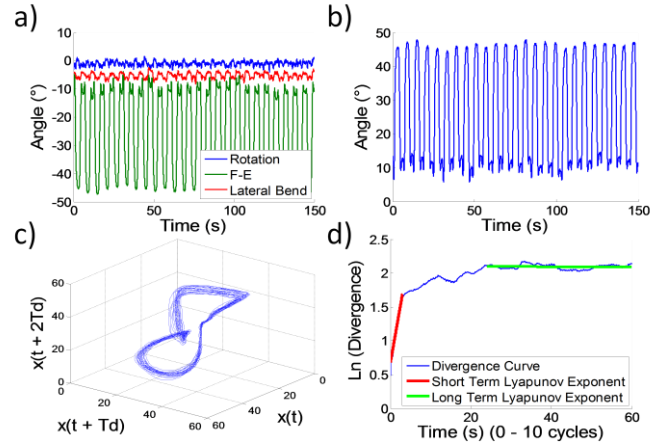

Figure 1: Schematic representation of: a) 3-D trunk angles, b) Euclidean norm of the trunk angles, c) state space embedding, and d) calculation of the short and long term λ_{max} values.

Table 1. Repeated-measures ANOVA results.

	Mean Results		P-Value Results		
	0 Load	**10% Load**	**Load**	**Sex**	**Load*Sex**
λmax short	0.379	0.335	< 0.001*	0.842	0.902
λmax long	4.58E-04	2.41E-03	0.055	0.463	0.308

* Indicates significance at $p < 0.05$

DISCUSSION AND CONCLUSIONS

To the best of the authors' knowledge, this study was the first to characterize dynamic trunk stability when lifting under different loading conditions. Results indicated that the short term λ_{max} was significantly reduced when lifting a load of 10% of max strength when compared to no load, demonstrating an increase in dynamic trunk stability when lifting a load. In other words, without a load-in-hands subjects' abilities to respond to a perturbation were diminished. This finding may be explained by reduced muscular co-contraction requirements around the spine, which act to augment spinal stability [1]. Furthermore, these results support the notion of greater spinal instability during movement with low loads due to decreased muscular demand [5], and should aid in understanding how lifting various loads contributes to occupational low back pain.

REFERENCES

[1] Granata & England (2006). *Spine*, *31*(10), E271-76.
[2] Granata & Gottipati (2008). *Ergonomics*, *51*(8), 1258-71.
[3] Lotz et al. (2009). *JEK*, *19*(2), 331-40.
[4] Rosenstein et al. (1993). *Physica D*, *65*, 117-34.
[5] Cholewicki & McGill (1996). *Clin. Biom*, *11*(3), 170-72.

ACKNOWLEDGEMENTS

We would like to acknowledge OGS, NSERC, and the WSIB.

GROUND REACTION FORCES DIMINISH IN MICE AFTER BOTULINUM TOXIN INJECTION

Sarah L. Manske[1], Steven K. Boyd[1,2], Ronald F. Zernicke[1,2,3]
[1]Faculty of Kinesiology, University of Calgary, Calgary, Canada
[2]Schulich School of Engineering, University of Calgary, Calgary, Canada
[3]School of Kinesiology, University of Michigan, Ann Arbor, United States, zernicke@umich.edu

INTRODUCTION

Botulinum toxin type A (BTX) is increasingly being used to investigate the interaction between muscle and bone [1, 2]. BTX may provide a unique opportunity to isolate the effects of muscle disuse on bone without affecting load-bearing, as mice begin to recover normal ambulation patterns one week post-injection. Few studies have measured ground reaction forces in mice [3, 4]. However, load-bearing activity has not been examined after BTX injection. We hypothesized that BTX injection to the posterior hindlimb would not have a significant effect on the mouse's ability to bear weight in the affected limb one week post-injection.

METHODS

Female BALB/c mice (N = 6, 16-17 wk old) were injected with 20 µL of BTX (1 U/100 g) in the left hindlimb, targeting the gastrocnemius, soleus, and plantaris. The right hindlimb served as an internal control. Vertical ground reaction forces, hindlimb muscle cross-sectional area (MCSA), and tibial bone micro-architecture were assessed at baseline, one, and three weeks following injection.

Peak vertical forces were measured in independent limbs as mice travelled along a walkway constructed with four custom-built force platforms (Figure 1). The force platforms employed load cells with a 200 g full scale capacity with a 3000 Ω thin film strain gauge (S250 Miniature Platform Load Cell, Strain Measurement Devices Inc., Meriden CT). Data were collected at 500 Hz using WinDaq data acquisition and playback software (Dataq Instruments, Akron, OH). Force data were low-pass filtered at 60 Hz. Four-to-ten trials were collected and averaged per mouse at each time point..

MCSA and bone micro-architecture were assessed using micro-CT (vivaCT40, Scanco Medical, Brüttisellen, Switzerland). Two-way ANOVAs and simple effects tests were used to examine differences between time points and legs.

Figure 1: Mouse crossing the walkway with 4 force platforms.

RESULTS

Vertical hindlimb forces were initially 58% (SE 2%) of body weight (BW) and declined to 50% BW (SE 2%, p = 0.01) in the BTX-injected leg one week post-injection (Figure 2). After three weeks, there was a non-significant trend toward lower vertical forces in the BTX-injected leg compared with baseline and the contralateral limb. There were no significant changes in either forelimb or contralateral hindlimb forces over time.

In contrast, MCSA declined 15% at one week and 46% at three weeks from baseline values in the BTX-injected leg. Similar trends in bone volume fraction were observed.

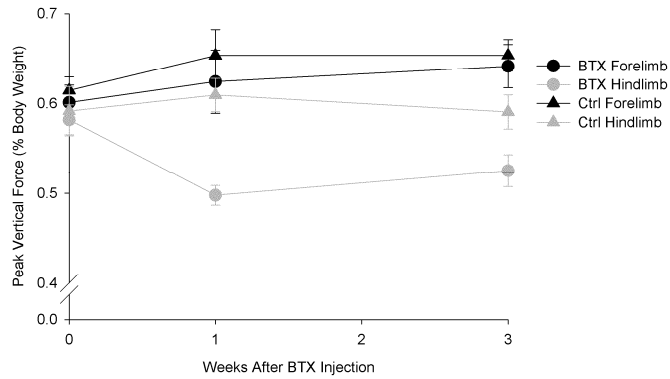

Figure 2: Peak vertical ground reaction forces for the left BTX-injected hindlimb (Hind), the corresponding forelimb (BTX Fore) as well as the contralateral control legs (Ctrl).

DISCUSSION AND CONCLUSIONS

To our knowledge, this was the first study to examine changes in mouse ground reaction forces after an intervention. A larger sample size may be required to detect subtle changes in gait because of the large inter-trial variation in peak forces. For example, the trend towards lower peak forces in the BTX-injected hindlimb was not significant 3 weeks post-injection.

We found that peak vertical forces were lower in the BTX hindimb compared with the contralateral hindlimb one week post-injection. This study suggested that weight-bearing ability was largely maintained in a BTX-affected limb despite significant muscle atrophy. The ability to ambulate somewhat normally may have been due to the maintenance of soleus mass and function after a relatively high dose of BTX.

Although BTX does not isolate the effects of muscle force on bone, it serves as a viable model to investigate the relative interactions of muscular and weight-bearing forces on bone adaptation.

REFERENCES

[1] Warner SE, et al. (2006). *Bone* Vol(2); p. 257-64.
[2] Manske SL, et al. (2010). *Bone* Vol(1); p. 24-31.
[3] Clarke KA, et al. (2001). *Behav Res Methods Instrum Comput* Vol(3); p. 422-6.
[4] Zumwalt AC, et al. (2006). *J Biomech* Vol(15); p. 2877-81.

ACKNOWLEDGEMENTS

Thank you to Andrzej Stano and Dr. Craig Good for assistance in constructing the force platforms. Funding was provided by AHFMR, NSERC and the University of Michigan.

WALKING TRUNK POSTURES DURING HEAD LOAD CARRIAGE FOR PREGNANT WOMEN IN WEST AFRICA

Erica Beaucage-Gauvreau[1], Geneviève Dumas[1], Mohamed Lawani[2]
1. Department of Mechanical and Materials Engineering, Queen's University, Kingston, ON, erica@me.queensu.ca
2. Institut National de la Jeunesse, de l'Éducation Physique et Sportive, Université D'Abomey-Calavi, Porto-Novo, Bénin

INTRODUCTION

Women in Benin commonly participate in agricultural and commercial chores that require strenuous physical work involving heavy loads carried on the head and back. These demanding tasks combined with pregnancy can result in back pain that may persist after delivery in some cases [1, 2]. The primary objective of this study was to examine how the trunk postures of pregnant women in West Africa were affected by their daily occupational activities with a focus on the head carriage task.

METHODS

Trunk postural data during the specific task of carrying loads on the head were collected using a Virtual Corset (MicroStrain, Williston, VT, USA) in Porto-Novo, Benin. This device is an inclinometer system capable of monitoring trunk angles with respect to the vertical in two directions. Twenty-six pregnant (age 26 ± 5 years, mass 63 ± 15 kg, height 159 ± 6 cm) and 25 non-pregnant (age 26 ±7 years, mass 57 ±11 kg, height 159 ± 6 cm) women were instrumented with two devices at the sacrum and C7 levels, respectively. These two landmarks, C7 and sacrum, were chosen to measure the flexion-extension and lateral bending angles of both the upper trunk and pelvis region with respect to the subject's upright neutral position. The subjects were asked to lift and carry a load corresponding to approximately 20% of their body weight on their heads in three different trials. The two subject groups also performed three trials where they walked without any load on their heads to compare the trunk postures between the loaded and unloaded conditions. The mean trunk angles and the standard deviations during the walking portions of the trials were compared between the subject groups and conditions using a mixed-design ANOVA.

PRELIMINARY RESULTS

During walking, load on the head significantly increased trunk extension ($p<.001$) (Fig. 1) and decreased the standard deviations ($p<.001$) (Fig. 2) of the sagittal trunk angles at C7, while pregnancy did not have a significant effect on those trunk angles (Fig. 1&2). Conversely, load significantly increased the standard deviation of the sagittal angles at the sacrum ($p<.001$) but did not have a significant effect on the mean angles. Similarly to the measurements at C7, pregnancy had no significant effect on the mean sagittal walking angles and mean standard deviation of the angles measured at the sacrum.

CONCLUSION

The significant decrease in the mean standard deviations of the walking trunk angles at C7 in the loaded condition suggests that both subject groups reduced their upper trunk movements to provide better stability for the load. The significant increase of the mean standard deviation at the sacrum could be explained as a compensation mechanism for small upper trunk motion to allow normal gait.

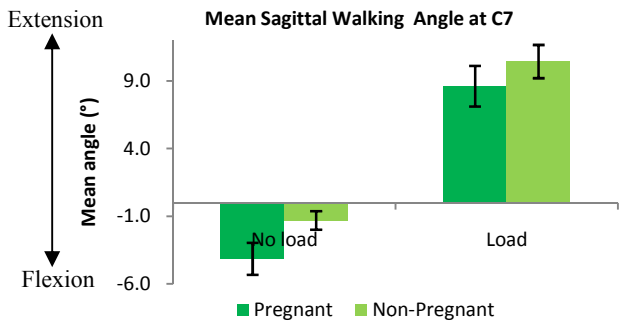

Figure 1: Mean trunk angles in the sagittal plane with their standard error of the mean for the walking portion of the trials with and without load on the head for pregnant and non-pregnant subjects.

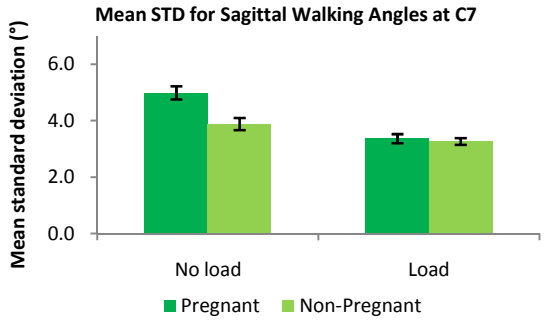

Figure 2: Mean standard deviation of the trunk angles in the sagittal plane with their standard error of the mean for the walking portion of the trials with and without load on the head for pregnant and non-pregnant subjects.

REFERENCES

[1] Worku, Z., J Manipulative and Physiological Therapeutics, 23 (2003) 147-154.
[2] Poole, J.L., Work, 10 (1998) 157-166.

ACKNOWLEDGEMENTS

This study was supported by the ISB travel grants fund, NSERC research grant 6858, and the Human Mobility Research Center, Kingston, Ontario.

DEVELOPMENT OF AN OFFICE ERGONOMIC CHECKLIST: THE RAPID OFFICE STRAIN ASSESSMENT (ROSA)

Michael Sonne[1,2], David Andrews[1], Dino Villalta[1,2]
[1]Department of Kinesiology, University of Windsor, Windsor, Ontario, Canada, sonne@uwindsor.ca
[2]LeadErgonomics, Windsor, Ontario, Canada

INTRODUCTION

Work-related computer use has increased in the past 2 decades, along with an increase in musculoskeletal disorders [1]. Ergonomic checklists such as RULA (Rapid Upper Limb Assessment) [2] do not account for office-specific factors, and can therefore not necessarily be used to accurately identify risk factors in this environment. The purpose of this study was to develop and evaluate a tool to identify office ergonomic hazards quickly and reliably.

METHODS

Risk factors and ideal postures were identified using the CSA standards on office ergonomics (CSA Z412) [3], as well as other literature from the field. Images reflective of these postures and equipment configurations were created (figure 1), and risk scores were assigned to each posture (1 for neutral or ideal, increasing up to 3 for poor postures). Factors that could be used in conjunction with other postures were scored as +1 or +2. Scoring charts were created similar to those in RULA [2]. ROSA final scores increase in magnitude from 1-10, with each level representing an increased presence of overall risk factors.

Seventy two offices were assessed, with subjects being administrative staff at a local hospital. Correlations between ROSA scores and discomfort scores from a questionnaire [4] were examined. Additionally, 3 expert observers performed simultaneous assessments of 14 separate workstations in the field, and 3 other mock workstations once a week for 4 weeks to examine the inter- and intra-rater reliability of the ROSA scores, respectively.

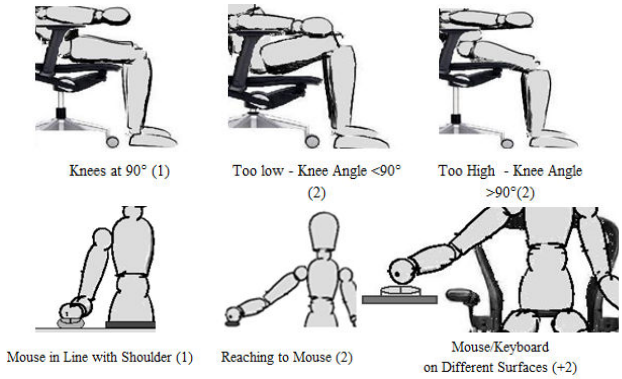

Figure 1 – Example of Diagrams in ROSA

RESULTS

The total discomfort and ROSA scores were significantly correlated (R=0.384). The total ROSA scores exhibited high inter- and intra-rater reliability, with ICCs of 0.83 and 0.91, respectively. A significant difference in mean discomfort occurred between levels 3 and 5 of the total ROSA score, and mean discomfort increased over all tested total ROSA score levels. Table 1 displays correlations between ROSA values and localized discomfort.

ROSA Score	Correlation with Discomfort
Total	R=.384*
Chair	R=.23
Monitor and Phone	R=.321*
Keyboard and Mouse	R=.366*

Table 1 – ROSA and Discomfort Correlations (*Significant at p=.01)

DISCUSSION AND CONCLUSIONS

ROSA is an effective, quick and easy to use method of identifying office configurations that may contribute to worker discomfort. A significant increase in mean discomfort was reported at ROSA final score 5, thus it is recommended that a ROSA final score of 5 should be used as the threshold value to signal that immediate assessment of a workstation is required. The ROSA scores were very reliable between and within raters, and compare favourably to other methods used to assess office workstations [5].

REFERENCES

[1] Bayeh, A., Smith, M., 1999. Int J Hum-Comput Int. 11, 109-135.

[2] McAtamney, L., Corlett, E.N., 1993. Appl Ergon. 24, 45-57.

[3] Canadian Standards Association, 2000. CSA-Z412: Guideline on Office Ergonomics. CSA International, Toronto, Canada.

[4] Hedge et al., 1999. Ergonomics. 42, 1333-1349.

[5] Robertson, M., et al., 2009. Appl Ergon. 40, 124-135.

ACKNOWLEDGEMENTS

Thanks to CRE-MSD for funding this project.

BIOMECHANICS OF LEANING FORWARD AGAINST AN EXTERNAL SUPPORT WITH MILD FORWARD FLEXED TRUNK IN STANDING

Mohammad Abdoli-Eramak[1], Caroline Damecour[1,2], Ahmad Ghasempoor[3]
[1] School of Occupational and Public Health, Ryerson University, Toronto, Ontario, Canada, m.abdoli@ryerson.ca
[2] School of Kinesiology and Health Studies, Queen's University, Kingston, Ontario, Canada K7L 3N6
[3]Department of Mechanical Engineering, Ryerson University, Toronto, Ontario, Canada. M5B 2K3

INTRODUCTION

A forward-bent trunk position in standing requires continuous postural muscle effort to counterbalance the external flexion moment that is created by the trunk. Mild forward bent standing postures are difficult to avoid when workspaces are shared and precise matching of work height to individuals is impossible. Two external trunk supports are investigated for their effect on the L4/5 and hip external moments using link segment modeling.

METHODS

Five healthy males with an average age of 37 (SD 5) years, height of 1.7m (SD 0.3m), and weight of 87 Kg (SD 7) bent forward from the hips to 30 degrees flexion in standing, lifted a bottle from a shelf (normalized to shoulder height), and held this position for positional data collection. Four masses equal to 0, 30, 40, and 60N were tested in three standing conditions; no support, leaning forward against a table with the height adjusted to the anterior superior iliac spine (ASIS) of the pelvis, and leaning against the prototype Dynamic Trunk Support (DTS) with the contact point for leaning adjusted to the upper portion of the sternum (Figure 1). The spring resistance on the DTS was adjusted to provide partial trunk support based on comfort and without pushing into the device (i.e. tightening abdominal muscles). An electromagnetic human motion capture system, Fastrak™ (Polhemus, Colchester, VT, USA) was used to determine changes in body segment orientation and position. Fastrak™ sensors were positioned in the upwards and anterior direction using Velcro straps. Linear and angular displacement (6 DOF) at 70Hz sampling frequency was continuously collected for 10 seconds of data collection identified by a manually activated switch. Body segments included right foot, leg, thigh, anterior pelvis, L5, T9, T1 and head (using a baseball cap). After positional data was captured, rib girth was measured at maximal inspiration for 3 repetitions using a tape measure and the zxyphoid landmark. Low back discomfort was rated using a 10 point visual analog scale (VAS).

The external moment at L4/5 was estimated using a downward link segment model that consisted of a single trunk segment and single leg model. The external moment at the hip was estimated using an upward link segment model and ground reaction force measured using a force. The load transfer from leaning was estimated as a horizontal reaction force. Values were used from a previous study. The external moment at the hip was estimated using an upward link segment model and ground reaction force measured using an Accusway forceplate (AMTI, MA, USA). Leaning against the pelvis-height support had no effect on the external moment at L4/5 since the support was too close to the L4/5 joint.

RESULTS

Repeated measures ANOVA revealed a main effect for load (P=0.001) and support condition (P=0.001) on the L4/5 moment with no interaction. A 40 Nm (SD 2) reduction in moment was seen for all load conditions therefore the percentage reduction ranged from 29% when the load in hand was 0 N, to 19% when 60 N was held in the hand.

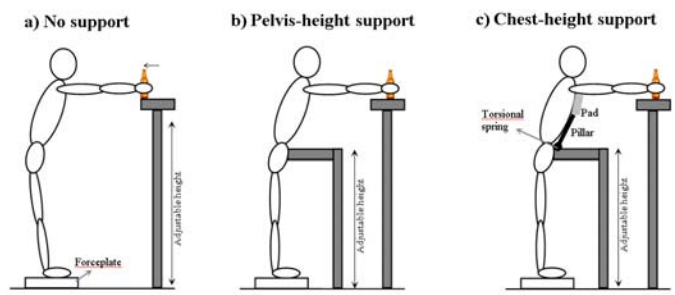

Figure 1. Three standing conditions tested with static forward bent standing with the trunk in 30 degrees flexion.

Repeated measures ANOVA showed effects for load in hand (P=0.001) and support condition (P=0.001) for the external moment at the hip, with an interaction effect (P=0.001). With increasing hand loads, the moment increased, as did the horizontal resultant force from leaning. The corresponding reduction in the external hip flexion moment was 27% while leaning against the DTS and 8% with pelvis-height support.

Ribcage expansion showed no difference between standing conditions. Low back discomfort increased as the load in the hand increased, however the rate of increase was lowest for DTS at 1 VAS interval compared to 3 VAS intervals for both no support and leaning on the pelvis-height support.

DISCUSSION AND CONCLUSION

The chest-height support was designed to optimize the biomechanical advantage from leaning and transferring weight by maximizing the lever arm. The results show a 29% reduction in the external L4/5 moment with partial support. EMG results from an earlier study [1] showed that this reduction is adequate to effectively lower postural muscle activity below 10% MVC. Subjective findings of back discomfort also demonstrate the effectiveness from this height of support. Ribcage expansion does not appear to be compromised however more comprehensive testing is suggested. Leaning against the desk, produced a small biomechanical benefit for the hip joint.

REFERENCES

[1] Damecour C., et al. (2010) Comparison of two heights for forward placed trunk supports with standing work. *Applied Ergonomics*. (in press).

SPATIAL DEPENDENCYOF SHOULDER MUSCLE DEMANDS IN HORIZONTAL PUSHING AND PULLING

Alison McDonald, Bryan B. Picco, Amy Y. Chow, Alicia L. Belbeck, Clark R. Dickerson
Department of Kinesiology, University of Waterloo, Waterloo, ON

INTRODUCTION

Inadequate work designs can limit worker performance by creating postural constraints, which subsequently may result in awkward postures, static muscle loading, reduced force production capability, muscular insufficiency, increased muscular fatigue and increased worker discomfort [1,3]. Pushing and pulling are often ergonomically problematic exertions, and are estimated to account for nearly half of all manual material handling tasks[2]. The purpose of this investigation was to develop a 3-D spatial map of the muscle activity for the right upper extremity during specific pushing and pulling tasks.

METHODS

12 university-aged males participated. Bipolar surface electrodes were placed on 14 different sites on the right upper extremity and electromyographic (EMG) activity was recorded with a T2000 EMG system (Noraxon, Arizona, USA). 140 40N ramped directional 7-second push tasks were performed (70 push; 70 pull) at specific locations at 20 cm intervals along three axes: x (frontal plane); y (saggital plane); and z (coronal plane), with the origin at the center of the trunk at the umbilicus. Force feedback was provided during the exertions. EMG data were linear enveloped using a 4 Hz cutoff and normalized to activity levels recorded during three maximal voluntary contractions for each muscle. One-second central windows for each task were evaluated for each muscle during each trial. Two directional (push, pull) 3-way repeated measures ANOVAs were used to assess the influence of X, Y and Z positions on muscle activity.

RESULTS

There is a clear influence of both hand position and push direction on total muscle demand, calculated as the sum of all muscle EMG activity from all monitored muscles (Figure 1). The influence of handle location was significant for nearly every direction for nearly all individual muscles (Table 1), though this varied slightly with direction, particularly with respect to the anterior deltoid and infraspinatus data.

DISCUSSION AND CONCLUSIONS

The data reveals the importance of hand location and force direction on specific and overall muscular demands for horizontal force generation in the saggital plane. It will help to estimate specific and general muscle demands for different work scenarios. It also provides novel evaluation data for existing predictive biomechanical models. The data is useful for proactive workplace design that aims to balance minimizing shoulder loading within constrained workspaces.

REFERENCES

[1] Grant K.A., Habes J., 1997. An electromyographic study of strength and upper extremity muscle activity in simulated meat cutting tasks. *Applied Ergonomics* 28, 129-137.
[2] Baril-Gingras G., Lortie M., 1995. The handling of objects other than boxes: univariate analysis of handling techniques in a large transport company. *Ergonomics* 38, 905-925.
[3] Dickerson C.R., Martin B.J., Chaffin D.B., 2007. Predictors of perceived effort in the shoulder during load transfer tasks. *Ergonomics* 50, 1004-16.

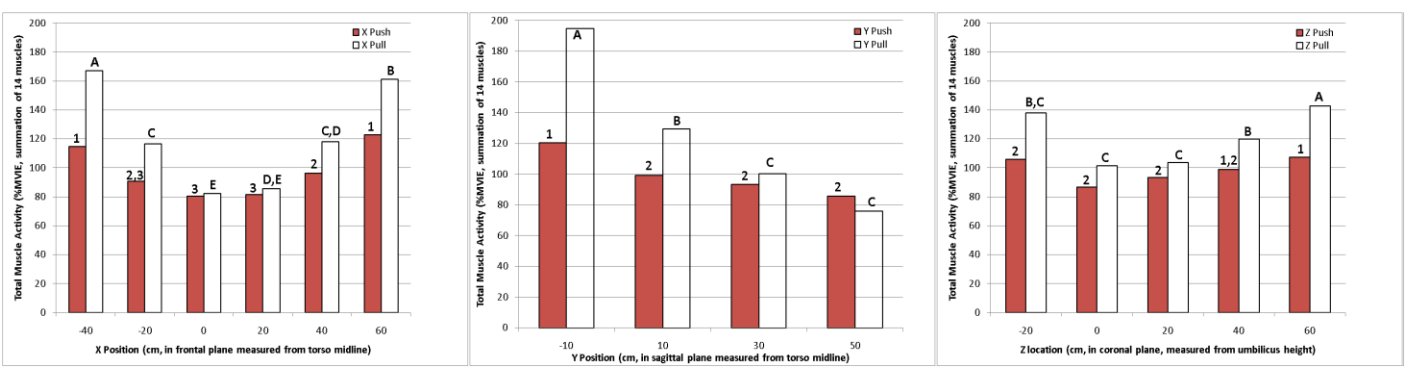

Figure 1. The influence of hand location on total muscle activity occurred for both pushing and pulling. Within direction (push/pull), significant differences are indicated by different letters/numbers above columns.

Table 1. Table of significant influences ($p < 0.05$) of X, Y, and Z handle location on specific muscle activity for pushing and pulling. PSH = significant influence for pushing; PLL = significant influence for pulling; B = significant influence for both

Handle Location	Ant Del*	Mid Del	Post Del	Bic	Tri	Infra	Supra	P Maj (S)	P Maj (C)	Lat	Serr	L Trp	M Trp	U Trp
X	B	B	B	B	B	B	B	B	B	B	B	B	B	B
Y	PSH	B	B	B	B	PLL	B	B	PLL	B	B	B	B	B
Z	PLL	B	B	B	B	PLL	B	B	B	B	B	B	B	B

*Muscles, from left: Anterior, Middle, Posterior deltoid, biceps, triceps, infraspinatus, supraspinatus, pectoralis major (sternal then clavicular heads, latissimus dorsi, serratus anterior, lower, middle, and upper trapezius

COMPARISON OF TWO FORWARD-PLACED TRUNK SUPPORTS FOR STANDING WITH REACHING TO A FIXED, EXTREME DISTANCE IN A DIAGONAL DIRECTION

Caroline Damecour[1], Mohammad Abdoli[2], Ahmad Ghasempoor [3], Joan Stevenson[1]
[1]School of Kinesiology and Health Studies, Queens University, Kingston, Canada, email: 7cmd@queensu.ca
[2]School of Occupational Health and Safety, Ryerson University, Toronto, Canada
[3]Department of Engineering, Ryerson University, Toronto, Canada

INTRODUCTION

Reaching is required for many work tasks in assembly, repair, sorting, and material handling with distances varying depending upon product size and workstation design. In standing, forward reaching is coordinated with a backwards shift of the pelvis when a hip sway strategy is used for balance. This backwards shift restricts the reach distance. Leaning against a forward-placed support, allows the pelvis to shift in the same direction as the reach while remaining balanced thereby extending reach distance[1]. The purpose of this study was to investigate if a forward placed support is beneficial while reaching to a fixed distance. Two supports were tested that differed for contact height. A workbench was used to study the effect of a lower height reflective of typical work postures. A prototype upper trunk support called the Dynamic Trunk Support (DTS) (Fig 1) was used to determine whether a new type of assistive device could be helpful for stationary standing work.

Fig 1. DTS

METHODS

Ten females with an average age of 31 years (SD 9), performed a slow-paced, two-handed horizontal reach at waist height and a vertical reach from waist to shoulder height, lifting 5kg 50-55 cm forward in a 45 degree diagonal. This task was performed while standing with no support, standing and leaning against a rigid support normalized to the anterior pelvic crest, and leaning against partial support with the contact normalized to the manubrium. Fastrak™ (Polhemus, VT) was used to track 3D body segment motion of the head, upper and lower back, pelvis and thigh. Postural muscle activity was recorded using a Bortec AMT8-channel (Bortec Biomedical Ltd., AB) for the bilateral lumbar erector spinae at L4, bilateral gluteus maximus and right hamstring. EMG was calibrated to a maximal voluntary contraction. A forceplate (AMTI, MA) was used to track center of pressure (COP) as an indicator of postural balance. Low back discomfort was rated using a 10 point VAS. Repeated measures ANOVA tested for differences of the average relative and absolute peak angles in 3D between standing conditions at terminal reach. Similar testing was completed for the lower back and hip extensor peak muscle activity and their APDF.

RESULTS

At terminal horizontal reach, the upper back was forward flexed 52 degrees (SD 13), side flexed 41 degrees (SD 12) and rotated 33 degrees (SD 16) with no support. With vertical reach, the upper back orientation was half of forward and side flexion, and a third in rotation to terminal horizontal reach. Leaning against a support reduced the upper back flexion angle by an average of 11 (SD 10) and 13 (SD 9) degrees for lower and upper trunk support respectively for horizontal lifting only. No effect was seen with vertical lifting. The absolute angular orientation of the pelvis and relative orientation of the lower and upper back at terminal reach were unchanged from no support while leaning against the upper trunk support for both heights. Leaning against the lower support changed 3D movement with the desk blocking rotation of the pelvis. This was compensated by an 8 degree (SD 6) increase of relative upper back rotation (Fig 2).

Figure 2: Trunk kinematics at terminal reach.

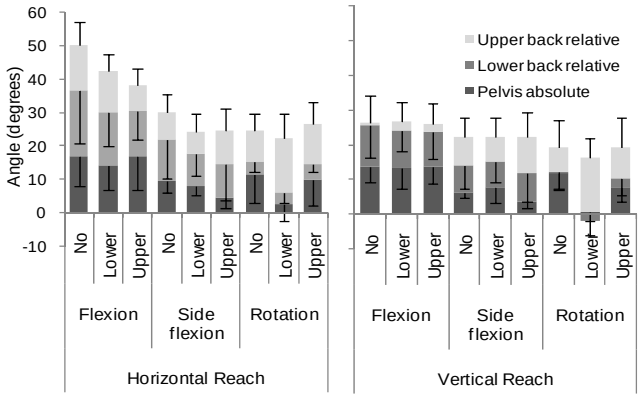

Muscle activity of the right L4 erector spinae decreased by 28% with leaning but only a small difference existed between the two support heights. APDF analysis revealed similar findings. The COP excursion was least while leaning against the upper trunk support. Lower back discomfort ranged from 0 to 9 with lowest average of 0.7 for upper trunk support and horizontal reach and the highest of 3.5 with no support and horizontal reach with a significant difference (P=0.05) between no support and upper trunk support horizontal lifting.

DISCUSSION AND CONCLUSIONS

The findings show a favourable change in trunk posture at terminal reach that appears to be secondary to a longer reach suggesting that leaning forward against a support is beneficial. A higher placed support appears to be favourable since there was no disruption of the 3D terminal reach posture. The forward shift of the pelvis appears to have more benefit than weight transfer from the support provided by the upper trunk support, however these finding may have been influenced by design limitations of the older prototype. Results were influenced by lift height and balance strategy.

REFERENCE

[1]Damecour C., et al. (2010) Comparison of two heights for forward placed trunk supports with standing work. *Applied Ergonomics*. (in press).

ACKNOWLEDGEMENT

Scholarly, Research & Creative Activities, Ryerson University

A BIOMECHANICAL ANALYSIS OF COKEOVEN STANDPIPE CLEANING LEADING TO DESIGN OF TARGETED ENGINEERING INTERVENTIONS

Micha Wallace[1], Michele Oliver[1], Mark Munro[1], James R. Sexsmith[2]
[1]School of Engineering, University of Guelph, Guelph, Canada, wallacem@uoguelph.ca, moliver@uoguelph.ca
[2]Faculty of Kinesiology, University of New Brunswick, Fredericton, Canada, sexs@unb.ca

INTRODUCTION

To chip carbon build-up on the walls and lid of a cokeoven standpipe, standpipe cleaners must use high-frequency, high-impact forces while under high heat loads requiring them to use full body safety gear, including a respirator and NOMEX™ suit. Awkward postures result from the geometry and height of the standpipe. The job is comprised of many subtasks: platform or ladder positioning, latch and lid opening, opening floor lids, lid chipping, lid scraping, mouth cleaning, sides scraping, back scraping, floor lid closing, standpipe lid and latch closing, and damper rocking. The purpose of this project was to quantify the biomechanical requirements in order to intelligently design a series of ergonomic interventions.

METHODS

Peak external load requirements were determined 'N' times (Table 1) using a customized Chatillon™ FCE Force Gauge (AMETEK, Largo, FL, USA) and averaged for several tasks. Four standpipe cleaners (mean age 42±8 years) consented to be monitored during their job using MyoMonitor™ (Delsys Inc, Boston, USA) electromyography (EMG) electrodes, bilaterally, on the upper trapezius, anterior and posterior deltoid, biceps brachii, triceps brachii, flexor carpi radialis and erector spinae (Figure 1) as only the upper body supplies required motions. Reference voluntary contraction (RVC) normalization was done with 7 and 5lb weights, as maximal voluntary contractions were contraindicated due to unknown cardiovascular risk factor status, and may have also served to fatigue the worker prior to their shift thus potentially compromising safety. EMG was matched to digital video, sectioned according to subtask, the peak and integrated EMG values were calculated and averaged across trials and subjects.

RESULTS

The Chatillon Force gauge indicated that the average impact force on standpipe scraping was 1624N, while lid scraping required 1730N (Table 1). Lifting the floor lid required forces upwards of 405N. EMG subtask results revealed that average peak ranged between 300-1300%RVC for most muscles on both sides, with one subtask peak reaching 4100%RVC, indicating that the job is extremely intense.

Table 1: Peak Force Measurement - Chatillon FCE Force Gauge

Job Task	Action	Average Peak Force (Newtons)	N
Lid Latch Open	Push	503	1
Scraper Pole to Break Lid Seal & Push Open	Push	354	1
Standpipe Scraping	Push	1624	4
Lid Scraping	Push	1730	5
Lid Close with Scraper Pole in Latch Loop while standing on ladder	Pull	178	1
Lid Close with Scraper Pole on Counterweight while standing on the ground	Push	185	1
Lid Latch Handle Pull	Pull	738	3
Pulling Damper	Pull	426	3
Pushing Damper	Push	367	3
Lift & Remove Ground Lid	Push	330	3

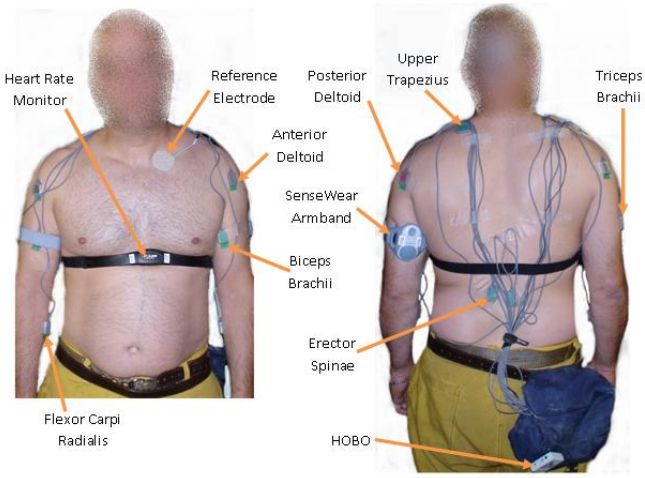

Figure 1: Instrumentation Setup including Electrode Locations

DISCUSSION AND CONCLUSIONS

One of the more interesting findings from the EMG task analyses showed that closing the lid on the ladder puts a higher strain on the neck and forearms than closing from the ground. Obviously closing from the ground would also help to prevent falls.

A number of engineering interventions are warranted. A sturdier platform may help to reduce corrective posture adjustments experienced on the ladder. A scissor-lift would allow for maximum adjustability and safety while potentially alleviating above-shoulder arm movements. Obviously the loading produced while cleaning should be reduced. An adjustable pivot point could act as a levering point for the scraper tool, reducing loading of the arms during cleaning of the pipe and lid. This could be in the form of an adjustable arm with a cuff for the tool, or a set of alternately placed pegs. A pneumatically actuated tool could be similarly mounted, with consideration for isolation from vibration exposure. A wheeled lever would help pry the floor lid and reduce the load to move it. A companion paper briefly describes the design, implementation and effectiveness of the engineering interventions.

Cokeoven standpipe cleaning requires high-force exertion thus requiring extremely high muscle loads while in awkward postures. Advanced measurement and analysis techniques such as external force determinations, EMG and video have provided an intensive analysis of job subtasks thus allowing for targeted engineering intervention design and assessment.

A BIOMECHANICAL ANALYSIS OF COKEOVEN STANDPIPE CLEANING ASSESSING EFFECTIVENESS OF TARGETED ENGINEERING INTERVENTIONS

Micha Wallace[1], Michele Oliver[1], Mark Munro[1], James R. Sexsmith[2]
[1]School of Engineering, University of Guelph, Guelph, Canada, wallacem@uoguelph.ca, moliver@uoguelph.ca
[2]Faculty of Kinesiology, University of New Brunswick, Fredericton, Canada, sexs@unb.ca

INTRODUCTION

To chip carbon build-up on the walls and lid of a cokeoven standpipe, standpipe cleaners must use repetitive, high-impact forces while under high heat loads requiring them to use full body safety gear, including a respirator and NOMEX™ suit. Awkward postures result from the geometry and height of the standpipe. The cleaning job is comprised of many subtasks: platform or ladder positioning, latch and lid opening, opening floor lids, lid chipping, lid scraping, mouth cleaning, sides scraping, back scraping, floor lid closing, standpipe lid and latch closing, and damper rocking. A companion study quantified the biomechanical requirements in order to intelligently design a series of ergonomic interventions. The purpose of this paper is to report on the effectiveness of the Mechanical Scraper Holder (MSH, Figure 1).

METHODS

Three standpipe cleaners (mean age 38±8 years) consented to be monitored while doing their job using MyoMonitor™ (Delsys Inc, Boston, USA) electromyography (EMG) electrodes, bilaterally, on the upper trapezius (UT), anterior and posterior deltoid (AD & PD, respectively), biceps brachii (BB), triceps brachii (TR), flexor carpi radialis (FCR) and erector spinae (ES). Reference voluntary contraction (RVC) normalization was done with 7 and 5lb weights, as maximal voluntary contractions were contraindicated due to unknown cardiovascular risk factor status, and may have also served to fatigue the worker prior to their shift. Over approximately one hour of data collection, the standpipes were cleaned once using the existing method 'old way' (OW) and twice using the MSH (MSH1 and MSH2). EMG was matched to digital video, sectioned according to subtask, and peak and integrated EMG (iEMG) values were calculated and averaged across trials and subjects.

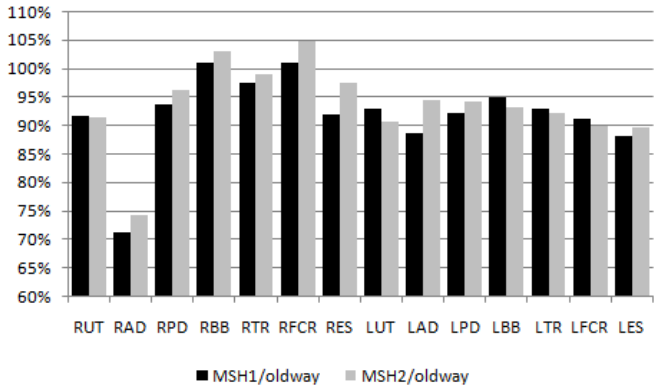

Figure 2: Averaged iEMG for the entire cleaning process using the MSH the first and second times as a percentage of the existing method, for right (R) and left (L) muscles

RESULTS

The introduction of the MSH reduced muscle loading on almost all of the muscles during the whole cleaning process, with the AD reduced to just over 70% of OW (Figure 2). When individual chunks of cleaning in recognizable postures using the MSH were dissected out, removing times when workers did not use the MSH, the iEMG of MSH cleaning were all reduced when compared to the same postures in OW, to an average of 86% across all muscles and postures. Individual EMG subtask results revealed that average peak EMG values ranged between 65-1060 %RVC with one maximum subtask peak reaching 3845%. When used while cleaning the lid and averaged across all muscles, the MSH was 110% of OW when chipping but 98% of OW when scraping the lid.

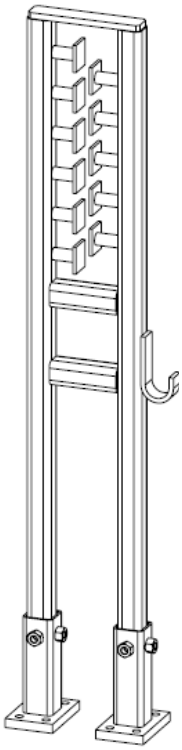

Figure 1: Mechanical Scraper Holder

DISCUSSION AND CONCLUSIONS

Overall, the MSH is a positive change to the standpipe cleaning procedure, reducing muscle loading. The MSH may not be as practical when used to clean the lid, though replacing the platform solid fall rail with a chain fall rail would allow for added range of motion allowing a better posture to achieve a mechanical advantage with the scraper bar.

This loading may be further reduced with more experience. The workers had not previously used the MSH, so the experience gained in MSH1 could account for a reduced muscle loading on MSH2. On the other hand, an increased muscle loading during the MSH2 is to be expected due to the fatigue from MSH1.

Cokeoven standpipe cleaning involves high force exertions, requiring extremely high muscle loads while in awkward postures. Advanced measurement and analysis techniques such as EMG and video have provided for an intensive analysis of job subtasks. It was a rare opportunity to test both before and after intervention implementation on the actual job site. This post-intervention study has allowed for confirmation of the effectiveness of the current targeted modifications engineering interventions and to pinpoint future design modifications to further improve this performance.

Kinematics and kinetics of the lower limb during stair ambulation in older adults

Samantha M. Reid[1], Patrick A. Costigan[1]
[1]School of Kinesiology and Health Studies, Queen's University, Kingston, ON, Canada , samantha.reid@queensu.ca

INTRODUCTION

The mechanics of stair negotiation by young adults has received a great deal of attention [1,2], while few studies have examined these same mechanics in an older adult population [3,4]. Currently, a comprehensive understanding of the biomechanics of the lower limb in both the frontal (responsible for medio-lateral stability) and sagittal (responsible for forward progression) planes in an older adult population is lacking. The objective of this investigation was to provide normative profiles of the lower limb during stair ascent and descent in a healthy older adult population.

METHODS

The lower limb mechanics of 28 (13M) healthy older adults (66.4 ± 8.3 yrs) were analyzed while they ascended and descended a custom 4-step staircase. Participants completed three stair ascent and descent trials at a self-selected pace. An optoelectric camera (Northern Digital, Waterloo, Canada) tracked clusters of 3-4 infrared emitting diodes secured to the thigh, shank and foot. Ground reaction forces were recorded with a force plate mounted on concrete blocks on the second step of a standard dimension four-step staircase.

The Visual three-dimensional (3-D) motion analysis software (C-motion Inc., Germantown, MD) processed the kinematic and kinetic data. The three-dimensional net hip, knee, and ankle joint forces and internal moments were calculated using typical inverse dynamics. While net joint angles were calculated using a Cardan/Euler rotation matrix. For each participant the hip, knee, and ankle joint force and moment curves were normalized to body weight. As well joint force, angle and moment curves were normalized to 100% of the gait cycle and then ensemble average to provide a single representative trial.

RESULTS AND DISCUSSION

Hip, knee, and ankle net joint internal moment data during stair ascent and descent are presented in Figures 1-2, angles and forces are not presented due to space constraints. Angle, moment and force waveform curve profiles for both ascent and descent are similar in shape to those previously reported, with discrepancies in the magnitudes being noted. Discrepancies in the magnitudes reported in this study compared to those previously reported could be due to the fact that previous studies examined younger adults. Thus the noted differences may be a result of age-related differences.

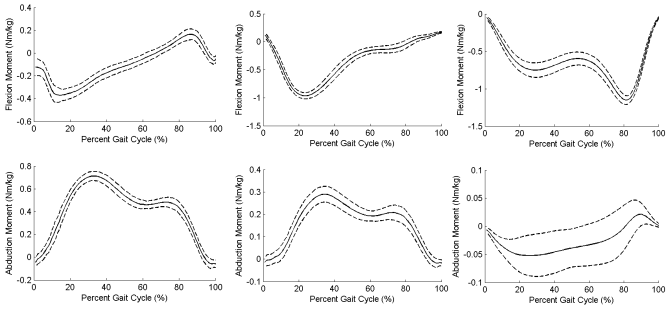

Figure 1: From left to right hip, knee, and ankle mean (solid line) joint sagittal and frontal plane internal moments during stair ascent. The dashed lines represent ± one standard deviation. Positive values of the Y axis refer to flexion or abduction moments.

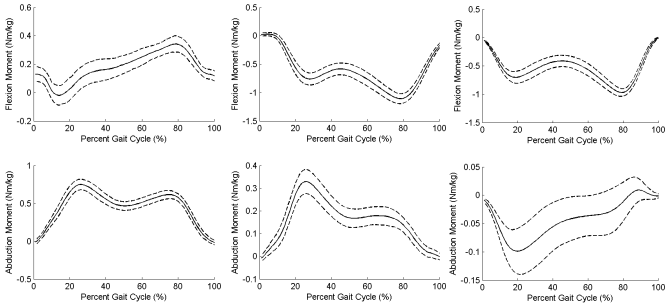

Figure 2: From left to right hip, knee, and ankle mean (solid line) joint sagittal and frontal plane internal moments during stair descent. The dashed lines represent ± one standard deviation. Positive values of the Y axis refer to flexion or abduction moments.

CONCLUSIONS

The current study used healthy older adults to establish normative lower limb net angle, moment, and force profiles for stair ascent and descent of an older adult population, adding to the current literature available by providing detailed information about the lower limb particularly in the frontal plane and also at the ankle that was lacking previously. To the authors' knowledge, this is the first study to examine the lower limb about the sagittal and frontal plane and may be effective in evaluating changes that may be occurring due to pathologies or compensations present in older adult and patient populations.

REFERENCES

[1] Andriacchi et al. (1980). J Bone and Joint Surgery 62A(5):749-57.
[2] Protopapadaki et al. (2007). J Clinical Biomech 22:203-210.
[3] Nadeau et al. (2003). Clinical Biomechanics 18:950-959.
[4] Reeves et al. (2007). J of Electromy Kinesiol 18(2):218-27.

ACKNOWLEDGEMENTS

Authors would like to thank Alison Novak for her assistance with data collection. We would also like to acknowledge the financial contribution of Ontario Graduate Scholarship.

TRANSVERSE PLANE KINEMATICS AND UNDER-CORRECTION IN HIGH TIBIAL OSTEOTOMY

Rebecca Moyer, Trevor Birmingham, Ian Jones, J. Robert Giffin
[1]Wolf Orthopaedic Biomechanics Laboratory, Fowler Kennedy Sport Medicine Clinic,
University of Western Ontario, London, Canada,
rmoyer@uwo.ca

INTRODUCTION

Medial opening wedge high tibial osteotomy (HTO) is a biomechanically focused surgery designed to correct varus alignment of the lower limb and reduce load on the medial compartment of the knee. The angle of correction is planned based on the goal of shifting the weight bearing line (WBL), measured on standing anteroposterior (AP) radiographs as the line connecting the centre of the hip to the centre of the ankle, laterally across the tibiofemoral joint. However, the accuracy of frontal plane alignment measured from AP radiographs can be compromised by transverse plane rotations, particularly in varus alignment [1]. Lower limb rotations not captured by radiographs may explain differences between patients where planned correction angles are achieved and patients with under-corrected malalignment after HTO. The purpose of this study was to compare pre- and post-operative transverse plane kinematics during gait in patients who reached planned radiographic correction angles in HTO and those who did not.

METHODS

40 patients having undergone medial opening wedge HTO were selected from a large cohort of patients participating in an ongoing study of osteotomy procedures. 20 participants had a post-operative WBL that was <50% (from medial to lateral) across the tibial plateau and considered "under-corrected". These patients were compared to those with optimal post-operative corrections (WBL approximately 62.5%) matched for pre-operative sex, age, body mass index, limb alignment and disease severity. All participants underwent 3-D gait analysis using an 8-camera motion capture system and modified Helen Hayes markers set (Eagle EvaRT; MAC, Santa Rosa, CA) synchronized with a floor-mounted force plate (AMTI, Watertown, MA) before and 6 months after surgery. The average hip, knee and ankle transverse plane rotations and foot progression angle from 10-to-60% of the gait cycle were calculated using commercial software (Orthotrak 6.2.4; MAC, Santa Rosa, CA) and custom post-processing techniques. Static frontal plane alignment was quantified using hip-to-ankle standing long-cassette radiographs.

RESULTS

Independent t-tests confirmed that post-operative WBL ratio and mechanical axis angle (MAA) were significantly different ($p<0.01$) between patients who reached planned correction angles (WBL= 65.1±4.2%; MAA= 3.0±1.0º) in HTO and those who did not (WBL= 40.9±8.3%; MAA= -2.0±1.8º). There were no significant differences in transverse plane kinematics between groups pre-operatively (Table 1). Only hip rotation was significantly different ($p<0.05$) between groups post-operatively (Table 1). For patients with under-corrected malalignment, paired t-tests indicated significant changes after surgery for knee and ankle rotations ($p<0.05$). Patients who reached planned correction angles displayed significant change after surgery for hip rotation only ($p<0.01$).

Table 1: Means (SD) for pre- and post-operative hip, knee and ankle transverse plane rotations (deg) and foot progression angle (deg) during mid-stance (mean of 10-60% of gait cycle). Negative values represent external rotation.

	WBL < 50% n=20	WBL > 60% n=20
Pre-Operative		
Hip Rotation	-1.8 (10.4)	-1.1 (9.2)
Knee Rotation	-2.1 (10.6)	-3.8 (9.6)
Ankle Rotation	-4.8 (8.0)	-2.0 (8.5)
Foot Progression	-8.7 (5.8)	-7.6 (6.0)
6 Month Post-Op		
Hip Rotation	-0.4 (13.0)	-7.0 (9.6)*†
Knee Rotation	-12.1 (10.4)†	-6.5 (19.0)
Ankle Rotation	0.9 (5.4)†	2.2 (15.1)
Foot Progression	-9.8 (4.9)	-8.6 (5.4)

*denotes statistical significance between groups
†denotes statistical significance after surgery

DISCUSSION AND CONCLUSIONS

These findings suggest that pre-operative differences in transverse plane kinematics do not explain differences in radiographic correction angles achieved during HTO. However, the amount of radiographic correction achieved does appear to affect transverse plane kinematics post-operatively. The clinical significance of changes in transverse plane kinematics on long-term outcomes after HTO warrants further study.

REFERENCES

[1] Swanson KE, et al. (2000). Does axial limb rotation affect the alignment measurements in deformed limbs? *Clinical Orthopaedics and Related Research* Vol **371**; p. 246-252.

EVALUATION OF GAIT SYMMETRY AFTER STROKE: A COMPARISON OF ANKLE-FOOT ORTHOTIC USERS AND NON-USERS.

Amanda E Kay[1,2], Stephen D Perry[1,2,3], William E McIlroy[1,2,4,5]
[1]Graduate Department of Rehabilitation Science, University of Toronto, Toronto, Canada
[2]Toronto Rehabilitation Institute, Toronto, Canada
[3]Kinesiology & Physical Education, Wilfrid Laurier University, Waterloo, Canada
[4]Department of Kinesiology, University of Waterloo, Waterloo, Canada
[5]Heart & Stroke Foundation Centre for Stroke Recovery, Canada

INTRODUCTION

Improved walking function is the goal most often stated by individuals living with stroke [1]. Patients with residual impairments may utilize assistive devices, such as walkers, canes and ankle-foot orthotics (AFO) to achieve independent walking. Evidence shows that AFOs may have a beneficial effect by improving walking speed; however other important issues such as symmetry have not been addressed [2]. Gait symmetry measures can provide insight about the quality of walking function and may be used to inform treatment decisions. The purpose of this study was to compare spatial and temporal symmetry measures of gait between chronic stroke survivors who use an AFO and those who do not.

METHODS

Twenty-nine chronic stroke survivors (64.4±12.2 years old and 40.4±27.6 months post stroke) completed three walking trials at each of their preferred and fast speed over a pressure sensitive mat (GAITRite®, CIR Systems Inc., Pennsylvania, USA). Participants were encouraged to walk without any assistive devices if possible.

Gait symmetry ratios (affected limb/unaffected limb) were calculated for swing time, stance time and step length. Participants were stratified into two groups for the analysis; AFO vs. non-AFO. A two-factor repeated measures ANOVA was utilized to compare gait symmetry measures between groups and walking conditions.

RESULTS

Nine participants used an AFO; 3 prefabricated and 6 custom made AFOs. Within this group, seven participants used other walking aids; 5 canes and 2 wheeled walkers. Of the twenty people in the non-AFO group, 7 used a cane and 3 used a wheeled walker.

The main group comparisons for swing time symmetry revealed a significant effect ($p=0.021$). Average swing time symmetry for the AFO and no AFO groups are 1.47 and 1.2, respectively. Stance time symmetry was significantly different between AFO users and non-AFO users (0.85 and 0.94, $p=0.009$). Step length symmetry scores were not significantly different between groups ($p=0.182$). Comparisons between walking conditions were similar for all symmetry measures ($p>0.05$).

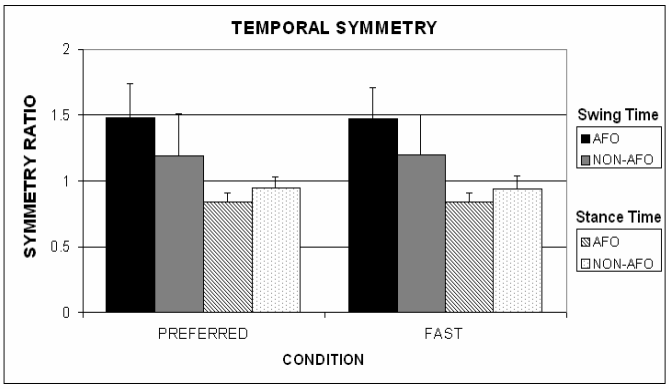

Figure 1: Swing and stance time asymmetry was significantly more severe for the AFO compared to the non-AFO group ($p<0.05$). A ratio of 1.0 indicates 'perfect' symmetry between limbs.

DISCUSSION AND CONCLUSIONS

Our analysis of gait symmetry revealed that stroke survivors who use an AFO demonstrate greater temporal asymmetry compared to non-AFO users. For example, the affected limb swing duration was approximately 1.5 times greater than the unaffected limb for the AFO group, as compared to 1.2 times for non-AFO users. Stroke survivors with asymmetric gait may be at increased risk for developing other musculoskeletal health consequences. Continued study is warranted for investigating immediate effects of AFOs on spatial and temporal gait asymmetry within stroke survivors.

REFERENCES

[1] Bohannon RW et al. (1988). Rehabilitation Goals of Patients with Hemiplegia. *Int.J.Rehabil.Res.* Vol **11**; p. 181-183.
[2] Leung J and Moseley A. (2003). Impact of ankle-foot orthoses on gait and leg muscle activity in adults with hemiplegia. *Physiotherapy*. Vol **89**(1); p. 39-55.

ACKNOWLEDGEMENTS

This work is support by NSERC, University of Toronto and CIHR operating grant. Also, we acknowledge the support of the Toronto Rehabilitation Institute which receives funding under the Provincial Rehabilitation Research Program from the Ministry of Health and Long Term Care in Ontario.

DYNAMIC STABILITY DURING GAIT AND SIT-TO-WALK ASSESSED WITH STABILIZING AND DESTABILIZING FORCES

Cyril Duclos[1], Pierre Desjardins[1], Hélène Corriveau[2], Brenda Brouwer[3], Sylvie Nadeau[1]
[1]Centre for Interdisciplinary Research in Rehabilitation/Institut de Réadaptation Gingras-Lindsay-de-Montréal, Montréal, Canada, and School of Rehabilitation, Université de Montréal, Canada, cyril.duclos@umontreal.ca,
[2]School of Rehabilitation, Université de Sherbrooke, Canada
[3]School of Rehabilitation Therapy, Queen's University, Kingston, Canada

INTRODUCTION

Falls often happen during diplacement tasks such as transition from sitting to standing and walking [1]. How these tasks challenge postural control is not well known. By determining the destabilizing and stabilizing forces [2], we quantified how the body position and the kinetic energy produced during gait and sit-to-walk (StW) performance contribute to dynamic instability. With this stability model, the lower the destabilizing force, the more unstable the body position; the higher the stabilizing force, the more difficult to maintain the centre of mass within the base of support.

METHODS

Seven older adults (73 ± 6 years old, 2 men; mean height: 161 ± 13 cm, mean weight: 70 ± 13 kg) participated in the study. Their balance was good according to clinical tools; mean Timed up & go: 9.8 ± 1.1 sec (range: 8.3-11.2 sec) and median Berg Balance scale: 53 (range: 52-56). Dynamic stability was also measured during gait and StW at preferred speed.

For this, kinematic recordings were obtained with an NDI Optotrak 3020 system, sampling at 60 Hz, from three non-collinear infrared markers placed over the feet, legs, thighs, pelvis, trunk and head segments and one over each wrist, elbow and shoulder joint. Kinetic data were collected from force platforms embedded in the floor (AMTI OR6-7-1000) at a frequency of 600 Hz, filtered with a 4th-order Butterworth zero-lag filter with a cut-off frequency of 10 Hz and re-sampled at 60 Hz to match the kinematic data.

The StW task was normalised from 0-100% using the seat-off event to the first heel contact after standing. For the gait task, the cycle was conventional (two consecutive contacts of the same foot with the ground). Minimal destabilizing and maximal stabilizing forces, as well as their means, were computed from kinematic and kinetic data during single limb support (SLS) of gait and StW. The minimum destabilizing force occurs at the time in the gait or StW cycle where it is easiest to displace the body's centre of pressure to the limit of the base of support whereas the maximum stabilizing force occurs when the theoretical force required to cancel the kinetic energy of the body is the greatest. Values were compared between the two tasks with Wilcoxon ranked tests.

RESULTS

The duration of StW was 0.78 ± 0.15 sec and the gait cycle was 1.13 ± 0.11 sec. During the tasks, the SLS phase was shorter for StW (0.29 ± 0.07 sec; 38± 6% of the task) than for gait (0.37 ± 0.04 sec; 33 ± 2% of the gait cycle). The mean speed of the centre of gravity was faster during SLS in gait (1.08 ± 0.13 $m.s^{-1}$) than in StW (0.58 ± 0.11 $m.s^{-1}$, $p<0.05$).

The destabilizing force was lower during gait (Mean: 112.4 ± 46.3 N; Min: 88.3 ± 23.4 N) than during StW (Mean: 183.3 ± 33.5 N, $p<0.05$; Min: 109.2 ± 15.8 N, $p<0.05$). The stabilising force was greater during gait (Mean: 252.8 ± 122.0 N; Max: 470.8 ± 165.6 N) than during StW (Mean: 119.7 ± 56.0 N, $p=0.063$; Max: 157.4 ± 82.7 N, $p<0.05$).

During gait, the minimum destabilizing force appeared at 32 ± 3% of the gait cycle (mid SLS phase) and the maximum stabilizing force at 41 ± 5% (second half of the SLS phase), close to the point of the minimum velocity of the centre of gravity (34 ± 1%). During StW, the minimum destabilizing and maximum stabilizing forces appeared after toe-off at 67 ± 4% and 74 ± 5% of the task, respectively close to the minimum velocity of the centre of gravity (66 ± 7%).

DISCUSSION AND CONCLUSIONS

At preferred speed, older adults were less stable during the SLS phase of gait than StW task. The instability of the body was due to both components of dynamic balance: the posture of the body (lower destabilising force) and the control of the centre of gravity velocity (higher stabilising force).

Contrary to what was expected, the most unstable time during both tasks appeared when the velocity of the centre of gravity was close to its lowest value over the entire task duration.

Future studies will need to assess the dynamic balance requirements of other functional tasks with this approach. Moreover, the amplitude of the forces should be analysed in relation to known determinants of postural control such as sensation, strength and reaction time.

REFERENCES

[1] Talbot, LA *et al.* (2005).Falls in young, middle-aged and older community dwelling adults: perceived cause, environmental factors and injury. *BMC Public Health* **5**; p. 86.
[2] Duclos, C *et al.* (2009).Destabilizing and stabilizing forces to assess equilibrium during everyday activities. *Journal of Biomechanics* **42** (3); p. 379-382.

ACKNOWLEDGEMENTS

C. Duclos received a postdoctoral scholarship from the REPAR/FRSQ for this project. Funding for the study was provided by CIHR. S. Nadeau is a Senior researcher supported by the FRSQ.

Strategies and Adaptations during Level Ground Walking and Obstacle Clearance Tasks with Limb Mass

Marc D.M. DeRochie, Jonathan C. Singer, Jeremy W. Noble, Stephen D. Prentice
Department of Kinesiology, University of Waterloo, Waterloo, ON, Canada, sprentic@uwaterloo.ca

INTRODUCTION

Previous lower limb weighting studies have placed a load on the legs bilaterally and tested its influence at different placement locations. It was previously determined that kinematic changes occur with greater masses and at joints proximal to weight placement [1]. Other studies have identified that these changes exist for a short adaptation period before parameters revert to a steady state [2]. Tasks that require voluntary gait modifications such as obstacle clearance have also been performed with lower leg bilateral weight addition [4]. In cases of normal obstacle clearance, increased flexion at all three joints in the lower limb was needed to safely traverse the obstacle [3]. The goal of the current study was to investigate joint kinematics and kinetics of unilaterally weighted participants using level ground force platform collection techniques, rather than a treadmill. It was hoped that this would allow for new insight into the adaptation periods and strategic motor pattern changes seen at the ankle, knee and hip.

METHODS

Kinematic and force platform data were collected on two groups of 10 healthy male subjects. Group 1 (mean age = 23yrs, mean wt. = 82.18kg, mean ht. = 1.79m) was a normal walking group and group 2 (mean age = 24.8yrs, mean wt. = 79.90kg, mean ht. = 1.77m) was an obstacle clearance group. Both participated in 20 trials each of three different conditions; normal, weighted and weight off using a 2.27kg limb mass attached just proximal to the right maleoli markers. A repeated-measures two-way ANOVA was carried out on relevant variables in order to determine statistical significance.

RESULTS

Weight addition and removal affected the kinematics and kinetics of the normal walking and obstacle clearance groups. This effect was more prominent in the normal walking group. If changes were seen, trials 1 through 5 were the locations showing a quick adaptation followed by a leveling off back to a new steady state in later trials.

ACKNOWLEDGEMENTS

This work was funded by a grant from NSERC.

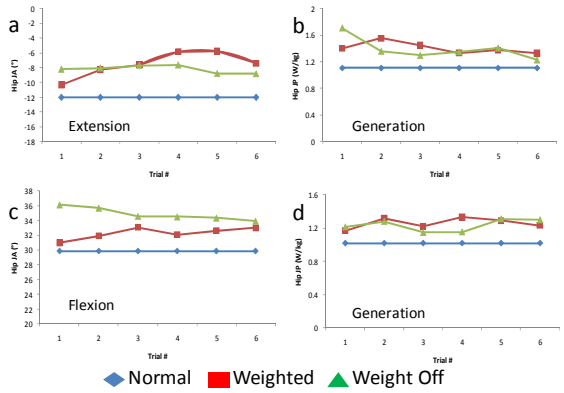

Figure 1: Peak hip angle during stance a) & swing c). Peak hip power during stance b) & swing d).

DISCUSSION

Participants in the normal walking group utilized the hip joint in order to account for weight addition and removal. Kinematically, changes in the hip angle occurred at all instances analyzed throughout the gait cycle with this effect being more prominent in the weight off condition (Figure 1). In conjunction, the hip energy generation increased during all phases of the gait cycle (Figure 1) while the ankle and knee either decreased generation or increased absorption. The obstacle group also increased flexion at the hip. However, the ankle had either decreased plantarflexion or increased dorsiflexion at all instances analyzed during the gait cycle. In this group, increases in energy generation at these joints were only found during stance and at heel contact. The toe-obstacle clearance values also showed a marked increase in trial 1 for the weighted condition demonstrating a voluntary gait modification made by participants to safely clear the obstacle that was quickly adapted for. Overall, there was evidence of recalibration of limb parameters that have been previously found by treadmill studies; however, they were not as robust during overground walking and obstacle clearance tasks.

REFERENCES

[1] Martin PE et al. J Biomech. 1990; 23(6): 529-536.
[2] Noble et al. Exp Brain Res. 2006; 169: 482-495.
[3] Patla AE et al. Exp B. Res. 1995; 196: 499-504.
[4] Reid MJ et al. Neurosci R C. 2001; 29(2): 79-87.

THE ASSESSMENT OF GAIT DISORDERS IN CHILDREN WITH AUTISM

Matthew Calhoun and Vicky Chester
Faculty of Kinesiology, University of New Brunswick, Fredericton, Canada, vchester@unb.ca

INTRODUCTION

Autism is considered the most common neurological disorder in Canadian children. This developmental disability is characterized by impaired social and communication skills. While lesser known, autism can also be characterized by numerous neuromuscular problems that affect gross motor skills such as walking. This study quantified and assessed the gait patterns of children with Autism and compared the data to age-matched controls. Objective clinical gait analyses were conducted using hi-tech motion analysis systems.

METHODS

Twelve children (n=12) aged 5 to 9 years with Autism Spectrum Disorder participated in the study (mean age = 5.8 yrs; mean height = 121.03 cm; mean weight = 29.31 kg). The following exclusion criteria were used in this study: 1) children diagnosed with Asperger's or Otherwise-Non Specified Disorder and 2) toe walkers. Previously published control data was used for data comparisons (Chester et al., 2008). An eight camera Vicon MCam motion capture system (Oxford Metrics Group Ltd.), sampling at 60 Hz, was used to track the three-dimensional trajectories of twenty reflective markers placed on the subjects' skin. Four force plates (Kistler 9281B21, 9281CA, Kistler Instruments, Winterthur, Switzerland) embedded in the lab floor measured the three-dimensional forces and moments during gait. A rigid body model was used and consisted of the left and right foot, shank, thigh and the pelvis and trunk. Joint center locations and joint angles were estimated in accordance with Davis et al. (1991). Net joint moments and joint power for the hip, knee, and ankle joints were estimated using an inverse dynamics approach.

Gait patterns in the Autism and control group were compared based on temporal-spatial data and principal component scores. Significant ($P<0.05$) differences in temporal-spatial parameters were tested using a one-way ANOVA. A series of one-way ANOVA's with Bonferroni adjustments were used to test for significant differences for the principal component (PC) scores that were normally distributed with equal covariance matrices, while the Kruskal-Wallis Test was used to analyze the principal component scores that failed to meet these assumptions. All statistical tests were performed using SPSS (SPSS Inc).

RESULTS

Significant differences ($P<0.05$) were found between the Autism and control for cadence (Table 1) and three of the principal component scores, namely sagittal ankle moment PC1, sagittal ankle angle PC1, and sagittal hip moment PC2. The Autism group showed decreased plantarflexor moments during the first half of the gait cycle, followed by increased plantarflexor moments until after toe-off. The decreased plantarflexion moments in stance coincided with increased dorsiflexion angles in stance. The Autism group showed decreased extensor moments during the initial 20% of the cycle and decreased peak hip flexor moments compared to the control group.

Table 1: Temporal-spatial data for the Autism and control group

Gait parameter	Autism		Control	
	Mean	SD	Mean	SD
Cycle time (s)	0.97	0.12	0.91	0.13
Cadence (steps/min)	125.52	14.39	134.27	18.25
Velocity (cm/s)	99.45	21.96	99.89	17.20
Opp foot strike (%)	49.23	1.77	50.81	2.09
Stride length (cm)	58.15	7.18	54.71	7.93
Toe-off (%)	60.10	2.16	61.06	2.35
Double stance (%)	20.32	3.03	21.31	3.37

DISCUSSION AND CONCLUSIONS

This work has identified kinematic and kinetic parameters that differ between high-functioning Autism and age-matched control group data. Significant differences in cadence and three PC scores were found between the two groups. It is likely that the increased dorsiflexion angles and decreased plantarflexor moment are related to hypotonia, confirmed in 33% of the individuals in the Autism group. Decreased hip extension moments and increased hip flexion moments were also found for the Autism group. The initial hip extensor moment is used to generate hip extension, while the peak hip flexor moment at midcycle facilitates the reversal of hip motion from extension to flexion. Given the lack of significant differences in walking velocity and hip and knee kinematics using PCA, the clinical significance of the reduced hip moments is unclear. To date, few studies have examined the gait patterns of children with Autism. To our knowledge, this is the first study to 1) examine kinetic parameters in a paediatric Autism population, and 2) examine Autism patterns of movement using waveform analyses. A greater understanding of the gait deviations associated with Autism is clearly beneficial for treatment planning.

REFERENCES

[1] Chester V et al. (2008). The identification of age-related differences in kinetic gait parameters using principal component analysis. Clin Biomech 23; p. 212-220.
[2] Davis R et al. (1991) A gait analysis data collection and reduction technique. Hum Mov Sci 10; p. 575–587.

The effects of aging on behavioural strategies when walking through apertures

Amy Hackney[1], Dr. Michael Cinelli[2]
[1,2]Kinesiology and Physical Education, Wilfrid Laurier University, Waterloo, ON, CA hack7780@wlu.ca

INTRODUCTION

Avoiding collisions with objects is a requirement of everyday locomotion. The actions individuals take to move through a cluttered environment are governed by how passable one perceives the open space to be. Naturally, people want to avoid colliding with objects to reduce the risk of injury. Previous research has found that young adults have a Critical Point ((ie. the aperture width that elicited a shoulder rotation) to be 1.3 times their shoulder width [1].

The objective of the study was to determine: if the behaviours of older adults (critical point, velocity change onset, & shoulder rotation onset) are different from those previously reported with young adults [1,2,3].

METHODS

Ten healthy older adults (mean age 72) with normal or corrected to normal vision, free of physical disabilities limiting limb movement and shoulder rotation and no reported neurological disorders volunteered for the study. Testing procedures were approved by the WLU Research Ethics Board.

Participants walked along a straight path at a self selected speed toward a static door aperture located 6m from the start. The participants were instructed to safely pass through the aperture without hitting the doors. The width of the aperture varied from 45-85cm in 5cm increments (ie. 9 aperture widths) and were presented in randomized order. Participants preformed 3 trials of each aperture width. The shoulder width of each participant was taken using a measuring tape.

Shoulder rotation magnitude about the vertical axis was calculated for each trial. The initiation of shoulder rotation was determined to be the point (distance) at which shoulder rotation magnitude fell outside 2SD from the average magnitude during the first second of the trial. In order to determine the Critical Point across all participants using the dimensionless Pi value: Aperture Width (A)/ Shoulder Width (S) [1].

RESULTS

Average shoulder rotation magnitudes were plotted against the Pi value (A/S) and data points were fit using a 2nd order polynomial (Fig.1). The Critical Point was determined to be 1.7.

Results indicated a main effect of aperture width on shoulder rotation magnitude ($p<0.001$) and onset of shoulder rotation ($p<0.001$). Smaller apertures produced a larger shoulder rotation and these larger rotations occurred earlier than small rotations.

An interaction between shoulder rotation onset and a velocity change onset was found in older adults ($p<0.05$). On average older adults change their velocity (walking speed) prior to producing a shoulder rotation.

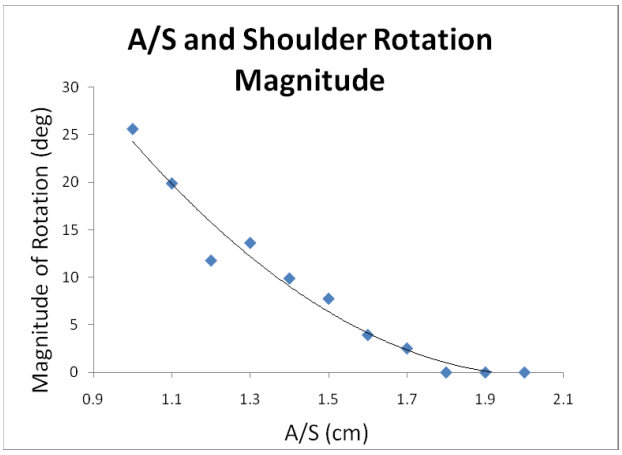

Figure 1 Average shoulder rotation magnitude at each Pi value (ie. A/S) for all participants

DISCUSSION AND CONCLUSIONS

The current study determined the aperture width at which a shoulder rotation was needed for older adults to be successful. It appears that older adults have a greater Critical Point than previously reported in younger adults (1.7 vs 1.3 [1]). This Critical Point indicates that with apertures that are less than 1.7 times one's shoulder width, an older adult will rotate this or her shoulders. This conservative behaviour indicates a cautious approach to walking through cluttered environments.

The study also determined that older adults initiate a shoulder rotation later for larger rotation magnitudes. This is different than what was biomechanically expected. Instead, it was found that older adults rotation their shoulders at similar rates regardless of the size of the rotation requires. Therefore a large shoulder rotation requires more time to perform and therefore would be initiated earlier.

In conclusion, older adults are using different behavioural strategies to walk through small spaces (ie. apertures) then what has been previously reported in young adults.

REFERENCES

[1] Warren, W.H., & Whang, S. (1987). Visual Guidance of Walking Through Apertures: Body Scaled Information for Affordances. *J. Exp Psychol Hum Percept Perform*. Vol **13** (3); p 371-83
[2] Higuchi, T. et. Al (2006). Locomotion through apertutres when wider space for locomotion is necessary: adaption to artificially altered body states. *Exp Brain Res,* Vol 75; p 50-59
[3] Cinelli, M.E., and Patla, A.E. (2007). Task specific modulations of locomotor action parapmeters based on on-line visual information during collision avoidance with moving objects. *Hum Move Sci,* Vol **27**: p 513-531 .
[4]Higuchi, T. et. al. (2009). Gaze behaviour during lomcomotion through apertures: The effect of locomotion forms. *Hum Mov. Sci.* Vol 28: p 760-771

ACKNOWLEDGEMENTS

WLU Science Technology and Endowment Program

Dynamics of unexpected slip perturbations during barefoot walking

Jessica M.R. Berrigan[1], Stephen D. Perry[1, 2, 3]
[1]Dept of Kinesiology & Physical Education, Wilfrid Laurier University, Waterloo, ON;
[2]Toronto Rehab Inst, Toronto, ON; [3]Grad Dept of Rehab Sci, University of Toronto, ON

INTRODUCTION

Slips are considered one of the most common causes of major accidental injuries [1]. It is generally accepted that pronation and supination, generated at the subtalar joint, are involved in the normal gait cycle [2]; however, this triplanar motion has yet to be investigated with respect to a slip perturbation. This study focused on the ankle muscle activity during a heel contact slip in barefoot individuals.

METHODS

Ten participants (8 females) were recruited from a university aged population (21.8 yrs ± 1.7, 1.7 m ± 0.1, and 71.1 kg ± 10.7). Each participant performed 28 walking trials over a 10 m walkway with rectangular sheets of sandpaper placed at each foot contact (Figure 1). Wax paper adhered to the underside of a sandpaper sheet was exchanged on the second force plate to cause an unexpected heel contact slip perturbation. Electromyography (EMG) signals were collected (sampling freq 1000 Hz) from eight lower limb muscles. Kinematic data was collected using a 20 marker set-up with a two OptoTrak 3020 camera banks (NDI, Waterloo, ON, Canada). Marker triads were placed on the tibia, calcaneous and forefoot to determine foot motion. Kinetic data was collected using embedded forces plates (AMTI, Watertown, MA, USA).

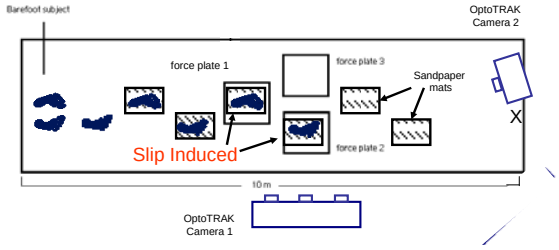

Figure 1: Walkway setup.

RESULTS

Eight participants had at least one entirely unexpected slip, of varying magnitudes, within their 28 trials. Three participants experienced a second slip for a total of 11 slip trials. In non-slip trials, maximum heel velocity occurred approximately 23.7 ms after heel contact. During slip trials, maximum heel velocity occurred 1.08s after heel contact, averaging 1.0 m/s. Onset of the slip occurred approximately 50 ms after foot contact. Stance leg muscle activity (tibilias anterior, rectus femoris and medial hamstrings) demonstrated simultaneous activation onset at approximately 150 ms after foot contact on the slip mat. Additionally, multiple bursts of muscle activity (> non-slip walking trials) were observed in tibialis anterior and perneous longus in slip trials (as indicated in Figure 1).

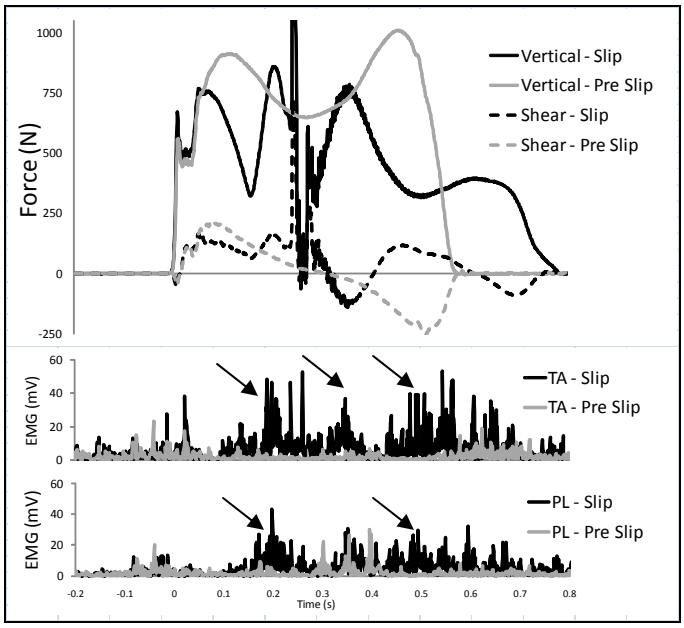

Figure 2: A typical participant vertical and anterioposterior shear forces and tibialis anterior (TA) and perneous longus (PL) muscle activity during a pre slip and slip trials.

DISCUSSION AND CONCLUSIONS

These results demonstrate similar findings in the literature with respect to heel contact slips. The onset of the slip was similar to that reported by Cham et al [1]. The muscle timing and magnitudes of the ankle and knee extensors/flexors of the stance leg support postural strategies targeted at reducing the forward translation of the heel to maintain the COM within the BOS as previously illustrated by Redfern et al. [3]. The presence of tibialis anterior and perneous longus activity during the slip may indicate a role for foot pronation/supination during the reaction. Therefore further analysis of foot motion should be preformed and evaluated in tandem with the muscle activity results to understand the potential importance of the interaction between the muscle activity and the motion of foot pronation/supination to understand the dynamics of a successful reaction to the slip event.

REFERENCES

[1] Cham & Redfern (2001). *J Biomech* **34**(11): 1439-45.
[2] Hamill & Knutzen, *Biomechanical basis of human movement, 2nd Ed.*; Williams & Wilkins, 1995.
[3] Redfern *et al*. (2001). "Biomechanics of slips." Ergo 44(13): 1138-66.

ACKNOWLEDGEMENTS - This study was supported by a CIHR operating grant (MOP-77772).

EFFECT OF FOOT ORTHOSES AND NANICULAR DROP MEASURES ON FOOT SEGMENT COUPLING PATTERNS

[a] Mansour Eslami, [b, c] Reed Ferber, [d]Mohsen Damavandi

[a] Department of physical education and sport sciences, University of Mazandaran, Iran;

[b]Faculties of Kinesiology and Nursing, University of Calgary, Canada, T2N 1N4;

[c] Running Injury Clinic, University of Calgary, Canada, T2N 1N4

[d] Faculty of Physical Education and Sport Sciences, Sabzevar Tarbiat Moallem University , Sabzevar , Iran

INTRODUCTION

Several studies have investigated the kinematic effects of foot orthoses on rearfoot and tibia coupling motions. Rearfoot eversion and tibia internal rotation ratio [1] as well as vector coding measurement techniques [2] have been used to examine lower limb joint coupling motion to provide new insight into the mechanisms behind the success of foot orthotic interventions in preventing and treating running-related injuries. Nonetheless, these mechanisms are not still very well understood since the previous studies have utilized limited biomechanical foot models. The purpose of this study was to examine the effect of a semi-rigid foot orthotic device on variations in forefoot- rearfoot joint coupling patterns in individuals with different navicular drop measures during the stance phase of running. We hypothesized that forefoot-rearfoot coupling patterns would be different between individuals with different navicular drop measures during orthoses and no orthoses conditions.

METHOD

Ten running trials were collected from eleven male subjects who ran shod at 170 steps per minute with orthoses and without. Forefoot–rearfoot coupling motions were assessed using a vector coding technique during four intervals across the first 50% of stance. Subjects were divided into two groups based on navicular drop measures. A three way ANOVA was performed to examine the interaction and main effects of stance interval, orthoses condition and navicular drop ($p < 0.05$).

RESULTS

There were no interaction effects among stance interval, orthoses conditions or navicular drop ($p=0.14$) whereas an interaction effect of orthoses condition and stance interval was observed ($p=0.01$; effect size= 0.74). Forefoot-rearfoot coupling motion in the no orthoses condition increased at a rate faster than orthoses condition from heel-strike to foot-flat phase. Orthotic modified this rate by decreasing coupling angle at phase 4 of stance phase during running ($p=0.02$).

DISCUSSION

During phase 4 of stance, the use of orthoses significantly reduced the forefoot-rearfoot coupling angle indicating reduced forefoot motion relative to the rearfoot during peak loading. Specifically, a significant interaction effect of conditions and phases, with a large effect size (0.74), could be the finding of most interest of this study. The large effect size suggests that orthoses have a systemic effect on forefoot-rearfoot coupling, regardless of inter-subject differences in coupling angle. The slope of the forefoot-rearfoot coupling angle in the no orthoses condition increasing sharply with a rate faster than the orthoses condition from phase 2 to phase 4. We suggest that the semi-rigid foot orthotic device functions to stabilize the mid-foot joint axes early at the foot-flat phase causing this joint complex to lock into a rigid lever, thus influencing the forefoot-rearfoot coupling relationship.

REFERENCES

[1] MacLean C., Davis IM., Hamill J.,(2006). Clin Biomech 21 (6), 623-630.

[2] Ferber R., Davis IM., Williams III, DS., (2005). J Biomech 38, 477-483.

ATTITUDE INTERPOLATION USING CRAWFORD AND CARDAN ANGLES ON PELVIC MOTIONS AFTER REMOVING THE "GIMBAL LOCK" CONDITION

Pierre Desjardins[1,2,3], Sylvie Nadeau[1,2], André Plamondon[3]
[1]Centre de Recherche Interdisciplinaire en Réadaptation (CRIR/IRGLM), Montréal, Québec, Canada
[2]École de réadaptation, Faculté de médecine, Université de Montréal, Montréal, Québec, Canada
[3]Institut de Recherche Robert-Sauvé en Santé et en Sécurité du Travail (IRSST), Montréal, Québec, Canada

INTRODUCTION

The aim of this paper is to analyze the use of the Cardan and Crawford angles to interpolate the attitude of a moving pelvic segment using cubic splines. There are 12 possible expressions for the Euler angles, each giving a different path when we plot the data, with the result that a judicious choice is needed to describe the degrees of freedom of the motion to be interpolated. There are six possibilities of the Cardan kind (xyz, xzy, zxy, zyx, yzx, yxz), six of the Crawford [1] kind (zxz, zyz, xyx, xzx, yzy, yxy). One potential problem is that the Euler angle can experience "gimbal lock" (i.e. two axes effectively lining up, resulting in the temporary loss of a degree of freedom) as observed when the second rotation is near 90° or 270°. Crawford exposes a method to shift the gimbal lock problem from 90° to 180°, the tilt/twist planar angles. This method has demonstrated stability over twice the range of the corresponding Euler angles.

As the order of the rotation affects the result, it is important to select the order that best describes the motion so as to correctly interpolate the attitude. However, if the interpolation deals with unconstrained objects, there is no preferred order.

METHODS

The data were obtained from a cluster of nine LEDs fixed by a harness to the pelvis of a healthy subject. The 3-D space positions of marker clusters were measured by five Optotrak cameras (Northern Digital, Waterloo, Canada) at a sampling rate of 50 Hz. A 5-min trial (walking, jumping, turning around and picking objects off the floor) was analyzed. Retaining the original frequency, the data from this trial were re-sampled at ~27 to 3 Hz, replacing data with missing values. All 12 possibilities were used. The quaternion angular metric distances [2] between the interpolated and the original data were computed and used for comparison between conditions.

When interpolating a curve, it is important to include all peak values in the process. Since these values depend on the choice of angles, all 36 possible paths (3 angles for each 6 Cardan and 6 Crawford) were analyzed. An algorithm based on the derivatives obtained from a cubic spline [3] with a root of variance set at 25° was used to detect the frames where these peaks happened and these key frames were never removed from the files to be interpolated. To eliminate the gimbal lock, all data with the critical angle at 20° or less near the gimbal lock conditions were removed.

RESULTS

The results are presented in Table 1. The mean frequency of the unmissing data in the files varies from 27 - 3 Hz. Despite the greater stability range of the Crawford angles, there is no difference in the percentage of missing interpolations. Only 4% data were removed when the gimbal lock was eliminated. The percentages of the interpolated data with an error lower than 1° and 5° vary with the gap length but are very similar between Crawford and Cardan. The percentage of interpolated data with >80° error increased with the gap between data. Some points had a >170 ^{o} error even with the gimbal lock removed and all signal peaks preserved. Visual inspection of plotted curves shows that this occurs in a relatively flat region of the original data.

Table 1: Comparison of interpolated with original data

Nb=15000 at 50 Hz	Freq.	Percentage of the interpolated data				Nb. Pts D > 170°
		Miss.	D <1°	D <5 ^{o}	D >80 ^{o}	
Crawford	26	3	91	97	0	7
Cardan	27	3	90	97	0	5
Crawford	12	4	86	96	1	0
Cardan	12	4	83	93	1	7
Crawford	7	4	68	92	1	18
Cardan	8	4	66	90	2	28
Crawford	3	4	26	68	4	53
Cardan	5	4	30	71	5	54

Nb: Number of samples; Freq.: mean of the approx. frequency of the known data before interpolation; D: angular metric distances between original and interpolated data, Miss.: % of data removed by gimbal lock condition

DISCUSSION AND CONCLUSION

The results showed no advantage of one method over the other. We found no way to predict the occurrence of errors over 170°. Use of these angular procedures to interpolate the missing orientation of a segment is therefore questionable. To use angular interpolation, it is essential to check the validity of the resulting motion. We therefore recommend visually inspecting the motion with an avatar after interpolating the attitude.

REFERENCES

[1] Crawford N. R. et al. (1999). A new technique for determining 3-D joint angles: the tilt/twist method. *Clinical Biomechanics* Vol **14**; p. 153-165.

[2] Ales, Ude (1999). "Filtering in a unit quaternion space for model-based object tracking". Robotics and Autonomous Systems, vol. 28, no. 2-3, pp. 163-172.

[3] H.J. Woltring (1986), A Fortran package for generalized, cross-validatory spline smoothing and differentiation. Advances in engineering software 8(1986)2, pp. 104-113.

OPTIMAL MARKER LOCATION FOR LANDING ANALYSIS

Arsène Thouzé[1,2,3], Mickaël Begon[1,3], Tony Monnet[2], Matt Pain[4]
[1]Department of Kinésiologie, University of Montréal, Montréal, Québec, arsene.thouze@gmail.com
[2]Institut P' UPR 3346, University of Poitiers, Chasseneuil, FRANCE
[3]C.H.U Ste Justine, Montréal, Québec, Canada.
[4]School of Sports Exercise and Health Sciences, Loghborough University, Leics, United Kingdom.

INTRODUCTION

Whatever the studied movement, skin movement artefact is a major source of inaccuracy in human movement analysis. If three markers put on bony landmarks are sufficient to calculate three dimensional kinematics, a redundant marker set placed over the body segment increases significantly the accuracy [1]. While marker sets for gait analysis are daily used in clinics, they have shown several limits that are amplified when applied to movements with larger impacts, range of motion and muscle contraction such as jumping or landing. More accurate marker sets should be determined. The aim of this study is to assess the intra- and inter-subject reproducibility of the marker deformations during landing trials. Since subjects have different morphologies, markers are ranked from the most and least deformed for inter-subject comparison instead of analysing the raw deformations.

METHODS

Twenty six markers were put on the thigh defined five vertical lines of four to six equidistant markers (Fig a) of nine male subjects (23±2.9 years old, 178±3.7 cm, 73.6±5.6 kg). They performed a static trial, thigh setup movements for locating hip joint centre and five landing trials from a 0.92 m-high box. The kinematics was collected using a 10 camera Vicon system (T40, 4Mpx). The local frame of the thigh was defined using condyles and hip joint centre positions. Static acquisitions allowed to record condyle positions in the technical frame composed of the 26 markers and obtain the geometry of reference of the markers in the local frame.
The measured positions during landing trials were compared with the solidified positions in the local frame to obtain the mean marker deformations expressed by:

$$\overline{d} = \sum_{i=1}^{n} \frac{1}{n} \left\| {}^{m}P - {}^{s}P \right\|, \qquad (1)$$

where ${}^{m}P$ is the measured positions for each i moment of trials and ${}^{S}P$ is the solidified positions in the local frame [3]. Then markers were ranked from the most to the least deformed markers for each trial. The agreement of ranking between trials and subjects was analysed with the Kendall coefficient of concordance (W). To test W for statistical significant, the χ^2 statistic was used for a p value of 0.001.

RESULTS

Results shows a repeatability between trials of each subject, the minimal value of W was 0.88 for a χ^2 of 110.1 (χ^2 =52.6 for p =0.001) whereas no reproducibility was observed between subjects (W =0.18 for χ^2 =40.7).

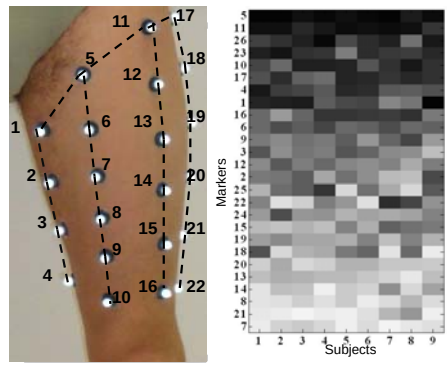

a) b)

Figure 1: a) Marker placement on the thigh; b) Marker rankings for each subject, black box means that marker was the most deformed whereas white box are for least deformed.

DISCUSSION AND CONCLUSIONS

Marker deformation was calculated with respect to the global kinematics of the thigh based on 26 markers. No concordance between inter-subject marker rankings was found but there are tendencies to show common worst such (#5, #11 and #26 put close to knee and hip joints) and the least deformed markers (#7, #8 or #21 put on the middle of the anterior and lateral faces) to consider the thigh as a rigid segment. We suppose that low repeatability could be a consequence of different soft tissue distributions and various techniques during landing (e.g. knee range of motion and landing duration).
Although intracortical pins enable to quantify the actual marker displacement with respect to the bone, this method is invasive and presents experimental limits in walking (e.g. anaesthetics or pain affects the coordination, pins bending, loosening or vibrating) [2]. The risks increase in sports movements with larger impacts and range of motion.
This study could be considered as an alternative method for assessing marker deformation during tasks with impacts and velocity.

REFERENCES

[1] T. Monnet et al. in Levy, T.H. *Biomechanics : Principles, Trends and Applications* (2010) Improvement of the input data in biomechanics : Kinematic and body inertial parameters.

[2] C. Reinschmidt et al. (1997) Tibiofemoral and tibiocalcaneal motion during walking : external vs. Skeletal markers. *Gait and Posture,* Vol **6 ;** p.98-109.

IMPLICATIONS OF MARKER SIZES DURING GAIT ANALYSIS

Arsène Thouzé[1, 2], Marine Gaihlard[1], Rachel Cotton[1], Mickael Begon[1, 3]
[1]Département de Kinésiologie, University of Montréal, Montréal, Québec, Canada, arsene.thouze@gmail.com
[2]Institut P' UPR 3346, University of Poitiers, Chasseneuil, France
[3]C.H.U Sainte Justine, Montréal, Québec, Canada

INTRODUCTION

Skin movement artefacts are a major source of error in human movement analysis [1]. Several studies propose a large number of markers over the body segments to obtain to improve accuracy [2]. Marker inertia could induce in a traction on the skin during movement and increase skin movement artefact. To our knowlegde, no study has assessed marker placement reproducibility on the subjects. The purposes of this study are to assess the reproducibility in marker placement and the effect of marker size on skin deformation. We hypothesize that bigger markers increase skin deformation.

METHODS

Thirty-two markers were put on the thigh of a subject (Fig. 1a). The markers were positioned into 6 vertical lines of 4 to 6 equidistant markers. Their placement was defined by anatomical landmarks: femoral condyles (#5 and #24), greater trochanter (#18), crotch, gluteus maximus insertion on the femur and popliteal fossa. The subject was filmed in a static upright position, for lower limb motions to estimate the hip center of rotation and for 10 walking trials using a 8-camera 512 Vicon system at 60 Hz. This protocol was repeated with two marker diameters commonly used in motion analysis namely, 14 mm *vs* 7 mm (2.16 g *vs* 0.990 g) – in 18 paired sessions in the same experimental conditions Markers positions are expressed in the local frame of the thigh. Marker positions of each static were grouped together within a sphere of a minimal radius, determined with the distance between the two farthest markers for all the sessions. If there was no intersection between the spheres, marker placement was considered as reproducible.

During the gait, the marker deformation was expressed by:

$$\frac{1}{100}\sum_{t=1}^{t=100}\left(\frac{1}{32}\sum_{m=1}^{m=32}\left(\sqrt{(P_{m,t}^{a}-P_{m}^{s})^{2}}\right)\right), \quad (1)$$

Where $P_{m,t}^{a}$ is the measured position of the mth marker at normalized time t and P_{m}^{s} is its solidified position [3] (Fig. 1c) for each time among the hundreds of our normalized gait cycle. The effect of the marker size on this deformation was assessed using a paired t-test using a p value of 0.05.

RESULTS

Since there is no intersection between all the spheres (Fig. 1b), marker placement was considered as reproducible. Their radii vary from 11.7 to 30.1 mm. For the upright standing condition, there was no statistical difference between marker size (p=0.813).During gait, marker deformations showed cyclic patterns and the mean deformation was 7.42±0.47 mm *vs* 7.39±0.39 mm for 7 and 14 mm-diameter markers, respectively.

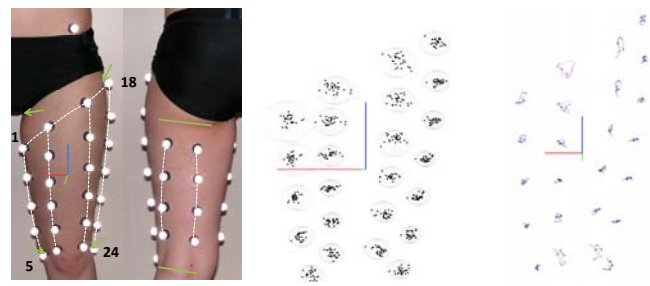

a) b) c)

Figure 1: a) Marker placement on the thigh; b) Fitting spheres for each marker; c) Marker deformation: red crosses for static position and blue dashed lines for their displacement during one walking cycle.

DISCUSSION AND CONCLUSIONS

Using 32 markers on the thigh is reproducible technique and can be used on several subjects to determine optimal marker locations for gait analysis. However some locations showed a larger variability because of a lack of bony landmarks: e.g., marker under the crotch in anteroposterior direction or those under the gluteus maximus in the mediolateral direction. A bigger marker does not increase skin movement artefacts 57% of the mass for 7 mm and 29% for 14mm marker is in located in the plastic base plate (0.565 and 0.640 g for 7 and 14 mm), while a 3 mm hemispherical marker weights only 0.205 g and have no base. It could make the difference with & and. Inaccuracy in motion analysis systems and actual skin movement artefact seem to be more important than the marker size effect. New motion analysis systems make use of 3-mm marker and smaller, and could reduce skin movement artefacts.

REFERENCES

[1] A. Cappozzo et al. (1996). Position and orientation of bones in space during movement: experimental artefacts. *Clinical Biomechanics* Vol **11**(2); p. 90-100.
[2] A.Van der Zidjen et al. (2009). The introduction and development of the FAMP-coach; A tool to guide marker placement in gait analysis, *Gait and Posture* 30S, S1-S153.
[3] T. Monnet et al. (2008). Iterative solidification procedure to determine the optimal markers location. 10th international symposium on the 3D Analysis of Human Movement. Amsterdam 28-31 October.

SHOULDER MAXIMUM VOLUNTARY ELECTRICAL ACTIVITY: EFFECT OF BILATERAL VERSUS UNILATERAL EXERTIONS ON SIGNAL AMPLITUDE AND INTRAPARTICIPANT REPRODUCIBILITY

Tej-Jaskirat Grewal, Steven L. Fischer, Richard Wells & Clark R. Dickerson
Department of Kinesiology, University of Waterloo, Waterloo, Canada

INTRODUCTION

Measurement of maximum voluntary electrical excitation (MVE) during a maximum voluntary isometric contraction (MVIE) is a common approach used to determine reference electrical activity values for a muscle. The accuracy of MVE values is often criticized due to their high variability. To maximize accuracy, a standardized approach is required to describe specific MVIE tests. While MVEs increase with training, verbal encouragement and visual feedback, concerns remain regarding the specific postures used during MVIE tests. This study compared the amplitude and intraparticipant reproducibility of MVE values measured during MVIE tests in both unilateral and bilateral postural configurations.

METHODS

16 (8 males and 8 females) university-aged, right-hand dominant participants performed five repeats of three specific MVIE tests (empty can, palm press, and external rotation tests) using bilateral and unilateral configurations. MVIE tests were performed against a custom handle. All 30 exertions were performed in a completely randomized order, and took place over 5 seconds, in which participants ramped up to their peak during the first two seconds and sustained the peak for the remainder of the trial.

Surface electromyographic (EMG) signals were recorded from upper trapezius (UT), anterior (AD), middle (MD), and posterior (PD) deltoids, pectoralis major clavicular head (Pec), supraspinatus (Supra) and infraspinatus (Infra) of the dominant arm with a Noraxon Telemyo 2400T T2 system (Noraxon, Arizona, USA). Force was measured using an AMTI transducer (MC3A, AMTI MA, USA), fixed to the handle. These data were synchronously sampled at 1500Hz. Verbal encouragement and visual force feedback was provided during each exertion.

EMG was linear enveloped by full wave rectifying and digitally filtering the raw signal at 4Hz using a 4th order single pass Butterworth filter. A two factor repeated measures ANOVA ($\alpha<0.05$) was used to examine the effects of postural configuration, gender and MVIE test on the peak linear enveloped EMG for each muscle and hand force. Coefficients of variation (CV), determined using average peak activity and standard deviation obtained over 5 repeats of each test, were used to compare within-participant reproducibility.

RESULTS

Test configuration influenced MVE amplitude for the upper trapezius and supraspinatus during the empty can MVIE test, with the bilateral performance eliciting significantly higher muscle activity than the unilateral configuration (Figure 1). Bilateral configuration generated higher hand forces only during the palm press test.

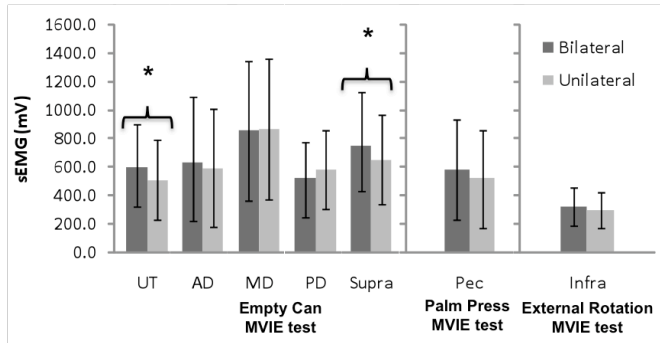

Figure 1: The MVE for each muscle as determined bilaterally (black bars) and unilaterally (grey bars), within the prescribed MVIE tests for each muscle.

The posterior deltoid and pectoralis major MVEs were less reproducible (CV=12-15%) than those of anterior and middle deltoids, upper trapezius, and supraspinatus (CV=10-12%), independent of configuration. Configuration had a small effect on the repeatability of MVEs during MVIE tests. In a bilateral configuration, the CV decreased by 1-2% for the upper trapezius, anterior and middle deltoids, and the infraspinatus.

DISCUSSION AND CONCLUSIONS

This study helps to objectively establish preferred configurations to expand existing recommended standardized protocols[2] for collecting MVEs. A significantly higher muscle activity for selected muscles for the bilateral empty can test and a moderately improved or similar reproducibility of MVEs during bilateral tests suggests that if possible, bilateral configurations may be preferred over unilateral configurations.

Higher MVE values during a bilateral configuration than a unilateral test configuration agree with previous research[3] but contradict some upper extremity research[1]. Continued evaluation is still required to determine whether it is muscle function, muscle size or neural activation that causes muscle-specific activity variations during bilateral exertions.

REFERENCES

[1] Herbert RD, Gandevia SC. Muscle activation in unilateral and bilateral efforts assessed by motor nerve and cortical stimulation. *J Appl Physiol,* 80: 1351-1356, 1996

[2] Mathiassen SE, Winkel J, Hagg GM. Normalization of surface EMG amplitude from the upper trapezius muscle in ergonomic studies – A review. *J Electromyogr Kinesiol*, 5: 197-226, 1995.

[3] Van Dieen JH, Ogita F, De Haan A. Reduced Neural Drive in Bilateral Exertions: A Performance-Limiting Factor? *Med Sci Sports Exerc,* 35:111-118, 2003.

MRI DATA REGISTRATION USED IN INTRASUBJECT COMPARISON OF PELVIC CONFIGURATION

Pavel Ruzicka[1], Petra Bendova[2]
[1]Faculty of Mechanical Engineering, CTU in Prague, Prague, Czech Republic, pavel.ruzicka@fs.cvut.cz
[2]fyzioP - Physiotherapy Clinic, Klatovy, Czech Republic, info@fyziop.cz

INTRODUCTION

The present study aims to project universal magnetic resonance imaging data processing tool (MPT), which would enable to register effectively MRI data within individual subject. The relative configuration of pelvic bony segments is detected.

METHODS

From an operational view, the inputs of registration are the two views to be registered: the basic view assumed as fixed and the secondary view assumed as registered. The output is a geometrical transformation, which is merely a mathematical mapping from points in one view to points in the second view (Figure 1). The transformation is in our case accomplished by registration of landmark coordinates of the same structure, i.e. point-based method.

Two approaches were tested to find a transformation that performs the match between geometrical data: interactive reposition performed by means of CAD package NX™ (Siemens PLM Software, Köln, Germany) and computational approach based on rigid-body point-based registration method minimizing the sum of squared relative distances between the corresponding reference points, by singular value decomposition of weighted covariance matrix [1], realized by means of MS Excel™ spreadsheet (Microsoft Corp., Redmond WA, USA). Specific diameter parameters were monitored for 18 subjects and 46 MRI studies.

RESULTS

The precision of registration was evaluated by residual distances between the corresponding reference points after registration procedure. When using L5 vertebra as the reference body, achieved average values were 0.69 mm in the case of interactive procedure and 0.31 mm in the case of computational approach. Then the target registration errors were calculated on basis of existing matching inaccuracy of reference bodies. On average, the registration error was 0.57 mm. West et al. proposed registration error lower than 1 mm as high registration accuracy [2]. Fitzpatrick et al. suggested a method of registration error estimation based on estimation of localization inaccuracy within reference bodies [3], which would represent an average of 0.52 mm in our conditions.

DISCUSSION AND CONCLUSIONS

The study has demonstrated benefits associated with processing of MRI data in terms of highly accurate image registration, provided by designed MPT. The convenience of MPT is direct data analysis, automatic spatial visualization, accurate error calculation and outcome comparison with predefined parameters. The ability to adjust MPT settings makes it universal in processing of any image data and may favour its application in clinical practice.

REFERENCES

[1] Sonka M, Fitzpatrick JM (Eds.). *Handbook of Medical Imaging, vol.2: Medical Image Processing and Analysis*; SPIE press, Bellingham, WA (USA), 2000
[2] West JB et al. (1997). Comparison and Evaluation of Retrospective Intermodality Brain Image Registration Techniques. *Journal of Computer Assisted Tomography* Vol **21**; p. 554–66.
[3] Fitzpatrick JM et al. (1998). Predicting Error in Rigid-Body Point-Based Registration. *IEEE Transactions on Medical Imaging* Vol **17**; p. 694-702.

ACKNOWLEDGEMENTS

This research has been supported by research plan of the Ministry of Education of the Czech Republic MSM 6840770012 “Transdisciplinary research in the field of biomedical engineering II”.

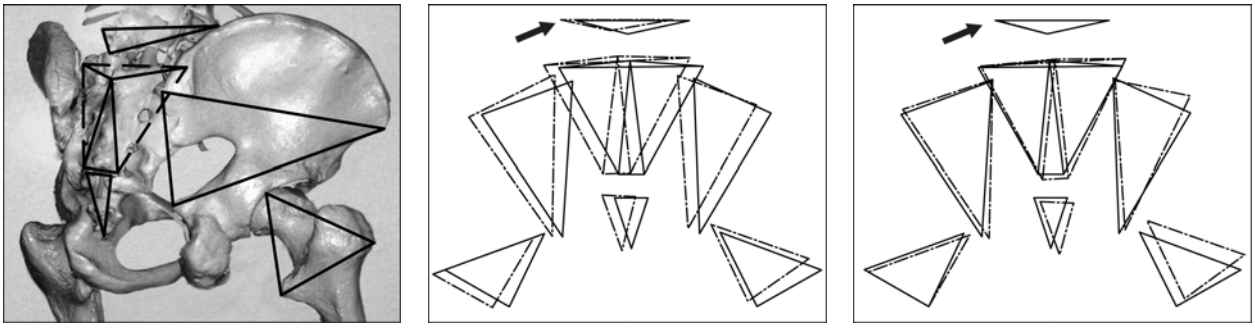

Figure 1: Localized anatomical landmarks: vertebra L5; pelvic bones; femoral heads; coccyx; sacrum (left). Spatial visualization of unregistered data (middle) and registered data (right).

THE INCLUSION OF A 30 HZ HIGH-PASS FILTER AS A UNIVERSAL EMG DATA PROCESSING COMPONENT

Chad E. Gooyers & Jack P. Callaghan
Department of Kinesiology, University of Waterloo, Waterloo, ON, CA
Email: cgooyers@uwaterloo.ca

INTRODUCTION

The frequency spectrum of electrocardiogram (ECG) is encompassed in the bandwidth of surface electromyography (sEMG) signals and often contaminates sEMG data collected from trunk muscles [1,2,3]. It has been previously shown [3] that failing to remove ECG artifact can alter the interpretation of sEMG data. Although numerous techniques exist to reduce this ECG contamination, [1,2,4,5,6] few studies have quantified the changes that occur when these techniques are universally applied on all collected data, including uncontaminated sEMG signals. The purpose of this investigation was to characterize both amplitude and spectral changes that occur when uncontaminated sEMG signals are dual-pass filtered with a second-order high-pass Butterworth filter (HPF) with a cutoff frequency of 30 Hz [2] to assess whether the inclusion of a 30Hz HPF has merit as an integral data processing stage for trunk EMG data.

METHODS

One healthy male (age = 24 years, height = 183 cm, mass = 91 kg) participated in this investigation. Surface EMG was collected during one test session from the dominant side Vastus Lateralis muscle using one pair of bipolar electrodes (30 mm diameter; 25 mm inter-electrode spacing) placed according to the SENIAM guidelines. Raw data were band-passed filtered from 10Hz – 1kHz, differentially amplified and sampled at a rate of 4096 Hz. In total, four different activities were examined. These included: (1) isometric knee extension (2) isoinertial knee flexion / extension (3) cycling at a cadence of 60 rpm and (4) isometric knee extension performed at 50% MVIC until exhaustion. For each of the four activities, direct comparisons were made between dependent measures calculated from data processed with a 30 Hz HPF and control set of data without the HPF.

RESULTS

From the static isometric exertions, mean RMS differences of 0.74, 1.00, 1.69, 3.61, 5.70 and 10.48 %MVIC were calculated for exertions of 2.5, 5, 10, 20, 40 & 80 %MVIC respectively (Figure 1). From the isoinertial knee flexion and extension data, mean relative percent differences of -7.9, -6.6, -11.21% were revealed in the 10th, 50th and 90th percentile muscle activities. In performing a gaps analysis [7] on three minutes of cycling data, it was discovered that the number of gaps identified (0.2 seconds of consecutive data < 0.5 %MVIC) was impacted by including the 30 Hz HPF in the data processing sequence. From the control data only one gap was found, compared to 13 gaps that were identified in the HPF data. Lastly, from the fatigue trial data notable changes in median power frequency (MPF) of the signal were detected when the HPF was applied. Consequently, this altered the slope and y-intercept of a least-squares trend line calculated to describe MPF data over the course of the trial.

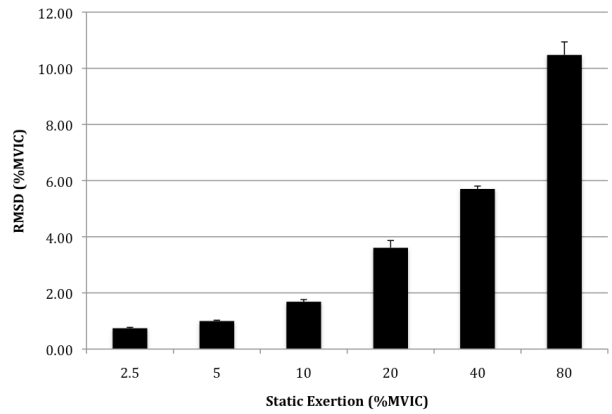

Figure 1. Mean (+ 1SD) RMS differences for static exertion trials.

DISCUSSION AND CONCLUSIONS

The results of the present study suggest that for some applications it may be acceptable to universally implement a HPF (fc = 30 Hz) on all sEMG data collected from muscles that are routinely contaminated by ECG artifact. However, the addition of an ECG removal filtering approach can appreciably alter EMG data, especially at higher activation levels. A universal approach is recommended over intermittent use of a HPF to ensure that accurate comparisons are made between signals that have been treated in the same manner. Selectively treating different trials from the same participant could introduce interpretation discrepancies of both the amplitude and frequency spectrums that are unrelated to changes in muscle activation.

REFERENCES

[1] Redfern et al. (1993). *Clinical Biomechanics.* 8: 44-48.
[2] Drake et al. (2006). *J Electromyogr Kinesiol.* 16: 175-187.
[3] Butler et al. (2009). *J Electromyogr Kinesiol.* 19: 102-113.
[4] Aminian et al. (1988). *Med Biol Eng Comput*. 26: 658-662.
[5] Bortolo et al. (1996). *Med Biol Eng Comput*. 34: 76-81.
[6] Hof (2009). *J Electromyogr Kinesiol.* 19: 554-555.
[7] Veiersted et al. (1990). *Int Arch Occup Env Health.* 62(1): 31-41.

Overground Walking Step Length Estimation with Inertia Measurement Unit

Shuozhi Yang and Qingguo Li
Department of Mechanical and Materials Engineering, Queen's University, Kingston ON, Canada

INTRODUCTION

Any motion in space can be decomposed to six measurable quantities: linear motions along three orthogonal axes and angular velocities about the axes. An inertia measurement unit (IMU) is a device that provides measurement of above-mentioned quantities in terms of linear accelerations and angular velocities. Previous studies were conducted to evaluate the performance of the treadmill walking speed estimation with shank-mounted IMU [1]. An overground walking experiment was implemented in this study to investigate the performance of this IMU-based method with constrained step length and step frequency.

METHODS

Three female and three male participants (age: 23.5 ± 1.5 years; height: 171.00 ± 11.00 m; tibia length: 40.00 ± 2.00 m) were recruited for overground walking experiment. All participants were healthy and exhibited no clinical gait abnormalities. A wireless IMU (MicroStrain, Inc., Williston, VT, USA) was mounted on the lateral side of the left shank of the participant to measure the shank acceleration and angular velocity in the sagittal plane (Figure 1). The IMU measurement data were transmitted to a computer in real time and and recorded at a sampling rate of $100Hz$. The measurements were processed in MATLAB (The MathWorks, Natick, MA, USA) after the experiment. A $2.5Hz$ butterworth filter was used to remove the noise from the data. The walking speed estimation method with shank-mounted IMU developed by Li *et. al* [1] was modified to estimate the step length. The y-intercept of the linear regression model of the resulting data was then used to compensate the systematic error. Two-way ANOVA was implemented to test the effects of different step lengths and step frequencies on the estimation results.

The experiment was conducted on the floor of a flat hallway ($35m$). Prior to the experiment, we used yellow adhesive tape to label four different step lengths ($0.7m$, $0.8m$, $0.9m$ and $1.0m$) on the floor with the aid of a tape ruler. For each step length, four walking trials at different step frequencies were designed, which were approximately 80%, 90%, 100% and 110% of the preferred step frequencies. The beat sound from the metronome provides an indication of the designated frequency. In the walking trials, the participants were instructed to walk along the hallway stepping on the tape markers on the floor while following the beat sound from the metronome, such that the step lengths and step frequencies were respectively constrained at the designated values.

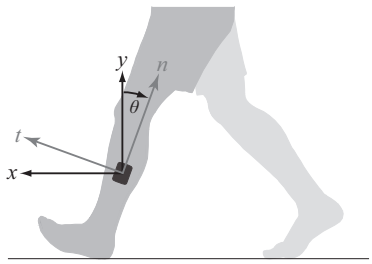

Figure 1. IMU configuration on the left shank.

RESULTs

The linear regression on the estimation results from one representative participant gives a linear model ($y = a * x + b$) with slope 1.03 and y-intercept 0.14 ($R^2 = 0.92$). After adjustment the representative estimation result is shown in Figure 2. The reference step lengths are indicated with the step line, while the thick lines show the average of the estimates for each step length. An overall RMSE of $0.04m$ was obtained.

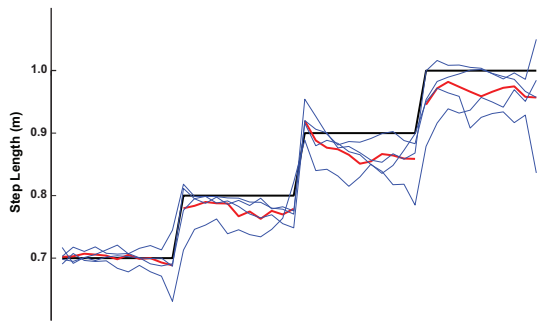

Figure 2. Step Length Estimation Result.

DISCUSSION and CONCLUSION

The linear regression model with slope 1.03 presents a linear trend of the estimation results. However, the amount of underestimation throughout different walking conditions, as shown in Figure 2, indicates some systematic error in this method. The loss of information can be one reason for the underestimation. Only motions on the sagittal plane are considered in our study; however, the shank is not restricted in 2-D motion during walking. With accelerations along two axes and angular velocity about one axis, the IMU sensor might not capture the complete shank motion information. Another reason can be the zero initial condition assumption of the estimation algorithm, referring to [1], in the integration of each gait cycle. In conclusion, this IMU-based step length estimation method can provide accurate estimation with overall RMSE of $0.04m$.

References

[1] Q. Li, M. Young, V. Naing, and J. M. Donelan, "Walking speed estimation using a shank-mounted inertial measurement unit." Accepted by Journal of Biomechanics.

TRANSMISSION OF ACCELERATION FROM VIBRATING EXERCISE PLATFORMS TO THE LUMBAR SPINE AND HEAD

Robert Caryn BA[1,2], J.P. Dickey PhD[1,2], Alan Salmoni PhD[2], Peter Lemon PhD[2], Tom J. Hazell MSc[2]
[1]Joint Biomechanics Laboratory, [2]School of Kinesiology, the University of Western Ontario, London, ON

INTRODUCTION

Whole body vibration exposure has been proposed as a physiological training stimulus for the musculoskeletal system [1,3]. In contrast, whole body vibration has also been identified as a cause of injury in occupational settings [4]. The goal of this study was to quantify the accelerations experienced by the axial skeleton during standing vibration. This study investigated the specific range of knee angles needed to effectively dampen vibration to the upper body.

METHODS

Healthy male and female subjects completed whole body vibration trials on a vibrating platform (WAVE, Windsor, ON) that generated vertical vibrations of 2 or 4 mm amplitudes at specific frequencies between ranges of 20 and 50Hz. Subjects were asked to complete static or dynamic squats at knee angles between 0 and 60 degrees of knee flexion while standing on the platform.

An electrogoniometer (Biometrics SG 150, Gwent, UK) was used to monitor knee flexion during static squat and dynamic squat trials. Triaxial accelerometers (Biometrics ACL 300, Gwent, UK/PCB Piezotronics, NY, USA) were placed on the platform surface, greater trochanter, lumbar spine (L5) and forehead.

The magnitudes of the accelerations were calculated using root-mean-square (RMS). Transfer functions describing the magnitude and phase frequency response of the skeleton were calculated for the platform-to-spine and platform-to-head accelerations. A published transfer function was used to predict bone accelerations from skin accelerations [2].

RESULTS

Pilot data revealed that the platform vibrations were non-sinusoidal. Peak vertical accelerations of the platform ranged from 1.0 to 6.5 g depending on the amplitude and frequency settings. The axial skeleton RMS measurements were strongly related to the knee flexion angle (Fig. 1); knee flexion angles less than 30 degrees were associated with increased skeletal accelerations (due to increased transmissibility).

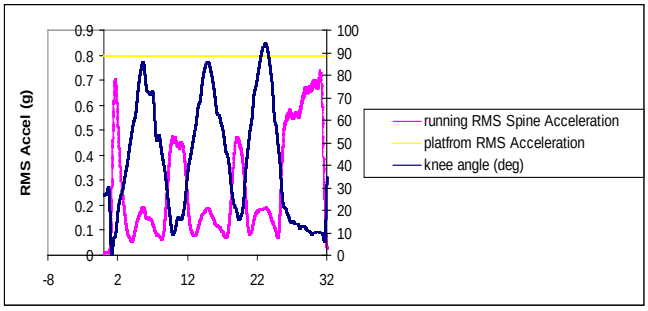

Figure 1. RMS acceleration measured at the spine and platform (left axis), and knee joint angle (degrees: right axis) during dynamic squat trials.

DISCUSSION AND CONCLUSIONS

The transfer functions illustrated that the body is a nonlinear system (data not presented here). The skeletal acceleration amplitudes showed that the axial skeleton is exposed to large amounts of mechanical energy; full knee extension should be avoided. Failure of lower extremity muscles and soft tissue to adequately absorb mechanical energy may lead to excessive energy storage and subsequent injury to the passive structures.

More research is needed to develop guidelines for safe use of vibrating platforms and to explore the long term health effects that may be caused by whole body vibration through the feet.

REFERENCES

[1] Hazell, T., Jakobi, J., Kenno, K. (2007). "The effects of Whole Body Vibration on Upper-and Lower-Body EMG during static and dynamic contractions". *Applied Physiology Nutrtrition and Metabolism*, 32, pp. 1156- 1163.
[2] Kitazaki, S., and Griffin, M.J. (1995). "A Data Correction Method for Surface Measurement of Vibration on the Human Body," *J. of Biomechanics*, Vol. 28, No. 7, pp. 885-890.
[3] Mester, J., Kleinoder, H., Yue, Z. (2006). "Vibration Training: Benefits and Risks". *J. of Biomechanics*, 39, pp. 1056-1065.
[4] Randall, J.M., Matthews, R.T., and Stiles, M.A. (1997). "Resonant Frequencies of Standing Humans," *Ergonomics*, Vol. 40, No. 9, 879-886.

Address correspondence to Robert Caryn, rcaryn@uwo.ca

TRI-AXIAL ACCELEROMETERS FOR THE MEASUREMENT OF LUMBAR SPINE AND PELVIC ANGLES

Diana E. De Carvalho, Jack P. Callaghan
Department of Kinesiology, University of Waterloo, Waterloo, Canada, ddecarva@uwaterloo.ca

INTRODUCTION

The accurate estimation of lumbar curvature during functional tasks is necessary to gain a better understanding of low back injury mechanisms and physical exposures. External measures of the lumbar lordosis are preferable over invasive imaging procedures for reasons of harmful exposures and functionality, however, to date they have been found to have varying levels of accuracy [1, 2]. This study compares the measurement of lumbar and pelvic angles by tri-axial accelerometers to those calculated from radiographs in standing and seated postures.

METHODS

Eight male subjects, recruited from a student population, were instrumented with two tri-axial accelerometers fixed to the skin over the spinous processes of L1 and S1. They were then radiographed in 4 postures: standing, sitting in an automobile seat with 0% lumbar support prominence (LSP), 50% LSP and 100% LSP. A foot switch controlled by the radiology technician triggered the collection of a 20s accelerometer trial during the radiographic exposure. Accelerometer data were processed using custom written software and measures of lumbar angle and pelvic tilt were calculated. Radiographic measures of lumbar lordosis and sacral tilt were completed from the plain film digitally converted radiographs. A 2-way ANOVA (posture by measurement technique) with a level of significance $p \leq 0.05$ was conducted. Fisher's Least Significant Difference post hoc test was used on all significant main effects. Pearson's Correlation Coefficients were calculated for the two methods of measurement.

RESULTS

Lumbar angles, measured by accelerometer, were significantly less than the lumbar lordosis angles measured from the radiographs ($p<0.001$, Figure 1). The average difference between lumbar measures was 33º (+/- 13º). Despite the differences between these measures they were found to be strongly correlated ($r = 0.80301$). Pelvic angle was not significantly different between accelerometer and radiograph measures ($p = 0.4238$, Figure 1), however, a significant interaction was found for the measures between standing and sitting ($p < 0.001$). The average difference between pelvic measures was 28º (+/- 19º). The pelvic angles for each measurement method were strongly negatively correlated ($r = -0.9517$).

DISCUSSION AND CONCLUSIONS

The results of this study suggest that measurement of the lumbar angle by tri-axial accelerometers in standing and sitting accurately reflect true lumbar spine motion. The triangular shape of the sacrum likely is the cause of the negative correlation between pelvic measures. Despite both angles being taken with respect to the vertical, the lines follow quite different parts of the sacrum. The radiographic measure is taken from the posterior aspect of the sacral vertebral bodies which is typically angled anteriorly while the accelerometer mounted over the spinous process senses a posterior rotation in the same position. The interaction of measurement with the standing and seated position could be a result of skin movement and soft tissue contour differences between standing and sitting. Further work will develop a regression model that can be used to adjust accelerometer measures of spine curvature in future studies.

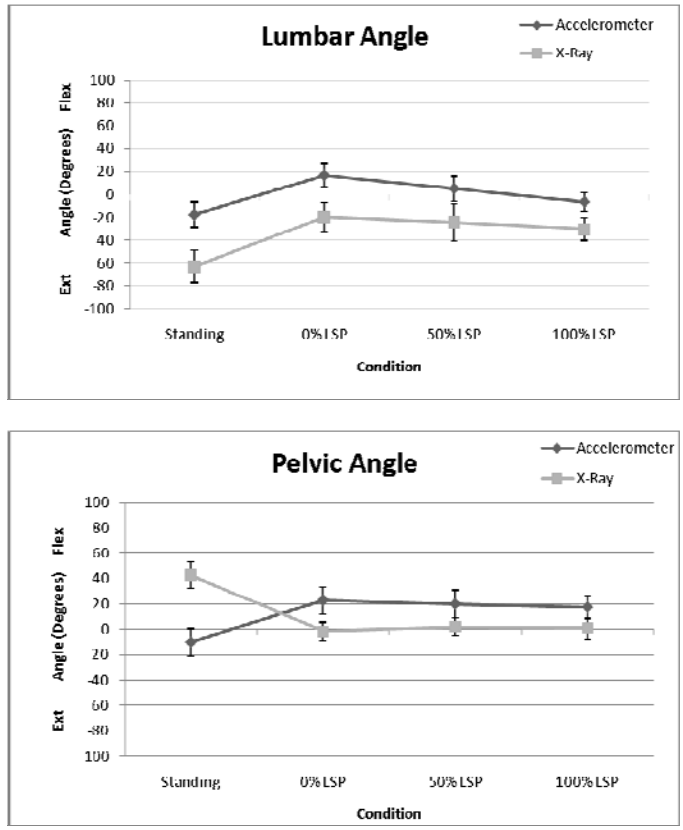

Figure 1: Angles measured by accelerometer and x-ray.

REFERENCES

[1] Harrison et al. (2005). JMPT **28**; p. 597-603.
[2] Hansson et al. (2001). Med Biol Eng Comp **39**; p.405-413.

ACKNOWLEDGEMENTS

AUTO21, CIHR, FCER and Schukra of North America

DEVELOPMENT OF A SYSTEM FOR MOBILE 3D RECONSTRUCTION.

Emílio Cipolli[12], Tamotsu Hirata[1]
[1]UNESP, Guaratinguetá, Brasil, eac.cipolli@santanna.br
[2] UNISANT'ANNA, São Paulo, Brasil.

INTRODUCTION

Most of the time the sports movements are performed at great distances, but the 3D reconstruction systems are limited to actual filming of a small sample of the actual distance traveled (LAFONTAINE and LAMONTAGNE, 2000). Some procedures developed can capture most of the movements performed in sports, such as panning the camera (YU, 1993), but still requires extensive calibration and large field of view, which can lead the evaluator to establish measures to lower accuracy (Allard, Stokes and BIANCHI, 1995). The mobile capture system (moving camera) is an alternative to more traditional approaches, where the dimensions of the field of view of the image remain constant and the athlete's movements are tracked throughout their length. This study aims to verify the accuracy and precision of the kinematic measures of a mobile system for 3D reconstruction.

METHODS

The test was conducted inside a room in which it was built a trail through PVC pipes with 3m long. Were used for image capture two cameras, 1m away from each other, apart 4m the calibration object, with capture rates of 30Hz and set the car that ran on the track (Fig. 1). The cameras were positioned so as to fit any object calibration built with plumb lines of dimensions 1.5 m x 1.4 m x 0,75 m and 54 control points. It was used for calibration only 1 frame of the original used as a reference in all positions in the pair of cameras was moving, even outside the area calibration. The object with known dimensions was moved alongside the cameras at the same speed of cameras. After shooting the images were captured and stored on computer. Was used for manual tracking of markers and reconstruction of the coordinates of object software Dvideow (CAMPOS et al, 2005). 30 frames were reconstructed. The array of coordinates were exported to MATLAB software that through a function held data processing.

RESULTS

The percentage difference (% diff) between the actual measurement and was rebuilt about 5%, the percentage indicated as acceptable limit (LAFONTAINE and LAMONTAGNE, 2000). The results reached values between 1.47% - 5.49%. (Table 1).

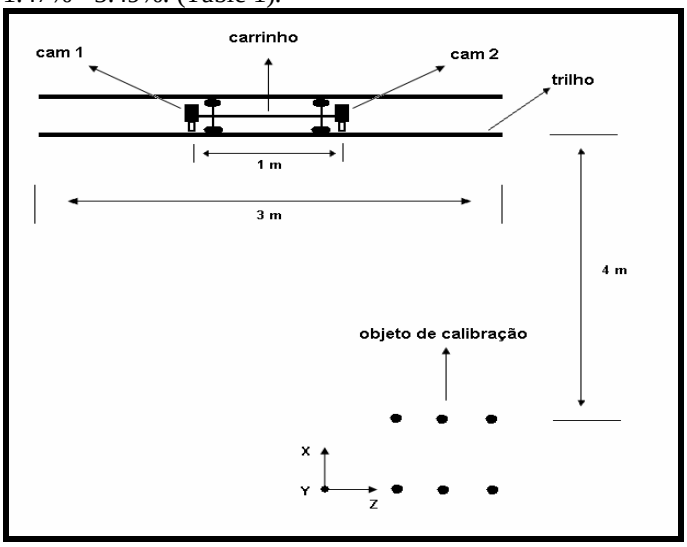

Figure 1: representative scheme of the cart and shooting rail.

DISCUSSION AND CONCLUSIONS

The data proved satisfactory for measuring kinematic variables with camera in motion, but more studies need to be done to improve the system and for future applications in the sport.

REFERENCES

ALLARD, P., STOKES, I.A., & BIANCHI, J.P. Three-dimensional analysis of human movement. Human Kinetics, 1995.

CAMPOS, M. H. ; MENEZES, R. P. ; SILVATTI, A. P. ; MARINHO, P. C. ; CIPOLLI, E. A. C. ; BARROS, R. M. L. . Análise cinemática tridimensional da fase submersa do nado crawl. Revista brasileira de ciência e movimento, Londrina/ Maringá - PR, v. 13, n. 4, p. 85, 2005.

LAFONTAINE, D., LAMONTAGNE, M. Development and validation of a mobile video capture system for spatial kinematics. Archives of Physiology and Biochemistry, 108, 99, 2000.

YU, B. A Panning DLT procedure for tree-dimensional videography. Journal Biomechanics, 741-751, 1993.

Table 1: Data reconstruction of the object for 30 frames.

Distances Sides of the object	Dimension Real (cm)	Reconstructed (cm)	Absolute Difference RMS (cm)	Difference (%) RMS (%)
1	24,0	25,02	1,31	5,49
2	45,0	44,89	0,66	1,47
3	50,0	51,35	1,47	2,94

A MODEL OF THE EXTRA-CELLULAR MATRIX OF ARTICULAR CARTILAGE

Malika Bongué Boma[1], Marcelo Epstein[1], Salvatore Federico[1,*]
[1]Department of Mechanical and Manufacturing Engineering, The University of Calgary, Calgary, Canada
* salvatore.federico@ucalgary.ca

INTRODUCTION

The extra-cellular matrix of articular cartilage is a gel-like material constituted of a proteoglycan meshwork saturated by a fluid, and is responsible for most of the resistance of cartilage to compression. The aim of this work is to propose a model describing the electro-mechanical interactions between the negatively charged lateral chains of the proteoglycans, PGs (the glycosaminoglycans, GAGs), and the positively charged electrolytes dissolved in the fluid. We take inspiration from Poisson-Boltzmann models [1] and consider the GAGs as freely floating in the fluid (thus neglecting that they are attached to the protein backbone of the proteoglycans). We do not describe the pre-stresses applied by the collagen fibres.

METHODS

We recall to principles of theories of generalized continua [2] and suppose that cartilage forms a continuum of material elements including one cylindrical GAG and a surrounding variable volume of water. We thence examine two different scales: a macroscopic one (when the global properties of the tissue are considered), and a microscopic one (when one GAG is observed).

We assume that the evolution of each material element is fully determined by the macroscopic gradient of transformation denoted **F**, and we suppose that mass and energy must be the same whether we use the micro- or the macroscopic descriptions. The latter assumption will allow us to express the constitutive assumptions of the model in terms of variables describing the microstructure of the GAGs matrix.

RESULTS

The balance equations of the model read

$$\operatorname{div}\mathbf{B} + \rho\mathbf{b} = \mathbf{0}\,, \tag{1}$$

where **B** is a symmetric stress tensor, **b** is the external body force per unit mass, and ρ is the apparent mass density of the continuum. If ω denotes the domain occupied by one material element, the relations between masses and energies calculated from both macro and microscopic descriptions read

$$\rho = \alpha\,\rho_{GAG} + (1-\alpha)\rho_{Liq}\,, \tag{2}$$

$$\mathbf{B}\cdot[\dot{\mathbf{F}}\mathbf{F}^{-1}] = -\upsilon\left[\frac{\partial}{\partial\mathbf{F}}\int_{\omega} e_E\right]\mathbf{F}^T\cdot[\dot{\mathbf{F}}\mathbf{F}^{-1}]\,, \tag{3}$$

where υ and α are the number density and solid fraction of the GAG, respectively, and e_E is the electrostatic energy of one material element, per unit volume. The integral of e_E over ω gives the total energy accumulated by one material element; it is a function of the orientation and charge density of the GAG, of the composition of the interstitial solution, and of υ and α.

The identification term by term of equation (3) leads to the final constitutive equation

$$\mathbf{B} = -\upsilon\left[\frac{\partial}{\partial\mathbf{F}}\int_{\omega} e_E\right]\mathbf{F}^T\,. \tag{4}$$

We tested the model on the confined compression of a typical homogeneous network of chondroitin sulfate GAGs consisting of 43 disaccharide units [3], and characterized by a GAG radius 0.55 nm, an intercharge space 0.64 nm, and an inter-GAG spacing 6.5 nm; Figure 1 shows the evolution of the normal stress for increasing values of stretch λ.

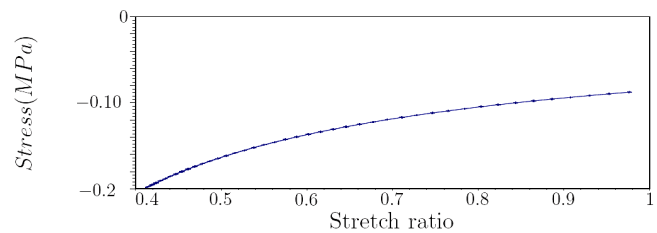

Figure 1: Stress-stretch curve obtained from the model.

DISCUSSION AND CONCLUSIONS

Numerical results are similar to the typical stress-stretch curves available in the literature [4]: the stresses are in the same order of magnitude, and variations of the material stiffness are well represented (note that we did not recall any fitting parameter). The stress is not null in the undeformed configuration (stretch $\lambda = 1$): indeed, the present model depicts the evolution of the GAGs matrix, without taking into account the action of the collagen fibres which are supposed to balance the repulsive forces created by the GAGs by undergoing tension. Further steps in this research will be the inclusion of the PG backbone protein linking the GAGs and the fibres.

REFERENCES

[1] Buschmann M.D. and Grodizinsky, A.J. (1995). A molecular model of proteoglycan-associated electrostatic forces in cartilage mechanics. *J. Biomech. Eng*. Vol. **117**; p. 179-192.
[2] Capriz G. *Continua with Microstructure;* Springer, 1998.
[3] Quinn T. M. et al. (2001). Glycosaminoglycan network geometry may contribute to anisotropic hydraulic permeability in cartilage under compression. *J. Biomech.* Vol. **34**(11); p. 1483-1490.
[4] Huang C.Y. et al (2005). Anisotropy, inhomogeneity, and tension compression nonlinearity of human glenohumeral cartilage in finite deformation. *J. Biomech.* Vol. **38**; p. 799-809.

ACKNOWLEDGEMENTS

The AIF New Faculty Programme (Alberta Ingenuity Fund, Canada), the NSERC Discovery Programme (Natural Sciences and Engineering Research Council of Canada)

NON-LINEAR MODEL FOR COMPRESSION TESTS ON ARTICULAR CARTILAGE

Salvatore Federico[1,*], Alfio Grillo[2], Amr Guaily[1]
[1]Department of Mechanical and Manufacturing Engineering, The University of Calgary, Canada
[2]G-CSC Goethe-Universität Frankfurt am Main, Germany
* salvatore.federico@ucalgary.ca

INTRODUCTION

Based on the linear biphasic model of articular cartilage [4], Armstrong et al. [1] derived an analytical solution for the unconfined compression test. In this work, based on the large-strain governing equations of a biphasic mixture (e.g., [2]) and on Ogden's [5] solution for monophasic unconfined compression, propose a solution to the differential equations of unconfined compression problem with isotropic homogeneous non-linear elasticity [4] and deformation dependent permeability, and, after removing the hypothesis of homogeneity to the confined compression.

SPATIAL BALANCE EQUATIONS

For a biphasic mixture of incompressible solid and fluid, the true mass densities ρ_T^s and ρ_T^s remain constant during the motion, and the role of the apparent mass densities ρ^s and ρ^f is played by the volumetric fractions $\phi^s = \rho^s / \rho_T^s$ and $\phi^f = \rho^f / \rho_T^f$, obeying the saturation condition $\phi^s + \phi^f = 1$. If $\boldsymbol{v}^s$ and $\boldsymbol{v}^f$ are the velocities of solid and fluid, the balance of mass (continuity equation) of the mixture reads

$$\operatorname{div}(\phi^s \boldsymbol{v}^s + \phi^f \boldsymbol{v}^f) = 0 . \qquad (1)$$

The Cauchy stresses in the solid, fluid and whole mixture are

$$\begin{aligned} \boldsymbol{\sigma}^s &= -\phi^s p \boldsymbol{i} + \boldsymbol{\sigma}^{el}, \\ \boldsymbol{\sigma}^f &= -\phi^f p \boldsymbol{i}, \\ \boldsymbol{\sigma} &= -p \boldsymbol{i} + \boldsymbol{\sigma}^{el}, \end{aligned} \qquad (2)$$

where p is the fluid pressure, $\boldsymbol{i}$ the identity tensor, $\boldsymbol{\sigma}^{el}$ the elastic stress. Neglecting inertia and external volume forces, the balance of momentum in the solid, fluid and mixture is

$$\begin{aligned} \operatorname{div} \boldsymbol{\sigma}^s &= -\phi^f \boldsymbol{k}^{-1} \boldsymbol{w} + p \operatorname{grad} \phi^s, \\ \operatorname{div} \boldsymbol{\sigma}^f &= \phi^f \boldsymbol{k}^{-1} \boldsymbol{w} - p \operatorname{grad} \phi^s, \\ \operatorname{div} \boldsymbol{\sigma} &= 0, \end{aligned} \qquad (3)$$

where $\phi^f \boldsymbol{k}^{-1} \boldsymbol{w}$ is the dissipative part of the drag force, depending on the permeability $\boldsymbol{k}$ and the filtration velocity $\boldsymbol{w}$, according to Darcy's law

$$\boldsymbol{w} = -\boldsymbol{k} \operatorname{grad} p , \qquad (4)$$

and $-p \operatorname{grad} \phi^s$ is the conservative part of the drag force. Combination of Eqs. (1) to (4) yields the spatial equations

$$\operatorname{div} \boldsymbol{v}^s = \operatorname{div}(\boldsymbol{k} \operatorname{grad} p) , \qquad (5)$$

$$\operatorname{div} \boldsymbol{\sigma}^{el} = \operatorname{grad} p . \qquad (6)$$

MATERIAL BALANCE EQUATIONS

If χ is the configuration map of the solid, $\boldsymbol{F}$ is the deformation gradient ($F_{iI} = \chi_{i,I}$) and $J = \det \boldsymbol{F}$, the material balance equations read, after some manipulation,

$$\dot{J} = \operatorname{Div}(J \boldsymbol{K} \operatorname{Grad} p) , \qquad (7)$$

$$\operatorname{Div} \boldsymbol{P}^{el} = J \boldsymbol{F}^{-T} \operatorname{Grad} p , \qquad (8)$$

where $\boldsymbol{K} = \boldsymbol{F}^{-1} \boldsymbol{k} \boldsymbol{F}^{-T}$ is the material permeability, $\boldsymbol{P}^{el} = J \boldsymbol{\sigma}^{el} \boldsymbol{F}^{-T}$ is the first Piola-Kirchhoff elastic stress, Div and Grad are the material divergence and gradient operators. Equations (7) and (8) constitute a system of 4 scalar equations in the 13 scalar unknowns χ_i, P_{iI}^{el}, p.

CONSTITUTIVE EQUATIONS, CONSTRAINTS

The closure of the differential system given by Eqs. (7) and (8) is obtained by adding the 9 hyperelastic constitutive equations for $\boldsymbol{P}^{el}$, conveniently expressed in terms of Biot stress $\boldsymbol{T}^{el}$ [5],

$$\boldsymbol{P}^{el} = \boldsymbol{R} \boldsymbol{T}^{el} = \boldsymbol{R} \left(\partial W / \partial \boldsymbol{U} \right) , \qquad (9)$$

where $\boldsymbol{U}$ is the right Cauchy stretch tensor (from the polar decomposition $\boldsymbol{F} = \boldsymbol{R} \boldsymbol{U}$). Because of the incompressibility of both phases, the system is subjected to the unilateral constraint

$$J - \phi_{ref}^s \geq 0 , \qquad (10)$$

where $\phi_{ref}^s = J \phi^s$ is the referential solid volumetric fraction.

DISCUSSION

The system obtained from Eqs. (7), (8) and (9), with the constraint (10), reduces to that of Armstrong et al. [1] for the case of small displacements, and therefore is its generalisation. It enables us to study problems with simple geometry, such as unconfined compression of isotropic homogeneous samples and confined compression of inhomogeneous samples, based on non-linear cartilage models, such as that proposed by Holmes and Mow [3].

REFERENCES

[1] Armstrong, C.G., et al. (1984), An Analysis of the Unconfined Compression of Articular Cartilage. *J. Biomech. Eng.*, Vol. **106**, p. 165-173.
[2] Grillo, A. et al. (2009), Evolution of a Fibre-Reinforced Growing Mixture, *Nuovo Cimento C*, Vol **32C**, p. 97-119.
[3] Holmes, M.H. and Mow, V.C. (1990), The Non-linear Characteristics of Soft Gels and Hydrated Connective Tissues in Ultrafiltration, *J. Biomech.*, Vol. **23**, p. 1145-1156.
[4] Mow, V.C., et al. (1980), Biphasic Creep and Stress Relaxation of Articular Cartilage, Theory and Experiment, *J. Biomech.*, Vol. **102**, p. 73-84.
[5] Ogden, R.W. (1984), *Non-Linear Elastic Deformations*, Dover Publications Inc., Mineola, New York, USA.

ACKNOWLEDGEMENTS

The Alberta Ingenuity New Faculty Programme the NSERC Discovery Programme.

Investigation of the Compliance Mismatch and Wall Shear Stress Distribution effects on Graft Failure Initiation in a distal end-to-side femoral bypass graft anastomosis

Mostafa Toloui
School of Mechanical Engineering, Sharif University of Technology, Tehran, Iran, m_toloui@mech.sharif.ir

INTRODUCTION

To overcome blockage in femoral artery, bypass surgery may be undertaken to bypass the blockage and return blood to the limb, either using a vein from the person or a synthetic graft. However, these grafts have a tendency for restenosis.
The development of IH in bypass grafts depends on several factors such as injury, hemodynamics, and graft-artery compliance mismatch [1]. There are a number of different theories which suggest how disease develops due to hemodynamics [2,3], however, what is common is that abnormal hemodynamic conditions and Material mismatch are causing the disease [4,5].
In the present work, the influence of three rheology models (i.e., Newtonian, power law and Carreau-Yasuda) are investigated to represent the shear rate dependence of blood viscosity and clarify the role of WSS in the formation of intimal hyperplasia (IH) in a distal end-to-end femoral bypass graft, by the use of Computational Fluid Dynamics (CFD) technique. That is, the objective of present research is to investigate the effect of the various constitutive equations representing blood on the wall shear stress distribution along the bed of the distal end-to-side vascular bypass graft anastomosis. Further, FSI (Fluid-Solid Interaction) analysis was used to investigate the effect of material mismatch on IH in a distal end-to-end femoral bypass graft.

METHODS

The distal end-to-side anastomosis ideal model was used as the simulations geometry. In this model (Figure 1), two rigid, straight, cylindrical tubes of constant diameter 6mm intersecting with an anastomotic angle of 45°.
Steady, Pulsatile & FSI simulations: a parabolic velocity profile was prescribed as the axial inlet velocity in the inlet, and Neuman boundary condition was applied to DOS and no-slip to the walls. The POS was assumed to be fully occluded.

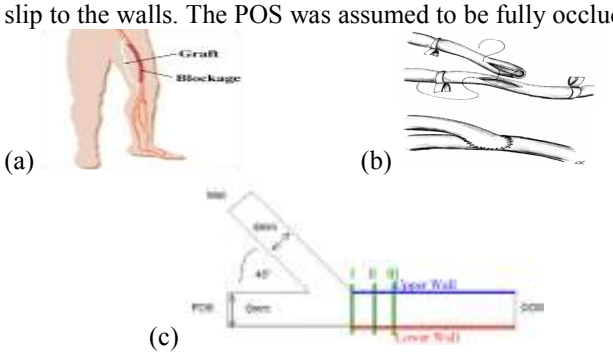

Figure 1: (a) Schematic position on femoral bypass graft **(b)** ypical arterial bypass graft and **(c)** an ideal geometry of femoral bypass graft s end-to-side anastomosis.

CSS modeling: By the use of our FVM modeling's results, a spatially uniform luminal pressure waveform of femoral artery is applied onto the inner walls of the graft and host arteries which have different Young modulus.

RESULTS

The areas most prone to intimal hyperplasia are the toe, heel and bed of the distal anastomosis, as shown in *Figure 3*.

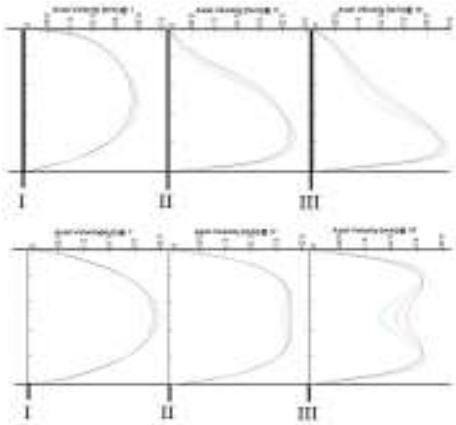

Figure3 : Velocity profiles at three different positions in (a) the symmetry plane and (b) the perpendicular to this plane in the host artery(-Carreau-Yasuda, - Power-Law, Newtonian)

DISCUSSION AND CONCLUSIONS

Present study's results show that IH at the heel, toe and suture line can be attributed to compliance mismatch between the graft material and host artery. That at the bed is attributed to local abnormal hemodynamics or more specifically abnormal wall shear stress (WSS) distribution. That is, both of these factors are playing the important roles in IH, although WSS has more significant and critical role.
Further, FSI simulations showed that , WSS shows a great sensitivity to the arterial wall's stiffness. Stiffening of the arterial wall occurs in diseased arteries or by aging, and it can cause a great decrease in blood flow rate

REFERENCES

[1] Eleyas Shaik, Klaus A. Hoffmann, Jean-Francois Dietiker, Numerical Simulations of Pulsatile Non-Newtonian Flow in an End-to-Side Anastomosis Model, Journal of Simulation Modeling Practices and Theory, 2008.
[2] Hayashi K, Yanai Y, Naiki T. A 3D LDA study of the relation between WSS and intimal hyperplasia in a human aortic bifurcation. J Biomech Eng 1996;118:273–9.
[3] Hazel AL, Pedley TJ. Alteration of mean wall shear stress near an oscillating stagnation point. J Biomech Eng 1998;120:227–37.
[4] O'Brien T, Walsh M, McGloughlin T. On reducing abnormal hemodynamics in the femoral end-to-side anastomosis: the influence of mechanical factors. Ann Biomed Eng 2005;33(3):309–21.
[5] Ballyk PD, Walsh C, Butany J, Ojha M. Compliance mismatch may promote graft-artery intimal hyperplasia by altering suture-line stresses. J Biomech 1998;31:229–37.

Deformation and Fluid Pressure Analysis of Knee Cartilages In-situ

Gu, K B and Li, L P

Department of Mechanical and Manufacturing Engineering, University of Calgary, Alberta, Canada
LePing.Li@ucalgary.ca

INTRODUCTION

The load response of a knee joint is predominantly determined by the mechanics of articular cartilage and meniscus, which consist of proteoglycan matrix, collagen fibre network and a fluid. The interplay of the three constituents has been investigated using tissue explants in confined, unconfined, indentation and tensile testing geometries. The mechanics of cartilage in real knee contact geometries, however, has only been modeled as elastic [1, 2]. The fluid flow and collagen fibre orientation were not considered in computational knee modeling. The objective of this study was to determine the influence of collagen network on the deformation and fluid pressure in intact cartilages with real knee contact geometry.

METHODS

The solid model of a right knee was constructed from the MRI data of a healthy male, which consists of tibia, distal femur, menisci, femoral and tibial cartilages. Our focus for this study was the femoral cartilage (Fig. 1), because of the available measurement for the fibre orientation [3]. The finite element model contains a total of 88,096 elements. The cartilages and menisci were meshed in ABAQUS with C3D20P element; they were modeled as fibre-reinforced fluid-saturated materials using a user-defined procedure, UMAT in ABAQUS [4]. Collagen fibres in menisci were aligned in radial and circumferential directions, while fibre orientations in articular cartilage were assumed to follow the split-line pattern [3]. Because of their greater stiffness as compared with other tissues, the bones were considered as linearly elastic.

The interactions between the cartilaginous tissues were defined as surface-to-surface contacts, which allow low frictional sliding between the surfaces, as formulated in ABAQUS. The ends of menisci were assumed to be fixed to the tibia using the TIE option in ABAQUS.

RESULTS

A relaxation loading protocol was used to gain insight of the mechanics before physiological loadings are considered. A compression of 100μm was applied in 1s on the top of the distal femur while the bottom of the tibia was fixed; the compression was then held unchanged.

The surface displacement of the cartilages exhibited a complex pattern that was not only determined by the surface and boundary geometries, but also by the collagen network (not shown). This pattern was time-dependent in nature. The complex displacement pattern may also be associated with the complicated shearing patterns in the cartilage, a consequence of the complex contact geometry and site-specific fibre orientations.

The fluid pressure distribution demonstrated the effects of the multiple contacts in the knee joint (Fig. 1). The maximum fluid pressure was approximately 0.2MPa with the small compression applied. It occurred at 9s after the unset of relaxation (Fig.1). The pattern of fluid pressure was different when fibres were absent (not shown). The fibre orientation also affect the fuild pressure distribution (not shown).

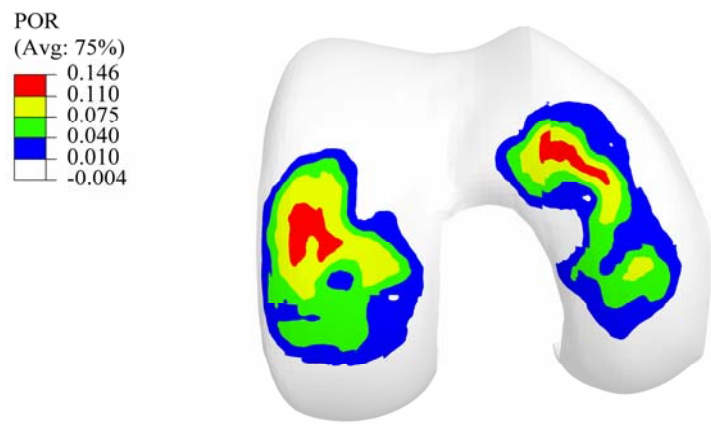

Figure 1 Pore fluid pressure in the femoral cartilage at the depth of 0.75mm from articular surface (inferior view).

DISCUSSION

The deformation and fluid pressure for cartilage in the knee joint contact geometry is obviously highly non-uniform, exhibiting a complex fluid flow pattern. The preliminary results also indicated that the collagen network changed the patterns and magnitudes of tissue deformation and fluid pressure in the knee cartilage. The site-specific collagen orientation may play an important role of improving the joint load bearing. The current case was limited to small deformation and small inter-articular sliding to avoid difficulties in obtaining numerical solutions. Large deformation and large sliding will be considered later. Physiological loadings should also be used in further studies.

REFERENCES

[1] Bendjaballah MZ +, 1995, *Knee* **2**, 69.
[2] Li G +, 1999, *J Biomech Eng* **121**, 657.
[3] Below S +, 2002, *J Arthrosc Relat Surg* **18**, 613.
[4] Li LP +, 2009, *Med Biol Eng Comput* **47**, 607.

ACKNOWLEDGEMENTS: NSERC and CIHR.

THEORETICAL SIMULATION OF SPONGY BONE REMODELING UNDER OVERLOAD USING A SEMI-MECHANISTIC BONE REMODELING THEORY

Xianjie Li[1], Gholamreza Rouhi[2]

[1, 2]Department of Mechanical Engineering, University of Ottawa, Canada

INTORDUCTION

Bone adapts to mechanical loads through bone remodeling process which includes bone resorption and subsequent bone formation, carried out by basic multi-cellular units (BMUs). Osteoclast resorption is activated at the bone surface where inhibitive osteocyte signals no longer reach [1]. This can occur not only when external loads are reduced, but also when the osteocytic network is blocked because of overloading microdamage [2,3]. Many mathematical models have been proposed to describe bone remodeling process, but very few attempts were made to study bone resorption due to overload. In this study, we proposed a mathematical model for overloaded bone resorption and simulated overload resorption in spongy bone using a semi-mechanistic bone remodeling theory [4,5]. Two- and three-dimensional computer models are used to simulate spongy bone remodeling.

METHODS

The mathematical expression of semi-mechanistic bone remodeling theory is:

$$\frac{dm(x,t)}{dt} = \frac{dm_{ob}(x,t)}{dt} - \frac{dm_{oc}(x,t)}{dt} \quad (1)$$

where $dm_{ob}(x,t)/dt$ and $dm_{oc}(x,t)/dt$ are local change of relative bone density (m) caused by osteoblasts, bone forming cells, and osteoclasts, bone resorbing cells, respectively.

The second term in Eq.1 can be expressed as follows:

$$\frac{dm_{oc}(x,t)}{dt} = r_{oc} \quad (2)$$

where r_{oc} is the amount of resorption at the bone surface caused by stochastic osteoclastic activation. Huiskes et al.'s model includes a probability $p(x,t)$ of osteoclastic resorption, in which $p(x,t)$ caused by microcracks was considered spatially random and selected to be 10% [4].

It is assumed here that microdamage caused by overloading was performed when external loads exceed a critical value [6]. Since experimental results found a positive quadratic relationship between microdamage and local strain energy density [7], we hypothesize that resorption probability, $p(x,t)$, caused by overloading is a quadratic function of total remodeling stimulus ($P(x,t)$) [5]. Thus, the overload resorption probability can be stated as follows:

$$p(x,t)=a[P(x,t)]^2+b \quad (3)$$

where a and b are empirical constants.

RESULTS

There are three computer simulations (see Fig.1). In the 1st simulation (process A, Fig. 1), a trabecular-like structure was resulted from an initial configuration when external load was 2MPa. In the 2nd simulation (process B, Fig. 1), trabeculae became thicker when the magnitude of external loads was increased by 20%. In the 3rd simulation (process C, Fig. 1), trabeculae became much thinner than that in A when external load exceeded a critical value, 6 MPa in this study. Thus, when spongy bone is under extremely large load, due to excessive resorption, its relative density would decrease substantially.

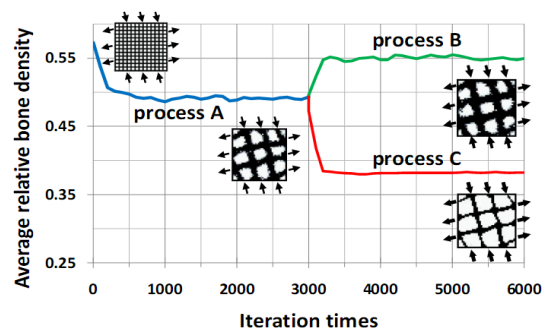

Figure 1: Alteration of average relative bone density during bone remodeling process

DISCUSSION AND CONCLUSIONS

The model proposed in this study can simulate remodeling process in spongy bone. Results of this current study show that when bone is under extreme external load, there will be a considerable reduction in spongy bone density; and this is in agreement with some other researcher (e.g. with [8]). Based on the hypothesis presented here, a 3D computer model of spongy bone is also built and our investigation is in process.

REFERENCES

[1] Burger EH et al. (1999). *The FASEB J* **13**; 101-112.
[2] Tanck E et al. (2006). *J Biomech* **39**; 2631-2637.
[3] Martin RB (2003). *Calcified Tissue Int.* **73**(2); 101-107.
[4] Huiskes R et al. (2000). *Nature* **405**; 704-706.
[5] Vahdati A and Rouhi G (2009). *Mech. Res. Comm.* **36**(3); 284-293.
[6] Rouhi G et al. (2006). *Int. J Eng Sci.* **44**(7); 456-469.
[7] Nagaraja S et al. (2005). *J Biomech.***38**; 707-716.
[8] Li J et al. (2007). *Dental Materials* **23**; 1073-1078.

NECK MOTION DUE TO THE HALO-VEST IN PRONE AND SUPINE POSITIONS

Paul C. Ivancic[1] and Connor J. Telles [1]
[1]Biomechanics Research Laboratory, Department of Orthopaedics and Rehabilitation,
Yale University School of Medicine, New Haven, CT, USA; email: paul.ivancic@yale.edu

INTRODUCTION

The halo-vest orthosis, introduced in 1959 to treat scoliosis or neck muscle paralysis, has been used since then to treat a variety of cervical spine injuries including Jefferson, odontoid, facet, and compression fractures. Previous clinical studies have suggested snaking motion due to the halo-vest during activities of daily living may lead to inadequate healing or nonunion. Snaking motion is defined as rotation in opposing directions throughout the cervical spine. The objectives of this study were to evaluate motion of the injured cervical spine with normal halo-vest application and vest loose in the prone and supine positions.

METHODS

The halo-vest was applied to a Human Model of the Neck (HUMON), which consisted of a cervical spine specimen (n=4) mounted to the torso of an anthropometric test dummy and carrying a surrogate head (**Fig. 1**). HUMON was transitioned from prone, to upright, to supine with the halo-vest applied normally and with the vest loose. Average peak spinal motions were computed in the prone and supine positions and contrasted with the physiologic rotation range, obtained from the intact flexibility test, and statistically compared ($P<0.05$) between normal halo-vest application and vest loose.

Fig. 1. Photograph of the Human Model of the Neck (HUMON) with the halo-vest. Motion tracking flags were fixed to the head, cervical vertebrae, and pelvis.

RESULTS

Snaking motion of the neck was observed in the prone and supine positions, consisting of extension at head/C1 and C1/2 and flexion at the inferior spinal levels (**Fig. 2**). The largest peak motions were generally observed in the prone position. The intervertebral rotation peaks generally exceeded the physiologic range throughout the cervical spine due to the loose vest in the prone position. Significant increases in the extension peaks at head/C1 (16.9° vs. 5.7°) and flexion peaks at C4/5 (6.9° vs. 3.6°) and C7/T1 (5.2° vs. 0.7°) were observed in the prone position due to the loose vest, as compared to normal halo-vest application. Average peak head/T1 rotation remained within the physiologic limit however the loose vest caused significantly greater head/T1 anterior shear and axial separation in the prone position, as compared to normal halo-vest application. Axial separation was observed at all spinal levels due to the halo-vest, consistent with tensile load that has been observed clinically in halo-vest patients.

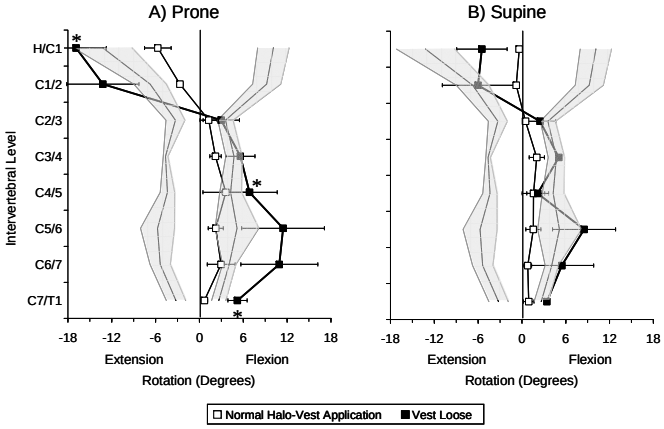

Fig. 2. Average peak rotations of spinal levels head/C1 through C7/T1 in **A**) prone and **B**) supine positions with normal halo-vest application and with the vest loose. The physiologic rotation range (average $\pm$ 1 SD) is indicated in grey shading for flexion and extension. Significant differences ($P<0.05$) in average peak motion between normal halo-vest application and vest loose are indicated with asterisks.

DISCUSSION AND CONCLUSIONS

The present results underscore the importance of proper vest fit and continued monitoring of strap tightness to reduce snaking motions of the neck in those treated with the halo-vest.

ACKNOWLEDGEMENTS

We gratefully acknowledge a gift from Ossur Americas, Aliso Viejo, CA, USA, which made this research possible.

AGE EFFECTS ON TRUNK MUSCLE ACTIVATION RESPONSES TO A SYMMETRICAL LIFT AND REPLACE TASK IN HEALTHY ADULTS

Ruth Pelleg-Kallevag[1], Heather L. Butler[1], Ed Hanada[1] and Cheryl L. Hubley-Kozey[1]
[1] Dalhousie University, Halifax, NS

INTRODUCTION

The role of abdominal and back muscles in lumbo-pelvic control of young adults is well established, however, little data exists regarding their function in older adults. A recent electromygraphic (EMG) study showed altered motor control among trunk muscle sites in older adults during an abdominal exercise [1]. To further understand aging effects on muscle responses this study examined EMG differences in abdominal and back muscles in older and younger adults performing a controlled functional task.

METHODS

Fifty-five healthy young adults (age 32±8.7; BMI=24.4±4; aerobic sessions/week=6±4.6) and 12 healthy older adults (age 68±3.5; BMI=27.2±3.5; aerobic sessions/week=3.2±3) consented to participate. EMG data were collected from 24 muscle sites while subjects performed a symmetrical lift and replace task. Twenty-four pairs of surface Ag/Ag Cl electrodes (Meditrace™ Canada) were placed over left and right trunk muscle sites of: lower and upper rectus abdominus; external oblique (anterior lateral and posterior fibres); internal oblique; longissimus and iliocostalis muscles at L1 and L3 lumbar levels; multifidus and quadrates lumborum [1,2]. Three trials of a symmetrical lift and replace task were performed in normal reach position using a 2.9kg container. A FOB™ system (Ascension Technology, VT, USA) was used to monitor participants' spine and pelvic motion.

EMG signals were differentially amplified (3 AMT-8 Bortec, Calgary, Canada), digitized at 2000 Hz using Labview™ (National Instruments, Texas USA) and processed using Matlab™ software (Mathworks Inc.). An event marker system was used to divide the task into 3 phases (lift, transition, and replace). Nine standardized maximal voluntary isometric contractions (MVICs) were performed for normalization [1,2]. Root mean square amplitudes were calculated for each of the phases and total task, and normalized to the highest amplitude recorded over a 500ms window from the MVIC. Pattern recognition techniques were applied to activation amplitude patterns (discrete amplitudes of 24 muscle sites) [2], and principal patterns (PPi) and *scores* were calculated. PP *scores* that explained over 95% of the variability in the measured amplitude patterns were entered input to repeated measures ANOVA models to determine significant effects and interactions. Bonferonni post hoc corrections were done on all significant effects ($p<0.05$).

RESULTS

Four PPs explained 95% of the variance. PP1 captured the overall magnitude of the amplitude patterns. PP2 featured co-activation between abdominal and back muscles (Figure 1), whereas PP4 featured a more specific co-activation strategy between the internal oblique and L1 muscle sites. PP3 captured an asymmetric response between left and right muscle sites (Figure 2). For PP1, 2 and 4, significant group by phase interactions were found. When accounting for sex, PP3 *scores* were significant for a sex by group by phase interaction showing asymmetrical back muscle responses for older adults that were different for men and women (Figure 2).

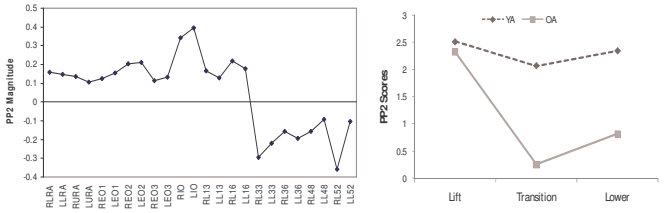

a) b)

Figure 1: a) PP2 b) group*phase interaction (p=0.007).

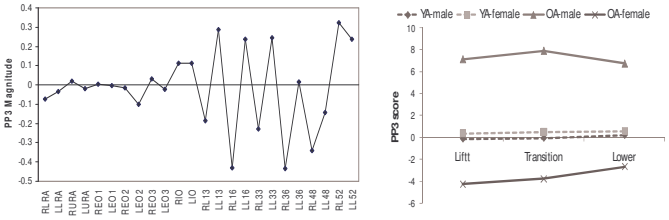

a) b)

Figure 2: a) PP3 b) group*sex*phase interaction (p=0.044).

DISCUSSION AND CONCLUSIONS

The task used in this study resembles activities that are commonly used daily. Older adults demonstrated overall higher amplitudes (PP1) and reduced co-activation strategies between abdominals and back extensors during the lowering phase of the task. The former is most likely related to strength differences whereas the latter could have implications for decreased control and possibly decreased stability. Consistent with previous reports [2] the younger adults showed no asymmetry for this bilateral task, whereas we found the older adults did (PP3). Sex differences for the older adults indicating that men had higher left compared to right amplitudes and women had higher right than left amplitudes requires further investigation. These altered neuromuscular responses for older adults and between sexes may help explain high incidence of low back pain in older adults as well as decreased function, providing information for therapeutic exercise interventions.

REFERENCES

[1] Hubley-Kozey CL et al. (2009). Differences in abdominal muscle activation patterns of younger and older adults performing an asymmetric leg-loading task. *PM&R;* 1(11).
[2] Butler HL et al.(2009). Electromyographic assessment of trunk muscle activation amplitudes during a simulated lifting task using pattern recognition techniques. *JEK*, 19 e505-e512.

ACKNOWLEDGEMENTS

M McKeon, N Hill, Nova-Scotia Health Research Foundation.

A NEW SURROGATE BONE MODEL FOR TESTING INTERVERTEBRAL DEVICES

Anthony G. Au[1], Ameet K. Aiyangar[1], Paul Anderson[2], Heidi-Lynn Ploeg[1]
[1]Department of Mechanical Engineering, University of Wisconsin-Madison, Madison, WI, USA, email: aau@cae.wisc.edu
[2]Department of Orthopaedic Surgery, University of Wisconsin-Madison, Madison, WI, USA

INTRODUCTION

Chronic low back pain is commonly treated by spinal fusion surgery augmented with intervertebral devices. Device subsidence into surrounding vertebrae is a common surgical complication and is often investigated with benchtop tests employing human cadaveric vertebrae. Polyurethane foam is recommended as a bone surrogate for subsidence tests [1], but the absence of a vertebral endplate and cortical shell limits clinical applicability of the conclusions. This can be improved by employing a new surrogate with more representative geometry and material properties, i.e. a polyurethane foam vertebra encased in a fiberglass-reinforced epoxy shell. This study investigated the efficacy of this synthetic vertebra bone surrogate for benchtop subsidence tests of intervertebral devices.

METHODS

Two sizes of custom-made aluminum-alloy implants were compressed into 10 synthetic L5 vertebrae (Sawbones, Vashon Island, WA) using a materials testing machine (858 Bionix, MTS, Eden Prairie, MN). Implants seated either centrally (smaller diameter implant) or peripherally (larger diameter implant) on the endplate were axially compressed into synthetic vertebrae at a displacement rate of 2.5 mm/min up to a displacement of 5 mm. For comparison, the same implants were similarly compressed into 10 human lumbar vertebrae and 12 polyurethane foam blocks. Failure load, subsidence, and failure mode were observed. Subsidence was measured using custom-made extensometers attached between the implant and sample.

RESULTS

Synthetic vertebrae shared several subsidence characteristics with human vertebrae: the implant severely deflected the endplate until the endplate fractured and failed, characterized by a load drop on the force-displacement curve (Fig 1); also, peripherally seated implants generated a lower subsidence than centrally placed ones (Table 1). By contrast, subsidence in foam was insensitive to placement, as were failure load and implant-foam construct stiffness.

Synthetic vertebrae required the largest forces to fail and also generated the lowest subsidence (Table 1). The synthetic vertebral endplate did not fully fail under loading by the large implant therefore no failure load was recorded.

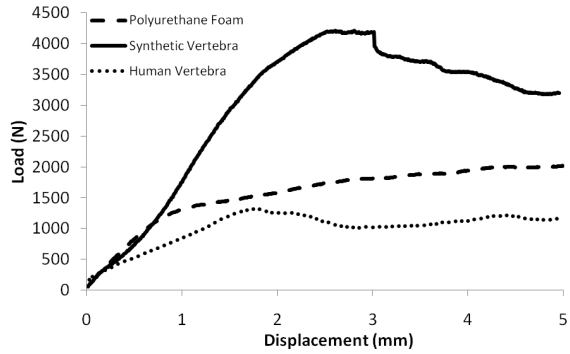

Figure 1: Load-displacement curves from centrally-placed implants.

DISCUSSION AND CONCLUSIONS

Polyurethane foam is a readily available bone surrogate for human vertebrae but its simplicity obviates extrapolation of results to clinical situations. The synthetic vertebrae of this study were more resistant to subsidence than both foam and human vertebrae. However, they replicated some key subsidence aspects observed with human vertebrae, due to the presence of an artificial endplate. The endplate shielded the foam core from localized forces thereby reducing subsidence levels. More importantly, implants seated on the edge of the vertebrae encountered lower subsidence [2].

Understanding the failure mode associated with synthetic vertebrae can foster a better understanding of subsidence. Subsidence in the synthetic vertebra can be modeled as a combination of bending and indentation commonly seen in composite materials [3]. Subsidence of the peripherally placed larger implant was dominated by bending whereas indentation was more influential in subsidence of the centrally placed smaller implant. Endplate fracture generated large subsidence but its absence did not completely eliminate it since the foam core could plastically deform without endplate fracture. This new surrogate is appropriate for benchtop subsidence testing and will help facilitate a more comprehensive understanding of subsidence etiology.

REFERENCES

[1] ASTM F 2267-04
[2] Tan J.-S. et al. (2005) *Spine* 30; 638-644.
[3] Shuaeib F. M. and Soden P. D. (1997) *Composites Science and Technology* 57; 1249-1259.

Table 1: Failure load and subsidence generated from centrally and peripherally placed implants (Mean±SD).

Specimen	Failure Load (N)		Subsidence (mm)	
	Central	Peripheral	Central	Peripheral
Foam	1128±144	1169±152	2.72±0.04	2.66±0.04
Synthetic	4497±296	N/A	1.01±0.33	0.40±0.30
Human	1196±207	1946±487	3.55±0.37	2.24±0.47

RELATIONSHIP BETWEEN LUMBAR REGION KINEMATICS DURING A CLINICAL TEST AND A FUNCTIONAL ACTIVITY IN PEOPLE WITH AND WITHOUT LOW BACK PAIN – A PILOT STUDY

Sara P Gombatto[1], Mark E Kroll[1], Kara E McCallum[1], Melissa N Shiffer[1]
[1]Department of Physical Therapy, Nazareth College, Rochester, NY, USA, sgombat4@naz.edu

INTRODUCTION

Lumbar region movement tests often are included in a clinical examination for a person with low back pain (LBP) because movement during the test is assumed to reflect movement during a related functional activity. To our knowledge, no one has examined this relationship. The purpose of the current pilot study was to examine the relationship between lumbar region kinematics during a clinical test of trunk lateral bending (TLB) and while lifting a 10-pound suitcase placed to the side in people with and without LBP.

METHODS

Five people with chronic or recurrent LBP and 3 people without LBP were tested (24.3 ± 6.6 years). People without LBP were matched to people in the LBP group based on age, sex, height, and weight. People with LBP were not in a flare-up of the LBP problem on the day of testing; average symptoms were 1.4 ± 2.2 on a numeric rating scale (0-10) and modified Oswestry scores were 13.0 ± 8.0 %.

Three-dimensional kinematics of the upper and lower lumbar regions were measured during test movements using a 3-D motion capture system (Vicon Inc., Denver, CO, USA). Participants performed 3 repetitions of the following movements to each side: TLB, self-selected functional movement, and instructed functional movement. For the self-selected functional movement, the participant used a self-selected movement strategy to lift a 10-pound suitcase placed to the participant's side. For the instructed movement, the examiner instructed the participant to pick up the same suitcase by primarily using a lateral bending movement.

A spine model was developed to analyze kinematic data using Visual 3-D software (C-Motion Inc., Kingston, ON, Canada). Kinematics of the lower lumbar segment (L4-L5) were examined relative to the pelvis. Kinematics of the upper lumbar segment (L1-L3) were examined relative to the lower lumbar segment. Maximum angle of the upper and lower lumbar segments in the frontal plane were calculated. An average of the measures from the 3 repetitions was calculated for each test movement.

T-tests and chi-square analyses were conducted to test for differences between groups on anthropometric and demographic characteristics. To examine reliability of measures between repetitions of each test movement within a single session, interclass correlation coefficients (ICC) and standard errors of the measure (SEM) were calculated for each angle. To examine the relationship between lumbar region kinematics during the clinical test of TLB and each functional movement, pearson product-moment correlation coefficients were calculated between maximum lower and upper lumbar segment angles during the clinical test and each functional movement. Correlation coefficients were calculated first for the entire sample (N=8) and then separately for the LBP group (N=5).

RESULTS

There were no differences between groups on demographic or anthropometric characteristics (Ps>0.4). Across conditions, ICC values for maximum upper and lower lumbar region angles ranged from 0.88-0.97 and SEM values ranged from 0.6°-1.3°. Values for pearson product-moment correlation coefficients are presented in Table 1. Overall, correlations between the TLB and instructed condition were greater than between the TLB and the patient-preferred condition. Also, correlation coefficients for only people with LBP were consistently higher across conditions and regions (P=.007-.29).

Table 1 Pearson product-moment correlation coefficients for maximum angles between conditions.

	Participants	
Conditions	**All (N=8)**	**LBP(N=5)**
TLB vs. Patient-Preferred		
Lower Lumbar	0.593	0.594
Upper Lumbar	0.106	0.835
TLB vs. Instructed		
Lower Lumbar	0.871	0.969
Upper Lumbar	0.683	0.919

DISCUSSION AND CONCLUSIONS

Lumbar region kinematics during a clinical test and a related functional activity are moderately correlated. The correlation coefficients are higher for people in the LBP group and when the functional movement is constrained. Lumbar region movement during a clinical test appears to reflect movement during a related functional activity, particularly in people with LBP. Understanding this relationship will assist physical therapists in selecting relevant movement tests to include in an examination and in identifying the relevant functional activities to address with intervention. A limitation of the current study is that only 3 people without LBP were included.

REFERENCES

[1] Cyriax J. *Textbook of Orthopaedic Medicine*, Bailliere Tindall,1982.
[2] Delitto A et al. (1995). A treatment-based classification approach to low back syndrome: Identifying and staging patients for conservative treatment. *Phys Ther* Vol 75(6); p.470-485.
[3] Sahrmann SA. *Diagnosis and Treatment of Movement Impairment Syndromes*; Mosby Inc., 2002.

EFFECT OF COUPLED POSTURES ON LUMBAR MUSCLE ACTIVIY: DOES THE FLEXION RELAXATION PHENOMENON PERSIST?

Tara Diesbourg[1], Janessa Drake[2], & Nadia Azar[1]
[1]Department of Kinesiology, University of Windsor, Windsor, ON, Canada, azar5@uwindsor.ca
[2]School of Kinesiology and Health Science, York University, Toronto, ON, Canada

INTRODUCTION:

The Flexion-Relaxation Phenomenon (FRP) is characterized by the myo-electric silencing of the erector spinae muscles in moving from upright standing to full trunk flexion[1]. "Coupled" postures (combinations of flexion and axial twist) are commonly encountered in occupational settings, and are known to place the lumbar spine at a greater risk of injury than postures along pure flexion-extension axes[2]. Research has been conducted on various postures and their effect on FRP; however, little focus has been placed on movements along axes other than pure flexion-extension. This study examined whether FRP is present when the lumbar spine is placed into coupled postures, in comparison to pure flexion.

METHODS:

Nine male participants (age 17-28) volunteered for this study. A Vicon motion capture system (Oxford Instruments Group, Oxford, UK) was used to collect full-body kinematics (75 markers) and EMG from the upper (UES) and lower (LES) erector spinae, rectus abdominus (RA), internal (IO) and external (EO) obliques, latissimus dorsi (LAT), and gluteus maximus (GMAX) and medius (GMED) muscles bilaterally. Visual 3D software (C-Motion Inc., Maryland, USA) was used to output trunk angle data, and EMG data was processed using customized LabView 8.6 software (National Instruments, Austin, TX). In random sequence, participants performed three trials of each of three bending movements, including pure forward flexion and combined flexion/lateral bend/axial twist to both the left and right sides. EMG data from each muscle were normalized to a maximum voluntary contraction, and a flexion-relaxation ratio (FRR) was generated for each trial by taking the ratio of the peak activation of the muscles in the extension phase to the mean activation in the full flexion phases[3].

RESULTS:

In the pure flexion trials, six of the eight muscles consistently exhibited FRP (UES, LES, EO, LAT, GMAX, & GMED). In the left coupled posture trials, there was more evidence of FRP in the muscles on the right side of the spine compared to the left side, as evidenced by the silencing of more muscles on the right (UES, LES, RA, GMAX, & GMED) than on the left (LES, RA, & GMAX). A similar trend of greater contralateral FRP was observed in the right coupled posture trials.

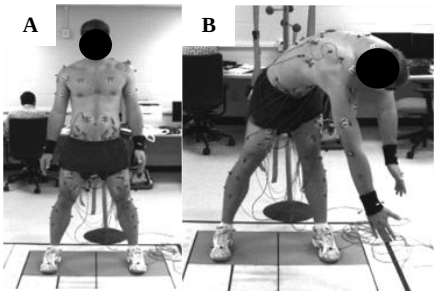

Figure 1: A) EMG electrode and Vicon marker placement. B) Participant at maximum position in the left coupled posture.

DISCUSSION AND CONCLUSIONS:

The presence of the FRP in healthy individuals is thought to represent a temporary transfer of the load-supporting role of the muscles to the passive elastic components of the spine[1]. The asymmetrical muscular response to coupled lumbar flexion/axial twist, particularly the lack of relaxation in the ipsilateral musculature, may be a contributing factor in the development of low-back pain. Further analysis comparing the EMG time-histories of the ipsilateral and contralateral sides of the spine in the coupled posture trials may provide additional insight. Future research could involve the investigation of these postures as well as pure lateral bend and axial twist motions as they apply to these and other muscles, with more focus on work-related tasks (such as lifting).

REFERENCES:

[1] Colloca CJ, Hinrichs RN (2005). The biomechanical and clinical significance of the lumbar erector spinae flexion-relaxation phenomenon: a review of literature. *J Manipulative Physiol Ther* Vol 28: p. 623-631.

[2] Drake JDM, et al. (2005). The influence of static axial torque in combined loading on intervertebral joint failure mechanics using a porcine model. *Clin Biomech* Vol 20(10): p. 1038-1045.

[3] Alschuler KN, et al. (2009) Flexion-relaxation and Clinical Features Associated With Chronic Low Back Pain: A Comparison of Different Methods of Quantifying Flexion-relaxation. *Clin J Pain* Vol 25(9): p. 760-766.

DAY TO DAY RELIABILITY OF KICKING ACCURACY IN SOCCER

Katharina Althoff, Ewald Hennig, Simon Batz, David Bürgel
Biomechanics Laboratory, University of Duisburg-Essen, Essen, Germany, katharina.althoff@uni-due.de

INTRODUCTION

Kicking the ball accuratly is a fundamental skill of soccer players. Accuracy, defined as the absolute distance between a given target point and ball impact, can be determined with different methods. In the literature 3 different approaches for measuring kicking accuracy are found. Finnoff et al. [1] constructed a wooden target covered with carbon paper for marking ball impacts. Sterzing et al. [2] located ball impact with a high speed camera (200 Hz), positioned behind a goal. In this study an electronic target was used (Hennig et al. [3]).

METHODS

40 experienced male soccer players from the 3rd to 10th German league (26.1 ± 4.2 yrs, 1.83 ± 0.06 m, 80.3 ± 9.3 kg) participated in this study. In each of 3 conditions (own soccer shoe OW, assigned soccer shoe AD, barefoot BA) subjects performed 30 repetitive kicks on a circular target (Figure 1) at a distance of 8m as accurately as possible. The target had a diameter of 120 cm. Electrically conducting wires with a distance of 2 cm were arranged in a concentric pattern on a wooden board. During ball contact electrostatic charges were transferred to these wires, connected to charge amplifiers. A computer program determined the distance between target center and ball impact location. For achieving best accuracy, kicking technique was self-chosen by the subjects. Five trials were recorded in each condition with a high speed camera (Casio Ex-F1, 600 Hz) to identify the used kicking technique. To examine repeatability of kicking accuracy, measurements were performed on two different days. A repeated measures ANOVA and Pearson correlation coefficients were used for statistical evaluation.

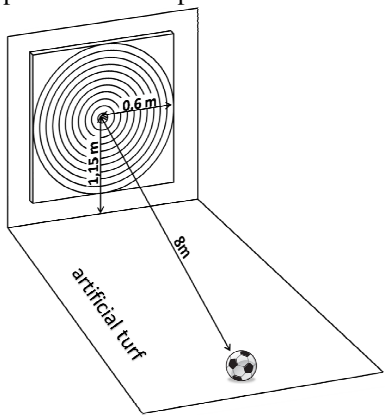

Figure 1: Experimental setup

RESULTS AND DISCUSSION

Subjects kicked the ball either with the inside (n=22) or inner instep (n=18) of the foot. No one chose full instep or the outside. The kicking technique was independent from skill level. Compared to barefoot, kicking with shoes shows a strong trend to better accuracy (ANOVA, p=0.06; Table 1).

Table 1: Kicking accuracy (cm) in two shoes and barefoot

	Mean	SD
AD	47.18	8.80
BA	49.23	10.84
OW	46.67	8.83

Significantly lower accuracies for barefoot kicking were reported before [3].

To kick the ball accurately depends primarily on the technical skill of the soccer player. In this study players with different skill levels (from 3rd to 10th German league) were tested. Differences in accuracy were significant ($p<0.001$) between higher and lower leagues (3rd - 6th league, n=8: 39.5 cm, 9th - 10th league, n=19: 52.2 cm).

No statistical significant differences were found for the accuracy measurements across all conditions between the first and second day. A coefficient of r=0.84 shows a good day to day repeatability of kicking accuracy (Figure 2).

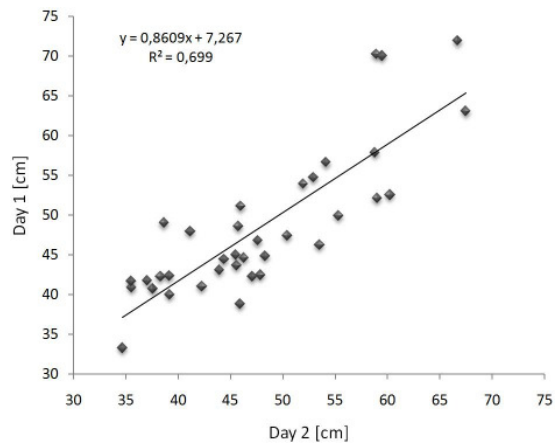

Figure 2: Mean values of kicking accuracy (in cm) for all conditions at two different days.

Interestingly, when analyzing repeatability separately for each condition the barefoot and the assigned shoe conditions were as repeatable as the own shoe condition. Therefore, a possible learning effect when wearing a new or no shoe seems to be of minor importance.

CONCLUSIONS

Although kicking accuracy is highly variable between soccer players [2], it is repeatable from day to day. Furthermore, kicking with unfamiliar conditions (assigned soccer shoe, barefoot) is as repeatable as kicking with own, used shoes. These results are helpful for further accuracy studies.

REFERENCES

[1] Finnof JT et al. (2002). A valid and reliable method for measuring the kicking accuracy of soccer players. *Journal of science and medicine in sport* **5** (4); p. 348-353.

[2] Sterzing T et al. (2009). Velocity and accuracy as performance criteria for three different soccer kicking techniques. *27. International Society of Biomechanics in Sports Conference;* p. 243-246.

[3] Hennig EM et al. (2009). Soccer footwear and ball kicking accuracy. *Footwear science* **1** (S1); p. 85-87.

ACKNOWLEDGEMENTS

This research was supported by Adidas / Germany.

Acute Effects of Whole Body Vibration on Accuracy of Motor Performance

Nina Völkel, Ewald M. Hennig
Biomechanics Laboratory, University of Duisburg - Essen, Essen, Germany, nina.voelkel@uni-due.de

INTRODUCTION

Vibration training becomes increasingly popular in fitness studios and rehabilitation centers. Based on a literature review, Jordan et al. [1] conclude that vibration training can serve to augment the performance and training of athletes. As an acute effect increased post vibratory power output was observed in several studies. Improvement in gait as well as fine coordination performance (handwriting) after Whole Body Vibration (WBV) was reported for Parkinson patients [2]. The stochastic resonance phenomenon has been suggested as an explanation for this improvement in neuromotor performance. The present study was conducted to investigate the acute effect of WBV on the accuracy of movement execution in a simple jumping task onto a target.

METHODS

20 female and 20 male sports students (age 24.5 +/- 2.2 years) from the University Duisburg-Essen jumped from a table (70 cm) onto a target before and after three different treatments. The jumping distance to the target center was 120 cm for the women and 155 cm for the men. All subjects were instructed to land with the back of their heel on the centerline of the target (Figure 1). After landing from the jumps the distances from both heels to the centerline were measured and the values from both heels were averaged. The absolute deviation from the centerline was calculated for statistical evaluation.

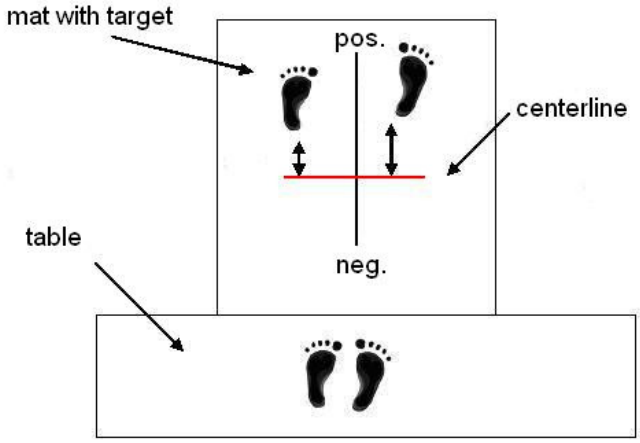

Figure 1: Experimental set-up

Whole body vibrations at 5 Hz (treatment 1) and 26 Hz (treatment 2) were used with a "Galileo" vibration platform. The subjects stood for 1 minute on the platform and performed dynamic knee bends without shoes. For another minute they sat on the platform. A 2 minute concentration task for improving attentiveness was added as placebo (treatment 3).

All subjects came on three different days. After familiarization with the task 5 jumps were performed before the treatments on each day (Pre). Thereafter, the WBV (5 Hz or 26 Hz or Placebo) was applied. Treatment order was randomized across the three test days. After the treatments the students performed a second set of 5 jumps (Post) onto the target. The mean values from the 5 Pre and Post jumps were calculated and used for statistical evaluation (dependent t-test).

RESULTS

A significant improvement ($p < 0.05$) in landing precision was found after the 5 Hz vibration treatment. A non significant improvement in precision was found following the 26 Hz treatment. For the placebo concentration task no changes were observed (Figure 2).

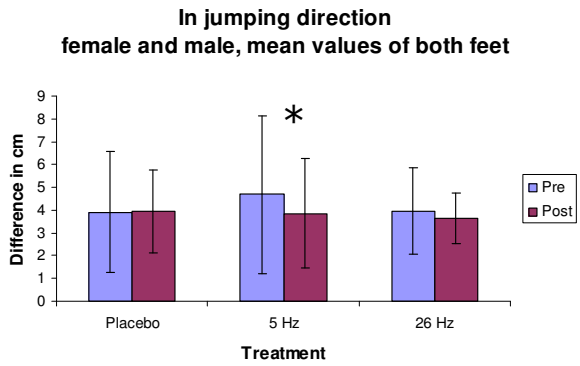

Figure 2: Absolute deviation from target in cm (* $p = 0.014$)

DISCUSSION AND CONCLUSIONS

The more accurate movement after the 5 Hz treatment may be explained by the introduction of stochastic noise with its influence on brain and peripheral neural mechanisms. An improvement of the precision of movement execution by WBV may enhance performance in various sports. Future research will explore the duration of the better movement accuracy after WBV. For Parkinson patients the positive effect of WBV lasted from several hours to up to 2 days for some subjects [2].

REFERENCES

[1] Jordan M.J. et al. (2005). Vibration training: an overview of the area, training consequences, and future considerations. J. Strength & Cond. Res. **19** (2); p. 459-466.
[2] Haas C.T. and Schmidtbleicher D. (2002). Zu den Effekten mechanischer Schwingungsreize bei Morbus Parkinson. Rheuma Aktuell 3; p. 8-10.

SLAP AND WRIST SHOTS: THE EFFECT OF PLAYER CALIBRE ON STICK STRAIN GAUGE RESPONSE

Ashley Hannon[1], Yannick Michaud-Paquette[1], David J. Pearsall[1], Rene A. Turcotte[1]
[1]Department of Kinesiology & Physical Education, McGill University, Montreal, Canada
ashley.hannon@mail.mcgill.ca

INTRODUCTION

Physical properties of the ice hockey stick can be greatly controlled using composite materials. [1] . Optimal slap (SS) and wrist shot (WS) puck speed depends largely on the player's calibre and technique [2] as well as how the user interacts with the mechanical properties of the stick [3]. How a player adapts to different stiffness properties is not known. To address this question, players from high to low calibre (HC,LC) performed SS and WS where dynamic stick shaft deflection (strain) was measured. It was hypothesized that differences in stick strain would be observed based on calibre of player and stick stiffness.

METHODS

Healthy adult male subjects (n=17) were tested. HC and LC players were categorized by max puck velocity during SS and WS execution ($p \leq 0.0001$),Table 1.

Table 1: Descriptive statistics based on calibre of player

	HC	LC
	M± SD	M± SD
Height (cm)	182.61 ± 2.17	174.30 ± 2.30
Mass (kg)	84.43 ± 3.71	77.39 ± 3.93
SS Velocity (m/s)	26. 43 ± 0.97	21.94 ± 1.06
WS Velocity (m/s)	24.31 ± 0.97	19.78 ± 1.06

Three WS and SS were taken with each stick (77 and 102 flex) per subject on a synthetic ice surface. Kinematic data were recorded at 300Hz using a Vicon™ system, obtaining puck velocity. Shaft flexion was measured using five half-active Wheatstone bridges at 150, 300, 450, 600 and 850 mm (SG1-SG5 respectively) along the shaft central axis and recorded with LabView™ at 10KHz.

RESULTS

Mean max strain values were statistically significant(df=1, n=17, $p<.05$) when comparing both calibres(LC<HC); for SG1(F=9.8), SG2(F=6.1), SG3(F=14.9), SG4(F=14.6), and SG5(F=12.4); Fig 1, 2. Strain differences were also significant when comparing stick(flex 102<flex 77); for SG1(F=8.0), SG2(F=6.6), SG3(F=5.4), and SG5(F=22.3) and shot(WS<SS;) for SG1(F=9.9), SG2(F=30.6), SG3(F=96.1), SG4(F=70.8), and SG5(F=186.8).

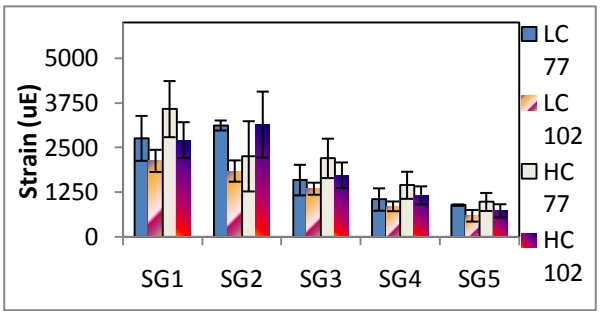

Fig 1: Maximum strains by calibre and stick for WS

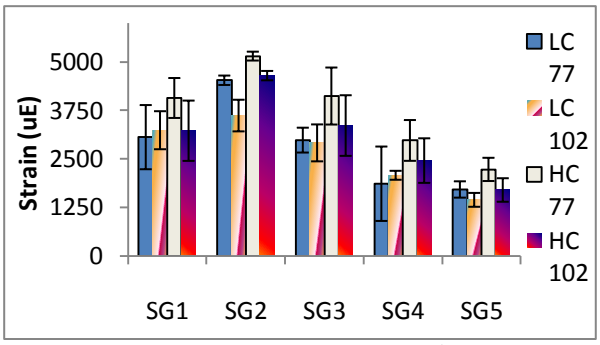

Fig 2: Maximum strains by calibre and stick for SS

DISCUSSION AND CONCLUSIONS

As anticipated, HC players produced more flexion strain along the shaft than LC; as well, HC and LC players flexed the stick differently along the shaft's length. Hence, both player skill level and shaft stiffness interaction play an important role determining the dynamic response of composite ice hockey sticks during WS and SS skills. Further study is needed to identify the optimal stick behaviour(s).

REFERENCES

[1] Montgomery,D, et al. (2004). *Safety in ice hockey 4th vol*, ASTM STP 1446
[2] Wu,T. et al. (2003) Sport Eng **6**(1):31-39
[3] Woo (2004). *ISBS Conference*, Ottawa

ACKNOWLEDGEMENTS Funding provided by NSERC and Bauer Hockey Corp

ANGULAR IMPULSE DURING BALLET TURNS

April Karlinsky,[1] François D.Beaulieu[2] and DGE Robertson[3]
School of Human Kinetics, University of Ottawa, Ottawa, Canada
Email: [1]akarl017@uOttawa.ca, [2]fdbeauli@uOttawa [3]dger@uOttawa.ca

INTRODUCTION

Turns or spins are fundamental skills in ballet and dance.[1] Yet few biomechanical studies have determined the angular impulses necessary to initiate turns.[1,2,3] The two most common turns in ballet are the *pirouette* and the *fouetté*. The main difference being that the *fouetté* can be a continuous series of turns whereas the *pirouette* is a one shot turn that typically permits one or more rotations. The purpose of this study was to measure the angular impulses produced by ballet dancers in the performances of various *pirouettes* and during the initiation of series of *fouettés*.

METHODS

Four subjects (two female, two males), all with years of ballet experience, performed *pirouettes* and/or *fouettés* from a choice of three force platforms (Kistler). In most cases, each foot was placed on a different force platform. The data from multiple force platforms were mathematically combined[4] in Visual3D to determine the total vertical ground reaction moment of force (M_z). The start and end of each impulse was identified and the interval integrated to obtain the total angular impulse delivered immediately before single-support on the support leg began.

Each trial was then evaluated to determine, approximately, the number of turns achieved before touchdown of the gesture (non-supporting) leg. The data from all subjects' *pirouettes* were combined and correlated with the number of turns produced.

RESULTS

Figure 1 shows the relationship between the number of turns and the initial angular impulse. The linearity of the turns and angular impulse was (r =) 0.920, which was statistically significant (P>0.001). Regression analysis yielded a slope of 6.20 N.m.s/turn and an intercept of 5.2 N.m.s. Table 1 shows the mean angular impulses for 1, 2 and 3-turn *pirouettes*.

DISCUSSION AND CONCLUSIONS

The fact that the regression line had a non-zero intercept (i.e., it took 5.2 N.m.s to produce no turns) may be due to the necessity to overcome static friction at the start of any spin.

It is clear from Figure 1 that there was a strong linear relationship between the number of turns and the required angular impulses for the *pirouettes*.

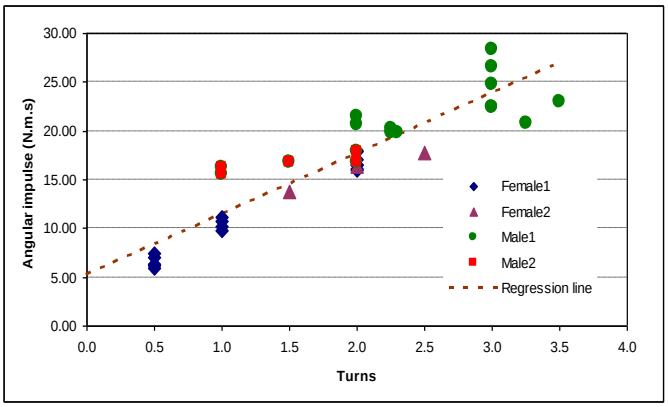

Figure 1: Angular impulse versus number of turns

The only other study that has also correlated these factors suggested a parabolic relationship[2] but since that study used single subject and only 4 *pirouettes* the parabolic relationship was not well supported. Of course, more subjects and trials are necessary to confirm the linearity suggested by this study. The data from Imura *et al.*[3] were normalized to mass and stature and so could not be compared to the current study.

Notably the *fouettés* for the two subjects that performed this skill required larger impulses than what the subjects needed for 2 or even 3-turn *pirouettes*. This may be necessary to provide enough momentum for the subsequent turns since addition angular momentum will be limited to what is acheivable from a single leg's angular impulse. Obviously, a single foot cannot create the same angular impulse as two feet and a wider base of support. Dancers must therefore supply greater impulses at the start of a series of *fouettés*. Dancers should therefore use a wider base at the start of *fouettés* to permit larger angular impulses as compared to *pirouettes*.

REFERENCES

[1] Laws KL. *Dance Res J* 11:12-19, 1978
[2] Laws KL. *Med Probl Perform Art* 13:136-145, 1998
[3] Imura A, *et al*. *Human Mvt Sci* 27:903-913, 2008
[4] Gerber H, Stuessi E. *Biomechanics X-B*, 1055-1058, 1987

Table 1: Mean (SD) angular impulses (N.m.s) for *pirouettes* and *fouettés*.

Subject	Female1	Female2	Male1	Male2
fouettés	none	(n=3) 16.5 (4.23)	(n=2) 26.1 (1.70)	none
1-turn pirouette	(n=4) 10.4 (0.58)	none	none	(n=2) 16.5 (0.40)
2-turn pirouette	(n=5) 16.7 (0.72)	none	(n=4) 20.6 (0.70)	(n=2) 17.3 (1.72)
3-turn pirouette	none	none	(n=4) 25.5 (2.57)	none

MUSCLE ACTIVATION/RELAXATION CYCLES AND THE SPEED/STRENGTH PARADOX

Stuart McGill, David Frost, Tom Hubrecht
Department of Kinesiology, University of Waterloo

INTRODUCTION

The main issue addressed here is the paradox of muscle contraction to optimize terminal segment speed and force. When muscle contracts both force and stiffness are increased. Force creates faster movement but the corresponding stiffness slows the change of muscle length and shape together with joint velocity. The purpose of this study was to investigate how this speed-strength is accomplished at elite levels of performance. Five elite MMA athletes were recruited given that they must create high strike force very quickly.

METHODS

Two data sets were collected for this analysis. In the first set muscle activation and 3 dimensional spine motion was measured in elite MMA fighters who were all UFC veterans with one World Champion. Fighters were asked to hand strike and kick a heavy bag using different styles that they felt would result in both speed and a high contact force. Each fighter has their own arsenal of striking styles. Hand strikes included combinations such as a jab/hook. Foot strikes included the roundhouse kick to the opponents' knee, hip, and head (simulated by appropriate strike zones on the bag) and also a side kick and a spinning back kick. In addition, they created muscle "twitches" while laying supine so that muscle activation/relaxation rates could be quantified in a more controlled manner but still in an unfamiliar novel task to neutralize the effect of a learned skill. The second data set involved eight "normal" subjects (undergraduate students) who repeated the controlled twitches. Both muscle activation and relaxation rates were quantified and compared between the elite athletes and "normals".

RESULTS

Examples of different hand and foot strikes together with some ground and pound techniques often revealed the "Double peak" pattern of muscle activation (see figure). The first peak of muscle activity was often associated with initiation of motion. As the hand or foot gained speed a relaxation phase was sometimes observed followed by a second peak associated with the body stiffening at impact to create a harder impact. Kicks created more distinct double peaked activation profiles. Quantification of muscle activation/relaxation twitch dynamics showed that the elite athletes contracted their torso muscles up to 6 times faster, on average, than the normal subjects, and they relaxed up to 6 times faster, depending on the muscle.

DISCUSSION AND CONCLUSION

Optimizing strike force and reducing the time taken for the hand or foot to reach the opponent require paradoxical muscle variables. It appears that speed and strike strength depend on

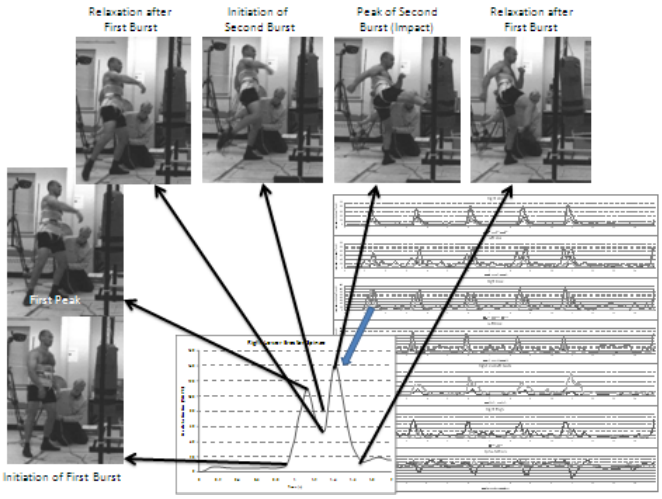

Figure: The first pulse initiates leg motion, the relaxation phase facilitates speed, the second pulse enhances impact.

the muscles "pulsing" within a single strike effort. The first pulse often occurs just before, or during, initiation of the first limb motion. A subsequent relaxation phase appears to assist increased limb velocity. Then a second pulse occurs very close to the impact. The reaction of the accelerating limbs, either the arms for hand strikes or the legs for kicks, must be buttressed by an opposing force which appears to be created by a stiff torso – this is known as enhancing the "effective mass" (Neto et al, 2007). In this way, it would appear that elite fighters' performance is determined not only by the rate of muscle contraction but also the rate of muscle relaxation.

If speed-strength is dependent upon activation/relaxation dynamics we also wondered if the elite athletes were inherently faster at contracting and relaxing muscle in a novel twitch task. They were faster at both. It has been suggested that elite sportsmen are twice as fast in contracting muscle but about eight times faster in relaxing muscle (Matveyev, 1981 as quoted by Siff, 2003). This appears to be reasonable.

The implications of these combined results is that elite performance requiring speed strength may be enhanced with training to enhance both the rate of muscle contraction and relaxation, if this is even possible. We continue this work.

REFERENCES

Neto, et al, The role of effective mass and hand speed in the performance of Kung Fu athletes compared with non-practitioners, J. Appl. Biomech. 23:139-148, 2007.
Siff, M., Supertraining, Supertraining Institute, Denver, 2003.

EFFECTS OF THE LOCATION OF INSTABILITY ON MOTION PATTERNS AND ELECTROMYOGRAPHICAL ACTIVITY IN BENCH PRESS EXERCISES

Brian Nairn[1], Chad Sutherland[2], Janessa Drake[1]
[1]School of Kinesiology and Health Science, York University, Toronto, Canada, jdrake@yorku.ca
[2]Department of Kinesiology, University of Windsor, Windsor, Canada

INTRODUCTION

Instability training is widely used in rehabilitative, recreational, and competitive environments though few studies have examined the effects of unstable surfaces [1-3]. Use of unstable load or surface may stimulate similar muscle activation with less load [1, 3], however practical applications are debatable [2, 3]. Any modulating effects should be analyzed to ensure training occurs properly and safely. Therefore, the purpose of this study was to evaluate and compare three-dimensional motion patterns and electromyography (EMG) of a bench press exercise when performed using an unstable load (fluid-filled Attitube® bar), unstable surface (stability ball), and a stable load (standard Olympic bar) and stable surface (exercise bench).

METHODS

Ten male participants from a university population who train regularly were recruited. Three bench press repetitions of 20.5 kg (45 lbs) were performed with a standard Olympic bar (BAR), on a stability ball (with Olympic bar: BALL) and with an Attitube® bar (TUBE). A Vicon motion capture system (Oxford Instruments Group, Oxford, UK) was used to collect full body kinematics (75 marker set) and EMG (12 muscles bilaterally: biceps, triceps, anterior deltoid, medial deltoid, pectoralis major, upper trapezius, latissimus dorsi, rectus abdominis, internal oblique, external oblique, upper erector spinae, lower erector spinae). Kinematic data was processed using Visual3D (C-Motion, Inc., Maryland, USA) and EMG data was processed using Visual Basic (Microsoft Corporation, Washington, USA). A maximum voluntary contraction (MVC) was used to normalize EMG data.

RESULTS

Electromyography of four participants showed they did not differ from one another overall ($p>0.08$). The right and left anterior deltoid activations were shown to be 3.2 and 3.7 times larger respectively in the Ball condition, and 1.5 and 1.3 times larger than the Tube conditions compared to the Bar ($p<0.014$).

Trajectory analysis of the mean range from four participants revealed certain trends. There were no differences in the average range of the vertical ($p>0.853$) or the anterior-posterior ($p>0.595$) movements between exercises. The difference of the mean mediolateral range was statistically significant between the Tube and both Bar ($p<0.02$) and Ball ($p<0.013$) exercises; whereas the Bar and Ball trials were not statistically significant ($p>0.673$). The Tube trial showed a range of 2.6 times greater than the Bar and 1.7 times larger than the Ball. The Ball range was 1.6 times greater than the Bar (Figure 1).

DISCUSSION AND CONCLUSIONS

The changes in muscle activation may be due to the instability of both the surface and the load, with greater instability requiring an increase of anterior deltoid activation. Also, the near significance of some trunk muscles may be indicative of a stabilizing response. The changes in the mediolateral bar and Attitube® trajectories are an indication of a stabilizing attempt as the liquid moves through the Tube from one end to the other. These results suggest that it may be easier to control the rigid bar regardless of surface stability as compared to an unstable load, where as both an unstable surface and load both may require an increase of muscle activation to perform the exercise. Future work will focus on analysis of remaining data, as well as elbow joint angles and time varying kinematic and EMG data to gain a more complete understanding of the role instability plays in the bench press exercise.

REFERENCES

[1] Drake, J.D.M. et al., (2006). *J Manipulative Physiol Ther*, 29(5); 354-362.
[2] McBride, J.M. et al., (2006). *J Strength Cond Res*, 20(4); 915-918.
[3] Behm, D.G. et al., (2002). *J Strength Cond Res*, 16(3); 416-422.

ACKNOWLEDGEMENTS

The authors would like to acknowledge Balance Modus Inc. for providing the Attitube® bar.

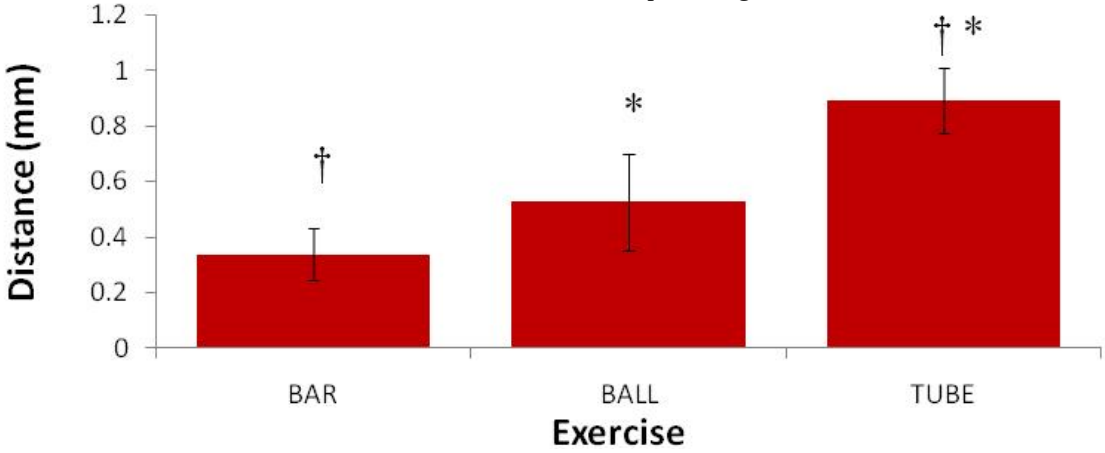

Figure 1: Mean mediolateral range of bar/tube motion during the exercises across participants. The † represents statistical significance between the Tube and Bar ($p<0.02$) and * represents significance between Tube and Ball ($p<0.013$).

LOWER EXTREMITY TISSUE MASS RATIO DIFFERENCES IN ATHLETES OF SPORTS INVOLVING REPETITIVE IMPACTS

Alison Schinkel-Ivy[1], Timothy A. Burkhart[1,2], David M. Andrews[1,2]
[1]Department of Kinesiology, University of Windsor, Windsor, Ontario, Canada, schinke@uwindsor.ca
[2]Department of Industrial and Manufacturing Systems Engineering, University of Windsor, Windsor, Ontario, Canada

INTRODUCTION

Lower extremity injuries have been associated with certain anthropometric measurements and sports that involve repetitive foot impacts [1]. However, the effect that different loading patterns (i.e. between sports) have on the specific ratios of tissue masses and the relationship to injury has not been explored. Therefore, the purpose of this study was to compare lower extremity tissue mass ratios of athletes across sports involving impacts with different repetitive loading characteristics.

METHODS

Male and female varsity athletes (N=104) from the volleyball (VB) (F=10), cross country (CC) (M=18, F=13), soccer (S) (M=29, F=7), and basketball (B) (M=18, F=9) teams at the University of Windsor participated in the study. Anthropometric measurements (lengths, circumferences, breadths, and skinfolds) were taken for the left and right lower extremities, which were then used as inputs to regression equations to predict bone mineral content (BMC), lean mass (LM), fat mass (FM), and wobbling mass (LM+FM=WM) for the leg and leg+foot segments [2]. Tissue mass ratios (LM:FM, LM:BMC, and FM:BMC) for the right and left (side) leg and leg+foot (segment) were compared across sports.

RESULTS

A significant sport effect was found across all combinations (side and segment) of tissue mass ratios. Bilaterally, for both the leg and leg+foot segments, VB players had significantly smaller LM:FM and LM:BMC ratios than the CC, BB, and S participants with a mean difference of 3.6 (Figure 1); the maximum difference occurred with CC in all instances. The VB/CC disparity was most pronounced in the left leg LM:FM ratio, where CC participants had approximately 9 times more LM than FM, compared to VB players who were found to have only 3 times more LM than FM. For the FM:BMC ratios, VB was found to have significantly higher values compared to the other three sports; the maximum difference occurred with S (1.1) (Figure 1).

DISCUSSION AND CONCLUSIONS

The VB athletes, who engage primarily in jumping, had tissue mass ratios that were significantly different from the athletes who engaged in purely running (CC, S) or a combination of running and jumping (BB). The differences in tissue mass ratios may help to explain the variability in injury rates and injury types between the sports. Finally, subject-specific biomechanical models used to analyze impacts experienced in these sports should be developed to better represent the morphological differences in leg tissues that exist in the participating athletes.

REFERENCES

[1] Milner, C.E. et al. (2006). Biomechanical factors associated with tibial stress fracture in female runners. *Med. Sci. Sports Exerc., 38*(2), 323-328.
[2] Holmes, J.D. et al. (2005). Predicting in vivo soft tissue masses of the lower extremity using segment anthropometric measures and DXA. *J. Appl. Biomech., 21*, 371-382.

ACKNOWLEDGEMENTS

Thanks to NSERC for funding this study and to Robyn Bertram for her help with data collection.

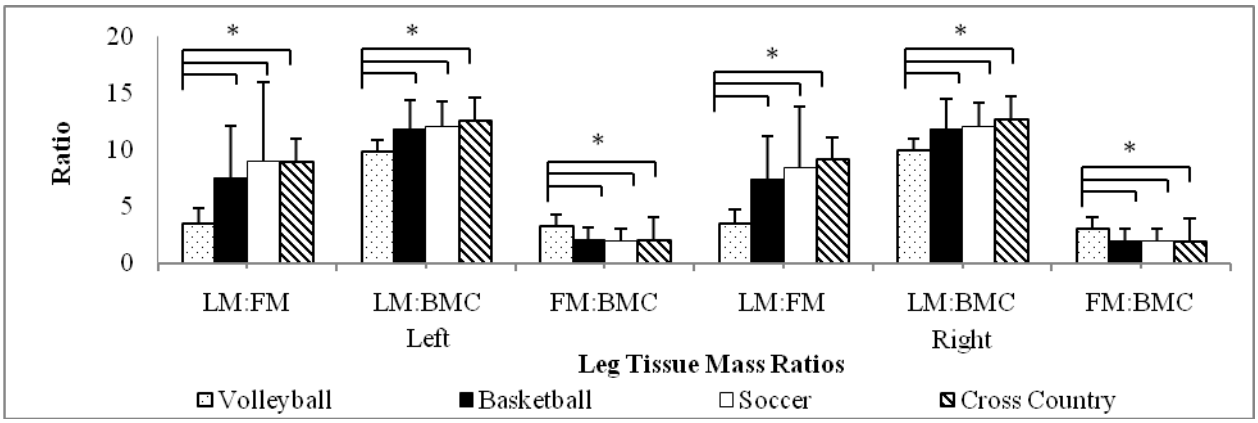

Figure 1: Differences in tissue mass ratios of the left and right leg segments across the sports (* p<0.05).

THE EFFECT OF PERSPIRATION ON THE sEMG AMPLITUDE AND FREQUENCY SPECTRUM

Mohammad Abdoli[1], John Christenson[1], Caroline Damecour [2], Joan Stevenson [2]
[1]School of Occupational Health and Safety, Ryerson University, Toronto, Canada, m.abdoli@ryerson.ca
[2]School of Kinesiology and Health Studies, Queens University, Kingston, Canada

INTRODUCTION: Sweat will influence on the surface EMG (sEMG) signal if an electrical conduction shortcut occurs directly through the sweat between the electrode contacts. As sEMG is increasingly used in the workplace where environmental conditions are difficult to control, the accumulation of sweat under the electrodes may be an important source of error in field studies. This study examines the effect of sweat on both the amplitude and median frequency (MF) of the EMG signal. Since the use of antiperspirants to reduce sweating has been problematic with reduced adherence of the electrodes with the skin, a medical adhesive is tested as an isolator to prevent signal shortcuts.

METHODS: Twelve males performed 3 maximal voluntary contractions (MVC) of the right quadriceps in a sitting position with the foot flat on the floor. EMG was collected using a Bortec AMT8-channel. The average peak value was used for statistical comparison. Four participants were tested using 11 pairs of single snap electrodes (Meditrace 135) positioned adjacent to each other and 4 participants were tested using 11 double snap electrodes (Bortec Biomedical). Another 4 participants were tested with an isolator (Kryolan #2100) applied between the electrode snaps. The volume of sweat applied directly to the skin surface under the electrode varied in increments of 0.4µL/cm^2 from 0, or dry condition, to 4µL/cm^2. This range was selected based upon a literature review of sweat volumes for medium intensity work ranges (Fig. 1). Artificial sweat was prepared according to ISO 3160-2 and spread evenly under the electrode using a Hamilton Microliter #705 glass GC syringe. EMG was normalized to a calibration MVC under dry conditions with the average of 3 repetitions used. Each contraction was passed through a Hanning window prior to determining the power spectrum through a Fast Fourier Transformation. The resulting power spectrum was converted to a single-sided power spectrum before calculating MF. The average MF from the three epochs was used to evaluate the change in EMG signal and was normalized with respect to the dry MF. Skin resistance was measured using a voltmeter. One way analysis of variance was used to compare electrode conditions for skin resistance, peak EMG amplitude, and MF.

RESULTS: As the volume of sweat under the electrode was increased, the amplitude of the sEMG signal decreased with a statistical difference emerging between dry and wet conditions when the volume of sweat was greater than 1.2µL/cm^2 for both electrode types ($F_{single\ snap}$ = 10.83, P < 0.01; $F_{double\ snap}$=27.67, P < 0.01) (Fig 1). When the isolator was applied, no significant difference in peak amplitude was seen between wet and dry electrode conditions for both types of electrodes.. As the volume of sweat increased, the skin resistance and signal amplitude decreased in a linear relationship with a R^2 of 0.86 ($EMG_{reduction}$=0.9191 Skin $resistance_{increase}$+14.732, R^2=0.86). With the isolator, no relationship between sweat volume and skin resistance was seen. The MF remained unchanged with no significant difference between sweat volumes for either electrode type (Fig 2).

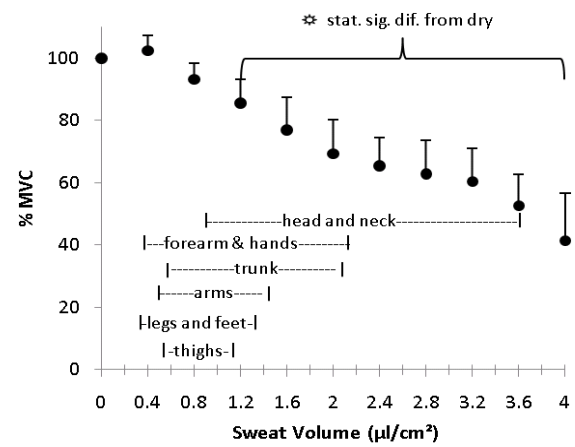

Fig. 1 Change in sEMG signal with increasing sweat volumes applied under the double snap electrodes. Similar findings were seen for single snap electrodes. Sweat volumes according to body part are shown based on a literature review.

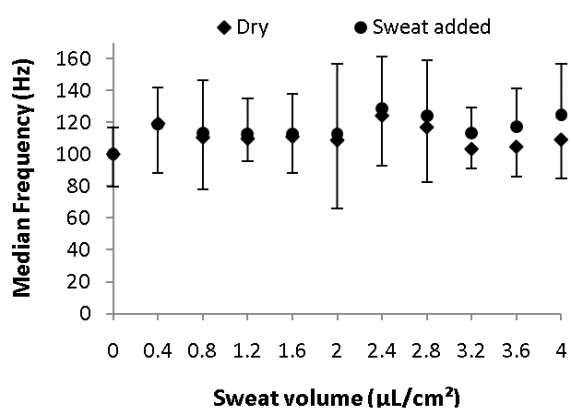

Fig. 2 Change in MF of the sEMG signal with increasing sweat volumes applied under the double snap electrodes. Similar findings were seen for single snap electrodes.

DISCUSSION AND CONCLUSION: These findings, given the small number of subjects, suggest that sweat accumulated under the sEMG electrodes is a potential source of error for signal amplitude. Statistical differences emerged with sweat volumes that have been reported in the literature for most body parts. Skin resistance appears to be a reliable indicator of EMG signal error and therefore should be continuously monitored during testing. An isolator appears to be an effective barrier limiting signal interference from electrical shortcuts when sweat accumulates under the electrode. This study controlled for temperature associated with muscle work since the sweat was added and therefore these changes are directly attributed to sweat. Further study is needed to identify other possible isolators and the effect of the sweat on other types of electrodes.

PASSIVE STRESSES GENERATED BY MYOFIBRILS FROM DILATED CARDIOMYOPATHIC HAMSTERS

Audrée McKenzie[1], Appaji Panchangam[2] and Walter Herzog[2]
[1] Faculty of Kinesiology, University of Calgary, Calgary, AB, Canada, amckenzie@kin.ucalgary.ca
[2]Faculty of Kinesiology, University of Calgary, Calgary, AB, Canada

INTRODUCTION

Dilated cardiomyopathy (DCM) is a frequent heart disease characterized by ventricular dilation, contractile dysfunction and symptoms of congestive heart failure. It is estimated that one fourth of the cases of congestive heart failure in the USA are due to DCM. It is likely the end result of myocardial damage produced by three basic mechanisms: genetic factors, cytotoxic insults and immunological abnormalities.[1]

Reduced passive tension has been reported in failing human myocardium due to DCM compared to non-failing myocardium. Protein isoform changes have also been implicated in the development of heart failure, more specifically, an increased N2BA/N2B titin isoform ratio and a shift from α-MHC to β-MHC.[2] In a single myofibril, titin is thought to be responsible for essentially all of the passive stress response to stretch [3].

The Bio TO-2 Syrian hamster is a valuable genetic model of human DCM. Its lifespan is about 42 weeks.

The purpose of this research is to study the progression of DCM by comparing, over time, the passive mechanical properties of experimental cardiac myofibrils from Bio TO-2 hamsters to those of control myofibrils from Bio F1B hamsters, and relating these findings to changes in titin and myosin protein isoforms.

METHODS

Left ventricular wall muscle samples are collected from age and sex matched Bio TO-2 and Bio F1B hamsters. Muscle strips are skinned in a solution containing 1% v/v triton, then washed and stored at 0-4°C in a relaxing solution containing an antiprotease cocktail. Myofibrils are isolated from these muscle strips by homogenization at 24 000 RPM for 7 seconds. A few drops of the myofibril suspension are placed onto a cover slip chamber on top of an inverted microscope. Single myofibrils are attached at one end to a glass needle fixed to a motor for stretching and shortening, and to a nanolever of known stiffness at the other end, allowing for force measurements. The striation patterns formed by sending light vertically through the myofibrils are captured with a photodiode array for sarcomere length (SL) determination. The resolution of the system is 6 nm. The myofibrils are subjected to ramp stretches. Protein isoforms are determined by gel electrophoresis.

ACKNOWLEDGEMENTS
NSERC, CFI, Canada Research Chair Program

RESULTS

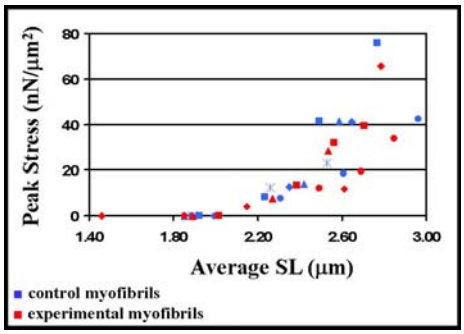

Figure 1: Peak passive stresses as a function of average SL for normal and experimental myofibrils at 18 weeks of age.

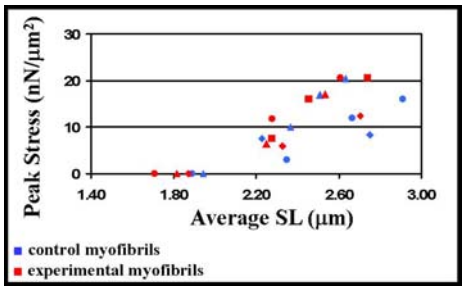

Figure 2: Peak passive stresses as a function of average SL for normal and experimental myofibrils at 38 weeks of age.

DISCUSSION AND CONCLUSIONS

Thus far, the passive mechanical properties of 5 control and 4 experimental myofibrils at 18 weeks of age (Figure 1), and of 3 control and 4 experimental myofibrils at 38 weeks of age (Figure 2), have been tested.

At 18 and 38 weeks of age, the following passive mechanical properties of experimental myofibrils do not appear to differ from those of control myofibrils: the peak and steady state stress – SL relations, SL distributions, and rates and magnitudes of stress decay. More myofibrils will need to be tested to confirm this result.

REFERENCES

[1] Braunwald E, Heart Disease: a textbook of cardiovascular medicine, Elsevier-Saunders, 2005.
[2] Linke WA et al. (2004). Passive stiffness changes caused by upregulation of compliant titin isoforms in human dilated cardiomyopathy hearts. Circ Res Vol 95(7); p. 708-716.
[3] Linke WA and Pollack GH. (1997). Basis of passive tension and stiffness in isolated rabbit myofibrils. AM J Physiol Vol 273(42); p.C266-C276.

Effect of Extrinsic Finger Flexor and Extensor Interconnection on Force and Muscle Activity

Kia Sanei, Peter J. Keir
Department of Kinesiology, McMaster University, Hamilton, Ontario, Canada, saneik@mcmaster.ca

INTRODUCTION

Biomechanical and neural factors have both been suggested to contribute to the limited independence of finger movement and the involuntary force production [1]. The lack of independence is thought to be due to tendinous interconnections or synchronous firing of the motor units in different compartments of the extrinsic finger flexors and extensors [2]. Muscle activity and force measures have been used to investigate the extent to which biomechanical restrictions and neural factors contribute to the lack of independent finger movement and the involuntary force production. The evaluation of involuntary force production in fingers has not yet examined antagonist muscle activity. The purpose of this study was to evaluate the activity of the four compartments of extensor digitorum (ED) and flexor digitorum superficialis (FDS) using surface EMG and finger forces during isometric finger flexion and extension exertions.

METHODS

Fifteen male participants performed a series of finger flexion and extension exertions after providing informed consent. The four fingers were placed in adjustable metal rings oriented vertically and attached to force transducers. The forearm rested on an adjustable table with an elbow angle of 120°, mid-prone forearm and neutral wrist. During the finger extension exertions, the rings were placed around the proximal phalanges. Two sets of flexion exertions were performed in which the metal rings were placed around the middle and distal phalanges. Each trial was repeated three times for each finger. The maximal and sub-maximal exertions were 5 seconds each and alternated between fingers with 5 seconds between exertions of different fingers. Sub-maximal exertions were performed at 5, 25, 50 and 75 % MVC.

Force and surface EMG were recorded from all 4 fingers and muscular compartments of ED and FDS (Biometrics Ltd, Gwent, UK). Detailed anatomical and functional testing allowed the muscle compartments to be identified for electrode placement. EMG and force were collected at 1000 Hz. The forces and EMG were processed in various ways to determine the "selectivity index" [2] and enslaving effects. For this communication, EMG was linear enveloped at 3 Hz, normalized to maximum and averaged over the middle 3 seconds of the 5-second exertions.

RESULTS

Preliminary results suggest that involuntary force and muscle activity were higher in adjacent versus non-adjacent fingers and muscular compartments. Both EMG and force in the adjacent fingers/compartments increased with increasing level of exertion. Involuntary force production was much lower in flexion than extension exertions. At every force level, involuntary force was greatest in the ring finger (5-45 %MVC) when the little finger was exerting force in both extension (Figure 1) and flexion. Involuntary force was lowest during the flexion exertions of the index finger. ED compartments had higher activity during flexion exertions compared to the activity of FDS compartments during extension exertions. Occasionally, the non-task fingers exerted forces in the opposite direction than the task finger.

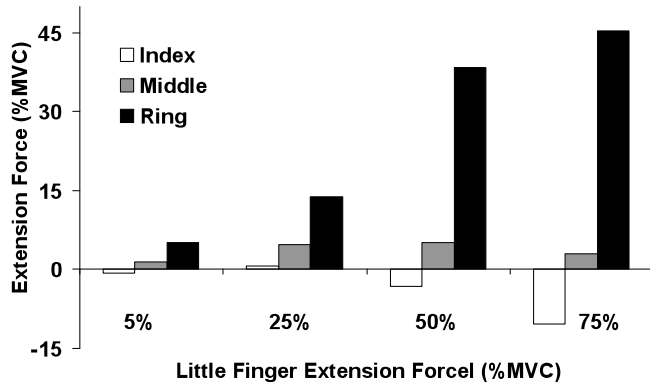

Figure 1: Involuntary force production of the fingers during extension exertions of the little finger. A negative value indicates a force in the flexor direction.

DISCUSSION AND CONCLUSIONS

Our initial results suggest that the fingers exert force more independently in flexion than extension, as was expected. The little finger was least capable of exerting independent force than all other fingers in extension while the index finger was the most independent finger during flexion exertions. As seen by high extensor EMG in flexion exertions, a functional co-contraction may be present which limits the involuntary flexion forces at the expense of increased muscle activity.

REFERENCES

[1] Zatsiorsky et al. (2000). Enslaving effects in multi-finger force production. *Exp Brain Res* Vol **131** (2); p. 187-195.
[2] Keen and Fuglevand (2003). Role of intertendinous connections in distribution of force in the human extensor digitorum muscle. *Muscle Nerve* Vol **28** (5); p. 614-622.

ACKNOWLEDGEMENTS

This study was funded by an NSERC Discovery grant.

ELECTROMYOGRAPHIC ACTIVITY FOR TWO PARTS OF GLUTEUS MAXIMUS DURING SQUAT

B Singh[1], A Hefferman[1] , N Naraine [1], S Nolte [1], JJ Callaghan [2], HJ Yack[1]
[1]Program in Physical Therapy & Rehabilitation Science
[2]Department of Orthopaedic Surgery,
The University of Iowa, Iowa, USA
bhupindersingh@uiowa.edu

INTRODUCTION

The squat exercise is a classic multi-joint exercise that has become an integral part of many lower extremity strengthening and postoperative rehabilitation programs. Studies have shown the monoarticular gluteus maximus (GM) and vasti muscles to be prime movers during ascent while performing a squat.(1) The GM, rather than the hamstrings or quadriceps becomes more active in concentric contraction as squat depth increases. There has, however, been little attention paid in either research or clinical settings, to the impact of the functional differentiation of the segmentation of the GM muscle on joint mechanics and the prescription of therapeutic exercise [2]. Various studies have been performed to identify kinematic and electromyographic (EMG) characteristics, but there is limited literature regarding gluteal muscle activity during therapeutic exercises.

The purpose of this study was to describe the activation of the two parts of the gluteus maximus muscle during a single and double leg squat.

METHODS

Ten subjects (7 females, 3 males, mean age 23.6 years), without current neuromuscular or orthopaedic ailments participated in this study for a single testing session. Kinematic data, used to define movement events, were collected using the Optotrak motion analysis system (Model 3020, Northern Digital Inc., and Waterloo, Ontario, Canada.) Electromyographic activity was assessed with surface electrodes (2 cm spacing), incorporating a preamplifier (Model EMG-55, Therapeutics Unlimited, Iowa City, IA; gain x35), Electrodes were placed over the upper and lower parts of Gluteus Maximus. Subjects performed double leg and single leg squats to a predetermined height. Proper electrode placements were confirmed by observing the EMG signal amplitude during manual muscle tests. Visual 3D software (C-Motion) was used for processing, EMG signals which were rectified and low pass filtered at 6 Hz. The EMG data were scaled to maximum EMG reference values (maximum amplitude obtained during max voluntary isometric contraction held for 3 seconds) and represented as %MVIC hip extension contraction.

Statistical Analysis

Paired t-tests ($p-<0.05$) were performed to determine significant differences between the levels of muscle activation for two parts of G.max during two types of squat.

RESULTS

GM activation during the single leg squat for the upper (mean 38.1+/- 5.1 %) and lower (25.8+/- 4.0) parts was greater than seen for the double leg squat (upper 19.6+/-.09, lower part 19.4+/- 3.6) ($p < 0.01$). Mean activation was greater for the Upper GM compared to the Lower GM for the single leg squat. ($p < 0.01$). (Fig 1)
Correlation between upper and lower parts for single and double leg squat were 0.82 and 0.4 respectively.

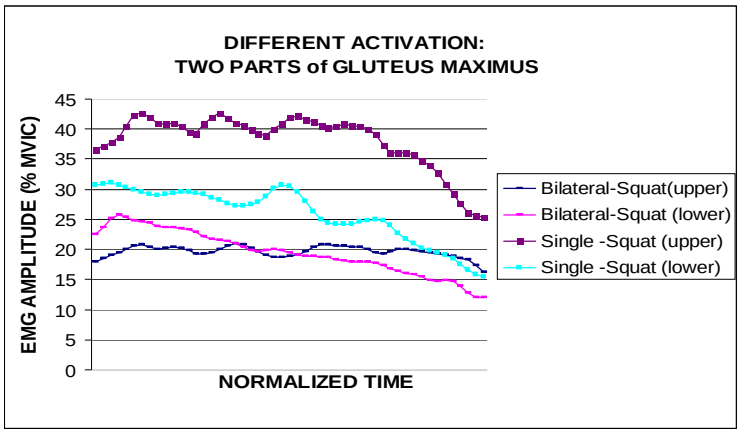

Figure 1: Mean ensemble EMG activation patterns for the Upper and Lower parts of the Gluteus Maximus Muscle during ascent phase of single and double leg squat.

DISCUSSION AND CONCLUSIONS

Differences are seen in the activation levels and patterns for upper and lower parts of the GM for the single leg squat which may suggest that segmentation of bigger muscles should be taken into consideration for muscle modeling and to develop more specific effective therapeutic exercises.
Anatomically, the upper portion of the GM muscle arises from the posterior iliac crest, while the lower portion of the GM muscle arises from the inferior sacrum and upper lateral coccyx, and the upper GM, acts more like a hip abductor than extensor (2) Significantly higher and symmetrical differences in amplitude were seen for single leg squat for other hip muscles tested, which relates to the higher hip moments during this task as compared to the bilateral squat.

REFERENCES

[1] Robertson DG (2008) Appl Biomech. Nov;24(4):3339
[2] Alison Grimaldi.(2009). Manual Therapy 14 (611-17)

MUSCLE ACTIVATION PATTERNS OF TRANSRADIAL AMPUTEES USING HIGH DENSITY EMG

Heather Daley[1], Usha Kuruganti[1], Kevin Englehart[2]
[1]Faculty of Kinesiology, University of New Brunswick, Fredericton, Canada, ukurugan@unb.ca
[2]Institute of Biomedical Engineering, University of New Brunswick, Fredericton, Canada

INTRODUCTION

Myoelectric prosthetics have been accepted by upper limb amputees for many years. Using conventional myoelectric control systems with one or two electrodes sites, prosthetic users often have the ability to perform open and close motions of the myoelectric hand however further functionality of upper limb myoelectric prosthetics is desired (Atkins et al., 1996). While pattern recognition myoelectric control systems provide prosthetic users with the ability to control multiple functions of the prosthetic device, there has been limited research using clinical populations to test advanced devices and control systems. The purpose of this study was to look for distinct and repeatable muscle activation patterns (required for pattern recognition myoelectric control) using amputee subjects. A high density EMG system was used to investigate muscle activation patterns during wrist and hand motions.

METHODS

Eight normally limbed subjects and four amputee (traumatic and congenital) subjects participated in this study. A high density EMG system (TMS International) was used for data collection. Twelve wrist and hand motions were performed during testing and were classified as gross, medium and fine movements. Normally limbed participants performed 20, 5-second contractions of each movement for a total of 240 contractions. The testing protocol for amputee subjects varied because each individual presented a unique case. During the familiarization stage amputee subjects were given time to imagine performing all movements with the missing limb. Up to 64 channels of EMG were used with the high density EMG` system and the electrodes were placed in a grid formation over the forearm to collect as much data from a large surface area. The areas on the forearm that experienced muscle activity during given movements were illustrated in energy maps. The number of electrodes (and consequently the grid formations) used with transradial amputee subjects varied because of different residual limb lengths. The number of electrodes used for each amputee subject is listed in Table 1.

Table 1: Subject information, number of electrodes placed on the forearm of each subject and the movements performed during testing. CG – congenital amputee, TR – traumatic amputee, Movements: 1 – pronation, 2 – supination, 3 – flexion, 4 – extension, 5 – abduction, 6 – adduction, 7 – hand – open, 8- chuck grip, 9- key grip, 10- power grip, 11-fine pinch grip, 12- tool grip, 13- no movement.

Subject	Gender/Age	Number of Electrodes	Movements Performed
CG1	Female/17	16 (8 X 2)	1-13
CG2	Male/24	32 (8 X 4)	1-7, 10, 11, 13
TR1	Female/41	24 (8 X 3)	1-7, 10, 12, 13
TR2	Male/61	24 (8 X 3)	1-7, 9-11,13

RESULTS

This study focused on within subject analysis due to the variability of the amputee subjects. Three of the four amputee subjects did not perform all 13 movements involved in this study. Classification accuracies for the movements performed were obtained and the average classification accuracy for the amputee subjects was 66.39 ± 14.26% compared to the classification accuracy of normally limbed subjects of 80.02 ± 5.52%. Classification accuracies for the amputee subjects increased when only a subset of movements performed were included in the analysis. For amputee subjects, the movements with the strongest classification accuracies were chosen to be included in the subsets; minimum classification accuracies were not required because of lower results. Both of the congenital amputee subjects could perform four movements with strong classification accuracy. The traumatic amputee subjects were able to perform six movements with strong classification accuracy. By reducing the number of movements included in the analysis, the chance of misclassifications was decreased, and therefore allowed for better classification accuracies (92.63 ± 2.54% for normally limbed subjects and 94.22 ± 2.66% for amputee subjects).

DISCUSSION AND CONCLUSIONS

The purpose of this study was to determine if transradial amputees could produce distinct and repeatable muscle activation patterns required for successful pattern recognition myoelectric control. It was hypothesized that amputee subjects would be more challenged to elicit distinct and repeatable muscle activation patterns as compared to normally limbed subjects. It was also hypothesized that channel reduction would identify optimal electrodes sites for pattern recognition control and that classification accuracies would not be compromised by reduced electrode information. The data found in this study support these hypotheses and indicate promise for the future use of pattern recognition control of multifunction myoelectric prosthetics.

REFERENCES

[1] Atkins D.J. et al. (1996). Epidemiologic overview of individuals with upper-limb loss and their reported research priorities. *Journal of Prosthetics and Orthotics* Vol **8**(1); p. 2.

INVERSE DYNAMICS ANALYSIS OF TWO SNOW SHOVEL DESIGNS UNDER NO-FATIGUE CONDITIONS

Ryan T. Lewinson[1,a], D. Gordon E. Robertson[1,b], Gholamreza Rouhi[2,c]
[1]School of Human Kinetics, [2]Department of Mechanical Engineering ,University of Ottawa, Ottawa, Canada
[a]rlewi066@uottawa.ca, [b]dger@uottawa.ca, [c]grouhi@uottawa.ca

INTRODUCTION

Snow shovelling is necessary in many areas of the world, but occasionally results in back pain and/or cardiac sudden death even for healthy people. The bent-shaft shovel allows for a more upright posture [1], but whether it helps reduce fatigue and back pain is questionable. Investigations on muscle activity while snow shovelling have shown that there in an increase in biceps brachii EMG, a decrease in biceps femoris EMG and no change in lower back erector spinae EMG while shovelling with a bent-shaft shovel compared to a straight shaft shovel [2]. The present study aimed to expand upon these findings by assessing joint kinetics while snow shovelling. The purpose of this study was to compare the bent-shaft shovel to a typical straight-shaft shovel by assessing the mechanical work done in the lower extremities and lower back while snow shovelling.

METHODS

Nine subjects participated in this study where 7 Vicon MX cameras captured marker trajectories of the lower extremities. Subjects stood on two force platforms and shovelled a 3-kg load to simulate an average load of snow. This was repeated for 3 trials with both straight and bent-shaft shovels (Figure 1). Net moments and powers were computed for the ankle, knee, hip and L5/S1 joints using Visual3D. Powers were then integrated over time to determine the work done by each joint. For each joint and axis, the percent contributions were determined by comparing with the total body work done (external+internal). Paired-sample *t*-tests were performed on the works that contributed over 5% of total body work in the either *x* (sagittal), *y* (frontal) or *z* (axial) directions.

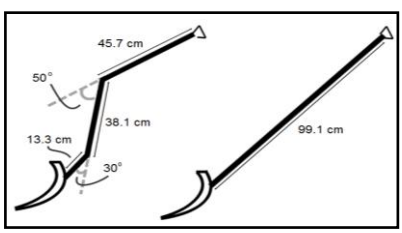

Figure 1: The bent-shaft and the straight-shaft shovels.

RESULTS

Figure 1 shows the averaged lead (coloured) and rear (black) hip and L5/S1 angular velocities, moments and powers for a typical subject using the straight-shaft shovel. Table 1 holds the mean-difference work results, *P*-values and percentage contribution of the five major moments of force. Difference values represent the bent-shaft value minus the straight-shaft value.

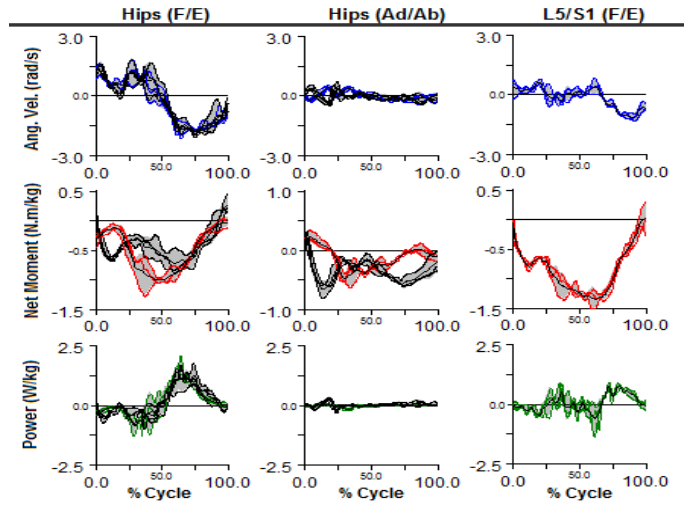

Figure 2: Hip and L5/S1 angular velocities (top), moments (middle) and powers (bottom) for the straight-shaft shovel.

A positive difference indicates the bent-shaft shovel required more work. No statistical significances were found between shovel designs for the amounts of work needed at any of the joints tested (arms were not tested).

DISCUSSION AND CONCLUSIONS

The hip extensors collectively contributed 36.5% of the total work; the L5/S1 moment contributed 29.0%; while all the other moments collectively added 34.5%. Results of this study are consistent with our previous work[2] on the L5/S1 joint where no significant differences in lower back muscular activity (erector spinae and gluteus maximus) were detected with these shovel designs. This occurred even though there was the potential for larger lower back moments because the bent-shaft shovel does not allow for hand positions near the blade. This lack of statistical differences between the two shovel designs may be a due to a compensatory mechanism produced by the biceps brachii muscles or trials being too brief to observe the effects of muscle fatigue. The present study concludes there were no significant differences between the bent and straight-shaft shovel designs in terms of the amount of mechanical work done by the lower extremity and L5/S1 moments.

REFERENCES

[1] Huang C, Paquet V. (2002). Kinematic evaluation of two snow-shovel designs. *Int J Industrial Ergon.* Vol **29**. p. 319-330.
[2] Lewinson R *et al*. (2009). EMG comparison of two types of snow shovels. *ISB XXII*, Cape Town, South Africa. p. 39.

Table 1: The statistical *P*-values (α=0.05) are displayed below along with their respective mean difference values.

	L5/S1 *x*	L5/S1 *y*	L5/S1 *z*	Lead hip *x*	Rear hip *x*
Mean Diff. Work Percent (%)	1.58%	0.22%	0.13%	-1.64%	0.10%
***P*-values**	0.1532	0.739	0.867	0.1423	0.895
Mean component contribution (%)	14.6%	7.5%	6.9%	20.1%	16.4%

THE IMPACT OF A SLOPED SURFACE ON LOW BACK PAIN AND MUSCLE ACTIVATION PATTERNS DURING STANDING WORK

Erika Nelson-Wong[1] and Jack P. Callaghan[2]
[1]School of Physical Therapy, Regis University, Denver, USA, enelsonw@regis.edu
[2]Department of Kinesiology/Faculty of Applied Health Sciences, University of Waterloo, Waterloo, Canada

INTRODUCTION

Occupational standing has been strongly associated with low back pain (LBP) development [1]. Increased muscle co-activation of the bilateral gluteus medius muscles has been previously identified for LBP development during standing using an induced pain protocol [2]. The purpose of this study was to investigate the subjective and biomechanical responses of known pain developers (PD) and non-pain developers (NPD) when exposed to the same prolonged standing task protocol completed while standing on a ±16° sloped surface (eQ Almond, Deltabalance Inc., Alberta, Canada).

METHODS

Eight males and 8 females (average age 22.2 ± 3.06 years, female mass 62.5 ± 9.3 kg, male mass 83.1 ± 9.4 kg, female height 1.64 ± 0.07 m, male height 1.85 ± 0.07 m, BMI 23.6 ± 2.34 kg/m^2) volunteered for this study. Participants had previously been categorized as PD/NPD during level standing on an initial testing day. PD/NPD were equally distributed between genders.

On an initial testing day, participants stood on a level floor, and on a second day they stood on the ± 16° sloped surface. Continuous electromyography from 6 bilateral trunk and hip muscle groups, lower extremity and trunk kinematics, and kinetics (force plate) were recorded during both standing exposures. Participants completed visual analogue scales (VAS) every 15-minutes for LBP, and were categorized as PD on the first (level) standing day if VAS increased > 10 mm from baseline.

Muscle co-activation was quantified for each possible muscle pair by co-contraction index (CCI) [3]. Lower extremity and global pelvis angles, relative trunk angles, forces and moments at the L_5S_1 segment were calculated with an 8-segment rigid link inverse dynamic model using Visual3D software (C-Motion Inc., Kingston, ON). Participants completed a satisfaction survey at the end of the second testing day. Multifactorial (repeated measures) general linear models were used for statistical analyses, with significance criterion set at $p < 0.05$.

RESULTS

There was a significant interaction between PD/NPD group and standing condition ($F_{1,12}$ = 10.5, p < 0.01) with participants identified as PD in level standing having an overall decrease in VAS of 59.4% when standing on the sloped surface. There was a non-significant decrease in CCI for bilateral gluteus medius muscles in the PD group when standing on the sloped surface compared with level standing ($F_{1,14}$ = 3.304, p = 0.09, effect size f = 0.49). The NPD group responded in the opposite direction by having an increase in gluteus medius CCI, although they did not have a commensurate increase in LBP. Post hoc pairwise comparisons were significant (Bonferroni corrected α) and are shown in Figure 1. There were statistically significant changes in both the postural and joint-loading variables examined, however these were of very small magnitudes and therefore not considered to be clinically meaningful.

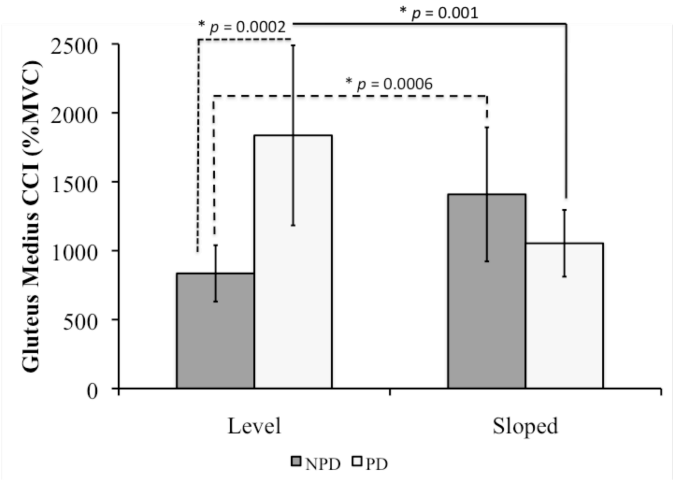

Figure 1: Differences in bilateral Gluteus Medius Co-Contraction Index (CCI) between standing conditions. Significant differences on pairwise comparisons denoted by *.

DISCUSSION AND CONCLUSIONS

The sloped surface resulted in decreased subjective LBP during prolonged standing in prior pain reporters. There were also associated biomechanical changes resulting from using a sloped surface during prolonged standing. These positive findings were supported in an exit survey satisfaction rating with 87.5% indicating that they would use the sloped surface if they were in an occupational setting that required prolonged standing work.

REFERENCES

[1] Andersen, et al. (2007). Risk Factors for More Severe Regional Musculoskeletal Symptoms. *Arthritis & Rheumatism* **56** (4); 1355-1364.
[2] Nelson-Wong, et al. (2010). Is muscle co-activation a predisposing factor for low back pain development during standing? *J Electromyography and Kinesiol* **20**; 256-263.
[3] Lewek M, et al. (2004). Control of frontal plane knee laxity during gait in patients with medial compartment knee osteoarthritis. *Osteoarthritis and Cartilage* **12**(9);745-7

POSTURE CATEGORY SALIENCE POSITIVELY AFFECTS ANALYST DECISION TIME AND ERROR RATE

Krysia M. Fiedler[1], David M. Andrews[1], Patricia L. Weir[1], Jack P. Callaghan[2]
[1]Department of Kinesiology, University of Windsor, Windsor, ON
[2]Department of Kinesiology, University of Waterloo, Waterloo, ON

INTRODUCTION

Video-based posture assessment methods such as 3DMatch [1] require body postures to be classified into posture categories. Biomechanical loads can be quantified using this information to evaluate worker injury risk. Posture classification errors can have a sizable effect on biomechanical load calculations [2] and increased classification time can prolong analyses. Introducing geometrical elements and color into tasks requiring visual search can improve observer performance [3], but the effect that posture category salience has on analyst performance using posture-based ergonomic tools has not been assessed to date. Therefore, the purpose of this study was to investigate the effect that posture category salience (borders, shading and colour) has on the error rates and decision times of analysts during a posture sampling task on computer.

METHODS

Ninety students (45 males/45 females) with no experience in body posture evaluation selected posture categories (as quickly and accurately as possible) that best described the postures (trunk, shoulder, elbow) provided on the screen of a computer interface similar to 3DMatch. Each participant was randomly shown posture diagrams with categories in 5 different salience conditions: the current 3DMatch diagrams (plain), the posture categories with grey borders, red borders, fully shaded grey and fully shaded red. The analysts' performances were quantified in terms of their decision time and error rate.

RESULTS

There was a main effect of salience condition for decision time, with the mean decision time for the grey border and red shading conditions being the fastest and slowest, respectively (range from 2.10 to 2.24 s) (Figure 1). Overall, participants responded quickest in the two border conditions. Responses in the plain condition (current 3DMatch posture diagrams) took 0.12 s longer on average than the grey border condition.

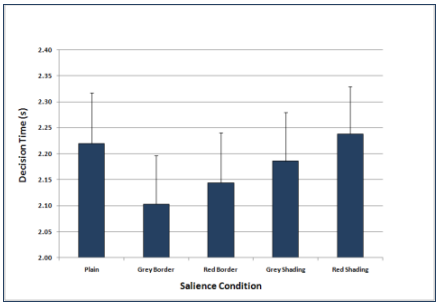

Figure 1: Decision time as a function of salience condition. All conditions were significantly different from one another ($p<0.05$), except plain and red shading.

Error rates ranged from a low of 23.6% for the red border and red shading conditions to a high of 25.1%, for the plain condition (Figure 2). Adding the colour red to the posture categories had the largest positive effect on error rates, but grey borders did reduce error rates by approximately 1% compared to the diagrams currently used in 3DMatch.

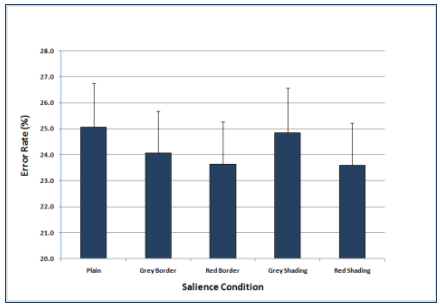

Figure 2: Error rate (% error) as a function of salience condition. All conditions were significantly different from one another ($p<0.05$), except plain and grey shading, grey border and red border, grey border and red shading, and red border and red shading.

DISCUSSION AND CONCLUSIONS

Visual search studies [3] have reported reductions of 15% in search time for letters in color backgrounds, but no difference in errors when using grey or color. The results of this study show that increasing the salience of the posture categories by adding a border will reduce classification time by 5%. This is a significant time savings if considered over long sampling cycles using 3DMatch. The addition of colour also significantly reduced classification errors. Adding a border (both grey and red) helped to improve both decision time and error rate over the plain diagrams, and would be a simple change that could be made to current posture matching based methodologies to improve analyst performance and the accuracy of results.

REFERENCES

[1] Callaghan, J.P. et al. (2003). Proceedings of XXIV ACE Conference, London, Ontario
[2] Andrews, D.M. et al. (2008). Occupational Ergonomics, 8:11-25.
[3] Michalski, R & Grobelny, W. (2008). Industrial Ergonomics, 38:321-332.

ACKNOWLEDGEMENTS

Funding for this study was provided by

DIFFERENCES IN VERBALLY ESTIMATED HAND FORCES AFFECT PEAK AND CUMULATIVE LOW BACK AND SHOULDER LOADS OF NURSES IN AN ACUTE CARE HOSPITAL SETTING

Jennifer Lembke[1], Krysia Fiedler[1], Patricia Weir[1], David M. Andrews[1]
[1]Department of Kinesiology, University of Windsor, Windsor, ON

INTRODUCTION

Hand forces are required as inputs into most biomechanical models used in workplace settings. Traditional methods of measuring hand forces, such as hand held force transducers, are not practical in many occupations, such as patient handling in nursing, where the work can't be interrupted and physically interacting with patients is not always possible. Verbalizing hand forces has been studied previously in a lab setting with some promise [1, 3], but this type of approach has not been attempted in a field setting to date. Therefore, the purpose of this study was to examine the relationship between verbally estimated and actual hand forces and quantify the resulting effect on peak and cumulative low back and shoulder loads of nurses in an acute care hospital.

METHODS

Ten female nurses (mean age 40.6 years) at a Southwestern Ontario acute care hospital were taught to verbalize their hand forces (in kg, as a %MVC) using a portable device, by providing visual feedback of applied forces during standardized push and pull exertions against resistance [1]. After training, the nurses commenced work and verbalized their peak hand forces during normal work activities over a 2 hour period. Nurses were videotaped and actual hand forces were measured when possible (non-patient handling tasks). Video clips of 150 tasks were analyzed using 3DMatch [2] to determine the peak and cumulative low back and shoulder loads when using both actual and verbally estimated hand forces. Actual and verbalized hand load magnitudes were compared and the resultant differences between peak and cumulative low back and shoulder loads (e.g. moments, compression and shear forces) were quantified as a percentage of actual low back and shoulder loads.

RESULTS

On average, nurses overestimated the actual hand loads required to perform the tasks about 83% of the time (Figure 1). Over 52% of the verbalized hand loads had magnitudes within 5 kg (+/-) of the actual hand loads, and over 92% had magnitudes between -5 kg and +15 kg of the actual hand loads. The percent of hand loads overestimated by each nurse was highly variable, with a range of 42% to 100% (i.e. 1 nurse underestimated on average across all of her tasks).

The consistent overestimation of actual hand loads by most of the nurses when verbally reported, translated into sizable differences in peak and cumulative low back and shoulder loads across subjects. Overall, approximately 45% of the actual peak and cumulative model outputs were overestimated in magnitude by more than 25%. For the low back, more than 50% of the actual peak and cumulative loads were overestimated by more than 25% when the nurses' verbalized hand loads were used in the model.

Similar trends were noted for the shoulders. Between 37% and 43% of all peak and cumulative left and right shoulder loads that were determined from verbalized hand forces were found to have magnitudes that were more than 25% greater than would have been if actual hand forces had been used.

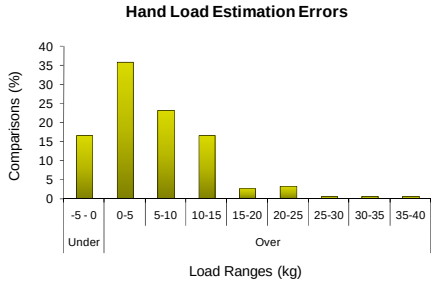

Figure 1: Range of verbalized hand load errors.

DISCUSSION AND CONCLUSIONS

Verbalizing hand loads in an occupational setting has the advantage of not disrupting normal work activities, such as those that occur between nurses and patients in a hospital. However, errors in verbalized hand forces resulted in relatively large peak and cumulative loads at the low back and shoulders in many cases, which could have significant implications for risk assessment. Refinement to the portable training device might help to improve the accuracy of verbalized hand forces in occupational settings like hospitals and should be evaluated further to see if the lower error rates consistent with laboratory evaluations can be realized in the field [1]. Individual training efforts should also target different workers as some people are much worse at perceiving how much effort they are exerting than others.

REFERENCES

[1] Burkhart, T.A. et al. (2009). Proceedings of the 22nd ISB Congress, Cape Town, South Africa.
[2] Callaghan, J.P. et al. (2003). Proceedings of 24th ACE Conference, London, Ontario, Canada.
[3] Marshall, M. et al. (2004). Human Factors, 46(4); p. 697-710.

ACKNOWLEDGEMENT

Thanks to the CRE-MSD for funding this project.

IS A LINKED, UPPER BODY MODEL APPROPRIATE FOR ESTIMATING KINEMATIC AND KINETIC PARAMETERS FOR FIELD APPLICATIONS OF INERTIAL MOTION SENSORS

Alison Godwin[1], Joan Stevenson[2,], and Susan Reid[2]
[1]School of Human Kinetics, Laurentian University, Sudbury, Canada, agodwin@laurentian.ca
[1]School of Kinesiology and Health Studies, Queen's University, Kingston, Canada

INTRODUCTION

New wireless sensors called inertial motion sensors (IMS) can be used to create motion capture systems from field applications. To acquire the required six degrees of freedom for biomechanical applications, researchers have needed to estimate positional information in some way [1]. Using a segment's rotation matrix expressed in the global coordinate system combined with a set segment length [1] can produce relative positional coordinates with error ranging from 2cm to 8cm [2]. These positions can be used in a 3-D, inverse dynamic model to calculate forces and moments for any joint of interest in the linked model. Working with a lower-body, upwards model, error in knee adduction moment representing 10% of the peak moment during walking was considered unacceptable [3].

The purpose of this study was to compare the predicted positional coordinates generated with an upper-body linked model to the same coordinates calculated with gold standard, optoelectronic data. Kinetic comparisons are also made.

METHODS

The gold standard kinematic data were acquired from six infrared video cameras recording at 60Hz. The subject was outfitted with three non-collinear markers on each of the seven segments in the upper-body model. Tracking markers were related to internal joint locations using a calibration trial with additional markers used to demarcate specific anatomical landmarks. Using set segment lengths and global rotation matrices for each segment, relative joint locations were calculated by defining the base joint (L5/S1) as a (0,0,0) starting point and adding segment endpoint coordinates together from the first joint to the last in the upper-body model. Both sets of positions were input into a recursive inverse-dynamic link-segment hands-down model. The joint positions predicted from the upper-body model are expressed as RMS error compared to the reconstructed, true joint positions.

RESULTS

RMS values for positional coordinates during sweeping and table-washing trials ranged from a low of 2.1 mm at the first estimated joint position (T12/L1) to maximal values of 71 mm in the right wrist joint during table-washing motion (Table 1).

Using the predicted coordinates to calculate joint moment resulted in RMS errors in lumbar extensor moment ranging from 2.8-6.1Nm (6-19% of peak) during a lifting motion. Lateral bend moment errors were between 2.2Nm-5.9Nm RMS.

Table 1: RMS positional error (mm) for all joints in upper-body model during sweeping and table-washing motions

	Positional Error					
	Sweeping Motion			**Table-Washing Motion**		
Joint	X	Y	Z	X	Y	Z
T12/L1	2.1	5.5	6.3	10.3	6.9	15.7
C7/T1	3.3	12.1	5.9	17.2	15.9	18.0
R. Shoulder	3.3	12.2	5.9	17.9	15.6	22.6
Right Elbow	30.9	23.2	29.6	36.5	33.7	44.9
Right Wrist	54.1	56.8	26.9	62.1	66.0	71.0

DISCUSSION AND CONCLUSIONS

Given the existing attempts to reproduce relative position, the errors in position estimation for our experiment were not unreasonable considering that the upper-body model is more complex than previous two-link systems modeled [1,3].

The upper-body model approach using predicted segment endpoints shows good potential compared with other attempts at a feet-up system [3,4]. Optimizing the calibration method using a more advanced method and improving the anatomical model assumptions could greatly improve lumbar moment estimation in the proposed system.

REFERENCES

1. Z. H. & H. H. (2007). Upper limb motion estimation from inertial measurements. *International Journal of Information Technology, 13*(1), 1-14.
2. Z. H. et al. (2006). Inertial measurements of upper limb motion. *Medical and Biological Computing, 44*, 479-487.
3. v. J. et al. (2008). Ambulatory estimation of knee adduction moment: Accuracy and sensitivity. Proceedings from 3DMA: 10th International Symposium on 3D Analysis of Human Movement. Santpoort: The Netherlands.
4. F. G., et al. (2008). Determination of 3D L5-S1 moments using instrumented shoes. Proceedings from 3DMA: 10th International Symposium on 3D Analysis of Human Movement. Santpoort: The Netherlands.

ACKNOWLEDGEMENTS

Funding was provided by the Workplace Safety and Insurance Board of Ontario, Canada.

PRELIMINARY ASSESSMENT OF LIFTING TECHNIQUE CHANGES IN A PROLONGED LIFTING TASK

Robin Hampton, Matthew Cochran, Usha Kuruganti, Wayne J. Albert
Faculty of Kinesiology, University of New Brunswick, Fredericton, Canada, c244y@unb.ca

INTRODUCTION

Manual material handling has been associated with musculoskeletal disorders of the back and shoulders. Currently, there is minimal understanding of the postural and neuromuscular adaptations experienced during a fatiguing task, and the combined effects of joint loading changes. The etiology of these types of disorders is considered to be multifaceted [1] requiring a complete investigation into the kinetic, kinematic and neuromuscular changes, in order to better understand the underlying effects of fatigue. The purpose of this pilot project was to investigate the muscular and lifting kinematic changes that occur during a prolonged fatiguing lifting task.

METHODS

Eight healthy male participants (Mean age 26 years; height 177cm; weight 81kg)) were recruited from the University student population. The participants performed a repetitive upper extremity task which involved lifting and lowering an 8.4 kilogram crate from waist to shoulder height. The subjects performed this task at a rate of six lifts per minute over a 90-minute period. Neuromuscular and movement data were collected for one minute samples at the beginning of the experiment and at 15-minute intervals for the remainder of the experiment. Motion tracking was performed using an electromagnetic tracking system (Polhemus Liberty Latus, Vermont, USA). The 6 DOF motion tracking sensors were placed at the centre of gravity of the hands, forearms, upper arms, and trunk.

Neuromuscular activity was recorded using an 8-channel electromyography (EMG) system (Bortec Octopus, Bortec Biomedical LTD., Alberta, Canada). Bipolar surface electrodes (Duotrode silver silver-cloride electrodes, Myo-tronics, In., Kent, WA; interelectrode spacing = 21.0 ± 1mm) electrodes were placed at sites based on established electrode placements (SENIAM) for the anterior deltoid, middle deltoid, upper trapezius, lower trapezius, biceps brachii (long head), triceps brachii (lateral head), erector spinae at the thoracic (T8) and lumbar (L1 & L5) levels. The myoelectric signal was collected at 1500 samples per second and the raw signal was band pass filtered from 20-500 Hz. A metronome was used to influence the lifting rate of the subjects. Data was imported and processed using Labview (National Instruments Corp., Texas, United States of America). A trigger was incorporated into the programs to allow for synchronization of the motion and EMG data.

Preliminary analysis of the data included assessment of muscular activity, specifically the amplitude of the signal quantified with the root mean square (RMS) value and median frequency (MF) between the first and final collection interval as well as lifting kinematics.

RESULTS

Initial assessment of group data indicated that there was no observed change in either the RMS or MF over the 90-minutes of prolonged lifting suggesting that there was no neuromuscular fatigue detected [2]. In fact some participants exhibited an increase in MF in selected muscles. In terms of kinematics, the group data showed no change in the lift time by revealed a significant difference in the trunk range of motion namely an increase in trunk extension. There were also changes in the lift trajectory of the load indicating a change in motion pattern.

Observation of the RMS data for each person across the eight muscle group suggests significant fluctuation in muscle recruitment patterns. There is a clear indication of muscle trade-off occurring during the entire lifting time, but the pattern is rather individual in nature. For example, the anterior and middle deltoid RMS patterns were mimics of each other with three participants demonstrating a continuous increase (suggesting the presence of some fatigue), three with a continuous decrease and the other increasing and decreasing activity at each collection period. These differences are likely due to individual differences and the lack of constraint in completing the activities. Three participants demonstrated an increase in RMS for all muscles over the entire lifting period, except for the final collection period, suggesting an increase in motor unit recruitment, while the other 5 a pattern was less clear as there was continuous tradeoff between the deltoids, biceps and trunk muscles. Future work will examine the role of muscle co-contraction and the changes between the relative contributions of muscle activity to further elucidate evidence of fatigue.

REFERENCES

[1] Fuller, J. et al. (2009). Posture-movement changes following repetitive motion-induced shoulder muscle fatigue. Journal of Electromyography and Kinesiology 19(6); 1043-1052

[2] C. J. De Luca. 1997. *The use of surface electromyography in biomechanics.* Journal of Applied Biomechanics. 13(2): 135-163.

ACKNOWLEDGEMENTS

This project was funded in part by an NSERC Discovery Grant and AUTO21 Network Centres of Excellence funding.

EARLY-STANCE DIFFERENCES BETWEEN TOTAL ANKLE ARTHROPLASTY AND ARTHRODESIS

Jason Fong[1], Janie L Astephen Wilson[1], Kory Arsenault[2], Patricia Francis[2], Mark Glazebrook[1,2]
[1]School of Biomedical Engineering, Dalhousie University, Halifax, Canada, jason.fong@dal.ca, http://bme.medicine.dal.ca
[2]Department of Surgery, Division of Orthopaedics, Dalhousie University, Halifax, Canada

INTRODUCTION

End-stage ankle arthrosis is typically treated with ankle arthrodesis (AA) (i.e. joint fusion) [1,2,4]. However, AA has been related to ipsilateral degeneration of the contiguos foot joints [1]. There is renewed interest in total ankle arthroplasty (TAA) as a treatment due to design innovations and improvement in gait characteristics [2,4]. One study has compared TAA and normal gait with kinematics and kinetics [2], and another study has compared AA, TAA, and normal gait with ground reaction force and range of motion [4]. Neither of these studies compares AA and TAA gait with kinetics and kinematics. The objective of this study was to compare post-operative ankle and knee joint kinematics and kinetics in the early-stance phase (ESP) between AA and TAA.

METHODS

Sixteen patients participating in a randomized control trial for TAA and AA underwent postoperative (2-4 years) gait analysis. Eight patients had undergone TAA implanting the Mobility Total Ankle System (DePuy, Indiana, USA) and eight had undergone AA using the fibular-sparing Z-osteotomy technique. One surgeon performed all of the surgeries. Each subject performed five walking trials at their self-selected velocity, and in their comfortable walking shoes. Gait data was collected using an Optotrak® motion capture system (NDI, Waterloo, Canada) and an AMTI force platform (AMTI, Massachusetts, USA). Ankle and knee joint kinematics were calculated according to the joint coordinate system, and net resultant moments were calculated using an inverse dynamics approach. A single-segment foot model was used. Peak ankle and knee joint angles and moments during ESP were extracted and compared between the AA and TAA groups using one-way ANOVA (ESP was defined as 0-20% gait cycle) ($p<0.05$).

RESULTS

There was a significant difference in the peak abduction angle during ESP of the ankle ($p=0.019$) and of the knee ($p=0.029$) between TAA and AA (Table 1). In both of these cases, the angles were larger in the TAA group than in the AA group. There were also significant differences in the ESP knee peak flexion angle ($p=0.045$) and the ankle peak abduction moment ($p=0.035$) (Figure 1).

Table 1: Mean (standard deviation) early-stance phase (ESP) TAA and AA peak and total mean joint angles and moments (‡ denotes statistically significant difference).

Description	TAA	AA	p
Joint Angular Positions [°]			
ESP Peak Ankle Abduction‡	8.1 (3.6)	4.4 (1.5)	0.019
ESP Peak Knee Abduction‡	1.9 (1.8)	-0.3 (1.9)	0.029
ESP Peak Knee Flexion‡	11.5 (5.9)	17.2 (4.2)	0.045
Joint Moments [N • m / B. Wt.]			
ESP Peak Ankle Abduction‡	0.02 (0.01)	0.05 (0.03)	0.035

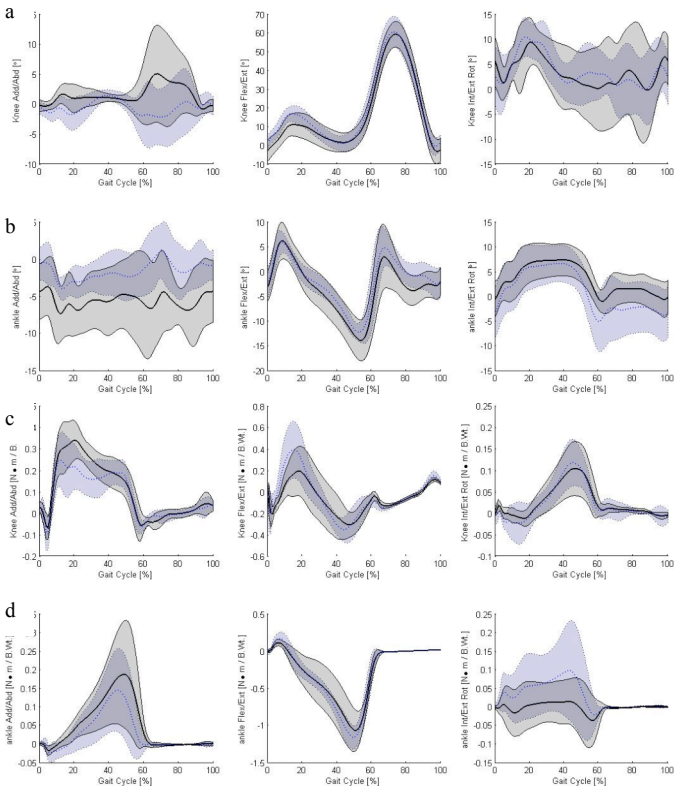

Figure 1: Knee (*a,c*) and Ankle (*b,d*) Mean Joint Angles (*a,b*) and Moments (*c,d*) for the TAA (*black solid*) and AA (*blue dotted*) gait trials. *Left to right*: add/abd, flex/ext, and int/ext rotation. Shaded regions are the respective standard deviations.

DISCUSSION AND CONCLUSIONS

The reduced ankle peak abduction angle in the AA patients is intuitively related to the fused talocrural joint. However, the intuitive changes in the flexion-extension angles and moments had not been discriminated between TAA and AA likely due to the nature of the single-segment foot model used and the limited statistical power of this pilot study. Higher ESP ankle peak abduction moments in AA patients can likely be attributed to the reduced force attenuation following the high impact heel contact in the fused joint. Changes in the knee peak abduction and flexion angles may be due to compensation associated with the limited movement in the fused ankle. Improved gait characteristics in TAA over AA are supported by this study; however further investigation into changes at the contiguous foot joints with both surgeries should be investigated with multi-segment foot models [3].

REFERENCES

[1] Coester LM et al. (2001). *JBJS Am* **83-A**; p. 219-28.
[2] Doets HC et al. (2007). *FAI* **28**; p. 313-22.
[3] Leardini A et al. (2007). *Gait & Posture* **25**; p. 453-62.
[4] Pirou P et al. (2008). *FAI* **29**; p. 3-9.

TOWARDS THE REDUCTION OF FALL-RELATED INJURY RISK: NOVEL COMPLIANT FLOORS DO NOT INFLUENCE RATE OF BALANCE CONTROL RESPONSES IN OLDER WOMEN

Alexander D. Wright[1], Andrew C. Laing[1]
[1]Department of Kinesiology, University of Waterloo, Waterloo, Canada, a9wright@uwaterloo.ca

INTRODUCTION

Fall-related injuries in adults over the age of 65 years cost the Canadian Health Care system in excess of $2.0 billion per year in direct costs [1]. To minimize the social and economic burden associated with the aging of Canada's population, interventions must be developed to minimize the projected rise in incidence of fall-related injuries over the next 25 years. Novel compliant flooring systems provide a promising intervention approach. During simulated sideways falls on the hip, they have been shown to attenuate the impact force applied to the proximal femur by 25-50% [2]. The purpose of this study was to determine if such benefits are achieved at the expense of impaired underfoot centre-of-pressure (COP) position and rate responses in older women.

METHODS

Thirteen women between 65-90 years of age stood on flooring samples (rigid, SmartCell and SoftTile (novel compliant floor products), Firm-Foam, Soft-Foam) mounted on a motorized perturbation platform. Using ankle and/or hip strategies while keeping the feet stationary, participants were required to maintain balance following a sudden 26.5 cm posterior floor surface translation. A force-plate and motion capture system recorded centre-of-gravity (COG) and COP (Figure 1). Rates of change in COP displacement from the pre-perturbation position were calculated for 4 regions of the response curve: 0 to 2 cm, 2 to 4 cm, 4 to 6 cm, and 6 to 8 cm. We also measured how closely the COG and COP approached the anterior base-of-support limit defined by the participant's toes (margin-of-safety (MOS)).

RESULTS

Repeated measures ANOVA indicated that flooring type was significantly associated with COP displacement rates in all four regions (Table 1). Compared to the rigid floor, paired t-tests indicated that COP rates were significantly slower only for the SofTile ($p=0.025$), Firm-Foam ($p<0.001$) and Soft-Foam ($p=0.001$) conditions in the 4 to 6 cm region, and the Firm-Foam ($p=0.002$) and Soft-Foam ($p<0.001$) conditions in the 6 to 8 cm region. Repeated measures ANOVA also indicated floor condition was associated with COG and COP margin-of-safety. Compared to the rigid floor, paired t-tests demonstrated that *COP_MOS* was significantly smaller for the Firm-Foam condition ($p=0.009$), and *COG_MOS* was significantly smaller for Firm-Foam ($p<0.001$) and Soft-Foam ($p=0.001$) conditions.

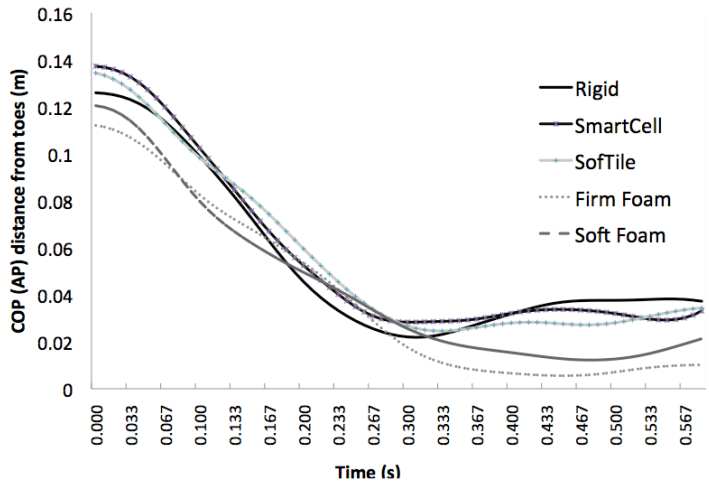

Figure 1: Sample plot of COP position with respect to toes versus time for one subject.

DISCUSSION AND CONCLUSIONS

Novel compliant flooring systems including SmartCell and SofTile can attenuate impact force by 50% during simulated falls on the hip, and have limited influence on clinical measures of balance including quiet stance sway and the Timed Get Up and Go test [2]. The current study demonstrates that these benefits may be achieved without concomitant impairments in COP balance control responses in older women. Together, these results provide further support for the potential for appropriately designed compliant floors to reduce the incidence and severity of fall-related injuries in seniors.

REFERENCES

[1] SMARTRISK (2009). Economic Burden of Injury in Canada. SMARTRISK: Toronto, ON.
[2] Laing, A.C., and Robinovitch, S.N. (2009). Low stiffness floors can attenuate fall-related femoral impact forces by up to 50% without substantially impairing balance in older women. *Accid Anal Prev* Vol **41**(3); p. 642-650.

Table 1: Mean (SD) of COG and COP margin of safety and COP displacement rate for each floor condition

	p for RM ANOVA	Rigid	SmartCell	SofTile	Firm-Foam	Soft-Foam
COG_MOS (cm)	<0.001	5.81 (1.29)	6.21 (0.99)	5.12 (1.29)	*2.68 (1.29)	*4.45 (0.98)
COP_MOS (cm)	0.006	2.56 (0.80)	2.95 (0.74)	2.10 (1.15)	*1.66 (1.45)	1.93 (1.07)
COP_0to2 (cm/s)	<0.001	22.5 (0.02)	22.8 (0.03)	*27.0 (0.04)	23.7 (0.03)	*27.2 (0.03)
COP_2to4 (cm/s)	0.034	52.1 (0.07)	53.8 (0.07)	57.2 (0.08)	45.3 (0.08)	61.6 (0.17)
COP_4to6 (cm/s)	<0.001	57.1 (0.10)	55.6 (0.10)	*49.8 (0.06)	*32.5 (0.06)	*37.9 (0.08)
COP_6to8 (cm/s)	<0.001	49.7 (0.15)	49.5 (0.11)	47.1 (0.10)	*30.0 (0.04)	*24.2 (0.06)

* indicates significant difference ($p<0.05$) from rigid condition based on paired t-tests

HEEL COMPLIANCE AND WALKING MECHANICS USING THE NIAGARA FOOT PROSTHESIS

Valérie Wellens[1], Joel L. Lanovaz[1, 2], J. Tim Bryant[3]
[1]Division of Biomedical Engineering; [2]College of Kinesiology, University of Saskatchewan, Canada, v.wellens@usask.ca
[3]Department of Mechanical and Materials Engineering, Queen's University, Canada

INTRODUCTION

The Niagara Foot, a new prosthetic foot design constructed from injection-molded thermoplastic, was developed to fulfill the need for improved foot prosthesis in developing countries. The Niagara Foot combines low cost and durability with high performance energy return features. One of the unique features of the Niagara Foot is that the stiffness of both the keel and heel are adjustable. This can be done directly by the prosthetist by removing material from selected portions on the foot. Keel stiffness has been studied fairly extensively, however less is known about the effect of heel compliance of a prosthetic foot [1], especially in vivo. The current study is designed to characterize the effect of the heel stiffness modifications on gait mechanics during walking in persons with unilateral below-knee amputations using the Niagara Foot.

METHODS

Five active male subjects (mean: 52.8 yrs, 81.31kg), each with a unilateral below-knee amputation (average time post amputation: 12 years) walked at a self-selected pace across a 6-meter walkway. A force platform (OR6, AMTI, Watertown, MA) embedded in the walkway recorded the ground reaction forces (SR 2000 Hz). At the same time, the 3D kinematics of both lower limbs as well as pelvis were recorded (SR 100Hz) using an 8-camera motion capture system (Vicon Nexus, Vicon Motion Systems, CO.). Static and functional dynamic calibrations were used to locate the positions of the hips, knee and ankle centres.

Standard inverse dynamics methods were used to calculate hip and knee torques and joint powers for both the affected and unaffected limbs for each subject. Peak moments during the stance phase were identified along with joint power peaks typically associated with walking [2].

The experiment was a within-subjects design examining two levels of heel stiffness using the Niagara Foot. The first heel stiffness level corresponded to the standard unmodified Niagara Foot (NF1). The second, more compliant heel stiffness condition (NF2) was generated by reducing the standard heel thickness by 20%. Each subject underwent two separate data collection sessions for NF1 and NF2, each preceded by a two-week adaptation period. For each condition, five trials for each limb of each subject were analyzed.

RESULTS

The average velocity between conditions was not significantly different within subjects (mean 1.13 m/s SD 0.13 m/s). There were considerable inter-individual differences in gait patterns although intra-individual patterns were fairly consistent. Most of the effects of the compliant heel could be seen during the early stance phase of the affected limb. At this time point, 4/5 subjects showed an increase in energy absorption at the knee (K1 peak) which was accompanied by a decrease in energy generation at the hip in both the affected (H1) and unaffected limbs (H3).

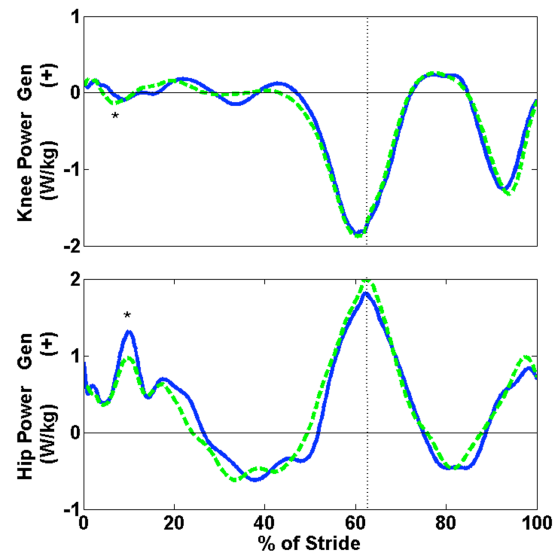

Figure 1: Knee and hip power during the stance phase (Solid blue line: stiff heel NF1, Dash green line: compliant heel NF2, Vertical dotted line delineate stance and swing)

DISCUSSION AND CONCLUSIONS

This study is the first to examine the effect of heel compliance on walking gait characteristics in subjects with below-knee amputations using the same prosthetic foot for both rigidities. High inter-individual variability precluded statistical tests in this small study. However, consistent differences were seen during the weight acceptance phase of the affected limb which is the most logical time point when considering the change to heel compliance.

A K1 power peak is not typically reported in gait patterns of subjects with below-knee amputations [3,4] although this is not always the case [5]. The increase in K1 magnitude seen in this study may indicate that a more compliant heel on a prosthetic foot like the Niagara Foot moves knee mechanics towards a gait pattern similar to the unaffected side.

REFERENCES

[1] Klute G.M. et al. (2001) J Rehabil Res Dev **41** (4); p. 535-546.
[2] Winter D.A. Biomechanics and motor control of human movement, 4rd ed., Waterloo, ON (1991)
[3] Winter D.A. & Sienko S.E. (1988) J Biomech **21** (5); p. 361-367
[4] Powers C.M. et al. (1998) Gait & Posture **8** (1); p.1-7
[5] Gitter A. et al. (1991) Am J Phys med Rehabil **70** (3) p. 142-148.

BIOMECHANICAL CHANGES DUE TO TOTAL KNEE ARTHROPLASTY WITH TWO IMPLANT DESIGNS

Allison L. Clouthier, Scott C.E. Brandon, Kevin J. Deluzio*, John F. Rudan
Department of Mechanical and Materials Engineering, Queen's University, Kingston, Canada
*deluzio@me.queensu.ca

INTRODUCTION

Patients with knee osteoarthritis often receive total knee arthroplasty (TKA) surgery to increase function and reduce pain. It has been shown that there is a significant improvement in the activities of daily living for these patients following surgery [1]. In this randomized study, knee kinematics and kinetics were compared pre- and post-operatively for two implant designs in order to determine the effect TKA has on gait as well as biomechanical differences between the two implant designs.

METHODS

A group of 30 subjects (16 male, 14 female; height 1.70 ± 0.10 m; weight 91.3 ± 15.4 kg) walked at self-selected speed within 6 months before, and again within 1 year after TKA. A fixed-bearing implant (Sigma Fixed-Bearing, DePuy, Warsaw, IN) was randomly assigned to 13 subjects, while the remaining 17 subjects received a rotating-bearing design (Sigma Rotating-Bearing, DePuy, Warsaw, IN). Subjects were assessed using the WOMAC, SF-36, and KSS grading scales. 3D gait analyses were performed using an Optotrak motion analysis system (Northern Digital Inc., Waterloo, ON) and an AMTI force platform (Advanced Mechanical Technology Inc., Watertown, MA) operating at 100Hz and 1000Hz, respectively. External knee moments were calculated using standard 3D inverse dynamics approach [2]. Principal component analysis was used to extract features of knee moments and angles that differentiated between pre-and post-operative conditions, as well as implant types. Fixed- and rotating- implant groups were compared using a two-way ANOVA with surgery as the repeated measure at a significance level of $P = 0.05$. Post-Hoc comparisons were performed in SAS 9.2 (SAS Institute Inc., Cary, NC, USA) using the Sidak adjustment.

RESULTS

After surgery, subjects showed significant improvement in pain and function as measured by WOMAC, SF-36, and KSS scores. Self-selected walking speed was significantly faster post-operatively (1.03 vs 0.96 m/s). Three biomechanical features that were significantly different after surgery are shown in Figure 1. The knee adduction moment during stance (Figure 1a) was significantly reduced post-operatively, but only in subjects with a rotating-bearing implant. Conversely, only subjects who received the fixed-bearing implant exhibited an increased range of motion and stance magnitude for knee flexion angles (Figure 1b). Regardless of the type of implant, subjects walked with greater flexion moment amplitudes after TKA (Figure 1c). A post-operative decrease in frontal plane adduction angle was not significant ($P = 0.07$), regardless of implant type.

DISCUSSION AND CONCLUSIONS

Fully randomized trials are rare in orthopaedic studies. This study was able to identify three implant-specific biomechanical changes due to TKA. The finding of increased postoperative walking speed is in accordance with previous investigations [3]. The knee adduction moment is perhaps the most important biomechanical factor as it relates directly to surgical outcome [4]. In this study, the knee adduction moment was reduced after TKA only for subjects who received a rotating-bearing implant. However, the rotating-bearing subjects also had significantly greater knee adduction moment magnitudes before surgery. While the difference between rotating- and fixed-bearing implants could be important for future implant design and selection, it is necessary to expand this study to eliminate the possibility of a bias in the subject groups.

REFERENCES

[1] Kane RL et al. (2005). *JBJS.Am.* **87:** 1719-24.
[2] Landry SC et al. (2007). *J.Biomech.* **40:** 1754-61.
[3] Börjesson M et al. (2004) *The Knee* **12:** 121-27.
[4] Miyazaki T et al. (2002) *Ann.Rheum.Dis.* **61:** 617-22.

ACKNOWLEDGEMENTS

This study was funded by DePuy Canada Inc.

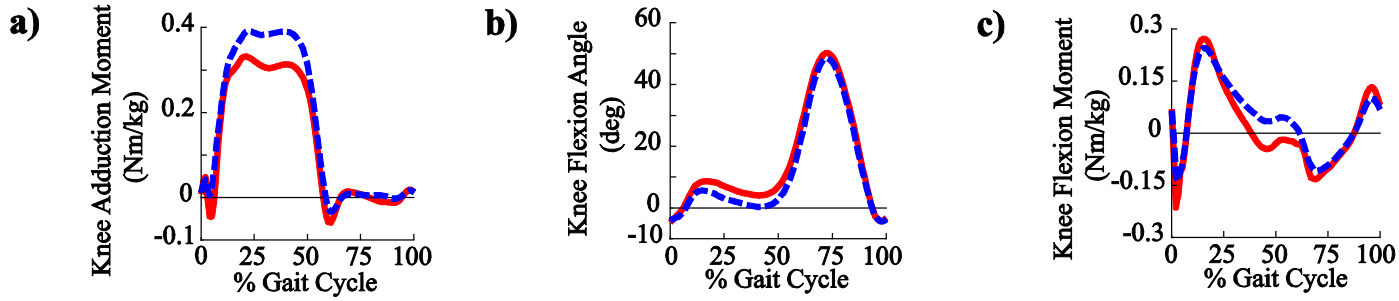

Figure 1: Mean gait waveforms before (dashed blue line) and after (solid red line) unilateral total knee arthroplasty. The knee flexion angles shown in figure (b) include only subjects who received the fixed-bearing implant

SHEAR AND VERTICAL FORCE CONTRIBUTIONS TO FRONTAL PLANE BALANCE WITH A ROLLATOR

James Tung (james.tung@utoronto.ca) [1,4], Brian Maki[2,4], William McIlroy[3,4]
[1]Graduate Department of Rehabilitation Science, University of Toronto, Toronto, Canada, james.tung@utoronto.ca
[2]Centre for Studies in Aging, Sunnybrook Health Sciences Centre, Toronto, Canada
[3]Department of Kinesiology, University of Waterloo, Waterloo, Canada
[4]Toronto Rehabilitation Institute, Toronto, Canada

INTRODUCTION

Rollators, or 4-wheeled walkers, are frequently used to assist with maintaining balance by permitting the upper limbs to be involved in sensing instability and generating stabilizing moments [1]. When using a rollator, the upper limbs are important effectors of frontal plane balance control in quiet standing [2] and straight-line walking [3]. While previous studies have demonstrated the importance of upper limb involvement to compensate for restricted lower limb capabilities, the contributions of shear and vertical loading to generate stabilizing moments have not been examined.

Upper limb stabilizing torques in the frontal plane can be generated by applying: i) shear forces (H_{x1}, H_{x2}; see Figure 1) through the moment arm defined by the height of the handles; and/or ii) vertical forces (H_{z1}, H_{z2}) acting through the distance between the hands and the COM (d). Since the height of the handles is considerably larger than d, applying shear forces would have a greater mechanical advantage. Conversely, excessive shear forces could result in tipping the rollator frame. We hypothesize that upper limb balance control would select a strategy that maintains stability of the support surface to minimize the risk of tipping. Specifically, we predict that the stabilizing moments generated through shifts in vertical loading would be significantly higher than moments generated through shear forces in quiet standing, particularly when reliance on upper limb involvement is greater.

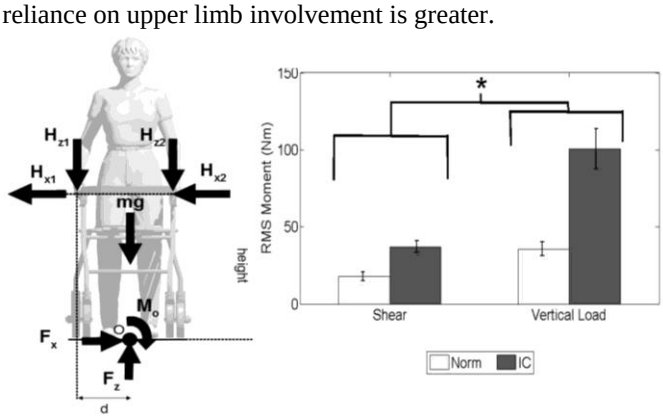

Figure 1: Frontal plane free body diagram (left) and RMS moment contributions of shear and vertical loading components (right). Norm = normal stance; IC = increased challenge condition.

METHODS

Eleven (11) healthy, young adults (7F, 20-35y, 50-100 kg) without history of musculoskeletal or neurological impairments participated in this study. Participants performed a stationary standing task while holding the rollator under 2 conditions: i) a normal (Norm) condition (feet apart; eyes open; and ii) an increased challenge (IC) condition (feet together; on foam; eyes closed). The rollator handles were adjusted to the height of the radial styloid with arms straight.

Upper limb forces were measured from ground reaction forces acquired from 3 forceplates under the rollator (i.e., isolated from the feet) and resolved into shear (F_x), vertical (F_z), and frontal plane moment (M_o) components. Forceplate data was acquired for 60s in each condition, and low-pass filtered (2nd order Butterworth; 10 Hz cutoff) prior to analysis. To separate the two components of the net righting moment, the shear component was calculated by multiplying the shear force record (F_x) with the height of the handles. The vertical load component was calculated by taking the difference between the net moment (M_o) and the calculated shear contribution. RMS values of the final 30 seconds of each trial were calculated to measure the torque contributions to stability. A 2-way ANOVA was computed with component (shear/vertical load) and condition (Norm/IC) as main factors.

RESULTS

As hypothesized, the vertical loading component (Mean±SE; Norm: 32.6±4.1 Nm, IC: 100.7±13.1 Nm) was significantly higher ($p < 0.001$) than the shear component (Mean±SE; Norm: 27.1±3.7 Nm, IC: 35.7±4.6 Nm). Furthermore, the relative contribution of the vertical loading component increased more under IC conditions than the shear contribution, indicated by a significant interaction effect ($p = 0.004$).

DISCUSSION/CONCLUSION

The main finding of the study was that stabilizing moments generated through shifts in vertical loading were significantly greater than the shear contribution in quiet standing. Understanding the relative contributions of these forces will impact the assessment of the effectiveness of current rollator assistive device designs, influence prescription guidelines, and recommendations for device training and safety.

REFERENCES

[1] H. Bateni and B.E. Maki (2005). Assistive devices for balance and mobility: benefits, demands, and adverse consequences. *Archives of Physical Medicine and Rehabilitation*, Vol. **86**, p. 134-45.
[2] Tung, JY et al. (2006) Balance Related to Rollator Use. *14th Canadian Society of Biomechanics*, Waterloo, ON.
[3] Tung, JY et al. (2009). Frontal Plane Stabilizing Moments During Assisted Walking: Older Adult Assistive Device Users and Beam-Walking Controls," *19th Int'l Society Posture & Gait Research*, Bologna, Italy.

CHARACTERIZING FOOT PLACEMENT PATTERNS DURING REAL-WORLD ROLLATOR USE: INITIAL DEVELOPMENT AND VALIDATION

Justin Chee[1], James Tung[1], William Gage[2], William McIlroy[1,3], Karl Zabjek[1]
[1]Graduate Department of Rehabilitation Science, University of Toronto, Toronto, ON, justin.Chee@utoronto.ca
[2]School of Kinesiology and Health Science, York University, Toronto, ON
[3]Department of Kinesiology, University of Waterloo, Waterloo, ON

INTRODUCTION

Mobility impairments often become manifested during gait as changes in step width or step width variability[1]. Assistive mobility devices are commonly prescribed to enhance medio-lateral stability and prevent falls in patients with poor lateral balance control. Through quantifying rollator-assisted gait characteristics, without using a laboratory-based motion capture system, we may enhance our understanding of how these devices influence their user's gait patterns in a real-world environment. The purpose of this study was to assess the validity of a novel algorithm to extract step width from video data recorded directly on-board an instrumented walker (i.e. iWalker).

METHODS

Five able-bodied young adults (mean: 27±3 years) were recruited to ambulate across an in-laboratory walkway at their preferred step width and walking speed. Step width was quantified using both an Archos 404 digital video camera (Archos, CO, U.S.A.), mounted on-board the iWalker (i.e. the footcam) (Figure 1), and a 7-camera Vicon MX Motion Capture System (Vicon, CO, U.S.A.). The footcam was oriented backwards towards the user's feet to capture the position of toe markers (Figure 2). Matlab code was applied to correct for parallax error in the video image and the 2-D marker position was extracted using Peak Motus software (Vicon, CO, U.S.A.). Step widths were calculated and compared to those obtained using Vicon.

RESULTS

The average step widths calculated by the iWalker and Vicon systems were 14.9 ± 4.7 cm and 14.2 ± 4.4 cm respectively, with an average root mean square (RMS) difference of 0.70 cm. As such, there was a strong correlation between the two methods (R2=0.9817) (Figure 3).

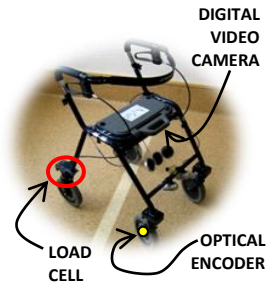

Figure 1: The i-Walker

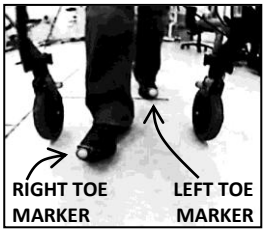

Figure 2: Footcam View

DISCUSSION AND CONCLUSIONS

Due to the high agreement between the Vicon and iWalker systems, we believe that our camera-based process of calculating step width provides an accurate assessment of foot placement during rollator use. Ongoing work is being conducted to characterize the real-world step width patterns of balance-impaired patient populations, such as individuals with multiple sclerosis, traumatic brain injury, stroke, and THA.

REFERENCES

[1] Brach, J.S. et al. (2008). Stance time and step width variability have unique contributing impairments in older persons. *Gait & Posture* Vol 27(3); p. 431-9.

ACKNOWLEDGEMENTS

CIHR Pilot Projects in Aging grant awarded to Dr. Zabjek & Dr. McIlroy.

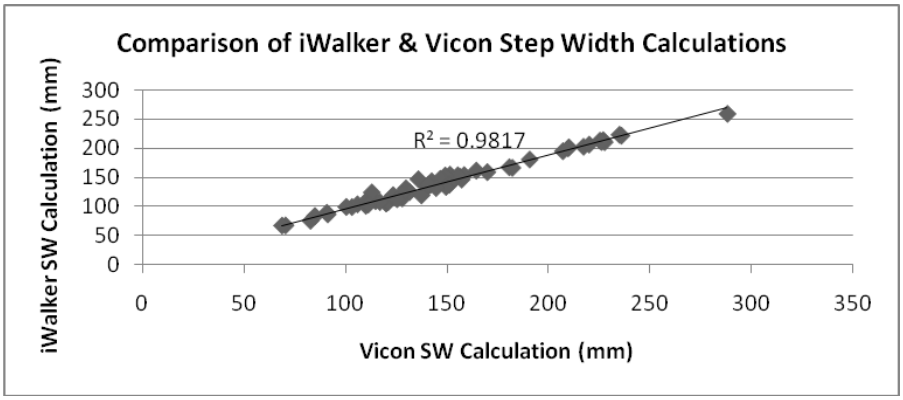

Figure 3: Comparison of iWalker & Vicon step width calculations.

EFFECT OF TOTAL KNEE ARTHROPLASTY ON THE TOTAL SUPPORT MOMENT DURING GAIT

Gillian Hatfield[1], Cheryl Hubley-Kozey[1], Michael Dunbar[1,2]
[1]School of Biomedical Engineering, Dalhousie University, Halifax, Canada, GHatfield@dal.ca
[2]Department of Surgery, School of Biomedical Engineering, Dalhousie University, Halifax, Canada

INTRODUCTION

The total support moment represents the magnitude of extensor synergy of the lower extremity needed to prevent collapse during stance phase of gait. It has been reported to be less variable than any of the individual joint moments [1, 2]. A decrease in the first peak of the total support moment has been reported six months following total knee arthroplasty (TKA), in combination with decreased contributions from the knee and increased contributions from the hip to this peak [2]. No studies have examined longer term changes to the total support moment of the lower extremity following TKA, and no studies have used pattern recognition techniques to quantify changes to the total support moment. The purpose of this study was to use principal component analysis (PCA) to investigate changes in the total support moment at one and two years post-TKA. In addition, the contributions of the hip, knee and ankle to the first peak in the total support moment were investigated.

METHODS

30 patients (mean age 66 ± 6 years) had their gait analyzed within one week of TKA surgery, and 1 and 2 years post-TKA. Ground reaction forces were measured using an AMTI™ force platform (Advanced Mechanical Technology Inc, Watertown MA) sampled at 1000 Hz. Segment motion was recorded at 100 Hz using an Optotrak™ motion capture system (Northern Digital Inc, Waterloo ON) synchronized with the force platform. Motion and force data were used to calculate three-dimensional moments at the hip, knee and ankle using inverse dynamics [3]. The internal extensor moments at each joint were summed to calculate the total support moment of the lower extremity [1,2]. The total support moment waveform and the extensor waveforms for the hip, knee and ankle were analyzed using PCA [3]. Repeated measures (test) ANOVA models (α=0.05) were used to detect significant changes in the PC *scores* for each waveform separately at each testing period. The contribution of the extensor moments from each lower extremity joint to the first peak in the total support moment was determined and compared at each testing period using a repeated measures ANOVA (α=0.05).

RESULTS

Walking velocity increased significantly from pre to 1-year post-TKA (0.91 m/s to 1.07 m/s), but was not different between 1 and 2 years post-TKA (1.08 m/s). The total support moment waveforms can be seen in Figure 1. The overall magnitude of the total support moment waveform decreased 2 years post-TKA (significantly lower PC1 *scores*). The decreased magnitude could be attributed to the significant decrease in magnitude of the hip extensor moment 2-years post-TKA (significantly lower PC1 *scores*). There were no magnitude changes in the knee or ankle extensor moments.

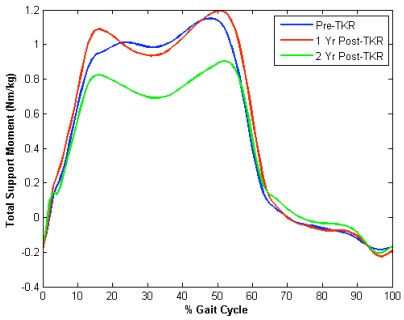

There was also a change in shape of the waveforms. The peaks in the total support moment waveform were more prominent post-TKA (significantly higher PC3 *scores*). The hip and knee extensor moment waveforms were more biphasic post-TKA (significantly higher PC2 *scores*). The ankle extensor moment waveform was also more biphasic (significantly higher PC3 *scores*) post-TKA. In agreement with the PCA results, the magnitude of the first peak in the total support moment was significantly lower at 2-years post-TKA. At each testing period the hip was the biggest contributor to the first peak. By 1-year post-TKA the ankle contribution had significantly decreased, and by 2-years post-TKA the knee contribution had significantly increased.

DISCUSSION AND CONCLUSIONS

Consistent with previous work [2], the amplitude of the total support moment decreased post-TKA. This is the first study to report temporal changes in the waveform, which can be attributed to more biphasic patterns of the individual joint extensor waveforms post-TKA. The decrease in mid-stance moment represents a more typical pattern. In contrast to previous findings [2], no changes in contribution to the total support moment were seen at the hip post-TKA. Instead, the ankle contribution decreased (at 1-year post-TKA), and knee contribution increased (at 2-years post-TKA).

REFERENCES

[1] Winter DA (1983). Biomechanical motor patterns in normal walking. *Journal of Motor Behaviour*. **15**(4);p. 302-30.
[2] Mandeville D et al (2007). The effect of total knee replacement on dynamic support of the body during walking and stair ascent. *Clinical Biomechanics*. **22**; p. 787-794.
[3] Landry S et al. (2007). Knee Biomechanics of Moderate OA Patients Measured During Gait at a Self-Selected and Fast Walking Speed. *Journal of Biomechanics* **40**(8); p. 1754-61.

ACKNOWLEDGEMENTS
NSERC and CIHR for funding.

TIBIAL BONE DENSITY IS ASSOCIATED WITH TOTAL KNEE IMPLANT MIGRATION

D. Konadu[1], J.L. Astephen Wilson[1], M.J. Dunbar[1,2], E. Laende[2], A Hennigar[2], M. Gross[2]
[1]School of Biomedical Engineering, Dalhousie University, Halifax, Canada, dv897764@dal.ca
[2]Department of Surgery, Dalhousie University, Halifax, Canada

INTRODUCTION

Aseptic loosening of the tibial component of total knee prosthesis is a common cause of revision surgery [1]. While micromotion at the bone-implant interface can now be accurately measured with Radiostereometric Analysis (RSA), mechanisms responsible for loosening remain poorly understood. It is intuitive that tibial bone quality and strength may affect implant fixation; however the literature is equivocal. One previous study has shown a positive association between intraoperative tibial bone fracture strength and implant longevity [2]. Another found no correlation between implant migration measured with RSA and bone quality [3]; however, only limited tibial regions of interest were considered in this previous analysis. The purpose of this study was to investigate the association between bone density in multiple regions of interest in the proximal tibia and post-operative knee implant migration measured with RSA.

METHODS

Thirty subjects who received total knee arthroplasty (TKA) surgery with the Wright Medical Medial Pivot Biofoam (Wright Medical Inc., TN, USA) implant (uncemented) were recruited. The subjects were stratified into two groups with one having screws (n=17) and the other with no screws (n=13) affixed with the implant. Bone mineral density (BMD) of several regions of interest (ROIs) of the proximal tibia (Figure 1) was measured with DEXA postoperatively at 2, 6, 12 and 24 weeks (GE LUNAR; GE Healthcare, UK). RSA exams were also taken immediately post-operatively and at 6, 12 and 24 weeks. Bone density was analysed with enCore software (GE Healthcare, UK) and RSA analyses were performed with model-based RSA software (Medis Specials b.v, Netherlands). Correlations between bone mineral density in various regions and RSA migration at 24 weeks ($P < 0.05$) were examined..

RESULTS

Subject data and RSA summary results are presented in Table 1. ***All subject data:*** There were significant correlations between low BMD in the medial region (ROI 2AP) and high distal (r^2=0.28, p =0.003) and anterior translations (r^2=0.22, p =0.008) of the implant relative to bone. High distal translation of the implant was also correlated with low BMD in the ROI 2 LAT (r^2=.14,p=0.04) and ROI 1 AP (r^2=0.15,p=0.04) regions. Low BMD in the ROI 5 AP region was associated with high lateral translation (r^2=0.29, p=0.002) and high rotation about the long axes of the implant was associated with low BMD in the ROI 1LAT region (r^2=0.14, p=0.05). ***Screws:*** There were significant correlations between low BMD in the medial region (ROI 2 AP) and high distal translation (r^2 = 0.48, p=0.002), high anterior translation (r^2 = 0.38, p=0.008) and high maximum total point motion (MTPM) of the implant (r^2=0.23, p=0.05). ***No screws:*** A significant correlation was found between low BMD in the region under the tip of the implant (ROI 5 AP) and lateral translation of the implant (r^2 = 0.42, p= 0.016).

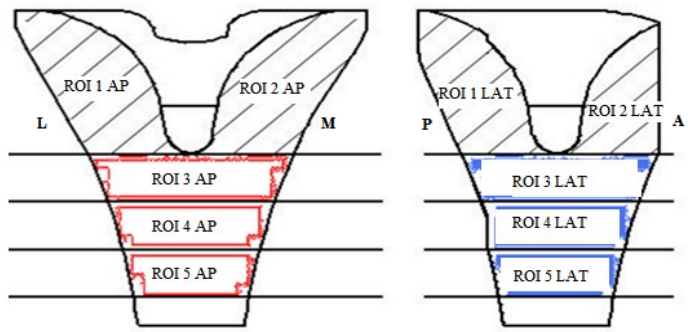

Figure 1: Regions of interest (ROIs) for the BMD analysis (Anterior posterior view - left and Lateral view -right).

DISCUSSION AND CONCLUSIONS

Our results show that the stability of implants, as measured with RSA, is related to the quality of the surrounding bone. Less micromotion was observed with increase in the density of the bone, contrary to the results of Li et al. [3], likely due to our more comprehensive capture of subchondral bone density. These results have important implications for post-operative treatment strategies to prevent aseptic loosening.

REFERENCES

[1] Berend ME et al (2008), *J Arth.*,23 (6);104-109
[2] I Hvid (1988), *Clin Orthop* 227; 210-221.
[3] Li M et al, (2001), *JArth.,*893-900

Table 1: Subject Demographic and RSA Results

			BMD			*RSA Results*			
Group	***Age (yrs)***	***Sex (m/f)***	***BMI (kg/m^2)***	***AP ROI 2 (gcm^{-2})***	***AP ROI5 (gcm^{-2})***	***X (mm)***	***Y (mm)***	***Z (mm)***	***MTPM (mm)***
All	70.8 (6.0)	18/12	29.3(3.9)	0.03	0.12	-0.03(0.18)	-0.41(0.58)	0.05(0.33)	1.29(1.15)
No screws	69.5 (4.4)	6/7	29.3(2.6)	0.06	-0.03	-0.04 (0.12)	-0.46(0.60)	0.06(0.26)	1.41(1.51)
Screws	71.8 (7.0)	12/5	29.3(4.4)	0.01	-0.06	-0.02(0.22)	-0.38(0.58)	0.05(0.39)	1.21(0.84)

Passive knee joint kinematic patterns during computer-assisted TKA surgery depend on choice of kinematic model

Richard D Roda[1], Janie L Astephen Wilson[1], Michael J Dunbar[1,2], C Glen Richardson[2]
[1]School of Biomedical Engineering, Dalhousie University, Halifax, CA, rroda@dal.ca
[2]Department of Surgery, Dalhousie University, Halifax, CA

INTRODUCTION

Computer assisted total knee arthroplasty (TKA) surgery is a novel method for accurate measurement of intraoperative passive joint kinematics, component placement, and protocol recording[1]. A goal of TKA surgery is to restore the frontal plane alignment of the knee joint to neutral, and the direct and dynamic measurement of this alignment is now possible with computer-assisted surgery. The objective of this study was to determine if the representation of frontal plane alignment during passive knee flexion/extension movement during TKA surgery is dependent on the particular kinematic model chosen to represent joint angles.

METHODS

A retrospective analysis of 172 individuals (mean age 66.8±8.2 yr) diagnosed with end-stage knee osteoarthritis who underwent primary computer assisted TKA between 2007 and 2009 was performed. During TKA, pre-implant 3D knee joint angles during a passive flexion/extension range exercise were recorded using a computer assisted surgery system (Stryker® Orthopedics, NJ). 3D knee kinematics were calculated using three joint kinematic models: tibia-based (1) and femur-based (2) cardan ZYX models, and the joint coordinate system (3) [2]. The primary difference between kinematic models was the cardan sequences used and mediolateral/AP-axis definitions. The cardan models' AP axes were based on an axis digitized by the surgeon, while the JCS uses an orthogonal axis calculated from the mediolateral and distal/proximal axes of each segment. Patterns of the frontal plane angles relative to changing flexion/extension angles during the movement were compared by calculating the mean values over the entire range and for 3 different intervals of flexion (0-20°, 30-60°, 70-90°).

A one-way ANOVA was performed to test for differences in mean frontal plane angles over the flexion/extension range between the kinematic models. A two-way ANOVA was also performed to test for differences and interaction between the models and flexion interval (0-20°, 30-60°, 70-90°, n=152). Tukey HSD post-hoc comparisons were performed.

RESULTS

ANOVA results are summarized in Table 1. The mean frontal plane curve for each kinematic model is shown in Figure 1. Total mean frontal plane angles were -2.0°±5.6, 5.3°±7.2, and -10.0°±8.1 for the Tibia-based, Femur-based, and JCS-Femur models respectively. Mean frontal plane angles were significantly different between all kinematic models ($p < 0.001$) (Table 1). There were also statistically significant differences between all model and flexion/extension interval pairs, as well as significant interactions between model and interval ($p < 0.001$) (Table 1).

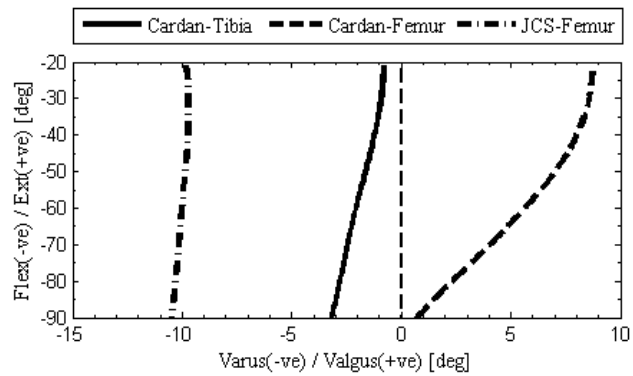

Figure 1: Mean frontal plane curve for each kinematic model

DISCUSSION AND CONCLUSIONS

All three kinematic models resulted in significantly different frontal plane angle patterns over a passive range of knee flexion/extension during TKA. The Joint Coordinate System in particular appeared to shift the curves into more varus relative to the two cardan models. This may be a result of differences in the definitions of the mediolateral axis between the malleoli for the distal segment. Further study should be focused on determining which model(s) appropriately captures intraoperative frontal plane alignment for surgical decision making.

REFERENCES

[1] Choong FP, Dowsey MM, Stoney JD. (2009) J Arthroplasty. 24(4): 560-569
[2] Grood ES, Suntay WJ. (1983) J Biomech Eng. May;105(2):136-44

ACKNOWLEDGEMENTS

Stryker® Orthopedics for their collaboration

Table 1: Results of one and two-way ANOVA's to test for differences between kinematic models and curve position.

ANOVA	Dependent Variable	Factor	*p*
1-way	Mean Frontal Plane Angle over flexion/extension range	Model	$p < 0.001$
2-way	flexion/extension interval (0-20°, 30-60°, 70-90°)	Model	$p < 0.001$
		Interval	$p < 0.001$
		Interaction	$p < 0.001$

The Pre-operative Knee Adduction Moment during Gait is Associated with the Dynamic Varus/Valgus Angle of the Knee during Computer-Assisted TKA Surgery

Richard D Roda[1], Janie L Astephen Wilson[1], Michael J Dunbar[1,2], C Glen Richardson[2]
[1]School of Biomedical Engineering, Dalhousie University, Halifax, CA, rroda@dal.ca
[2]Department of Surgery, Dalhousie University, Halifax, CA

INTRODUCTION

The dynamic knee adduction moment during gait is the gait parameter most associated with knee osteoarthritis (OA) and surgical outcome, however knee adduction moment information has not yet been incorporated into surgical decision making. Static frontal plane alignment of the knee joint (varus/valgus) is more commonly used as a surgical metric, and frontal plane alignment is generally restored to neutral during total knee arthroplasty (TKA) surgery based on preoperative radiographic measurements. Computer-assisted orthopedic surgery is a new technology that allows the surgeon to measure 3D pre and post implant joint kinematics intraoperatively. Quantifying a relationship between pre-TKA gait measures and intraoperative joint kinematics may be a first step towards developing patient-specific preoperative treatment strategies based on the dynamic mechanical environment of the knee rather than static parameters alone.

METHODS

Eight male and 6 female subjects (age 67.1±8.6 yr, BMI 30.7±4.9) diagnosed with end-stage knee osteoarthritis who underwent primary computer-assisted TKA between August 2009 and January 2010 also visited the Dynamics of Human Motion laboratory for pre-operative gait analysis testing within the week of their surgery.

Three-dimensional gait patterns were recorded during gait analysis using a Optotrak 3020 motion capture (Northern Digital, Inc.), and force platform (AMTI, Watertown, MA) system. Knee joint angles and net resultant moments were calculated using an inverse dynamics procedure.

During the TKA procedure, pre-implant passive three-dimensional knee joint kinematic data was recorded for each subject during a passive flexion/extension exercise using a computer-assisted surgery system (Stryker® Orthopedics, NJ, USA). Three-dimensional knee kinematics were calculated using the joint coordinate system[2]. The mean frontal plane angle was calculated for all values recorded at <60° flexion. The passive frontal plane range of motion (ROM) of the knee was defined as the maximum range of motion of the frontal plane angle recorded at <60° flexion. The interval <60° flexion was selected as it is comparable to a typical range of knee flexion during the gait cycle.

Two-tailed Pearson correlation coefficients were used to test for significant associations between the mean dynamic knee adduction moment during pre-operative gait and the mean passive frontal plane angle / frontal plane ROM over 60° flexion/extension during the TKA ($p < 0.05$).

RESULTS

The Pearson correlations between the mean stance phase external knee adduction moment and the intraoperative passive ROM / mean frontal plane angle were both significant ($r^2 = 0.244$, $p = 0.048$; $r^2 = 0.442$, $p = 0.009$ respectively). Scatter plots of the two relationships are shown in Figure 1.

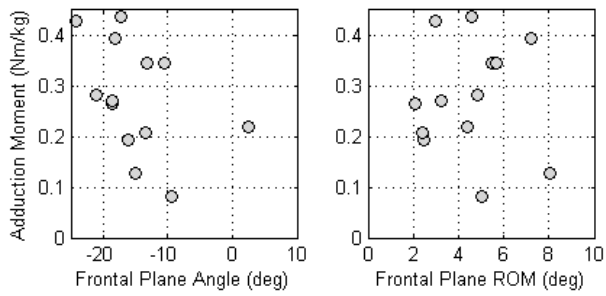

Figure 1: Scatter plot of the knee adduction moment with intraoperative parameters: passive knee frontal plane ROM and mean frontal plane angle (varus -ve, valgus +ve)

DISCUSSION AND CONCLUSIONS

Radiographic static alignment has been shown to correlate with the second stance-phase peak external knee adduction moment during gait[1]. We found a similar trend between the dynamic knee adduction moment during gait and the dynamic frontal plane alignment during TKA surgery. Thus, increasing mean varus alignment correlated with the mean stance-phase external adduction moment during gait, despite limitations in power due to sample size. The relationship was not as pronounced with the passive ROM of the knee. This may be due to the changes in kinematics associated with loading the knee joint during gait, such as muscle contraction and ground reaction force, or in the nature in which it was parameterized.

Unlike static radiographs, computer-assisted surgery can record passive dynamic kinematics intraoperatively and presents a unique opportunity for further study of intraoperative kinematic waveforms and their relationship to preoperative gait measures. These systems hold the potential of allowing surgeons to incorporate dynamic information on the mechanical environment of the knee joint into their surgical planning.

REFERENCES

[1] Hurwitz DE. (2002) J Orthopaedic Research. 20:101-107s
[2] Grood ES, Suntay WJ. (1983) J Biomech Eng. May;105(2):136-44

ACKNOWLEDGEMENTS

Stryker® Orthopedics for their collaboration

Knee Joint Mechanics Improve Two Years after Total Knee Replacement Surgery

Janie L Astephen Wilson[1], Cheryl L Hubley-Kozey[1,2], Michael J Dunbar[1,3]
[1]School of Biomedical Engineering, Dalhousie University, Halifax, Canada, Janie.Astephen@Dal.Ca
[2]School of Physiotherapy, Dalhousie University, Halifax, Canada
[3]Department of Surgery, Division of Orthopedics, Dalhousie University, Halifax, Canada

INTRODUCTION

Total knee replacement (TKR) is a successful surgery in terms of post-operative pain relief [1]. While some previous work has characterised simple functional characteristics post-TKR such as walking velocity and range of motion [1,2], there remains a paucity of objective information on postoperative in vivo lower limb joint function. The knee adduction moment, which has been highly associated with loading on the medial compartment of the knee during gait [3], is the gait measure that has been most implicated in the initiation and progression of knee osteoarthritis (OA) [4]. Many conservative and surgical treatment options for knee OA aim to reduce the knee adduction moment; however, little information exists on the effect of the TKR on the knee adduction moment during gait. The objectives of this study were to investigate i) changes in the knee adduction moment and ii) changes in other joint kinematic and kinetic gait measures from the pre-operative period to one and two years post-TKR.

METHODS

Three-dimensional gait analysis was performed on thirty patients who underwent TKR within one week prior to surgery and at one and two years post-TKR. Patterns of 3D joint angles and net moments at the knee, hip and ankle during gait were measured. Principal component analysis (PCA) was used to extract major patterns of variability in each of the kinematic and kinetic gait measures [5]. Principal component scores (PC scores) were calculated as the projections of original gait waveforms onto the principal patterns. One-way ANOVA was used to determine any changes in gait measure patterns (i.e. PC scores) between the pre-TKR and one and two year post-TKR time points ($P < 0.01$).

RESULTS

The pattern of the knee adduction moment at two years post-TKR was significantly different than that pre-TKR, characterised by a higher first peak adduction moment in early stance relative to the moment in late stance ($P = 0.007$) (Figure 1a,b), which is more similar to a healthy, asymptomatic knee adduction moment pattern. There was no significant difference between pre-operative and one-year post-TKR knee adduction moment patterns during gait. The overall magnitude of the knee flexion angle over the gait cycle was significantly increased at both post-operative times relative to pre-TKR ($P = 0.003$) (Figure 1c). Knee adduction angles were lower during swing phase at two years relative to pre-TKR ($P = 0.003$) (Figure 1d). The hip adduction angles and flexion angles were significantly lower during stance at one and two years post-TKR relative to pre-TKR ($P = 0.001$ and 0.006 respectively).

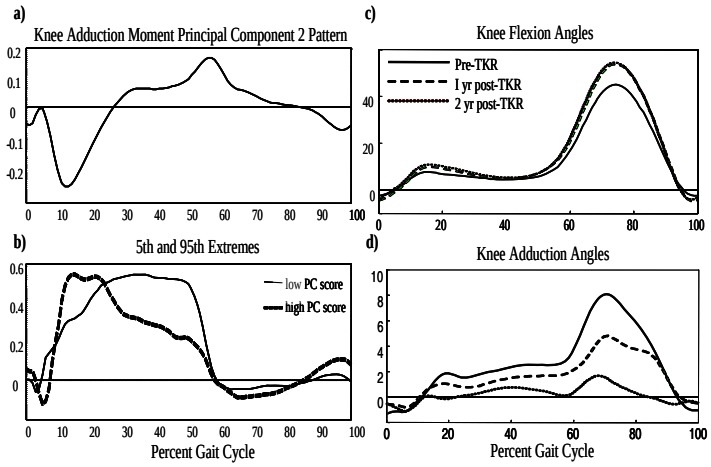

Figure 1: Principal component pattern 2 of the knee adduction moment (a) and example knee adduction moments with high and low PC2 scores (b) are shown for interpretation. Mean group waveforms of the knee flexion (c) and adduction (d) angles are also shown.

DISCUSSION AND CONCLUSIONS

Our results show that a number of post-TKA lower limb kinematics and kinetics move toward asymptomatic profiles. However, many changes appear to take more than one year post-operatively to occur, which highlights the importance of improved post-TKA rehabilitation strategies.

REFERENCES

[1] Yoshida et al. (2008). *Clinical Biomechanics;* Vol **23**(3); p. 320-328.
[2] Smith et al. (2006). *Clinical Biomechanics*; Vol **21**(4); p. 379-386.
[3] Zhao et al. (2007). *J Orthopedic Research;* Vol **25**(6); p. 789-797.
[4] Miyazaki et al. (2002). *Annals of the Rheumatic Diseases;* Vol **61**(7); p. 617-622.
[5] Deluzio and Astephen (2007). *Gait & Posture;* Vol **25**(1); p. 86-93.

ACKNOWLEDGEMENTS

We would like to acknowledge CIHR for funding.

OSTEOARTHRITIS KNEE PAIN DURING ISOKINETIC TESTING AT DIFERENT VELOCITIES

Scott C.E. Brandon[1], Sivan Almosnino[2], Alison Chalmers [3], Elizabeth A. Sled[3]
[1]Department of Mechanical Engineering, Queen's University, Kingston, ON
[2]School of Kinesiology and Health Studies, Queen's University, Kingston, ON
[3]School of Rehabilitation Therapy, Queen's University, Kingston, ON
brandon@me.queensu.ca

INTRODUCTION

Isokinetic testing and conditioning of the knee musculature in those suffering from knee osteoarthritis (OA) is of great interest due to possible favourable effects on patient self-efficacy [1]. However, pain experienced during exercise may affect patients' performance during testing and adherence to a training program. Selection of an optimal angular velocity for isokinetic testing and conditioning in OA populations should consider the fact that at lower testing velocities, the exposure time to the mechanical load imposed is greater, which could increase pain [2]. The purpose of this investigation is to assess whether pain intensity during isokinetic testing performed by knee OA patients is velocity dependent. Specifically, we hypothesize that pain intensity experienced during testing will be higher when performing isokinetic efforts at lower testing velocities.

METHODS

35 individuals with tibiofemoral OA volunteered to participate in this study. The participants met the following inclusion conditions: age ≥ 40 years, self-reported pain in the knee(s) for most days of the month, and either radiographic evidence of knee OA as indicated by definite osteophytes in the medial and/or lateral tibiofemoral compartment in one or both knees, or documented evidence of cartilage loss in the knee by arthroscopy or magnetic resonance imaging (MRI).

After a short warm-up, each participant performed 5 maximal concentric knee extension/flexion trials of the involved leg at 60°/sec, 90°/sec, and 120°/sec using a Biodex System 3 isokinetic dynamometer (Biodex Medical Systems., Shirley, NY, USA). Testing was performed through each participant's available range of knee motion. Testing velocities were randomized both within and between participants.

The intensity of knee pain during testing was recorded using standard 100mm Visual Analog Scales (VAS). Pain was assessed prior to testing (baseline) and immediately after each velocity of testing. Participants were instructed to make a vertical mark along the horizontal scale to denote any knee pain experienced with the specific test administered just previously. Clean copies of VAS scales were administered after each testing velocity such that the participants were not able to view previous marks on the scales. For each participant, representative pain scores were calculated as the difference between baseline and immediately after each testing velocity. Based on standardized skewness and kurtosis scores, visual observation of histogram plots, and Shapiro-Wilk tests the data were not normally distributed . As such, differences between pain scores obtained for different testing velocities were evaluated using Friedman's analysis of variance.

RESULTS

Pain scores did not significantly change as a result of performing knee extension/flexion trials at the 3 different velocities ($\chi^2(2) = 4.97$, $p = 0.086$). However, as shown in Figure 1, there were clusters of subjects who exhibited no change in pain (n=21, black lines), decreasing pain (n=7, red lines), and increasing pain (n=4) with increasing testing velocity.

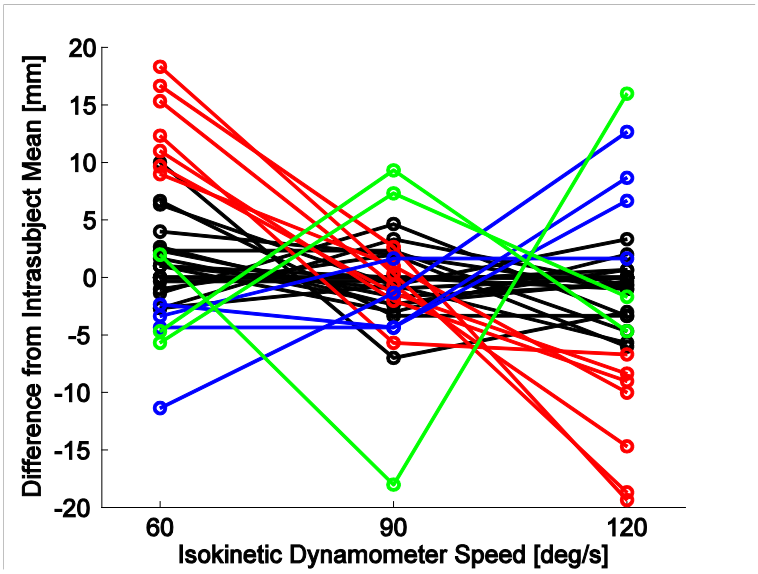

Figure 1: Pain scores from 100mm visual analog scale (VAS), relative to intrasubject mean across three isokinetic testing speeds. Only subjects whose pain scores varied less than 10mm across the speeds are placed in the 'no-change' group.

DISCUSSION AND CONCLUSIONS

Although there was no consistent effect of speed, it is possible that for some subgroups of patients pain is correlated with speed. All scores not coloured black in Figure 1 (n=14/35) exhibited a clinically relevant change in pain of 10mm [3]. However, a direct relationship cannot be applied to all subjects with knee OA. It appears that pain should be assessed on a subject-specific basis in order to prescribe an optimal operating speed for conditioning. Future work will establish whether groups identified in Figure 1 may be associated with either OA severity or the order of testing.

REFERENCES

[1] Maly et al . (2006). *Arthritis Rheum.* 55: 94-101.
[2] Dvir Z. *Isokinetics:* Churchill Livingstone, 2004.
[3] Barthel et al. (2010). *ArthritisResTher.* 12: R7

Understanding Wolff's Law via micro-level Topology Optimization

Chris Boyle[1], Il Yong Kim[2]
[1]Department of Mechanical and Materials Engineering, Queen's University, Kingston, Canada, boyle@me.queensu.ca
[2] Department of Mechanical and Materials Engineering, Queen's University, Kingston, Canada, iykim@me.queensu.ca

INTRODUCTION

Internal bone architecture, with its unique complex material matrix, has long been studied to determine the underlying principles of its formation and adaptation. Wolff proposed that trabecular bone functionally adapts to external mechanical loading stimuli; orientating to align with the principal stress trajectories [1]. Wolff's observed the "self-optimizing" property of bone, which achieves maximum mechanical efficiency with minimal mass. Recently, computational techniques have been developed that utilize the finite element (FE) method to simulate the bone remodeling and trabecular adaptation process in the proximal femur. Most previous studies have simplified the analysis by either utilizing a two-dimensional model or a macro-level (large finite elements) approach to simulate the adaptation process. These can provide adequate insight into overall mechanical properties but cannot represent realistic trabecular architecture. The objective of this study is to conduct the first micro-level three-dimensional bone remodeling simulation using the topology optimization approach, which will allow accurate representation of the trabecular architecture at a near cellular level.

METHODS

Topology optimization [2] seeks to minimize global compliance resulting in a structure of uniform strain energy. It achieves this by iteratively distributing a finite amount of material in a given domain; thus, the procedure can be illustrated as "layout optimization". The areas of highest loading will attract more material to maximize overall structural stiffness. This method is comparable to actual bone remodeling, as areas of highest loading (and strains) will be more susceptible to fatigue damage and micro-fractures; thereby, activating remodeling and resulting in acquisition of more bone mass. In this study, a specialized topology optimization called design space optimization (DSO) was utilized. It emulates the cellular level surface remodeling through micro-finite element expansion and reduction at the trabecular surface. An anatomically correct three-dimensional femur model was subjected to realistic loading conditions based on the daily activities of walking and stair climbing.

RESULTS

The proximal femur model adapted to the two daily loading conditions during the optimization process; reorienting the trabecular to align with these external loadings. As a result, the final trabecular structure obtained the anisotropic structure similar to natural bone (Figure. 1).

The simulation results were compared to natural femur cross-sections and radiographs, revealing corresponding key features of trabecular architecture. The four main loading groups (i.e. – principal compressive, secondary tensile, etc.), according to Ward's classification [3], are clearly visible. In addition, the bone material distribution is comparable; with more density in high loading areas, such as the high compressive region in the proximal head. The unique, low density area known as "Ward's triangle" is also visible.

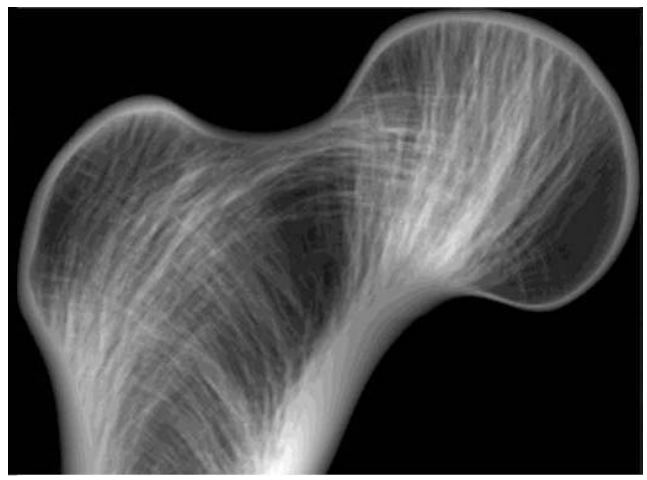

Figure 1: Femur trabecular architecture achieved through topology optimization with two daily loading conditions

DISCUSSION AND CONCLUSIONS

The femur geometry achieved through optimization reveals the same key features as natural human bone. The simulated adaptation process reoriented the trabecular reaching equilibrium with the applied loads as according to Wolff's Law. This study suggests that topology optimization can accurately model the trabecular adaptation process due to biomechanical stimulus, which plays the dominant role in adaptation as Wolff hypothesized.

REFERENCES

[1] J. Wolff. (1986). (Translated by P. Maquet, R. Furlong), Das Gesetz Der Transformation Der Knochen (Translated as The Law of Bone Remodeling), Springer.
[2] O. Sigmund. (2001). A 99-line topology optimization code written in Matlab. *Struct. Multidisc. Opt.* **21**; p.120-127.
[3] W.J. Whitehouse *et. al.* (1974) Scanning electron microscope studies of trabecular bone in the proximal end of the human femur. *Journal of Anatomy*, ***118***(3); p.417-444

A NEW BIOMIMETIC COMPOSITE MATERIAL STEM IN SURFACE REPLACEMENT OF THE HIP

Christiane Caouette[1], Martin N. Bureau[2], Pascal-André Vendittoli[3], Martin Lavigne[3], Natalia Nuño[1]
[1]Génie de la production automatisée, École de technologie supérieure, Montréal, canada, natalia.nuno@etsmtl.ca
[2]Industrial Materials Institute, National Research Council, Boucherville, Canada
[3]Maisonneuve-Rosemont Hospital, Montréal, Canada

INTRODUCTION

The short metaphyseal stem of current surface replacement arthroplasty (SRA) of the hip are designed for alignment purposes and was not bonded to adjacent bone. To prevent early femoral head loosening some surgeons suggested to cement the metaphyseal stem to allow a more distal fixation[1]. The adverse effects of this fixation method may be increased stress shielding in the femoral head[2] (bone is less stressed and resorbs as a result) and possibly compromised long term results.

A possible solution to reduce potential stress shielding of bonded metallic stems in SRA implants would be the use of a composite material with bone-matching mechanical properties to fabricate the metaphyseal stem. Such a stem could be osseointegrated and provide the same kind of stable fixation as a cemented metallic stem without increasing stress shielding in the femoral head. The objective of this study is to verify the validity of this claim using a finite element model.

METHODS

A finite element model (FEM) was constructed; the femur was obtained from CT-scans of a patient and modeled with heterogenic mechanical properties. All material properties were modeled as isotropic and linearly elastic; trabecular bone heterogeneity was also modeled. Three models of a commercially available implant were constructed: an unfixed metallic stem, a cemented metallic stem (cement mantle is 1 mm thick) and an osseointegrated stem made of composite material. All bone-cement and osseointegrated interfaces were modeled as perfectly bonded; implant-cement and bone-metal interfaces were modeled as frictional interfaces. A static load case representing healthy gait was applied to evaluate stress shielding in the trabecular bone of the femoral head.

RESULTS

Trabecular bone underneath the spherical part of the implant was divided into four zones; the same was done with the trabecular bone in the femoral neck. Maximal compressive stress (σ_3) in these zones for the cemented and biomimetic stems was compared with that of the unfixed stem. The decrease in stress varied from 1.8% to 21.5% in the femoral head of the cemented stem; the infero-posterior and infero-anterior zones were the most severely stress shielded with -16.4% and -21.5% of stress respectively (see A and B on figure 1). The same two zones in the biomimetic stem saw decreases of 5.5% and 0.2% respectively. The femoral neck regions did not show a clear trend.

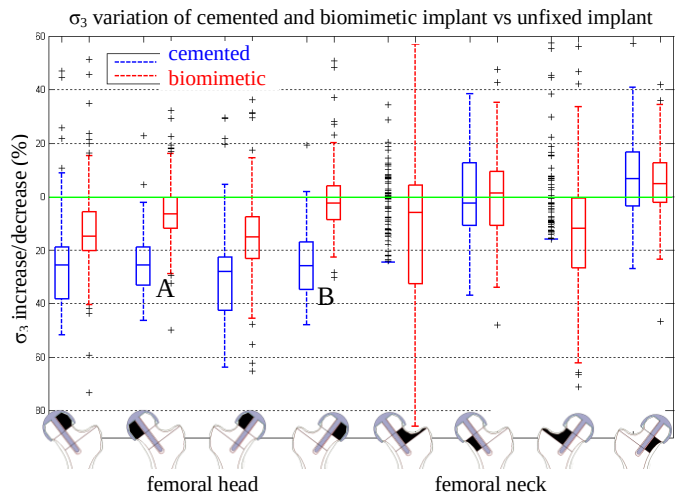

Figure 1: Increase/decrease of maximum compressive stress when comparing cemented metallic stem and biomimetic stem with unfixed stem.

DISCUSSION AND CONCLUSIONS

The FEM model has showed increased stress shielding in the femoral head and neck when the metallic stem of the implant was cemented; it has also shown that this stress shielding can be reduced if a composite material with bone-matching properties is used to fabricate the stem. The main limitation of this study is that it has been done with only one patient-specific femur, which may not represent clinical situations. Also, the interfaces were modeled with bonded contacts, which cannot simulate aseptic loosening (bonded contacts will always remain attached regardless of load, micromotions or bone resorption).

Further studies will be necessary to confirm these findings; bone remodelling simulations will have to be done in order to assess the severity of long term bone resorption resulting from stress shielding.

An osseointegrated metaphyseal stem made of biomimetic material seems to reduce the stress shielding effect observed in the femoral head in comparison with a bonded chromium-cobalt metallic stem. Such a biomimetic stem could become an interesting alternative when fixation extension is desired.

REFERENCES

[1] Amstutz, H.C., et al. (2007). The Effects of Technique Changes on Aseptic Loosening of the Femoral Component in Hip Resurfacing. *J Arthroplasty* Vol **22**(4): p. 481-489.
[2] Ong, K.L., et al. (2006). Biomechanics of the Birmingham hip resurfacing arthroplasty. *JBJS Br* Vol **88B**(8): p. 1110-5.

Greater trochanteric plate design refinement using finite elements method

Yan Bourgeois[1,2], Yvan Petit[1,2], Yves Laflamme[2]
[1]Mechanical engineering department, École de Technologie Supérieure, Montreal, Canada, yvan.petit@etsmtl.ca
[2]Research center, Hôpital du Sacré-Coeur, Montréal, Canada

INTRODUCTION

Greater trochanteric reattachement (GTR) is needed after a fracture or an osteotomy performed during hip revision surgery. Studies [1][2] have shown healing issues to using wire cerclage or cable grip systems. Approximately 30% of complex arthroplasties show a trochanteric fiber union [1]. To solve the problem a new trochanteric plate (Y3) was developed using cables, screws and a unique geometric design. The Y3 plate is especially designed to reduce anterior displacements without compromising the fragment stability in other directions. The objective of this study is to refine the design of Y3 plate to obtain a low-profile with increased flexibility.

METHODS

A finite element model (FEM) was used to perform design iterations. The FEM represents a 4th generation composite femur (Sawbones) with a GT osteotomy and instrumented with a femoral implant and the Y3 GTR plate (Fig 1). Fixation of the GTR plate to the femur uses four cortical locking head screws (CLHS) in GT and four CLHS in femoral shaft. A total of 141 645 tetrahedral elements were used to represent the FEM geometry. Contact elements assuming no friction were defined between the GT and femur and bounded contacts were defined at the screw-bone interfaces. Fixed joints were defined between screws and Y3 plate. Simultaneous loads were applied on the femoral head (2400 N) and the GT (650 N). Two load cases simulating different GT force orientations were defined: proximal and anterior direction. Maximum displacements of the GT relative to the femur and Von-Mises stresses were analysed.

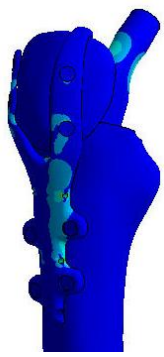

Figure 1 FEM of femur and GTR assembly

GT displacement direction and amplitude from the FEM were compared with experimental results for validation purpose. Experimental results were achieved by using a test bench comprising 2 hydraulic pistons and cable systems to apply the loads on the femoral head and the GT. GT and femur displacements were recorded by a 2D camera and GT displacement relative to the femur was calculate using a rigid body method.

Y3 design refinement targets the thickness and wideness at 3 zones: posterior, anterior and femoral shaft branches. Output results are the maximum GT-femur displacement and maximum Von-Mises stresses. The first design criteria was to obtain Von-Mises stress lower than 500 MPa into Y3 plate corresponding to a design safety factor (SF) of 1.6 on yield strength and of 1.3 for endurance limit after $3x10^6$ cycles (~1 year walking). The second design criteria was to keep GT displacements amplitude below the initial Y3 design (1.32 mm and 2.04 mm for anterior and proximal loading direction respectively)

RESULTS

Numerical simulation results are consistent with the experiments. In all loading situations the GT move exclusively anteriorly (0.33 to 0.83 mm) and proximally (0.48 to 0.85 mm) with a counter clockwise rotation (0.48 to 0.96°). In average, simulated displacements are 45% lower than experimental results.

After 8 Y3 design refinement iterations, Von-Mises stresses reach 498 MPa in anterior direction and 312 MPa in proximal direction. Maximum GT displacements relative to the femur are 1.30 mm and 2.03 mm for proximal and anterior loading directions respectively, which is in agreement with the second design criteria.

The final design provides a plate 30% thinner and 10% narrower. In general, the refinement reduced the initial volume of Y3 plate by 29%.

DISCUSSION AND CONCLUSIONS

This study presents the refinement of a GTR system using a validated FEM. The results show that GT rotation is sensitive to changes in Y3 geometry. Specifically, a change in geometry of the transition between anterior, posterior and femoral shaft branches particularly affected GT rotation. Other zones were less critical for displacements, but maximum Von-Mises stresses were observed in the femoral shaft branch, close to the proximal cable holes. Since the Y3 design includes the possibility to use cables in addition to self-locking screws, a next step will be to investigate the design refinement using cables and screws in the construct. Nevertheless, the FEM presented in this study proved useful for the design refinement of a GTR system from systematic criterion. This sophisticated tool will be used to evaluate different designs and investigate new GTR designs.

REFERENCES

[1] Barrack, R. L. and R. A. Butler (2005). Current status of trochanteric reattachment in complex total hip arthroplasty. *Clin Orthop Relat Res* Vol **441**; p. 237-242.

[2] Bal, B. S., P. Kazmier, et al. (2006). Anterior trochanteric slide osteotomy for primary total hip arthroplasty. Rev. of nonunion and complications. *J Arthroplasty* Vol **21**(1); 59-63.

ACKNOWLEDGEMENTS

This research was funded in part by NSERC and CFI. The authors also thank M. Yannick Baril for his technical work.

RADIUS MOVEMENT SIMULATION AND EVALUATION BASED ON ARTICULAR SURFACES

Julien Leboucher[1,2], Mathieu Lempereur[2,3], Valérie Burdin[1,2], Olivier Rémy-Néris[2,3]
[1] Telecom Bretagne, Brest, France, julien.leboucher@univ-brest.fr; [2] LaTIM, Brest, France;
[3] Service de Médecine Physique et Réadaptation, Hôpital Augustin Morvan, Brest, France

INTRODUCTION

Radial bone movement, which is the main contributor of forearm prono-supination, has been suggested to occur around various axes[1], mobile or not, with respect to the humerus-ulna complex. The purpose of our study was to compare the results of rotation of the radius around a number of stationary axes.

METHODS

Eight different axes of rotation were designed using six joint surfaces, two distal and four proximal. These surfaces were segmented from a CT scan performed on the right upper limb of a volunteer with no history of disease or trauma. Quadric shapes were fitted[2] to these surfaces in order to obtain their centers used rotation axes extremities. Distal ends of rotation axes were obtained by fitting ellipsoids on the ulnar head and the ulnar notch of the radius. Capitellum, humeral notch, head of radius and radial notch surfaces were used to fit ellipsoids and spheres which centers were the four proximal ends.

Different axes are used to simulate movements evaluated using an index of articular coherence. Coherence indices were proposed in [3]. They are based on the spatial configuration of facing joint surfaces and computed using the quantity of paired vertices on these surfaces and their separating distances. The coherence index value runs from 0 to 1, the latter meaning perfect congruence and being set using a reference position (e.g. CT scan position). Pairs of joint surfaces under investigation were capitellum and humeral notch, head of radius and radial notch and ulnar head and ulnar notch for the humero-radial, proximal and distal radio-ulnar joints, respectively.

RESULTS

Results shown on Figures 1 to 3 are index averages with respect to rotation angle. Averages over two or four axes are presented as small differences were found while opposite end of axes were modified (e.g. proximal ends for distal joint).

Coherence indices for the distal radio-ulnar joint dropped quickly as the radius moved out of the reference position (Figure 1) for the axes passing through the ulnar head centre.

Humero-radial joint indices are shown on Figure 2. Axes running through the centre of the head of the radius and the centre of the fitted sphere on the ulnar notch performed fairly from -30° and -10°, respectively, until the complete pronation; while other axes performed better until 60° of pronation.

Concerning the proximal radio-ulnar joint (Figure 3), only the axes using the head of the radius presented suitable indices for a range of motion of 100° (from -60° to 40°).

DISCUSSION AND CONCLUSIONS

Distal ends of rotation axes did not exhibit important influence over the coherence index for the proximal joints, and vice versa. The best results for the proximal joints were obtained using the axes running through the head of the radius' centre. This landmark should be used with the ulnar notch when a fixed axis is chosen to simulate the movement of the radius.

REFERENCES

[1] Tay SC et al. (2008) A method for *in-vivo* kinematic analysis of the forearm. *Journal of Biomechanics* **41**, p. 56-62.
[2] Allaire S et al. (2007) Robust quadric fitting and mensuration comparison in a mapping space applied to 3D morphological characterization of articular surfaces. *Proc. 4th IEEE ISBI*, Washington, April 2007, pp. 972-975.
[3] Schwartz C (2009) Contribution à l'élaboration d'un espace commun de représentation pour l'analyse morpho-fonctionnelle du membre supérieur : application à l'articulation gléno-humérale. *Ph.D. Thesis*, Telecom Bretagne.

ACKNOWLEDGEMENTS

We acknowledge the Medical Imaging Unit of Clermont-Tonnerre Hospital (Brest, France) for CT data.

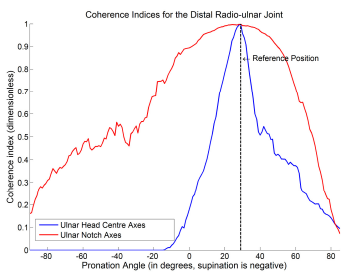

Figure 1: Distal radio-ulnar indices

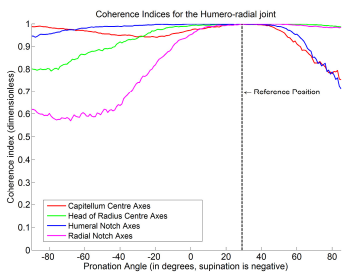

Figure 2: Humero-radial indices

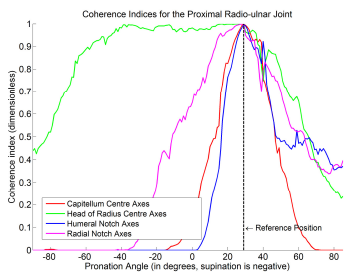

Figure 3: Proximal radio-ulnar indices

KINEMATIC MODEL OF A SHOULDER FITTED WITH AN ORTHOSIS

Maryline Doyon[1,2], Rachel Cotton[1], Mickael Begon[1,2], Jacinte Bleau[3], Paul Allard[1,2]
[1]Département de kinésiologie, Université de Montréal, Montréal, Canada, maryline.doyon@umontreal.ca
[2]Centre de recherche de l'Hôpital Sainte-Justine, Montréal, Canada
[3]Laboratoire Orthopédique Médicus, Montréal, Canada

INTRODUCTION

Rotator cuff injuries may require surgery followed by orthotic immobilization to decrease muscle tension and protect healing tissues. Since the desired arm abduction is not always maintained during daily-life activities [1] a kinematic shoulder model could be used to assess the efficiency of orthoses. Current models are difficult to apply because some markers are occluded by the orthosis during data acquisition. Furthermore, these models do not include all the shoulder joints: sternoclavicular, acromioclavicular and scapulohumeral. The purpose of this study is to develop a three-dimensional (3D) kinematic model that includes all three shoulder joints and can be used when patients are fitted with an orthosis.

METHODS

First, 31 reflective markers were put over the pelvis (4), thorax (6), clavicle (4), scapula (5), upper-arm (5) and lower-arm (7) as shown in Fig. 1A to be tracked by an eight-camera 512 Vicon^{TM} system (OMG plc, Oxford, UK) at 60 Hz. To determine the centers of rotation (CoR) of the shoulder joints using the method described by Ehrig [2], the subject performed arm elevations in 5 different vertical plans (every 45°, starting with arm flexion) followed by a circumduction, 5 shoulder shrugs and 5 protractions-retractions. The subject also performed 5 elbow flexions to determine its axis of rotation (AoR) by the method of O'Brien [3]. These analytical methods require rotation matrix optimization [4] to minimize soft tissue artefacts at each body segment. The translation vector is defined as the centroid of all the marker vectors of the segment. Additional markers placed on anatomic landmarks of the acromioclavicular joint (AC), root of the spine of the scapula (RS), inferior angle (IA), sternoclavicular joint (SC) and humeral epicondyles (EP_L, EP_M) help to define anatomical systems of coordinates and verify the coherence of the CoR and AoR. The Cardan sequence of flexion, abduction and axial rotation was used to calculate the joint angles.

RESULTS

Fig. 1B illustrates the corresponding 3D kinematic shoulder model. Motion at the sternoclavicular (SC) and acromioclavicular (AC) joints are presented in Fig. 2. Time histories for the scapulohumeral joint angles are not shown due to space limitation.

DISCUSSION

To minimize skin movement artefacts, segment position and orientation were calculated using at least four markers. With the use of optimisation techniques, it was possible to adjust marker locations to avoid large soft tissue areas and comply with the orthosis geometry and functions. The calculated position of the centers of rotation and axes of rotation were comparable to anatomical ones. To our knowledge, these are the first results on sternoclavicular and acromioclavicular in-vivo motions obtained with skin markers and shoulder complex modeled as three ball-and-socket joints. However, the model is sensitive to marker occlusions, especially when the subject performs maximal flexion because the camera view is obstructed by the neck and skin folds on the top of the shoulder. This limitation could be overcome using a link-model associated with an inverse kinematic procedure.

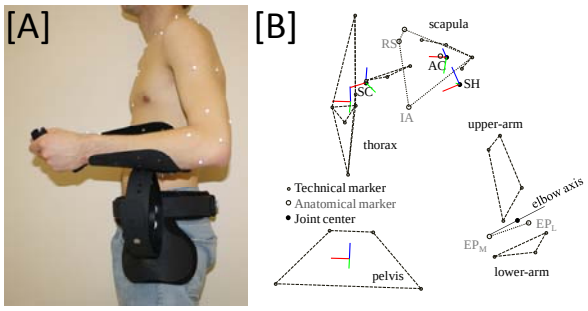

Figure 1: A) Markers position and B) kinematic model of the shoulder.

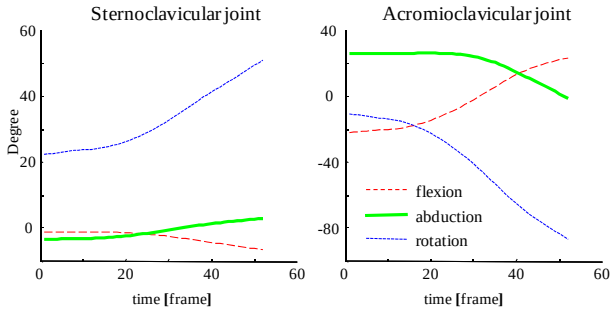

Figure 2: SC and AC joint angles.

REFERENCES

[1] Sullivan L et al. (2007). An Evaluation of Shoulder External Rotation Braces. *Arthroscopy: The Journal of Arthroscopic & Related Surgery* Vol **33**(2); p. 129-134.

[2] Ehrig RM et al. (2006) A survey of formal methods for determining the centre of rotation of ball joints. *Journal of Biomechanics* Vol 39; p. 2798-2809.

[3] O'Brien J et al. (2000). Automatic Joint Parameter Estimation from Magnetic Motion Capture Data. *Proc. Graphics Interface Conference*; p. 53-60.

[4] Monnet T et al. Improvement of the input data in biomechanics: kinematic and body segment inertial parameters. In *Biomechanics: Principles, Trends and Applications*; Nova Science Publishers, 2010.

ACKNOWLEDGEMENTS

This work was funded in part by the Laboratoire Orthopédique Médicus.

In Silico Nanomechanics of Collagen Peptide Bending and Microunfolding

Jonathan W. Bourne[1,2] and Peter A. Torzilli[1,2]
[1]Department of Physiology & Biophysics, Weill Graduate School of Medical Sciences, Cornell University, NY, NY, USA
[2]Tissue Engineering, Regeneration and Repair Program, Hospital for Special Surgery, NY, NY, USA, TorzilliP@HSS.EDU

INTRODUCTION

Collagens contribute to the mechanical properties of biological tissues, such as blood vessels, tendons, ligaments, and cartilage, and are generally loaded *in vivo*. Single molecule loading experiments, like those using optical tweezers, help to characterize collagen in uniaxial tension, but lack the spatial resolution to visualize protein conformation. Crosslinking of collagen, both enzymatically during tissue maturation and spontaneously during aging, plays a critical role in enhancing the strength of the structural network. However, there is a paucity of molecular data when mechanical force is not colinear with the long axis, as would likely occur in a crosslinked collagenous structure. We hypothesize that mechanical force perpendicular to the long axis results in bending and then microunfolding of the collagen helical structure. To test this we used Steered Molecular Dynamics (SMD) simulations to model the conformation of a collagen molecule when subjected to external forces.

METHODS

The 1BKV pdb structure file, describing an enzyme cleaved region from collagen type III, was visualized and manipulated using VMD 1.8.6. CHARMM22 chemical parameters were amended to include hydroxyproline as described by In 't Veld and Stevens [1]. The molecule was placed in a cylinder of water, and Na^+ and Cl^- ions added to bring the solution to 150 mM, and the total system was 18,267 atoms. Using SMD software (NAMD 2.6) [2], the system was minimized for 5,000 steps, then equilibrated at 37°C before beginning loading.

Loading conditions were designed to simulate a peptide within the context of a higher order (multi-scale) fibril structure. Thus, the C-α atoms of all three chains at both the N and C-termini were fixed. External force was applied through the C-β of an arginine side chain in the middle of the molecule directed away from the long axis. This residue was chosen as these side chains spontaneously crosslinks as advanced glycation end products during aging.

RESULTS

In silico loading showed that the collagen peptide has minimal resistance to bending, exhibiting increasing curvature (Figure 1A and 1B) and no distinct helical disruption at forces below 750 pN. As force increased, we observed the characteristic collagen triple helix began to fail and the pulled chain underwent a microunfolding event, where a loop pulled out from the helix (Figure 1C). Local helix disruption far below peptide bond strengths suggests potential hidden conformational changes occur within the collagen molecule as structures are loaded. We speculate that these changes are plastic and represent nano-damage to the structure and these local conformational changes might reveal new motifs for protein binding or change enzyme susceptibility.

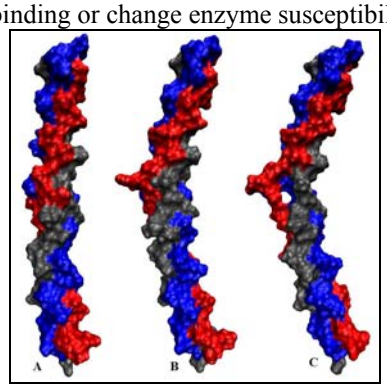

Figure 1: A collagen peptide is shown (A) before loading, (B) bending during loading, (C) exhibiting microunfolding during bending.

DISCUSSION AND CONCLUSIONS

SMD integrates many physical variables, including an external force vector, over femtosecond time steps to predict atomic movements of a system [2]. Using SMD, our results provide conformational predictions about nanoscale structural changes that occur during collagen loading and failure. The microunfolding predicted by this study correlates with published experimental data that mechanical overload of collagenous tissue (tendon) decreases thermal stability of some individual molecules within the structure [3]. These predictions suggest a model where mechanical properties and crosslinking in a structure might enable biological systems to dynamically tune enzyme-substrate, protein-protein and even cell-matrix interactions *in vivo*.

REFERENCES

[1] In 't Veld P and Stevens MJ (2008). Simulation of the Mechanical Strength of a Single Collagen Molecule. Biophys J 95 (1):33-39

[2] Phillips JC, *et al.* (2005). Scalable molecular dynamics with NAMD. J Comput Chem 26 (16):1781-802

[3] Willett TL, *et al.* (2008). Mechanical overload decreases the thermal stability of collagen in an in vitro tensile overload tendon model. J Orthop Res 26 (12):1605-10

CHANGES IN FOOTWEAR PROPERTIES AFTER 50, 200, 500, AND 1000 KM OF RUNNING

Ewald M. Hennig, Stefan Fischer
Biomechanics Laboratory, University of Duisburg-Essen, Essen, Germany, ewald.hennig@uni-due.de

INTRODUCTION

Good running shoes shall be comfortable and prevent overuse injuries by providing good shock absorption properties and counteract excessive pronation. Depending on individual anatomy and running style cushioning or stability running shoes are recommended. Deterioration of shoe properties has been documented by mechanical tests [1] and a biomechanical evaluation after 220 km of running [2]. The purpose of our study was the determination of changes in shoe properties over a total distance of 1000 km in 5 stages (0, 50, 200, 500, 1000 km).

METHODS

Three quality cushioning running shoe models from Adidas, Asics, and Nike (same price category) were used by 5 runners for a total distance of 1000 km. To guarantee a similar wear of the shoes a rotation protocol was used. During the first 50 km the 5 runners used each shoe for 10 km, during the next 150 km for 30 km, up to 500 km for another 60 km and during the final 500 km for 100 km. Biomechanical laboratory tests were performed with the three shoes when they were new and after 50, 200, 500 and 1000 km. A second unused pair of each of the three shoe models served as reference shoe. 20 experienced male runners (75.3 kg, SD 10.8) participated in the 5 tests and ran in each of the 3 experimental as well as the 3 reference shoes at a speed of 3.3 m/s across two adjacent "Kistler" force platforms with a target area of 120 cm by 40 cm. Tibial acceleration was measured with a miniature "Entran" EGAX-25 accelerometer. An electrogoniometer determined the changes in Achilles tendon angular motion (pronation, pronation velocity) during ground contact. Miniature piezoelectric force transducers measured the pressures under seven anatomical locations of the foot. A repeated measures ANOVA was used for statistical evaluation.

RESULTS AND DISCUSSION

In figures 1 and 2 the relative changes in peak tibial acceleration and maximum pronation are shown. These changes are calculated as ratios of the used shoe models AU, BU, CU against the reference shoes AR, BR, CR and shown in percent. For shock absorption (figure 1) almost no changes were found in peak tibial accelerations for the shoe models A and C. For shoe B a significant ($p < 0.05$) increase in maximum acceleration was found after wearing the shoe for 50 km. It appears that the major change in shock absorption properties occurs within the first 50 km. In all shoe models, small overall changes (below 10%) were found for the used against new reference shoes after 1000 km. Maximum pronation for shoe B increases the most during the first 50 km ($p < 0.01$) and remains almost the same up to 1000 km of wear. Shoe C does not show changes in pronation values across all tests. For shoe A increases in pronation occur between 500 and 1000 km of use ($p<0.05$). However, for all shoe models the increase in pronation is small and below 10%. For the heel and forefoot pressures similarly small changes were found for the used shoes after wearing them for 1000 km.

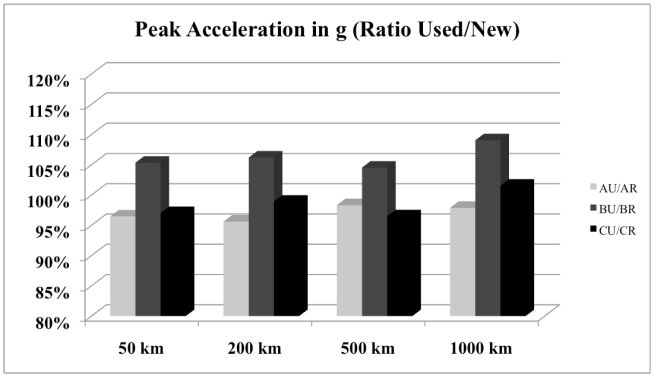

Figure 1: Changes in peak tibial acceleration of used shoes (AU, BU, CU) against the new reference shoes (AR, BR, CR)

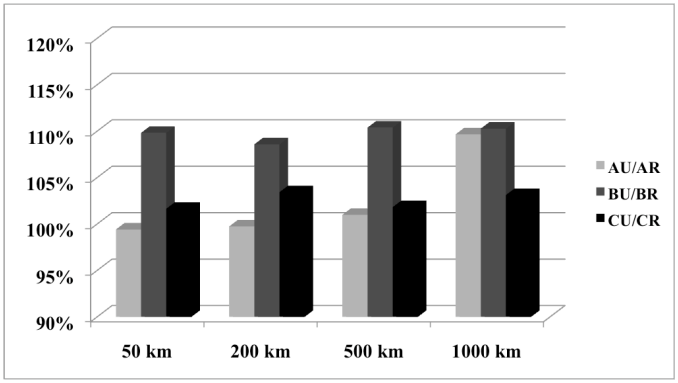

Figure 2: Changes in maximum pronation of used shoes (AU, BU, CU) against the new reference shoes (AR, BR, CR)

CONCLUSIONS

Surprisingly small changes in footwear function occur by using modern running shoes for a distance of 1000 km. The biggest changes happen within the first 50 km of running, probably by breaking the shoes in during this early period of use. Modern midsole materials, chamber structures with air and gel, and stable rearfoot counters are likely reasons for the longevity of modern high quality running shoes.

REFERENCES

[1] Cook SD et al. (1985). Shock absorption characteristics of running shoes. *Am J Sports Med* **13**(4); p. 248-53.
[2] Hennig EM and Milani TL (1995). Biomechanical profiles of new against used running shoes. In: Williams KR, Stanford University. ASB Proceedings, Palo Alto; p. 43-44.

ACKNOWLEDGEMENTS

This research was supported by Stiftung Warentest / Germany

IMPACT FORCES IN MARTIAL ARTS BRICK BREAKING

Joel L. Lanovaz, Blair F. Healey, David S. Kobylak, Mike J. Smith
College of Kinesiology, University of Saskatchewan, Saskatoon, Canada, joel.lanovaz@usask.ca

INTRODUCTION

Competitive martial arts brick breaking is a sport which exposes participants to high levels of impact forces. This unique loading regime provides an opportunity to study tolerances of the human body and investigate how exposure to high intensity/short duration loading may influence bone health. However, to date, few studies have measured the mechanical loads experienced during brick breaking [1]. The goal of this study was to examine the characteristics of the impact event during brick breaking when using common techniques employed in competitions.

METHODS

Nine experienced male black-belt level participants (mean: 31.1 yrs, 95.0 kg) made a total of 13 attempts to break as many bricks as possible by striking the top of a vertical stack of 8 standard concrete patio bricks (50 x 200 x 400 mm, 6.52 kg each). The bricks were separated using 10 mm thick hex nuts placed at the corners. The stack was supported from the bottom at the edges by two cinderblocks such that the top of the stack was ~60 cm above the floor. The participants used one of two standard striking techniques; elbow (n=6) or palm (n=7).

The stack was set up on a rigidly mounted force platform (OR6-7, AMTI, Watertown, MA) to record the applied forces (4000 Hz). An 8 camera motion capture system (F20/Nexus, Vicon, Centennial, CO) was used to track clusters of reflective spheres placed on the upper arm, forearm and hand of the striking arm (400 Hz). Static kinematic calibration data were combined with the dynamic trials to track the locations of the elbow and wrist joint centres. Force and 3D kinematic data were collected simultaneously. A separate high speed video camera (PCI 1000, Redlake MASD, San Diego, CA, 1000 fps) filmed the brick stack and was triggered using the vertical force data from the force platform.

Vertical force profiles were obtained for each attempt along with the vertical velocity of the striking point at impact (either elbow or wrist). Vertical impulse was also calculated and combined with the impact velocity to estimate an effective impact mass for each trial.

RESULTS

The number of bricks broken ranged from 3 to 7 (mean: 5.4) and was higher with the elbow technique. Impact duration ranged from 26 to 84 ms (mean: 59 ms). Peak vertical forces ranged from 2075 N to 4496 N (1.74 – 5.72 x BW) and were also higher in the elbow technique. Using the high speed video, 3 distinct phases were identified in the vertical force data (regardless of technique); an initial impact spike, a secondary loading phase and a post break deceleration spike (Figure 1). In all but 2 trials, the peak vertical force occurred after the final brick had broken. Impact velocities ranged from 7.13 to 10.56 m/s (mean: 9.02 m/s) and were not different between techniques. Vertical impulse during the breaking phases was not different between techniques but was highly correlated to the number of bricks broken. The effective impact mass was 5.1% BW for the palm technique which was different from the 9.4% BW calculated for the elbow technique.

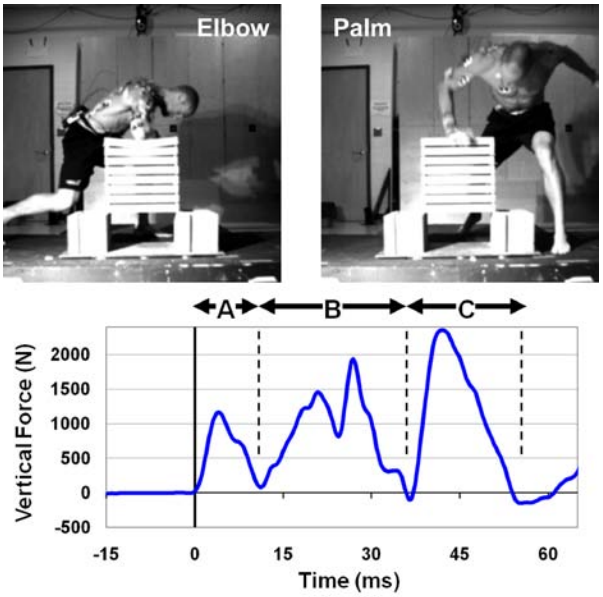

Figure 1. Breaking techniques (above), Exemplar vertical force tracing: A:Impact B:Loading C:Post-break (below)

DISCUSSION AND CONCLUSIONS

This study is the first to measure loading and kinematics in a standard competition brick breaking configuration and the first to compare the elbow and palm striking techniques. Data were comparable to previous work with different techniques and brick set ups [1]. The results of this study indicate that successful breaks are dependent on the impulse generated rather than the peak impact force or impact velocity alone.

Peak forces recorded in this study are at the upper end of estimated fracture loads in the arm [2] and are potentially greater than other high impact sports such as gymnastics [3]. This population could therefore serve as a unique model to examine the relationship between extreme loading and bone remodelling.

REFERENCES

[1] Wilk SR et al. (1983). *Am. J. Phys.* **51** (9); p. 783-790.
[2] Augat P et al. (1998). *J. Orthop. Res.*. **16**; p. 629-635.
[3] Daly RM et al. (1999). *J. Bone Miner. Res.* **14** (7); p. 1222-123

QUANTIFICATION OF LOAD DISTRIBUTION IN HELMET PADDING MATERIALS

Ryan Ouckama & David J.Pearsall
Department of Kinesiology and Physical Education, McGill University,
Montreal, QC, Canada, ryan.ouckama@mail.mcgill.ca

INTRODUCTION

Multiple-impact helmet certifications for sport (CSA, ISO, and ASTM) rely on metrics of global acceleration and puncture prevention. However, there exist situations where high velocity, low mass projectiles (e.g. hockey puck) may cause high focal forces at the impact site while headform acceleration remains within the 'safe' zone [1]. Of particular concern are stiff padding materials that perform well for high energy impacts but for mid to low energy impacts allow high focal forces to the cranium. To assess the helmet-to-head force transfer, conventional force sensor matrices can provide high spatial resolution; however, they typically lack the high sampling rates and durability needed for multiple impact measurements. The purpose of this study was to demonstrate a valid measurement system to record impact force distribution of padding materials used in helmets.

METHODS

A custom amplifier was designed to power an array of 13 Flexiforce® sensors (Tekscan, Boston, MA). A USB data acquisition device powered by a portable laptop recorded synchronized force readings providing both higher speed (15kHz/sensor) and signal resolution than most available commercial systems. Each sensor was dynamically calibrated from 0-1000N using a material testing machine (Sun 1000, Galdabini, VA, Italy). Vertical acceleration and global force were recorded in addition to the 13 force channels. Global force was recorded through use of a force plate (Kistler 9215M113, NY, USA) secured to the impact surface. The individual force sensors were arranged in a 3-2-3-2-3 square array. Various 10x10 cm foam samples were then placed on top on this array for testing. A drop tower meeting CSA requirements was used with a 5 kg spherical impactor to provide 5-10J of energy. A 3D surface was fit to the force-location data to interpolate force values between sensors and provide visual interpretation of the data. 5-10 samples of 10 different helmet foam materials were tested for 2 conditions of energy (5,10J), temperature (21,-25°C), and repeated impacts (2). To demonstrate the variance in load distribution, two conditions resulting in similar acceleration profiles will be presented.

RESULTS

Acceleration and force distribution profiles are presented in Figure 1 for expanded polypropylene (EPP) and urethane type foams. Both foams represent 5J energy first impacts. The EPP was cold (-25°C) and the urethane ambient (21°C). The average (n=5) peak acceleration was nearly identical at 37.857g and 37.854g respectively. At the same instant in time average (n=5) peak focal force was 33.3N for the EPP foam and 62.8N for the urethane foam. The global impulse (F>50N) was greater for the EPP foam at 10.4 kg·m/s compared to 9.1 kg·m/s for the urethane foam. Severity index was 32.6 for EPP versus 31.9 for the urethane foam.

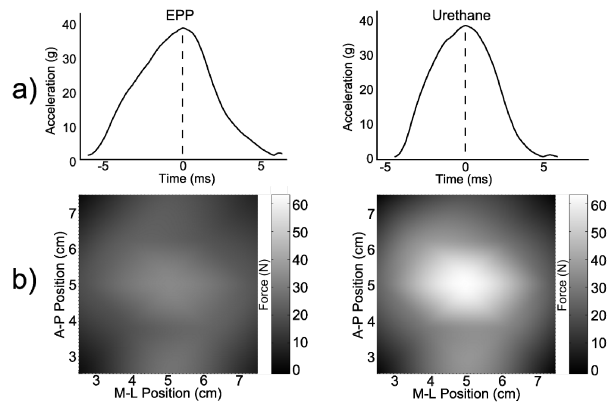

Figure 1: Acceleration (a) and peak load distribution profiles (b) for EPP and urethane foam types.

CONCLUSIONS AND DISCUSSION

Using only peak acceleration as a criterion assessment, one may assume that the above two foams examples (Fig 1a) have similar impact attenuation properties. However, load distribution analysis shows these foams behave differently, particularly with regards to a two-fold magnitude discrepancy in focal force maxima. In turn, one may speculate that the underlying tissue (scalp, cranial bone, cerebral tissue) response may vary with foam type due to these differential stresses induced during impact when worn by a person. By testing a range of common foam types, we hope to catalogue the unique load distribution properties of different padding materials across all tested conditions. Initial findings indicated that further study of helmet materials using this system is warranted. To date, preliminary testing involving over six hundred impact trials have been recorded and are currently in analysis.

REFERENCES

[1] Bishop, P.J. and J. Arnold. 1993. *Safety in Ice Hockey: 2* ASTM STP 1212: 175-182.

ACKNOWLEDGEMENTS

Funding provided by the NSERC/FQRNT Industrial Innovation Scholarship and by Bauer Hockey Corp

GATE IMPACT AND SIT-SKIER PERFORMANCE
A TOP SECRET 2010 PROJECT

Marc Denninger, Eve Langelier, Cécile Smeesters, Cyntia Doré and Denis Rancourt
Human Performance and Safety Research Group (PERSÉUS), Sherbrooke QC, Canada
Department of Mechanical Engineering, Université de Sherbrooke, Sherbrooke QC, Canada
e-mail: Denis.Rancourt@USherbrooke.ca web: http://eureka.gme.usherb.ca/perseus/

INTRODUCTION

Gate impact is one of the critical phases in slalom competitions. Athletes must learn to impact the gate to shorten the course but they must do it in such a way to minimize destabilizing impact forces on their sit-ski. The purpose of our study was to determine the extent of gate impact on skier performance and to determine a minimal impact height to reduce destabilizing effects.

METHODS

An ANSYS 2D finite element model was elaborated to represent the impact of a sit-skier on a certified 1740mm long slalom gate. The gate is a homogenous flexible plastic gate connected to a flexible coupling grounded to the snow cover. Both components include damping based on the decay of step responses of the isolated sub-system. The skier and sit-ski were modeled as a solid 80Kg mass. A simili mass-spring-damper bumper system represented the impedance of the sit-ski leg cover structure. Impact simulations were computed for various impact velocities (15 to 60km/h in 5km/h increments) and various impact heights (20 to 100cm in 5cm increments), for a total of 170 simulations.

RESULTS

Following impact, the gate progressively deforms and exerts an interacting force F(t). At impact, the force is horizontal and tends to slow down the sit-ski. A typical sequence of gate deformations is shown in Figure 1.

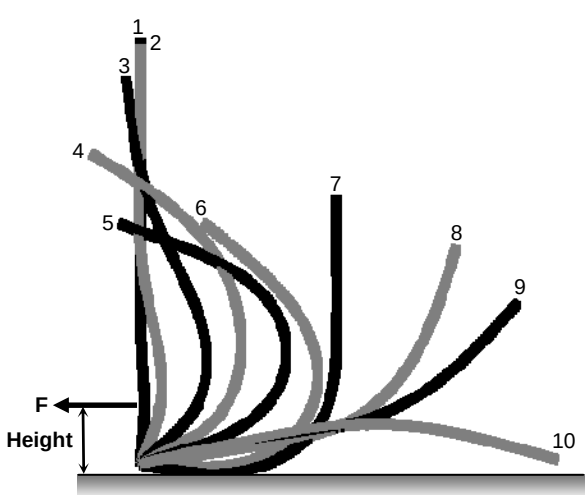

Figure 1: Typical gate deformation following impact.

The first consequence of the interacting force is to slow down the sit-ski. The percentage of velocity reduction is illustrated in Figure 2 for the various impact conditions. Overall, the velocity reduction is between 1 to 2km/h. Figure 3 illustrates the impact force magnitude.

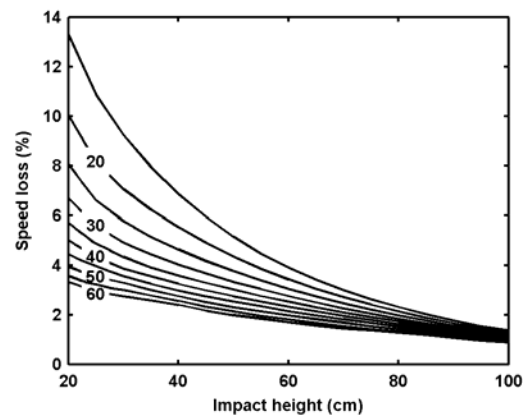

Figure 2: Velocity reduction following impact as a function of impact height and impact velocity.

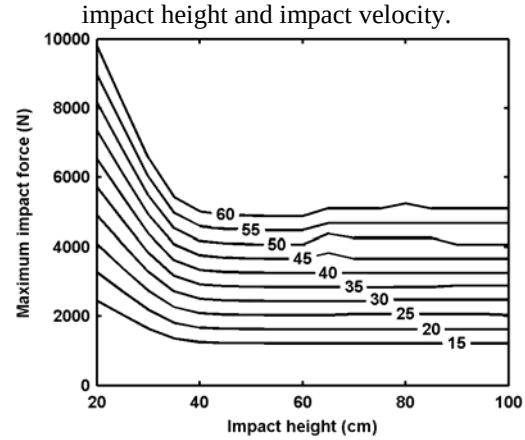

Figure 3: Maximum impact force on sit-ski leg cover as a function of impact height and impact velocity.

DISCUSSION AND CONCLUSIONS

Given the number of gates in a slalom run, impact height must be as high as possible. Straight impact on a gate may induce impact forces as high as 9 000N for low impact heights. To minimize impact force, impact height should be over 40cm. Impact height should therefore be addressed with care to avoid performance reduction and possibly safety issues.

ACKNOWLEDGEMENTS

This work was funded by the Own the Podium – Top Secret 2010 program from the Canadian Olympic Committee. We also thank Jean-Luc Lessard for technical help.

GROUND REACTION FORCE ADAPTATIONS DURING CROSS-SLOPE WALKING AND RUNNING

Mohsen Damavandi, Philippe Dixon, David Pearsall
Department of Kinesiology and Physical Education, McGill University, Montreal, Canada, mn_damavandi@yahoo.com

INTRODUCTION

Ground reaction force (GRF) measurements are commonly used for assessment of normal and pathological gait in level surfaces [1]. Though transverse inclined (cross-sloped) surfaces are a common characteristic of our environment, only a few studies have evaluated cross slope design [2,3]. Thus, the purpose of this study was to determine the GRF adaptations in level and cross-slope walking and running.

METHODS

Nine male subjects participated in this study. Four different gait conditions were observed: walking and running on a 0° and 10° cross slope surface. A minimum of five bare foot trials for each condition were collected. A 7m inclinable walkway with an embedded force plate (AMTI, model OR6-5-1000) was used. The force plate was secured into the walkway via a number of bolts and covered with Mondotrack (Mondo America Inc.) to avoid slippage. GRF data were collected at 960Hz. The force parameters of each GRF component for walking at heel strike (HS), the first and second maximum GRF values (MaxFy1 and MaxFy2, respectively), at the minimum GRF between them (MinFy), and toe off (TO); and running at HS, maximum GRF (MaxFy), and TO were extracted using Matlab (The Mathworks Inc.). GRFs between cross-slope conditions (0° versus 10°) for walking and running were compared using repeated measure ANOVA.

RESULTS

Statistically significant differences were observed generally in mediolateral component of GRF (Fy) as shown in Table 1. Fy was significantly different among the conditions during walking at MaxFy1, MinFy, and MaxFy2 ($p < 0.002$) (Figure 1). For running, Fy values were significantly different among the conditions at MaxFy ($p < 0.000$) (Table 1).

DISCUSSION AND CONCLUSIONS

This study shows that compared to horizontal locomotion, 10º cross-slope walking and running require substantial and asymmetrical adaptations of the GRF (from –17 to +29% body weight (BW) for walking and –38 to +53% BW for running). These adaptations are necessary to enhance dynamic stability in order to prevent down slope slippage and/or vertical body instability. The adaptations required for walking could be difficult for populations with restricted mobility, while those for running may represent a challenge for athletes with existing lower-limb injuries or asymmetries. From these findings, further study is warranted to identify the effects of varied slopes, surface frictions, and walking and running speeds for different populations.

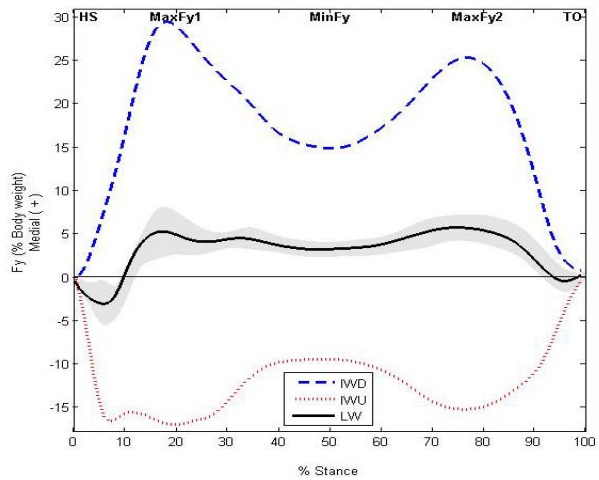

Figure 1: Average mediolateral GRF component (Fy) in flat and inclined walking conditions. Gray area indicates the standard deviation of level walking trials.

REFERENCES

[1] Giakas G et al. (1997). Comparison of gait patterns between health and scoliotic patients using time and frequency domain analysis of ground reaction forces. *Spine* 21(19); p. 2235-42.
[2] Pearsall DJ et al. (2007). Effects of cross slope on gait ground reaction forces. *Proceedings of the International Society for Posture & Gait Research*, Burlington, VT.
[3] Dixon CD and Pearsall DJ. *J Appl Biomech,* in press.

Table 1: Means (SD) of Fy (%BW) across the intervals of stance phase of walking and running in level (LW and LR), inclined up-slope (IWU and IRU), and down-slope (IWD and IRD). Negative values indicate lateral direction. [a] and [b] represent significant differences between level and cross-slopes, and up- and down-slopes, respectively.

Plane	Event	LW	IWU	IWD	LR	IRU	IRD
Mediolateral	HS	−0.4 (0.4)	0.0 (0.2)	−0.2 (0.2)	−0.2 (0.9)	0.4 (0.4)	0.1 (0.5)
(Fy)	MaxFy1	4.7 (2.4)	−17.5 (1.7) [a]	29.3 (5.4) [a,b]	---	---	---
	MaxFy	---	---	---	8.7 (4.3)	−37.9 (5.9) [a]	52.7 (7.0) [a,b]
	MaxFy2	5.5 (1.4)	−15.6 (2.7) [a]	25.3 (1.6) [a,b]	---	---	---
	TO	0.2 (0.4)	−0.4 (0.5) [a]	0.8 (0.6) [b]	0.3 (0.4)	0.2 (0.7)	0.5 (0.4)

Investigation of dynamic stability during the transition from level ground walking to a change in surface height in healthy young adults.

Kathleen O'Reilly[1], Rachel Campbell[1], Kristen MacDonell[1], Katherine Norrish[1], Kristen Whitney[1] Karl F Zabjek[1,2]
[1]Department of Physical Therapy, University of Toronto, Toronto, Canada, k.zabjek@utoronto.ca
2 Bloorview Kids Rehab, Toronto, Canada

INTRODUCTION

Falls are prevalent amongst populations with neuromuscular disorders and are attributed to decreased dynamic stability and environmental barriers such as curbs [1,2] However, very few studies have investigated the transition in walking from level ground to a change in surface height. [3-5] The purpose of this study is to identify differences in dynamic stability using medial-lateral center of mass (COM) and center of pressure (COP), inclination angles (COP-COM) during level ground walking, curb ascent, and curb descent.

METHODS

Ten healthy young adults were recruited to perform level ground walking, curb ascent and descent tasks in a Biomechanics Laboratory. Three AMTI force plates (A-Tech, Instruments, Scarborough, ON) were used to capture ground reaction forces (GRF) during the three tasks. Force plate one (FP1) was placed at ground level, and two additional force plates (FP2 and FP3) were embedded side by side into the platform of a curb that was fifteen centimetres in height. Each force plate was used to calculate the COP under each foot. A multi-camera Vicon Mx motion capture system (Vicon, Denver CO, USA) was used to track the motion of thirty four reflective markers that defined the feet, shank, thigh, pelvis, trunk and arms and used to calculate the COM. The 3D marker trajectory was collected at a sampling frequency of 50 Hz. The COP-COM inclination angle was calculated from heel contact to toe off for the Trail Limb (push off foot from the ground), and Lead Limb (foot stepping up onto the curb.

RESULTS

Peak medial-lateral COM-COP inclination angles were significantly larger ($P<0.01$) during both curb ascent and descent compared to level ground walking. (see Figure 1)

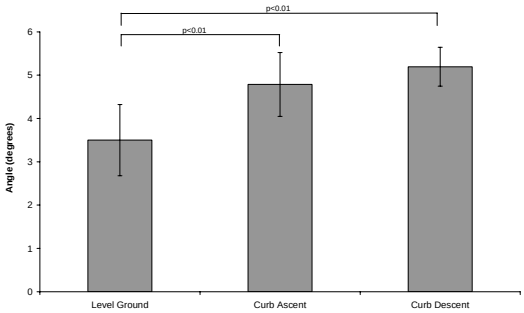

Figure 1. Peak M-L COM-COP inclination angles between level ground walking, curb ascent and curb descent. Values are mean ± standard deviation (SD).

In addition, average medial-lateral COM-COP inclination angles were significantly greater in the lead limb during curb ascent and the trail limb during curb descent ($P<0.01$). (See Figure 2)

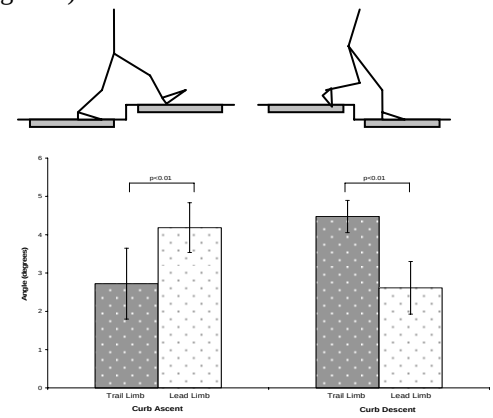

Figure. 2. Mean M-L COM-COP inclination angles for trail limb and lead limb during the single stance phases of curb ascent and descent. Values are mean ± standard deviation (SD).

DISCUSSION AND CONCLUSIONS

Curb negotiation poses a greater challenge to dynamic stability in the medial-lateral direction compared to level ground walking in able-bodied young adults. Decreased medial-lateral stability exists during single leg support of the lead limb during curb ascent and of the trail limb during curb descent. This finding is in agreement with current physiotherapy clinical practice, which encourages patients to step up with the unaffected limb, and down with the affected limb.

REFERENCES

[1] Berg, W.P., Alessio, H.M., Mills, E.M. & Tong, C. 1997, *Age and Ageing*, vol. 26, no. 4, pp. 261-268.
[2] Campbell, A.J., Borrie, M.J., Spears, G.F., Jackson, S.L., Brown, J.S. & Fitzgerald, J.L. 1990, *Age and Ageing*, vol. 19, no. 2, pp. 136-141.
[3] Collen, et al., 2005 *Physiotherapy research international : the journal for researchers and clinicians in physical therapy*, vol. 10, no. 2, pp. 81-92.
[4] Crosbie, J. & Ko, V. 2000, *The Australian journal of physiotherapy*, vol. 46, no. 2, pp. 103-112.
[5] Lythgo, N, Begg, R, Best, R. 2007, *Gait & Posture*, vol. 26, pp. 82.

ACKNOWELDGMENTS

The authors gratefully acknowledge William Gage, Justin Chee and Sonya Allin and for their generous contributions.

STATIC & DYNAMIC KNEE KINEMATICS IN HEALTHY WOMEN WITH KNEE HYPEREXTENSION

P Teran-Yengle, R Birkhofer, M Sinnott, K Patton, B Singh, & HJ Yack
Program in Physical Therapy & Rehabilitation Science, University of Iowa, Iowa, USA
Email: patricia-teranyengle@uiowa.edu

INTRODUCTION

Abnormal knee kinematics can result in excessive loading of structures of the knee joint, such as menisci, ligaments, or cartilage. Associated change to these structures, due to the abnormal stress, can be detrimental to the integrity of the knee joint [1, 2]. Knee hyperextension implies increased stress to the posterior joint capsule of the knee [3] and to the anterior cruciate ligament (ACL) [4]. Studies also point out that there is an increased contact stress on the tibial-femoral joint in the straight knee or when the knee joint is extended [5]. Normative knee extension passive range of motion (PROM) values for women ages 18 to 29 (2º ± 8º) and 30 to 39 (5º ± 5º) have been established [6]. Several studies have reported that compared with men, women demonstrated greater incidence of knee hyperextension [7]. Female athletes with knee hyperextension patterns are five times more likely to injure their ACL [8]. The purpose of this study was to investigate the kinematics of the knee joint in healthy young women with asymptomatic knee hyperextension at passive range of motion (PROM), standing, and walking.

METHODS

Eleven women with asymptomatic knee hyperextension PROM greater than 5° [3] participated in this study. Participants underwent a physical and gait evaluation. The physical evaluation assessed lower limb muscular strength and PROM using standard techniques. Joint laxity was assessed using the Beighton and Horan Joint Mobility Index (BHJMI). The gait evaluation was conducted along an 8 m walkway using a three-dimensional motion analysis system (Optotrak, NDI; Kistler) with subjects walking at their self selected (SS) speed and at 3 mph. Gait data was processed using Visual 3D software (C-Motion).

RESULTS

Eleven women (age 26.6 ± 6.8; weight 74.3 ± 17.6 Kg; height 1.64 ± 0.1 m) took part in this study. Muscular testing showed normal values for knee extensors (145 ± 11 N), and flexors (128 ± 23 N). Based on the BHJMI 64% of subjects had moderate joint laxity and the remaining 36% had high joint laxity. The PROM showed 9.5º ± 3.1 (from 6º to 14º) of knee hyperextension in subjects' right knee and 9.5º ± 2.4º (from 7º to 14º) in subjects' left knee. Peak knee extension values in right or left knee at either initial contact or toe off of gait cycle were used for further analysis. PROM data showed that four subjects had greater knee hyperextension values in their right knee and three subjects had the same degree of knee hyperextension in both knees. The peak knee hyperextension value at PROM was 10º ± 2.7º (from 7º to 14º). Standing data showed that nine subjects had peak knee hyperextension values in their right knee (from -2.2º to 11.3º). Gait data showed that seven subjects had greater hyperextension range of motion in their right knee at SS (8.4º ± 2.1º) and 3 mph (10.5º ± 2.4º). Six of these seven subjects showed maximum knee hyperextension at initial contact (8.8º ± 2º) when walking at SS and four subjects showed greater knee hyperextension at toe off when walking at 3 mph (10º ± 1.7º). Peak knee extension during standing, walking at SS speed and at 3.0 mph were 6.6 ± 4.1º, 8.1 ± 2.5º and 8.5 ± 3.1º, respectively (Fig. 1). There was a low correlations between PROM and standing (r= 0.09), walking at SS speed (r=0.28), and walking at 3 mph (r=0.28).

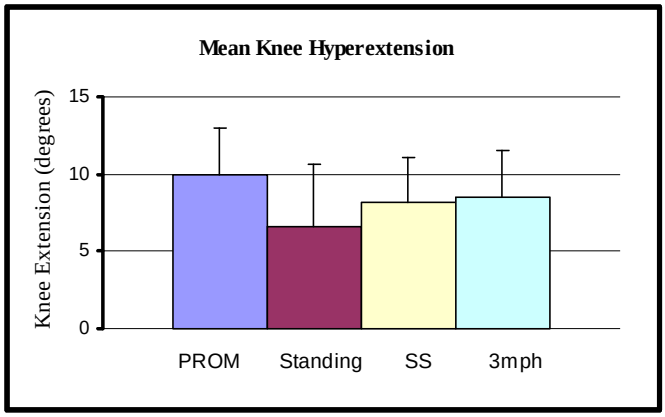

Figure 1: Mean values of knee hyperextension at PROM, standing, and walking at self selected speed and 3 mph with standard error.

DISCUSSION AND CONCLUSIONS

The results of this study indicate that peak knee extension range of motion varies in the different conditions: PROM, standing, walking at SS speed and at 3 mph. The majority of subjects have moderate joint laxity. The maximum knee hyperextension values occurred in subjects' right knee. The results show that, while clinical assessment of knee PROM enables the identification of individuals with knee hyperextension, it may not predict the amount of knee hyperextension achieved during walking at self-selected and faster speed or other functional activities.

REFERENCES

[1] Hunter DJ et al. (2009). *Journal of Bone and Joint Surgery* 91(1); p. 85-89
[2] Tanamas S et al. (2009). *Arthritis & Rheumatism* 61(4); p. 459-467
[3] Oatis CA. Kinesiology.: Mechanics & Pathom of human movement (2004)
[4] Senter C et al. (2006). *Sports Medicine* 36(8); p. 635-641.
[5] Nisell R et al (1986). Acta Orthop Scand 57; p. 41- 46.
[6] Gazzi Macedo et al. (2009). *Physiotherapy Theory and Practice* 25(2)
[7] Medina McKeon J M et al. (2009). *Journal of Athletic Training*, 44 (3) 249
[8] Myer GD et al. (2008). *Am J Sports Med* 36:1073-1080.

Nonlinear time series analysis of human gait under cognitive interference conditions

Karelia E. Tecante G., Peter A. Federolf, Benno M. Nigg
Human Performance Laboratory, Faculty of Kinesiology, University of Calgary, 2500 University Drive N.W., Calgary, Alberta, Canada, T2N 1N4

INTRODUCTION

Dual task situations occur when cognitive and motor control tasks are shared simultaneously. Prior studies suggest that gait can be a reflex-controlled task but may also deteriorate due to the level of the cognitive task challenge [1]. Therefore, quantifying dynamic stability during dual task activities is important for assessing people that may be at a greater risk of falling in order to prevent such falls. Traditional gait analysis neglects the temporal information in gait waveforms. To examine the effects of a cognitive task (CT) during the complete gait cycle, a more complex analysis is required. The present research combined two techniques for this purpose. First, principal component analysis (PCA) was used to find the main gait features in order to reduce data of high dimension. Secondly, the largest Lyapunov exponent (LE) was computed in order to detect very small fluctuations during gait. A greater LE indicates a less periodic movement over the time interval studied [2]. The hypotheses tested are: (H1) the LE increases according to the level of the CT and (H2) greater LEs are found in higher principal components (PCs).

METHODS

Twenty-two healthy subjects, ten old (age 59.8±4.6, weight 72.9±13.2 kg, height 165±0.09 cm) and twelve young adults (age 26.5±2.9, weight 73.3±20.0 kg, height 168±0.09 cm) participated in the study . All subjects walked on a treadmill while performing a CT (numbers memory test) with four levels of difficulty (CT1 to CT4). A baseline measurement was captured in which no cognitive test was applied (CT0). To obtain and quantify the walking pattern variability, a total of thirty-seven reflective markers were placed on selected bony landmarks of the body. Kinematic data was captured by an eight video high speed camera system (Hawk Digital RealTime System, Santa Rosa, CA USA) at a sampling rate of 240 frames per second. Data analysis involved custom MATLAB (Version R2008a) routines to perform PCA and LE calculation. A total of 60 steps were used. The PCA resulted in ten PCs (PC1-PC10). Each PC represented a coefficient time series describing the walking patterns during a dual task situation. With these time series the LE was calculated based on Kantz algorithm. To compute the LE the appropriate time delay (τ=10) and embedding dimension (d=5) were obtained with the average mutual information (AMI) and false nearest neighborhood (FNN) algorithm respectively.

RESULTS

The old and young group showed a significant decrease in the CT test score as the level of difficulty increased ($p<0.05$). In both groups the LEs for each CT tended to increase when comparing the first five PCs and slightly decrease for the last five suggesting an increase in chaotic behavior but again a more periodic behavior for the last PCs, however these differences are not enough to be significant ($p>0.05$). No significant differences were found when increasing the difficulty level of the CT and no significant differences were found when comparing between groups.

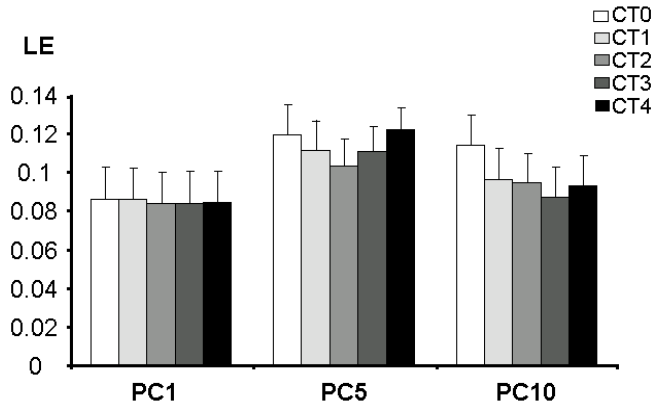

Figure 1. Mean LEs for each time series (PC1, PC5 & PC10) when walking under CT0 to CT4 for the old group. Error bars indicate standard error.

DISCUSSION AND CONCLUSIONS

A new way to analyze gait variability not reported in the actual literature was explored. Although the hypotheses were rejected, it remains interesting to observe in both groups that the fluctuations among cognitive tests in PC1 seem more stable compared to the rest of the PCs. A possible explanation might be that usually the first three or four PCs are highly regular oscillations. Also, high scores found for CT1 and CT2 could suggest that some attention is needed to perform a cognitive test during walking but not demanding enough, thus a more automated walking occurs. This can be a possible explanation for the trend observed from PC3 to PC10 where the LE starts decreasing from CT0 to CT3 and increases again for CT4. Nevertheless, this was not always the case for the young group and this observation can not be proved since the LE technique seems to not sensitive enough to detect significant fluctuations among different cognitive tests. To determine the relationship between the LE and locomotor performance may be highly complicated. Future research should evaluate more extensively factors such as the type of LE logarithm used and its restrictions, noise, multiple attractors, time delays in the dynamical system and the type of CT applied. Despite these first results, previous studies have shown that the LE technique remains a powerful approach to analyze dynamic locomotor stability [3].

REFERENCES

[1] Woollacott et al. (2002). Attention and the control of posture and gait: a review of an emerging area of research. Gait Posture; 16: 1-14

[2]Nessler et al. (2009). Nonlinear time series analysis of knee and ankle kinematics during side by side treadmill walking. Chaos 2009; 19: 026104-1-026104-11

[3] Dingwell et al. (2000). Nonlinear time series analysis of normal and pathological human walking. Chaos; 10

EFFECT OF SENSORY FEEDBACK ON WALKING PATTERNS OF A NEUROMECHANICAL MODEL

Jeremy W. Noble[1,2] & Stephen D. Prentice[1]
[1]Department of Kinesiology, University of Waterloo, Waterloo ON, Canada, jwnoble@uwaterloo.ca
[2]Department of Physical Therapy, University of British Columbia, Vancouver BC, Canada

INTRODUCTION

Recently neuromechanical simulations have been developed to further understand the mechanisms involved in the control of human locomotion [1]. Most of these simulations have tried to replicate normal walking patterns in attempt to reverse engineer the control mechanisms used for normal walking. For this study, we will not focus on reproducing the exact kinematics involved in human walking, but rather explore some basic issues in its neural control. The goal of this study was to systematically manipulate the magnitude of the sensory feedback originating from muscle receptors and cutaneous receptors and use a neuromechanical model to investigate the effect on the walking pattern. The specific objective was to compare the effects of feedback being applied over the whole gait cycle to phase dependent feedback, where the feedback gain was manipulated over the gait cycle.

METHODS

The neuromechanical model consisted of separate represntations of the musculoskeletal system and the neural control system. The musculoskeletal model consisted of 5 segments (HAT, 2 Thighs & 2 Legs), and was actuated by a flexor and extensor muscle at each hip joint. The range of motion of the knee was controlled only by passive moments at the knee joint.

The neural control model consisted of a Central Pattern Generator (CPG) that consisted of a flexor and extensor neuron for each hip joint. Sensory signals from muscle receptors were based on a weighted combination of each muscle's length and velocity that was subject to a first order delay for smoothing purposes. A stance sensor was located at the distal end of each leg segment, this sensor was capable of blocking sensory feedback from muscle receptors under certain circumstances.

Two sets of simulations were carried out to determine the effect of sensory feedback on the walking pattern of the neuromechanical model. In both sets of simulations, the feedback gain and the intrinsic frequency of the CPG was manipulated across the working range of these variables. In the first series of simulations, sensory information from the muscle receptors was provided across the entire walking cycle. In the second series of simulations, phase dependent feedback was used, such that extensor muscles only received sensory receptors during the stance phase, and flexor muscles only received sensory feedback during the swing phase. The simulations were carried out at four different magnitudes of CPG output.

RESULTS

The highest walking speeds were observed when only feedforward control was used, the application of sensory feedback over the whole walking cycle led to a significant decrease in the walking speed of the model. The use of phase dependant feedback led to a more moderate walking speed, approximately halfway between the feedforward control and constant feedback simulations.

The walking pattern was most variable when feedforward control was used exclusively, while the most stable walking pattern was observed when feedback was applied over the whole gait cycle. Phase dependent feedback allowed for a faster walking speed, at the expense of a slightly more variable walking pattern.

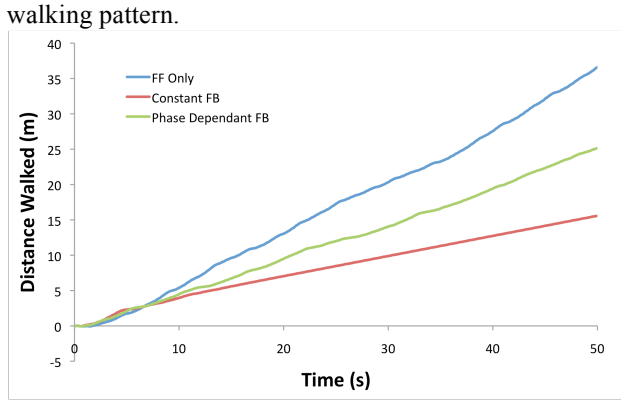

Figure 1: Illustration displacement of the HAT segment over 50s for feedforward control (blue), when feedback was applied over the whole gait cycle feedback (red) and phase dependent feedback was used (green).

DISCUSSION AND CONCLUSIONS

This work illustrates the importance of phase dependent feedback in the development of neuro-mechanical simulations of walking. Phase dependent feedback, is a significant feature of locomotor control, and allows the control system to make corrective responses when a perturbation will disrupt the walking pattern, but ignore the perturbation if there will not be a large effect on the walking pattern [2].

REFERENCES

[1] Paul, C. et al. (2005). *Biol Cybern.* Vol **93**(3). p. 153-70.
[2] Capaday, C. & Stein, R. (1986). *J Neurosci.* Vol **6**(5). p. 1308-13.

ACKNOWLEDGEMENTS

This work was funded by a grant from NSERC.

A MODEL FOR FORWARD DYNAMIC SIMULATION OF RAPID TAPPING MOTION OF INDEX FINGER

Mohammad Sharif Shourijeh[1], John J. McPhee[1], Richard Wells[2]
[1]Systems Design Engineering Department, University of Waterloo, ON, Canada, msharifs@uwaterloo.ca
[2]Department of Kinesiology, University of Waterloo, ON, Canada

INTRODUCTION

A model for the forward dynamic simulation of rapid tapping motion of the index finger is presented. It consists of a 1-DOF horizontal pendulum along with two muscles, one as flexor and the other as extensor. The goal is to solve the force-sharing problem during a desired motion so we can investigate the maximum motion frequency at which the assumed muscles can move the finger.

METHODS

The model has only two muscles and the moment arms of them are assumed to be constant during the motion defined, since the range of motion is small. Desired motion is defined as $\theta = 0.21\sin(f \cdot t)$ where 0.21 rad is the amplitude of the periodic motion which has a good agreement with [2], and f is the motion frequency. Anthropometric properties of the index finger like length, mass and moment of inertia are according to [3].

Muscle models are Hill-type (consist of three elements) and activation and contraction dynamics have been considered within the contractile element.

The pattern of each muscle neural input (excitation) signal is assumed to be a sixth-order polynomial as a function of time. The first reason for assuming such a pattern is that the neural input acts as the rectified, smoothed and normalized EMG [1], which is smooth and can be curve-fitted by medium and high-order polynomials, and the second is that assuming a continuous and continuously differentiable function like a polynomial will smooth the nonlinear constraints of the excitation signal within the optimization problem definition.

The optimization process looks for the coefficients of the polynomial terms, which are 14 variables, in order to minimize the objective function which is defined as a linear combination of a physiological cost function (sum of activation states) and motion tracking error. The optimization Toolbox of Matlab® is used for solving the problem. For the initial guess needed, results of the same case using a Genetic Algorithm as the optimizer were used. Consequently, the optimization approach applied to solve for the muscle force-sharing was a hybrid method.

RESULTS

Sensitivity analyses were done by changing model parameters, e.g. finger mass, to investigate the effects of each on the values of both cost functions and other results. One separate simulation was run to study how gravity affected the results. Another simulation studied the effects of weighting factors in the linearly combined objective function.

The main results were caught for motion frequency variation to see how muscle coordination changed when a faster motion was desired. Starting from 2Hz, frequency was increased to 4, 5, and 6 where the model could not follow the desired motion anymore. Figure 1 shows the results of motion and the extensor values when motion frequency is 2 Hz.

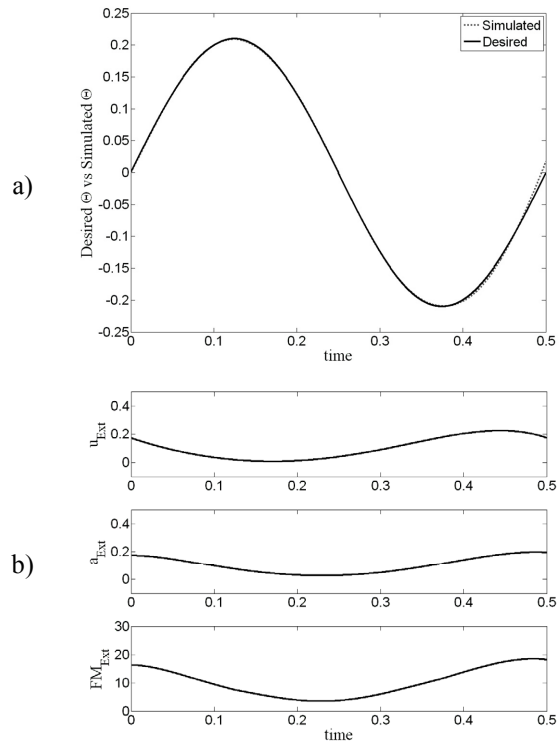

Figure 1: f =2 Hz a) theta, desired and simulated motions vs. time b) the extensor excitation, activation, and force

DISCUSSION AND CONCLUSIONS

The maximal frequency for which the model can follow the desired motion was found to be around 6, which means from this frequency on, muscles are not able to contract fast enough as desired. This agrees well with the maximum frequencies presented in the literature, e.g. [4] which claims 6.92 ± 0.56 Hz.

REFERENCES

[1] He, J., Levine, W.S., &Loeb, G.E. (1991). Feedback gains for correcting small perturbations to standing posture. *IEEE Transactions on Autonomic Control*, 36, 322-332.

[2] Kuo, P.L., Lee, D.L., Jindrich, D.L. and Dennerlein, J.T., 2006, Finger joint coordination during tapping, *Journal of Biomechanics*, 39(16), 2934-2942.

[3] Buchner, H., Hines, M. and Hemami, H., 1988, A dynamic model for finger interphalangeal coordination. *Journal of Biomechanics*, 21(6), 459–468

[4] Morrison, S.., Hong, S.L. and Newell, K.M., 2009, Upper frequency limits of bilateral coordination patterns, *Neuroscience Letters*, 454, 233–238

MUSCLE AND FASCICLE EXCURSIONS IN CHILDREN WITH CEREBRAL PALSY

Marlee Hahn[1], Megan Yaraskavitch[1], Walter Herzog[1]
[1]Department of Kinesiology, University of Calgary, Canada
mhahn@kin.ucalgary.ca

INTRODUCTION

Cerebral Palsy (CP) is a group of conditions caused by a static lesion in the brain, leaving children with permanent cognitive and motor impairments [1]. Spasticity, a velocity-dependent resistance of muscle to stretch [2], is a common manifestation of CP. Although much research has been aimed at discovering the cause of CP, little attention has been paid to determine the influence of spasticity on muscle architecture. Recently, we discovered that myoibrils from CP patients were much stiffer than myofibrils from control muscles, suggesting that excursion of fascicles in CP patients is limited [3]. However, there is no information on fascicle excursions in CP patients compared to age- and sex-matched controls. The purpose of this study was to measure fascicle lengths (FL), and fascicle and muscle excursions for full range of motion testing in CP patients and typical age- and sex-matched subjects.

METHODS

Children between the ages of 10 and 16 were recruited from the Calgary Cerebral Palsy Association (experimental group n=7) and the Calgary community (control group n=13). Five of the 7 experimental group children had a sex-matched sibling that was used for the control group. Testing was performed on the medial gastrocnemius (MG), a unipennate muscle that is often spastic in CP patients. EMG electrodes were placed on the proximal MG and the tibialis anterior. Subjects were seated in the chair of the Biodex™ System III (Biodex Medical Systems Inc., New York, USA). The probe from the Philips™ EnVisor Ultrasound System (Koninklijke Philips Electronics N.V., The Netherlands) was secured to the lower leg to visualize either mid-belly MG fascicles or the myotendinous (MT) junction. Four passive trials covering the full range of motion were performed. Active trials were conducted with the subject performing an 8-second ramp-up isometric contraction at 10-degree intervals over the full range of motion. Torque, ankle angle and EMG data were collected. In cases where FL was not fully visible, trigonometric relationships were used to calculate fascicle lengths from the measured pennation angle (α) and muscle thickness (Tm) (Figure 1). FLs and MT position were measured through the full range of motion. Non-parametric Mann-Whitney U-statistics (α=0.01) were used to test for differences in fascicle lengths, fascicle excursions and muscle excursions between experimental and control group children.

RESULTS

Fascicle lengths at reference position were shorter for CP children (23±6mm) than control (37±6mm), while fascicle excursions over a control range were greater for CP children (14±8mm) than control children (11±5mm). Finally, fascicle excursion as a percentage of muscle excursion was twice as big in CP children (87±37%) than the control group children (43±20%).

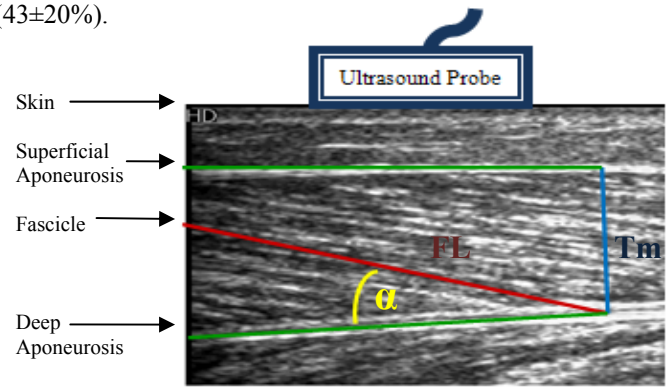

Figure 1: FL calculation from an ultrasound image of the MG: FL=Tm/sin(α). Green delineates superficial and deep aponeuroses. Blue shows muscle thickness (Tm). Red traces the fascicle (FL). Yellow (α) defines the pennation angle.

DISCUSSION AND CONCLUSIONS

Here we confirm previous results that fascicle lengths in CP children are shorter than those in age-matched controls [4]. New, is the result that fascicle excursions are greater in absolute terms and greater compared to the muscle excursion in CP children than control children. Combined these results indicate that the excursion of fascicles compared to the resting length of fascicles is much bigger in CP children (61%) compared to normal children (30%), thereby covering a much greater range of sarcomere lengths. Since spastic myofibrils [3] and fascicles [4] are known to be much stiffer in CP patients than normal, such large excursions of fascicles in the CP patients is likely associated with tremendous resistance, and thus inefficiency of movement. Since sarcomere lengths at rest in spastic muscles of CP children have been found to be greatly elongated in the arm [4] and leg musculature [3], and since muscles are much more prone to injury at long lengths, we can further assume that the large excursions in the CP patients may cause stretch-induced injuries in the spastic musculature.

REFERENCES

[1] Miller, F. *Cerebral Palsy*: Springer, 2005.
[2] Sanger, T.D. et al. (2003) *Classification and Definition of Disorders Causing Hypertonia in Childhood*. *Paediatrics* 1; e89-97.
[3] Yaraskavitch, M. *Changes in Passive Muscle Properties and Titin in Spastic Cerebral Palsy*. (2008). University of Calgary, AB. MSc Thesis.
[4] Friden, I. (2003). *Muscle and Nerve*. vol **27**; p. 157-164.

THE EFFECT OF ANTAGONISM ON THE CALCULATION OF MUSCLE MODEL PARAMETERS

Ross H. Miller, Graham E. Caldwell
Department of Kinesiology, University of Massachusetts, Amherst, USA, rhmiller@kin.umass.edu

INTRODUCTION

In musculoskeletal modeling, subject-specific Hill muscle model parameters have been calculated by minimizing the difference between simulated joint moments and those measured on a dynamometer [1,2]. Both agonist and antagonist muscles contribute to resultant joint moments, and the antagonistic muscles are active during isolated joint actions [3]. It is thus important to consider antagonistic co-activation when calculating muscle model parameters, yet most modeling studies have assumed no co-activation [1,2].

Therefore, the purpose of the study was to quantify the effect of including antagonistic co-activation on the calculation of muscle model parameters from isolated joint actions.

METHODS

Five adult females (age 29±5 yrs, height 165±3 cm, mass 60.3±3.4 kg) performed a series of maximum isovelocity joint actions (ankle plantar/dorsiflexion, knee and hip flexion/ extension) on a dynamometer (System 3, Biodex, Shirley, NY, USA). Each action was performed at three concentric and one eccentric velocity (10, 90, 150, and -90 deg/s). Gravitational, passive, and inertial effects were subtracted from the measured moments to calculate the net active muscle moment.

For each subject, the joint actions were simulated using a 2D computer model with nine Hill muscle models that represented iliopsoas, glutei, vasti, knee flexor, tibialis anterior, soleus, rectus femoris, hamstrings, and gastrocnemius. Joint angles were drawn from the experimental data, and 100% activation was assumed for all agonist muscles. Muscle model parameter optimizations were performed with no antagonistic co-activation, and with all antagonists activated at either 10% or 50%. In each case, muscle parameters for maximum isometric strength (F_o), optimal CC length (L_o), unloaded SEC length (L_u), and fiber type ratio (FT) were optimized until the average RMSE between the simulated and measured joint moment time series was under 20 Nm for all speeds. Differences between conditions were assessed by repeated measures ANOVA and, due to the small number of subjects, by effect sizes (ES), with ES > 0.50 deemed significant [4].

RESULTS

Table 1 compares the gastrocnemius parameters for the three simulated co-activation conditions. There was a significant condition effect for muscle strength, with increased F_o for both 10% (~1500 N, p = 0.04, ES = 0.52) and 50% (~1700 N, p = 0.01, ES 1.73) antagonistic co-activation compared to no antagonism (~1400 N). Gastrocnemius results were typical, with F_o consistently higher in the 10% (ES > 0.50 for 8/9 muscles) and 50% (ES > 0.90 for all muscles) antagonism conditions. In contrast, the parameters L_o, L_u, and FT remained relatively constant across all antagonism conditions, with p > 0.05 and ES < 0.25 for 7/9 muscles.

Table 1. Muscle model parameters (mean±SD) calculated for gastrocnemius with 0, 10, and 50% co-activation (CA) of the antagonist muscle (tibialis anterior). * indicates p < 0.05 and ES > 0.50 in comparison to CA=0%.

Parameter	CA=0%	CA=10%	CA=50%
F_o (N)	1420±155	1494±129*	1729±202*
L_o (cm)	5.1±1.0	5.4±1.3	5.4±0.9
L_u (cm)	37.5±4.9	38.5±5.0	38.7±5.3
FT (%)	55±5	54±6	57±7

DISCUSSION AND CONCLUSIONS

Not surprisingly, the maximum isometric strength parameter of Hill muscle models calculated from dynamometer data depends on the degree of assumed antagonistic co-activation. The simulated 10% antagonism condition is comparable to that observed experimentally (*e.g.* [4]), while 50% co-activation is likely not physiological, but does serve to demonstrate the sensitivity of the calculations. In the 50% co-activation condition, none of the simulations could meet the optimization termination criterion at the hip and knee (RMSE < 20 Nm) unless the upper bound on F_o was increased to unrealistic levels for these subjects (*e.g.* vasti Fo = 5000 N).

The other parameters (L_o, L_u, and FT) did not depend on the degree of co-activation. This result suggests that if F_o is known *a priori* (*e.g.*, if F_o is calculated from MRI data), then co-activation may be reasonably neglected without compromising the validity of the muscle model parameters.

Previous research has indicated that antagonistic co-activation during human motion is not negligible [3], and that muscle model outputs are sensitive to parameter values [5]. Therefore, we suggest that future modeling efforts consider antagonism, both during the experimental protocols and in the simulations to compute the subject-specific model parameters.

REFERENCES

[1] Hatze H (1981). Estimation of myodynamic parameter values from observations on isometrically contracting muscle groups. *European Journal of Applied Physiology and Occupational Physiology* **46**(4); p. 326-338.
[2] Garner BA and Pandy MG (2003). Estimation of musculotendon properties in the human upper limb. *Annals of Biomedical Engineering* **31**(2); p. 207-220.
[3] Simoneau E et al. (2009). Antagonist mechanical contribution to resultant maximal torque at the ankle joint in young and older men. *Journal of Electromyography and Kinesiology* **19**(2); p. e123-e131.
[4] Cohen J (1990). *Statistical Power Analysis for the Behavioral Sciences*. USA: Routledge Academic.
[5] Scovil CY and Ronsky JL (2006). Sensitivity of a Hill-based muscle model to perturbations in model parameters. *Journal of Biomechanics* **39**(11); p. 2055-2063.

A COMPARISON OF PLATFORM MOTION WAVEFORMS DURING CONSTRAINED AND UNCONSTRAINED STANDING IN A MOVING ENVIRONMENTS

Carolyn A. Duncan[1], Scott N. MacKinnon[2], Wayne J. Albert[3]
[1] Faculty of Engineering and Applied Science, Memorial University of Newfoundland, St. John's, NL, Canada,
carolyn.duncan@mun.ca
[2] SafetyNet, Memorial University of Newfoundland, St. John's, NL, Canada
[3] Human Performance Lab, Faculty of Kinesiology,
University of New Brunswick, Fredericton, NB, Canada

INTRODUCTION

Recent research suggests that operator stability and subsequent postural adjustments in marine environments cannot be described as purely physics predictable reactions [1]. The strategy of continuous operator correction is not consistent with classical definitions of a motion induced interruption (MII) used to define change-in-support strategies that occur while working in marine environments, which in marine literature is a motion induced correction (MIC). To the author's knowledge no studies have examined the differences in platform motions between MIIs and MICs at the time of their occurrence. Research is needed to investigate timing of MII and MIC incidents and how to overcome the inaccuracies of current MII models to predict the magnitude and timing of these events. Therefore, the purpose of the study is to determine the differences in platform motion waveforms between MICs and MIIs occurrences when standing on a 6 degree of freedom motion platform. A principal component analysis (PCA) was incorporated permitting the preservation of temporal characteristics unique to each motion curve in the analysis.

METHODS

Twenty participants (ten male, ten female) with limited experience working in marine environments performed two stationary standing tasks were exposed to three different motion conditions varying in magnitude and frequency. The first standing task permitted the participants to move their feet only when it was absolutely necessary to prevent loss of balance (constrained). During the second standing task participants were instructed to move their feet when they felt it was best to maintain postural stability (unconstrained). Participants were videotaped to determine timing of MIIs and MICs. A custom built motion pack capable of measuring changes in all six degrees of freedom was used to monitor the motion of the platform in a location near the subject. Motion waveforms in each degree of freedom during each event was entered as a row vector and normalized to 100 data points for each degree of freedom to form a 100 x number of events matrices. These waveforms were then converted to principal components using eigenvector analysis of the covariance matrix. An ANOVA was performed on the derived significant principal component scores to determine if significant differences exist between these events during different motion profiles with. This will determine if these components are significantly different between groups.

RESULTS

Preliminary results of the pitch and roll axes suggest that most of the variability of platform motions between MIIs and MICs can be described by two principal components. The first of the components, which accounts for approximately 90% of the variability in the pitch axis, and approximately 80% of the variability for roll, respectively axes, is a magnitude operator which affects the entire event (Figure 1). Statistical analysis shows that this magnitude operator is significantly greater, ($p<0.05$), during MIIs when compared to MICs along both axes.

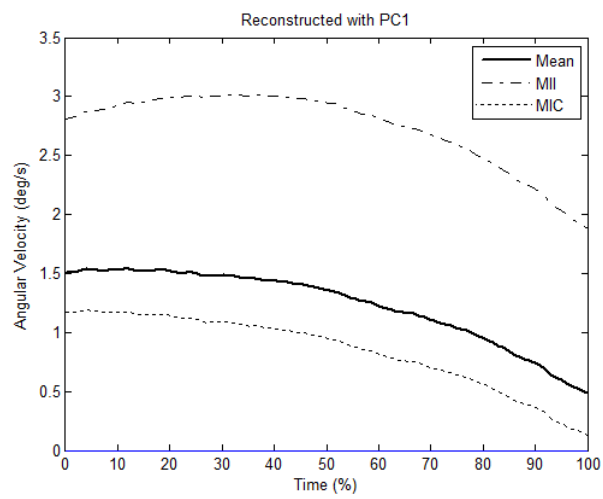

Figure 1: Reconstructed principal component for pitch axis

DISCUSSION & CONCLUSIONS

Results of this study suggest that there are significant quantifiable differences in the platform motions that cause MIIs and MICs, with generally greater angular velocities required to initiate an MII event. Therefore it is likely that these events are distinctly different and should be considered as such when examining the human response to wave-induced ship motions and ship operability.

REFERENCES

[1] Langlois et al. Modelling sea trial motion induced interruption data using an inverted pendulum articulated postural stability model; *International Journal of Maritime Engineering*. *In Press.*

POSTURAL AND BALANCE CONSTRAINTS INFLUENCE HAND FORCE CAPABILITY

Bryan Picco, Steve Fischer, Clark Dickerson, Richard Wells
Department of Kinesiology, University of Waterloo, Waterloo, Canada, bpicco@uwaterloo.ca

INTRODUCTION

Scientists have measured pushing, pulling, and pressing capabilities under a variety of conditions to better understand human capability often with respect to the work environment [1]. Joint strength is one mitigating factor of manual force production, but the importance of whole body balance and localized stiffnesses should not be ignored [2]. The purpose of this study was to assess the influence of different task constraints on hand force capability and muscle demand. This was accomplished by applying progressively restrictive postural constraints to the feet, lower limbs and torso, thereby systematically removing degrees of body control until only the upper limb is free to move. This allowed objective comparison of the influence of multiple limiting factors (friction, balance, and local joint strength) on manual force capability.

METHODS

Nine university-aged males without shoulder pain performed a series of maximal isometric hand exertions against a force transducer handle with their right shoulder flexed 90°, elbows slightly bent, and shoulders square in combinations of direction (press-down, pull medial, pull-in) and postural constraint (feet taped, feet shoulder-width, participant preference, legs braced, torso braced). Each exertion was selected at random and repeated once for a total of 30 efforts. When required, friction was controlled by taping the soles of the participants shoes to the floor, and the legs and torso were braced by strapping each segment to a rigid board. Hand force was measured using a MC3A transducer (ATMI, MA, USA). Surface electromyography (EMG) was recorded from selected right shoulder muscles, and symmetrically from torso, and upper leg muscles. Raw EMG signals were full wave rectified, low pass filtered at 4 Hz using a 4th order Butterworth filter and then normalized to maximal voluntary exertion EMG. A two-factor ANOVA was used to identify the main effects of direction and postural constraint on hand force and EMG.

RESULTS

Changes in postural constraint influenced both force production and muscle demand (Figure 1). Constraining the legs and trunk resulted in increased force capability in the pull-in direction (542.5 ± 111.9 N and 587.9 ± 83.0 N respectively), and EMG of the primary movers for this exertion was also increased within the two constraint conditions as seen in Figure 1B ($p < 0.05$). Balance as a constraint did not significantly affect hand force capability in the medial or downward exertion directions. Similarly, EMG was also unchanged between constraint conditions within the medial and downward exertion directions. Increasing friction did not increase hand force capabilities.

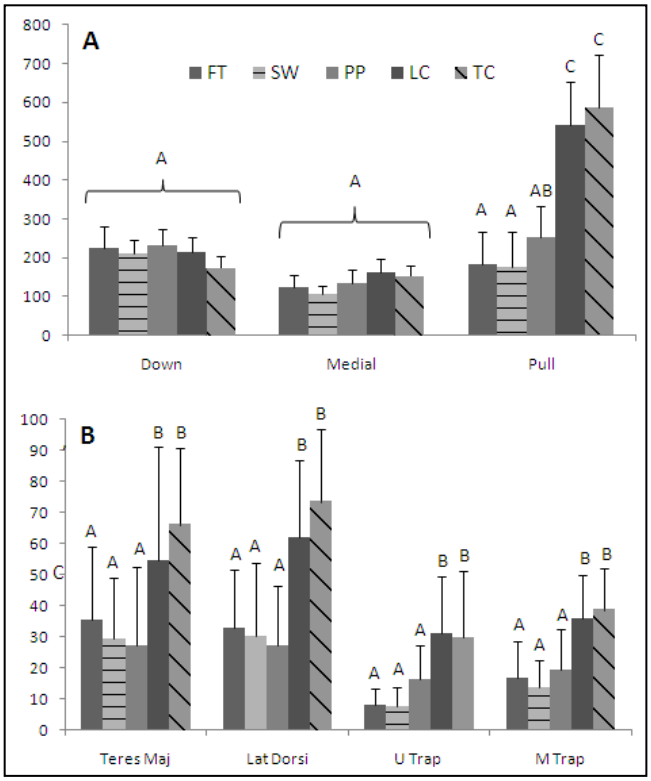

Figure 1: Effect of constraint condition on A) maximum isometric hand force for all directions and B) normalized EMG of primary movers for the "pull-in" direction ($p < 0.05$). FT = foot taped; SW = feet shoulder width; PP = participants preference; LC = legs constrained; TC = torso constrained. Dissimilar letters indicate significant differences.

DISCUSSION AND CONCLUSIONS

Hand force capabilities were only limited by balance in the pull-in condition. For other directions, joint strength appears to be the limiting factor. The increase in force was accompanied by an increase in EMG of the humeral and scapular movers for the action (Figure 1B). EMG did not change when balance was not a limiting factor. This finding has implications in designing studies, as bracing may be required to illicit maximal muscle activation for normalization, or for producing maximal static pulling forces. Also, results give insight into postural and balance effects when predicting human joint strength and hand force capabilities in occupational settings.

REFERENCES

[1] Peebles L et al. (2003). Filling 'gaps' in strength data for design. *Applied Ergonomics* Vol **34**; p. 73-88.
[2] Kerk CJ et al. (1998). Stability as a constraint in sagittal plane human force exertion modeling. *Occupational Ergonomics* Vol **1**(1); p. 23-29.

COMPARISON BETWEEN ISO 2631-1 PREDICTED COMFORT AND SELF-REPORTED COMFORT VALUES DURING OCCUPATIONAL EXPOSURE TO WHOLE-BODY VEHICULAR VIBRATION

Katherine Plewa[1], James P. Dickey PhD[1], Tammy Eger PhD[2], Michele Oliver PhD[3]
[1]Joint Biomechanics Laboratory, University of Western Ontario, London, ON, kplewa@uwo.ca
[2]Ergonomics & Kinesiology Lab, Laurentian University, Sudbury, ON
[3]School of Engineering, University of Guelph, Guelph, ON

INTRODUCTION

Exposure to whole-body vibration is strongly associated with health and comfort problems. Understanding how workplace vibration exposure affects comfort is an important factor in worker health and performance. International standards (ISO 2631-1) predict comfort based on vibration magnitudes, frequencies and durations. The objective of this study was to determine whether the ISO 2631-1 prediction method produces similar results to self-reported field comfort levels during occupational exposure to whole-body vehicular vibration.

METHODS

6 degree of freedom seat-pan acceleration data was recorded in various industrial machines in forestry [1], mining [2], and construction [3] industries. These machines were performing normal operations under actual working conditions. Following an audio tone at 5-minute intervals, operators reported their comfort level on a ten-point scale [4] based on the preceding minute of vibration exposure.

Corresponding one minute profiles of raw acceleration data were processed using the appropriate filtering and multiplying factors [5]. Frequency weighted RMS accelerations and point vibration total values were then calculated for each axis and combined as a vector sum. Comfort was predicted from the overall vibration total value for each acceleration profile.

RESULTS

We collected 45 matched sets of comfort and vibration data from 10 mining LHD vehicles, 18 sets from 6 forestry skidders and 60 sets from 15 construction scrapers. Each industry showed consistent trends between the predicted and self-reported comfort; however, there were different relationships between the industries. The data from the construction industry showed a weak positive relationship between predicted and self-reported comfort values, whereas the data for both the forestry and mining industries showed no clear relationships between predicted and self-reported comfort.

DISCUSSION AND CONCLUSIONS

It is difficult to predict comfort because comfort is subjective and identical vibration exposures may be perceived quite differently between subjects. The predicted comfort levels did

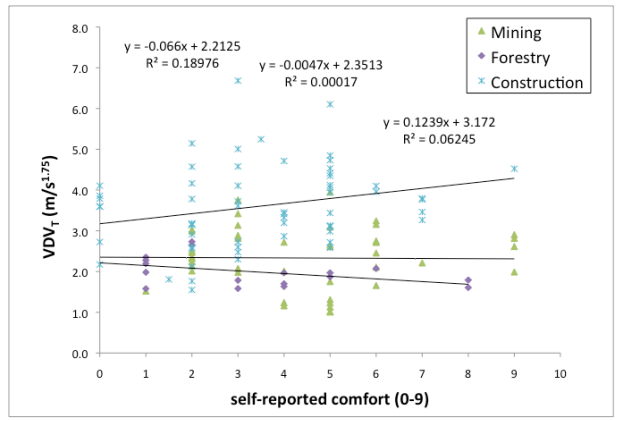

Figure 1: Vibration Dose Value versus Self-Reported Comfort for in the mining, construction and forestry industries.

not accurately represent self-reported comfort. This finding is similar to some previous studies [4], but contrasts with other studies [6]. This may be due to discrepancies with the prediction equations or perhaps that the operators were incorporating additional factors such as temperature, noise and fatigue into their self-reported comfort ratings. In order to improve our understanding of the relationship between multi-axis vibration and comfort, a more controlled study should be done in the laboratory where workplace vibrations are simulated and subjects rate their comfort given a certain acceleration profile.

REFERENCES

[1] Cation, S. et al. *Int J Industrial Ergo*. Vol. 38, No 9-010, pp. 739-757, 2008.
[2] Eger, T. et al. *Int J Industrial Ergo*. Vol. 38, No. 9-10, pp. 726-738, 2008.
[3] Cann, A. P., Salmoni, A. W., Vi, P., and Eger, T. R., *Appl Occup Enviro Hygiene*, Vol. 18, No. 12, pp. 999-1005, 2003.
[4] Dickey, J.P. et al. *J Low Freq Noise Vib Act Control.* Vol. 26, No. 3, pp. 195-204, 2007.
[5] ISO 2631-1. *International Standards Organization, Geneva*, 1997.
[6] Fairley, T E, *Ergonomics*, Vol. 38, No. 10, pp. 2091-2106, 1995.

ACKNOWLEDGEMENTS

This study was funded by a grant from the Ontario Workplace Safety and Insurance Board.

A MODEL TO PREDICT CARPAL TUNNEL SYNDROME RISK

Justin A. Weresch, Peter J. Keir
Department of Kinesiology, McMaster University, Hamilton, Ontario (werescj@mcmaster.ca)

INTRODUCTION

Carpal tunnel syndrome (CTS) remains an issue in the workplace. Increased carpal tunnel pressure (CTP) and nerve impingement are known to play roles in the symptoms and development of CTS. CTP of 30 mmHg or higher is associated with CTS symptoms when induced experimentally, and resting CTP in CTS patients is above this pressure. Thus 30 mmHg has been used as a threshold limit value, above which median nerve function may be compromised and risk of CTS increased [1]. In healthy individuals, CTP has been reported to be lowest in a neutral or slightly flexed wrist posture and a semi-pronated forearm. CTP increases with deviations from this posture in wrist flexion-extension (FE), radioulnar deviation (RUD), finger posture, finger force, and to a lesser extent forearm rotation [1]. Fingertip loading has also been shown to increase CTP independently of posture [3], more so when a pinch grip is used. The purpose of this project was to develop a model to predict median nerve (CTS) risk using CTP and nerve compression based on data in the literature.

METHODS

Of the 19 CTP studies that investigated the effect of wrist posture, forearm posture and/or fingertip loading, only 7 met the criteria of examining healthy wrists, using active motion and had consistent study protocols. Additional cadaver and clinical studies were used in specific instances to bolster the relationships. As an initial step, regression equations (up to 3rd order polynomial) were developed for wrist posture (FE, RUD), forearm rotation, finger posture and load (SPSS Inc., IL, USA). In addition to regression equations, multiplicative or additive models were created to fine tune CTP predictions based on interactions between variables (Fig. 1).

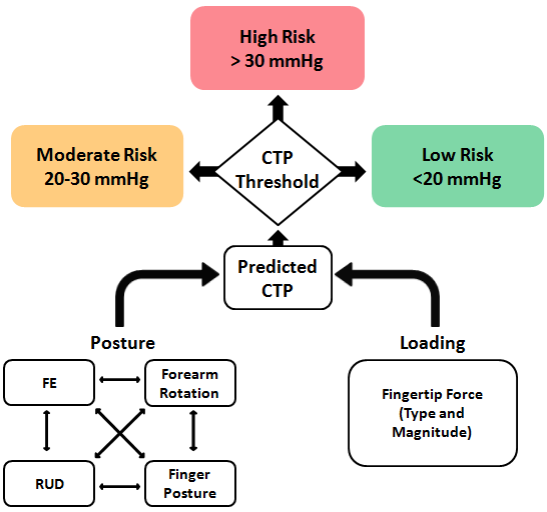

Figure 1. CTS risk model based on CTP.

RESULTS

Preliminary equations were developed for individual factors (Fig. 1) from a single series of studies based on the same subject pool [1]. Most variables were well fit by 2nd order regression equations (e.g. FE and RUD), were consistent with the literature and show greater effects with wrist extension and ulnar deviation. However, there is a need to adequately represent the variability in the data since only summary data from the literature was used. The complex effect of MCP angle was first addressed by individual regression equations and then by creating an additive model for wrist extension only as MCP posture has been shown to have little effect during wrist flexion [2]. The effect of fingertip loading was addressed by developing an additive model that was independent of wrist angle.

DISCUSSION

At present, preliminary equations (wrist FE, RUD, finger posture, pronation/supination), rudimentary additive (fingertip loading and finger posture) and multiplicative (combined postures) models have been developed. However, it is clear that strict confidence intervals are needed, and may be derived from the literature [1]. Work is underway to further apply the evidence that low level fingertip loads (< 12 N) have an additive effect to CTP, independent to the effect of posture [3]. The effect of movement in multiple planes has the least supporting data and will require a complex relationship. Mechanical compression also plays a large role in median nerve trauma during wrist flexion, thus the completed model will also incorporate mechanical compression of the median nerve. The final phase of this project will test the model predictions of risk with injury, posture, and loading data obtained from a manufacturing environment. A risk model for median nerve trauma is needed in the workplace since measuring CTP is not feasible in most occupational settings. This model will ultimately be used to predict CTS risk based on wrist/hand posture and fingertip loading for use in ergonomic assessments.

REFERENCES

[1] Keir, P.J., et al. (2007). *Human Factors* 49 (1); 88-99.
[2] Keir, P.J., et al. (1998). *J. Hand Surg.* 23 (6); 1004-1009.
[3] Rempel, D. et al. (1997). *J. Orthop Res.* 15 (3); 422-426.

ACKNOWLEGEMENT

This study was funded by AUTO21 Grant #AE403.

BIOMECHANICAL AND ERGONOMIC ASSESSMENT OF URBAN TRANSIT OPERATORS

Donald Everson[1], Michelle Rae[1], Usha Kuruganti[1], Jack, P. Callaghan[2], Wayne J. Albert[1]

[1]Faculty of Kinesiology, University of New Brunswick, Fredericton, CANADA, donald.everson@unb.ca
[2] Department of Kinesiology, Faculty of Applied Health Sciences, University of Waterloo, Waterloo, Ontario, CANADA

INTRODUCTION

Previous research has identified urban bus drivers as being at a high risk for occupational disorders, due to exposure to a variety of musculoskeletal hazards and occupational stressors that can significantly and negatively affect their overall health. Few comprehensive studies have been conducted in the field regarding musculoskeletal risk in the transportation occupations, with much of the existing literature limited to studies involving questionnaire-based evaluations of musculoskeletal symptoms. The use of high-tech equipment in ergonomic studies is a relatively new endeavour, with the availability of small, wireless devices allowing researchers to obtain significant data in the field. This study was designed to examine the specific workload and health implications of urban bus drivers in Fredericton, New Brunswick by obtaining objective data in the field. This research project investigated the health and wellness of city bus drivers in terms of biomechanical (postural) and musculoskeletal stress (muscle activity), while also examining psychosocial factors (workplace stress). The main goal of this work was to obtain effective pressure, EMG, and subjective ratings for a better understanding of driving demands in urban transit operators.

METHODS

15 Participants (13 male, 3 female), average age 44.4 years (7.7) with an average of 14.8 years (9.7) driving experience Participants drove a preselected 60 minute bus route once at the same time each day, in a preselected bus (2004 Nova Low Floor). For each trial interface pressure (at a sampling rate of 5 Hz) and video were recorded continuously by two Xsensor pressure mats (model X3 LX100:36.36.02) and a Panasonic digital video camera respectively. Interface pressure was measured in the seat pan and back rest (total sensing area 45.7cm x 45.7cm) with thin pads (0.81mm when compressed) that could conform to the contours of the driver's seat. X3 PRO electronics connected to a laptop computer and X3 PRO version 5.0 software were used to show a real-time image of the driver's pressure distribution and posture (Figure 2).

A comprehensive questionnaire provided insight into the neck and back pain experienced by these drivers, as well as supplying health and lifestyle data. This equipment allowed for a comprehensive biomechanical monitoring of the bus driver while completing a scheduled 1-hour bus route without interfering with the driver's normal work functions.

RESULTS

Pressure data were unique to drivers and dependant on individual anthropometrics and driving style. Average pressures tended to increase in the seat pan in the majority (78%) of participants throughout the 60 minute driving trial (Figure 1). Drivers often began in a symmetrical balanced position and throughout the driving period changed to having the majority of their weight on one hip and one shoulder in the seat pan and on the backrest respectively (Figure 2).

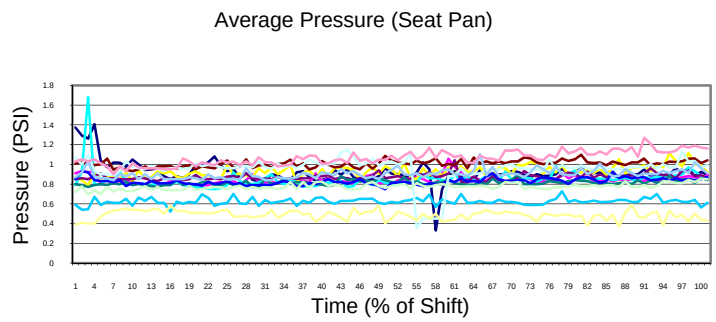

Figure 1: Average pressure recorded in the seat pan

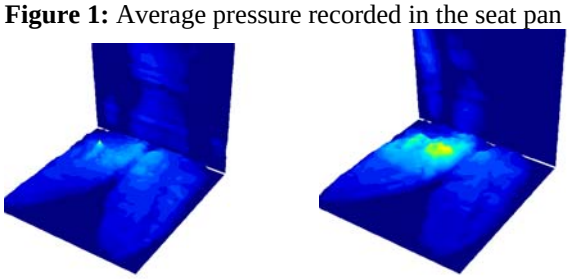

Figure 2: 3D pressure distribution image of a drivers posture at beginning of shift (left) and toward the end of shift (right).

DISCUSSION AND CONCLUSIONS

Drivers are likely to shift position more frequently when they experience discomfort. Therefore, postural changes observed by drivers may evidence discomfort. Not all movement represents discomfort, and (short term) changes in position may be a function of performing certain driving tasks. Long term changes in posture observed could be evidence of discomfort and an attempt to alleviate pain by finding a more comfortable sitting position.

ACKNOWLEDGEMENTS

The authors would like to acknowledge the support of the City of Fredericton and the cooperation of Fredericton Transit.

COORDINATION OF SHOULDER MUSCLES IN RESPONSE TO GRIPPING AND BICEPS ACTIVITY DURING STATIC AND DYNAMIC SHOULDER EXERTIONS

Joanne N Hodder, Peter J Keir
Department of Kinesiology, McMaster University, Hamilton, ON, hodderjn@mcmaster.ca

INTRODUCTION

The addition of a gripping task to a shoulder exertion has been shown to decrease deltoid activity and in some cases increase rotator cuff muscle activity as measured via surface EMG [1,2]. Redistribution of muscle activity may result in increased load on the rotator cuff muscles, thus increasing the risk of injury. However, the mechanism by which coordination of muscle activity changes has yet to be determined. Given that the long head of biceps crosses both the elbow and shoulder joints, it may transfer load from the forearm, across the elbow and to the shoulder. In addition to this effect, it was hypothesized that gripping may increase biceps activity, requiring increased rorator cuff activity to oppose the action of biceps, specifically, supraspinatus and infraspinatus. Previous investigations have been limited to isometric shoulder exertions. Thus the purpose of this study was twofold. First, to investigate the effects of voluntary biceps contractions and concurrent gripping on rotator cuff muscle activity during static shoulder and isokinetic shoulder exertions.

METHODS

A series of static and isokinetic shoulder exertions were performed. Isometric exertions (40% maximum) were performed at 30°, 60° and 90° shoulder angles in both sagittal and scapular planes using neutral and supinated forearm postures. Shoulder exertions were performed alone or in conjunction with a 30% maximal grip effort or a 30% MVE biceps effort using visual feedback. Concentric dynamic exertions were performed at 30°/s in both sagittal and scapular planes with the same conditions as the static trials (neutral and supine forearm postures with (i) no hand load, (ii) 30% grip, (iii) 30% biceps contraction). For each trial, three cycles of concentric contractions (ie. up/down) were performed. Surface EMG was collected from the anterior (AD), medial (MD) and posterior (PD) deltoids, trapezius (TR), long head biceps (BI) and long head triceps (TRI), while fine wire electrodes were used for the supraspinatus (SUP) and infraspinatus (INF) muscles (AMT-8, Bortec Biomedical Ltd., AB, Canada). All signals were sampled at 4000 Hz. EMG signals were linear enveloped at 3 Hz and normalized to maximum voluntary excitation (MVE). EMG was then found at 30°, 60° and 90° for flexion and extension in the sagittal plane and abduction and adduction in the scapular plane.

RESULTS

The addition of a grip or biceps contraction decreased AD activity during isokinetic shoulder flexion with both forearm postures. The greatest reduction in activity was found at 30°, where AD activity decreased from 57.0 ± 17.4% MVE to 37.7 ± 9.5% MVE (grip) and 39.8 ± 11.5% MVE (biceps contraction) with neutral forearm, and from 67.2 ± 22.6% MVE to 42.7 ± 9.6% MVE (grip) and 40.9 ± 16.8% MVE (biceps) when supinated. In the scapular plane, concurrent gripping lowered MD activity (abduction, neutral forearm) by 8.5-13.3 % and PD by 8.2-13.2% MVE depending on angle. In extension efforts, AD activity increased with both the concurrent gripping and biceps contractions. The supinated forearm yielded the greatest increases in AD with grip which was most prominent at 90° (+ 29.3 %MVE), while biceps contraction increased AD activity by 10.2% MVE at the same angle. With adduction, all 3 heads of the deltoid increased near twofold with gripping. For example, with a neutral forearm at 90°, AD increased from 11.3 ± 6.6 to 23.6 ±8.3% MVE, MD from 15.2 ± 12.2 to 27.5 ± 18.4% MVE and PD from 15.4 ± 13.6 to 24.7 ± 18.2% MVE.

In the sagittal plane, INF generally followed the pattern of AD, most prominently when the forearm was supinated (Fig. 1). In flexion exertions, INF decreased by 14.8% MVE (30°), 7.3% MVE (60°) and 12.0% MVE (90°) with the addition of grip. In extension exertions, INF increased with the addition of grip by 5.0% MVE (90°), 2.5% MVE (60°) and 0.9% MVE (30°).

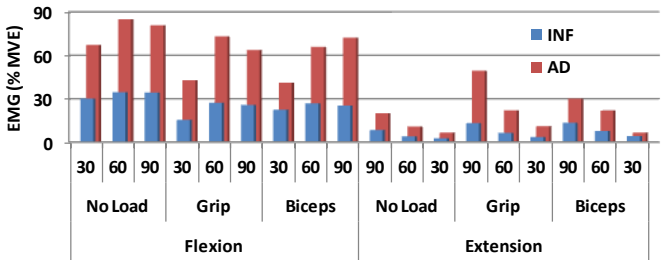

Figure 1: AD and INF activity (% MVE) during shoulder exertions in flexion plane with supinated forearm posture.

DISCUSSION AND CONCLUSIONS

Reductions in deltoid activity were found during flexion and abduction contractions with the addition of gripping or biceps contraction. It was anticipated that reductions in deltoid muscle activity would be accompanied by increased rotator cuff activity. Instead, it appears that the INF synergistically contracts with the deltoids. INF activity followed AD in the sagittal plane and followed MD and PD in the scapular plane; thus suggesting a mechanism to maintain glenohumeral stability. Further analysis of muscle activity throughout the dynamic trials will provide greater insight into the coordination of the muscles of the shoulder complex.

REFERENCES

[1] Au & Keir (2007). *JEK.* 17(5):578-586.
[2] Smets et al (2009). *Ergo.* 52(9):1144-52.

ACKNOWLEDGEMENTS

NSERC (Canada) Discovery Grant #217382 (PJK)

NUMERICAL IMPLEMENTATION OF A NON-LINEAR MICROSTRUCTURAL MODEL OF CARTILAGE

Jan Pajerski[1], Amr Guaily[1], T. Christian Gasser[2], Salvatore Federico[1,*]
[1]Department of Mechanical and Manufacturing Engineering, The University of Calgary, Canada
[1]Department of Solid Mechanics, KTH Royal Institute of Technology, Stockholm, Sweden
[*]salvatore.federico@ucalgary.ca

INTRODUCTION

Articular cartilage is the load-bearing tissue covering the articular surfaces of bones in diarthrodial joints, in order to distribute stresses and minimise joint wear. The tissue's health depends largely on the functioning of its cells (chondrocytes), which synthesise the macromolecules composing the extracellular matrix: proteoglycans and collagen fibres. The biosynthetic response of the chondrocytes is influenced by their mechanical environment. Therefore, understanding the stress-strain fields in the chondrocytes is a basic step towards understanding articular cartilage adaptation and degeneration.

Articular cartilage is known to be anisotropic and inhomogeneous, with depth dependent mechanical properties. However, early theoretical-numerical studies of chondrocyte mechanics were based on linear, isotropic, homogeneous material models [2]. More recently transversely isotropic, transversely homogeneous (TITH) models for linear elasticity, characterised by a statistical description of the depth-dependent fibre orientation, have predicted cellular deformation [3] in closer agreement with experimental results [1]. Nonetheless, linearity implied that fibre stiffness in tension and compression was unrealistically assumed to be the same. The most recent step towards a continuum model for cartilage is the Non-Linear TITH (NLTITH) model [6], which preserves the mathematical framework for the description of the statistical fibre orientation, but overcomes the inherent limitations of the TITH model for elasticity.

The purpose of this work is to analyse chondrocyte mechanics using an extended NLTITH model, inclusive of a theory for permeability under large strains [5].

METHODS

The non-linear cell mechanics model is achieved in steps:

A) The NLTITH model is originally monophasic, and it is turned into biphasic by including the fluid phase (f); the solid phase (s) is comprised of matrix (0) and fibres (1); the efflux of fluid outside the boundaries of the system implies an overall compressibility, although solid and fluid are both incompressible; the constraint of incompressibility is taken into account by the inequality constraint

$$J - \phi_{sR} > 0\,, \tag{1}$$

where $J = \det \boldsymbol{F}$ is the volumetric deformation ratio and ϕ_{sR} is the volumetric fraction of solid in the reference configuration; the elastic potential is still in the form [6]

$$W(\boldsymbol{C}) = \phi_{0R} W_0(\boldsymbol{C}) + \phi_{1R} W_{1i}(\boldsymbol{C}) + \phi_{1R} W_{ea}(\boldsymbol{C}, \boldsymbol{A}) \tag{2}$$

where this time reference volumetric fractions were used, and

$$W_{ea}(\boldsymbol{C}) = \int_{\mathbb{S}^2} \psi\ \mathcal{H}(I_4(\boldsymbol{C}, \boldsymbol{A}) - 1)\ W_{1a}(\boldsymbol{C}, \boldsymbol{A})\ dS \tag{3}$$

is the anisotropic ensemble fibre potential, governed by the orientation probability ψ and such that the contribution of the fibres in compression is filtered by the Heaviside step $\mathcal{H}$.

B) The formulation for the permeability under large strains [5] shares the same structure seen in Eq. (3):

$$\boldsymbol{K} = \int_{\mathbb{S}^2} \psi\ \boldsymbol{Z}_0 [\phi_{1R}(1-\phi_{1R})\boldsymbol{A} + (1-\phi_{1R})^2 \boldsymbol{I}]\ dS \tag{4}$$

where $\boldsymbol{A}$ is the structure tensor describing the local fibre direction, and $\boldsymbol{Z}_0$ is the local permeability in the neighbourhood of a fibre. Both $\boldsymbol{K}$ and $\boldsymbol{Z}_0$ are permeabilities in the reference (undeformed) configuration. For the case of articular cartilage, $\boldsymbol{Z}_0$ is constructed as a function of J and the fractions ϕ_{sR}, ϕ_{fR} [4].

C) Based on the extended NLTITH model built in steps (**A**) and (**B**), cell mechanics is studied by means of the multi-scale approach [2][3]: the macroscopic results (displacements, fluid pressure) obtained from an indentation test of a cartilage sample are used as boundary conditions for the microscopic model including one cell and its neighbouring extracellular matrix.

RESULTS AND DISCUSSION

The cell deformation model of Han et al. [3] was able to qualitatively reproduce the experimental results of Clark et al. [1]. However, because of the limitations imposed by linearity of the early TITH model, it could not model the actual deformations (over 40% nominal strain) imposed in the experiments. The NLTITH model will enable us to more accurately compare the predictions of the theory with experiments, in particular in terms of cell stresses and strains, which are responsible for the overall cellular behaviour.

REFERENCES

[1] Clark AL et al. (2003). In situ chondrocyte deformation with physiological compression of the feline patellofemoral joint. *J Biomech* Vol **36**(4); p. 553-568.
[2] Guilak F et al. (1995). Chondrocyte deformation and local tissue strain in articular cartilage: a confocal Microscopy study. *J Orthop Res* Vol **13**(3); p. 410-421.
[3] Han SK et al. (2007). The mechanical behaviour of chondrocytes predicted with a micro-structural model of articular cartilage. *Biomech Model Mechanobiol* Vol **6**(3); p. 139-150.
[4] Holmes MH and Mow VC (1990), The Non-linear Characteristics of Soft Gels and Hydrated Connective Tissues in Ultrafiltration, *J Biomech* Vol **36**(11); p. 1145-1156.
[5] Federico S (2009). Porous fibre-reinforced materials under large deformations. *Proc. AIMETA*; p.612-613.
[6] Federico S and Gasser TC (2010). Non-linear elasticity of biological tissues with statistical fibre orientation. *J Roy Soc Interface*, in press, DOI: 10.1098/rsif.2009.0502

ACKNOWLEDGEMENTS

AIF New Faculty Programme, NSERC Discovery Programme.

IMPROVED PREDICTION OF STRESS RELAXATION INDENTATION RESPONSE OF CARTILAGE USING A NONLINEAR BIPHASIC POROVISCOELASTIC MODEL

A, Seifzadeh[1], D.C.D. Oguamanam[1]and M. Papini [1, 2]
[1]Department of Mechanical and Industrial Engineering, Ryerson University, Toronto, ON, mpapini@ryerson.ca
[2]Canadian Institutes of Health Research (CIHR)-Bioengineering of Skeletal Tissues Team

INTRODUCTION

Articular cartilage (AC) permeability depends on strain [1], introducing a nonlinearity that must be taken into account when modeling its response to applied loads. As the compressive strain increases, the interstitial space in the cartilage decreases and the drag forces experienced by the interstitial fluid increase. Linear biphasic theory assumes that cartilage consists of two immiscible solid and fluid phases with a constant permeability coefficient, irrespective of the level of deformation in the tissue. In this study, a nonlinear biphasic finite element model utilizing a strain-dependent permeability coefficient was compared to a linear model, in order to determine which model best predicted the response of ovine AC tissue in a stress relaxation indentation test.

METHODS

A finite element (FE) model was coupled to an optimization scheme in order to determine the flow-dependent and flow-independent material parameters for ovine cartilage from an indentation test under the both linear and nonlinear biphasic poroviscoelastic (BPVE) models. The stress-relaxation response for 10 native 0.34-0.7 mm thick ovine cartilages harvested from 6-9 month sheep was determined using a 0.5 mm diameter cylindrical indenter to compressively indent the cartilage tissue in a Mach-1TM mechanical tester (Biosyntech, Laval, PQ) .The compressive force was applied in 10 steps, each step corresponding to 1–2% strain. This was repeated for each of the 10 deformation steps for a total of 20% strain. The nonlinear biphasic model incorporates strain-dependent permeability in the biphasic model [2] as $k = k_0 \exp\left(M \frac{e - e_0}{1 + e_0} \right)$.The dependence of void ratio through the thickness of the cartilage found based on the water content along it, was assumed to determine the void ratio along the tissue thickness. k_0 (initial permeability), M (constant number)and e_0 (initial void ratio) were determined from optimization in an iterative scheme and used to determine k and *e*. The tissue viscoelasticity was defined by Prony series coefficients including dimensionless bulk and relaxation amplitudes, k_i and g_i respectively and time constants τ_i .

RESULTS

The material parameters and the predicted stress relaxation indentation of a 0.41 mm thick ovine cartilage using the nonlinear BPVE model were determined with a maximum error of 2% between the FE model and the experiment, as shown in Table 1 and Fig. 1 respectively.

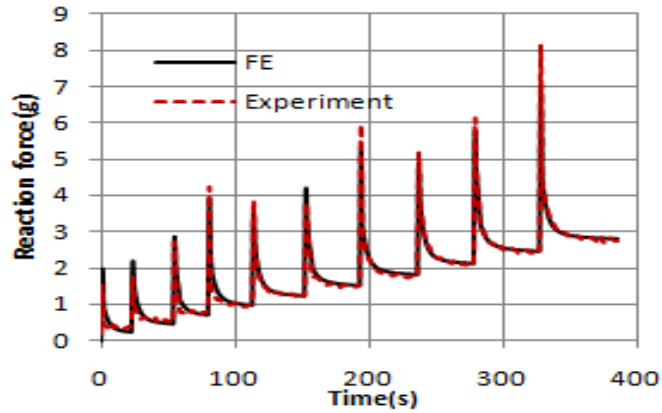

Figure 1: Predicted FE and experimental stress relaxation for the nonlinear BPVE model of a 0.41 mm thick ovine cartilage.

DISCUSSION AND CONCLUSIONS

Using the nonlinear BPVE model that incorporates strain-dependent permeability phenomena for cartilage improved the predicted response of the tissue in the stress relaxation indentation experiment. Using the presented nonlinear model decreased the error between predicted finite element response and experiment by 2% compared to the linear model.

REFERENCES

[1] Spilker RL, Suh JK and Mow VC (1988).Finite element formulation of the nonlinear biphasic model for articular cartilage and hydrated soft tissues including strain-dependent permeability. American Society of Mechanical Engineers, Bioengineering Division (Publication) BED, vol **9**, p 81-92.
[2] Lai WM and Mow VC (1980).Drag induced compression of articular cartilage during a permeation experiment. Biorheology, vol **17**, p. 111–123.

ACKNOWLEDGEMENTS

The financial support of the Canadian Institutes of Health Research (CIHR) is gratefully acknowledged.

Table 1: Optimized material parameters of nonlinear BPVE model of a 0.41 mm thick ovine cartilage layer.

e_0	$k_0 (m/s) \times 10^{-9}$	M	g_1	k_1	τ_1 (s)	g_2	k_2	τ_2 (s)
5.875	0.793	3	0.82	0.106	2.61	0.059	0.054	14

Quantification of change in thickness and shear modulus of articular cartilage after freezing

Trutiak, NWH[1]; Lowerison, MW[1]; Kunz, M[2]; Gordon, KD[1]; Hurtig, MB[1]
[1]School of Engineering & Clinical Studies, University of Guelph, Guelph, Canada, NTrutiak@uoguelph.ca
[2]Human Mobility Research Centre, Queens University, Kingston, Canada

INTRODUCTION

Due to the variation in loading and wear across the articular surface thicknesses, material and chemical properties vary considerably from site-to-site with some areas more prone to osteoarthritis than others. [1] Exhaustive mapping studies are needed to elucidate these mechanical and physical properties before osteochondral grafts or engineered tissue can be used to supply a repair with properties similar to the patient's tissue. Furthermore, fresh human joints are difficult to obtain for such mapping studies, whereas frozen samples are more readily available. The objective of this work was to determine the effects of a single 12h freeze thaw cycle on surface geometry and shear modulus of intact, untreated bovine cartilage.

METHODS

Nine pairs of fresh 23-27 month old bovine knee (stifle) joints were disarticulated for the harvesting of medial and lateral femoral condyles. Pairs of joints were assigned to biomechanical testing and assessment of surface geometry. The flattest (semilunar) area of each condyle was used for stress relaxation indentation testing using Biomomentum's Mach-1 Micromechanical Testing System with 3.2mm diameter hemispherical indenter. Indentation was performed medially and laterally to the center of the semilunar area. The indenter displacement was 0.1mm at a rate of 0.1mm/sec and was held until the relaxation rate dropped to 0.05g/min. Hayes' method was used to calculate the relaxed shear modulus by recording the load on the indenter at the point where equilibrium was established. [2]

Thickness measurements where a needle probe mounted on the Mach-1 and Seedhom's method [3]. Samples were frozen in layers of Ringers solution soaked gauze and plastic food wrap, then frozen for 12hrs at -20ºC, thawed and retested.

The effect of freeze-thaw on cartilage geometry was investigated using a GE explore Locus µCT at 93µm resolution to image the left and right femoral condyles, in air. An isosurface routine and thresholding in MicroView (v2.1.2, GE Healthcare 2003) were used to create stereo-lithographic (STL) files representative of the bone surface and the cartilage surface of each condyle before and after freezing. The STL files were then imported to IMinspect (v8.0, InnovMetric 2003) where they were aligned with one-another in reference to bony landmarks which do not change with freezing.

Statistics were then performed in R (v2.8.1, 2009), a linear mixed effect model was used where shear modulus was a function of treatment, animal, site and strain of the cartilage thickness.

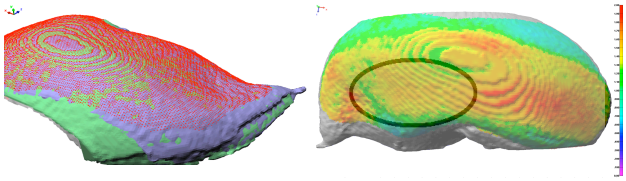

Figure 1: Bony marker coordination and cartilage thickness color map (2.0-0.0mm, red-purple), semilunar area circled

RESULTS

The mean equilibrium shear modulus decreased in the lateral condyle and increased slightly in the medial condyle after one freeze-thaw cycle (n=9, p=0.14), shear modulus of lateral condyles proved consistently higher than the medial, this agrees with literature. [4]. Mean shear modulus for the lateral femoral condyle, fresh and frozen, was 0.33MPa+/-0.01 and 0.29MPa+/-0.07 respectively. The medial femoral condyles showed slightly lower values of 0.21MPa+/-0.06 and 0.21MPa+/-0.04 for fresh and frozen shear modulus. Strain varied by 4.1-7.8% and was considered a factor in the mixed effect model but showed no significance (p=0.37).

Thickness measurements, n=8 area +/-, were taken using IMinspect and mean thickness values varied only slightly between treatments of lateral and medial condyles with mean fresh thicknesses of 1.31mm+/-0.10 and 1.59mm+/-0.13 respectively and decreases in thickness due to freezing of 0.01mm+/-0.05 and 0.01mm+/-0.06 respectively. Linear mixed effect models show that significant changes in thickness were due to condyle ($p<0.001$) rather than treatment (p=0.87).

DISCUSSION AND CONCLUSIONS

The objective of this work was to determine if changes occurred in bovine articular cartilage geometry or shear modulus after a single freeze-thaw cycle of untreated intact bovine cartilage. Results indicate that after a single 12h freeze-thaw cycle there is negligible change in geometry or equilibrium shear modulus.

This method of indentation was chosen for large osteochondral segments due to its versatility and simplicity. Additional work on human tissue is warranted but these data support the use of cadaveric knee joints that have undergone one freeze-thaw cycle for mapping of articular cartilage thickness and shear modulus via indentation.

REFERENCES

1. [Walton et al, Arthroscopy: The J. of Arthros. & Related Surg., 1997]
2. [Hayes et al, Journal of Biomechanics 1972]
3. [Ann Rheum Dis 1999;58:27-34]
4.[Brama et al, Equine Veteranary Journal 2000]

EFFECT OF SAMPLE PREPARATION ON THE MODULUS OF BOVINE LUMBAR CANCELLOUS TISSUE

Andrew C. Engbretson*, Geneviève A. Dumas
Mechanical and Materials Engineering, Queen's University, Kingston, Canada

INTRODUCTION

Bone, as a material, is generally well-researched; however much of the work done has involved whole bone, cortical bone, or bulk testing of cancellous bone. Additionally, results from previous work on the properties of cancellous bone tissure are not in agreement [1]. Previous studies relied on aggressive sample preparation, the effects of which were not examined [2]. The present study sought to determine the elastic modulus of single trabeculae obtained through minimal machining. In addition, the effect of machining was examined.

METHODS

Samples were obtained from the inferior anterior portion of a fresh-frozen bovine L4 vertebra. Slices ~0.7 mm thick were made using an Allied TechCut 4™ (Allied High Tech Products, Inc., California, USA) low speed saw with constant lubrication. The slices were cleaned of fat and marrow using a low-pressure stream of deionized water and individual struts were manually dissected and measured under a Zeiss (Zeiss Canada, Ontario, Canada) stereomicroscope. Samples were stored in tissue culture wells with saline solution to maintain hydration until testing.

Samples were tested using a Mach1™ A class single-axis load frame (BioMomentum Inc., Quebec, Canada) with custom attachments to create a three-point bending setup. A flexural strain rate of 0.01 min^{-1} was kept constant between samples by changing the crosshead rate according to sample dimensions. Load and displacement data were analyzed using a MATLAB® (The MathWorks Inc., Massachusetts, USA) program to determine the samples' moduli.

The majority of trabeculae did not have an aspect ratio (length:thickness) greater than the ideal minimum of 16:1 [3]. To compensate for the short beam and the shear force present in a three-point flexural test, a modified flexural modulus formula was used [4]

$$E = \frac{L^3 m}{48I}\left[1 + 2.85(d/L)^2 - 0.84(d/L)^3\right]$$

where L is the span length, m is the slope of the load-displacement curve, d is the sample thickness, and I is the second moment of inertia.

PRELIMINARY RESULTS

Trabeculae with either square or round cross-sections were observed. "Square" samples had been machined on more than one side of the strut's midsection, while the "round" ones had not. Ten square and four round samples were tested. Round samples had an average modulus of 16.84 ± 1.19 GPa, while the modulus for square samples was found to be lower ($p = 0.012$) at 1.233 ± 0.711 GPa (Figure 1).

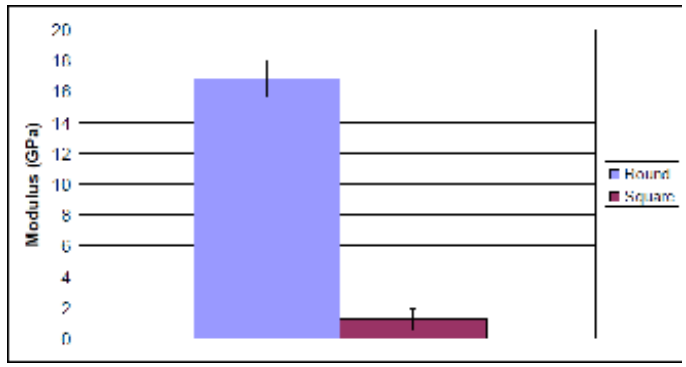

Figure 1: Mean (SD) experimental moduli for "round" and "square" samples.

DISCUSSION AND CONCLUSIONS

The modulus of the round specimens is comparable with the results of nanoindentation studies, often considered the "gold standard" for small-scale testing, while the square specimens have a modulus comparable to those on the lower end of published results [1]. We have shown that the modulus of cancellous bone tissue is close to, but still somewhat lower than, that of cortical bone [1] and that the machining of trabecular bone tissue samples may result in a lower modulus due to microdamage. These results should be confirmed with a larger sample pool, while future studies should monitor potential damage due to sample preparation.

REFERENCES

[1] Rho JY *et al* (1998). *Medical Engineering and Physics* Vol **20** (2); p .92-102.
[2] Kuhn *et al.* (1989). *Journal of Orthopaedic Research* Vol **7** (6); p. 876-884.
[3] ASTM Specification D790-86. In: ASTM Standards. Philadelphia: American Society for Testing and Materials; 1995: 62-68.
[4] Timoshenko SP, Goodier JN. *The Theory of Elasticity*; McGraw-Hill, NY, 1987.

ACKNOWLEDGEMENTS

This study was funded by NSERC research grant 6858 in lab space provided by the Human Mobility Research Centre, at Queen's University, Kingston, ON

*Person to whom all correspondence should be addressed: engbretson@me.queensu.ca

YOUNG MODULUS EFFECT ON BONE STRESSES IN TOTAL HIP ARTHROPLASTY USING FINITE ELEMENT ANALYSIS

Michael Reimeringer, Natalia Nuño
Imaging & Orthopaedic Research Lab., École de technologie supérieure, Montréal, Canada, mickareim@gmail.com

INTRODUCTION

Finite Element Analysis (FEA) tools are increasingly used in Total Hip Arthroplasty (THA) to evaluate the behaviour of the femur. Various factors are crucial for the reliability of FEA results [1]: 3D geometry, boundary conditions, and material properties. 3D geometry can be reconstructed from medical images or a composite bone can be used as proposed by [2]. This eliminates geometric variance problems and mechanical variability between cadaveric or human bones when performing experiments. The composite femur behaviour has been validated by [3, 4]. Boundary conditions of daily activities have been defined by [5] and are steadily used in FEA studies. Regarding the material properties, measurements from experimental studies result in a large range of Young modulus *E* for cortical and cancellous structures to characterize the behaviour of femurs (Table 1). This large range can be explained by various factors like origin, age, gender of the donors, apparent density of bone, location of the specimen tested (proximal, neck,...)... Although the natural bone has an anisotropic heterogeneous behaviour [6], for simplicity most FEA describe it as isotropic homogeneous. Only a small difference has been found on the maximum equivalent Von Mises stress and displacement with an assignment of isotropic and orthotropic materials compared to the real anisotropic heterogeneous behaviour of bone [7]. Among numerical studies, the range of *E* is also wide (Table 1). The aim of this study is to investigate using FEA the effect of Young modulus of cancellous and cortical bones, on Von Mises (VM) stress distribution within the femur.

Table 1: Range of Young modulus for cancellous and cortical bones found in experimental and FEA studies

	Cancellous bone *E* (GPa)	Cortical bone *E* (GPa)
Experimental studies	0.051→3.47	11.8→20
FEA	0.05 →20	2 →20

METHODS

FEA was carried out using a Sawbones® 4th generation (Pacific Research Lab., Vashon Island, WA, USA) for the loading condition simulating the heel strike of the gait cycle [5]. The mechanical properties of the femur Sawbones® 4th generation have been used as reference, namely the Young modulus *E*, 155 MPa and 16 GPa for the cancellous and cortical bones, respectively. The Von Mises (VM) stresses distribution inside the femur was analyzed. Then, keeping E for the cortical bone fixed at 16 GPa, the effect of cancellous E on the VM stresses inside the femur was analysed. Finally, keeping *E* for the cancellous bone fixed at 155 MPa, the variation of the cortical *E* on the VM stresses distribution inside the femur was investigated.

RESULTS

VM stresses within the cancellous Sawbones® 4th generation are lower than 0.5 MPa with the exception of the head (under the bearing surface), where the stress reaches a maximum of 1.1 MPa. When the cancellous *E* increases up to 1.7 GPa, VM stresses within the cancellous structure increase up to 5.4 MPa (under the bearing surface): first in the head, followed by the greater trochanter and then in the rest of the cancellous structure. On the contrary, VM stresses within the cancellous bone decrease from 1.3 MPa to 1 MPa with the increase of the cortical *E* (12 GPa up to 16.8 GPa). Regarding the VM stresses within the cortical structure, the variation of the cortical *E* has no significant impact on the VM stresses distribution. However, the increase of the cancellous *E* decreases the VM stresses within the cortical bone, mainly in the head and the greater trochanter.

DISCUSSION AND CONCLUSION

Overall, VM stresses within the cancellous bone increase with the increase of the cancellous *E*. The opposite effect is observed within the cancellous structure with the increase of the cortical *E*. As expected, the variations of the mechanical properties have a significant impact on the VM stresses distribution within the femur. This makes comparisons between FEA studies difficult.

To conclude, FEA are widely used to predict the behaviour of the bone. Results provided by these tools are greatly dependent on the pre-processing defined by users. There is a general agreement among the scientific community on the selection of 3D geometry and boundary conditions. However, there is still no agreement on bone material properties selection, which prevents comparison of stresses distribution within FEA. Indeed, the present study demonstrates that there are large differences in the assignments of Young modulus *E* between numerical studies. Thus, it would be useful to develop a database of human bone material properties obtained from experimental data and adapted to the geometry of the composite bone like Sawbones® 4th generation for FE studies.

REFERENCES

[1] Baca et al., 2008, Med. Eng. Phys., 30, 924-930
[2] Viceconti et al., 1996, J. Biomech., 29, 1241
[3] Cristofolini et al. 1996, J. Biomech., 29, 525-535
[4] Heiner et al., 2008, J. Biomech., 41, 3282-3284
[5] Bergmann et al., 2001, J. Biomech., 34, 859-871
[6] Wirtz et al., 2000, J. Biomech., 33, 1325-1330
[7] Peng et al., 2006, Med. Eng. Phys., 2006, 28, 227-233

AN INVESTIGATION INTO THE REMODELING PROCESS IN AN ARTIFICIALLY-MADE BONE TISSUE

Nima Jamilpour[1], Abdolhosein Fereidoon[1], Gholamreza Rouhi[2]
[1]Mechanical Engineering Department, Semnan University, Semnan, Iran, nima.jamilpour@gmail.com
[2] Mechanical Engineering Department, University of Ottawa, ON, Canada

INTRODUCTION

Tissue regeneration on carbon nanotubes (CNTs) as a scaffold is increasingly favored [1] due to the suitable environment that the CNTs provide for growth and proliferation of bone cells [2]. Superior mechanical properties of CNTs compared to those of collagen fibers (CFs), certify that an artificial bone has a greater mechanical strength than its natural counterpart [3]. Nevertheless, bone is a very dynamic organ, and there is a continuous process of resorption and formation between bone actor cells, i.e. osteoclasts and osteoblasts, and its matrix. Furthermore, based on clinical observations, it is known that the rate of bone remodeling is dependent and related to the level of mechanical stimuli within the bone. Based on the bone remodeling related facts, also the superior mechanical properties of artificial bones; it is hypothesized here that there will be a disturbance in the normal rate of bone remodeling in an artificial bone compared to a natural bone. In this research, using a theoretical approach, we aim at shedding some light on the stated hypothesis. Based on semi-mechanistic bone remodeling theories [4, 5], it is assumed that osteocytes sense the strain energy (SE) within the bone, and subsequently send suitable stimulating signals to recruit osteoblasts to initiate bone formation process. So, any changes in the SE distribution within the bone can potentially alter the rate of bone formation, and ultimately change bone density and its strength.

METHODS

In this study, bone tissue is assumed as an isotropic and linear elastic material in which hydroxyapatite (HAp) performs as the matrix of the composite. Also, the bonding between the matrix and fibers is assumed to be perfect. Two 2D comparative finite element models are built, for the natural and artificial bone samples. In each, three holes, as lacunae, are considered where osteocytes can reside. First, using finite element method and "ANSYS10™ software", the amount of SE stored in each sample is calculated. Then, an investigation is made into the effects of the presence of micro-cracks on the strain energy distribution. The later investigation is made based on the hypothesis that osteoclasts are recruited where micro-cracks appear in bone [6]. Three randomly-located cracks [7], oriented in 5 different directions, are considered in our 2D model (Figure 1).

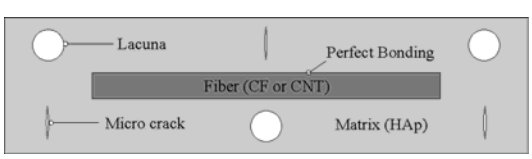

Figure 1: Schematic view of the 2D model for the crack analysis

RESULTS

Results of this research show that in the case of using CNTs, a significant reduction will occur in the amount of strain energy (SE) stored in the composite (see Table 1). It is also found that in an artificial bone, the maximum amount of SE is stored in the fibers, but in a natural bone it is stored in the matrix.

Table 1: Total SE stored in natural and artificial bone samples

Bone Sample	Total Strain Energy (Joule)
Natural bone (HAp+CF)	139.763
Artificial bone (HAp+CNT)	108.831

Results of the second step show, as expected, the existence of cracks makes a minute augmentation in the amount of SE stored in composites (see Table 2).

Table 2: Total SE stored in natural and artificial bone samples when cracks are present and distributed in different directions

Assumed angle between the crack and the loading direction	Total Strain Energy (Joule)	
	Natural bone	Artificial bone
0^0	140.149	109.085
30^0	141.690	110.193
45^0	143.351	111.392
60^0	144.948	112.549
90^0	146.667	113.740

DISCUSSION AND CONCLUSIONS

Considering the same geometry, loading and boundary conditions for the natural and artificial bones, the SE stored in the artificial bone will be less than that of a natural bone. Thus, based on the Wolf's law and semi-mechanistic bone remodeling models [4, 5], a reduction in the rate of artificial bone remodeling, compared to its natural counterpart, should be expected. Moreover, since the maximum amount of SE is stored in the fibers in an artificial bone, there would be more low SE areas in the matrix, which can promote osteoclast's activity and bone resorption [8]. Because of the stress concentration, cracks will add to the amount of SE stored in both natural and artificial bones. However, this research shows that the augmentation in SE due to the presence of micro-damages is not considerable. Experimental research is needed to shed more light on the problem tackled in this research.

REFERENCES

[1] Lobo AO et al. (2008). *Mater. Sci. Eng. C* 28; 264-269.
[2] Zanello LP et al. (2006). *Nano Lett.* 6; 562-567.
[3] Jamilpour N et al. (2009). *ICBME2009 Proceedings.*
[4] Huiskes R et al., (2000). *Nature* 405; 704-706.
[5] Vahdati A and Rouhi G (2009). *Mech. Res. Comm.* 36(3); 284-293.
[6] Burr D B and Martin R B (1993). *J Biomech.*26 (4-5); 613-616.
[7] Vashishth D *et al*. (2000). *Bone* 26; 147–152.
[8] Burger E et al. (1999). *FASEB J* 13; 101-112.

QUANTIFICATION OF MUSCULAR, POSTURAL, AND UPPER LIMB MOVEMENT DEMANDS DURING CRANE OPERATION IN AN INTEGRATED STEEL MANUFACTURING PLANT

Mark Munro[1], Michele Oliver[1], Micha Wallace[1], James R. Sexsmith[2]
[1]School of Engineering, University of Guelph, Guelph, ON, munrodm@uoguelph.ca, moliver@uoguelph.ca, wallacem@uoguelph.ca
[2]Faculty of Kinesiology, University of New Brunswick, NB, sexs@unb.ca

INTRODUCTION: Crane operators work long hours in constrained workspaces often requiring deviated postures. Neck extension, trunk flexion and repetitive arm movement are associated with increased risk of developing neck and shoulder pain [1, 2]. While reports of injuries in these regions are common amongst other workers [1], there is a dearth of information regarding injuries in crane operators, however, given their working conditions it seems reasonable to assume that they might also be at risk. The objective of this work was to quantify the muscular, postural and upper limb movement demands of crane cab operation.

METHODS: 7 male crane operators aged 25-54 years (42.4±9.4 yrs) were observed in an elevated crane cab during the loading and unloading of sheet steel for 60 minutes per operator. The task of loading and unloading a plate was segmented into four subtasks: 1) Maneuvering the cab into position over the work area; 2) Positioning the electromagnets onto the plate steel; 3) Lifting and travelling to the unload area; and 4) Positioning and release of the plate steel. Posture and hand movements were recorded for each subtask using a video camera. EMG was recorded bilaterally from the **(1)** upper trapezius, **(2)** anterior and **(3)** posterior deltoid, (4) biceps brachi, **(5)** lateral triceps brachi, (**6)** flexor carpi radialis, and **(7)** erector spinae using a Delsys MyoMonitor IV System (Delsys Inc., Boston, MA, USA) and a Toshiba Toughbook running the EMGworks 3.5 data acquisition software package (Delsys Inc., Boston, MA, USA). EMG data were normalized using reference voluntary contractions since MVC's are contraindicated in this population of workers due to unknown cardiovascular risk factor status.

RESULTS: Completion of each cycle (comprised of 4 subtasks) took approximately 2 minutes. The trunk flexion angles adopted within and between subjects were relatively constant throughout each subtask ranging between 19˚ and 30˚ (22.8±0.8˚). The average total joystick inputs were 2234±748.3/hour, with 89.3% of the inputs made with the right hand and 10.7% made with the left. Most movements were made during subtasks 2 and 4, averaging 39.4% and 42.4% respectively of the total. Integrated EMG (RMS) for the left trapezius was 28.23% of RVC compared to 30.51% of RVC for the right and remained relatively constant across the four subtasks. A Factorial ANOVA analysis revealed that %RVC was significantly different ($p \leq 0.01$) between Muscles. Subsequent Bonferroni post-hoc analyses showed that the upper trapezius muscle activation was significantly larger (**1>2,3,6,7** $p \leq 0.01$) than the other muscles in the study.

DISCUSSION AND CONCLUSIONS: Despite the higher movement frequency seen on the right hand side, the upper trapezius muscle activity remained relatively constant during the work cycle. While it is expected that the contralateral upper trapezius would display some degree of muscle activity due to its function in stabilizing the shoulder, the muscle activity observed seems to be much higher than would be expected. Bonferroni post hoc procedures showed that different combinations of muscle, subtask and side, required different levels of muscle activation to complete the task; however, the upper trapezius was observed to remain at a higher level throughout. While the sample size is quite low, these results indicate that operators might be at increased risk of developing neck and shoulder pain possibly due to the forward neck and trunk flexion.

These field data have been used in a project that involved the development of a laboratory mockup which approximated the crane cab geometry and movement demands. The mock-up was used to determine if a camera vision system allowed operators to sit in a more neutral trunk posture in order to try to concomitantly reduce muscular demands.

REFERENCES:

[1] Hagberg, M. (1984). Int Arch Occup Environ Health. Vol 53; pp. 269-278.
[2] Ariëns G. et al. (2000). Scandinavian Journal for Work, Environment and Health. Vol 26; pp7-19.

COUPLING DOES NOT INFLUENCE LIFTING AFFORDANCES

Doan, JB[1], Gausman, SJ[1], Flindall, JS[1]
[1]Engineering and Human Performance Laboratory, Department of Kinesiology and Physical Education
University of Lethbridge, Lethbridge Alberta Canada
email: jon.doan@uleth.ca

INTRODUCTION

Coupling has long been identified as a contributive factor to musculoskeletal loading and injury in occupational settings [1]. Experimental evidence has shown that gross changes in coupling can modify grip contact forces and musculoskeletal loading [2]. A learned reciprocity may exist such that individuals control physical demands and behaviours to mitigate the increased loading associated with poor or fair coupling [3]. This homeostasis may be modelled as an affordance – individuals should perceive limited coupling as affording lower lifting demands and limit the demands and/or behaviour of their lifting accordingly. The purpose of this study was to examine how coupling affects affordances of safe lifting, and lifting behaviour.

METHODS

Subjects: Sixteen healthy subjects (22.5 ± 2.3 years, 71.5 ± 10.5 kg, 174 ± 10 cm, 7 females) were randomly assigned to GOOD (n=7) and FAIR (n=9) coupling groups. Both groups lifted the same load (10 kg) in the same style container, modified only at the handles. Participants were specifically directed to the design of their hand holds, and were unaware of the existence of the other lifting container. *Affordance protocol*: While holding the load at waist level, participants were asked to determine their maximum acceptable distance for reaching to lift the load without moving their feet. Participants were given a mock task frequency (4 lifts per minute) and duration (1 hour), and were provided with 3 minutes of 4 beat per minute stimulus signal while holding the load (but not lifting). After participants had placed the load at their initial affordance threshold they were invited to increase or decrease that distance. Any changes were done by the investigator, and subjects were not allowed to reach to or lift the load as confirmation. Final affordance threshold (AT) was recorded, and normalised to height (AT/H). *Lifting protocol*: All participants completed 3 lifting trials are each of 4 reach distances (70, 90, 100, and 110% AT). Trials were randomly presented to participants, and included flexion, extension, and steps to final placement of load. Lifting movements were quantified using bilateral Optotrak™ ireds positioned on posterior trunk (L4/L5 level), posterior neck (C7 level), and posterior upper arm (distal end of humerus).

RESULTS

Good and fair coupling groups did not differ on AT/H [Fig. 1] or spatiotemporal measures of lifting, including maximum trunk angle, maximum angular velocity during reach, and maximum angular velocity during lift [Fig. 2]. We subsequently collapsed across coupling type then reclassified based on AT/H, such that we had a HYPOaffordant group (AT/H < sample mean AT/H; n = 8) and a HYPERaffordant group (AT/H ≥ sample mean AT/H; n = 8). These perceptotype groups differed significantly on AT/H, and on maximum reaching and lifting velocities of the trunk.

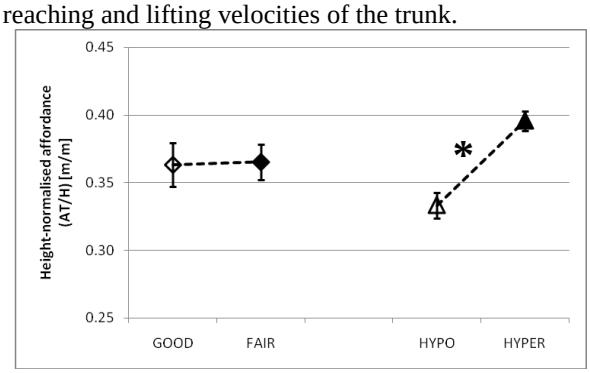

Figure 1: Normalised affordance thresholds for coupling-type and perceptotype groups (mean ± SEM).

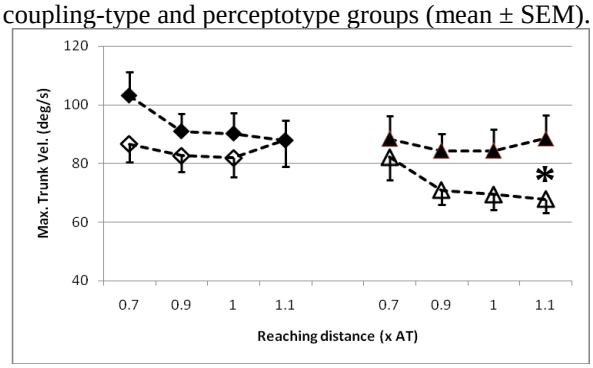

Figure 2: Maximum trunk velocity during lift (mean ± SEM). Coupling types are diamonds (open for GOOD), perceptotypes are triangles (open for HYPO).

DISCUSSION AND CONCLUSIONS

Affordance-based perceptotypes exist with respect to occupational lifting tasks. It appears these groups are biased in perception and action, such that hyperaffordants act in a manner previously associated with increased incidence of low back disability [4].

REFERENCES

[1] Waters T, Putz-Anderson V, Garg A, Fine L. (1993). Revised NIOSH equation for the design and evaluation of manual lifting tasks. *ERG, 36*, 749–776.

[2]Garg A, Saxena U. (1980). Container characteristics and maximum acceptable weight lift. *HUM FACTORS, 22*, 487 – 495.

[3]Jung HS, Jung H-S. (2007). Design of liquid container handles in accordance with user preferences. *ERG, 51*, 223-234.

[4] Marras WS, Lavender SA, Leurgans SE, Fathallah FA, Ferguson SA, Allread WG, Rajulu SL. (1995). Biomechanical risk factors for occupationally related low back disorders. *ERG, 38*, 377 - 410.

ON THE USE OF A SCALING FACTOR TO ESTIMATE CUMULATIVE SPINAL LOADING

Kaitlin M. Gallagher*[1], Steven L. Fischer[1], Samuel J. Howarth[1], Wayne J. Albert[2], Jack P. Callaghan[1]
[1]Department of Kinesiology, University of Waterloo, Waterloo, ON
[2]Faculty of Kinesiology, University of New Brunswick, Waterloo, ON
*Corresponding Author: kgallagh@uwaterloo.ca

INTRODUCTION

Despite recent advances that have looked to reduce the amount of data for workplace analyses, the estimation of cumulative spinal loading is still quite labour intensive[1,2]. The purpose of this investigation was to propose and evaluate an additional method for estimating cumulative spinal loading. The proposed method utilized a scaling factor related to the total cycle time of two tasks that were similar in their musculoskeletal demands, but differed in length. The rational for the investigated approach was to reduce the need for full analyses on jobs that incorporated similar task components to jobs that had been previously accessed.

METHODS

The proposed method was based on the hypothesis that cumulative spinal loads for a single task would be linearly proportional to its cycle time. As a result, cumulative loading of a task can be based on estimates from a similar or surrogate task that has already been analyzed. Two equations were created to estimate cumulative spinal loading:

$$\text{Interpolated Estimate} = \text{long task load} \times \frac{\text{short task cycle time}}{\text{long task cycle time}}$$

$$\text{Extrapolated Estimate} = \text{short task load} \times \frac{\text{long task cycle time}}{\text{short task cycle time}}$$

The interpolation equation is used to estimate cumulative spinal loads for a task based on the estimate made for a task with a longer cycle time. The opposite prediction can be made with the extrapolation equation. This allowed for the determinination of whether interpolating or extrapolating the analyzed estimates gave a more accurate result.

Fifteen subjects performing six tasks from four different job cells were analyzed by video analysis using 3DMatch (University of Waterloo, Waterloo, ON). These estimates acted as a criterion measure to compare the estimates made by the equations. Five cumulative loading variables were estimated using both methods – cumulative compression, extension moment, joint anterior and posterior shear, and reaction anterior shear. Absolute and relative percent error, as well as absolute magnitude of error and absolute magnitude of error per second were calculated to quantify the differences between the estimated and criterion measures of cumulative spinal loading.

RESULTS

The criterion estimates and estimates made by both the interpolation and extrapolation equations were not significantly different for four of the five outcome measures. Cumulative extension moment was overestimated by 19% (p = 0.0148) and under estimated by 16% (p = 0.009) when using the interpolation and extrapolation equations, respectively. Cumulative compression was shown to be the most accurately predicted variable (4%), while the remaining outcome measures showed a large range of relative percent errors (23 to 191%).

Despite relative and absolute percent errors that could be larger than 1000% for anterior joint and reaction shear, the absolute magnitude of error introduced per second ranged from 0.1 to 1.3 N*s/second for anterior joint shear and 0.2 to 3.4 N*s/second for anterior reaction shear. Similarly, the amount of error introduced per second for extension moment was small (0.5-2.9 Nm*s/second) despite the significant difference between the criterion and predicted measures.

DISCUSSION AND CONCLUSIONS

Using a scaling factor based on the cycle time of two similar tasks was most successful for interpolating and extrapolating cumulative compression. Moderate to large errors were found for posterior and anterior joint shear and anterior reaction shear. Slight postural differences in the task, potentially caused by unnecessary or different movements may produce poor predictions of variables (such as joint shear) that tend to oscillate around zero magnitudes in certain body positions.

The proposed method can potentially be used with other methods of data reduction to proactively estimate cumulative loading and quickly screen for tasks that are in need of a full and in-depth analysis. Future studies will investigate and define specific criteria that can be used to identify similar tasks that are candidates for this type of workplace analysis to determine their cumulative loads, as well as its validity in other areas of industry and with more complex tasks.

REFERENCES

[1] Allread WG et al. (2000). Ergonomics Vol **43**; p. 691-701.
[2] Andrews DM et al. (2003) Applied Ergonomics Vol **34**; p. 589-95.

ACKNOWLEDGEMENTS

The authors would like to acknowledge Erin Harvey for her assistance with the statistical analyses.

STEPPING RESPONSE DURING CONSTRAINED AND UNCONSTRAINED STANDING IN MOVING ENVIRONMENTS

Carolyn A. Duncan[1], Wayne J. Albert[2], Scott N. MacKinnon[3]
[1] Faculty of Engineering and Applied Science, Memorial University of Newfoundland, St. John's, NL, Canada, carolyn.duncan@mun.ca
[2] Human Performance Lab, Faculty of Kinesiology, University of New Brunswick, Fredericton, NB, Canada
[3] SafetyNet, Memorial University of Newfoundland, St. John's, NL, Canada

INTRODUCTION

Previous work at sea and in simulated motion environments has reported that wave-induced platform motions compromise postural stability [1]. Marine related literature generally views all postural responses as purely physics-based reactions to stability threatening events [2]. Research in the field of clinical biomechanics and motor control suggests that a to mediate upcoming disturbances to stability may be preferable over other strategies primarily due to the lower physiological requirements and greater biomechanical advantages of the strategy [3]. Research to examine the importance of stepping responses to maintain postural stability in motion-rich environments is needed. The purpose of this study is to determine the differences in response stepping reaction between constrained and unconstrained standing while being exposed to simulated wave-like motions.

METHODS

Twenty subjects (ten male and ten female) with limited experience working in moving environments, performed a constrained and an unconstrained standing task on a six degrees of freedom motion simulator while being exposed to three different simulated wave-like motion conditions. Motions varied in magnitude and frequency of the waveforms. During the constrained task subjects stood with their feet shoulder-width apart and were asked to only move their feet if absolutely necessary to prevent from stumbling or falling. During the unconstrained standing task subjects were told to move their feet whenever they felt necessary to retain necessary levels of stability. Constrained and unconstrained standing tasks were performed for each motion condition. Data were collected for ten minutes for each platform condition with a five minute rest between trials. Task order was randomized to minimize order effects.

All trials were videotaped to aide in the analysis of stepping occurrence. T-tests ($p<0.05$) were performed to determine if stepping occurrence differed significantly between standing tasks in each motion condition.

RESULTS

Occurrence of stepping differed significantly between unconstrained and constrained standing (Figure 1). Stepping occurrence was greater during unconstrained standing than constrained standing during all three motion conditions

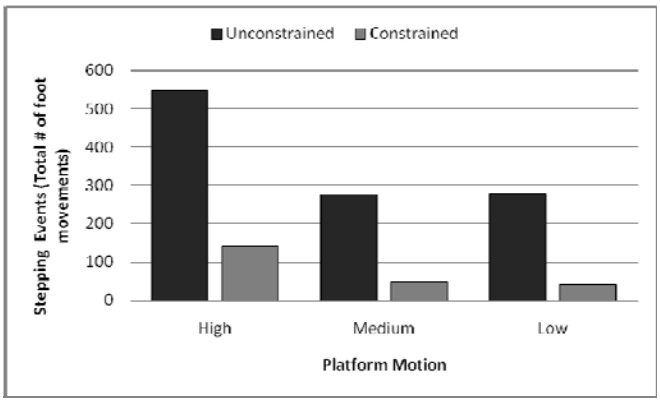

Figure 1: Stepping events during constrained and unconstrained standing tasks in high medium and low motion conditions

DISCUSSION & CONCLUSIONS

The premise of most motion-induced interruption prediction models is that when exposed to wave-induced platform perturbations, stepping need only occur once the physics based limits of stability had been surpassed and all other means of postural corrections had been exhausted. However, the results of this study suggest that stepping occurs more frequently, and also long before the limits of stability have been reached. Therefore, when examining the postural response to wave-induced ship motions, stepping should not be considered as a last resource when all fixed-support options have been exhausted.

REFERENCES

[1] Duncan et al.(2007). Occurrence of motion induced interruptions while performing common manual materials handling tasks. Presented at the 6th International Scientific Conference on Prevention of Work-Related Musculoskeletal Disorders - PREMUS 2007, August 27th-30th, Boston, USA.

[2] Langlois et al. Modelling sea trial motion induced interruption data using an inverted pendulum articulated postural stability model; *International Journal of Maritime Engineering*. *In Press.*

[3] Maki B E, McIlroy W E (1997) The role of limb movements in maintaining upright stance: the "change-in-support" strategy. *Physical Therapy* Vol **77**; p. 488-507.

POSTURAL ASSESSMENT OF CITY TRANSIT BUS DRIVERS

Michelle Rae, Donald Everson, Wayne J. Albert
Faculty of Kinesiology, University of New Brunswick, Fredericton, CANADA, walbert@unb.ca

INTRODUCTION

Previous research has identified urban bus drivers as being at a high risk for occupational disorders, due to exposure to a variety of musculoskeletal hazards and occupational stressors that can significantly and negatively affect their overall health. To date there have been limited studies that have observed transit drivers in their actual work environment, rather they have relied on questionnaires and simulated driving tasks to evaluate these stressors. The purpose of this study was to provide a postural assessment of transit drivers as they completed a full bus route.

METHODS

Fifteen city bus drivers (12 males, 3 females) volunteered to be monitored while completing a one-hour bus route during rush hour (5-6pm). The drivers have an average age of 44±8 years; average height of 179±10 cm and an average of 15±9 years of driving experience.

The full assessment included monitoring the muscle activity of the neck; shoulder and back, sitting seat pressure and body posture using standard video collection. Drivers also completed a health and lifestyle questionnaire that included both neck and low back pain status. This abstract has the video-based postural assessment as its focus.

A video camera was mounted to the dash of the bus, with the field of view directed at the seated driver only. An information poster was placed in the advertisement space behind the driver's seat to inform passengers of the study. Video was captured for the entire hour of the bus route. The video was then decimated to analyze turns, stops to disembark passengers and driving straight. The video records were converted to AVI format and imported into 3DMatch posture matching software (U.of Waterloo). On a frame-by-frame basis, postures were selected from pre-determned bins for the neck, arms and back.

Each posture bin represents a posture range. For example, 3 posture bins were provided for neck twist with the 1st bin for neck twist of less than 10°, the 2nd bin would be selected for posture greater than 10° but less than 40° and the third bin would be selected for postures greater than 40°. Depending on the range of movement afforded by a joint there were between three and five bins available. For analysis purposes, postural ranges were cumulated and percent times in each of three categories, neutral, mild, and severe posture were recorded. This was done to provide an assessment of musculoskeletal risk as outlined by Punnett et al. [2], who have provided odds ratios related to percent of cycle times spent in non-neutral postures.

RESULTS

Thirty percent of drivers reported having neck and/or low back pain on the health and lifestyle questionnaire. An examination of the percent time spent in non-neutral postures revealed that neck and arms reported higher times than the back. Trunk flexion, twist and bend were in a neutral posture for greater than 90% of the driving time. Arm flexion ranged from 30-50% of time in a non-neutral posture depending on the activity.

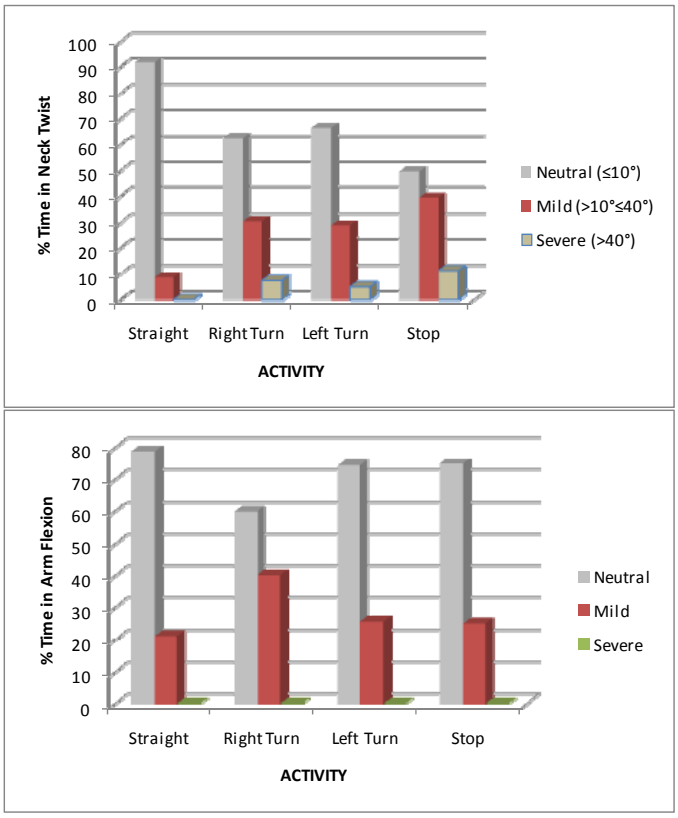

Figure 1. Percent time spent in neutral, mild and severe posture with respect to neck flexion (top) and arm flexion (bottom) for each driving activity.

DISCUSSION AND CONCLUSIONS

The physical size of the bus requires drivers to assume non-neutral postures of the neck and arms in order to make routine turns as well as to monitor seven mirrors to scan passenger activity and navigate the buses blind spots.

REFERENCES

[1] Punnett et al. (1991). Scand J Work & Environ Health 17:337-346.

ACKNOWLEDGEMENTS

The authors would like to acknowledge the support of the City of Fredericton and the cooperation of Fredericton Transit...

SEAT EFFECTIVE AMPLITUDE TRANSMISSIBILITY BASED SEAT SELECTION TO MINIMIZE 6 DOF WHOLE-BODY VIBRATION IN INTEGRATED STEEL MANUFACTURING MOBILE MACHINERY

Leanne Conrad[1], Michele Oliver[1,2], Robert J. Jack[2,4], James P. Dickey[2,3] Tammy Eger[4]
[1]School of Engineering,[2]Biophysics Interdepartmental Group, University of Guelph, Guelph, Canada, lconrad@uoguelph.ca
[3]School of Kinesiology, University of Western Ontario, London, Canada
[4]School of Human Kinetics, Laurentian University, Sudbury, Canada

INTRODUCTION

There is strong evidence linking whole-body vibration (WBV) to back, neck and shoulder injuries. Operators of mobile machinery are exposed to WBV along six axes (three translational and three rotational) (6DOF). Seats for these heavy machines are usually selected without field based 6DOF testing. The purpose of this project was to use Seat Effective Amplitude Transmissibility (SEAT) measures from field based vibration to help the steel industry make more appropriate seat selections for machine retrofitting.

METHODS

6-DOF chassis acceleration data were recorded for a variety of mobile machines from the steel making industry [1]. From these data, six, 20 second representative profiles (Table 1) were assembled from the 'worst' WBV machine for implementation on a lab-based 6 DOF Parallel Robotics System Corporation (PRSCO) robot. Subjects sat on one of three heavy equipment seats (BeGe7150, Grammar MSG 95G1721, and a 6801 Isringhausen in which the seat pan cushion was retrofitted with Skydex™ seating material) mounted on the PRSCO robot. Three randomized trials were conducted for each combination of seat and profile using 8 male (22.3±2.0 yrs) and 8 female (23.5±1.8 yrs) inexperienced operators (IEO) as well as 4 male (47.3±12.3 yrs) experienced operators (EO) from a participating steel making company. Six-DOF vibrations were recorded at the chassis by a MEMSense Mag3 Triaxial Accelerometer & Gyroscope (MEMSense, SD, USA) and at the seat by a custom seat pad transducer consisting of two ADXL320EB dual axis accelerometers and three single axis ADXRS150EB gyroscopes (Analog Devices Inc., MA, USA) [2]. Seat effective amplitude transmissibility (SEAT) was calculated from the ISO 2631-1 weighted 6DOF vibration dose value (VDV) [3,4].

RESULTS

Significant main effects from the factorial ANOVA procedures ($p \leq 0.01$) are presented in Table 2. The only consistent significant differences across all 7 SEAT variables in both the IEO and EO were for Profile.

DISCUSSION AND CONCLUSIONS

The large number of significant differences for the various main effects and interactions strongly suggest that there may not be one best seat for all of the different vibration profiles encountered in an operator's daily routine. Though a small number of subjects were tested, this appears to be particularly true for EO.

REFERENCES

[1] Oliver M et al. Quantification and characterization of 6-degree-of-freedom whole-body vibration exposure from the chassis of selected mobile machines used in the steel making industry. *Proc. of the 4th Int. Conf. on WBV Injuries*, 2009
[2] Cation, S., et al. Six degree of freedom whole-body vibration during forestry skidder operations. *Int. J. Ind. Ergon.* 38, 739-757, 2008.
[3] ISO 2631-1. *Mechanical vibration and shock – Evaluation of human exposure to whole-body vibration – Part 1: General requirements*: International Standards Organization 1997.
[4] Griffin MJ. *The Handbook of Human Vibration*: Academic Press INC. 1990.

Table 1: 6DOF Vibration total value (VTV) for each of the 6, 20 second vibration profiles and the field task from which they were obtained.

Field Task	Driving Loaded	Driving Loaded	Driving Unloaded	Driving Unloaded	Slag Pot Pickup	Pot Banging
6DOF Unweighted Chassis VTV (m/s^2)	2.122	1.247	2.168	1.442	1.028	1.816

Table 2: Summary of statistically significant results from factorial ANOVA procedures ($p \leq 0.01$).

Response Variable	Significant Main or Interaction Effect ($p \leq 0.01$)	
	Experienced Operators (EO)*	Inexperienced Operators (IEO)
6DOF	Profile	Profile
X	Profile	Profile, Sex*Profile
Y	Profile	Profile, Sex, Chair, Chair*Profile
Z	Profile	Profile
Roll	Profile	Profile, Chair, Chair*Profile
Pitch	Profile	Profile
Yaw	Profile, Chair, Chair*Profile	Profile, Chair, Sex*Profile, Chair*Profile

***note that all experienced operators were male so the analysis did not evaluate the effect of sex.**

OCCUPATIONAL VIBRATION EXPOSURE AT THE FEET: CHARACTERISTICS AND HEALTH IMPLICATIONS

Tammy Eger[1], Ron House[2], Aaron Thompson[2], Mallorie Leduc[1], and Alison Godwin[1]
[1]School of Human Kinetics, Laurentian University, Sudbury, Canada, teger@laurentian.ca
[2]University of Toronto and St. Michael's Hospital, Toronto, Canada

INTRODUCTION

Workers in mining and contruction can be exposed to vibration through their feet. Prolonged exposure to hand-transmitted vibration has been shown to cause vascular, neurological, and musculoskeletal problems of the hand-arm[1]. Workers who are exposed to vibration via the feet could also be at risk for similar health problems[2]; however, limited research has examined the characteristics (frequency content, acceleration) of vibration entering the body via the feet. Documented case histories of workers with "white-feet" are also limited.

METHODS

Vibration at the feet was measured during the operation of locomotives, bolting platforms, wood raise platforms, and metal raise platforms using a tri-axial accelerometer according to ISO 2631-1 guidelines. Participating workers were also asked to complete a musculoskeletal disorders questionnaire.

The case report of a worker with prolonged exposure to foot-transmitted vibration with complaints of pain, blanching and cold intolerance in his toes is also described. Digital photocell plethysmography of the hands and feet of the worker after a 2-minute 10 º C cold immersion bath was conducted to determine if the worker had evidence of vascular impairment in the feet and/or hands.

RESULTS

Frequency-weighted r.m.s. acceleration values and dominant frequency measured at the feet are reported in Table 1. Workers operating the jumbo drill and raise platform were exposed to higher frequency vibrations and indicated they had been diagnosed with hand-arm vibration syndrome and white-feet.

The worker presenting with pain and blanching in the feet was 54 yrs old and had worked as a miner (including bolting platform operation) for 18 years. Digital plethysmography post cold provocation showed moderate dampening of all toe waveforms and no changes of the hand waveforms (see Figure 1). These results indicate a vasomotor disturbance associated with cold sensitivity in the toes but not in the hands resulting in a diagnosis of "vibration white-foot".

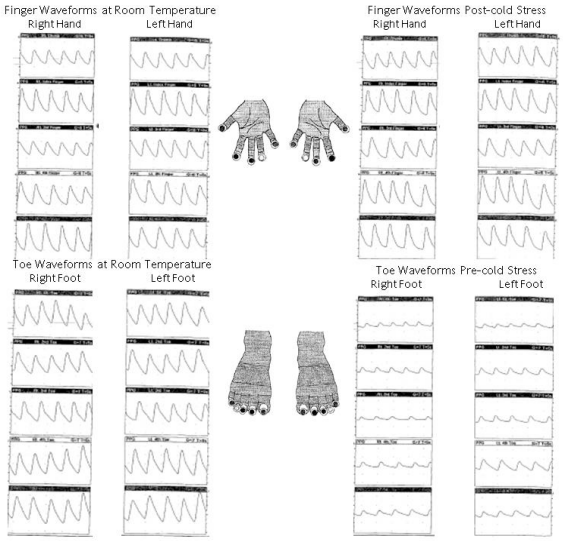

Figure 1: Plethysmography results showing finger and toe waveforms at room temperature and post-cold stress.

DISCUSSION AND CONCLUSIONS

Field measures and a case report provide evidence to suggest workers exposed to higher frequency vibration levels are more likely to report pain and discomfort in the feet and be diagnosed with "white-feet".

REFERENCES

[1] Griffin MJ, Bovenzi M.(2002). The diagnosis of disorders caused by hand-transmitted vibration: Southhampton Workshop 2000. *Int Arch Occup Environ Health.* 75: 1-5..
[2]Cooke, J.P. et al. (2005). Mechanisms of Raynaud's disease. *Vascular Medicine*. 10: 293-307.

Table 1: Vibration characteristics and musculoskeletal discomfort associated with equipment operation.

Machine	DF_z (Hz)	a_{wz} (m/s/s)	Reported Musculoskeletal Discomfort 1=mild discomfort; 4 = severe discomfort
Locomotive-2	3.15	0.36	L.Knee:1, R.Knee:1, L.Ankle:3, R.Ankle:1
Locomotive-1	6.3	0.43	Neck:1, Lower Back:2, R.Wrist:1, L.Wrist:1, L.Knee:1, R.Knee:1
Jumbo Drill	31.5	0.16	R.Shoulder, R.Wrist 2, L.Wrist:2, L.Feet:1, R.Feet:1 **(Diagnosed white hands and feet)**
Wood Raise Platform	40	1.1	R &L.Shoulder:2, R&L.Elbow:2, Upper Back:2, Lower Back:2, R&L.Wrist:2, Hips&Thighs:2, R&L.Knee:2, R&L.Ankle:2 **(Diagnosed white hands and feet)**
Metal Raise Platform	40	1.08	R&L.Ankle:2, R&L.Knee:2, R&L.Wrist:3, Lower back:1, Upper back:1

DIFFERING NECK POSTURES FOR OPERATING NORMAL AND LOW-PROFILE MACHINES

Alison Godwin[1], Tammy Eger[1,], and Sylvain Grenier[1]
[1]School of Human Kinetics, Laurentian University, Sudbury, Canada, agodwin@laurentian.ca

INTRODUCTION

The postures used by operators of load-haul-dump (LHD) machines have been examined in an effort to document design characteristics, and task requirements associated with musculoskeletal injuries. In previous investigations, operators were found to require greater than 40° of neck rotation for 85% and 89% of the work cycle for underground mining tasks [2]. These results have far exceeded the recommended amount [1,3] of neck rotation during a workshift. Manufacturers have started to design low profile mining machinery specifically for access in low-seam mines. Since the machines are restricted in vertical height, the cabs also have limited space for the operator, which further impacts the postures they may use. The purpose of this paper was to compare neck rotation during specific mining tasks for operators of a normal vs low profile LHD machine.

METHODS

Small digital video cameras (DCR-PC109 NTSC, Sony) were installed in the operator's cab of two LHDs – a normal machine and a low-profile machine. A 3DMatch analysis was subsequently carried out to determine the percentage of time spent in mild and severe neck rotation during the following tasks: driving forward, right turns, left turns, mucking, driving in reverse. The results were averages taken from two different operators.

RESULTS

LHD vehicle operators sit sideways to their direction of motion resulting in a large percentage of time spent with the neck in a severely rotated posture (Table 1). The normal cab machine required that the operator spend a greater percentage of the task cycle in severe neck rotation for driving loaded, mucking and right turns. Generally, the operators of the low-profile cab were able to spend more of the task cycle using mild neck rotation. Although not reported, the low-profile cab and the low seating position required the operator to use neck extension to view the opposite-side of the machine.

DISCUSSION AND CONCLUSIONS

Although it was anticipated that the low-profile cab would require greater twisting motion of the neck, these preliminary results have not shown this to be true. The operators of the low-profile cab were able to work with their necks in mild rotation for greater portions of the task cycle. The results may be compromised by the fact that low-profile testing occurred in a controlled above-ground test pit while the normal machine was tested underground. The restricted view available from the low-profile cab may also mean that the operators rely on different visual cues to navigate – a finding that could be corroborated by evaluation of eyetracking and point-of-regard results also gathered. The amounts of neck extension that were observed could be alleviated by mounting a reference mirror on the opposite-side of the machine. A full line-of-sight investigation on a low-profile cab in an underground environment is warranted.

Table 1: Percentage of task cycle spent in mild and severe neck postures for normal and low-profile LHD machines.

Posture Adopted	Percentage of task cycle in each posture							
	Driving Loaded		Mucking		Right Turn		Left Turn	
	LP	N	LP	N	LP	N	LP	N
Mild neck rotation (10 - 40°)	30	7	54	24	52	2	15	17
Severe neck rotation (>40°)	63	92	46	74	30	98	85	80

REFERENCES

1. S. G. et al. (1999) Ergonomic Guideline for Forest Machines. Handbook. SkogForsk, Uppsala, Sweden
2. T.E. et al. (2008). Predictions of health risks associated with the operation of load-haul-dump mining vehicles: Part 2—Evaluation of operator driving postures and associated postural loading. *International Journal of Industrial Ergonomics, 38* (9-10); 801-815.
3. J. E. et al. (1994). Head posture measurements among work vehicle drivers and implications for work and workplace design. *Ergonomics* **37** (4); 623–639.

ACKNOWLEDGEMENTS

Funding was provided by the Workplace Safety and Insurance Board of Ontario, Canada.

PRINCIPLE COMPONENT DECOMPOSITION OF POSTURAL CONTROL MOVEMENTS

Peter Federolf
Human Performance Laboratory, University of Calgary, Calgary, Canada

INTRODUCTION

The assessment of the stability in balance exercises is an important tool to characterise skills or deficites in postural control. The standard procedure in the assessment of stability is the chracterization of the center or pressure (COP) motion, which is determined from the ground reaction forces when subjects stand on a force plate. COP excursion is an appropriate measure to quantify stability since any departure of the COP from the support area under the feet requires the subject to take action in order to prevent a fall, e.g. to abort the balance exercise and step away. Unfortunately, analysis of the COP motion does not allow to draw conclusions about the actual postural control movements that the subject employed. Previous studies have identified, for example, ankle or a hip strategies. In the project presented here postural control movements were decomposd into principle movements using a principle component analysis. The aim of this project was to determine if dual task conditions, which were reported to affect postural control, would affect the range or the temporal characteristics of these principle movement patterns.

METHODS

Nine subjects (♀, age 55-60) were included in this study. All subjects gave informed written consent and the local ethics board has approved the study.
The subjects were equipped with 37 markers using a standard marker setup ("Plug-in-gait"). The balance exercise was an 80-second tandem stance on a force plate. The subjects were instructed to "stand as quiet as possible" with their hands on the hip. Single task (postural control only) and dual task conditions (subjects were solving an auditory n-back test in addition to the balance task) were tested. The marker positions were recorded at 240 frames/second using a system of 8 synchronized digital infrared high-speed cameras (Eagle and Hawk, Motion Analysis. Corp., USA). The kinematic data was post-processed using the software Eva Real-Time (EVaRT, Motion Analysis Corporation, USA). The data was not filtered. Gaps shorter than 0.1s in the trajectories of individual markers were reconstructed using either cubic interpolation or by determining the position of the missing marker from adjacent markers (for each gap the researchers selected the method that gave the subjectively best results). If the gaps were longer or numerous, then the whole trajectory of this marker was excluded from the analysis. The subsequent analysis was conducted for on the middle 70 seconds of each trial and 28 markers on anatomical landmarks were selected. In each frame of the video the posture of the subject was thus characterised by 84 variables (x,y,z-coordinates of 28 makers), which were interpreted as one 84-dimensional posture vector. Characteristic movements of the subject during each trial were then determined by performing a principle component analysis on the 16,800 posture vectors obtained during the analysed 70 seconds of each trial. The principle component vectors with large Eigen values represent the direction of the largest variance in the posture vector, which were interpreted as *principle movements*. These principle movements represent the main movement patterns that a subject executes while balancing. Projection of the posture vectors onto the principle component axes yielded time series that quantified the main balance movements executed by a subject. Range and temporal characteristics of these time series were analysed using classical statistics (standard deviation, interquartile range, mean velocity) and fractal analysis techniques (detrended fluctuation analysis).

RESULTS

An example of the principle movement patterns of one subject is shown in Figure 1. These patterns are subject specific but in many cases they were reproduced when the subject repeated the same test.

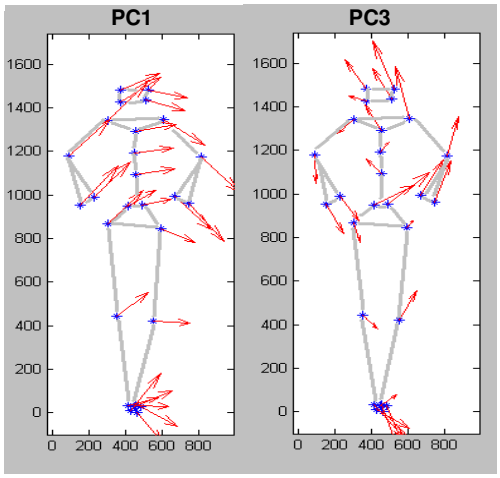

Figure 1: First and third principle movements of one subject shown in the frontal plane. The arrows indicate the direction of each marker's motion.

The classical statistical methods did not suggest that a concurrent cognitive task had an effect on the principle balance movements. However, the result of the detrended fluctuation analysis suggested that movement characteristics in the first, second and fourth principle movements changed due to the dual task situation ($p=0.04$, $p=0.007$, $p=0.001$).

DISCUSSION AND CONCLUSIONS

Principle component analysis conducted on the movement patterns during balance exercises appears to be a promising alternative to COP-based assessments of stability.

BIOMECHANICAL GAIT ANALYSIS USING HIGH-HEELED SHOES IN HORIZONTAL AND INCLINED WALKWAY

Glauce Gonzaga Silva[1], João Alberto de Oliveira[1]
[1]Department of Mechanics/Engineering College of Guaratinguetá, Universidade Estadual Paulista, Guaratinguetá, Brazil, fisioglau@gmail.com

INTRODUCTION

Actually it's large the number of women that make use of high-heeled shoes for several hours a day, often being subdued to gait different types of surfaces, smooth and/or inclined, subjecting the musculoskeletal system to a variety of efforts. The present study's intentions were: to analyze women's gait using high heels in comparison with the barefoot condition; to analyze the influence of a slope surface over the gait pattern of individuals and to relate the effect of high-heeled shoes utilization with the effect of a slope surface.

METHODS

Ten healthy young women volunteers participated on the study, walking on the treadmill with a force plate wearing shoes with heels of 5.0 cm (as shown in Figure 1) and shoeless condition in three conditions: on the horizontal plane, inclined surface with 1.83 ° and 3.61 °. Each condition was also analyzed during 10 seconds by film. The images were fragmented in Quintic Player ® (*Quintic Consultancy Ltd®/England*) software and relayed to the ImageJ ® (*National Institute of Mental Health/* USA) software through which were analyzed the angular variation of knee in the sagittal plane.

Figure 1: Shoe used in this study.

RESULTS

Statistical analysis Non-parametric (*Wilcoxon* test) by using significance $p < 0.10$ showed that the use of shoes with with 5 cm heels associated with gait in the horizontal plane and inclined surface with 1.83 ° and 3.61 ° does not amending the minimum angle of knee flexion, but applies influence on the maximum angle in the same horizontal plane downwards with the use of footwear. It was also found that such footwear is correlated with walking speed inversely proportional to the slope surface, except the slope of 3.61 ° with the same footwear, in which case there was a value close to the barefoot condition in the horizontal plane. The use of 5cm heel footwear on the slope of 3.61° leads to an increase of the First Force Peak (FFP). The same shoes however decreased both the Second Force Peak (SFP) on the horizontal plane as the two slopes studied.

DISCUSSION AND CONCLUSIONS

Prentice et al. (2004) and Leroux, Fung and Barbeau (2002) say the gait slope promotes postural changes such as increased flexion of the hip, knee and ankle. In this situation, the trunk control as well as the pelvis, are essential to body balance, so there is a proper reception of force by the lower limbs. Postural changes are directly proportional to the slopes of the surface. Despite the small slope adopted in the present study (1.83 °), was found the considerable influence of the slope on the kinematic behavior of this joint.

The gait in the slope of 3.61 ° with the use of footwear leads to an increase of the FFP, which possibly creates more strain on the musculoskeletal system. The same shoe generates, however, decreased both the SFP in the horizontal plane as the two slopes studied.

REFERENCES

[1] Leroux A Fung J Barbeau J (2002). Postural adaptation to walking on inclined surfaces: I. Normal strategies. *Gait and Posture* Vol 15; p. 64-74.
[2] McIntosh AS et al. (2006). Gait dynamics on an inclined walkway. *Journal of Biomechanics* Vol 39; p. 2491-2502.
[3] Menant JC et al. (2009). Effects of walking surfaces and footwear on temporo-spatial gait parameters in young and older people. *Gait and Posture* Vol 29; p. 392-397.
[4] Prentice et al. (2004). Locomotor adaptations for changes in the slope of the walking surface. *Gait and Posture* Vol 20; p. 255-265.

ACKNOWLEDGEMENTS

Thanks to CAPES (Improving Coordination of Senior Staff), in Brazil, for the scholarship granted.

GROUND REACTION FORCES IN ASSYMETRICAL GAIT USING SPLIT-BELT TREADMILL

Rachid Aissaoui[1,2], Philippe Gourdou[1], Sylvie Nadeau[2]
[1]Laboratoire de Recherche en Imagerie et Orthopédie, École de technologie supérieure, Montréal, rachid.aissaoui@etsmtl.ca
[2]Labortoire de Pathokinésiologie, École de réadaptation, Université de Montréal, Canada

INTRODUCTION

In the past, few studies have analyzed the spatiotemporal and electromyographical modifications when healthy/hemiparetic subjects walked in an asymmetric environment controlled by a split-belt treadmill [1,2]. Up to now, no data have assessed the effect of speed difference between limbs on ground reaction forces. The purpose of this study was to investigate the influence of the assymetry ratio in speed between the dominant and non-dominant side on ground reactions forces in a group of able-bodied subjects.

METHODS

Seventeen (17) healthy adult subjects took part in the experimentation: height 1.70 ± 0.06 m; weight 65.6 ± 7.1 kg; age 28.0 ± 7.1 years; leg-length 0.79 ± 0.04m. They were tested randomly at their comfortable speed Vconf on an instrumented treadmill with five asymmetric ratios. Each ratio corresponded to a decrement of 10% of the speed belt of the non-dominant side with respect to the dominant one. Each subject carried out a total of six walking conditions on a split-belt treadmill at different asymmetric ratio. Each trial lasts for 5 min, and the 30 last seconds were recorded. First, the speed of the belt located under the dominant leg was set to comfortable walking speed which was equal to 1.42 ± 0.08 m/s. Afterwards, the speed of the belt located under the non dominant contra-lateral leg was randomly set to 0%, 10%, 20%, 30%, 40%, and 50% less than the ipsilateral dominant side speed. For each reference speed, the experiment was repeated twice. Kinematics data was collected by an optoelectronic motion analysis system (Vicon M460) using six (6) cameras at 120 Hz. Two Kistler force plates recorded the ground reaction forces at 120Hz under a split-belt treadmill (Adal). The speed of each belt was controlled separately. The parameters extracted from the ground reaction forces are: peak amplitudes and timing of medial and lateral peak forces, anterior and posterior peak forces, as well as the 1st and 2nd vertical peak forces. ANOVA tests were used to determine the effect of speed asymmetry on each of the above parameter.

RESULTS

In the medial-lateral direction, the main results is that for the dominant side the lateral magnitude of the forces decreases at the heel strike instant when the ratio of asymmetry increases. However, the magnitude of the first medial peak is constant and did not vary with speed. In the non-dominant side, the medial peak significantly ($p<0.01$) decreases from 7.92 % BW to 6.39 % BW when the speed ratio varied form 0 to 50% at V_{conf} reference speed with respect to the dominant side. Figure 1 shows the anterior-posterior force in the dominant and non-dominant side for 5 asymmetrical ratio of speed at Vconf. For the dominant side, the posterior directed braking force decreases significantly ($p<0.007$) when the speed ratio increases and the instant of the posterior peak occurs significantly earlier during the stance phase ($p<0.001$). The push-off peak occurs earlier also ($p<0.001$). For the non-dominant side, the posterior and anterior peaks decrease significantly ($p<0.001$) when speed ratio increases.

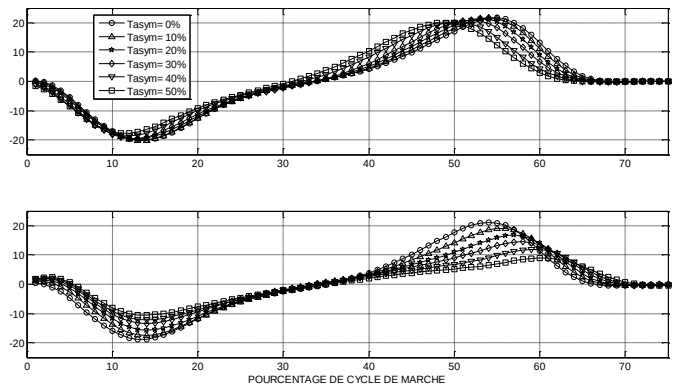

Figure 1: Anterior-posterior horizontal forces in dominant side (top) and non-dominant side (bottom) at Vconf. Tasym indicates the asymmetry ratio between dominant and non dominant side. Vertical axis indicates a (%) of body-weight; horizontal axis indicates the stance phase of the normalized gait cycle.

DISCUSSION AND CONCLUSIONS

In the dominant side, there is less time to achieve the support phase of gait that is why the AP peaks occur earlier during the stance phase. The findings suggest that the anterior-posterior forces are the most sensitive when compared to the vertical and medial-lateral directions; this could have an impact when developing therapeutic training methods for pathological cases such as hemiparesis conditions using asymmetrical speed between sides.

REFERENCES

[1] Reisman DS et al. (2007). Locomotor adaptation on a split-belt treadmill can improve walking symmetry post-stroke. *Brain*, Vol. **130** (7); p. 1861-1872.
[2] Zijlstra W., Dietz V. (1995). Adaptability of the human stride cycle during split-belt walking. *Gait & Posture*, Vol. **3**; p. 250-257.

ACKNOWLEDGEMENTS

This study was supported by the MENTOR program of the Canadian Institute of Health Research. S. Nadeau is supported by the FRSQ.

IMPLEMENTATION AND VALIDATION OF A NOVEL INERTIAL MEASUREMENT SYSTEM FOR KINEMATIC GAIT ANALYSIS

Brummund, MK[1, 2], Doan, JB[2], Block, E[3], Brown, LA[2], Hu, B[3]
[1]Institut für Sportwissenschaft, Otto-von-Guericke-Universität, Magdeburg, Germany
[2]Department of Kinesiology & Physical Education, University of Lethbridge, Lethbridge Alberta Canada
[3]Hotchkiss Brain Institute – Movement Disorders Program, University of Calgary, Calgary Alberta Canada
email: Martin.Brummund@uleth.ca

INTRODUCTION

Active and passive optical motion capture systems (OMS) represent the gold standard in kinematic gait analysis as they excel at accuracy and versatility. Despite their great value OMS are also accompanied by a number of temporal, financial and spatial constraints that hinder a routine clinical use. This gap can be bridged by inertial systems like the novel GaitMeter™ prototype (GM); a portable, low-cost, system of the Movement Disorders Clinic at the University of Calgary that was primarily developed to meet the requirements of clinicians. The purpose of the present study is to introduce analysis procedures that were implemented with the goal of automating the kinematic data processing and to validate the obtained output against a Vicon® system (Vicon, CA, USA).

METHODS

Subjects & Protocol: Ten healthy subjects (21.6 ± 1.8 years, mean ± S.D.) walked in stocking feet along a 9m long, straight line to the beat of three metronome paces (slow = 70Bpm, medium = 80Bpm, fast = 90Bpm) presented in random order. Each subject's gait was bilaterally tracked by the GM using one uniaxial accelerometer and one pitch gyroscope respectively. The sensors were firmly mounted on the participant's lower extremities aligning the accelerometers in anterior directions. As reference, a synchronized six camera Vicon® system tracked each participant over 3m within the walkway. One reflective marker was directly placed on the inertial sensors and additional markers were mounted on bony landmarks according to Winter's [1] full body model.

Data Analysis: The Vicon® data were analyzed with the help of manufacturer provided software. The inertial data were analyzed with custom-made GUIs in Matlab (Mathworks Inc., MA, USA) that aimed to minimize user interaction and to maximize processing pace while at the same time assuring highest accuracy. This was achieved through the steps signal conversion, signal filtering and mathematical refinement as depicted in Figure 1.

Statistical analysis: The horizontal translational and angular trajectories of the inertial sensors and the reflective markers were statistically analyzed through the determination of the coefficient of multiple correlation (CMC) and the root mean of the squared differences (RMS) [2].

RESULTS

The trajectory comparison of the rotational trajectories indicated overall very high CMCs and small percent RMS errors with the angle trajectories yielding slightly better statistical results than the angular velocity trajectories. Horizontal displacement trajectories also demonstrated very high CMCs, but larger RMS errors. The observed accuracies remained constant across varying cadences for both trajectory types.

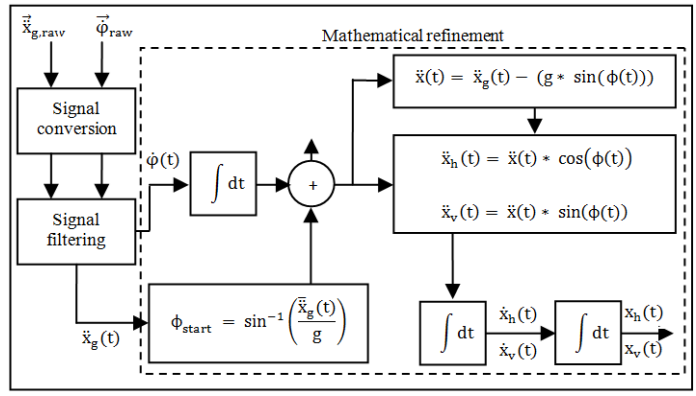

Figure 1: Autonomous offline data processing procedures.

Table 1: Statistical results of: angle, angular velocity, horizontal displacement, acceleration of left sides (mean ± S.D., Bpm=Beats per minute).

Left	70 Bpm	80 Bpm	90 Bpm
RMS [°]	3.75 ± 2.55	3.09 ± 0.91	3.91 ± 1.67
RMS [%]	6.21	5.11	6.25
CMC	0.98 ± 0.03	0.99 ± 0.00	0.99 ± 0.01
RMS [°/s]	25.68 ± 15.8	23.79 ± 6.1	33.61 ± 18.3
RMS [%]	7.99	6.54	8.49
CMC	0.96 ± 0.07	0.99 ± 0.01	0.97 ± 0.03
RMS [m]	0.35 ± 0.19	0.34 ± 0.18	0.38 ± 0.19
RMS [%]	19.13	17.82	18.81
CMC	0.92 ± 0.07	0.89 ± 0.09	0.90 ± 0.08
RMS [m/s^2]	2.28 ± 0.38	2.63 ± 0.31	2.95 ± 0.44
RMS [%]	17.20	17.31	16.33
CMC	0.85 ± 0.05	0.87 ± 0.02	0.89 ± 0.02

DISCUSSION AND CONCLUSIONS

The excellent results obtained from the rotational trajectories are in accordance with previous research findings [2]. The observed difference between linear and angular trajectories might mostly be caused by accelerometer vibrations during heel-strike and toe-off as well as the employed double integration. Nevertheless, the findings clearly indicate that the chosen approach is suitable to provide satisfying kinematic data in a timely manner.

REFERENCES

[1] Winter DA. *Biomechanics and Motor Control of Human Movement*; John Wiley & Sons, INC, 2005.

[2] Mayagoitia RE et al. (2002). Accelerometer and rate gyroscope measurement of kinematics: an inexpensive alternative to optical motion analysis systems. *J Biomech*, **35**(4), 537-542.

ACKNOWLEDGEMENTS

The support of CIHR and SAIPN is gratefully acknowledged

GAIT MODE RECOGNITION FROM ABLE-BODIED LOWER LIMB EMG

Dan Rogers[1], Kevin Englehart[1], Ann Simon[2], Levi Hargrove[2,3]
[1]Institute of Biomedical Engineering, University of New Brunswick, Fredericton, Canada, dan.rogers@unb.ca
[2]Rehabilitation Institute of Chicago, [3]Feinberg School of Medicine, Northwestern University, Chicago, USA

INTRODUCTION

The objective of this study was to use lower limb EMG collected from able-bodied participants during weight-bearing activities in order to distinguish among modes of locomotion including standing, walking, stair ascent/descent and contralateral/ipsilateral turn.

A linear discriminant analysis (LDA) classifier was chosen because of its ease of implementation as well as its reported success by Huang [2]. Hidden Markov models (HMM) are also well suited to the gait mode classification problem because they inherently model the temporal variation of signals without being sensitive to the rate at which these variations occur.

METHODS

Thirteen channels of surface EMG were collected from the intact lower limb from the gluteus maximus, sartorius, tensor fasciae latae, adductor magnus, gracilis, vastus medialis, rectus femoris, vastus lateralis, biceps femoris, semitendinosis, lateral gastrocnemius, soleus and tibialis anterior muscles. Stainless steel electrodes with inter-electrode spacing of approximately 2.5 cm were used and all signals were sampled at 1000 Hz.

Five participants performed 'data collection circuits' which began in standing and proceeded to level walking, stair ascent, contralateral turn, stair descent, level walking and ipsilateral turn. Two versions of the circuit were performed: a 'discrete' version in which each mode began and ended in standing and a 'continuous' version which had level walking transition directly to stair ascent and stair descent transition directly to level walking. Time-domain EMG features were calculated from 150 ms frames overlapped by 140 ms. The features included mean absolute value, zero crossings, slope sign changes and waveform length as described by Hudgins [1]. Features from 10 repetitions of the discrete circuit were used to train pattern classifiers and 5 repetitions of the continuous circuit were used for testing.

A single LDA as well as gait phase-specific LDAs were trained. A threshold applied to force sensors on the heel and toe defined 4 gait phases in a continuous manner: stance (both sensors above threshold), swing (neither sensor above threshold), heel and toe. A different LDA classifier was trained for each phase.

A HMM classifier with 4 states modeled as single-mixture Gaussian densities was trained for each locomotion mode.

RESULTS

The results are summarized in Table 1. Averaged across participants, the single LDA classifier had a classification accuracy of 63.8% while the phase specific LDA scored 76.7% which was improved to 80.3% with the addition of a 25-vote (250 ms) majority vote in post-processing. The HMM classifier was slightly better with an average classification accuracy of 81.7%.

Table 1: Classification accuracy by participant and classifier (m.v. denotes majority vote in post-processing)

Classifier\ Subj	1	2	3	4	5	Ave
LDA	67.3	62.3	64.7	71.3	53.3	63.8
LDA + m.v.	69.2	63.2	65.3	72.8	56.6	65.4
LDA phase	78.7	78.5	80.7	79.9	65.9	76.7
LDA ph + m.v.	82.1	80.7	83.9	83.6	71.3	80.3
HMM	83.2	84.2	81.6	83.5	76.2	81.7

DISCUSSION AND CONCLUSIONS

The reported classification accuracies are relatively low compared to those often cited in upper limb control strategies (> 95%). The decrease in class separability is largely the result of the dynamic nature of EMG during locomotion as well as the relative similarity of the various movements. The EMG-based mode recognition system is not intended to be the sole controller of a powered prosthesis but to supplement the information provided by force sensors, accelerometers and other physical sensors embedded in the prosthesis. Data fusion strategies will be explored as data become available.

Although classification accuracy offers some ability to compare the classifiers to each other, it gives limited insight into the classifiers' affect on the real-world usability of a prosthesis. Such tests will be conducted with appropriate hardware in the near future.

REFERENCES

[1] Hudgins B, Parker PA, Scott RN. (1993). A new strategy for multifunction myo- electric control. *IEEE Trans Biomed Eng* 40: 82–94, 1993.
[2] Huang H, Kuiken TA, Lipshutz R. (2009). A strategy for identifying locomotion modes using surface electromyography *IEEE Trans Biomed Eng* 51(1); p.65-73

ACKNOWLEDGMENT

This work is a preliminary study as part of a TATRC sponsored project, "Development of a Neural Interface for Powered Lower Limb Prostheses".

EFFECT OF ASYMMETRICAL LOAD CARRIAGE ON LOWER EXTREMITY JOINT KINEMATICS DURING NORMAL AND HIGH-HEELED GAIT IN FEMALES

Soul Lee & Jing Xian Li
School of Human Kinetics, University of Ottawa, Ottawa, Canada, slee087@uottawa.ca

INTRODUCTION

Balance is challenged during gait when body is forced to make a postural alteration and to compensate changes due to disturbances to the body. Often a load carriage challenges the balance during gait [1] especially when it is carried asymmetrically [2]. A purse on one shoulder is one of the most popular methods of carrying load employed by women. Balance is affected by load and exacerbated further when high-heeled shoes are worn. The effect of load carriage has been studied from previous studies, however, the effect of asymmetrical load carriage during high-heeled gait has not yet been studied.

METHODS

Seventeen healthy women (mean age 21.1 ± 5.1 years; mean height 164.2±4.8 cm; mean body weight 52.1±4.4 kg) were participated in present study. A 1.1 cm flat heeled shoes and 9.0 cm high-heeled stiletto shoes were used to represent two shoes conditions. A single strapped small purse was used in the study. 0%, 5%, and 10% of participant's body weight (BW) were employed to test the effect of asymmetrical loading. The purse was carried on right shoulder. Kinematic data were collected using Vicon Motion Analysis System (MX-13, Oxford Metrics, Oxford, UK). Nine high-speed infrared cameras were used to capture 3D view at 200 Hz. Participants walked across the testing area of approximately 6 m long at their comfortable speed. The order of conditions was randomly assigned, and data from five successive trials were recorded for each condition for both walking types. University of Ottawa Motion Analysis Model marker set, a modified version of Plug-in-Gait model, was adopted for a gait analysis. Two-way repeated measures ANOVA using SPSS software was conducted to compare the kinematic variables between the different loads in different walking conditions. When signifycant difference was found, a Tukey post hoc analysis was performed. The level of significance was chosen as $p < .05$.

RESULTS

In both normal and high-heeled walking conditions, the major differences in peak joint angle between different loading conditions occurred at the loaded-side limb (Table 1). When different loaded conditions were compared, a larger hip and ankle angle ($p < .05$) were displayed during the normal walking and a larger hip and a lesser knee and ankle angle ($p < .05$) were displayed during the high-heeled walking. In same loading conditions, the significant differences ($p < .05$) between normal and high-heeled walking were found at distal joints, ankle and knee. The difference in joint angles is more apparent between shoe conditions than loading conditions.

DISCUSSION AND CONCLUSIONS

The purpose of present study was to examine the effect of asymmetrical load on lower extremity joint kinematics during normal and high-heeled gait in females to determine whether asymmetrically carried load weight results in biomechanical disadvantage especially to high-heeled shoes wearer. From the results, it is evident that changes in load weight can greatly influence the kinematics of the lower extremity especially during the high-heeled gait. Asymmetrical load carriage of 10% BW alters knee and ankle joint kinematics which requires body to adjusts and compensate. The kinematic changes are greater once high-heeled shoes are worn by women. During the high-heeled gait, 5% BW alters the joint kinematics. Significantly altered ankle joint due to the raise heel could cause an increase in risk of fall and with the loading on one side disturbing the stability, the balance during the gait is challenged further.

REFERENCES

[1] Kinoshita, H. (1985). Effects of different loads and carrying systems on selected biomechanics parameters describing walking gait. *Ergonomics* Vol 28(9); p. 1347-1362.
[2] Hong, Y. & Li, J. X. (2004). Influence of load and carrying methods on gait phase and ground reactions in children's stair walking. *Gait and Posture* Vol 22; p. 63-68.

Table 1: Mean maximum angle (degrees) of the hip, knee, and ankle in sagittal (top) and frontal (bottom) plane

Walking type	Load	Hip Angle (SD)		Knee Angle (SD)		Ankle Angle (SD)	
		Left	Right	Left	Right	Left	Right
Normal Walking	0%	37.99 (0.34)	40.33 (0.46)	62.42 (1.02)	61.10 (0.40)	13.09 (0.74)	10.58§ (0.03)
		17.33 (6.18)	18.50 (1.11)	3.60 (4.07)	6.22 (2.21)	9.22 (1.55)	9.49 (1.03)
	5%	39.21 (0.52)	40.54§ (2.94)	64.40 (7.23)	61.36 (0.04)	12.45 (0.19)	10.70 (0.44)
		16.82 (4.15)	18.11 (0.29)	5.17 (2.38)	7.53 (1.05)	9.42 (0.98)	9.00 (2.00)
	10%	38.83 (5.22)	42.31§ (0.01)	64.36 (1.62)	61.87 (0.05)	13.22 (0.43)	12.29§ (1.34)
		18.23 (6.32)	18.26 (4.44)	4.22 (8.16)	6.28 (0.65)	13.97 (0.55)	13.11 (2.01)
High-heeled walking	0%	37.11 (0.90)	37.74*§ (0.36)	56.59* (1.10)	57.15* (0.01)	-10.74* (0.32)	-9.727*§ (0.06)
		18.99 (8.22)	18.12 (7.59)	4.95 (9.45)	7.72 (3.22)	16.58 (4.61)	17.10* (2.79)
	5%	37.65 (3.75)	39.88 (0.72)	55.23 (0.20)	58.62 (0.01)	-9.317* (0.06)	-9.044*§ (0.21)
		17.75 (4.09)	18.49 (5.64)	4.84 (3.81)	7.69* (3.27)	16.59 (0.82)	17.22* (3.55)
	10%	37.26 (2.99)	40.31*§ (0.07)	55.96* (0.02)	59.01* (0.02)	-9.624* (4.29)	-5.420*§¤ (3.98)
		17.71§ (7.13)	17.79 (4.12)	5.69§¤ (3.45)	6.51§ (2.11)	17.37 (2.91)	16.85* (1.04)

* $p<0.05$ as comparing normal walking with high-heeled walking in same load condition

§ $p<0.05$ as comparing between the different loads in same walking condition

¤ Tukeys post hoc test indicates means are significantly different

MECHANISMS OF ANGULAR MOMENTUM TRANSFER DURING THE FOUETTÉ

Coren Walters-Stewart[1], Gholamreza Rouhi[1], D.G.E. Robertson[2]
[1]Department of Mechanical Engineering, University of Ottawa, Ottawa, Canada, cwalt007@uottawa.ca
[2]School of Human Kinetics, University of Ottawa, Ottawa, Canada

INTRODUCTION

The *fouetté* is a two-count ballet step—on the first count, the dancer flexes the knee of his (or her) support leg and begins to raise the other leg (flexed at the hip, extended at the knee and ankle); on the second count, the raised leg moves laterally pulling the body into a clockwise rotation. The dancer uses his (or her) extended leg to drive the rotation of the body [1], as well as to create the appearance of a pause in his (or her) rotation when facing the audience [2]. Three-dimensional analysis of angular impulse and angular momentum using equations of motion in concert with gyroscopic equations will illustrate which components contribute to the desired motion of the fouetté, and which components detract from the maintenance rotation and balance necessary to perform this dance step.

METHODS

The body was modelled as a multi-link system comprised of 15 rigid-body segments. Data were obtained using a Vicon Motion Capture system in a 5-camera configuration. MATLAB was used to calculate and process most of the vector data executing calculations described by the governing equations of motion. Angular momentum, L, was calculated (Eq.1) about the body's centre of mass from the motion of the body's limbs (segment k =1 to 15):

$$\bar{L}_{O_k}(t) = \vec{r}_{CO_k}(t) \times m\eta_k \vec{v}_{\_CO_k} + \bar{L}_{C_k}(t) \qquad (1)$$

Changes in kinetic and potential energy were also calculated to quantify the provenance and transfer of energy and momentum during the turn. To further investigate the mechanisms of the turn, angular impulse (Eq.2) was also calculated in MATLAB and compared to torques generated at different joints.

$$\int_{t_1}^{t_2} M dt = \vec{L}_{O_b}(t_2) - \vec{L}_{O_b}(t_1) \qquad (2)$$

External forces and moments acting on the body throughout the *fouetté* (see Fig. 1) were compared to angular impulse to demonstrate an agreement between the action of the forces on the body and the reaction of the body (its motion).

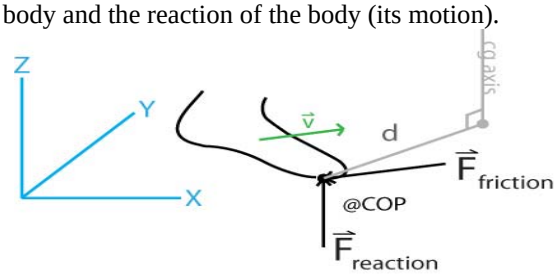

Figure 1: Diagram of the external forces acting on the foot of the dancer during the performance of the *fouetté*. The free moment (not shown) is also considered in the calculation.

The use of several different methods of calculation including gyroscopic equations of motion allows for validation of the calculations, and also can help demonstrate how different mechanisms are at play in to produce the rotation and balance when a dancer performs a *fouetté*.

RESULTS

As shown in Fig. 2, the x-component of angular momentum of the dancer averaged 0.0054 kg·m^2/s, the y-component average to 1.650 kg·m^2/s, and a vector comprised only of the x and y-components averaged 1.172 kg·m^2/s. The principal rotation of the dancer was driven by the z-component of angular momentum, which had an average of –14.99 kg·m^2/s (negative indicates CCW momentum).

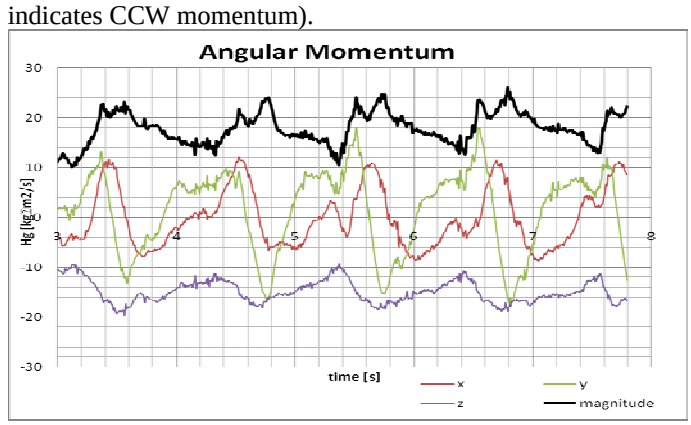

Figure 2: Shows small but significant momenta about both axes perpendicular to the rotation of the dancer in addition to a large amount of momentum about the main (z) axis of rotation.

DISCUSSION AND CONCLUSIONS

As expected, a large amount of angular momentum can be seen about the z-axis, the main axis of rotation of the dancer. Yet, it is important not to discount the small amounts of momenta around the x and y axes. Based on the gyroscopic effect, it is hypothesized here that the angular momenta about x and y, even though much less than that of z axis, have a considerable effect on the balance of the dancer resulting in a tilted axis of rotation, which may not be evident in a 2D analysis of the *fouetté*. Too much momentum about these minor axes and the torque generated at the dancer's ankle will not be sufficient to maintain his or her balance. In addition, since peaks in angular impulse coincide with local maximums in the magnitude of angular momentum, these impulses must occur in the correct direction, otherwise they will create momentum about the minor axes, which will cause the dancer to lose his/her balance. However, the occurrence of double peaks in the magnitude of angular momentum (black curve in Fig. 2) shows other significant contributing impulses in the direction of desired rotation (e.g., torque produced at the hip).

REFERENCES

[1] Laws KL. (1998). *Med Probl Perform Art* 13:136-45
[2] Imura A, *et al*. (2008). *Human Mvt Sci* 27:903-13

DIFFERENCES IN ANGULAR VELOCITIES, MOMENTS AND POWERS CAUSED BY USING DIFFERENT GAIT MARKER SETS

Li Zhang[1] and D. Gordon E Robertson[2]
School of Human Kinetics, University of Ottawa, Ottawa, Canada
[1]lzhan079@uottawa.ca, [2]dger@uottawa.ca

INTRODUCTION

Joint kinetics from biomechanical and rehabilitation studies are often derived from different marker sets. Each marker set uses various body landmarks and/or marker structures to define the underlying segments. Therefore, one could question whether discrepancies in joint kinetics from one study to another may be due to differences in the marker sets used. The present study compared the kinetics of 3 different locomotor tasks produced by three different marker sets: clusters [1], joint centre markers, and Vicon's Plug-in-Gait (PiG).

METHODS

A male participant with all three marker sets (cluster, joint centres, and PiG, no cluster was attached to the foot) walked twice and jogged and ran once while a Vicon MX motion analysis system (200 Hz) captured the marker trajectories. Each trial included at least one locomotor cycle. Segmental lengths and widths were measured with an anthropometer. Locomotion data were filtered by a Butterworth, zero-lag, 6 Hz low-pass filter. Angular velocities, net moments and powers of hip, knee and ankle joints were calculated using the Visual3D with three different marker sets.

RESULTS

Root-mean-square deviations (Table 1) and linear correlations were calculated to quantify the differences in joint angular velocities, moments and powers at ankle, knee and hip between the three marker sets (Table 1). All correlations were greater than 0.850 indicating strong phasic relationships between the kinetics derived from the different marker sets. Only the powers at the knee produced RMS errors greater than 30 W. The PiG marker set produced relatively larger hip moment RMS errors (> 25 N.m) compared to the other two marker sets but only for the walking trials while the cluster and joint centre markers were very similar (RMS <= 10 N.m)

Figure 1 shows the histories for 2 walking trials and all three marker sets. Note there were few differences between trials at the ankle but there were trial differences at the knee and hip.

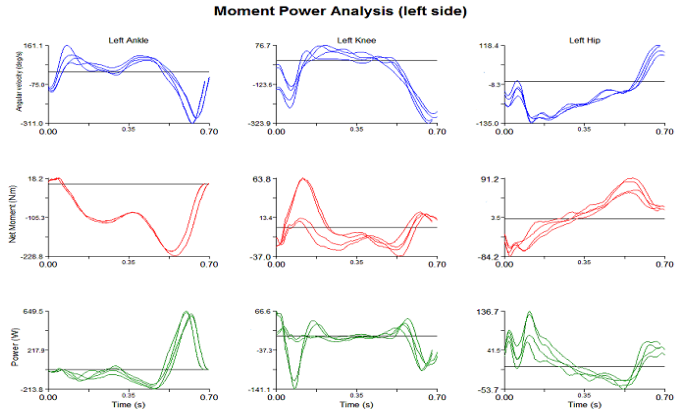

Figure 1: Angular velocities, net moments and powers of ankle, knee and hip joints were plotted as shown using three different marker sets

DISCUSSION AND CONCLUSIONS

Forces and moments are indirectly computed based on kinematic and anthropometric data [2]. The differences in kinetics between the three models may be attributed to inconsistency of orientation of joint centres and axes during locomotion. Six degrees-of-freedom are not possible with the PiG model since too few markers are used to define segments. Unlike the PiG, cluster markers were designed to minimize skin movement artifacts and photogrammetric errors by attaching 4 markers to a rigid structure. The cluster structure itself, however, can move relative to the underlying boney structures if attached loosely over muscle bellies. Using joint centres, where muscle tissue is scarce, reduces such errors. This study has shown few differences between the cluster and joint centre marker sets, however, the PiG marker set can produce different results. Thus, within a study a consistent marker set is advisable.

REFERENCES

[1] Cappozzo A *et al*. (1997). Surface-Marker Cluster Design for 3-D Bone Movement Reconstruction. *IEEE Transactions on Biomedical Engineering*, Vol 44; p. 1165.
[2] Robertson DGE *et al*. *Research Methods in Biomechanics*; Human Kinetics, 2004.

Table 1: Root Mean Square deviations between clusters (Cl), joint centres (Ce) and Plug-in-Gait (P) marker sets

Left leg	Knee moment (N.m)			Knee power (W)			Hip moment (N.m)			Hip power (W)		
	Cl-P	Cl-Ce	P-Ce	Cl-P	Cl-Ce	P-Ce	Cl-P	Cl-Ce	P-Ce	Cl-P	Cl-Ce	P-Ce
walk 4	11.4	5.3	8.6	10.5	9.2	4.5	**32.0**	8.8	**27.5**	15.8	10.8	16.1
walk 5	15.8	4.6	16.0	15.7	13.1	5.6	**31.1**	10.0	**25.4**	18.1	12.4	20.0
jog	10.6	9.7	1.0	9.8	10.2	1.6	15.0	18.1	5.2	15.0	18.1	5.2
run	2.2	2.9	2.4	**48.5**	**32.7**	**39.3**	9.3	10.4	16.2	9.3	10.4	16.2

LUMBER SPINAL COMPRESSION FORCE MODEL FOR LIFTING TASK

Danielle Rodrigues de Oliveira, Tamotsu Hirata, João Alberto de Oliveira
Mechanical Department/Faculty of Engineering, Paulista State University, Guaratinguetá, Brazil, *tamotsu@feg.unesp.br*

INTRODUCTION

Many computer model to simulate the loads acting in the spine have been developed for different posture and activities. Therefore most models cannot be validated, or even confirmed, because very few in vivo data exist for the intradiscal force. The purpose of this study was to evaluate a lumber disk compression force model during lifting task, using 3D movements data captured from two digital cameras. The validation of the model was confirmed in comparison with in vivo measured data selected 3 lifting posture and 1 natural standing posture.

METHODS

The lifting movements were captured from 2 digital cameras, in MPEG format and the sequence images were obtained using *Quintic Player* software. The each body segment position was calculated based on 3D reconstruction model with modified direct linear transformation (MDLT) described in MATLAB. The mass center of each segment and total mass were estimated with segmental anthropometric data [1]. The lumber compression force was determined based on the erector muscle force model proposed by Chaffin [2]. Due to the model validation 3 lifting posture with 200 N loads and 1 standing posture, selected by Wilke´s [3] photogrametric images and respected anthropometric data were used (Figure 1). To demonstrate the application of purposed model two cycle lifting sample (Figure 2) was selected, first cycle without trunk rotation and second cycle with trunk rotation.

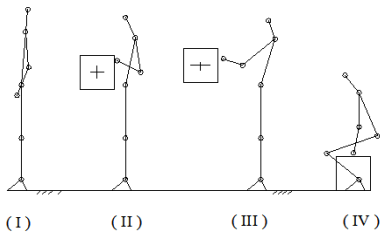

Figure 1: Schematic lifting posture for model validation.

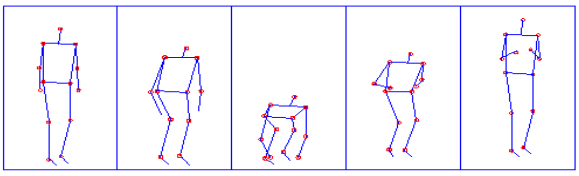

Figure 2: One cycle lifting posture (without trunk rotation).

RESULTS

The difference between Wilke´s measured data and the results of estimated compression force in lumber disk, L3/L4, were showed in Table 1. Figure 3 presents two peaks forces in two cycle lifting simulation followed by without trunk rotation where worker take squatting posture.

Table 1: Compression forces (Fc) comparison in L3/L4.

Posture	Fc (N) Wilke´s	Fc (N) Model	Difference (%)
I	900	976	+ 8,4
II	1.800	2.085	+ 15,8
III	3.240	3.095	- 4,5
IV	3.060	3.009	- 1,7

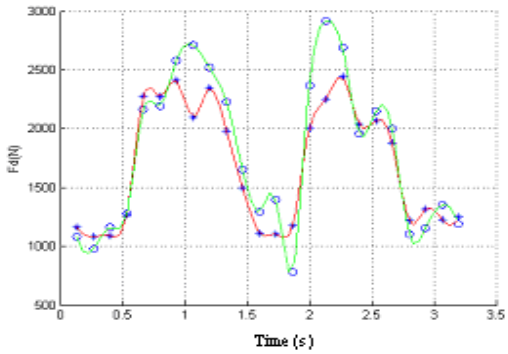

Figure 3: Two cycle lifting simulation results, * red line; without load, ° green line; with 200 N load.

DISCUSSION AND CONCLUSIONS

The significant difference in the table 1 is addressed by poor precision of one image photogrametric data that used oblique camera angle. Furthermore the rigid segment model will be contributed it difference. In the two cycle lifting simulation the image processing error was minimized by accurate 3D reconstruction model that registered bellow 1 % of coordinate calibration. Two peaks forces were observed in figure 3 when worker take squatting posture to handling load.
The study shows reasonable correlation with in vivo experimental data for the lumber disk compression force in different posture and the proposed model will be useful to simulate periodic lifting task.

REFERENCES

[1] Winter DA. Biomechanics and motor control of human movement; John Wiley-Sons, 1990.
[2] Chaffin DB. Occupational Biomechanics; John-Wiley-Sons, 1999.
[3] Wilke HJ. et al. (2000) Intradiscal Pressure together with anthropometric data. *Clin.Biomech.* Vol 16(1); p.111-126.

DEVELOPMENT AND VALIDATION OF A FOUR BAR LINKAGE KINEMATIC MODEL OF THE UPPER LIMB AND JOYSTICK FOR USE IN VIRTUAL PROTOTYPING

Lauren Bailey[1], Michele Oliver[1,2]
[1]School of Engineering, University of Guelph, Guelph, Canada, lbaile01@uoguelph.ca
[2]Biophysics Interdepartmental Group, University of Guelph, Guelph, Canada

INTRODUCTION

This paper describes the development and validation of a planar four bar linkage model of the upper limb and joystick. Allowing for virtual assessment of the kinematic effects of various joystick designs, the model represents the first human factors based joystick design protocol by permitting one to simulate the effects on fore-aft joystick and operator movements resulting from alterations to joystick and operator anthropometry. Previous studies have indicated that forward and backward directions are most strenuous on the shoulder musculature [1], therefore, this initial model represents fore-aft motion.

METHODS

The kinematic model was developed using a four-bar mechanism as pictured in Figure 1e [2]. To assess model efficacy, 15 right handed male subjects were divided into three groups according to stature representing thirds of the population [3]. Subjects sat in a mock-up of an excavator cab with a right hand side joystick mounted to the frame that supports the seat (Figure 1 in companion submission). An initial practice trial was conducted to provide the subject with feedback to ensure that off axis motion was minimized. Off axis motion was defined as an average over the motion cycle of greater than 20 mm of movement along the y-axis.

Kinematic data were captured using six VICON® M2 cameras at a frame rate of 100 Hz. Twenty-one retro-reflective markers placed on the upper body of the subject and joystick, using locations adapted from PlugInGait (VICON® Peak, Oxford, UK) were used to predict kinematics. Three markers placed on the base which housed the joystick and three markers placed on the joystick swash plate were used to calculate the joystick angle via the vectors perpendicular to both the base and swash plate planes. The angle between these perpendicular vectors was used as an input for the kinematic model. Subject segment lengths and the joystick angle were determined from VICON® data and used as inputs into the four-bar model. The model output, which included the angles of the shoulder relative to the torso, the upper arm relative to the forearm and the forearm relative to the hand and joystick complex were validated using kinematic data collected using the VICON® motion capture system.

RESULTS

Peak relative joint angle amplitudes of the shoulder, elbow, and wrist were analysed using factorial ANOVA procedures and when appropriate, Bonferroni post-hoc tests. Except for the shoulder, there were no significant ($p \leq 0.01$) differences observed between the modeled and the measured values. While significant, the difference between the means for the shoulder was only 1.1 degrees (Figure 1a). While the mechanism made the assumption of a fixed shoulder, in fact the model output proved to be relatively insensitive to vertical shoulder movement of up to ± 20 mm.

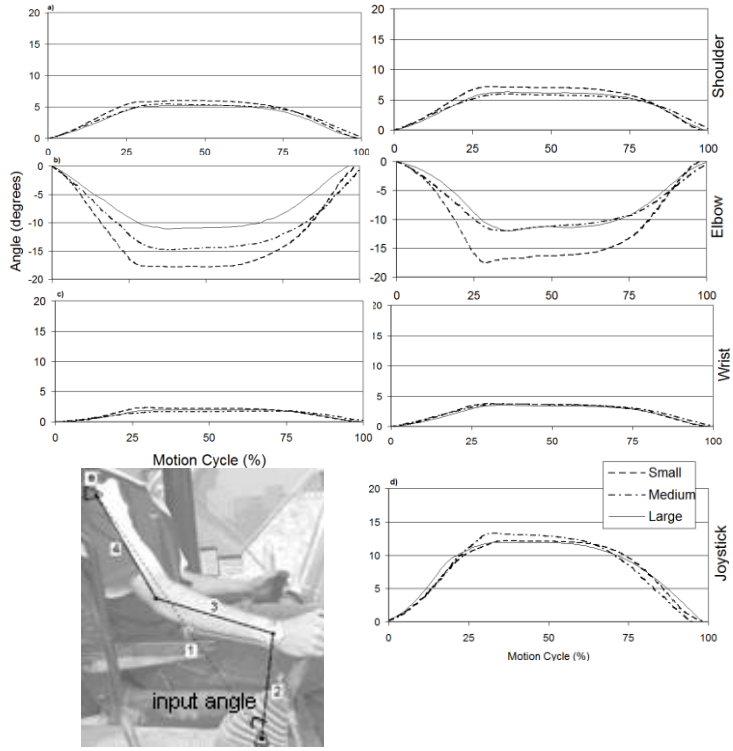

Figure 1: Model predicted (left) and VICON® (right) joint and joystick angles during forward motion for small, medium and large subjects

DISCUSSION AND CONCLUSIONS

The 4-bar model accurately represents the relative joint angles resulting from joystick use. Though not statistically different for elbow joint angle amplitude, Figure 1b shows relatively large differences in elbow angles between sizes particularly for small subjects. This probably results from the operators accomplishing the motion differently based on their segment lengths. Smaller subjects have to reach further than larger subjects to reach the same endpoint causing greater elbow extension. This validated kinematic mathematical model could be used to virtually prototype joysticks and other operator cab components such as armrests to optimize the cab configuration for a variety of users based on specific anthropometrics.

REFERENCES

[1] G.W. Northey, The effects of stiffness and speed on upper limb electromyography during joystick use. M.Sc.(Eng) Thesis, School of Engineering, University of Guelph, 2004.
[2] Wilson et al. USA. *Kinematics and Dynamics of Machinery*; Harper and Row, 1983.
[3] Kroemer et al. USA. *Ergonomics: How to design for ease and efficiency*; Prentice Hall, 1999

DEVELOPMENT AND VALIDATION OF A FOUR BAR LINKAGE KINETIC MODEL OF THE UPPER LIMB AND JOYSTICK FOR USE IN VIRTUAL PROTOTYPING

Lauren Bailey[1], Michele Oliver[1,2]
[1]School of Engineering, [2]Biophysics Interdepartmental Group, University of Guelph, Guelph, Canada,
lbaile01@uoguelph.ca

INTRODUCTION

This paper describes the development and validation of a planar four bar linkage model of the upper limb and joystick. Allowing for virtual assessment of the kinetic effects of various joystick designs, the model represents the first human factors based joystick design protocol by permitting one to simulate the effects on fore-aft joystick and operator movements resulting from alterations to the joystick and operator anthropometry.

METHODS

The kinetic model was developed by building on the kinematic four-bar mechanism described in the companion submission. Subject (n=15) input forces were monitored by strain gauges fixed to the joystick stem (Figure 1). Eight thin foil bending moment strain gauges (EA-06-060PB-350, Measurements Group Inc., Micro-Measurements Division, Raleigh, North Carolina; resistance 350±0.2% ohms; gauge factor 2.105±0.5%; transverse sensitivity 0.7±0.2%) in two, full Wheatstone bridge configurations were fixed to the joystick stem to allow for the assessment of the bending force being applied by the subject to the joystick in the both motion planes.

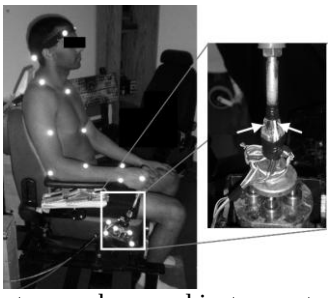

Figure 1: Excavator mock-up and instrumented joystick

The strain gauges were calibrated in the anterior (fore), posterior (aft), medial (left) and lateral (right) directions by incrementally adding mass from 0.5 Kg to 8 Kg, and recording the output voltage. A first order polynomial was then fit to each of the calibration data sets producing calibration curves, both the anterior/posterior and the medial/lateral R^2 values were greater than 0.99. An initial practice trial was conducted to provide the subject with visual feedback from the strain gauge signal to ensure that off axis motion was minimized. Off axis motion was defined as an average over the motion cycle of greater than 20 mm of movement along the y-axis.

The fore-aft forces measured by the strain gauges were used as the input, driving the four bar linkage model. The known values for force input and segment inertial parameters made it possible to determine the torque on the driving link which was considered to be an unknown value required for mechanism equilibrium in a given position under specified loads. While predicting the torque using inverse dynamic equations, the forces and moments at each joint of the mechanism, representing the shoulder, elbow, and wrist, were determined in the process [1]. The model was validated by comparing the model output dynamic torque to the torque calculated using the forces measured from the strain gauges multiplied by the distance between the point where the operator applied force and the universal joint of the joystick (T=Fd) over the motion cycle. Forces, moments and torques were analyzed using factorial ANOVA procedures, and when appropriate, Bonferroni post-hoc tests.

RESULTS

The peak torque output from the kinetic model was found to be significantly greater ($p \leq 0.01$) than the measured torque; however, the difference was only 1 N·m. Absolute forces at the shoulder were greater than forces at the wrist which were greater than forces at the elbow. Similarly, absolute moments at the shoulder were found to be highest, followed by the wrist and then the elbow, and forward motions had higher absolute moments than backwards ones.

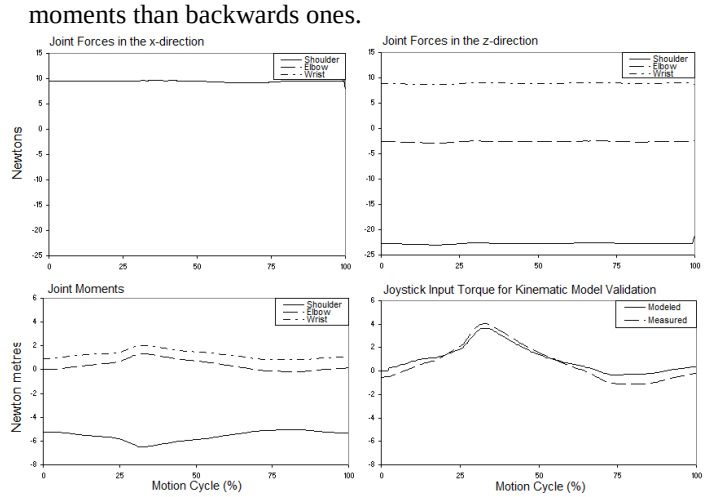

Figure 2: Forces and moments at the shoulder, elbow and wrist joints, including model validation using torque at the joystick input during forward motion

DISCUSSION AND CONCLUSIONS

A kinetic planar four bar linkage model of the upper limb and joystick was successfully developed and validated. The reflection of the pattern of the torque, especially the peak at the hard end-point (30% of the motion cycle) which is reflected in the moments found at joint warrants further investigation.

REFERENCES

[1] Wilson et al. USA. *Kinematics and Dynamics of Machinery*; Harper and Row, 1983.

TOWARDS AUTOMATED 3-D SCOLIOTIC SPINE RECONSTRUCTION BY USING BIPLANAR RADIOGRAPHIC IMAGES AND STATISTICAL MODLS

Behnam Heidari[1], Forough Madeh Khaksar[2], David FitzPatrick[1]
[1] School of Electrical, Electronic, & Mechanical Engineering, University College Dublin, Dublin, Ireland
behnam.heidari@ucd.ie
[2]School of Biomedical Engineering, Amirkabir University, Tehran, Iran

INTRODUCTION

Three-dimensional data of the musculoskeletal system is often required for diagnostic or research purposes. However, radiation dose is a limiting factor especially when dealing with complex & large structures such as spinal column. Bi-planar radiographic images are routinely used in diagnosis of pathological conditions such as Scoliotic deformity, which is characterized by combined frontal & lateral deformity of the spine together with rotational deformity of the vertebrae. Nevertheless, conclusion about a complex 3-D deformity requires a 3-D knowledge of the structure.

METHODS

In this paper, a 3-D reconstruction method of the thoracolumbar spine is presented by the use of bi-planar radiographic images (lateral & posterior-anterior). In this respect, a prior knowledge of the vertebrae, captured by statistical data, is used. This method has two stages: 1) determine the approximate location of each vertebra by selecting the centres of the superior & inferior endplates, and subsequently applying a rigid deformation on the statistical template of the vertebra; 2) a global deformation using a statistical modal analysis of the pathological deformations is applied to the model [4]. An energy based function is introduced to find vertebrae deformations [1]. Optimizing of this model is obtained with applying exploration/selection algorithm [2] [3], which lead to the 3-D reconstruction of each vertebra and spinal model.

This energy function depends on similarity between extracted external contours of deformed template and edge potential field [5] of two radiographic views together with a prior energy [1], which is dependent on variation modes yielded from statistical knowledge

RESULTS

Deformable statistical template used as a priori knowledge model obtained by conventional CT-scans and optical CMM of the vertebrae. The initial results of the reconstructed models are compared with 3-D models yielded by conventional CT-scans, demonstrating good geometry fitting. Characteristics of the initial results are demonstrated in Figure 1.

DISCUSSION AND CONCLUSIONS

Automated 3D-reconstruction of the spine is useful in orthopaedic application such as surgical planning and implant/orthotic design. Further development and proper application of this method will lead to 3-D reconstruction of the spine for clinical use, exposing lower radiation to the patient, saving time and resources.

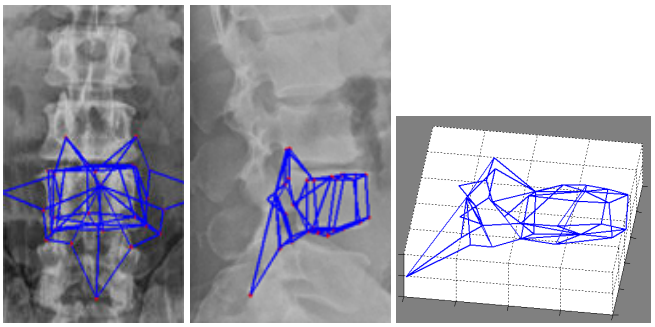

a) b) c)

Figure 1: A representative image demonstrating the initial results of the 3-D model for lumbar region; (a) & (b) are demonstrating the projection of vertebra template on frontal & lateral views, respectively; (c) is demonstrating the 3-D view of the reconstructed model.

REFERENCES

[1] Benameur S. et al. (2003). 3D/2D registration and segmentation of scoliotic vertebrae using statistical models. *Computerized Medical Imaging and Graphics*, Vol. 27(5); p.321–337.
[2] Olivier F. (2002). Global optimization with exploration/selection algorithms and simulated annealing. *The Annals of Applied Probability*, Vol. 12; p.248–271.
[3] Pena-Reyes C., Sipper M. (2000). Evolutionary computation in medicine: An overview. *Artificial Intelligence in Medicine*, Vol. 19; p. 1–23.
[4] Cootes T.F. et al. (1995). Active shape models – their training and application. *Computer Vision and Image Understanding*, Vol. 61(1); p.38–59.
[5] Jain A. K. Et al. (1996). Object matching using deformable templates. *IEEE Transactions on Pattern Analysis and Machine Intelligence*, Vol. 18(3); p.267–278.

KNEE MUSCLE CONTRIBUTIONS TO JOINT ROTATIONAL STIFFNESS

Joshua Cashaback, James Potvin
McMaster Occupational Biomechanics Laboratory, McMaster University, Hamilton, ON, cashabjg@mcmaster.ca

INTRODUCTION

The majority of research in quantifying mechanical joint stability has been directed towards the lumbar spine. However, much less research has focused on other joints, such as the knee, where injuries often occur. The purpose of this study was to examine the relative contributions of individual knee muscles to JRS, about three orthogonal axes, with changes in condition and moment about the knee. Using an equation developed by Potvin and Brown (2005), individual muscle contributions to stability were calculated. The summation of these contributions represents the total joint rotational stiffness (JRS) about the system, and dividing an individual muscle contribution by the total JRS yields relative muscle contributions to JRS.

METHODS

Twelve male participants generated isometric, extensor moments about the knee. These moments were matched in real-time to computer-generated templates, which were normalized to maximum voluntary exertion (MVE). There were two types of templates: 1) ramping (up/down) and 2) holding various plateaus. Muscle activity was recorded from nine muscles at 25%, 50% and 75% MVE for the ramp up, ramp down and plateau conditions, with an additional 100% MVE plateau trial. A biomechanical model of the lower limb was used to find muscle maximal force generating capacities, lengths and moment arms [2]. Normalized muscle activity was multiplied to maximal force generating capacity, and corrected based on its position on the force-length curve. These muscle forces were used to calculate JRS about the flexion/extension (FE), valgus/varus (VV) and axial (AX) axes.

RESULTS

For the FE axis, there was a significant linear relationship ($p<0.001$) between JRS and percent MVE for the plateau conditions (Figure 1). On average, the VV and AX axes were 32% and 14%, respectively, of the FE axis JRS, where the extensors accounted for more JRS than the flexors about all axes. Of all muscles, the vastus lateralis (VL) was the greatest contributor to JRS about all axes. Of the flexors, the semimembranosis (SM) was the greatest contributor to JRS about the FE and AX axes. About the VV axis, the gastrocnemius lateral (GL) had the highest contribution to JRS of the flexors, with an average contribution of 7.5%.

DISCUSSION AND CONCLUSIONS

Individual muscle activity increased linearly with increased moment demands, which translated to linear increases in JRS about all three axes. The VL had the greatest contribution to JRS about all axes because of its large force generating capacity. It was 37% greater than the next largest muscle crossing the knee joint. The SM provided the most JRS of the antagonists about the FE and AX axes. Of the flexors, the SM muscle has the largest force generating capacity and a large moment arm about the FE and AX axes, with the latter contributing a large role in providing JRS. The exception to the linear increases in muscle activity was the GL during the ramp down condition, where its relative contributions to JRS about the VV axis were 18.9%, 11.1%, and 8.0% at 25%, 50%, and 75% MVE, respectively. Despite an extensor moment, the GL had minor JRS contributions about the FE axis and it is postulated that this increase in activation was to stabilize about the VV axis.

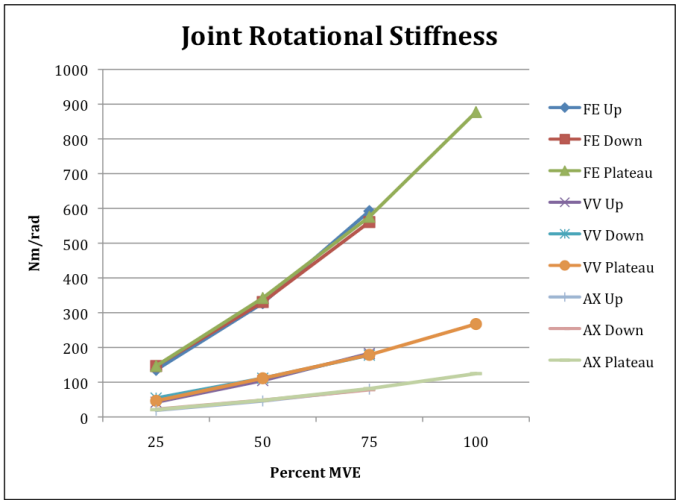

Figure 1: Average total joint rotational stiffness values for all conditions

REFERENCES

[1] Potvin, J.R., Brown, S.H.M., (2005). An equation to calculate individual muscle contributions to joint stability. J Biomech 38(5); p. 973-80.
[2] Delp, S.L., Loan, J.P., Hoy, M.G., Zajac, F.E., Topp, E.L., and Rosen, J.M. (1990). An Interactive Graphics-Based Model of the Lower-Extremity to Study Orthopedic Surgical-Procedures. *IEEE Transactions on Biomedical Engineering, 37,* 757-767.

ACKNOWLEDGEMENTS

The authors are grateful for the assistance of Derek Cheung and Fangchen Wang during the data collection process. The Ontario Graduate Scholarship and Natural Sciences and Engineering Research Council of Canada funded this research.

REPEATABILITY OF MOTOR CONTROL PATTERNS DURING PROLONGED STANDING IN PEOPLE WITH AND WITHOUT STANDING-INDUCED LOW BACK PAIN

Erika Nelson-Wong[1] and Jack P. Callaghan[2]
[1]School of Physical Therapy, Regis University, Denver, USA, enelsonw@regis.edu
[2]Department of Kinesiology/Faculty of Applied Health Sciences, University of Waterloo, Waterloo, Canada

INTRODUCTION

Many current musculoskeletal research efforts in biomechanics and kinesiology are focused on the identification of predictive factors for low back pain (LBP) development, and evaluating specific motor pattern responses to different interventions. As factors that are thought to be associated with or predictive of LBP development are identified and characterized, interventions can be targeted towards changing or modifying these factors, with the ultimate goal of improving LBP intervention effectiveness. In order to confidently differentiate changes in motor patterns in response to an intervention from natural variability however, the normal day-to-day stability of the motor patterns of interest must first be established. A prolonged standing protocol has been useful in identification of predisposing factors for LBP and evaluating the response of these factors to different intervention strategies [1]. Factors that were consistently found to be important discriminators between LBP developers (PD) and non-LBP developers (NPD) individuals were elevated co-contraction of the bilateral gluteus medius muscles, decreased resting time for the gluteal muscles and differences in modulation of trunk flexor/extensor co-contraction during prolonged standing exposure [1]. The purpose of this study was to assess the between-day repeatability of factors previously associated with LBP development, in both PD and NPD individuals, in the absence of any intervention.

METHODS

Forty-three participants (22 male and 21 female) participated in this test/re-test study. Participants were exposed to a 2-hr standing protocol during which continuous electromyography (EMG) from 8 bilateral trunk and hip muscle groups were recorded. Participants rated their LBP every 15-minutes on a 100 mm visual analog scale (VAS). Participants that had an increase of > 10 mm VAS from baseline were considered to be PD. Participants were randomly assigned to control (usual activity) or exercise groups for 4 weeks and then returned for an identical testing protocol. Outcome measures of interest included co-contraction index (CCI) [2], Gaps in muscle activation (< 0.5% MVC for > 0.2 ms) [3] and VAS. Only data from participants assigned to the control group were considered for these analyses. Statistical analyses consisted of calculating intraclass correlation coefficients (ICCs) to determine the between-day repeatability of these outcome measures.

RESULTS

For participants assigned to control, 6/8 PD and 13/15 NPD would have remained in their respective PD/NPD groups on the repeat testing day. There were no significant between day differences in VAS score for either PD/NPD group ($p > 0.05$.)

Between-day repeatability for bilateral gluteus medius CCI was excellent for both PD/NPD participants assigned to the control group. For the trunk flexor/extensor CCI however, between-day repeatability was excellent for the PD group but very poor for the NPD group (Table 1).

Table 1: Between-day ICC values for co-contraction index in PD/NPD participants assigned to control.

	Glut Med CCI	**Trunk Flex/Ext CCI**
NPD	ICC = 0.87	ICC = 0.09
PD	ICC = 0.90	ICC = 0.82

ICC values for muscle Gaps between-days was very good for both PD/NPD groups assigned to control, with values ranging from 0.62 to 0.86.

DISCUSSION AND CONCLUSIONS

The between-day repeatability of the assessed outcome measures in the control group was, in general, excellent. 83% of the participants remained in their original PD/NPD group on repeated testing indicating that individuals who are predisposed to develop LBP during a standing exposure remain fairly consistent in this response. Muscle activation profiles were very repeatable with the exception of trunk flexor/extensor CCI in the NPD group only. This indicates that there is more day-to-day variability in trunk muscle co-activation in individuals who are not predisposed to develop LBP during standing, while pain developers tend to utilize the same muscle co-activation pattern more consistently. These findings are important in that they increase confidence in attributing motor control and muscle activation profile changes following intervention as being directly related to the intervention. This provides further support for the utility of this induced LBP protocol as a model for studying LBP development and interventions.

REFERENCES

[1] Nelson-Wong, et al. (2010). Is muscle co-activation a predisposing factor for low back pain development during standing? *J Electromyography and Kinesiol* **20**; 256-263.
[3] Lewek M, et al. (2004). Control of frontal plane knee laxity during gait in patients with medial compartment knee osteoarthritis. *Osteoarthritis and Cartilage* **12**(9); 745-7.
[3] Veiersted, KB, et al. (1990). Pattern of muscle activity during stereotyped work and its relation to muscle pain. *Int Arch Occ Env Health* **62**(1); 31-41.

SHOULD A MOVEMENT SCREEN BE USED TO GUIDE EXERCISE PRESCRIPTION?

David M. Frost, Tyson A.C. Beach, Jack P. Callaghan, Stuart M. McGill
Department of Kinesiology, University of Waterloo, Waterloo, Ontario, Canada, d3frost@uwaterloo.ca

INTRODUCTION

Evaluating an individual's risk for injury or performance during a specific task is achieved in large part by assessing the way they move and coordinate their body in space. Many clinicians and performance coaches alike now include a "movement screen" to identify restrictions, asymmetries or compensatory patterns prior to the prescription of exercise. The Functional Movement Screen (FMS) is one such tool that has received widespread recognition as it has demonstrated efficacy in the prediction of athletic injuries [1]. Specific guidelines have been published to administer the seven-task test and grade the quality of movement [2]; however, it is not always clear how the findings should be used or interpreted. Individuals are given a task objective and scored from 0 to 3, whereby a 2 implies *any* compensation. Therefore, the FMS, in its current state, may not be sensitive to meaningful changes in movement quality, and thus, be appropriate to guide the prescription of exercise. This study compared the sensitivity of the incumbent grading scheme and that of a novel method to observable differences in movement using screening scores from before and after a 12-week exercise program.

METHODS

Sixty-five men were screened with the FMS and assigned to one of two groups (intervention and control). The intervention group (n=41) participated in a supervised exercise program for 12 weeks, but like the controls, were blinded to the results and overall objectives of the FMS. After the intervention all participants were screened a second time. Video was collected from the sagittal and frontal planes and 4 reps (2 forwards and 2 backwards) of each task were performed. Only the 'best' rep was scored. Aside from the verbal instructions no specific cues were given. Participants were graded on how they *chose* to perform rather than how they *could* perform the tasks given feedback or coaching.

Video was used to objectively assign scores using two methods: 1) Current - a 3 (perfect), 2 (compensation), 1 (can't perform) or 0 (pain) to each task and cumulative grade out of 21; 2) Novel – Each task was assigned a primary objective and secondary compensations. If the objective was met, one point was given for each compensation (0 was perfect). If it was not met, the base score was made to be one point higher than the total number of compensations possible. Scores for each task were given the same weight in the total score (100 was worst). The number of subjects demonstrating screen score differences was used to represent the sensitivity of each grading scheme.

RESULTS

The correlation between the grading schemes was 0.86 and 0.85 for the pre and post test respectively ($p<0.01$). The number of participants demonstrating a change in score was not only different between the two methods, but also task dependent (Table 1). For example, of the 65 subjects completing the hurdle step only 6 had a change in score (positive or negative) using the current method compared to 46 with the novel approach. However, there was also no difference in the number of changes between the intervention and control groups, using either method, perhaps implying that the grading criteria or tests themselves were not a reliable means to detect changes in movement quality.

DISCUSSION AND CONCLUSIONS

The novel approach to grading was more sensitive to changes in movement (based on explicit criteria), but it is not clear whether these detectable differences were in fact meaningful. Because the changes among the control group were similar to those of the men receiving supervised exercise it is difficult to speculate as to how the screening information can or should be used to guide the prescription of training. The FMS is not purported to be a diagnostic tool and perhaps the current findings are evidence that it is simply a screen capable of identifying pain and overt asymmetries and that additional tests must be used to guide exercise. Alternatively, by choosing to grade the 'best' repetition only, it is possible that valuable information was neglected. If the goal is to assess physical competence or capacity and to evaluate how an individual chooses to move, it is arguably more appropriate to examine their performance over multiple repetitions. And if used to guide the prescription of exercise the nature of the movement screening tasks may need to parallel the progression of loads/speeds of the physical skills being taught.

REFERENCES

[1] Kiesel K et al. (2007). *N Am J Sports Phys Ther*, 2:147-58.
[2] Cook G et al. (2006). *N Am J Sports Phys Ther*, 1:62-72.

Table 1: The number of subjects whose screen score went up (+), stayed the same (/) or went down (-) when graded with the A) current and B) novel method. One task is not presented as there were no differences between methods.

		Squat			Hurdle			Lunge			Leg Raise			Pushup			Rotary			Total		
		+	/	-	+	/	-	+	/	-	+	/	-	+	/	-	+	/	-	+	/	-
Train	A	1	33	7	0	40	1	9	30	2	9	24	8	8	23	10	12	25	4	18	14	8
	B	15	13	13	15	14	12	20	15	6	12	15	14	9	21	11	25	5	11	28	0	12
Control	A	2	18	4	2	19	3	2	20	2	6	14	4	1	15	8	3	13	8	8	3	9
	B	6	10	8	12	5	7	8	11	5	10	8	6	2	12	10	10	2	12	14	0	6

MOTOR IMAGERY USE DURING SIMPLE KNEE FLEXION-EXTENSION EXERCISES MAY ENHANCE KNEE EXTENSOR MUSCLE RECRUITMENT AMPLITUDES

Phillip McKeen, Krista Munroe-Chandler, Nadia R. Azar
Department of Kinesiology, University of Windsor, Windsor, Canada, azar5@uwindsor.ca

INTRODUCTION

Imagery is defined as "using all the senses to recreate or create an experience in the mind" [1]. Motor imagery (e.g. visualizing one's self performing an action without actually producing movement) is known to elicit muscle activity even in a muscle at rest [2, 3]; however there have been no studies to date which examine whether motor imagery affects muscle recruitment levels in actively contracting muscles. Simple visual aids are frequently used in exercise and rehabilitative settings to enhance a client/patient's understanding of how to properly execute an exercise, yet it is currently unknown whether these aids result in increased muscle recruitment. The purpose of this study was to examine whether the use of motor imagery during the performance of a simple exercise results in recruitment increases in the actively contracting muscles. Increased recruitment results in more effective muscular contraction, which may potentially enhance the effectiveness of training/rehabilitation.

METHODS

12 female participants (mean age: 21.2 ± 1.3 yrs; mean weight: 60.9 ± 7.5 kg; mean height: 1.7 ± 0.1 m) currently enrolled as undergraduate students at the University of Windsor were recruited for this study. All participants were of normal body weight and had no history of knee pain, injury, or surgery. Participants performed three repetitions of two different exercises (simple squats; and squats with external femoral rotation, also called "pliés"). Vastus Lateralis (VL), Rectus Femoris (RF), and Vastus Medialis Obliquus (VMO) recruitment amplitudes were recorded bilaterally using surface EMG (Octopus, Bortec Biomedical Ltd., Alberta, Canada), and knee flexion angles were monitored bilaterally with electrogoniometers (SG Series, Biometrics Ltd., Virginia, USA) throughout the movements. Participants were randomly assigned to an imagery group or a control group. Prior to executing the movements, all participants were given verbal instruction on how to properly complete the exercises. However, participants in the imagery group were also read a short imagery script designed to encourage the participants to focus on the function of these muscles while executing the movements. Participants in both groups completed the Vividness of Movement Imagery Questionnaire-2 (VMIQ-2) to assess motor imagery ability and an exit survey to collect participant demographics and self-reported imagery use during the trials.

RESULTS

There were no significant within-subject differences in recruitment amplitudes (% MVC) between the right and left limbs for any muscle, thus recruitment amplitudes were pooled by muscle for subsequent analyses. Between-group differences in recruitment amplitudes during the plié exercise were not statistically significant (VL: $p = 0.13$, RF: $p = 0.42$, VMO: $p = 0.12$). Between-group differences in VL ($p = 0.07$) and VMO ($p = 0.06$) recruitment amplitudes during the squat exercise approached significance, while RF failed to achieve significance ($p = 0.28$). Although participants in both groups reported using imagery during the execution of the exercises, between-group differences in motor imagery ability were not statistically significant ($p = 0.34$). Furthermore, participants in the imagery group reported using imagery that was specific to the target musculature (i.e. attempted to "see" and "feel" the VMO contracting, as requested in the imagery script), whereas participants in the control group reported using more general forms of imagery (e.g. imagined themselves or the investigator executing the proper exercise technique).

DISCUSSION AND CONCLUSIONS

The use of EMG biofeedback during VMO conditioning has been shown to improve VMO/VL activation ratios, in comparison to a group which did not use biofeedback [2].
However, the cost of biofeedback equipment may be prohibitive for many rehabilitation and/or exercise settings. The results of this study suggest that motor imagery may be a simple and cost-effective technique that may result in more effective training/rehabilitation practices. Although not statistically significant, the trends toward enhanced muscle recruitment in the imagery group are encouraging given the spontaneous use of imagery reported by the control group; the small sample size and the possibility that large standard deviations in recruitment amplitudes may have masked significant effects. While the spontaneous use of general imagery could not be prevented, use of imagery that is specific to the muscles involved in producing the movement appears to be beneficial. Furthermore, motor imagery is a learned skill and therefore one session of imagery may not be enough to see the desired effects. Future studies examining the effects of motor imagery training on knee extensor muscle recruitment amplitudes and timing, and force production are planned.

REFERENCES

[1] Vealey RS, et al. Imagery training for performance enhancement and personal growth. In JM Williams (Ed.) *Applied Sport Psychology* (2nd ed). Mayfield, 1993.
[2] Dickstein R, et al. (2005). EMG activity in selected target muscles during imagery rising on tiptoes in healthy adults and poststroke hemiparetic patients. *J Motor Behav* Vol 37(6); p. 475-483.
[3] Lebon F, et al. (2008). Modulation of EMG power spectrum frequency during motor imagery. *Neurosci Lett* Vol 435, p. 181-185.

EXHAUSTIVE EXERCISE IMBALANCES NEUROMUSUCLAR ACTIVATION PATTERNS OF KNEE EXTENSORS AND FLEXORS IN YOUNG AND MIDDLE-AGED WOMEN

Monica R. Maly,[1] Joanne Hodder,[2] Heather S. Linley,[1] Michael R. Pierrynowski,[1] Tova Plashkes[1]
[1]School of Rehabilitation Science, McMaster University, Hamilton Ontario, Canada, mmaly@mcmaster.ca
[2]Department of Kinesiology, McMaster University, Hamilton Ontario, Canada

INTRODUCTION

Fatigue protocols involve high-intensity contractions over short time intervals [1]; however, activities of daily living that induce fatigue involve prolonged and repetitive contractions. The purpose of this study was to evaluate the impact of exhaustive exercise on torque and neuromuscular activation of knee musculature in young and middle-aged women.

METHODS

Seven healthy young women (mean ± SD: 24.3 ± 0.8 years, BMI 24.2 ± 6.1 kg/m^2) and six healthy middle-aged women (55.3 ± 5.0 years, BMI 25.4 ± 3.2 kg/m^2) participated. Bipolar surface electrodes (AMT-8, Bortec Biomedical Ltd., AB, Canada) were placed over rectus femoris and biceps femoris of the dominant leg. Participants were positioned on an isokinetic dynamometer (Biodex Medical Systems, Shirley NY, USA). Electromyography (EMG) of rectus femoris and biceps femoris was normalized to maximum voluntary electrical activation during an isometric contraction at 60°. Measures included (1) peak torque during an isokinetic contraction at 60°/s, (2) average EMG (AEMG) during a 5s 25% maximum voluntary isometric contraction.

To induce fatigue, participants repeated sets of 50 concentric extensions and flexions at 60º/s. Immediately following each set, peak torque (isokinetic) and EMG (isometric) measures were repeated and pain and perceived exertion recorded on a self-report 0-10 scale. Fatiguing sets continued until peak torque of both muscles dropped by ≥25% from baseline, excessive pain or exertion, or the completion of 10 sets. After the fatiguing protocol, torque and EMG measures were repeated during a recovery period, at 5, 10, 15 and 30 minutes. Repeated measures analysis of variance followed by pair-wise comparisons were used to identify changes in peak torque and EMG during fatigue and recovery in flexors and extensors.

RESULTS

The same number of fatiguing contractions were completed by young (6.8 ± 2.1 sets) and middle-aged (6.9 ± 2.6 sets).

Peak Torque: Young women had greater baseline extensor and flexor torque (171.4 ± 29.5, 83.6 ± 11.5 Nm) compared to middle-aged women (119.5 ± 22.7, 58.1 ± 14.0 Nm). Thus, response to fatigue and recovery was split between groups. *Extensors:* The fatigue protocol reduced peak extensor torque from baseline in the young (F=28.1, p=0.002) and middle-aged (F=24.0, p=0.01). No recovery was noted in either group. *Flexors:* Fatiguing contractions reduced peak flexor torque in the young (F=46.9, p=0.001) and middle-aged women (F=7.8, p=0.04). No recovery was noted in either group.

Average EMG Amplitude: At baseline, the young group had baseline extensor and flexor AEMG activations (20.2 ± 9.0, 17.4 ± 6.7 %MVE) similar to the middle-aged group (20.1 ± 6.1, 18.5 ± 8.4 %MVE). Thus AEMG data was pooled. *Extensors:* The fatigue protocol did not increase extensor AEMG in the samples (Figure 1). Yet during recovery, both groups showed reduced extensor AEMG (F=3.4, p=0.05). *Flexors:* Flexor AEMG demonstrated the opposite pattern compared to extensor AEMG. During fatigue, flexor AEMG increased in both samples of women (F=14.3, p=0.001). Yet, no recovery of flexor AEMG was noted.

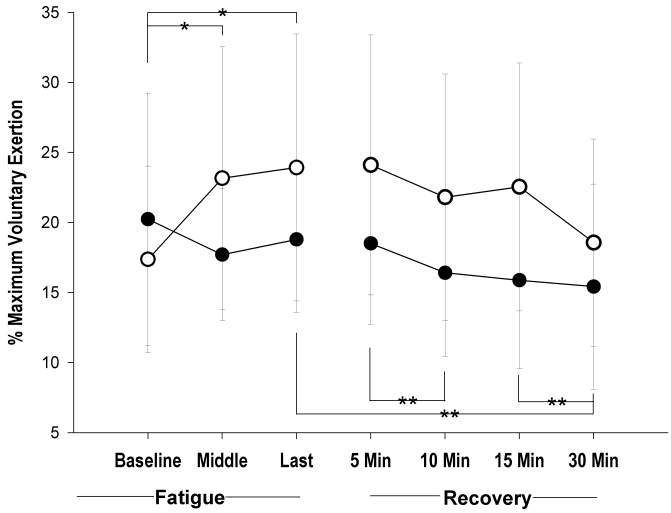

Figure 1: AEMG of rectus femoris (black circle) and biceps femoris (open circle) during fatigue and recovery. (p<0.05 rectus femoris, *p<0.05 biceps femoris).**

DISCUSSION AND CONCLUSIONS

Exhaustive exercise resulted in peak torque decrements that were not recovered after 30 minutes. Neuromuscular activation during fatigue differed between knee extensors and flexors. The blunt response by rectus femoris may reflect job sharing between the four heads of quadriceps, or recovery from the completion of isokinetic fatiguing contractions to the beginning of the isometric contractions for EMG analysis. Large variability in biceps femoris AEMG limited the ability to detect recovery. In addition to ongoing data collection for this study, future work should examine the impact of imbalanced neuromuscular activation across all knee extensors and flexors and the resultant pattern of knee joint loading.

REFERENCES and ACKNOWLEDGEMENTS

[1] Kent-Braun. (2008) *Exer Sports Sci Rev* **37**: pp 3-9.
NSERC Discovery #353715 (MM). The authors gratefully acknowledge J. MacDermid and P. Keir for use of equipment.

QUANTIFYING DYNAMIC POSTURAL STABILITY DURING SITTING PIVOT TRANSFERS USING A NEW EQUILIBRIUM MODEL IN INDIVIDUALS WITH A SPINAL CORD INJURY: A CASE STUDY

Dany Gagnon[1,2], Cyril Duclos[1,2], Pierre Desjardins[1,2], Michel Danakas[2], Sylvie Nadeau[1,2]
[1]School of Rehabilitation, University of Montreal, Montreal, Canada, dany.gagnon.2@umontreal.ca
[2]Center for Interdisciplinary Research in Rehabilitation (CRIR), Montreal, Canada www.pathokin.ca

INTRODUCTION

Individuals with a spinal cord injury (SCI) perform sitting pivot transfers (SPTs) about 20 times per day on average. While performing SPTs, these individuals need to exert substantial upper extremity effort and to preserve dynamic postural stability. While substantial research has been done over the past decade to better understand related physical demands on the upper extremities, no study has yet quantified the dynamic postural stability requirements during SPTs despite the considerable risk of falls and numerous fall-related injuries reported by individuals with a SCI, while performing these tasks. The objective of this study is to apply a recently-developed equilibrium model to provide preliminary data on the dynamic postural stability challenges individuals with a SCI encounter while performing SPTs.

METHODS

A 32-year-old male (weight = 75 kg; height = 1.68 m), who sustained a complete sensorimotor T4 SCI three years ago, and who executes SPTs independently, was recruited. During a comprehensive biomechanical laboratory assessment [1], the subject performed three SPTs between an initial and a target seat of similar height (50 cm) and three additional SPTs between an initial seat and a target seat 10 cm higher than the initial seat. Each phase (pre-lift, lift, and post-lift phases) of the SPTs were time-normalized to 100 data points using precise criteria for a total of 300 data points for the entire SPT duration [1]. Two transition phases of 20 data points (90-110; 190-210) were defined. To quantify dynamic postural stability during SPTs, a novel equilibrium model, measuring the stabilizing and destabilizing forces, was used [2]. The stabilizing force reflects the theoretical force (N) needed to maintain the center of mass (COM) within the limit of the base of support (BOS) and preserve balance at each instant of the SPT based on the kinetic energy needed to be neutralized. The greater the stabilizing force, the more effort the subject must exert to keep the COM within the BOS and remain stable. The destabilizing force is the theoretical force (N) required to move the COP to the limit of the BOS, and applied to the body in the direction of the velocity of the COM. The lower the destabilizing force, the easier it is to move the COP to the limit of the BOS and the more unstable the subject is. The two forces were computed using kinematic and kinetic data recorded during the SPT laboratory assessments [1].

RESULTS

The profile of the mean stabilizing and destabilizing forces reached during SPTs toward a target seat of similar and higher (+10cm) heights than the initial seat are presented (Figure 1). The mean stabilizing force reached its peak values around the transition phases (seat-off and seat-on) for both transfers. The mean destabilizing force rapidly declined during the transition phases (seat-off and seat-on) to reach its lowest values around the end of the transition phases.

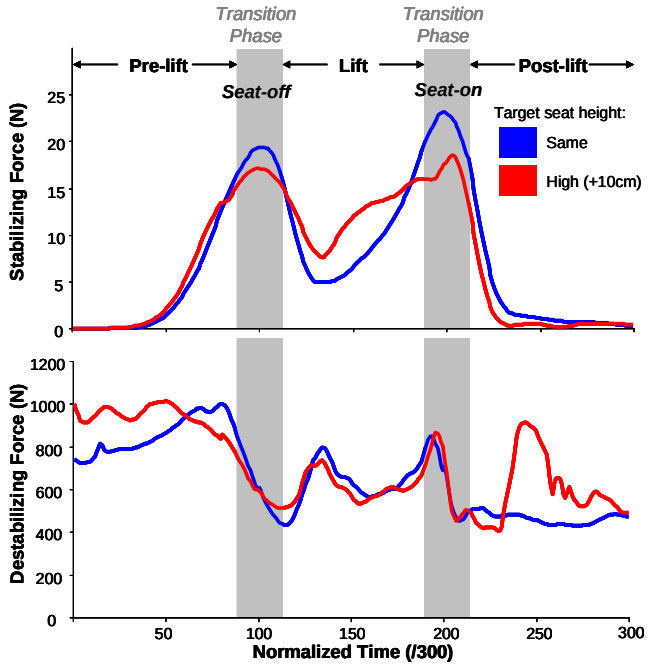

Figure 1: Stabilizing (top) and destabilizing (bottom) forces measured during sitting pivot transfers.

DISCUSSION AND CONCLUSIONS

Applying the equilibrium model to SPTs allowed, for the first time, to quantify how SPTs of distinct difficulty levels challenge dynamic postural stability and further validates the new equilibrium model itself. The model confirmed that the greatest postural stability challenges were reached around the two transition periods during SPTs. The computation of the stabilizing and destabilizing forces represent a key milestone that will allow researchers to refine comprehensive biomechanical assessments and improve understanding of the role of dynamic postural stability during SPTs. This new evidence-based knowledge is essential to strengthen clinical practice guidelines aimed at optimizing SPT performance.

REFERENCES

[1] Gagnon, D et al. (2008) Biomechanical assessment of sitting pivot transfer tasks using a newly-developed instrumented transfer system. J Biomech **41**(5); p.1104-10.
[2] Duclos C et al. (2009). Destabilizing and stabilizing forces to assess equilibrium during everyday activities. J Biomech **42**(3); p.379-82.

ACKNOWLEDGEMENTS

Funded by the Réseau provincial de recherche en adaptation-réadaptation (REPAR) du Québec and the Ordre professionnel de la physiothérapie du Québec (OPPQ).

UPPER BODY ACCELERATIONS DURING BALANCE RECOVERY IN RESPONSE TO LEAN AND RELEASE PERTURBATION WITH AND WITHOUT GALVANIC VESTIBULAR STIMULATION

Dmitry Verniba[1], William Gage[1,2]
[1]School of Kinesiology & Health Science, York University, Toronto, ON
[2]Toronto Rehabilitation Institute, Toronto, ON

INTRODUCTION

Previous research has suggested that the capacity of older adults to control upper body movement in response to postural perturbation may be diminished, indicated by a relative absence of attenuation of acceleration of the head compared with young adults [1]. Changes in vestibular signals and integration of sensory information within the balance response may contribute to diminished upper body control during balance recovery. Application of a small electrical current to the mastoid processes (Galvanic Vestibular Stimulation; GVS), provides a temporary error in the signal from the vestibular system; individuals perceive themselves to lean toward the cathodal (+) electrode side. The perceived lean is "corrected" by actually leaning toward the anodal (-) electrode side. Use of GVS in addition to absence of vision (eyes closed) during postural perturbations has shown that the CNS places a larger emphasis on the somatosensory information during balance recovery [2]. We hypothesized that healthy individuals would demonstrate increased head accelerations associated with altered vestibular information during balance recovery. Use of highly controlled postural perturbations to probe the control of balance has revealed complex, high velocity balance recovery strategies, even within mobility-compromised groups such as patients with stroke. A relatively low-cost, simple system to measure balance and balance recovery function within the clinical setting would provide a useful and relevant tool to evaluate patient recovery. We were also interested in contrasting the output of a wearable, wireless accelerometer system with a gold-standard optoelectronic motion capture system during balance recovery.

METHODS

Young healthy male participants (n=5; age=22.4 ± 1.5 years) underwent a forward lean-and-release postural perturbation. The angle of lean was adjusted to induce a stepping (change-in-support) balance recovery strategy. Release was effected using an electromagnet. Onset of GVS occurred 3 second prior to release. Participants maintained the position of their head turned to the left so that GVS would bias perception of verticality in the anteroposterior direction. Three GVS conditions were used: No GVS (CON), GVS with anode behind the left ear (L-GVS, posterior bias), and GVS with anode behind the right ear (R-GVS, anterior bias). Accelerations at the head, sternal notch, and xyphoid process were calculated using the motion capture-derived displacement data. In addition accelerations at the head and spine (C7 and T12 level) were measured using wireless accelerometers (Figure 1).

RESULTS

We have found that the output of the wireless accelerometer is qualitatively very similar to the output of the motion capture system (Figure 2). Furthermore, the descriptive statistics suggest an increase in acceleration at more superior locations with application of GVS (in particular, GVS-R), head acceleration may not be attenuated to the same degree as in the other conditions (Figure 3).

DISCUSSION AND CONCLUSIONS

The increase in head accelerations in the GVS-R condition may suggest that vestibular information is a contributor to control of head movement during balance recovery. Diminished attenuation of head acceleration among older adults might be a contributor to falls among this population. Hence, the development of a low-cost, simple, and portable accelerometer-based measurement system may provide a viable, clinically-relevant measurement system for evaluation of balance and balance recovery strategies.

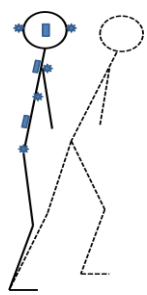

Figure 1: Step Recovery
- Reflective marker
- Accelerometer

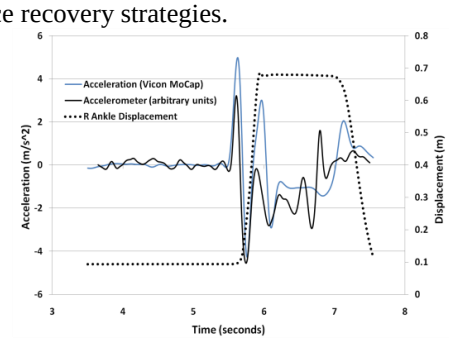

Figure 2: Head Acceleration Profile during Right Foot Step

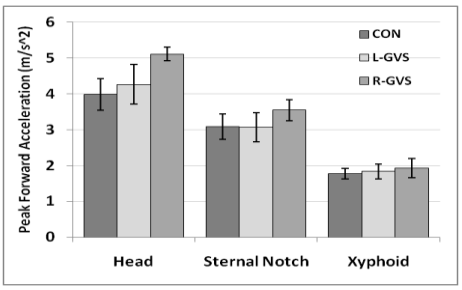

Figure 3: Peak Forward Acceleration during Step Balance Recovery with and without the GVS. Error bars: ± 1 SE.

If there are any remaining questions, please do not hesitate to contact us at whgage@yorku.ca.

REFERENCES

[1] Jensen et al. (2001). *Experimental Aging Research*, 27; p. 361-376
[2] Inglis et al. (1995). *Journal of Neurophysiology*, 73 (2); p. 896-901

ACKNOWLEDGEMENTS

We would like to thank CIHR, IA, and CFI.

TENSILE TESTING OF MEDICAL GRADE UHMWPE TO RUPTURE WITH UTILIZATION OF 3D OPTICAL CORRELATION SYSTEM

Tomas Bouda, Radek Sedlacek, Pavel Ruzicka, Svatava Konvickova
Faculty of Mechanical Engineering, Czech Technical University in Prague, Technicka 4, 16607 Prague, Czech Republic
radek.sedlacek@fs.cvut.cz

INTRODUCTION

The Ultra-high-molecular-weight polyethylene (UHMWPE) is the most used polymeric material in production of total joint replacements (TJR). As was many times addressed by other authors the lifespan of bearing component made from UHMWPE is the limiting factor of the whole TJR. During the service of a UHMWPE component there are recognized several modes of failure e.g. generation of mechanically induced polymer debris, delamination and pitting. Those modes of failure are coupled with cyclic nature of loading, lubrication, intrinsic mechanical properties and ageing of UHMWPE. When the lifespan of a component is considered from a perspective of material strength we are always trying to connect the state of stress which is observed in critical area and the number of cycles to failure under cyclic loading conditions. To evaluate the state of stress e.g. in tibial plateau under reasonable complicated loading conditions which could be found in total knee replacement (TKR) is possible to carry out a finite element analysis (FEA). Such FEA requires suitable constitutive model of UHMWPE which will be able reliably to predict relation between true stress and true strain during loading and unloading phase. A constitutive model which fulfills those conditions is Hybrid model developed by J.S. Bergström et al. (USA).

METHODS

The simple tensile test of flat specimens was carried out as the first intended experimental mechanical test of medical grade UHMWPE. Goal of the simple tensile testing was to receive relation curves between Cauchy stress (true stress) and Hencky strain (true strain) to the specimen rupture. There were tested 3 groups of flat specimens where each group was tested under different loading rate. Established testing loading rates were 30 mm/min, 75 mm/min and 150 mm/min according to CSN EN ISO 527-1. The UHMWPE specimens were prepared in the same manner as are manufactured and sterilized (by γ-radiation - dose of 30 kGy) tibial components of total knee replacement. The specimens were supplied by Czech producer of TJR Medin Orthopaedics a.s. The tensile tests were passed at ambient temperature 19°C. Generally all kinds of polyethylene can sustain large amount of deformation before they break. Therefore it was used optical digital 3D Correlation System Q-450 (by Dantec Dynamics) to measure such high magnitudes of strain. This system allows the dynamic measurement of full-field 3D displacements and the subsequent analysis of strains on almost any type of material and components. An analog connection between testing and optical measuring system was made to synchronize and record actual magnitude of force with 3D Correlation System.

RESULTS

The goal of the presented experimental testing was obtaining relation curve between Cauchy stress and Hencky strain of flat specimens from medical grade UHMWPE, evaluation of Poisson's ratio and verification of possibility using Correlation System Q-450 to measure large deformation of medical grade UHMWPE. The data gained by Q-450 in the form of image pairs were post-processed in intrinsic software of the correlation system Istra 4D (made by Dantec Dynamics) to evaluate the state of strain at the surface of each specimen during the time. Then the set of strain values for each specimen was exported to Matlab and in custom made script the construction of relation curves between true stress and true strain was finalized. The acquired true stress - true strain curves have confirmed the rate-dependency of UHMWPE and proved that the utilization of 3D correlation system was appropriate. It is needed to statistically evaluate the variance between specimens in each group and variance of all 3 groups between themselves. This was done by statistical evaluation (with the use of ANOVA) of material parameters of Hybrid model for each specimen.

DISCUSSION AND CONCLUSIONS

In these days when we are forced to extend the lifespan of TJR, we cannot omit any aspect which will significantly influence success of any implantation like chemical changes and mechanical properties of the material, corrosion of the material and reaction of the human body to an artificial material as well. According to authors belief there is a lack of knowledge about stress / strain state in components made from UHMWPE which is induced by cyclic loading during their service. The presented experimental work will be followed by next part of the project which is trying to evaluate stress / strain state in tibial plateau under dynamic loading conditions.

REFERENCES

[1] BERGSTRÖM JS et al. (2004). An augmented hybrid constitutive model for simulation of unloading and cyclic loading behavior of conventional and highly crosslinked UHMWPE. *Biomaterials* Vol. 25 (11); p. 2171-2178.
[2] KURTZ SM et al. (2002) Thermomechanical behavior of virgin and highly crosslinked UHMWPE used in total joint replacements. *Biomaterials* Vol. 23 (17); p. 3681-3697.

ACKNOWLEDGEMENTS

This research has been supported by the Ministry of Education of Czech Republic project No. MSM 6840770012.

A BIOMECHANICAL INVESTIGATION OF ANTERIOR AND POSTERIOR FEMORAL NECK NOTCHING

Zachary Morison[1], Gordon Higgins[2], Michael Olsen[1], Emil Schemitsch[1,3]
[1]Institute of Medical Science, University of Toronto, Toronto, Canada, zac.morison@rogers.com
[2]Orthopaedic Surgery, Birmingham, United Kingdom
[3]Orthopaedic Surgery, St. Michael's Hospital, Toronto, ON

INTRODUCTION

Optimal femoral component implantation is essential in reducing the risk of fracture after a hip resurfacing procedure. Improper component positioning can lead to a breach in the femoral neck cortex known as notching. This study was designed to determine risk of femoral neck fracture after anterior or posterior notching as a result of hip resurfacing arthroplasty.

METHODS

Fortyseven 4th generation synthetic femurs were implanted with Birmingham Hip Resurfacing prostheses (Smith and Nephew Inc., Tennessee, USA). Implant preparation was performed using imageless computer navigation (VectorVision SR, BrainLAB, Feldkirchen, Germany). The prosthesis was initially planned for neutral version and translated anterior, or posterior, to create a femoral neck notch. The femurs were fixed in a single-leg stance, flexion or extension and tested with axial compression using a mechanical testing machine (Instron, Ohio, USA). The synthetic femurs were prepared in 8 experimental groups:2mm and 5mm anterior notches, 2mm and 5mm posterior notches, neutral alignment with no notching (control), 5mm superior notch, 5mm anterior notch tested with the femur in 25° flexion and 5mm posterior notch tested with the femur in 25° extension.

Each femur underwent pre- and post-implant stiffness testing and load-to-failure testing. Statistical analysis was completed using SPSS 16 software (SPSS, Illinois, USA). A paired t-test was used to compare differences between the pre- and post-implant stiffness of each femur. A one-way analysis of variance (ANOVA) with Tukey's post hoc analysis was carried out to compare the difference in stiffness and load-to-failure between each experimental group and the control. A p-value of 0.05 was considered significant.

RESULTS

Superior notching significantly decreased the load-to-failure (2423 N, p=0.001). Both the anterior 5 mm notch group in flexion (3048 N, p=0.027) and the posterior 5 mm notch group in extension (3105 N, p=0.038) displayed significantly lower compressive loads than the axially tested controls (4539 N). There were no significant differences between axially loaded femurs prepared with anterior or posterior neck notches (3375-4208 N) and the control group ($p \geq 0.155$). There were no significant differences in stiffness values between post implant experimental groups ($p \geq 0.175$).

Testing Group	Mean load to failure	Significance
Neutral (Control)	4539.45 ± 911.04N	
Posterior 2mm	4208.09 ± 1079.81N	p=1.000
Posterior 5mm	3988.07 ± 728.59N	p=0.995
Anterior 2mm	3926.62 ± 894.17N	p=0.985
Anterior 5mm	3374.64 ± 345.65N	p=0.379
Posterior 5mm in 25° extension	3104.61±592.67N	p=0.038
Anterior 5mm in 25° flexion	3048.11 ±509.24N	p=0.027
Superior 5mm	2423.07 ± 424.16N	p=0.001

Figure 1: Mean load values causing femoral neck fractures for each experimental group.

DISCUSSION AND CONCLUSIONS

This work highlights the detrimental effect of femoral neck notching during hip resurfacing. Anterior or posterior neck notching does not appear to effect proximal femoral strength in axial loading but does significantly weaken the resurfacing construct when the femur is in flexion or extension. As a result, a fracture is more likely to occur with stair climbing rather than normal walking given the reduction in strength noted after testing in flexion. Hip resurfacing is commonly performed on active patients and 5mm notching of anterior cortex has clinically important implications.

WEAR TESTING OF A NOVEL TEMPOROMANDIBULAR JOINT IMPLANT

Ryan Frayne[1], James P. Dickey[1], Marv Schwartz[2], Gary Morphy[2]
[1]Kinesiology/ Faculty of Health Sciences, University of Western Ontario, London, Canada, rfrayne@uwo.ca
[2]4iBio, Pickering, Canada

INTRODUCTION

The temporomandibular joint (TMJ) is a bicondylar joint that is primarily used for mastication and speech. These functions are accomplished by two primary movements, translations in the anterior/posterior direction and rotations that elevate and depress the mandible [1]. TMJ disorders are caused by high compression and translational forces, and are associated with symptoms such as persistent pain, headaches, jaw clicking, and jaw locking. TMJ implants have been designed to decrease the severity of these conditions [2]; however, these implants break down under the physiologic loads experienced in the TMJ [3], and have not been clinically successful [2]. A newly developed implant has been designed to survive in this environment. The objective of this study was to perform wear testing of a novel TMJ implant and report damage to the articulating surface, implant thickness and surface roughness.

METHODS

Six implants were tested *in vitro* using swine TMJs, the best animal model for human TMJs [4]. Standard metal forming techniques were used to fabricate the implants from 0.127mm zirconium sheet using a positive model of the condyle. Holes were drilled at the base of the implant to accommodate a wire draw string to affix the implant over the condylar head. Implants were then inserted into the specimens and tested for 7 hours with a custom-designed mastication jig applying normal chewing movements [1] to the TMJ at a frequency of approximately 1 Hz (21,672 cycles or approximately 1.5 months of human chewing [6]). Compression forces were monitored to sustain a physiological amount of peak compression (70N) [5]. After the test, the implants were examined for damage using three analysis methods: percent surface damage [7], profilometry and implant thickness. Profilometry data was used to calculate surface roughness scores (SRS) for each implant. Photographs and scanning electron microscope images were taken to document implant damage. Implants were tested in sequence and findings from each implant were used to further the development of the next implant.

RESULTS

The implants had an average surface damage of 3.36% (SD=4.19%). The normalized average SRS from profilometry was 570.8 nm (SD=669.3 nm; Figure1). The implant thickness data showed that the implants were thinner in areas of concentrated articulation. Scanning electron microscope images of the implants showed evidence of cracking in implants 1 and 5. Dents were observed on implant 2, 3, 5 and 6, and were located on the anterior articulating surface (implants 3, 6) and the lateral anterior surface (implants 2, 5).

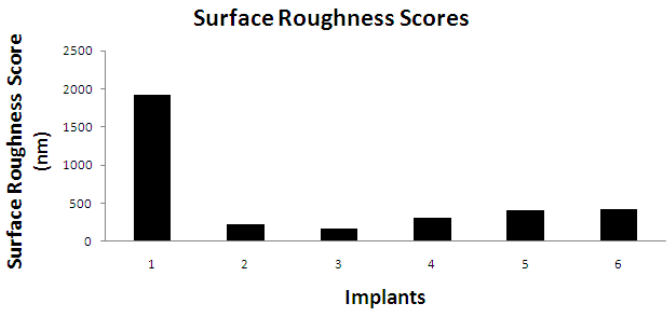

Figure 1: Surface roughness scores were normalized to the control implant. Implant one has a high SRS because it was the only implant that had catastrophic damage.

DISCUSSION AND CONCLUSIONS

All six implants completed the 7 hours of testing with catastrophic damage occurring to one implant (implant 1). This implant had a sub-optimal fit that may have played a role in its diminished performance. The percent surface damage values are a quantitative estimate of scratching and burnishing on the superior surface of the implant. The reported percent damage values are likely underestimates because the macroscopic images are unable to capture all of the damage including dents and small cracks. The next step for the development of this implant should be *in vivo* testing, perhaps using a swine model.

Overall, these implants received little damage throughout their 7 hours of testing and based on these results this novel implant may prove to be an alternative procedure for TMJ disorders.

REFERENCES

[1] Hylander W.L. (2006). TMDs an Evidence-Based Approach to Diagnosis and Treatment. Quintessence Publishing Co., Hanover Park, Illinois. p. 3-34.

[2] Fricton J.R. et al. (2002). *J.Oral Maxillofac.*Surg. Vol 60(12); p.1400-1411.

[3] Spagnoli D. et al. (1992). *Oral Surg. Oral Med.Oral Pathol.* Vol 74(4); p.411-421.

[4] Herring S.W. (1976). *Arch.Oral.Biol.* Vol 21(8); p. 473-480.

[5] Lagenbach G.E.J. et al. (2002). *J.Anat.* Vol 201(5); p. 383-393.

[6] Fontenot M.G. et al. (1992). *J.Oral.Maxillofac.Surg.* Vol 50(2); p. 133-139.

[7] Cornwall G.B., et al. (1995). *J.Appl.Biomater.*Vol 6(1); p.9-18.

QUANTIFYING THE TRADE-OFF BETWEEN WEAR AND KINEMATICS PERFORMANCE OF TOTAL KNEE REPLACEMENTS USING MULTIOBJECTIVE OPTMIZATION

Ryan Willing, Il Yong Kim
Department of Mechanical and Materials Engineering, Queen's University, Kingston, Canada, iykim@me.queensu.ca

INTRODUCTION

Total knee replacement (TKR) designs often experience premature failure due to wear or improper kinematics. Multiobjective design optimization is a way of considering both peformance measures simultaneously while generating optimum component shapes for TKR. Multiobjective optimization also provides useful information on the trade-off between competing performance measures, quantified using a Pareto curve. This abstract describes the use of multiobjective optimization to study the trade-off between wear and kinematics performance in TKR [1], as well as the optimal TKR shapes for either objective function.

METHODS

Candidate TKR finite element mesh and rigid body CAD models were created from a set of design variable parameters provided to a modelling script in HyperMesh (Altair Engineering, MI, USA). Wear performance was assessed using finite element contact analysis in ANSYS (ANSYS Inc., PA, USA) and a strain-hardening sensitive wear model developed by Willing and Kim [2]. Kinematics performance was assessed in terms of the maximum flexion range of motion and the ability to match natural knee anterior-posterior and internal-external rotational constraint characteristics. Kinematics assessments were performed using rigidy body dynamics simulations in MSC.Adams (MSC.Software Corp, CA, USA).

The weighted sum (WS) approach to multiobjective optimization was used in order to consider both wear and kinematics performance simultaneously during design optimization. The relative importance of the two performance measures was varied using a weighting factor (w) between 0 and 1. Optimization results at each different weighting factor were used to derive a Pareto curve, which graphically describes the trade-off between two performance measures while maintaining optimum designs.

Candidate TKR designs ($\bar{x}$) were simulated in terms of wear ($J_{wear}(\bar{x})$) and kinematics ($J_{kin}(\bar{x})$) performance. Optimization modified $\bar{x}$ in order to minimize the weighted sum of $J_{wear}(\bar{x})$ and $J_{kin}(\bar{x})$ while satisfying constraints on the maximum allowable damage depth ($\delta_{max}(\bar{x})$) and fatigue damage score ($D_{max}(\bar{x})$). The resulting mathematical multiobjective optimization problem statement was:

$$\text{Minimize } J_{MOO}(\bar{x}, w) = w\left[J_{wear}(\bar{x})\right] + (1-w)\left[J_{kin}(\bar{x})\right]$$

$$\text{such that } \quad \delta_{max}(\bar{x}) \le 1 \text{ mm}$$

$$D_{max}(\bar{x}) \le 150$$

$$\bar{x}_{min} \le \bar{x} \le \bar{x}_{max}$$

RESULTS

Optimum designs in terms of wear and kinematics performance alone were obtained by setting w to 1 and 0, respectively. The optimum shapes in terms of wear and kinematics are shown in Figure 1. The relationship between volumetric wear production (wear) and maximum flexion range of motion (kinematics) is shown in Figure 2 as an example of the trade-off between wear and kinematics performance. A similar relationship exists between volumetric wear and implant constraint characteristics.

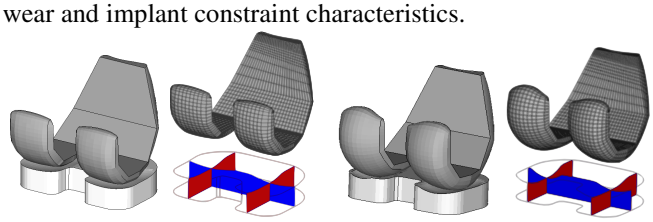

Figure 1: Optimum TKR design in terms of wear (left) and kinematics (right).

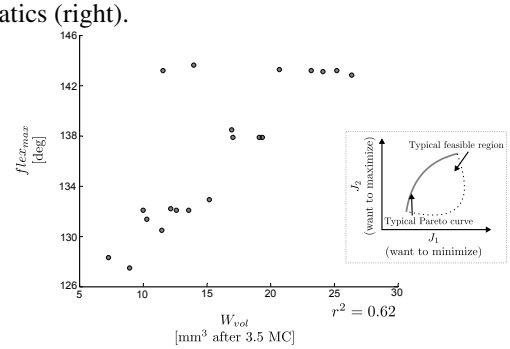

Figure 2: The relationship between flexion range of motion and volumetric wear in TKR.

DISCUSSION AND CONCLUSIONS

The trade-off between wear and kinematics performance was quantified using multiobjective optimization. Significantly different implant component shapes are required for optimal wear versus kinematics performance. Wear optimized designs featured larger radii of curvature in order to reduce contact stresses and crossing motions, while kinematics optimized designs feature smaller radii of curvature to allow greater flexion and femoral rollback and more natural constraint characteristics.

REFERENCES

[1] Sathasivam S. and Walker P.S. (1999). The conflicting requirments of laxity and conformity in total knee replacement. *J. Biomech.* Vol **32**; p. 239-247.

[2] Willing R. and Kim I.Y. (2009). A holistic numerical model to predict strain hardening and damage of uhmwpe under multiple total knee replacement kinematics and experimental validation. *J. Biomech.* Vol **42**; p. 2520-2527.

Finite Element Modeling of Cam Impingement Using Patient-Specific Data

K.C. Geoffrey Ng [1,2], Gholamreza Rouhi [2,1,3], Mario Lamontagne [3,1,2], Matthew J. Kennedy [3], Paul E. Beaulé [4]
[1] Department of Biomedical Engineering, University of Ottawa, kng035@uottawa.ca
[2] Department of Mechanical Engineering, University of Ottawa
[3] School of Human Kinetics, University of Ottawa
[4] Division of Orthopaedic Surgery, The Ottawa Hospital

INTRODUCTION

Femoroacetabular impingement (FAI) is recognized as a pathomechanical process that leads to hip osteoarthritis (OA) [1]. Despite many attempts in the past to characterize the mechanism by which cam FAI (aspherical femoral head-neck deformity) leads to OA, to the best of our knowledge, no *in vitro* study has integrated clinical patient-specific data to determine stresses and strains within the symptomatic hip joint. The aim of this research is to examine the effects of cam FAI towards hip OA using finite element analysis (FEA) and patient-specific CT, kinetic, and kinematic data.

METHODS

Net joint reaction forces were obtained from inverse dynamics, calculated from joint kinematics and kinetics, for a dynamic squat motion of a cam FAI patient [2]. CT radiographs of the patient's pelvic sections were compiled using 3D-DOCTOR (Able Software Corp, MA, USA). The symptomatic joint was segmented from each slice to assemble a 3D model, and then refined using SolidWorks (Dassault Systèmes, MA, USA) to minimize geometric artefacts. A cartilage layer, of varying thickness, was created using an offset method from the acetabulum [3]. The model was imported into ANSYS (ANSYS, PA, USA) for FEA. The assemblies were given tetrahedral SOLID187 elements, where bone was modeled as a linear elastic orthotropic material (elastic moduli: E_x = 11.6 GPa, E_y = 12.2 GPa, E_z = 19.9 GPa; shear moduli: G_{12} = 4.0 GPa, G_{13} = 5.0 GPa, G_{23} = 5.4 GPa; and Poisson's ratios: υ_{12} = 0.42, υ_{13} = υ_{23} = 0.23) [4] and cartilage as a linear elastic isotropic material (E = 12 MPa; υ = 0.45) [1]. The forces were applied onto the model, where two loading scenarios were considered: (1) stance and (2) maximum force endured during the impinged squat. Using the kinematics data, the femur was oriented with respect to the acetabulum according to the squat interval (Figure 1). Maximum-normal stresses were analyzed to determine adverse loading conditions within the joint. Strain energy density (SED) was determined to examine its effect on the initiation and rate of bone remodeling [5].

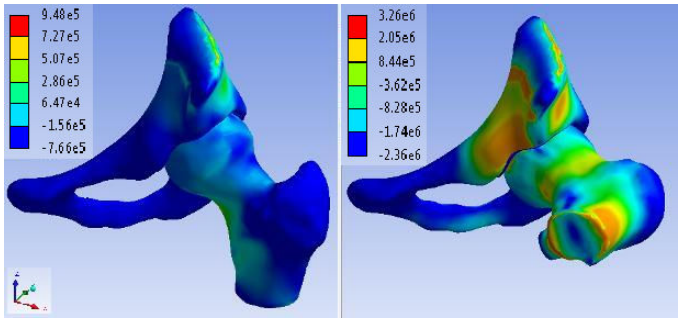

Figure 1: Left hip joint with cam FAI at standing position (left), and oriented femur at squat interval when highest force endured (right).

RESULTS

In both stance and squat scenarios, high mechanical stimuli regions were found along the femoral head-neck and in the acetabulum. Low levels of mechanical stimuli were found on the actual cartilage; however, high levels of stresses and strains were evident behind the cartilage layer, on the acetabulum's subchondral plate (Figure 2). At stance, the maximum-normal stress and SED were found to be 0.948 MPa and 0.721 kPa, respectively, located at the superior portion of the acetabulum. At squat, the highest stress and SED were found to be 3.258 MPa and 1.383 kPa, respectively, located at the antero-superior portion of the acetabulum, where the cam deformity was in most contact with the acetabular cartilage.

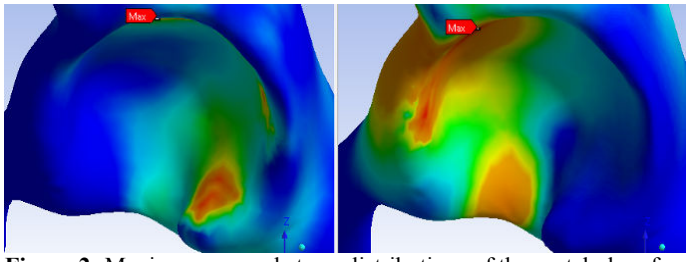

Figure 2: Maximum-normal stress distributions of the acetabulum for standing position (left) and for squatting position (right) (with cartilage and proximal femur hidden from view). Arrow denotes maximum stress region in each case.

DISCUSSION AND CONCLUSIONS

Resultant mechanical stimuli were found to be much higher in the squatting position than in the standing position, where the joint was at its impinged state. With the cartilage layer transferring the load onto the acetabulum, it is hypothesized that the elevated levels of mechanical stimuli could increase the rate of bone remodeling in the subchondral bone, causing stiffening of the subchondral plate, which would consequently accelerate the onset of cartilage degeneration. Since SED is proportional to the rate of bone remodeling [5], there will be varying rates of bone remodeling within the acetabulum, in order to establish a new suitable configuration, based on the level of SED and mechanical stimuli.

REFERENCES

[1] Chegini S, et al. (2008). The Effect of Impingement and Dysplasia on Stress Distributions in the Hip Joint during Sitting and Walking: A Finite Element Analysis. *J Orthop Res*, 27 (2): 195-201.
[2] Lamontagne M, et al. (2009). The Effect of Cam FAI on Hip and Pelvic Motion during Maximum Squat. *Clin Orthop Relat Res*, 467: 645-650.
[3] Russell ME, et al. (2006). Cartilage contact pressure elevations in dysplastic hips: a chronic overload model. *J Orthop Surg Res*, 1: 1-6.
[4] Taylor WR, et al. (2002). Determination of orthotropic bone elastic constants using FEA and modal analysis. *J Biomech*, 35: 767-773.
[5] Vahdati A and Rouhi G. (2009). A model for mechanical adaptation of trabecular bone incorporating cellular accommodation and effects of microdamage and disuse. *Mech Res Comm*, 36 (3): 284-293.

EFFECTS OF HIND LIMB MUSCLE WEAKNESS ON TIBIAL CARTILAGE DEGENERATION IN RABBITS

Aliaa Rehan Youssef [1], Tim Leonard[1], Walter Herzog[1]
[1]Faculty of Kinesiology, the University of Calgary, Calgary, Alberta, ayoussef@kin.ucalgary.ca

INTRODUCTION

Muscle weakness has been suggested to be a risk factor for the development of osteoarthritis (OA) [1]. Recently, isolated quadriceps muscle weakness was found to have no effect on tibial cartilage degeneration [2]. However, isolated muscle weakness is rare while general muscle weakness affects a large part of the population, particularly the elderly. Therefore, the purpose of this study was to investigate osteoarthritic changes in the rabbit knee cartilage following a period of general hind limb extensor weakness. We hypothesized that general muscle weakness is associated with degenerative changes in the knee cartilage, thereby providing evidence that muscle weakness might be an independent risk factor for joint degeneration leading to OA.

METHODS

Twenty-two skeletally mature New Zealand White rabbits were divided into an experimental and a control group. In the experimental group (n=11), hind limb extensor muscle weakness was induced by controlled injections of botulinum type-A toxin (BOTOX™, Allergan Inc., ON, Canada) into the quadriceps and plantar flexor muscles. The control group (n=11) received a matched volume of saline injections into the same muscles as the experimental group animals.

Rabbits in the experimental and control groups were followed for 1-month or 3-month periods. Isometric knee extensor torques and atrophy of the injected muscles were measured at the end of the experimental period. The degenerative changes in the medial and lateral tibial cartilages were assessed using the Mankin scoring system [3]. Statistical analyses were done using non-parametric tests (α=0.05).

RESULTS

Isometric knee extensor torques (Figure 1) and ***muscle mass*** (not shown) were significantly reduced in the experimental but not in the control animals' hind limbs.

The Mankin scores for the medial and lateral tibial cartilages were the same for corresponding hind limbs of the experimental and control group animals (Table 1).

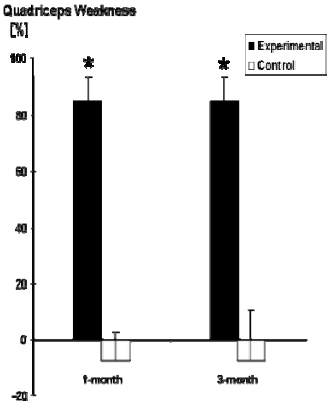

Figure 1: Percent quadriceps weakness for corresponding hind limbs of the experimental and control group rabbits. Group means and SD are shown (*p<0.05).

DISCUSSION AND CONCLUSIONS

Quadriceps and plantar flexor muscles weakness in a rabbit model did not increase tibial cartilage degeneration above control over a 3-months experimental period. This result is in accordance with previous findings reported in isolated quadriceps weakness introduced in the same animal model [2]. However, it is in contrast to suggestions based on work performed in human knees and quadriceps weakness [1]. This finding suggests that either the experimental period of muscle weakness was too short to produce an increased rate of cartilage degeneration in the rabbit model, or that muscle weakness affects joints differently in different species. We speculate that the four legged gait of rabbits might protect hind limb joints from muscle weakness induced joint degeneration, while muscle weakness is critical in the bi-pedal gait of humans.

REFERENCES

[1] Slemenda C et al. (1998) *Arthritis Rheum* **41**; 1951-1959.
[2] Rehan Youssef A et al. (2009) *Osteoarthritis Cartilage* **17**; 1228-35.
[3] Mankin H et al. (1971) *J Bone Joint Surg Am* **53**; 523-37.

ACKNOWLEDGEMENTS

AHFMR, AHFMR Team Grant on Osteoarthritis, CIHR, Egyptian Ministry of Higher Education

Table 1: Mankin scores for the medial and lateral tibial cartilage. Median values ± 1SD are shown.

Groups	Medial Tibia		Lateral Tibia	
	1-month	3-month	1-month	3-month
Botox Injected	**6.5±0.9**	**7±2.1**	**4.5±2.4**	**6±2.8**
Botox Contra-lateral	**7±0.8**	**7±1.7**	**4.5±2.7**	**6±2.4**
Sham Control	**7±1.1**	**5.5±2.1**	**3±2.3**	**4±4**
Sham Contra-lateral	**6.6±1.6**	**6.5±1.2**	**5±1.9**	**3±3.7**

DETERMINING THE EFFECTS OF WALKING POLES ON THE KNEE ADDUCTION MOMENT USING AN INSTRUMENTED NORDIC WALKING POLE: A PILOT STUDY

Daniel J Bechard[1], Thomas Jenkyn, Ian C Jones, Trevor Birmingham
[1]Wolf Orthopaedic Biomechanics Lab, the University of Western Ontario, London, Canada, dbechard@uwo.ca

INTRODUCTION

Increasing aerobic fitness and decreasing joint loading are two important yet potentially paradoxical treatment strategies for individuals with knee osteoarthritis (OA). Although patients are encouraged to participate in activity, the potential for increased knee joint loading is substantial. Nordic walking poles are proposed by their manufacturer to decrease load on the weight baring joints and thereby promote increased levels of activity, however previous research contains conflicting evidence. Walking poles could plausibly decrease the external adduction moment about the knee (KAM), a proxy for the load on the knee medial compartment and a risk factor for disease progression. Thus, the aim of this study is to determine the feasibility of using instrumented walking poles to study their affects on the KAM.

METHODS

Two individuals (one male and one female) with Nordic walking experience and no health concerns related to mobility volunteered for this study. Subjects were asked to walk at a self selected pace over a seven meter walkway while kinetic and kinematic data were collected using an 8-camera motion analysis system at 60Hz (Motion Analysis Corporation, CA, U.S.A), and a floor mounted force plate (Advanced Mechanical Technology Inc., FL, U.S.A) at 1200Hz. Passive reflective markers were affixed to both subjects using a modified Helen Hayes marker set. Five successive right foot strikes for two conditions were collected: no poles (NP) and with poles (WP) NP and WP conditions were randomized. Poles were instrumented with two markers each and a compression load cell (Omegadyne Inc., OH, U.S.A) collecting at 100Hz. The load cell was located near the foot of the left pole and transmitted data through a custom wireless telemetry system. Data reduction and post processing was completed using EVaRT, Orthotrak (Motion Analysis Corp., Santa Rosa, U.S.A.) and custom software. Primary variables of interest were first and second peak KAM. Gait speed, vertical ground reaction force (VGRF), and force measured by the load cell were also collected.

RESULTS

First peak KAM showed a decrease in both subjects where second peak decreased in only one individual (Table 1). This corresponded to an overall increase in gait speed in both participants. VGRF was unchanged for subject one however increased for subject two. The load through the pole as measured by the load cell was 11.0 and 14.1%BW for subject one and two respectively.

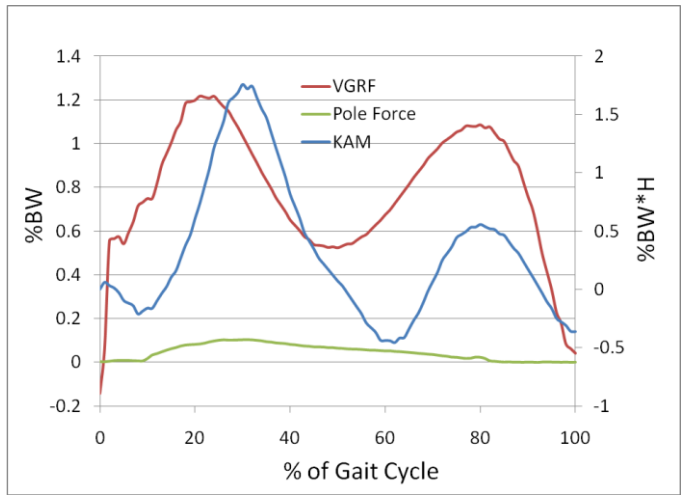

Figure 1: Illustration of the KAM, VGRF, and pole force during one step of a single trial for subject one.

DISCUSSION AND CONCLUSIONS

Through this pilot study, we have shown with the use of the instrumented Nordic walking pole that we can now accurately examine the effect of Nordic walking poles on the external KAM. Subject one depicts an example of an increased walking speed WP and an overall reduction of knee joint load. Subject two shows a higher KAM WP despite a higher reliance on the walking pole. This was due to a faster walking velocity that potentially masked the effects of the poles. Future studies will specifically focus on the contribution of the pole on the KAM and populations with disability.

REFERENCES

[1] Oakley, C. et al. (2008) Nordic poles immediately Improve walking distance in patients with intermittent claudication. *Eur J Vasc Endovasc Surg*; In Press
[2] Wilson, J. et al. (2000). Effects of walking poles on lower extremity gait mechanics. *Med and Sci in Sport and Exercise*. p. 142 - 147

Table 1: Subject demographics and variables of interest

				Gait Speed (m)		1st Peak KAM (%BW*H)		2nd Peak KAM (%BW*H)		VGRF (N)		Pole Force (%BW)
Subject	Sex	Age	BMI	NP	WP	NP	WP	NP	WP	NP	WP	
1	M	29	23.9	1.54	1.70	1.65	1.63	1.44	0.99	1.24	1.22	11.0
2	F	24	20.1	1.66	1.93	2.41	2.33	3.36	4.02	1.39	1.56	14.1

INFLUENCE OF MATERIAL PROPERTIES OF HIP PROSTHESIS FEMORAL COMPONENT ON STRESS SHIELDING

Ashkan Lakzadeh[1] , Tina Khazaei[2] , Ali Ataei[1]

[1]Department of Mechanical Engineering , Iran University of Science and Technology, Tehran , Iran , a.lakzadeh@gmail.com

[2]Department of Biomedical Engineering , Iran Azad University/Science and Research Branch, Tehran , Iran

Introduction : One of the most frequent complications of total hip replacement (THR) is aseptic loosening of hip prosthesis femoral component which is primarily due to changes of post-operative stress distribution pattern with respect to intact femur. The objective of the current study was to evaluate the influence of prosthesis material properties on stress shielding through the surrounding bone of the prosthesis which could cause aseptic loosening of the femoral component in long-term periods.

Method : Three different 3D finite element models i.e. an intact human proximal femur and two post-operative models were developed based on CT-scan images and the suggested surgery procedure for prosthesis placement . In the post-operative models ,a commercial cementless hip prosthesis with two different material properties (114 GPa for real Ti6Al4V prosthesis model and 1GPa for trial prosthesis model) was implanted in the human proximal femur. Hip joint ,abductors muscle and adductors muscle forces were applied on the all three models in the way in which simulate the critical toe off phase loading condition . Von Mises stress was measured in several predefined paths in bone to compare stress values in three different models.

Results : The results showed a significant reduction of Von Mises stress values in the both post-operative models with respect to the intact model. Although the stress values of the trial model were more similar to that of intact model, the reduction of bone Von Mises stress values in this post-operative model were still significant in comparison with the intact model. Conclusion : consequently , by comparison between stress distribution pattern of the all three different models, it is concluded that however , material properties of the prosthesis is one of the important factors which could influence on the stress distribution pattern and subsequent stress shielding effect through the femur bone , other factors such as prosthesis placement in bone , geometry of prosthesis and load placement , which were not investigated in the current study , might be some other important factors for hip prosthesis femoral component design and reduction of stress shielding which finally lead to better stability of fixation in long-term periods.

NEUROMUSCULAR APPROACH IN SPORT SPECIFICITY: ABILITY OF TWO OFF-ICE TRAINING DEVICES TO REPRODUCE THE FORWARD ICE HOCKEY SKATING STRIDE

Jacob Smith[1] and Scott Landry[1]
[1] School of Recreation Management and Kinesiology, Acadia University, Wolfville, N.S., Canada, scott.landry@acadiau.ca

INTRODUCTION

An off-ice forward skating training device, the SkateSIM, has recently been designed at Acadia University to enhance forward ice skating, specifically during the acceleration phase [1,2]. The purpose of this study was to use surface electromyography (EMG) to gain an understanding of the simularities and differences of muscle activity patterns for 7 lower limb muscles during both an acceleration stride (stride 2) and a constant maximum velocity stride (stride 5) and make comparisons between forward ice skating (IS), a running sprint (RS) and 2 different off-ice skating simulators (SkateSIM (SS) and slide board (SB)).

METHODS

14 healthy high level university hockey players participated in this study. A Delsys wireless Myomoinotor® IV EMG system was used to measure muscle activity patterns for the following 7 lower limb muscles: medial gastrocnemius (MGA), tibialis anterior (TAN), vastus medialis (VME), rectus femoris (REF), medial hamstring (MHA), gluteus medius (GME) and gluteus maximus (GMA). Participants performed 5-7 trials for each of the 4 conditions (IS, RS, SS and SB) and for the first 5 strides, a foot switch was used to divide each stride into a stance and swing phase. Activity levels for both phases, normalized to maximum voluntary contractions (MVC), were quantified for each condition by calculating the root mean square (RMS) for each phase separately. For the 2nd stride the athletes were accelerating and therefore 3 conditions (IS, RS and SS) were compared using a one-way repeated measures ANOVA. Stride 5 represented a constant maximum velocity and all 4 conditions were compared for this stride. Bonferroni corrected post hoc pairwise comparisons were performed when a condition effect was identified from the ANOVA. In addition to quantitative comparisons, qualitative comparisons of the activity waveforms were also performed for the 4 conditions for both phases (stance and swing) and both strides (2 and 5).

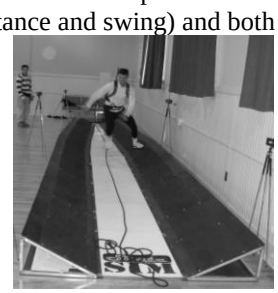

Figure 1: A participate performing a trial on the SkateSIM®

RESULTS

There were many similarities and differences identified in the activity waveform patterns and RMS activity magnitudes for the stance and swing phases, between the 3 conditions for the acceleration stride (Stride 2) and between the 4 conditions for the constant maximum velocity stride (Stride 5). For the stance phase of the acceleration stride, the waveform patterns and RMS activity magnitudes were similar across the 3 conditions for the VME, MHA, GME and GMA. For the MGA during stance, the running sprint generated larger activity magnitudes compared to ice skating and the SkateSIM. For the TAN and REF, waveform patterns and magnitudes during stance were similar for the SkateSIM and running sprint, with ice skating having larger activity magnitudes and different waveform patterns compared to the both the running sprint and SkateSIM.

For the stance phase of the constant maximum velocity stride (Stride 5), VME magnitudes across all 4 conditions were similar; however, the waveform patterns of the slide board were quite different from the other 3 conditions (Figure 2). The slide board waveforms peaked later in stance for the MGA, VME, REF, GME and GMA compared to the other 3 conditions, which all had peak muscle activity occurring earlier in the stance phase (Figure 2). Qualitatively comparing activity waveforms between the two phases, muscle activity for the 4 conditions tended to be greater during stance compared to swing for the MGA, VME, GME and GMA.

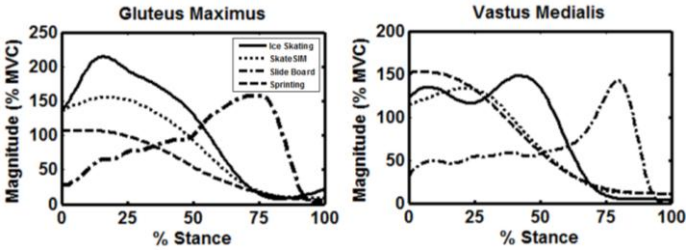

Figure 2. MVC normalized muscle activity patterns for the stance phase of the constant maximum velocity stride (Stride 5) for 2 selected muscles, showing all 4 conditions

DISCUSSION AND CONCLUSIONS

The SkateSIM produced gluteus maximus and medius activity patterns that were closer to ice skating compared to training on a slide board or during a running sprint. The SkateSIM and ice skating both involve forward propulsion and therefore gluteal activity is required to extend and control the hip. The slide board waveforms were quite different in shape because unlike the other conditions, a significant portion of stance was spent sliding on the board prior to the generation of the push off phase towards the end of stance. From a stance/swing perspective for select muscles, the SkateSIM appears to produce muscle patterns and magnitudes closer to ice skating compared to traditional slide board training.

REFERENCES

[1] Price M. (2003). Simulated skating to enhance skating performance and leg power in elite hockey players. *(Undergraduate Thesis).* Acadia University, Wolfville, NS.
[2] Farlinger CM et al. (2008). The effect of sequence of skating-specific training on skating performance. *Int J Sports Phsiol Perform.*

EVALUATION OF GAIT SYMMETRY AFTER STROKE: A COMPARISON OF ANKLE-FOOT ORTHOTIC USERS AND NON-USERS.

Amanda E Chisholm[1,2], Stephen D Perry[1,2,3], William E McIlroy[1,2,4,5]
[1]Graduate Department of Rehabilitation Science, University of Toronto, Toronto, Canada
[2]Toronto Rehabilitation Institute, Toronto, Canada
[3]Kinesiology & Physical Education, Wilfrid Laurier University, Waterloo, Canada
[4]Department of Kinesiology, University of Waterloo, Waterloo, Canada
[5]Heart & Stroke Foundation Centre for Stroke Recovery, Canada

INTRODUCTION

Improved walking function is the goal most often stated by individuals living with stroke [1]. Patients with residual impairments may utilize assistive devices, such as walkers, canes and ankle-foot orthotics (AFO) to achieve independent walking. Evidence shows that AFOs may have a beneficial effect by improving walking speed; however other important issues such as symmetry have not been addressed [2]. Gait symmetry measures can provide insight about the quality of walking function and may be used to inform treatment decisions. The purpose of this study was to compare spatial and temporal symmetry measures of gait between chronic stroke survivors who use an AFO and those who do not.

METHODS

Twenty-nine chronic stroke survivors (64.4±12.2 years old and 40.4±27.6 months post stroke) completed three walking trials at each of their preferred and fast speed over a pressure sensitive mat (GAITRite®, CIR Systems Inc., Pennsylvania, USA). Participants were encouraged to walk without any assistive devices if possible.

Gait symmetry ratios (affected limb/unaffected limb) were calculated for swing time, stance time and step length. Participants were stratified into two groups for the analysis; AFO vs. non-AFO. A two-factor repeated measures ANOVA was utilized to compare gait symmetry measures between groups and walking conditions.

RESULTS

Nine participants used an AFO; 3 prefabricated and 6 custom made AFOs. Within this group, seven participants used other walking aids; 5 canes and 2 wheeled walkers. Of the twenty people in the non-AFO group, 7 used a cane and 3 used a wheeled walker.

The main group comparisons for swing time symmetry revealed a significant effect ($p=0.021$). Average swing time symmetry for the AFO and no AFO groups are 1.47 and 1.2, respectively. Stance time symmetry was significantly different between AFO users and non-AFO users (0.85 and 0.94, $p=0.009$). Step length symmetry scores were not significantly different between groups ($p=0.182$). Comparisons between walking conditions were similar for all symmetry measures ($p>0.05$).

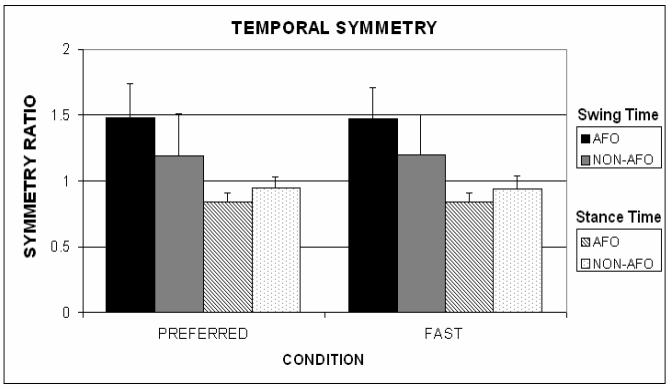

Figure 1: Swing and stance time asymmetry was significantly more severe for the AFO compared to the non-AFO group ($p<0.05$). A ratio of 1.0 indicates 'perfect' symmetry between limbs.

DISCUSSION AND CONCLUSIONS

Our analysis of gait symmetry revealed that stroke survivors who use an AFO demonstrate greater temporal asymmetry compared to non-AFO users. For example, the affected limb swing duration was approximately 1.5 times greater than the unaffected limb for the AFO group, as compared to 1.2 times for non-AFO users. Stroke survivors with asymmetric gait may be at increased risk for developing other musculoskeletal health consequences. Continued study is warranted for investigating immediate effects of AFOs on spatial and temporal gait asymmetry within stroke survivors.

REFERENCES

[1] Bohannon RW et al. (1988). Rehabilitation Goals of Patients with Hemiplegia. *Int.J.Rehabil.Res.* Vol **11**; p. 181-183.
[2] Leung J and Moseley A. (2003). Impact of ankle-foot orthoses on gait and leg muscle activity in adults with hemiplegia. *Physiotherapy*. Vol **89**(1); p. 39-55.

ACKNOWLEDGEMENTS

This work is support by NSERC, University of Toronto and CIHR operating grant. Also, we acknowledge the support of the Toronto Rehabilitation Institute which receives funding under the Provincial Rehabilitation Research Program from the Ministry of Health and Long Term Care in Ontario.

CLUB POSITION RELATIVE TO THE SWING PLANE SIGNIFICANTLY AFFECTS SWING DYNAMICS

Sasho MacKenzie
Department of Human Kinetics, St. Francis Xavier University, Antigonish, Canada, smackenz@stfx.ca

INTRODUCTION

It is common to read about the importance of being 'on-plane' during the golf swing. The correct plane of the golf swing has typically been illustrated using the orientation of the shaft at address, or the orientation of the shaft at impact. Perhaps neither the shaft position at address nor impact should be used to determine the swing plane? The club's position relative to these imaginary planes will not necessarily influence its motion during the swing. It may be more important to define the swing plane in a way that allows a greater understanding and prediction of the motion of the club. With this in mind, the swing plane may best be defined by the path traced out by the lead arm during the downswing. A three-dimensional (3D) model was used to investigate the importance of the positioning of the club relative to the swing plane formed by the motion of the lead arm. It was hypothesized that the position of the club relative to the swing plane would affect the model's ability to square the clubface for impact.

METHODS

A 3D, 4-segment (torso, upper arm, forearm, and club) forward dynamics model of a golfer was developed. Validity of a similar model has previously been established [1]. The model had four degrees of freedom: torso rotation, shoulder abduction, forearm supination, and ulnar deviation at the wrist. Autolev was used to generate the dynamical equations of motion into FORTRAN code according to Kane's Method. Three torque generators that adhered to the activation rate and force-velocity properties of muscle powered the torso, upper arm, and club segments. While the forearm was free to pronate and supinate, no muscular torques were present to directly produce these motions. The activation timing of each torque generator was optimized using a genetic algorithm to maximize clubhead speed at impact [1]. By manipulating the initial amount of forearm rotation, the affect of starting the downswing with the club 'above' and 'below' the swing plane was evaluated.

RESULTS AND DISCUSSION

Forearm angles of 9.6º and -5º (Fig. 1A), at the start of the downswing, placed the center of mass of the club 4.4 cm above and 4.4 cm below the plane, respectively (Fig. 1B).

If the center of mass of the club does not lie in the swing plane, then the component of force applied by the golfer to the club, within the swing plane, produces a torque on the club about the longitudinal axis of the lead arm. This torque will act until the center of mass of the club moves within the arm abduction plane. As the center of mass moves towards the arm abduction plane, the angular impulse generated by the torque creates angular momentum about the longitudinal axis of the lead arm (Fig. 1C). If the club was initially below the plane, then positive angular momentum is generated, which will aid in squaring the clubface at impact (Fig. 1A). If the club was initially above the plane, then negative angular momentum is generated, which will tend to prevent the clubface from squaring. It is important to note that the rotation of the forearm presented in this paper was generated in the absence of a muscle torque acting about the longitudinal axis of the lead arm. It seems likely that a properly timed muscle torque acting about the longitudinal axis of the lead arm would increase clubhead speed [1] but it is not necessary to attain the desired impact position with the club.

CONCLUSIONS

Minor deviations (< 5 cm) of the club from the swing plane can significantly affect the longitudinal rotation of the club, and thus a golfer's ability to square the clubface. The results also suggest that the club can rotate through 90º about the longitudinal axis of the forearm in order to square the clubface for impact without a muscular torque producing supination.

REFERENCES

[1] MacKenzie, SJ et al. (2009). A three dimensional forward dynamics model of the golf swing. *Sports Eng.,*11; p. 165-175.

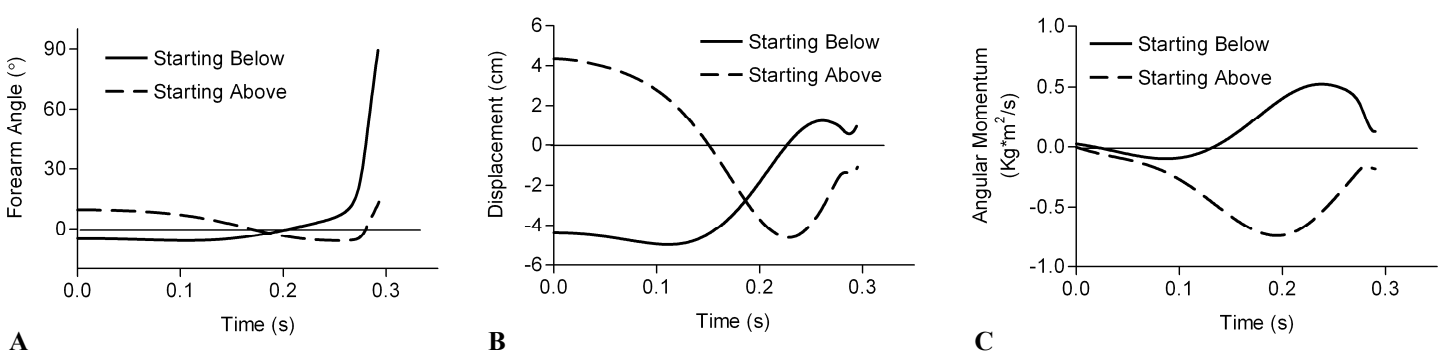

Figure 1: Each graph starts at the initiation of the downswing and ends at impact **A** Forearm rotation during the downswing. An angle of 90º at impact results in a square clubface **B** The distance from the club's center of mass to the plane traced out by the lead arm **C** Angular momentum of the golf club about the longitudinal axis of the forearm.

Kinematic Comparison of the Underwater Dolphin Kick Between Swimmers With Different Levels of Competitive Ability

Ryan Atkison, Volker Nolte
Health Sciences/Kinesiology, University of Western Ontario, London, Canada, ratkison@uwo.ca

INTRODUCTION

In order to be competitive in elite swimming competition, underwater dolphin kick (UDK) is considered an essential skill to master [1]. Despite obvious advantages of the UDK, swim researchers and coaches claim that the mechanics of UDK is poorly understood and is often overlooked in training [1,2]. Thus, there needs to be more research invested in understanding the mechanics of UDK and its application in training and competitions.

The purpose was to identify kinematic differences in the underwater dolphin kick between experienced swimmers within a broad range of competitive abilities, using a model which more accurately represents UDK trunk undulations than models used in previous kinematic studies.

METHODS

Participants were four male swimmers, selected based on highest level of competitive success: one international level, one national level, one provincial level, and one recreational, ages 26, 22, 19, and 46 respectively.

Each swimmer was filmed performing two 10m trials of UDK at maximum effort in a ventral position. Participants maintained a constant depth of 1m to minimize the interference of surface waves. All trials were initiated from an in-water start to eliminate the effect of a dive.

Trials were filmed from a Lorex CVC-6991 (Lorex Technology Inc., Ontario, Canada) underwater video camera (UVC) at 30 Hz. The UVC was positioned 7.5m from the initial impulse wall. Videos were digitized using HU-M-AN™ digitizing software (HMA Technology, Ontario, Canada) using an adapted 12 segment model for digitizing [3]. Centre of mass velocity (v_{CM}), frequency (*f*), amplitudes (*A*), and joint angles were calculated and correlated in Microsoft Excel™ (Microsoft Corporation, Washington, Canada).

RESULTS

Table 1 highlights the variability in basic kicking parameters between swimmers of different ability. Correlations reveal that *f* and toe *A* are not highly related to v_{CM} (r = 0.73, r = -0.02), but the product of *f* and toe *A* is highly related with v_{CM} (r = 0.91). Velocity of the CM is negatively correlated with large finger (r = -0.89), wrist (r = -0.80), elbow (r = -0.75), and shoulder (r = -0.76) *A*. Other amplitudes show no correlation with v_{CM}. Angle ranges in the torso and lower body are unrelated to v_{CM}, however, skilled swimmers showed different patterns of extension and flexion than non-skilled swimmers.

DISCUSSION AND CONCLUSIONS

Skilled swimmers seem to use thoracic extension to attenuate upper body amplitudes while maintaining large amplitudes in the lower body. Consistent with the literature, skilled swimmers show greater similarities between their upkick (hip extension phase) and downkick (hip flexion phase) than less skilled swimmers [1,3]. It has been shown that the basic kick parameters (i.e., toe amplitude and frequency) are insufficient in evaluating UDK [3]. Rather, a focus on full body motion, especially at the trunk is necessary.

REFERENCES

[1] Arellano, R., Terres-Nicoli, J., & Redondo, J. (2006). Fundamental hydrodynamics of swimming propulsion. *Revista Portuguesa de Ciencias do Desporto*, Vol 6; p. 15-20.
[2] Collard, L. & Oboeuf, A. (2009). Comparison of expert and nonexpert swimmers' opinions about the value, potency, and activity of four standard swimming strokes and underwater undulatory swimming. *Perceptual & Motor Skills* Vol 108; p. 491-498.
[3] Naskashima, M. (2009). Simulation Analysis of the Effect of Trunk Undulation on Swimming Performance in Underwater Dolphin Kick of Human. *Journal of Biomechanical Science and Engineering*, Vol 4; p. 94-104.

Table 1. Summary of the basic parameters of UDK. CM velocity, toe amplitude, and frequency are presented as the average for 3 kick cycles. Vertical toe velocity is the product of frequency and toe amplitude.

Subject	Trial	10 m Time (s)	CM Velocity (m/s)	Toe Amplitude (m)	Frequency (Hz)	Vertical Toe Velocity (m/s)
Rec Swimmer	1	7.32	1.07	0.68	1.64	1.12
	2	7.38	1.07	0.68	1.58	1.08
Provincial Swimmer	1	5.56	1.47	0.47	2.45	1.16
	2	5.69	1.51	0.51	2.38	1.21
National Swimmer	1	4.57	1.96	0.61	2.34	1.42
	2	4.32	1.93	0.61	2.25	1.37
Olympic Swimmer	1	4.40	1.85	0.68	2.22	1.51
	2	4.49	1.97	0.70	2.21	1.55

THE EFFECT OF DRAG SUIT TRAINING ON 50-M FREESTYLE PERFORMANCE

Andrew Dragunas[1], Volker Nolte[1], James P. Dickey[1]
[1]Department of Kinesiology, The University of Western Ontario, London, Canada, adraguna@uwo.ca

INTRODUCTION

Resistive training in sport predominantly comes in the form of weight lifting. However, some coaches believe that weight room training is not specific enough to movements performed in their sport. Therefore, sport specific resistance exercises have been developed. For example, swimmers use bungee cords and drag suits, while runners use sleds and weighted vests. The drag suit was introduced to swimming in the 1980's as a method to increase resistance in the water [1]. Little research has been performed on the biomechanics of drag suit training. The current study examined the effects of drag suit training (TYR 2.0 Resistance Trainer) on 50-m freestyle performance as quantified by stroke rate, distance per stroke, and final time.

METHODS

Figure 1: TYR 2.0 Resistance Trainer.
Adapted from: Swim-shop.com, 2008

18 subjects from the UWO varsity swimming team completed the study protocol (10 men, 8 women mean ± SD, age: 19.2 ± 1.38 years, men 50m freestyle personal best avg: 25.99 ± 0.98 seconds, women 50m freestyle personal best avg: 29.24 ± 1.80). Subjects were quasi – randomly divided into two groups; Resistance and Control. Subjects performed three sprint style training sets three times a week for five weeks as part of their normal training regime. The resistance group wore the drag suit for the sets and the control group wore typical training attire. The test consisted of two sets of six 50-meter sprints: one set with the drag suit and one set without. All trials were filmed from above in the spectator area. Stroke rate and distance per stroke were extracted from video using a Video Performance Monitor II (VPM) device (Yokohama Sports Development Institute Ltd, Japan), and final times were collected using manual stopwatches. A 2 x 2 Split-plot MANOVA was performed.

RESULTS

In the regular suit, the resistance group did not exhibit any significant ($p < 0.05$) changes in stroke rate (+0.2%) or distance per stroke (+0.5%) (Figure 2). However, the control group showed a statistically significant decrease in distance

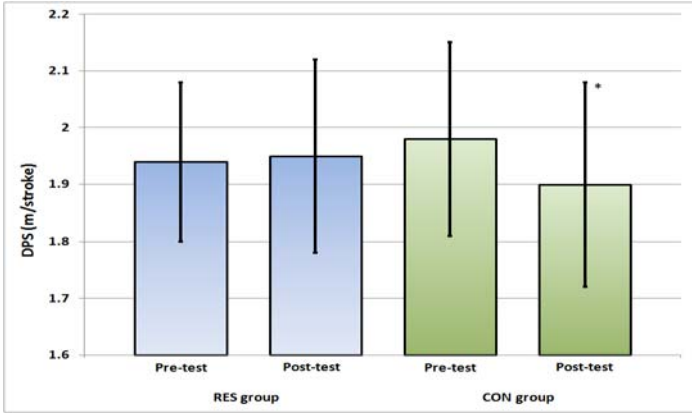

Figure 2: Pre and post-test results of distance per stroke (m/stroke) in the regular suit condition by group. The control group showed a significant ($p < .05$) decrease in distance per stroke at post-hoc test (*).

per stroke (-4%) and a significant change in stroke rate (+4%). In the drag suit condition, both the control and resistance group demonstrated significant ($p < 0.05$) decreases in distance per stroke, -6.3% and -3.5% respectively. Similar to results in the regular suit, only the control group showed a significant increase in stroke rate (6.4%) in the drag suit. The changes in final time were not statistically significant.

DISCUSSION AND CONCLUSIONS

In swimming, coaches desire athletes to maintain distance per stroke. Researchers have found that distance per stroke is the dominant factor in improved swimming performance [2]. This would be a strategy to enable swimmer to maintain velocity. We observed that drag suit training is an effective tool to maintain distance per stroke and stroke rate throughout training, since the resistance group showed no significant changes in the regular suit. Future studies should investigate the effect of drag suit and resistive swim training on swimming kinematics to gain an understanding of how the training effects swimming techniques.

REFERENCES

[1] Taguchi, N., Shibayama, H., & Miyashita, M. (1988). Added mechanical and physiological loads during swimming with a drag suit. Swimming Science V, Human Kinetics Publishers, c1988, p. 377-381
[2] Craig, A. B., & Pendergast, D. R. (1979). Relationships of stroke rate, distance per stroke, and velocity in competitive swimming. *Medicine and Science in Sports 11*(3), 278-283.

BIOMECHANICS OF THE CROSS-COUNTRY SIT-SKIER AND IMPACT ON SIT-SKI DESIGN
A TOP SECRET 2010 PROJECT

Marie-Pierre Leblanc-Lebeau[1,2,3], Denis Rancourt[1,2], Eve Langelier[1,2],
Marc-André Cyr[1,2,3], Jean-Luc Lessard[1,2] and Cécile Smeesters[1,2,3]
[1]Human Performance and Safety Research Group (PERSÉUS), Sherbrooke QC, Canada
[2]Department of Mechanical Engineering, Université de Sherbrooke, Sherbrooke QC, Canada
[3]Research Center on Aging, Sherbrooke QC, Canada
e-mail: Cecile.Smeesters@USherbrooke.ca web: http://eureka.gme.usherb.ca/perseus/

INTRODUCTION

In paralympic cross-country skiing, athletes in the sitting category compete on a sit-ski with 2 skis and use 2 poles. Even within this category there is a wide range of disabilities: from complete impairment of the lower limbs and minimal trunk muscle activity for LW10 sitting athletes, to only partial impairment of the lower limbs and normal trunk muscle activity for LW12 sitting athletes. Actual race time is thus multiplied by a percentage factor dependent on disability and the skier with the lowest calculated race time is the winner.

Disability obviously affects the muscle power produced by the athlete to increase and maintain speed, but for sit-skiers it also uniquely affects their ability to negotiate turns. An LW12 sit-skier can lean toward the inside of a turn to increase the centripetal force and thus avoid tipping over toward the outside of a turn. However, an LW10 sit-skier is physically unable to lean into a turn and can only avoid tipping over toward the outside of a turn by using his outside pole to push himself toward the inside of a turn. Their only other option is to slow down to negotiate turns, which is not the best strategy if they want to win a race.

The completely rigid structure of current sit-ski designs makes negotiating turns especially difficult. Indeed, whether it is because they under- compensate or over-compensate for a turn, sit-skiers will often find themselves precariously balancing on only one ski during turns, narrowly avoiding tipping over toward the outside or the inside of the turn. The purpose of this project was thus to improve sit-ski design to make it more stable and more agile during turns. To do so we studied the effect of adding a tilting mechanism to the sit-ski on maximum allowable turning velocities.

METHODS

So as to better understand the biomechanics of a cross-country skier negotiating a turn on a tilting sit-ski, a simple dynamic model was elaborated (Figure 1). We then determined the effect of centre of mass (h) and center of rotation (h_r) heights, turn radius (r) and lean angle of skier and sit-ski (θ) on the maximum allowable turning velocities (v_{max}) to avoid tipping over toward the outside of the turn:

$$v_{max} = \sqrt{rg\frac{t/2 - h - h_r \sin\theta}{h_r - h - h_r \cos\theta}}$$

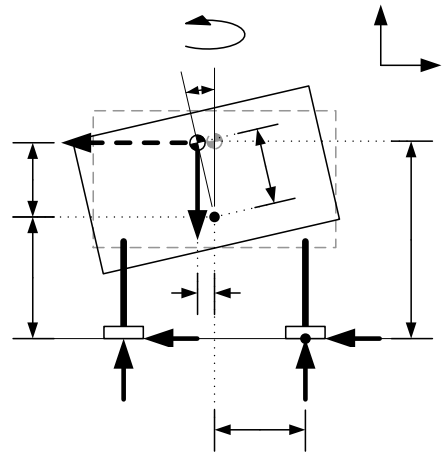

Figure 1: Free body diagram of a cross-country skier negotiating a turn on a tilting sit-ski. Internal (F_{zi} and F_{yi}) and external (F_{ze} and F_{ye}) ski forces, mass of skier and sit-ski (M), gravitational (g) and centripetal (a_y) accelerations, center of mass (h) and center of rotation (h_r) heights, distances between centre of mass and centre of rotation (y and h), distance between skis (t) and lean angle of skier and sit-ski (θ).

RESULTS

Our model showed that the maximum allowable turning velocity (v_{max}) to avoid tipping over toward the outside of the turn increased if centre of mass (h) and center of rotation (h_r) heights decreased, turn radius (r) increased and lean angle of skier and sit-ski (θ) increased.

DISCUSSION AND CONCLUSIONS

Therefore, to increase the maximum allowable turning velocity (v_{max}) a sit-ski with a tilting mechanism should have low centre of mass (h) and center of rotation (h_r) heights. A tilting sit-ski design would thus allow both skis to remain in contact with the ground when negotiating turns and could allow even LW10 athletes to lean toward the inside of a turn to go faster. These results were experimentally validated in the field and, to date, have resulted in a silver medal at the 2010 Paralympic Games in Vancouver.

ACKNOWLEDGEMENTS
This work was funded by the Own the Podium – Top Secret 2010 program from the Canadian Olympic Committee. We also thank the Canadian paralympic cross-country ski team.

BIOMECHANICS OF THE CROSS-COUNTRY SIT-SKIER AND IMPACT ON SIT-SKI DESIGN
A TOP SECRET 2010 PROJECT

Marie-Pierre Leblanc-Lebeau[1,2,3], Denis Rancourt[1,2], Eve Langelier[1,2],
Marc-André Cyr[1,2,3], Jean-Luc Lessard[1,2] and Cécile Smeesters[1,2,3]
[1]Human Performance and Safety Research Group (PERSÉUS), Sherbrooke QC, Canada
[2]Department of Mechanical Engineering, Université de Sherbrooke, Sherbrooke QC, Canada
[3]Research Center on Aging, Sherbrooke QC, Canada
e-mail: Cecile.Smeesters@USherbrooke.ca web: http://eureka.gme.usherb.ca/perseus/

INTRODUCTION

In paralympic cross-country skiing, athletes in the sitting category compete on a sit-ski with 2 skis and use 2 poles. Even within this category there is a wide range of disabilities: from complete impairment of the lower limbs and minimal trunk muscle activity for LW10 sitting athletes, to only partial impairment of the lower limbs and normal trunk muscle activity for LW12 sitting athletes. Actual race time is thus multiplied by a percentage factor dependent on disability and the skier with the lowest calculated race time is the winner.

Disability obviously affects the muscle power produced by the athlete to increase and maintain speed, but for sit-skiers it also uniquely affects their ability to negotiate turns. An LW12 sit-skier can lean toward the inside of a turn to increase the centripetal force and thus avoid tipping over toward the outside of a turn. However, an LW10 sit-skier is physically unable to lean into a turn and can only avoid tipping over toward the outside of a turn by using his outside pole to push himself toward the inside of a turn. Their only other option is to slow down to negotiate turns, which is not the best strategy if they want to win a race.

The completely rigid structure of current sit-ski designs makes negotiating turns especially difficult. Indeed, whether it is because they under- compensated or over-compensated for a turn, sit-skiers will often find themselves precariously balancing on only one ski during turns, narrowly avoiding tipping over toward the outside or the inside of the turn. The purpose of this project was thus to improve sit-ski design to make it more stable and more agile during turns. To do so we studied the effect of adding a tilting mechanism to the sit-ski on maximum allowable turning velocities.

METHODS

So as to better understand the biomechanics of a cross-country skier negotiating a turn on a tilting sit-ski, a simple dynamic model was elaborated (Figure 1). We then determined the effect of centre of mass (h) and center of rotation (h_r) heights, turn radius (r) and lean angle of skier and sit-ski (φ) on the maximum allowable turning velocities (v_{max}) to avoid tipping over toward the outside of the turn:

$$v_{\max} = \sqrt{rg\,\frac{t/2 + (h - h_r)\sin\phi}{h_r + (h - h_r)\cos\phi}}$$

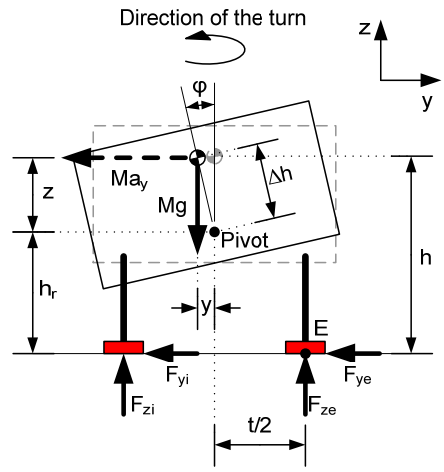

Figure 1: Free body diagram of a cross-country skier negotiating a turn on a tilting sit-ski. Internal (F_{zi} and F_{yi}) and external (F_{ze} and F_{ye}) ski forces, mass of skier and sit-ski (M), gravitational (g) and centripetal (a_y) accelerations, center of mass (h) and center of rotation (h_r) heights, distances between centre of mass and centre of rotation (z, y and Δh), distance between skis (t) and lean angle of skier and sit-ski (φ).

RESULTS

Our model showed that the maximum allowable turning velocity (v_{max}) to avoid tipping over toward the outside of the turn increased if centre of mass (h) and center of rotation (h_r) heights decreased, turn radius (r) increased and lean angle of skier and sit-ski (φ) increased.

DISCUSSION AND CONCLUSIONS

Therefore, to increase the maximum allowable turning velocity (v_{max}) a sit-ski with a tilting mechanism should have low centre of mass (h) and center of rotation (h_r) heights. A tilting sit-ski design would thus allow both skis to remain in contact with the ground when negotiating turns and could allow even LW10 athletes to lean toward the inside of a turn to go faster. These results were experimentally validated in the field and, to date, have resulted in a silver medal at the 2010 Paralympic Games in Vancouver.

ACKNOWLEDGEMENTS
This work was funded by the Own the Podium – Top Secret 2010 program from the Canadian Olympic Committee. We also thank the Canadian paralympic cross-country ski team.

CENTER OF MASS CONTROL IN PARALYMPIC ALPINE SKIING
A TOP SECRET 2010 PROJECT

Stéphane Martel, Denis Rancourt, Cécile Smeesters, Jean-Luc Lessard, Nicolas Huppé and Eve Langelier
Human Performance and Safety Research Group (PERSÉUS), Sherbrooke QC, Canada
Department of Mechanical Engineering, Université de Sherbrooke, Sherbrooke QC, Canada
e-mail: Eve.Langeliert@USherbrooke.ca web: http://eureka.gme.usherb.ca/perseus/

INTRODUCTION

Center of mass control is a critical issue in alpine sit-ski design. As a matter of fact, athletes constantly adjust the position of the combined skier – sit-ski center of mass over the ski in order to control the sit-ski trajectory.

Compared to able body skiers, disable skiers are significantly limited in their ability to control their center of mass. Aside from tilting the trunk fore and aft, they can use their upper limbs to control the center of mass. These control inputs must however not be used to offset an incorrect nominal center of mass location due to the particular sit-ski design.

METHODS

Given the variation in the location of the skiers' center of mass, an adequate sit-ski design must include sufficient features to adjust the nominal location of the center of mass. To that end, we have designed the support structure of the bucket with a fore and aft slider, which can be rigidly connected to the remaining structure at every 0.5 inch (Figure 1). That resolution was determined based on blinded tests with the athlete seated in the bucket, and the sit-ski connected to a standard alpine ski. A 2 inch cylinder was then inserted under the combined system and the bucket slider was positioned in such a way that when the system is at equilibrium, the cylinder is in the middle of the bindings.

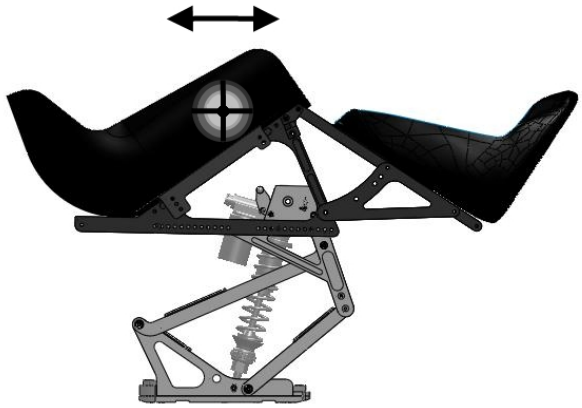

Figure 1: Fore and aft slider on the bucket.

However, the previous approach does not take into account suspension movements that occur during racing which can lead to significant center of mass motion depending on sit-ski design. Again, one does not want the skier to compensate for suspension effects on the center of mass motion. To that end, we optimized the four bar linkage design in order to minimize fore and aft center of mass motion during suspension compression.

RESULTS

Repeatability in identifying the nominal location of the center of mass of the skier – sit-ski system on the 2 inch cylinder was within 0.5 inch. However, results showed that although a nominal positioning of the skier – sit-ski system was successful, further adjustments were required during training and depended on the racing discipline.

Our four bar linkage design provides less than 1 inch of fore and aft center of mass motion during suspension compression (Figure 2). Based on athletes' feedback, such motion can be easily compensated by body segment movements. Our four bar linkage design also led to satisfactory behaviour in jump situations, leading to negligible rotational velocity at take-off.

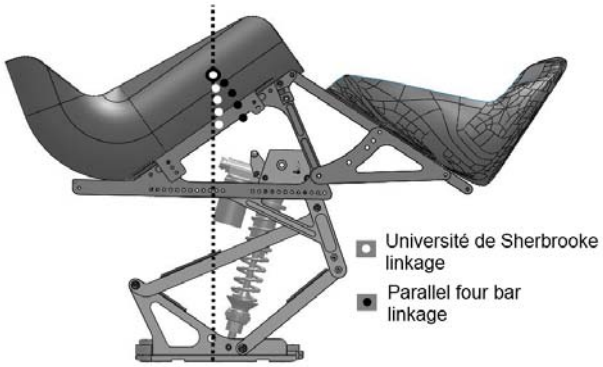

Figure 2: Center of mass motion during compression of the suspension.

DISCUSSION AND CONCLUSIONS

A combined fore and aft slider on the bucket with a properly dimensioned four bar linkage design provides sufficient center of mass management to avoid offsetting center of mass location by control inputs. To date, these features have resulted in a silver medal in slalom at the 2010 Paralympic Games in Vancouver.

ACKNOWLEDGEMENTS
This work was funded by the Own the Podium – Top Secret 2010 program from the Canadian Olympic Committee. We also thank the Canadian paralympic alpine ski team and the Eastern Townships Disabled Skiers Foundation.

MECHANISMS OF WHIPLASH INJURY PREVENTION ATTRIBUTABLE TO ENERGY-ABSORBING SEAT

Paul C. Ivancic[1] and Ming Xiao[1]
[1]Biomechanics Research Laboratory, Department of Orthopaedics and Rehabilitation,
Yale University School of Medicine, New Haven, CT, USA; email: paul.ivancic@yale.edu

INTRODUCTION

Motor vehicle crashes remain the leading cause of spinal injury. In attempt to reduce whiplash injuries, manufacturers have incorporated active injury prevention systems in newer automobiles, such as the Whiplash Protection System (WHIPS) introduced by Volvo in 1998. Epidemiological studies have indicated potential benefits of WHIPS in reducing neck injury risk between 21 to 47%, as compared to conventional seats. The majority of previous biomechanical studies were manufacturer-sponsored or contain limited data. The goals of this study were to investigate whiplash injury prevention mechanisms attributable to WHIPS using simulated rear crashes of a Human Model of the Neck (HUMON).

METHODS

HUMON consisted of a neck specimen (n=6) mounted to the torso of BioRID II and carrying a custom anthropometric head stabilized with muscle force replication (**Fig. 1**). HUMON was seated and secured in a 2005 Volvo XC90 minivan seat, which included WHIPS and a fixed head restraint. The main components of the WHIPS recliner included the energy-absorbing element; return spring; and pivot shaft, guide pin, and window for control of WHIPS motion. The WHIPS was activated by HUMON's momentum pressing into the seatback during the crash, causing rearward translation and extension of the seatback relative to the seat base and plastic deformation of the bi-lateral energy-absorbing elements. Rear crashes (9.9, 12.0, and 13.3 g) were simulated and motions of the head, neck, torso, pelvis, sled, seatback, and WHIPS were monitored. Significant increases ($P<0.05$) in the spinal motion peaks relative to physiologic limits were determined.

Fig. 1. Photograph of the Human Model of the Neck (HUMON) and rear crash apparatus.

RESULTS

- Average WHIPS motions are presented graphically for the 13.3 g crashes (**Fig. 2**). For all crashes, rearward and upward translations of the WHIPS guide pin within the control window were observed, with peaks reaching 4.1 cm for -Tz and 1.6 cm for +Ty, occurring as early as 76 ms. Motions of the seatback relative to the sled consisted of extension and rearward and downward translations. Peak plastic deformation of the energy-absorbing elements, ranging between 0.6 and 1.2 cm, occurred at 72 ms. WHIPS motion caused simultaneous: rearward and downward translations and extension of the seatback; deformation of the bi-lateral WHIPS energy-absorbing elements; and reduction in distance between the head and head restraint.

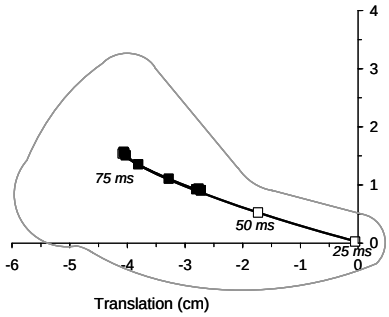

Fig. 2. Average motions of the right WHIPS guide pin during the 13.3 g rear crashes.

- A 42% reduction in peak T1 horizontal acceleration, as compared to sled acceleration, demonstrated the energy-absorbing capacity of WHIPS.
- Average peak C7/T1 rotations significantly exceeded physiologic limits during the 13.3 g crash. The cervical spine maintained its S-shaped curvature throughout the duration of contact of the head with the head restraint. Lower cervical spine injuries due to excessive motion may occur prior to or during contact of the head with the head restraint, even in the presence of WHIPS.

DISCUSSION AND CONCLUSIONS

The present study provided insight into the crash-dynamics of the occupant, seatback, and WHIPS. These data may be useful for refining seat design to reduce neck injuries. Future whiplash injury prevention systems will most likely integrate beneficial design features, such as active head restraint and energy-absorbing seat, with more advanced features, such as accident avoidance technology.

ACKNOWLEDGEMENTS

This research was supported by grant 5R01CE001257 from the Centers for Disease Control and Prevention (CDC).

TEMPORAL ACTIVATION LAGS OF ADJACENT FIBRE COMPARTMENTS SUGGEST SEPARATE BIOMECHANICAL FUNCTION AND CONTROL IN IPSILATERAL LUMBAR ERECTOR SPINAE

Marilee Nugent[1*], Theodore E. Milner[1]
[1]Department of Kinesiology & Physical Education, McGill University, Montreal, Canada, *marilee.nugent@mail.mcgill.ca

INTRODUCTION

A problem with simplified models of trunk muscle function and control is that they may omit important aspects of voluntary trunk movements such as the neuromotor system's capacity for very specific resolution of segmental articulation. The muscles that extend the lower back are generally believed to activate synchronously as a functional unit. Structure and innervation of this muscular region suggest the possibility of more segmentally specific biomechanical function [1, 2, 3] than has previously been found in simple spine bending tasks [4, 5]. In pilot studies we found temporal asynchrony of erector spinae (ES) activation between lower thoracic and lumbar levels during specific bellydance movements. The goal of the present study was to determine whether we could record even finer levels of segmental specification of control within ipsilateral lumbar spine extensors.

METHODS

Twelve healthy female subjects ranging from 4 weeks to 29 years of training in bellydance were recruited to perform two frontal plane "figure 8" pelvic isolation movements (maya and serpentine) differing in direction of motion. The movement cycles were performed at frequencies of .5, .7 and 1 Hz. Eight custom-made bipolar surface electrodes were placed on the right lumbar region to record activity in multifidus, longissimus thoracis and iliocostalis lumborum at all lumbar vertebral levels (L1 to L5). Two comparison tasks—forward bends/rises and alternating side bends—were also recorded. By-trial cross correlations between recorded EMG signal pairs were performed to calculate lags representing differences between muscle activation times.

RESULTS

Results showed four temporal patterns of activation, corresponding with the four tasks and consistent across subjects and levels of training (Figure 1). Forward bends showed synchronous ES activation across lumbar levels. Side bends showed ~190 ms earlier activation at L4-L5-multifidus compared to activation synchrony at higher lumbar levels. For one figure 8 direction (maya), muscle activity recorded below the third lumbar (L3) spinal level occurred an average of ~800 ms prior to muscles recorded from the four electrodes above L3. In the other figure 8 direction (serpentine), this pattern was reversed, with the muscles recorded below L3 firing an average ~500 ms later than muscles above L3. These temporal activation patterns characteristic of the figure 8 movements were not dependent on level of training in the .5 Hz tempo condition. The pattern of asynchrony was reduced or disappeared completely in some advanced subject trials in the 1 Hz (faster tempo) condition. Certain subjects, across training levels, could not achieve asynchrony in one of the figure 8 tasks, with resulting lags all near zero as in forward bends.

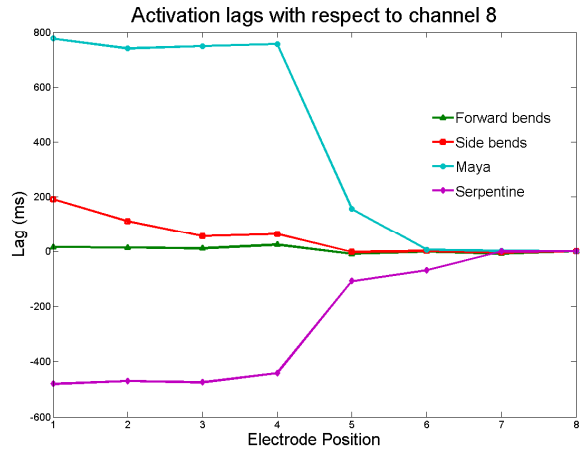

Figure 1: Temporal activation lags at each electrode compared to electrode 8.

DISCUSSION AND CONCLUSIONS

Complex multi-segmental trunk coordination tasks elicit temporal asynchronous activation of ipsilateral lumbar spine extensors above and below L3. This temporal asynchrony is interpreted as two separate ipsilateral control signals being directed to separate muscle compartments with differing biomechanical functions at adjacent levels of the lumbar ES. The control patterns required to perform the movements appear to be innate and not a function of learning, despite observable differences in performance between novice and trained dancers. However, loss of asynchrony at faster tempos suggests greater control difficulty at specifying individual compartments. The findings provide support for previous dissection studies that have suggested the possibility of specific biomechanical functional capabilities in different portions of the lumbar ES and thus a compartmental independence of control not previously elucidated in spine extensor function studies using simpler tasks.

REFERENCES

[1] Macintosh, J. E., & Bogduk N. (1986). The morphology of the lumbar erector spinae. *Spine* Vol 12 (7); pp. 658-668.
[2] Bogduk, N. (1980). A reappraisal of the anatomy of the human lumbar erector spinae. *Journal of Anatomy* Vol 131 (Pt 3); pp. 525-540.
[3] Bustami, F. M. (1986). A new description of the lumbar erector spinae muscle in man. *Journal of Anatomy* Vol 144; pp. 81-91.
[4] Jonsson, B. (1973). Electromyography of the Erector Spinae Muscle. *Medicine and Sport* Vol 8; pp. 294-300.
[5] Donisch, E. W., & Basmajian, J. V. (1972). Electromyography of deep back muscles in man. *American journal of anatomy* Vol 133 (1); pp. 25-36.

THE EFFECTS OF ACTIVE RELEASE TECHNIQUE® ON TIGHT HIP FLEXOR GROUPS WITH AND WITHOUT LOW BACK PAIN

Daniel Avrahami[1], Jim R. Potvin[1]
[1]Department of Kinesiology, McMaster University, Hamilton, ON, Canada
dr.danavrahami@gmail.com

INTRODUCTION

The iliopsoas complex is structurally and functionally important in providing spine stability [1]. Many low back pain patients present with a tight and shortened iliopsoas complex [2]. A common treatment by many clinicians is to correct this dysfunction by lengthening the iliopsoas complex through a technique named Active Release Technique® (A.R.T®).

METHODS

Four treatments of A.R.T® were performed on two groups of subjects (asymptomatic tight hip flexor group (A-THF) and a low back pain tight hip flexor group (LBP-THF)), over a two week period, and various outcome measures were take and compared with a control group (CON). The outcome measures for this study included: 1) maximum voluntary trunk flexor and extensor moments ($Flex_{Max}$ and Ext_{Max}), 2) disability and pain measurements (Roldand-Morris Disability Questionnaire (RMDQ) and 10-cm Visual Aanalogue Scale (VAS)), 3) passive hip extension mobility and 4) trunk muscle EMG measurements during an Unstable Standing (US) perturbation.

RESULTS

There was a significant short term and sustained improvements in trunk $Flex_{Max}$ and Ext_{Max}. Comparing baseline values for Ext_{Max} with day 2, 3, 4 and 5, there were sustained increases of 18.3%, 14.2%, 12.9% and 25.0% respectively. The effects immediately after each treatment demonstrated significant increase in Ext_{Max} on day 1, 3 and 4, by 20.6%, 11.9% and 12.3% respectively. The baseline values of $Flex_{Max,}$ compared with day 1 and day 2 post-treatment results, showed an increase of 12.8% and 10.9% respectively. The LBP-THF group demonstrated a reduction in disability by 2.8 points on the RMDQ (55%) and pain by 2.9 points on the VAS (65%) over the course of the treatment program. There was a significant increase in passive hip extension over the course of the treatment program for the LBP-THF and A-THF groups by 13.1° (±1.1°) and 8.0° (±1.0°) respectively. The US perturbation trials for both THF groups showed a decrease in muscle activity (%MVE) for the external oblique, internal oblique, thoracic erector spinae, lumbar erector spinae, multifidus and gluteus maximus by 1.8%, 1.6%, 2.3% and 1.5% respectively.

Figure 1: Active Release Technique® of the iliopsoas complex

DISCUSSION AND CONCLUSIONS

The outcome measures from this study are very promising to support the utilization of A.R.T® for tight hip flexor patients, with and without low back pain. Some of the theories for the mechanism behind the therapy include: 1) restoring the patient's normal fascio-muscular interface, 2) decreasing the inhibitory effect on the hip flexors antagonist and surrounding trunk musculature, 3) removing excessive, painful spinal compression and 4) removing the fear-avoidance behaviour of the subjects. The results from this study demonstrated improvements in trunk strength, decreases in disability and pain, increases in passive hip extension mobility and normalization of average trunk muscle activity.

REFERENCES

[1] Juker,D., McGill,S., Kropf,P., and Steffen,T. (1998) Quantitative intramuscular myoelectric activity of lumbar portions of psoas and the abdominal wall during a wide variety of tasks. *Med.Sci.Sports Exerc.* **30,** 301-310.
[2] Janda,V. Muscle weakness and inhibition (pseudoparesis) in back pain syndromes. *Modern Manual Therapy of the Vertebral Column.* Churchill-Livingston., New York. 1986.

ACKNOWLEDGEMENTS

None

LUMBAR MOTION AND MUSCLE ACTIVITY ON THE ELLIPTICAL TRAINER DIFFERS FROM WALKING

Janice Moreside, Stuart McGill
Spine Biomechanics Laboratory, Dept. of Kinesiology, University of Waterloo, Waterloo, Canada

INTRODUCTION

The elliptical trainer has gained widespread popularity as a low impact exercise modality. However, anecdotal evidence indicates that it provokes low back pain in a segment of the population. The purpose of this study was to analyze the effect of different hand positions, stride length and speed on spine kinematics and muscle activity on the elliptical trainer and compare them with those found in walking.

METHODS

Forty healthy males (age: 27 ± 3, height: 178 ± 7 cm, mass: 79 ± 13 kg) who were free of back or hip pain volunteered to participate. Surface EMG signals were collected from 16 trunk and gluteal muscles, and processed as a % of MVC. Participants were asked to exercise on the elliptical trainer [Octane Fitness LLC™ MN, USA], while hand position (3), speed (2) and stride length (2) were randomly varied. Motion was captured with Vicon MX System [Vicon Motion Systems, Oxford, UK] with orthopaedic angles being processed with Visual 3D™ software [C-Motion, Inc., MD, USA]. Walking trials were collected at a self-selected speed. For each of the 3 lumbar axes and forward lean, a 2X2X3 repeated measures ANOVA was used to determine significant effects. Peak and minimum EMG for each of the muscles was similarly processed with a repeated measures ANOVA. Bonferroni adjustments were applied.

RESULTS

Using the elliptical trainer resulted in more lumbar twist, flexion/extension and average forward lean than walking, but less lateral bend. Hand position, stride length and velocity significantly affected motion (Table 1, Figure 1). All muscles demonstrated greater peak activations on the elliptical compared to walking, with Glut Med and Glut Max showing the highest (51% and 32%MVC compared to 17% and 10% MVC respectively in walking).

DISCUSSION AND CONCLUSIONS

Speed of elliptical trainer, stride length and hand position affect forward trunk lean and total spine motion about the 3 orthopaedic axes of flexion/extension, lateral bend and twist.

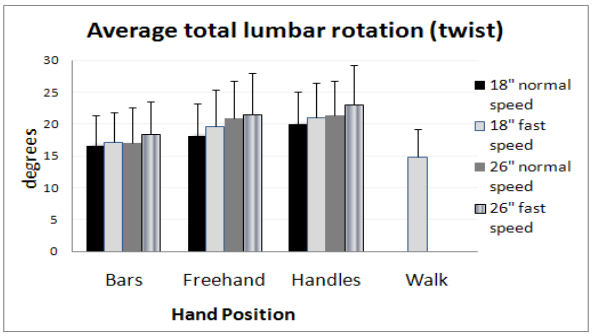

Figure 1: Average lumbar twist on the elliptical compared to walking; demonstrating the effect of changing hand position, speed, and stride length.

Specifically, an increase in speed resulted in greater trunk motion in all axes except lateral bend. Increased stride length produced more spine motion in all 3 axes, but did not significantly affect the average forward lean. The effect of hand position varied with the axis: the greatest lumbar flexion angle was elicited when holding onto the bars, the least with freehand. Both total flexion/extension and lumbar twist increased from bars to freehand to handles, but only significantly so with rotation. Freehand elliptical resulted in the greatest lateral bend angles, nearing those found in walking. Muscle activation levels in all muscles except rectus abdominis were significantly greater on the elliptical than walking, while demonstrating a strong phasic pattern: despite the higher %MVC, each showed an average minimum %MVC of less than 2.8%.

In conclusion, the elliptical trainer elicits lumbar spine motion and associated muscle activity which differs from walking. While providing a good muscular challenge, especially of the gluteal muscles, the user is cautioned to be aware of velocity, stride length and hand position modulators on spine motion and choose appropriately for the goals and capabilities of the user.

ACKNOWLEDGEMENTS

This research was supported by funding from NSERC.

Table 1: Significance levels for the effect of speed, stride length and hand position on average total lumbar motion in the 3 axes, as well as average forward lean.

	Speed	Stride length	Hand position	Significant interactions
Avg. flexion (forward lean)	0.005*	0.070	0.001*	Stride/hand 0.000*
Total flexion/extension	0.000*	0.000*	0.343	----------
Total lateral bend	0.074	0.000*	0.000*	Stride/hand 0.005*
Total rotation (twist)	0.001*	0.000*	0.000*	----------

PREDICTING VERTEBRAL SHEAR FAILURE TOLERANCES FROM MORPHOLOGY AND BONE DENSITY

Samuel J. Howarth and Jack P. Callaghan
Department of Kinesiology, University of Waterloo, Waterloo, ON, Canada, sjhowart@uwaterloo.ca

INTRODUCTION

The ability to predict spine joint failure strength is critical for both submaximal in-vitro injury testing and to provide individualized injury risk biomechanical models. Previous work has related vertebral body ultimate compressive failure tolerance with endplate area and measures of bone density [1,2]. The current investigation develops and tests a predictive model for ultimate anterior shear failure of the porcine vertebral joint.

METHODS

Forty porcine functional spinal units (FSUs) (C34 and C56) were tested. Facet angles and pars interarticularis (PI) length were measured from x-rays taken with respect to the transverse and sagittal planes. Bone density and cross sectional area for the PI were obtained using peripheral quantitative computed tomography (Orthometrix Inc., NY, USA). Measurements of the exposed endplates and posterior elements were also made using digital calipers. Specimens were mounted in aluminum cups using a combination of screws, steel wire and dental plaster for testing. A compressive load equivalent to 15% of the FSUs predicted compressive failure tolerance was applied (Instron, ON, Canada) while shear displacement was applied to each FSU at 0.15mm/s with two linear actuators (Tolomatic Inc., MN, USA) interfaced with brushless servomotors (Danaher Motion Inc., VA, USA) until ultimate failure. Vertebral kinematics were obtained at a rate of 128Hz from infrared emitting markers (Northern Digital Inc., ON, Canada) attached to metal plates that were rigidly affixed to the FSU vertebral bodies. Shear forces were measured at 1024Hz with uniaxial load cells (Transducer Techniques Inc., CA, USA). Each FSU was randomly assigned to either the prediction generation or testing group. Two factor analyses of variance (SAS Institute Inc., NC, USA) were performed to determine if differences existed between the prediction testing and generation groups. Stepwise linear regression was performed to identify the contributing factors to the predictive model for ultimate anterior shear failure.

RESULTS

None of the morphological measurements or average shear failure loads were statistically different between prediction generation and testing groups ($p \geq 0.1319$). Stepwise regression identified the superior PI length, facet angle and cortical bone area as the three measures for the regression model's first three steps (Table 1).

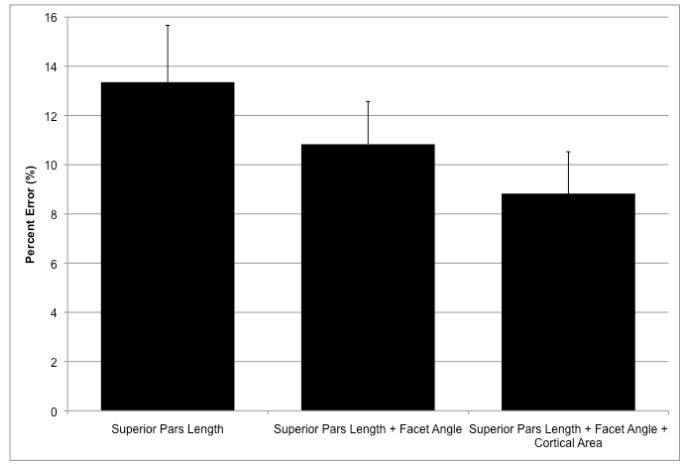

Figure 1: Percent error, for each regression model, between predicted and measured shear failure tolerances for the prediction testing group.

Prediction error decreased with successive steps in the regression analysis from 13.4% (one variable) to 8.8% (three variables (Figure 1).

DISCUSSION AND CONCLUSIONS

Bone density was not pivotal when predicting ultimate shear failure tolerance. Relative error magnitudes and explained variance of the predictive regression equations from this investigation are similar to prediction models developed for compressive loading [1]. The two-factor regression equation can be used as an effective method to scale shear load magnitudes in future repetitive loading studies as a percentage of the predicted failure tolerance. Future work should investigate possible relationships between the morphological factors identified in the current investigation and other factors such as bodymass, age and gender.

REFERENCES

[1] Biggemann M et al. (1988). Prediction of the compressive strength of vertebral bodies of the lumbar spine by quantitative computed tomography. *Skeletal Radiol* 17(4); 264-9.
[2] Parkinson RJ et al. (2005). Estimating the compressive strength of the porcine cervical spine: an examination of the utility of DXA. *Spine* 30(17); E492-8.

Table 1: Equation coefficients and explained variance from stepwise regression. X_1 = superior pars interarticularis length (mm); X_2 = facet angle (degrees); X_3 = cortical bone area (mm^2).

	Intercept	X_1	X_2	X_3	Partial R^2	Model R^2	p
STEP 1	181.12171	144.29936			0.4432	0.4432	0.0014
STEP 2	-1566.61338	140.84439	39.19734		0.1234	0.5666	≤0.0418
STEP 3	-1981.47622	137.88987	38.57859	12.97971	0.1194	0.686	≤0.0254

EFFECT OF THE RUPTURE OF THE TRANSVERSE LIGAMENT ON THE BIOMECHANICS OF THE CERVICAL SPINE IN COMPRESSION

Wissal Mesfar[1], Kodjo Moglo[1]
[1]Department of Mechanical Engineering, Royal Military College of Canada, Kingston, Canada, kodjo.moglo@rmc.ca

INTRODUCTION: The transverse ligament (TL) in the cervical spine is the primary structure acting as a stabilizer of the cranio-vertebrae joint and may be a subject of injuries and failure [1,2]. The atlas-dens interval exceeding 3 mm was found as an implication of either/both TL and Alar ligament failure [1]. However, the effect of the failure of the TL on the biomechanics of the head and neck complex is not widely studied. The aim of this study is to identify the role of the TL and the effect of its failure on the kinemactics and the kinetics of the head and neck complex under a static compressive load.

METHODS: A 3D nonlinear head and neck (HN) complex finite element (FE) model was developed and constructed based on a male adult, 39 years old, CT scan and MRI images. The FE model consists of bony structures (head, cervical vertebrae (C1-C7) and the first thoracic vertebra (T1)) and their cartilage facets joints, intervertebral discs and all the ligaments. The TL is modeled as a bundle and all the other ligaments are each modeled by a number of uniaxial elements with nonlinear material properties. The bony structures were considered as rigid bodies while the discs, each consisting of annulus and nucleus, were modeled with hexa solid elements. Both the cartilage and discs were modeled with homogenous isotropic material. For stable unconstrained boundary conditions, T1 is fixed while the cervical vertebrae and the head are left free. A compressive load (CL) was applied up to 57N at the centre of mass of the head. The analysis is performed for two cases; intact and ruptured TL.

RESULTS: The cervical spine moves anteriorly, proximally and flexes under CL. The anterior and proximal displacement and the flexion increase substantially in the case of the ruptured TL and when the CL increases (Fig. 1). At 40N CL, corresponding to the average of an adult head weight, an increase of 4 mm in the anterior displacement of the head was computed in the ruptured TL case. The flexion of the vertebrae according to T1 increases with CL and when the TL is ruptured. The flexion of the head reaches 9.6˚ and 11.5˚ and 24˚ and 29˚ at 40N and 57N CL and for the intact and injured case, respectively. The contact force (CF) increased with CL and was higher at the level of C1/C2 than C0/C1. It increases significantly after 40N at the level C1/C2 when the TL is ruptured and reaching 95N for the intact case and 120N for the ruptured TL case (Fig. 2). It was noticed that this contact force was nil for all other levels between the facets joints. In the intact case, the CF between the dens and the TL increased with CL and reaches 22.5N at 57N (Fig. 2).

DISCUSSION AND CONCLUSIONS: The CL on the HN complex joint induces a flexion, anterior and proximal displacements of the head and vertebrae. The lateral displacement and the two other rotations were found to be very small due to the asymmetry of the HN complex in the sagittal plane. The role of the TL was evaluated by the TL/Dens CF (Fig. 2). This CF restrains C1 to slide on C2 anteriorly. The absence of this CF affects not only the kinematics of the entire HN complex but also the magnitude of CF especially at the level C1-C2. The CF is nil at all the levels between C2 and T1 when the HN complex flexes. Indeed, the facets undergo a widening when the HN complex flexes; this is in good agreement with the experimental study [3].

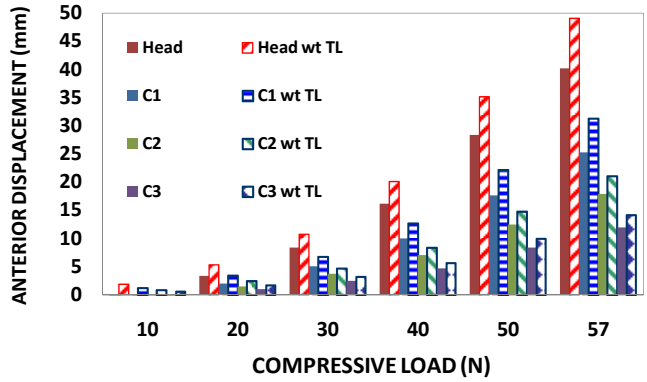

Figure 1: Displacement of the head and vertebrae under CL for two cases, intact and ruptured TL (wt TL).

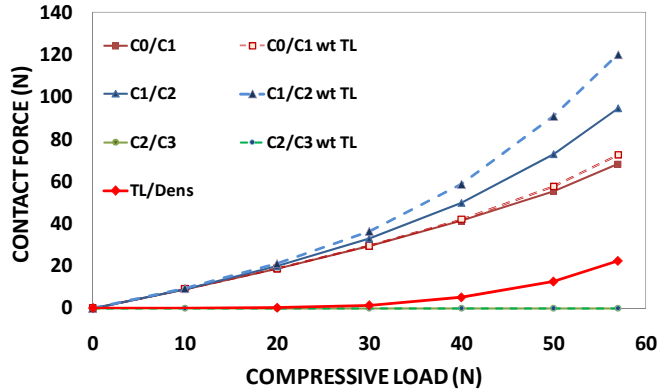

Figure 2: Total contact force at the facets joints (intact and ruptured TL cases) and at the TL/Dens (intact case) under CL.

REFERENCES

[1] Fielding JW *et al*. (1974). Tears of the transverse ligament of the atlas. A clinical and biomechanical study. *J. Bone Joint Surg. Am.*, Vol **56**(8); p. 1683-91.
[2] Heller JG *et al*. (1993). Transverse ligament failure: A biomechanical study. *J Spinal Disord*., Vol. **6**; p. 162–165.
[3] Wheeldon JA *et al*. (2006). Experimental flexion/extension data corridors for validation of finite element models of the young, normal cervical spine. *J Biomech*., Vol **39**(2); p. 375-80.

ACKNOWLEDGEMENTS: This study was supported by Department of National Defence, Aerospace Engineering.

HIP ABDUCTOR ACTIVATION AND COORDINATION WITH ABDOMINAL MUSCLES DURING WALKING IN CHRONIC LOW BACK PAIN AND ASYMPTOMATIC INDIVIDUALS

Algarni-Fahad S [1*], Hanada. EY [2*], Hubley-Kozey CL [3*]

[1*] King Saud University, Riyadh, Saudi Arabia, F.Algarni@Dal.Ca
[2*] Dalhousie University, Halifax, Canada
[3*] Dalhousie University, Halifax, Canada

INTRODUCTION

The importance of hip musculature in chronic low back pain (CLBP) may come from its significant role in transferring external forces from lower limbs to the spine in upright activities as well as providing lumbar-pelvic stability. CLBP patients have been shown to have neuromuscular impairments, and walking is a good model to study neuromuscular function as spinal stability demands are dynamically changing. Few studies have investigated trunk and hip muscle activation during walking in CLBP. There have been studies, albeit not walking studies reporting that GM had different muscle activation in LBP individuals compared to healthy individuals. As well, GM activation can be used as a predictor of LBP problems [1]. No study so far has examined GM muscle activation amplitudes or muscular coordination (co-activation synergism [2]) of abdominals and gluteus medius (GM) muscle in CLBP patients during walking. The research aims were to compare hip abductor muscle activation amplitudes between those with and without CLBP and to investigate whether there was coordination among hip abductor and abdominal oblique muscle sites.

METHODS

Electromyographic data were collected from (14) participants with a history of CLBP and (14) matched controls (CON) with no history of LBP. Both groups were 28 years old and mean BMI for CON (24.5 kg/m²) and CLBP (25.6 kg/m²) were not statistically different. Surface electrodes were placed over the anterior, middle, and posterior fibres of external (EO), internal oblique (IO), and GM bilaterally using standardized procedures. All participants walked on a pressure-sensor mat connected with the GAITRite™ system (CIR System Inc., Clifton, NJ, USA) to determine gait cycles during walking at a self-selected walking speed. Root mean square amplitudes for the right stance phase were normalized to maximums (NRMS). Ensemble average (EA) curves were calculated for the full wave rectified, low pass filtered (6 Hz) signals for 1.5 strides for each muscle site. A two (2×2) factor mixed model ANOVA tested differences between sides and groups for NRMS amplitudes of GM muscle (α=0.05). Coefficient of variation (CV) of the EA waveforms was calculated to quantify variability of the muscle activation pattern for each group. Correlation coefficient (r) were calculated between the waveforms of each oblique site and the GM and between the two sides for the GM. Confidence intervals were calculated for each group to assess coordination in temporal activation patterns among muscle pairs for each group.

RESULTS AND DISCUSSION

CLBP group reported mild disability (RMDQ,median=3, range 0 to 8) and low to moderate pain (VAS,median=4, range 3 to 7). T-test revealed no significant difference ($p>0.05$) between control and CLBP individuals' average self-selected walking speed (140.8±2.1 cm/s, 136.5±29.1 cm/s; respectively). CLBP group had a trend toward slightly lower NRMS amplitudes in both right and left GM but no significant differences ($p>.05$) between groups. Muscle activation patterns for hip abductor muscle did not differ functionally between those with CLBP and those without as shown from their temporal activation curves. Both groups had two peaks of GM coincide with ipsi-lateral heel strike. The CLBP group had higher CV of GM compared to controls. Positive correlations between sides illustrate co-activation synergy whereas negative correlation indicates trade-offs[2]. Significant correlations were recorded between right and left ipsi-lateral GM and the posterior fibers of EO for CON (r=.55-.60) and CLBP (r=.70-.79) indicative of a co-activation synergy. Significant negative correlations were found between right and left GM in both groups (r=-.40) indicating a trade off relationship between sides. All other correlations were not significant except a low negative (r=-.15 to -.17) between right IO and right GM in both groups.

CONCLUSION

GM muscle activation amplitudes during stance phase were similar between the CLBP and CON groups. This contrasts differences reported between groups for other muscles. Walking velocity was similar between groups in the present study possibly explaining this finding. Both groups were qualitatively similar in muscular activation patterns for GM muscle. CLBP group had higher variability compared to CON group for GM muscle. Heterogeneity of the location and duration of pain and disability may explain this variability. High muscular coordination among the posterior fibers of external oblique and hip abductor muscle pairs indicate synergies for both groups, although slightly higher for CLBP.

ACKNOWLEDGEMENTS

Funding from the Capital Health Research Fund and the Capital District Health Authority's Department of Medicine UIMRF Junior Investigator Grant.

REFERENCES

[1]Nelson-Wong E. *et al*., (2008). Gluteus medius muscle activation patterns as a predictor of low back pain during standing Clin Biomech (Bristol, Avon).23:545-553.

[2] Sirin & Patla, (1987) Myoelectronic changes in the triceps surae muscle under sustained contractions: Evidence for synergism. Eur. J. of Appl. Phys.56:238-44.

TEMPORAL RECRUITMENT PATTERNS REMAIN ALTERED IN INDIVIDUALS WITH A LOW BACK INJURY THAT RETURN TO WORK

Heather L. Butler[1], Cheryl L. Hubley-Kozey[1] and John W. Kozey[2]
[1] Schools of Physiotherapy and [2] Health and Human Performance, Dalhousie University, Halifax, NS, CANADA
hbutler@dal.ca

INTRODUCTION

The high rate of recurrent work related low back injuries (LBI) that become chronic suggest objective diagnosis and prevention of *repeated* episodes should be a research focus. Thus, the purpose of this study was to determine neuromuscular and biomechanical differences between asymptomatic controls and individuals with recurrent LBI that have returned to work. A secondary purpose was to examine sex differences.

METHODS

Fifty-four asymptomatic (females=57%) and 34 non-specific sub-acute (6±3weeks post-injury) LBI subjects (females=62%) provided informed consent. Surface electromyograms (EMG) were recorded from 12-bilateral trunk muscle sites: upper and lower rectus abdominus; anterior, lateral and posterior external oblique; internal oblique; longisimus and iliocostalis at spinal levels (L1,L3); multifidus and quadradus lumborum. Participants performed a right to left horizontal transfer task in maximum reach using a 2.9 kg load. Subject's spine and trunk motion were monitored throughout the movement using a FOB™ system (Ascension Technology, Burlington, VT) attached at T8, L5 and the iliac crest. A series of maximal voluntary isometric contractions (MVIC) were performed for normalization purposes.

EMG signals were amplified (AMTI-8, Bortec, Calgary, AB) and digitized at 2000 Hz using Labview™ . Angular motions were recorded at 50 Hz. Data processing algorithms were written in Matlab™ . EMG signals were corrected for subject bias and gains, full wave rectified, low pass filtered (Butterworth, zero lag, 6Hz), and time and amplitude (MVIC) normalized. Principal patterns (PP) were extracted from the measured EMG waveforms using pattern recognition techniques and *PPscores* were computed for each waveform (1). Separate analysis of variance models tested for sex, muscle and group main effects and interactions ($\alpha = 0.05$) for the abdominal and back extensor *PPscores*. Bonferonni post hoc tests determined pair wise differences.

RESULTS

No significant differences were found in total motion of the trunk or pelvis ($p>0.05$). Four PPs explained 98% of total variance. PP1 captured overall magnitude and PP2 captured an asymmetric response. PP3 showed a change in activity at the beginning and end of the movement while PP4 captured changes during the beginning, middle and end (Figure 1).

For the abdominals, there was a significant ($p<0.05$) group effect for PP1 and PP3, muscle-sex interaction for PP1, PP2 and PP3 and ***group-sex-muscle*** interaction for PP4. LBI subjects recruited their abdominal muscles with a higher overall magnitude with females showing sustained activity of the right external oblique muscle sites throughout the motion (Figure 2 A).

For back extensors, there were significant main effects for group, sex and muscle for PP1 as well as group and muscle for PP3. Also, there were significant muscle-sex (PP2) and ***group-sex-muscle*** (PP4) interactions ($p<0.05$). LBI subjects recruited their back muscles with higher overall magnitude with males having a more prolonged activation pattern (Figure 2 B).

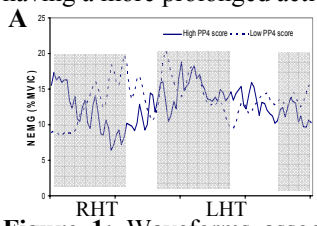

Figure 1: Waveforms associated with a "high" (solid) and "low" (dotted) PP4 *scores*. Right-hand transfer (RHT); left-hand transfer (LHT) phases.

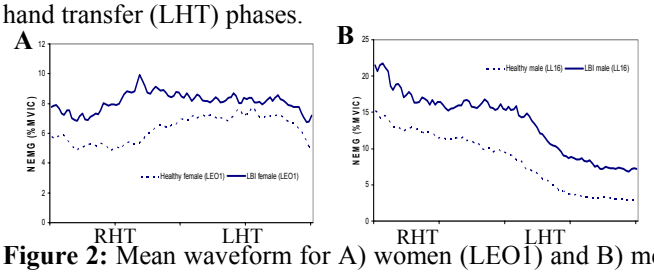

Figure 2: Mean waveform for A) women (LEO1) and B) men (LL16). Dotted is for healthy controls and solid for LBI.

DISCUSSION AND CONCLUSIONS

Despite similar task performance, altered temporal activation patterns were associated with LBI subjects that had returned to work. Interestingly, was that these altered patterns were sex specific. It appears that injured women co-activate their abdominals longer throughout the movement, whereas injured men co-activate their back extensors. These residual neuromuscular impairments may help to explain why individuals with a LBI tend to reinjure their back. Overall, these results suggest that therapeutic exercise goals for LBI patients should be individualized and based on objective neuromuscular findings.

REFERENCES

[1] Hubley-Kozey C and Vezina M (2002). Differentiating temporal electromyographic waveforms between those with chronic low back pain and healthy controls. *Clin Biomech* 17(10); p. 621-9.

ACKNOWLEDGEMENTS

Nova Scotia Health Research Foundation and Workers' Compensation Board of Nova Scotia.

MONITORING UPPER LIMB ACTIVITY DURING STROKE REHABILITATION WITH ACCELEROMETERS

Jeremy W. Noble, Janice J. Eng, & Debbie Rand
Department of Physical Therapy, University of British Columbia, Vancouver BC, Canada, Jeremy.Noble@vch.ca

INTRODUCTION

Recently accelerometers have been used to document activity levels over long periods of time [1]. These types of accelerometers have been used outside the laboratory to document the levels of upper limb and locomotor activity needed to accomplish activities of daily living (ADLs).

There are many ADLs that require bilateral use of the upper limbs to accomplish, which is often difficult for patients who have hemiparesis due to a stroke. The goal of this study is to document the activity of the upper limbs following stroke and apply a new analysis technique document the amount of time that individuals use each hand individually or a combination of both hands to accomplish a task. Measurements were taken at four different time points: immediately following admission to a rehabilitation hospital, after discharge from the rehabilitation program, and at 6 month and 12 months periods following discharge.

METHODS

A group of 22 patients (mean age = 57.8 yrs) who had experienced a stroke were recruited following admission to two rehabilitation centres. Participants wore Atical accelerometers (Mini-Mitter Co, USA) on each wrist to measure upper limb activity These accelerometers are the size of a wristwatch and log the total number of activity counts that occur every minute. A threshold filter is built in to record an activity count if the acceleration reaches a pre-determined level [2]. Participants wore the accelerometer for 4 consecutive days, on four occasions: at admission to the rehabilitation centre, following discharge from rehabilitation, and at six and twelve months following discharge. Data for this study was analyzed from a 12 hour window (8am-8pm) for the third day of wearing the accelerometer. Data was also collected and analyzed from 31 healthy older adults (mean age = 70.9 yrs).

For each minute of the analysis period the total number of activity counts was recorded, and a laterality index was calculated to show hand use preference for that minute (Laterality index = [R-L]/[R+L]). Data was organized such that the data from the paretic limb was represented by the right hand. To analyze how the of the laterality index varied over the day an amplitude probability distribution function (APDF) was used.

A repeated measures ANOVA was used to identify differences in activity points at across the time points and the probability levels at laterality indices of 0.7, 0.3,0, -0.3 & -0.7 to represent various levels of bilateral arm use.

RESULTS

There was a significant difference in the total number of activity counts at the 6-month and12-month follow-up periods when compared to the admission and discharge periods for both the affected and unaffected arms ($p < 0.05$).

The APDFs showed that the majority of the activity took place with the unaffected arm at the admission and discharge times, and activity became more bilateral during the follow-up periods. There as no statistically significant effects in the APDF data, due to high between subject variability.

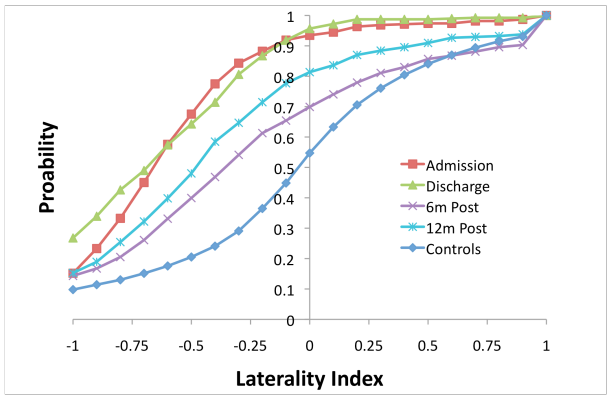

Figure 1: Example APDF illustrating that arm use occurred primarily with the unaffected hand at admission and discharge, and a shift to more bilateral use at the 6-month and 12-month time points. Average data is also shown for the older adults.

DISCUSSION AND CONCLUSIONS

The overall amount of activity increased at the 6 and 12 month periods following discharge, and tended to become more bilateral in nature. There was a large degree of variability in the APDF plots, which may be accounted for with factors such as the severity of the hemiparesis and whether the affected hand was the patients dominant hand.

REFERENCES

[1] Rand et al (2009). *Stroke* Vol **40**(1); p. 163-8.
[2] Uswatte et al. (2000) *Stroke.* Vol **31**(3); p. 662-7.

EVALUATION OF THE STEPPING LIMB CENTRE OF PRESSURE ON FOOT CONTACT DURING VOLITIONAL AND PERTURBATION-EVOKED STEPPING

Jonathan C. Singer, Stephen D. Prentice, William E. McIlroy
Department of Kinesiology, University of Waterloo, Waterloo, Ontario, jcsinger@uwaterloo.ca

INTRODUCTION

Compensatory stepping reactions are considered essential responses to recovering dynamic stabilty. While much research has focussed on the prevalence, onset and direction of such rapid stepping, there has been very little directed to the stabilizing events that occur after foot-contact. The occurence of multiple stepping, an index of instability, is likely associated with the control of stability after foot-contact. Specific research exploring compensatory stepping reactions to anteroposterior (AP) perturbations of standing balance have shown that these movements generally lack anticipatory postural adjustments [1], which may challenge mediolateral (ML) dynamic stability control, leading to multiple stepping. The present study focussed on advancing our understanding of the events that occur on foot contact, which may represent the earliest opportunity to alter ML centre of mass (COM) trajectory and velocity to control dynamic stability.

As a foundation for future work examining older adults, the aim of the present study was to characterize the centre of pressure (COP) on foot contact, under the stepping limb, during both volitional and perturbation-evoked stepping in young adults. We believed the inability to pre-plan movement parameters in perturbation trials should challenge stability control on foot contact and would lead to increased ML root mean square COP displacement (RMS-D), mean power frequency of COP displacement (MFP-D) and trial-to-trial variability, relative to volitional stepping trials. Secondarily, given research demonstrating adaptive responses to repeated perturbations [2], we believed that, over time, the magnitudes of these variables in the perturbation trials would diminish. This would further reinforce the need to expose individuals to 'novel' perturbations to maintain ecological validity.

METHODS

Four force platforms (AMTI, MA, USA), arranged in a rectangular array, were used to record reaction forces and moments during quiet stance and during/after stepping. Participants performed 30 trials for both volitional (VOL) and perturbation-evoked (PERT) stepping conditions. Prior to stepping, participants stood comfortably with feet shoulder-width apart. For VOL trials, a verbal command was given to prompt participants to take a single step with their preferred leg and, upon landing, maintain a stable position for 5 seconds. For PERT trials, participants wore a chest harness and were anchored to a rigid frame via a cable. An initial forward lean angle was established, standardized to a cable load of 15% body weight. The cable was released at random intervals. Participants were asked to regain their balance using a single step and maintain a stable position for 5 seconds.

RMS-D and MPF-D were calculated for each trial, using 3 seconds of data from the stepping-limb force platform, beginning at foot-contact. Trials were separated into 3 bins of 10 consecutive trials and mean trial-to-trial variability was calculated. Each variable was subsequently entered into a two-way repeated-measures ANOVA.

RESULTS

Contrary to our hypothesis, there were no differences in ML RMS-D by trial or condition. Trial to trial variability of RMS-D did, however, decrease in the PERT condition between the first and second blocks of trials and then became stable between second and third blocks (Figure 1). There were no changes in trial to trial variability in RMS-D within the VOL condition. There were also no differences by trial or condition in MPF COP displacement or trial-to-trial variability.

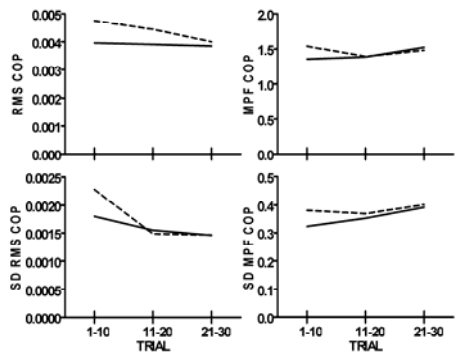

Figure 1: Mean (top) and standard deviation (bottom) of ML RMS-D (left) and MPF-D (right) for PERT (dashed) and VOL (solid).

DISCUSSION AND CONCLUSIONS

The lack of differences in RMS-D both between conditions and within the PERT trials would indicate that, on average, the magnitude of the AP perturbation utilized in this study poses little challenge to ML dynamic stability in this particular sample. However, the reductions in trial-to-trial variability in later trials in the PERT condition highlight adaptive changes with repeated exposure to the perturbation. These changes could involve various control parameters such as step width. These results also stress the importance of using only the initial trials when examining the effects of COM perturbations.

REFERENCES

[1] McIlroy, WE, et al. (1993). Neurosci Lett. Vol 164(1-2); p. 199-02.
[2] McIlroy, WE, et al. (1995). Gait Post. Vol 3; p. 43-50.

POSTURAL RESPONSES TO MULTIDIRECTIONAL PERTURBATIONS TO THE HAND DURING STANCE

Ali Forghani[1], Sheida Rabipour[2], Theodore E. Milner[2] and Paul J. Stapley[2]

[1]Department of Biomedical Engineering, [2]Department of Kinesiology and Physical Education

McGill University, Montreal, Quebec, Canada

INTRODUCTION

Humans are easily able to maintain their balance while applying force with their hands to move or stabilize objects. Based on Newton's laws, the applied force must be counteracted by ground reaction force (GRF) to maintain balance. However, because the GRF is partitioned between the two legs there is no unique solution. Furthermore, central nervous system (CNS) can employ an infinite number of muscle activation patterns to achieve ground reaction force (GRF) vectors needed to satisfy both the task-level goal and balance. This study examines the postural response when hand position must remain stable as an external force is applied in different directions during normal stance. We investigated whether the CNS uses an invariant strategy to compensate for forces acting in different directions.

MATERIALS AND METHODS

Ten healthy subjects participated in the present study. Subjects stood at their normal stance width on two multi-axis force plates while grasping the handle of a two degree-of-freedom robotic manipulandum with the dominant hand. A 6-axis force-torque sensor attached to the handle measured the reaction forces applied by the subject. The position of the handle was displayed on a monitor 50 cm from the subject. Surface EMG was sampled at 1 KHz bilaterally from leg muscles and unilaterally from the muscles of the dominant arm. At the beginning of each trial the subject was instructed to move the cursor into a target window and hold it there for a period of 4 seconds, during which a ramp-and-hold force was applied to the hand. There were 48 trials, comprising 8 force directions presented in random order. Force and EMG were analyzed for 3 intervals: 1) 500 ms before the increase in hand force 2) 100-300 ms from the onset of the force 3) 500 ms during the steady-state hold.

RESULTS

A typical steady-state response for one subject is shown in Figure 1. For each subject, the average GRF and root-mean-square EMG during interval 1 were calculated and subtracted from the corresponding values in intervals 2 and 3. The horizontal GRFs from individual trials and the average EMG across trials are plotted in polar coordinates as functions of the direction of applied force at the hand. The GRF directions and magnitudes are not uniformly distributed, unlike the force applied to the hand, although the resultant GRF vector is equal and opposite to the hand force for all directions (Figure 1A). The activity of leg muscles appears to be strongly tuned for specific hand force directions.

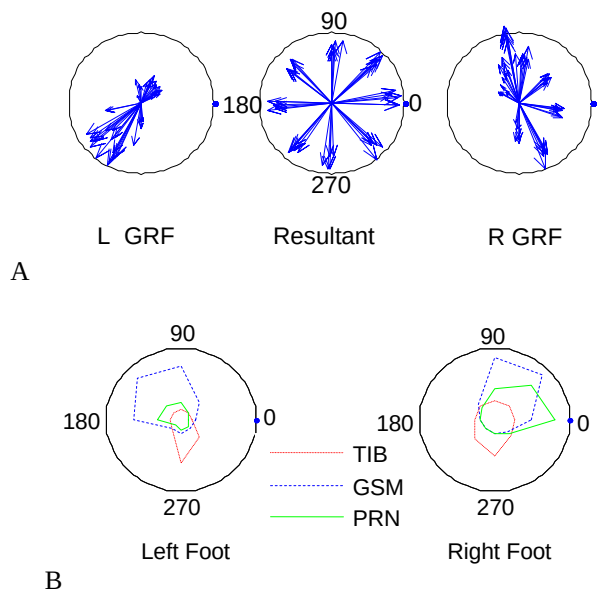

Figure 1: (A) GRF vectors, (B) EMG tuning curves

DISCUSSION AND CONCLUSIONS

GRFs of the left and right foot tend to be oriented in opposite directions with large components that cancel force but create torque. This may be needed to cancel torque created by the force applied to the hand. Similar GRF features have been reported to unexpected perturbations of the support surface [1]. Muscle tuning curves were narrowly tuned with a direction of maximum activation that showed mirror symmetry across the legs. The principal difference in muscle activation between legs is seen in Peroneus longus. Its action may be responsible for the difference in the medial/lateral component of the GRF between the left and right legs.

REFERENCES:

[1] Henry SM, Fung J, Horak FB (2001). Effect of stance width on multidirectional postural responses, *J Neurophysiol 85:559-570*

Assessment of the Postural Control Strategies Used to Play Two Wii Fit^{TM} Video Games

A. Michalski[1], C.M. Glazebrook[1], A.J. Martin[1], W.W.N. Wong[1], A.J.W. Kim[1], K. Moody[1,2]
N. Salbach[1], B. Steinnage[1,2], J. Andrysek[2], R. Torres-Moreno[1,2], K.F. Zabjek[1,2]
1. Department of Physical Therapy, University of Toronto, Toronto, Canada, k.zabjek@utoronto.ca
2. Bloorview Kids Rehab, Toronto, Canada

INTRODUCTION

Virtual reality, biofeedback and postural pertubation systems have been used widely to retrain motor function in different clinical populations.[1,2] The Wii Fit^{TM} Video Game (Nintendo of America, Redmond, Washington, USA) has the potential to be a useful rehabilitation tool for training dynamic balance control. This is of significant relevance for populations that have asymmetric weight bearing such as amputees. Before implementing the Wii Fit^{TM} rehabilitation tool, it is necessary to evaluate the movement and postural control strategies healthy young adults use when playing Wii Fit^{TM} video games. This is a necessary step because it is currently unknown which games challenge balance in a functionally appropriate manner. The objectives of this study are to: 1) evaluate the postural control strategies healthy young adults use when playing *Ski Slalom* and *Soccer Heading* games on the Wii Fit^{TM}; 2) compare the postural control strategies healthy young adults use across the first versus tenth trials of *Ski Slalom* and *Soccer Heading* games (Wii Fit^{TM}).

METHODS

Sixteen healthy young adults were recruited to participate in this research study (10 female, 6 male, aged 24 ± 2 years). Each participant attended one testing session in a Biomechanics and Assistive Technology Laboratory. During this session participants were asked to play 10 consecutive trials of Ski Slalom and Soccer Heading games on the Wii Fit^{TM}. The order of the games played was randomized. While playing each game, the participant stood on the Wii Fit^{TM} balance board which was situated on a multi-axial AMTI force-plate (A-Tech, Scarborough, ON). This force plate recorded the moments, and ground reaction forces which were used to calculate the Centre of Pressure (COP). The 3D motion of 14 individual body segments was tracked using a 32 reflective markers and a multi-camera Vicon Motion Capture system (Vicon, Denver, CO, USA). A Myomonitor IV (Delsys Inc, Boston, USA) was used to record surface EMG of 14 muscles of the lower extremities. Root mean square (RMS) over the duration of the first and tenth trials was calculated for the following parameters: 1) Medial Lateral (ML) COP displacement; 2) ML position of the Shoulders in relation to the Pelvis; 3) Rotation and Tilt of the Pelvis and Shoulders. A 2 Game x 2 Trial repeated measures analysis of variance was used to determine differences between the first and last game played and between games. Future EMG analysis will explore muscle activation patterns.

RESULTS

Centre of Pressure: Medial-Lateral Displacement

Significant main effects were observed for game ($F(1, 14)=19.7$, $p < 0.001$), and trial ($F(1, 14)=5.59$, $p<0.05$). This included a greater ML displacement for Soccer Heading vs Ski Slalom and decreased ML displacement from first to tenth trial. There was a significant interaction game by trial effect ($F(1,14)=70.46$, $p<0.0001$). *Specifically, Soccer Heading* increased vs *Ski Slalom* decreased across trials. There was no difference between games at the first trial, but a difference does exist at the tenth trial (See Figure 1.)

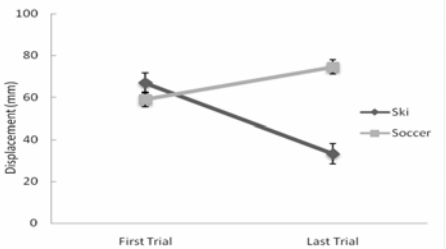

Figure 1: Centre of Pressure displacement in the ML direction for the first and tenth trial for 15 participants who played the *Skii Slalom* and *Soccer Heading* games**.**

Segment Motion: A significant main effects for game ($F(1,14)=5.67$, $p<0.05$), and trial ($F(1,14)=21.64$, $p<0.001$) were observed for ML displacement of the shoulders in relation to the Pelvis. Where, *Ski Slalom* led to greater coupling between shoulder and pelvis movement compared to *Soccer Heading* (individual game average across trials: 42.9 mm vs 61.7 mm). The coupling improved significantly from the first to the last trial. (individual trial average across games: 70.3 mm vs 34.3 mm). Additional changes in pelvic and shoulder tilt and rotation were also noted.

DISCUSSION AND CONCLUSIONS

Participants exhibited postural control strategies that were specific to the *Ski Slalom* and *Soccer Heading* games. Some of these strategies became more distinct as the participants gained experience with each game. Specifically: *Ski Slalom:* Participants demonstrated a tighter strategy to control their posture that was evident by decreased displacement of the COP and decreased rotation/tilt of the pelvis, shoulders and coupling between these two segments. *Soccer Heading:* Increased ML displacement of the COP suggests that participants altered their postural control strategy and challenged their limits of stability. These adopted postural control strategies highlight the clinical potential of the Wii Fit^{TM} video games to train balance control in patient populations such as amputees who have asymmetric weight bearing, and those who would need to challenge their limits of stability.

REFERENCES

[1] **Elion, O., et al.,** (2008). Virtual Reality, 50-53.
[2] Van Ooteghem, K., et al., (2008). Experimental Brain Research, 187, 603-611.

RESIDUAL FORCE ENHANCEMENT FOLLOWING STRETCH OCCURS IN A SINGLE SARCOMERE

Tim Leonard[1] and Walter Herzog[2]
[1]Kinesiology, University of Calgary, Calgary, Canada email: leonard@ucalgary.ca
[2]Kinesiology, University of Calgary, Calgary, Canada

INTRODUCTION

The force length relationship (1) and the cross bridge model of muscular contraction (2) predict that the isometric steady state force produced at a given sarcomere length will result solely from the amount of actin and myosin filament overlap present. However, a contracting muscle stretched to some final length produces more force than a muscle contracting purely isometrically at the same final length. Although several mechansims have been proposed for this property (typically refered to as residual force enhancement), such as the recruitment of a parallel elastic element and a change in the force produced by cross bridges, the most popular explanation for this force enhancement has been the "popping sarcomere" theory (3). In this theory, it is assumed that when a muscle is actively stretched, some sarcomeres become overly long (they pop) and are supported by passice structures exclusively, while others shorten little or not at all and are able to produce the enhanced force. The popping sarcomere theory is appealing for its simplicity but no direct experimental evidence exists to support it. Others have shown that although sarcomere length non-uniformites do exist in actively stretched muscles, popping of sarcomeres is not necessary for force enhancement to occur (4). Arguably the best way to test the popping sarocmere theory is by mechanically isolating a single sarcomere and stretch it actively and see if force enhancement is achieved without the sarcomere popping. The purpose of this study was to test if force enhancement could indeed be observed in a preparation consisting of a single sarcomere.

METHODS

Single sarcomeres were isolated from myofibrils of rabbit psoas (n=8). The isolated sarcomere showing clear A- and I-band regions and z-lines was attached at one end to a glass needle and a piezotube motor, while the other end was attached to a nano-lever force sensor of known stiffness (347 nN/µm). The sarcomere was situated on the stage of an inverted microscope with phase contrast optics and a 100 X objective (N.A. 1.3) with a 2.5 X optovar (Zeiss Axiovert 200M, Germany) equipped with a high resolution (6.7 nm/pixel) line scan camera (SK10680, Schafter and Kirschoff, Germany). Solutions and tissue preparation procedures are published elsewhere (5) but briefly, a high calcium solution (pCa 3.5) was used for activation and a low calcium concentration solution (pCa 8) was used for relaxation of the sarcomere.

Since the plateau of the force length relationship for rabbit psoas is from about 2.2 to 2.4 µm, all tests were started at this initial sarcomere length. Myofibrils were then activated, held isometrically for 15 seconds and then stretched approximately 1µm at a speed of 0.1 µm/sec followed by a hold at the new length of 20 seconds.

RESULTS

Each sarcomere was activated and its force was normalized to the isometric force prior to stretch and the corresponding sarcomere length in accordance with Gordon et al. (1). The steady state force at the stretched was greater for all sarcomeres than the initial force at the plateau or initial part of the descending limb (Figure 1).

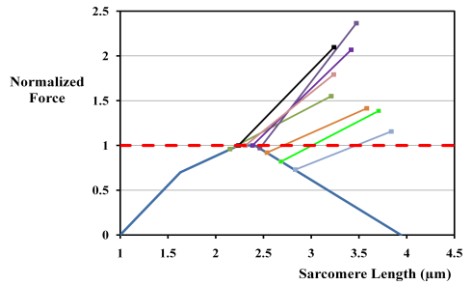

Figure 1: Normalized isometric steady state forces of 8 single sarcomeres before and after an active stretch of approximately 1 µm. Note that the purely isometric reference force prior to stretching was always substantially smaller than the force after stretching despite the loss of actin-myosin filament overlap during the stretch, and an expected decrease in isometric force (1, 2).

DISCUSSION AND CONCLUSIONS

Here we show for the first time force enhancement following stretch in a single sarcomere. Forces in the enhanced state do not merely exceed the expected forces at the final sarocmere lengths, but in all cases exceed the purely isometric forces at the initial lengths and the measured (or theoretically derived (1)) isometric forces at the plateu of the force-length relationship. This observation uniquely demonstrates that sarcomere "popping" cannot be the cause for this observation as we deal with a single sarcomere preparation. The results also exclude the idea that we have a non-uniformity between the two halves of the sarcomere, as the shorter half cannot exceed the purely isometric force at the plateau of the force-length relationship. Sarcomere popping and/or the development of sarcomere length non-uniformity has been thought to be the reason for residual force enhancement for more than 30 years, but this study proves that this theory cannot be correct.

REFERENCES

[1]Gordon et al. (1966) *J. Physiol* Vol **184**(Issue); p. 170-92.
[2]Huxley, A. (1957) *Prog. Biophys & Biophys Chem*. Vol **7**;p. 255-318.
[3]Morgan, D. (1990) *Biophys J.* **57**; p. 209-221.
[4]Joumaa et al. (2008) *Proc. R. Soc. B* 275; p. 1411-1419.
[5]Rassier et al. (2003) *Proc. R. Soc. B* 270; p. 1735-1740.

ACKNOWLEDGEMENTS

CIHR, NSERC, Canada Research Chair Program, CFI

NOVEL PROPERTIES OF TITIN IMMUNOGLOBULIN DOMAIN FROM HUMAN CARDIAC MUSCLE

Mike DuVall[1], Matthias Amrein[2], Jessica Gifford[3], Walter Herzog[1]
[1]Human Performance Lab, University of Calgary, Canada, mmduvall@ucalgary.ca
[2]Medicine, University of Calgary, Canada
[3]Biological Sciences, University of Calgary, Canada

INTRODUCTION

In North America, cardiac muscle diseases such as heart attacks and myopathies are financially burdensome and have a high incidence of mortality. In an attempt to contribute to work in this area, we have focused on a critical cardiac muscle protein called titin (connectin). Titin is responsible for all of the physiological passive force produced within muscle sarcomeres [1] by acting as a molecular spring that prevents muscle damage that may occur via over-extension. Titin is the largest protein known to date (3-4 Mda), and has the ability to vary its length in several different ways. By adjusting titin's extensible region, a muscle can vary its elastic properties and capability to produce the force necessary to withstand muscular stretch. One way for this passive force regulation is through calcium interaction. The calcium dependent elasticity of titin has been principally attributed to the PEVK region of titin [2], however other regions remain untested. We hypothesize that the immunoglobulin (Ig) domains of titin, have the potential to explain titin's calcium regulate passive force.

METHODS

E. Coli was used to produce the 27th Ig domain (I27) from the I-band region of human cardiac titin. Nickel charged column chromatography was performed to isolate his-tagged proteins. Fluorescence spectroscopy was conducted on tryptophan π electrons using a Hitachi™ F-2000 wavelength scanning spectrofluorimeter at 295nm. Atomic force microscopy (AFM) was done using a JPK™ (JPK Instruments, Berlin, Germany) AFM and software on an inverted Zeiss light microscope (Carl Zeiss Canada Ltd, Toronto, Canada).

RESULTS

Experiments using fluorescence spectroscopy revealed a distinct change in the microenvironment of the I27 protein when a physiological level of calcium was introduced. This calcium sensitivity arose from observations of π electron delocalization in the aromatic group of tryptophan. With the introduction of EDTA, a calcium chelating agent, the fluorescence intensity improved indicating reversibility. Using single molecule AFM, we evaluated the difference between Ig domain unfolding behaviour by stretching domains in the presence (Figure 1) and absence of calcium. The calcium induced conformational change mechanically translated into three novel properties: i – increased spring stiffness, ii – increased average force required for unfolding, iii – greater distance between forced unfolding events.

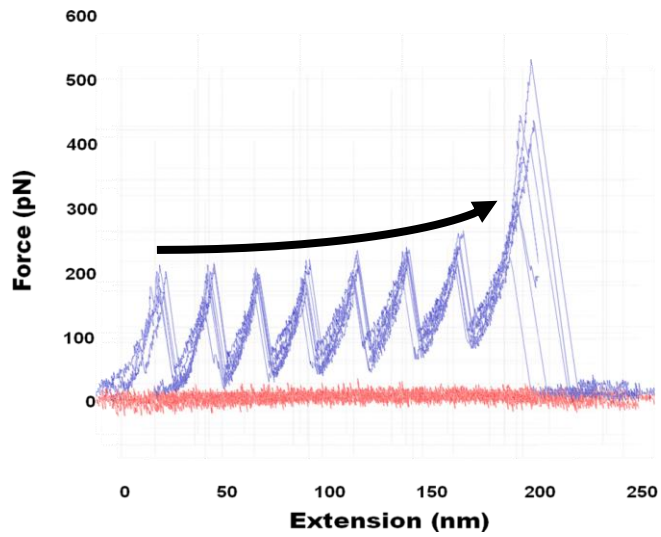

Figure 1: Seven overlapping force curves for I27 in the presence of Ca^{2+}. Pulling speed: 1µm/sec, 0.01M [Ca^{2+}]. Note the reproducibility of the gradual increase in force with Ca^{2+}

DISCUSSION AND CONCLUSIONS

Tryptophan fluorescence suggests that calcium binds to the I27 domain. This novel calcium responsive entropic spring within titin has further been shown to modulate its stiffness, passive force potential, and the peak to peak distance in the presence of calcium. Thus, Ig domains within titin may modulate their resting length, elasticity and also ligand binding properties [3], all of which are important for passive force regulation. This may be a further source of comparison between damaged and intact titin proteins and would help to better understand passive force regulation in cardiac muscle and the changes in passive properties associated with specific cardiac failure.

REFERENCES

[1] Joumaa V et al. (2008). The origin of passive force enhancement in skeletal muscle. *Am J Physiol Cell Physiol* Vol **294**; p. 74-78.
[2] Labeit D et al. (2003). Calcium-dependent molecular spring elements in the giant protein titin. *Proc. Nat. Acad. Sci*.; Vol **100**:(23); p. 13716-13721.
[3] Garcia TI et al. (2008) Mechanical stability and differentially conserved physical-chemical properties of titin Ig-domains. *Prot.:Struc., Func. and Bioinfo.*; Vol **75:**(3); p. 706-718.

SARCOMERE POPPING LIMITS FORCE LOSS IN STRETCH-INDUCED INJURY

Appaji Panchangam and Walter Herzog
Human Performance Laboratory, University of Calgary, Alberta, Canada

INTRODUCTION

Stretching of activated muscle results in loss of isometric force and has been found to be associated with focal sarcomere disruption [1]. In the absence of direct experimental support, the disruption of sarcomeres, often termed 'sarcomere popping', has generally been assumed to precede and cause the loss of force [2] and more popping was interpreted as more force loss. We showed earlier in myofibrils [3] that stretch-induced force loss can occur in the absence of sarocmere popping, thereby challenging the causal association between sarcomere popping and loss of force. The aim of this study was to test if sarcomere popping increases the loss of force in actively-stretched muscles.

METHODS

Isolated myofibrils (MF) were obtained from *psoas* muscles of rabbits using standard protocols [4]. Myofibrils were mounted with one end attached to a glass micro needle and the other end fixed to a silicon nitride cantilever of known stiffness. Cantilever deflection was optically projected onto a linear CCD array and the resulting line scan images were used to estimate the MF forces. Forces were normalized by cross-sectional area (kPa) to enable cross comparison among MFs.

Experimental MF (n=16) were maximally activated with a high-[Ca^{+2}] activating solution (pCa=3.5) at a mean sarcomere length (SL) of ~2.7 µm. At peak steady-state force, MF were stretched by 1 µm sarcomere^{-1} (~35%) at a speed of 1 µm sarcomere^{-1} s^{-1} (~3.7% s^{-1}). Myofibrils were immediately returned to the starting length at the same speed and relaxed after a few seconds. They were re-activated at the same length after 35 minutes and post-stretch isometric forces were re-measured (see *inset* in Figure 1). Force deficit, the percentage loss in maximum isometric force, was estimated from the two isometric force measurements before and after the stretch-release cycle. Control MF (n=6) were activated twice, but not stretched. All experiments were video taped and the SLs were computed from the video as the distance between the centroids of A-bands. A sarcomere is deemed as popped if its post-stretch length remained greater than 4.0 µm, whereafter myofilaments no longer overlap.

RESULTS

Experimental MF produced an isometric stress of 184 ± 43 kPa at a SL of 2.7 ± 0.25 µm. The stretch-release protocol resulted in a strain of 35 ± 6% that produced a force deficit of 27 ± 9%. Control MFs did not show any differences in isometric force between activations (p = 0.8553).

Eight out of the 16 experimental MF had no sarcomere popping, whereas the remaining 8 MF had one or two sarcomeres that had popped. When compared with the group of 8 that did not have sarcomere popping, the MFs with sarcomere popping had smaller force deficits (*p = 0.0397; Figure 1) while the strain (p = 0.5712), pre-stretch isometric stress (p = 0.9434), and SL at the onset of stretch (p = 0.1254) were not different.

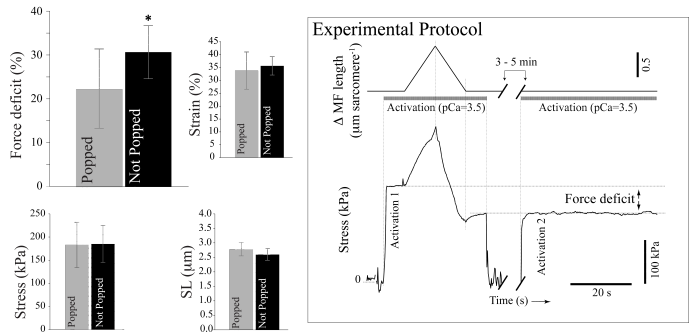

Figure 1: Comparisons between groups of MF with and without sarcomere popping. *Inset*: Experimental protocol

DISCUSSION AND CONCLUSIONS

The present findings contradict the commonly held view that sarcomere popping is the cause of stretch-induced force loss [2]. Coupled with our earlier findings that sarcomere popping is not necessary for stretch-induced force loss [3], the present results suggest that sarcomere popping is a protective mechanism limiting the amount of force lost during active stretch-induced muscle injury. As a potential mechanism, we suggest that the popped sarcomeres reduce the amount of stretch in adjacent intact sarcomeres, thereby reducing the force loss due to stretch by remaining at a more favourable position on the descending limb of the force-length realtionship.

REFERENCES

[1] McCully KK and Faulkner JA (1985). *J Appl Physiol*. Vol. **59**; p. 119-126. [2] Morgan DL and Allen DG (1999). *J Appl Physiol*. Vol. **87**; p. 2007-2015. [3] Panchangam A and Herzog W (2009). *ASB Conf Proc*. Vol. **33**; p. 876-877.[4] Joumaa V et al. (2007). *Pflugers Arch*. Vol. **455**; p. 367-371.

ACKNOWLEDGEMENTS

NSERC CREATE Programme, CIHR, and Canada Research Chair Programme.

MORPHOLOGICAL CHANGES IN CONTTRACTILE PROPERTIES OF MUSCLES SUBJECTED TO REPEAT INJECTIONS OF BOTULINUM TOXIN TYPE A (BOTOX)

Rafael Fortuna[1], Marco Aurelio Vaz[2], Aliaa Rehan Youssef, David Longino, Walter Herzog[1]
[1]Faculty of Kinesiology, University of Calgary, Calgary, Canada, email:rfortuna@kin.uclagary.ca
[2]Physical Education School, Federal University of Rio Grande do Sul, Porto Alegre, Brazil

INTRODUCTION

Botulinum toxin type A (BTX-A) is a toxin which paralysis muscles by preveting acetylcholine release at the motor endplate [1]. In the past two years, we developed a muscle weakness model in New Zealand White (NZW) rabbits to study the effects of weakness on joint loading and joint degeneration [2]. Using this model, we were able to control muscle activation effectively, but found that injected muscles atrophied severely and their force was greatly reduced. BTX-A injections are routinely used in a variety of muscular disorders to relax muscles [1], but contractility should not be affected so that muscles can be used effectively following BTX-A treatment. However, no systematic data on the effect of chronic BTX-A treatments on structure and functionality of the target muscles are available. Therefore, the aim of this study was to investigate the changes in mass, strength and structure of muscles exposed to chronic BTX-A injections.

METHODS

Twenty skeletally mature NZW rabbits were divided into four groups as follows: (i) control, (ii) 1 month post-single BTX-A injection, and (iii) 3 and (iv) 6 months post repeated monthly BTX-A injections. Outcome measures included mass, strength, and the proportion of contractile material of muscles. Mass and strength were assessed by weighing and by measuring isometric strength across the physiological range of knee joint motion. For assessment of structural integrity, 8μm histological sections were cut, stained with H&E, and analyzed under a light microscope. A custom written MatLab program was used to quantify the percentage of contractile material in each muscle.

A 3 way-ANOVA (α=0.05) with the main factors leg (BTXA-injected, non-injected contralateral, non-injected control), groups (control, 1, 3, and 6 months post BTX-A injections), and muscles (vastus lateralis VL, rectus femoris RF, and vastus medialis VM) was performed

RESULTS

Strength in the injected muscles was reduced by 88%, 89% and 95% in the 1, 3 and 6 months BTX-A injected limbs compared to controls. Muscle mass was reduced by 50%, 42%, and 31% for VL, RF, and VM, respectively at 1 month, by 68%, 51% and 50% at 3 months and by 76%, 44% and 13% at 6 months. An example of VL from the injected and non-injected limb of a 6 months BTX-A animal is shown in Fig. 1.

The percentage of contractile material was the same for control and the 1 month BTX-A treated animals and averaged 96% across all muscles. At 3 and 6 months of BTX-A injections, the contractile material of injected muscles was reduced to 72% and 56%, respectively and was replaced primarily by fat (Fig. 2).

The percentage of contractile material in the non-injected contralateral hind limbs was the same as for control at 1 and 3 months but was reduced to 78% after 6 months.

Fig. 1: Injected (L) and contralateral (R) VL after 6 months.

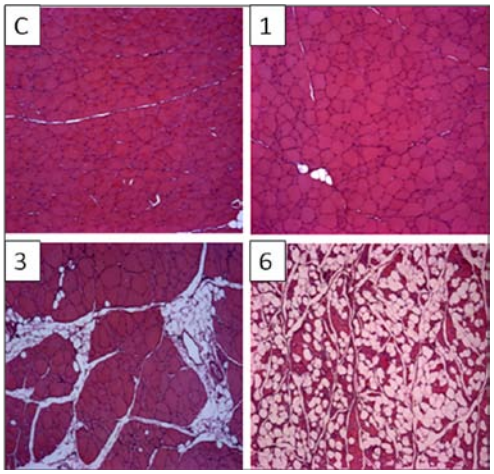

Fig. 2: Contractile material of the VL for control (C), 1 (1), 3 (3) and 6 (6) months group animals.

DISCUSSION AND CONCLUSIONS

BTX-A injections are a frequently used treatment modality in spastic muscles after stroke or in children with cerebral palsy. The idea is to chemically denervate muscles temporarily and then let them recover and take up normal function. However, the results of our study suggest that even a relatively short period of BTX-A injections may cause severe muscle atrophy, loss of contractile material and structural disintegration rendering the muscles virtually useless following BTX-A treatments. It seems important that these side effects of BTX-A injections can be prevented in clinical applications. This might potentially be achieved by supplementing BTX-A injections with simultaneous muscle stimulation training.

REFERENCES

[1]Brin, MF, 1991. Muscle & Nerve 6; 146-168.
[2]Longino et al, 2005. J. of Orthop Research 23;1411-1418.

AGING EFFECTS ON GRIP FORCE CONTROL: AN fMRI STUDY

Jeremy W. Noble, Janice J. Eng, Kristen J. Kokotilo & Lara A. Boyd
Department of Physical Therapy, University of British Columbia, Vancouver BC, Canada, Jeremy.Noble@vch.ca

INTRODUCTION

Functional Magnetic Resonance Imaging (fMRI) allows for the measurement of hemodynamic responses associated with neural activity within the CNS associated with a task. It has been observed that aging is correlated with an increase in bilateral activation (interhemispheric symmetry) of the primary motor cortex during various gripping tasks [1,2]. However it is not clear how the magnitude of the force influences brain activation in older adults, or how aging affects the activity of other areas of the CNS during a motor task.

The goal of this study is to analyze the effects of aging on the areas of neural activity associated with performing a gripping task at three different magnitudes

METHODS

A group of 13 right-handed older adults (mean age = 67.5 yrs) and a group of right-handed young adults (mean age = 26.1) were recruited to participate in this experiment. Participant's maximal grip force was measured with a Jamar hand dynamometer and with a custom MR-safe pressure transducer system. Participants then were asked to perform a series of sub-maximal contractions (10%, 40% and 70% MVC with a visual target) in a 3T fMRI environment. Participants performed four runs consisting of 24 gripping trials per run. Each squeeze lasted four seconds, with 10-16s of rest between each squeeze. In total the participant performed 6 squeezes with each hand at each force-level.

The fMRI analysis used a Region of Interest (ROI) approach to focus on 9 motor areas within the brain bilaterally: Caudate Nucleus, Putamen Nucleus, Thalamus, Primary Sensory-Motor Cortex, Supplementary Motor Area, Pre-Supplementary Motor Area, Pre-motor Cortex, Anterior Cerebellum and Posterior Cerebellum. The peak percent signal change (PSC) for each ROI was determined with the AFNI software package [3].

A two-way mixed MANOVA was carried out to determine group and force level differences in the PSC values and the behavioural force data. An additional two-way mixed MANOVA was carried out to determine group and hemispheric differences at each force level. Only the results of the right handed squeezes were analyzed for this abstract.

RESULTS

The maximum force produced by the older adults was equivalent to the force produced by the younger group with both the Jamar dynamometer and the MR-safe pressure transducer unit, for the right and left hands. Additionally, there were no group differences in either the relative or absolute force level produced during any squeeze task, with exception of the older group producing a lower absolute force on the 70% MVC trials.

In all ROIs, for both groups, the 70% MVC force level led to a higher level of neural activity when compared to the 10% and 40% trials. There was no significant difference in the PSC values between the 10% and 40% grip force trials. A general trend was observed where the older group had higher neural activity compared to the younger group for subcortical, but not cortical structures at matched grip force levels. PSC values of the older adults were statistically higher in 3 regions (both Putamen and the right Thalamus) when compared to the younger group.

DISCUSSION AND CONCLUSIONS

It was observed that there was a significant increase in neural activity in all of the analyzed ROIs when the grip strength increased. The activation for most ROIs was bilateral in nature with the exception of the primary motor areas, where the contralateral hemisphere shows significantly higher activity. The bilateral nature of the activation suggests that a substantial level of motor coordination is required to perform this motor task (involving several joints and muscles, and visual feedback).

A trend was observed where the older adults showed higher levels of activity in subcortical structures, when compared to the younger group. However this only reached significance in the right putamen and thalamus. This finding may indicate that a higher level of subcoritical processing is required by the older adults to achieve the same level of coordination as the younger group.

REFERENCES

[1] Ward NS et al. (2008). *Neurobiol Aging* Vol **29**(9); p. 1434-46..
[2] Talelli P et al. (2008). *Neuroimage.* Vol **40**(4); p. 1772-81.
[3] Cox RW. (1996). *Comput Biomed Res.* Vol **29**(3); p. 162-73.

MUSCLE ACTIVATION AT THE KNEE JOINT DURING CLOSED KINETIC CHAIN LOADING

Teresa Flaxman[1], M.Sc. Candidate; Andrew Speirs[2], M.Sc., Ph.D. Candidate; Daniel L Benoit[1,3], Ph.D.
[1]School of Human Kinetics, University of Ottawa, Canada,
[2]Department of Mechanical and Aerospace Engineering, Carleton University, Canada
[3]School of Rehabilitation Sciences, University of Ottawa, Canada. Contact: dbenoit@uottawa.ca

INTRODUCTION

Neuromuscular control plays a critical role in dynamic knee stability. The aim of this study was to investigate knee muscle activation strategies in response to voluntary direction-specific quasi-isometric closed kinetic chain (CKC) joint loading.

METHODS

Healthy young male and female adults stood with their dominant leg in a boot fixed to a force platform (Bertec Corp., OH, USA) (Figure 1A). A modified target matching protocol [1] required subjects to position a cursor (projected on a video screen) over a target and maintain the position for one second (Figure1B). To control the cursor, loads were applied against the force platform. Loads in the ±X, ±Y and ±Z axes corresponded respectively to anterior-posterior, varus-valgus and inferior-superior loads perpendicular to the shank's long axis. Eighteen targets randomly appeared one at-a-time about a circular trajectory, spaced by 20º. A successful target match required 50% of body weight and 30% of previously recorded peak loads made along the ±X and ±Y axes, triggering EMG (Delsys Inc., MA, USA) recording of eight muscles crossing the knee joint, force and moment data for the one second of target matching and three seconds pre-match.

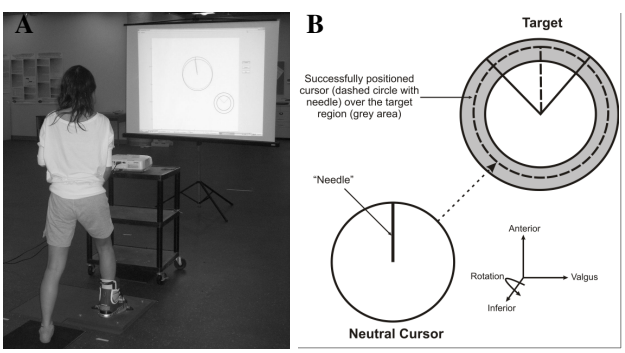

Figure 1: A) Laboratory setup **B)** Depiction of the cursor, target, and successful positioning of cursor over the target.

EMG was normalized to percent maximum voluntary isometric contraction, collected with a dynamometer (Biodex, New York, USA). Mean magnitude of muscle activity (REMG) (1), a mean direction of muscle activity (Φ) (2), and a specificity index (SI) (3) were calculated for each muscle using an EMG vector (i), where the mean EMG amplitude at each target location is represented in Cartesian coordinates:

$$REMG = (\Sigma EMGi)/n \quad (1)$$

$$\Phi = \arctan(\Sigma y_i/\Sigma x_i) \quad (2)$$

$$SI = REMG/\sqrt{(|\Sigma x_i|/n)^2 + (|\Sigma y_i|/n)^2} \quad (3)$$

RESULTS

Preliminary results indicate relatively high levels of activation for all muscles (Figure 2) during the target matching tasks. In terms of contributions to forces in specific directions, rectus femoris and semitendinosus had high specificities, SI=0.60 and 0.51, and activities were primarily oriented along the anterior and posterior axes, Φ=91° and 258°, respectively. Biceps femoris and medial gastrocnemius had lower specificity, SI=0.40 and 0.34, with activities greatly oriented in the varus plane, Φ=191° and 137º, respectively.

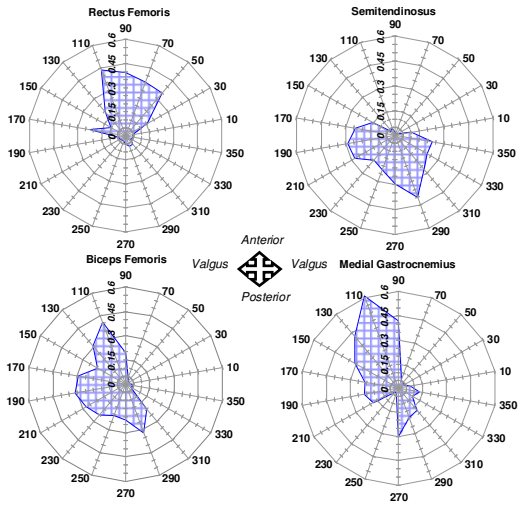

Figure 2: EMG polar plots where numbers along the circular trajectory identify target locations (º). Mean EMG amplitude at each target location is denoted by the EMG pattern's intersection on the target location radius.

DISCUSSION AND CONCLUSIONS

The findings display different knee stabilization strategies during CKC loading compared to open kinetic chain (OKC) [1]. Activation patterns may vary because CKC is more apt for simulating functional limb motion, regulating joint loads and contact areas, and reducing shear forces [2]. Of interest, the biceps femoris and medial gastrocnemius have Φ opposite to their moment arm orientation, demonstrating major stabilization roles during CKC loading with a varus component. During CKC knee extension, hamstring and gastrocnemius have shown higher and more simultaneous activities compared to OKC [2]. It is suggested that the CKC neuromuscular variation is indicative of greater cocontraction which increases joint stabilization.

REFERENCES

[1] Buchanan TS and Lloyd DG. (1997). Muscle activation at the human knee during isometric flexion-extension and varus-valgus loads. *J Orthop Res* Vol **15**; p. 11-17.
[2] Escamilla RF et al. (1998). Biomechanics of the knee during closed kinetic chain and open kinetic chain exercises. *Med Sci Sports Exer* Vol **30**(4); p. 556-569.

ACKNOWLEDGEMENTS: This work has been funded by the Canadian Foundations for Innovation and the Natural Sciences and Engineering Research Council.

Obesity Affects Gait Pattern Changes in Moderate Knee Osteoarthritis

Graeme Harding[1], Janie L Astephen Wilson[1], Cheryl L Hubley-Kozey[2,1]
[1]School of Biomedical Engineering, Dalhousie University, Halifax, Canada, graeme.t.harding@gmail.com
[2]School of Physiotherapy, Dalhousie University, Halifax, Canada

INTRODUCTION

Obesity is a highly cited risk factor for the progression of knee osteoarthritis (OA) [1], and excess weight contributes to an increased mechanical burden and altered dynamic movement and loading patterns at the knee. However, the role of obesity in the pathomechanics of knee OA remains unclear. The objective of this study was to examine the interacting role of moderate knee OA disease presence and obesity on knee joint mechanics during gait.

METHODS

Gait analysis was performed on 60 asymptomatic individuals and 60 diagnosed with moderate knee OA. Four subject groups (asymptomatic obese and healthy weight, OA obese and healthy weight) were defined according to BMI (BMI >=27, BMI <27) and disease presence. Using an Optotrak motion capture system (Northern Digital, Inc.) and force platform (AMTI, Watertown, MA), three dimensional joint kinematics and kinetics (angles and net resultant moments) were calculated. Waveform principal component analysis (PCA) was applied to the flexion angle, and the net moments at the knee to extract major patterns of variability between the patterns of subject angles and moments over the gait cycle [2]. PC scores for major patterns (projections of data onto these patterns) were calculated for the subset of PCs which explained at least 90% of the variance in the original data. These PC scores were compared between the 4 groups using a two-factor ANOVA.

RESULTS

Significant disease effects (Table 1) were found for the overall magnitude of the knee flexion angle during gait (OA lower), the overall magnitude of the knee adduction moment during stance (OA higher) (Figure 1), and patterns describing phase shifts in the peak knee flexion/extension and internal/external rotation moments during stance (OA peaks shifted later in stance). Significant BMI effects (Table 1) were found in the internal rotation moment peak phase shift (BMI shifted later stance), in the knee adduction moment pattern (BMI less difference between first and second peak moment during stance) (Figure 1), and in the knee flexion angle patterns (BMI peak flexion angle shifted to later in stance).

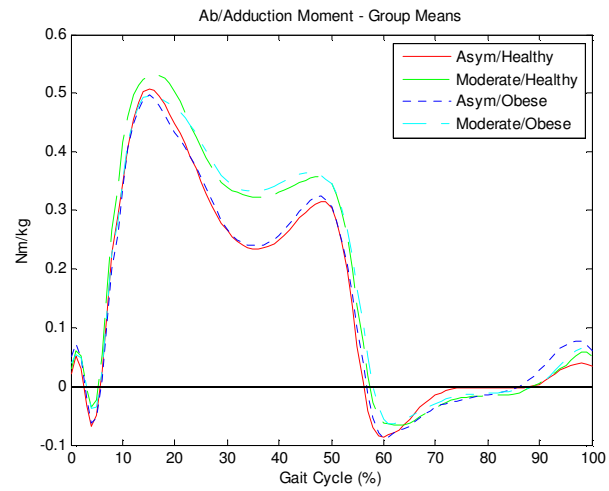

Figure 1: Mean external knee adduction moment patterns for the 4 subject groups.

DISCUSSION AND CONCLUSIONS

These results suggest that some changes in the biomechanical patterns of the knee joint during gait with OA can be attributed to the interacting effects of obesity on joint mechanics. While some effects, such as a decreased overall flexion angle and an increased overall knee adduction moment have previously been shown to be related to knee OA [2], the BMI effects shown here have not been previously demonstrated. These findings may have important implications for disease management and the development of treatment strategies.

REFERENCES

[1] Felson DT et al. (1997). *Arthritis & Rheumatism.* Vol **40**(4); p. 728-733.
[2] Astephen JL et al. (2007). *Journal of Orthopaedic Research.* Vol **26**(3); p. 332-341.

ACKNOWLEDGEMENTS

The authors wish to acknowledge Dr. Kevin Deluzio for his contributions to the development of this study.

Table 1: Significant disease (OA) and body weight (BMI) effects based on two-factor ANOVA of PC Scores.

Waveform	*Flexion Angle*	*Adduction Moment*	*Rotation Moment*	*Flexion Moment*
Disease Effect	lower overall magnitude (p=0.034)	higher overall magnitude (p=0.015)	peak later in stance (p=0.000)	peak later in stance (p=0.013)
BMI Effect	peak later in stance (p=0.036)	similar 1st and 2nd peak (p=0.017)	peak later in stance (p=0.000)	not significant

Obesity Does Not Alter Contact Forces in Tibiofemoral Joint With Moderate OA

Graeme Harding[1], Janie L Astephen Wilson[1], Cheryl L Hubley-Kozey[2,1]
[1]School of Biomedical Engineering, Dalhousie University, Halifax, Canada, graeme.t.harding@gmail.com
[2]School of Physiotherapy, Dalhousie University, Halifax, Canada

INTRODUCTION

Obesity is a commonly cited risk factor for OA, which has been associated with both increased radiographic and sypmtomatic OA [1]. While the pathomechanics of knee OA remain unclear, it is suspected that excess weight contributes to an increased mechanical burden at the knee [2], however the effect of obesity on dynamic loads within the knee joint of individuals with OA during gait has not yet been fully investigated. The objective of this study was to compare bone-on-bone contact forces in the tibiofemoral joint during gait between asymptomatic, healthy weight individuals, individuals with moderate OA who are of healthy weight, and those with moderate OA who are obese.

METHODS

Gait analysis was performed on three groups of subjects: i) healthy weight without OA (group 0, n=20), ii) healthy weight subjects with moderate OA (group 1, n=24), and iii) obese subjects with moderate OA (group 2, n=22). Subjects with a BMI of greater than 30 were considered obese. A system which included a synchronized Optotrak 3020 motion capture (Northern Digital, Inc.) and force platform (AMTI, Watertown, MA) were used to calculate 3D kinematics and net resultant moments of the lower limb.

From the knee flexion angle, the net external knee flexion moment, and the ground reaction forces, contact forces in the tibiofemoral joint were estimated in the horizontal (shear) and vertical (compressive) directions using a sagittal plane model [3]. Lines of action and moment arms of the patella ligament and the hamstrings tendon were determined from the equations of Herzog and Read [4]. The first and second peak values were extracted from the compressive bone-on-bone contact force during stance, and the minimum and maximum values during stance were extracted from the shear contact force (Figure 1). A one-way ANOVA was used to determine significant differences in these parameters between the three subject groups. Linear regression was used to assess the association between BMI and each of the four parameters.

RESULTS

Significant effects were found for both the first and the second peak compressive force during stance. The asymptomatic, healthy weight subjects (group 0) had lower compressive forces than the subjects with moderate OA (groups 1 and 2) (Table 1). Also, significant effects were found for the maximum shear force at the end of stance phase. Again, asymptomatic and healthy weight subjects (group 0) had lower contact forces than did obese subjects with moderate OA (group 2) (Table 1). Regression showed that 33% of the variability in the second peak compressive force could be explained by BMI.

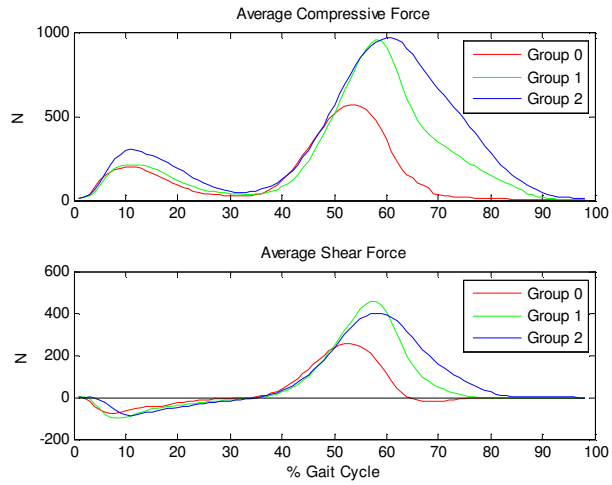

Figure 1: Average compressive and shear forces by group.

DISCUSSION AND CONCLUSIONS

These results are unexpected in that they do not indicate higher compressive or shear forces in obese subjects with moderate OA than in healthy weight subjects with moderate OA. The linear regression results show a trend of increasing compressive force with increasing BMI, but the effects of moderate OA disease presence appear to override any additional obesity effect.

REFERENCES

[1] [1] Felson DT et al. (1997). *Arthritis & Rheumatism.* Vol **40**(4); p. 728-733.
[2] Segal NA et al. (2009). *American Journal of Physical Medicine and Rehabilitation.* Vol **88**(3); p. 180-188.
[3] Thambyah A et al. (2005). *The Knee.* Vol **12**; p. 383-388.
[4] Herzog W et al. (1993). *Journal of Anatomy.* Vol **182**(2); p. 213-230.

ACKNOWLEDGEMENTS

The authors wish to acknowledge NSERC and CIHR for funding this work.

Table 1: Results of one-way ANOVA on bone-on-bone contact force parameters in the tibiofemoral joint.

Parameter	Max. Comp. 1	Max. Comp. 2	Min. Shear	Max. Shear
p-value	0.000	0.030	0.421	0.042
Direction of Difference	Group 0 < Group 1 and Group 0 < Group 2	Group 0 < Group 2	N/A	Group 0 < Group 2

Sagittal and frontal plane joint moment profiles associated with stair ascent and descent in young and older adults

Alison C. Novak[1], Brenda Brouwer[1]
[1]School of Rehabilitation Therapy, Queen's University, Kingston, Canada, alison.novak@queensu.ca

INTRODUCTION

Stair negotiation is an essential task required for independent mobility and is described by older adults as a challenging task, associated with high risk for falls [1]. It follows that to meet the higher demands, variation in moment patterns and the relative contribution of each joint to the overall net support moment produced may differ from young adults. The purpose of this study was to characterize joint kinetics associated with stair ascent and descent in young and older adults, providing insight into age-related alterations in movement control.

METHODS

Twenty three young adults (23.6 ± 3.0 years) and thirty two older adults (67.0 ± 10.8) completed the study. All subjects were free of any neurological or orthopaedic condition affecting their lower limbs or walking ability. Subjects were instructed to ascend and descend stairs several times at a self-selected pace in a step over step manner without the use of a handrail. Full lower limb, three dimensional, bilateral gait analysis (Optotrak 3020 motion analysis system) provided sagittal and frontal plane joint moment profiles of the ankle, knee, hip and support moment throughout stance. Mixed factor ANCOVA was used to compare kinetic variables of interest between the groups and sides, however data are reported for the dominant side only.

RESULTS

Cadence differences were detected groups ($p=0.031$), reflecting higher cadences among young adults compared to older adults.

During stair ascent, young adults demonstrated greater ankle extensor moments in early and late stance ($p<0.005$) contributing to a higher support moment in early stance ($p=0.04$) compared to older adults. The peak ankle extensor moment was also higher for young adults during pull up ($p=0.002$) during ascent, although the associated support moment peak was greater in older adults ($p=0.04$), as the older adults generated smaller knee flexion moments than their young counterparts ($p<0.001$). During stair descent, ankle extensor moments in older adults were low in early stance ($p=0<0.001$) and appeared to be compensated mainly by the hip extensors resulting in similar support moment peaks for both groups. During controlled lowering (descent), the peak extensor support moment was higher for older adults ($p<0.001$), reflecting a larger knee extensor moment ($p=0.02$) and smaller hip flexor moment ($p=0.001$).

In the frontal plane, young and older adults displayed similar joint moment profiles during stair ascent and during descent. No significant differences were detected between groups in the frontal plane ankle or knee kinetics. However, at the hip, the second hip abductor peak during pull-up and controlled lowering was larger in older adults ($p<0.04$).

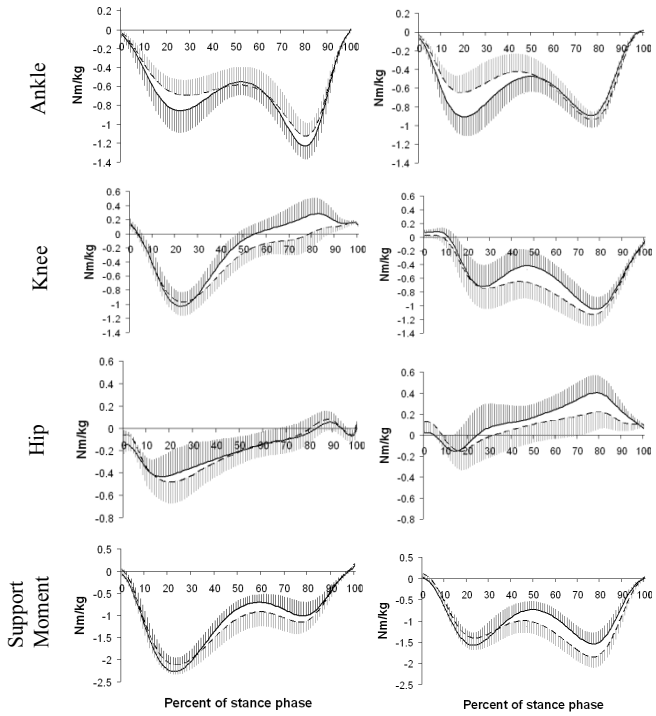

Figure 1: Ensemble averages of the sagittal plane joint moment curves during stair ascent (left) and descent (right) for young adults (solid line) and older adults (dashed line). Positive values represent internal flexion moments. Error bars represent ± 1 S.D.

DISCUSSION AND CONCLUSIONS

During stair negotiation, older adults rely less on their ankle musculature than young adults which may be due to age-related weakening of the distal muscles. The higher support moments in late stance in both ascent and descent in older adults could be a compensatory strategy to limit instability during transition from single to double support. Greater reliance on hip abductors in older adults suggests greater pelvic control is required as the opposite limb swings up and forward. Understanding age-related differences in the task requirements in terms of joint kinetics during stair negotiation can inform clinicians so they can better manage and assess patient populations.

REFERENCES

[1] Tinetti ME et al. Risk factors for falls among elderly persons living in the community (1998). *N Engl J Med* 319; p. 1701-1707.

ACKNOWLEDGEMENTS

The authors gratefully acknowledge Samantha Reid for her assistance with data collection and financial support of the National Sciences and Engineering Research Council (NSERC) PGS Doctoral Award.

IMPROVING GAIT CHARACTERISTICS IN OLDER ADULTS: THE EFFECT OF BIODEX BALANCE SYSTEM SD™ VERSUS WOBBLE BOARD BALANCE TRAINING

Brittney C. Muir, Shirley Rietdyk, Jeffery M. Haddad, Jessica M. Seaman
Health and Kinesiology, Purdue University, West Lafayette, Indiana, muir@purdue.edu

INTRODUCTION

Several interventions have shown promise in reducing the number of falls in older adults[1,2]. For example, balance training with center of pressure (COP) visual feedback resulted in improved balance control in frail elderly women[1]. It has been argued that accurate visual representation of the COP during standing can improve standing balance. However, the effect of balance training while standing on dynamic motor behaviours such as locomotion is less clear. Falls have been associated with changes in gait characteristics[3]. Therefore, it is important to determine if standing balance training can transfer to the more dynamic task of walking.

The purpose of this study was twofold. First, to examine if balance training while standing would translate to improvements in gait characteristics. Second, to examine if balance training with visual feedback (through the Biodex Balance System SD™ (Biodex Medical Systems, New York)), would result in greater gait improvements than similar training with no visual feedback on the traditional wobble board (WB).

METHODS

Eighteen participants (12 female, 6 male; mean age 81.1 ± 6.9 yrs) were matched for age, gender, activity level, timed-up-and-go (TUG) score and an initial Biodex Balance System score for placement into two groups. Groups received either training on a traditional WB or the Biodex Balance System. Participants trained 20 minutes, three times per week for six weeks.

Plantarflexor strength, ankle position matching and gait were assessed pre and post-training. The gait task required subjects to walk 3.2 m from a standing position. In some trials, an obstacle was present. This abstract will focus on the unobstructed trials only (six trials per subject both pre and post intervention). IREDs were placed bilaterally on the fifth metatarsal, heel, lateral malleolus, knee joint, greater trochanter, shoulder and on the right temple. IRED position data was collected with an Optotrak (Northern Digital, Inc., Waterloo, Canada) at 60 Hz. Position data was filtered with a fourth order dual pass low pass filter at 8 Hz. Step length (SL), SL variability, step width (SW), SW variability, minimum toe clearance (minTC), minTC variability and gait speed were calculated.

RESULTS

Following training, gait parameters of both groups moved closer to those of typical younger subjects. The two groups demonstrated similar changes for the following variables: gait speed (5.6% increase), SL (1.0% increase), and SW variability (12% decrease) (time main effect, $p<0.05$). However, the Biodex group showed greater improvements than the WB group in several variables: SW (Fig 1a), minTC (Fig 1b) and SL variability (Fig 1c) (group by time interaction, $p<0.04$). A decrease in minimum toe clearance variability was also observed for the Biodex group, although this was not significant.

DISCUSSION AND CONCLUSIONS

The observed changes reflect less cautious gait, or greater confidence, consistent with improved balance skills during gait. Therefore, balance training while standing did transfer to a gait task. The Biodex group achieved greater improvements in some of the variables, suggesting that visual feedback provides information that is used to improve performance. It is important to note that the Biodex group had values that were different from the WB group at the beginning indicting that the matching used (e.g. TUG score) did not result in similar gait scores. The difference in the pre-test allowed for greater improvement in the Biodex group in the minTC measure. However, the Biodex group had smaller SW pre-intervention, and still improved more than the WB group. We are in the process of collecting a control group to ensure that the differences following intervention were not due merely to experience with the task and/or the laboratory.

Overall, both groups improved, so standing balance training can transfer to the more dynamic task of walking. The greater changes in the Biodex group indicate that the visual feedback during training was relevant in improving gait performance.

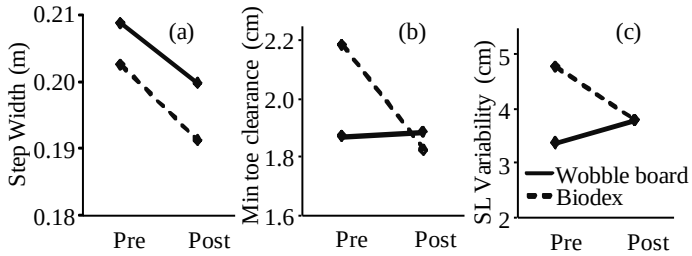

Figure 1: Step width (a), minimum toe clearance (b) and step length variability (c) during pre and post tests.

REFERENCES

[1] Sihvonen S et al. (2004). Changes in postural balance in Frail Elderly Women during a 4-week Visual Feedback Training: A randomized Controlled Trial. *Gerontology* 50:87-95.
[2] Srivastava et al. (2009). Post-stroke balance training: Role of force platform with visual feedback technique. *J of Neurol* 287: 89-93.
[3] Maki BE (1997) Gait changes in older adults: predictors of falls or indicators of fear? *J Am Geriatr Soc* 45: 313-320.

ACKNOWLEDGEMENTS

We would like to thank our participants for their enthusiasm and perseverance. We would also like to thank Jin Soo Kim, Tony Martin, Aaliyah Taylor, Tina Yang and Nick Zaleski for their help with training and data collection.

Are head rotations sufficient to cause a change in travel path in young and older adults?

Michael E. Cinelli[1], William H. Warren[2]
[1]Department of Kinesiology and Phys. Ed, Wilfrid Laurier University, Waterloo, ON, Canada, mcinelli@wlu.ca
[2]Department of Cognitive and Linguistic Sciences, Brown University, Providence, RI, USA

INTRODUCTION

Normally when one wants to change his or her travel path direction, the head and eyes initiate the turn and the body and feet follow. This has been termed the *Steering synergy* [1]. The objectives of the current study were: (1) to determine if self-initiated head rotations are sufficient to cause a change in travel path and (2) whether older adults responded differently to similar head turns. Previous research has shown that following a head perturbation, not a head turn, young adults deviate from their intended path direction [2,3]. It is hypothesied that older adults will have larger path deviations.

METHODS

Ten young healthy adults (19-21yrs) from WLU's Kinesiology and Physical Education department and 11 older adults (>65yrs) from the community participated in the study. All participants were free of any neurological disorders and had normal or corrected to normal vision. Participants were instrumented with 12 Optotrak Smart Markers: 3 on the head, xyphoid, left and right acromioclavicular joint, left and right ASIS, left and right ankle, left and right fifth metatarsal. Markers were used to calculate each participant's COM as well as head and trunk rotations about the vertical axis.

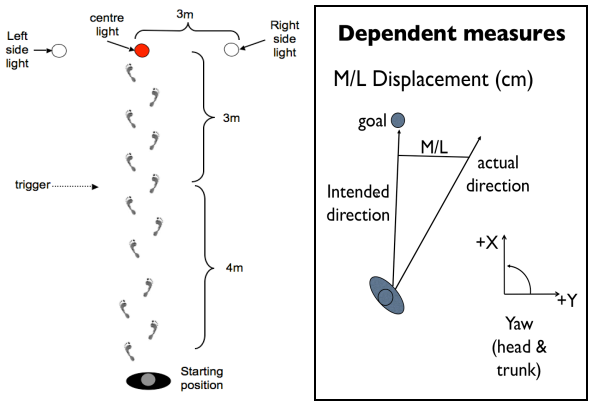

Figure 1- Experimental set-up (left). Dependent measures used include M/L path deviations and Yaw angles (right).

Participants walked 9m towards the goal light every trial, a trigger was place about half way down the path and was used to initiate a head turn (Fig. 1). The current study had five conditions: **(1)** control, **(2)** ATL- one of target lights illuminated, participants were told to turn their heads to face the target but walk towards the goal, **(3)** ATV- a verbal command instructed the participants to turn their heads towards one direction while walking towards the goal, **(4)** RG- the goal light would extinguish when the participants began to approach it, and **(5)** RGATL- participants walked towards a remembered goal and a target light would illuminate to indicate the direction of a head turn. The difference between ATL and ATV was to determine if path deviations are due to the mechanical effect of turning one's head or due to attentional capture (i.e. ATL).

Data analysis included the maximum and variability in M/L path deviations of the COM as well as head and trunk yaw rotations magnitudes.

RESULTS

The average maximum M/L deviations of the young participants when a head turn was initiated were not different from the control condition ($p>0.05$). However, the older adults displayed significant M/L path deviations in the direction of the head turn ($p<0.01$). These were similar regardless of the method used to initiate the head turn (Fig.2). The variability in M/L deviations was large for both groups, however, the older adults had significantly greater variability ($p<0.01$) (Fig. 2).

Both head and trunk rotation magnitudes were not different across the conditions ($p>0.05$), nor were they different between the two groups ($p>0.05$).

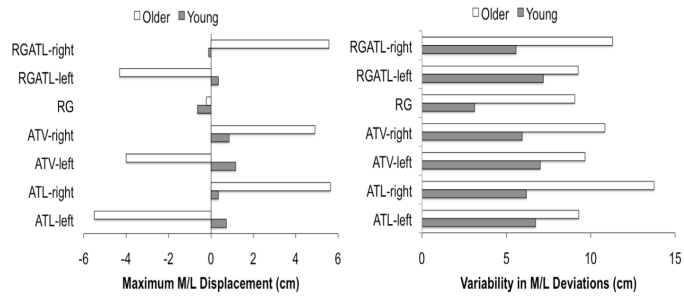

Figure 2- Average maximum M/L path deviations for each condition across the participant groups (left). Positive values indicate deviations to the right and negative to the left. Variability in maximum path deviations for both groups (right).

DISCUSSION AND CONCLUSIONS

Although head and eye rotations normally initiate a change in travel path, they are not sufficient to cause a systematic change in travel path in young highly trained adults. The high variability in the results proves that all individuals walk towards a goal with some small and inconsistent influences of eye and head rotations. These inconsistencies are centered around the intended travel path direction for young adults, but not older adults. The older adults tend to deviate in the direction of their head turns. Therefore, the steering synergy does hold with the older adults when their heads are actively turned away from the intended travel path direction. Thus indicating that the sensory signals from receptors in their heads interpret the mechanics of a head turn and not attentional capture as a signal to change travel path directions regardless of one's intentions.

REFERENCES

[1] Grasso R. et al. (1998). Eye-head coordination for the steering of locomotion in humans: an anticipatory synergy. *Neuroscience Letters.* Vol. **253**: p.115–118
[2] Vallis, LA & Patla, AE. (2004). Expected & unexpected head yaw movements result in different modifications of gait & whole body coordination strategies. *EBR.* Vol. **157**: 94–110
[3] Jahn, K. et al. (2006). Eccentric eye and head positions in darkness induce deviation from the intended path. *Exp Brain Res.* Vol. **174**: p.152–15.

USE OF PROGRESSIVE GLASSES WHEN GOING DOWNSTAIRS MODIFIES POSTURAL AND MOTOR STRATEGIES IN ELDERLY PEOPLE

Julie Lecours[1,2], Sylvie Nadeau[1,2], Benoît Frenette[3], Jacques Gresset[3], Guillaume Giraudet[4]
[1]Centre de recherche interdisciplinaire en réadaptation (CRIR), Institut de réadaptation Gingras-Lindsay-de-Montréal (IRGLM)
[2]École de réadaptation, Université de Montréal, Montréal, Québec, Canada, julie.lecours@umontreal.ca
[3]École d'optométrie, Université de Montréal, Montréal, Québec, Canada
[4]Essilor International - R&D Vision, Saint-Maur cedex, France

INTRODUCTION

Going downstairs is a particularly difficult task for the elderly and can be a dangerous one when the vision is impaired [1]. Studies have revealed that multifocal glasses could affect the behavior of elderly people in visuo-motor activities but to date almost only bifocal corrections have been considered [1,2].

This study compared postural and motor strategies used by two groups of elderly persons when going downstairs; one group used standard progressive glasses corrections, the other performed the task without glasses.

METHODS

Twenty elderly persons (65.1 ± 4.0 yrs; 10 short-sighted, 10 farsighted) who needed progressive glasses to perform daily living activities such as walking and negotiating stairs and 15 elderly controls (66.1 ± 3.6 yrs; emmetropes) who did not need glasses for these activities participated in the study. The participants in both groups had a high level of function and good balance (Berg: 56/56).

The subjects were required to go down the stairs at natural speed under different conditions: natural (no visual display), visual display testing close vision just before starting the descent (close condition) and visual display at 7.6 m in front of the staircase testing distant vision (far condition). The instrumented staircase comprised four steps and one removable footbridge (2.36 m) with handrails. The ground reaction forces under each foot were measured by three force plates; two in the steps (second and third steps when going down) and one in the floor just after the last step when going down. Two instrumented handrails allowed the forces applied on each of them to be recorded. Kinematic data of the head, trunk, arms and lower limbs were recorded with an Optotrak system and infrared markers.

Postural and motor strategies used when going down stairs were determined from certain parameters: speed of descent and patterns of movement at the head, trunk and lower limbs. Two-way repeated measures ANOVAs were used on the different outcomes to compare the two groups. The level of significance was fixed at values lower than 0.05.

RESULTS

The speed of descent was slower among the subjects with progressive glasses than among the controls for close ($p=0.04$) and far (tendency; $p=0.05$) conditions (Table 1). At the levels of the three steps (plateau transition to the first step, second and third steps), the head flexion was lower for the far condition compared to the close and natural conditions (ANOVA condition factor: $p<0.05$) in both groups (Table 2). This effect is more marked at the transition from the plateau to the first step. The trunk flexion (mean angle of 6.3°) does not differ between conditions and groups. Participants using progressive glasses presented a greater hip flexion at the three step levels ($p<0.05$ at the plateau level) than the controls (Table 2). No differences were found between groups regarding their ankle and knee movements.

Table 1: Speed of descent in both groups for the three conditions (m/s).

	Conditions		
	Natural	Far	Close
Controls	0.66 ± 0.10	0.74 ± 0.08	0.75 ± 0.11
Progressive glasses	0.63 ± 0.10	0.67 ± 0.10	0.68 ± 0.10

DISCUSSION AND CONCLUSION

When elderly participants using progressive glasses were compared with elderly controls, their walking speed was slower and their head and hip flexion were greater when descending the stairs. These findings point toward a reorganization of the postural control and motor strategies that might be required to ensure safe management of negotiating stairs among people who use progressive glasses.

REFERENCES

[1] Startzell et al. (2000). Stair negotiation in older people: a review. *J Am Geriatr Soc* Vol 48; p. 567-580.
[2] Lord et al. (2002). Multifocal glasses impair edge-contrast sensitivity and depth perception and increase the risk of falls in older people. *J Am Geriatr Soc* Vol 50; p. 1760-1766

ACKNOWLEDGMENTS

Project supported by Essilor International - R&D Vision.
Grateful thanks to J.-F. Pilon, M. Goyette and P. Desjardins.
S. Nadeau is a senior researcher funded by FRSQ.

Table 2: Head and hip flexion in the two groups for the three conditions and at the three stair levels (degrees).

		Controls (n=15)			Progressive glasses (n=20)		
		Natural	Far	Close	Natural	Far	Close
Head flexion	Plateau	37.6 ± 9.4	32.0 ± 10.4	35.8 ± 11.8	40.9 ± 9.3	36.9 ± 11.4	43.4 ± 12.1
	First step	34.0 ± 10.8	28.4 ± 12.7	32.2 ± 12.2	36.8 ± 11.5	35.2 ± 11.0	39.2 ± 11.9
	Second step	30.1 ± 11.4	26.7 ± 12.7	28.2 ± 11.7	31.3 ± 12.0	30.2 ± 11.6	36.5 ± 12.9
Hip flexion	Plateau	27.2 ± 18.1	26.9 ± 15.3	26.5 ± 16.4	41.2 ± 10.3	40.6 ± 9.1	39.2 ± 8.2
	First step	26.3 ± 17.9	28.5 ± 16.3	28.3 ± 18.1	35.2 ± 11.8	36.6 ± 10.5	37.7 ± 11.8
	Second step	22.3 ± 15.6	22.4 ± 16.9	21.4 ± 16.8	37.6 ± 11.0	38.1 ± 11.3	33.7 ± 9.5

IS THE GENESIS OF ROTATOR CUFF DISEASE (RCD) LINKED TO MUSCLE FATIGUE?

Clark R. Dickerson
Department of Kinesiology, University of Waterloo, Waterloo, ON, Canada, cdickers@uwaterloo.ca

INTRODUCTION

Although shoulder injuries and dysfunction are common, debilitating, and expensive, biomechanical study of shoulder function and injury mechanisms is historically limited. As a result, the ability to estimate or measure tissue-level exposures trails available methods in other body regions. However, specific tissue loads are known to closely relate to both the occurrence and aetiology of shoulder disorders [1].

Maintaining the subacromial space, which is between the superior humerus and inferior acromion, is critical to rotator cuff health. The supraspinatus and biceps tendons and the shoulder bursa occupy part of the space, and are implicated in RCD. Subacromial impingement (SAI) typically precedes RCD, and occurs when the space is decreased via cumulative or acute trauma, physically compressing the interposed tissues. Two primary mechanistic SAI initiation theories exist [2]: 1) superior humeral migration and 2) scapular dyskinesis. It is unknown which of the mechanisms dominates SAI initiation.

Superior humeral migration: This theory supposes that translation of the humeral head decreases the subacromial space, causing impingement. During abduction, if the rotator cuff muscles cannot maintain compression of the humeral head in the glenoid cavity, either due to fatigue or injury, the humeral head translates superiorly as a result of deltoid action. However, a functioning rotator cuff resists this translation due to force vectors that act largely in compression.

Scapular dyskinesis: This theory supposes that weak or dysfunctional scapular muscles (such as after fatigue) cannot properly guide scapular movement, resulting in geometric reduction of the subacromial space and tissue compression.

The purpose was to evaluate the role of muscular fatigue in enabling these mechanisms, thus establishing a potential work-relatedness of rotator cuff disease development.

METHODS

Two complementary studies were used to achieve the purpose:

I. Measuring fatigue-induced superior humeral migration

Twenty males performed a fatiguing task to exhaustion. Relative humeral position with respect to the glenoid was assessed radiographically at 4 elevation angles (in the scapular plane) while holding a load scaled to arm strength before and after fatigue. RPE, reported after each minute of performing the task was used to define exhaustion. EMG data was subsequently used to identify specific muscle fatigue.

II. Measuring fatigue-induced changes in scapular orientation

Twenty healthy males performed the same fatiguing protocol as in Phase I. 3-D scapular orientation was assessed at 3 arm elevations postures before and after fatigue.

RESULTS

Fatigue of the rotator cuff resulted in superior migration throughout the range of abduction (Fig 1), narrowing the subacromial space in all conditions but the 45° elevation condition, indicating heightened risk. This was pronounced at the 135° elevation, where the mean fatigue effect was 1.0 +/- 1.3 mm (approximately 12-25% reduction of the subacromial space). Scapular orientation changes existed for scapular tilt and scapular rotation (Fig 2), as much as 10° for rotation in the 90° elevation condition. These are meaningful changes given the initial dimensions of the subacromial space.

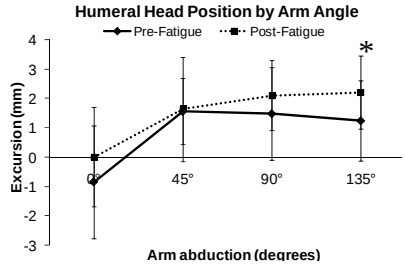

Figure 1: Humeral head excursion by arm angle and fatigue state [+ = upward] (* = significance at given arm angle)

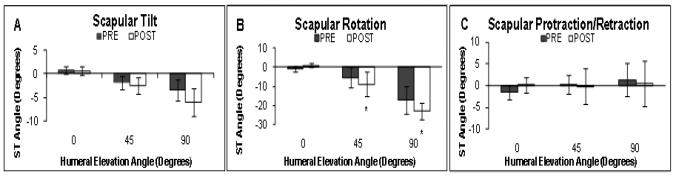

Figure 2: Scapular orientation after fatigue protocol [negative = posterior tilt, upward rotation, retraction] (* = significance)

DISCUSSION AND CONCLUSIONS

This work is the first to conclusively show that simulated work tasks leads to substantial changes in scapula-humeral relative position and orientation consistent with rotator cuff patients. As these characteristic changes are thought to precede SAI and RCD, the findings argue that work-related SAI likely occurs, particularly with overhead postures. In terms of magnitude of change, humeral translation appears to account for more SAI.

Integrated analyses must follow to clarify their links to injury initiation. The next step is to augment an existing shoulder model [3] with these empirical data and an original stochastic computerized shoulder morphometric database. The database has been developed using a unique 3-D white light digitizing system and cadaveric specimens. This will enable high-fidelity 3-D geometric recreation of the fatigue scenarios, including subacromial space volumes, for a population.

REFERENCES

[1] Hughes RE, An KN (1997) *Med and Bio Eng and Comp* 35:544-548.
[2] Michener LA et al. (2003) *Clin Biomech* 18(5):369-379.
[3] Dickerson CR et al. (2007) *Comp Methods Biomech Biomed Eng*, 10(6):389-400.

ACKNOWLEDGEMENTS

Funding for this research was awarded by CFI, ORF, NSERC, and CRE-MSD. Special thanks to Jaclyn Chopp, who played an essential role in completing this work.

BETWEEN-DAY RELIABILITY IN MEASUREMENT OF SHORT-LATENCY MUSCLE ACTIVATION AND FORCE-TIME VARIABLES OF THE NECK

Lucie Pelland[1], Sivan Almosnino[2], Joan Stevenson[2]
[1]School of Rehabilitation Therapy, Queen's University, Kingston, Canada, www.rehab.queensu.ca/
[2]School of Kinesiology and Health Studies, Queen's University, Kingston, Canada, www.queensu.ca/skhs

INTRODUCTION

Evidence of lasting effects of concussions on brain function [1] has prompted the need for effective risk management strategies to be implemented early in athletes' development. Simulation studies on the biomechanics of concussions demonstrate the important role that increased short-latency neck muscle strength could play in reducing the incidence and severity of concussion during a collision [2]. Population-based studies are needed at this time to provide empirical evidence regarding the implication of increased short-latency neck muscle stiffness on the risk for concussions in contact sports. The goal of our study was to determine the between-day reliability in measurement of discrete variables of short-latency neck stiffness necessary to this evaluation: rate of force development (RFD), time to 50% peak force (T_{50}PF) and latency of muscle activation (MA) to force onset.

METHODS

Twenty-six male athletes participated in two testing sessions, 7 to 8 days apart. Force and muscle activation measures were obtained under isometric conditions, with participants being asked to develop maximal force 'as fast as possible' and then to hold this force level until the end of the 5 s trial. Maximal efforts were produced in flexion, extension, protraction and lateral bending. The 3-dimensional components of force were recorded using a 6 degree-of-freedom load cell (MC5-2500, AMTI, Watertown, MA) mounted to a custom-built fixed frame [3] that includes a semi-spherical aluminium structure to which a hockey helmet (Bauer Nike, St-Jerome, QC) can be attached and used to couple the head and neck to the load cell (Figure 1); the helmet includes a face mask and reinforced chin strap to resist maximal efforts in flexion. The system is adjustable to participants' height and size. Surface electromyographic signals (sEMG) were recorded (Bortec AMT-8 amplifier, Bortec Biomedical, Calgary, AB) from the splenius capitis (SpC), upper trapezius (UT), and sternocleidomastoid (SCM) muscles bilaterally. The force and sEMG signals were sampled using a common 16-bit analog to digital converter (NI PCI-6036E, range of ± 5V) at 2048 Hz using custom-written software (Labview, version 8.6; NI Inc., Austin, TX). Outcome variables (RFD, T_{50}PF and MA) were extracted from the sampled signals using the Teager-Kaiser Energy Operator. Test-retest reliability was evaluated from the mean difference (95% CI) in score between the two session, the standard error of measurement (SEM), and intra-class correlation ($ICC_{3,3}$).

RESULTS

The discrete variables of short-latency force development, RFD and T_{50}PF, were measured with good reliability in all directions, with mean differences in between-day measures of -1.8% to 2.7%, and 95%CI below 10% and overlapping zero. SEM values of 4.8% to 9.0% for RFD and 7.4% to 9.3% for T_{50}PF were calculated, with $ICC_{3,3}$ scores ranging from 0.90 to 0.99. The corresponding smallest detectable difference (SDD) values, which indicate the smallest change in between-day measurement necessary for statistical significance, ranged between 13.3% and 25.0% for RFD, and 19.8% and 25.7% for T_{50}PF. Between-day measures of MA were also reliable, with test-retest differences of less than 4 ms, and a 95%CI range of -7.7ms to 9.2ms and overlapping zero. Between-day measures were most reliable in extension, with SEM values between 2.5 ms and 4.0 ms, and $ICC_{3,3}$ scores between 0.52 and 0.79. SEM increased in lateral bending and flexion, ranging between 3.4 ms and 4.8 ms, with $ICC_{3,3}$ scores of 0.23 to 0.71. Overall reliability was poor for protraction, with SEM values between 8.6 and 12.0 ms. Calculated SDD values ranged from 8.3 ms for the right SCM in extension to 14.0 ms for the right SCM in right lateral bending; values for protraction were not considered.

Figure 1: **Custom-built fixed frame dynamometer**, showing the coupling unit between the hockey helmet and the load cell; the standard position for testing is also shown.

DISCUSSION AND CONCLUSIONS

Short-latency force-time and muscle activation variables can be measured with sufficient reliability to be used in controlled studies to systematically investigate the relationship between active stabilization (or stiffening) of the neck and concussion biomechanics, as well as to evaluate the recommendation of including specific training protocols to improve short-latency neuromuscular response and neck force in the general conditioning programs of athletes in high-risk youth sports, such as ice hockey.

REFERENCES

[1] Marchie A, Cusimo MD. (2003) Bodychecking and concussions in ice hockey: Should our youth pay the price? *Canadian Medical Association Journal* Vol **169**(2); p.124-128.
[2] Viano DC et al. (2007) Concussion in professional football: Biomechanics of the struck player. *Neurosurgery* Vol **61**(2); p. 313-328.
[3] Almosnino et al. (2009) Retest reliability of force-time variables of neck muscles under isometric conditions. *Journal Athletic Training* (in press, JAT0155-09R).

ACKNOWLEDGEMENTS

Supported by the Ontario Neurotrauma Foundation to L.Pelland.

THE INFLUENCE OF FATIGUE ON TISSUE VIBRATION IN PROLONGED RUNNING

Bernd M. Friesenbichler[1], Lisa M. Stirling[1], Peter Federolf[1], Benno M. Nigg[1]
[1]Human Performance Laboratory, Faculty of Kinesiology, University of Calgary, Calgary, Canada, berndf@kin.ucalgary.ca

INTRODUCTION

In running, the impact shock at heel-strike is transferred to the skeletal system and to the connected soft tissues and causes it to vibrate. It has been shown that prolonged exposure to vibrations can have negative effects on these tissues [1,2]. It was suggested that soft tissues, therefore, are critically damped to minimize vibrations and that muscle activity within the tissues is damping those vibrations, a process referred to as *muscle tuning* [3]. The question which arises is whether the protective minimization of vibrations is negatively influenced by muscle fatigue, which is inherent with altered muscle activation. Thus, the aim of this study was to identify fatigue dependent changes in soft tissue vibration characteristics. The hypothesis to be tested was that the vibration intensity increases with fatigue.

METHODS

Ten healthy recreational runners were asked to complete as many laps as possible of a 230m outdoor course while maintaining a constant running speed (i.e. run to exhaustion). The running speed was determined for each subject based on their self-reported best 10km race time within the last year. All subjects were instrumented with two accelerometers (ADXL 78, range ±35g, Analog Devices USA). A single-axis accelerometer was secured with a vertical orientation to the heel-cup of the left shoe to detect heel-strike. A tri-axial accelerometer was secured to the muscle bulk of the triceps surae to measure the vibrations of that soft-tissue compartment. The axes of the tri-axial accelerometer were oriented to be parallel to the long axis of the tibia, medio-lateral (M-L) and anterior-posterior (A-P; i.e., normal to the skin). The frequency content of the data was calculated using Fast Fourier transformation and represented in power spectra, where local maxima of a non-fatigued (NF) to a fatigued (F) state of the subject were compared (Figure 1) with an independent Student's t-test (significance level: $p < 0.05$). Additional wavelet analysis allowed resolving fatigue dependent shifts of the time span starting from heel-strike until the time point when maximal vibration intensity was reached during stance phase.

RESULTS

In axial direction, 24 local maxima showed a significant intensity increase with fatigue, 8 showed a significant intensity decrease. Vibrations in M-L direction were affected in a similar way with 21 increasing and 9 decreasing local maxima. A-P vibration intensities showed the same amount of increases and decreases (Table 1). Maximal vibration intensity appeared in general later with fatigue, with significant results in all three vibration directions.

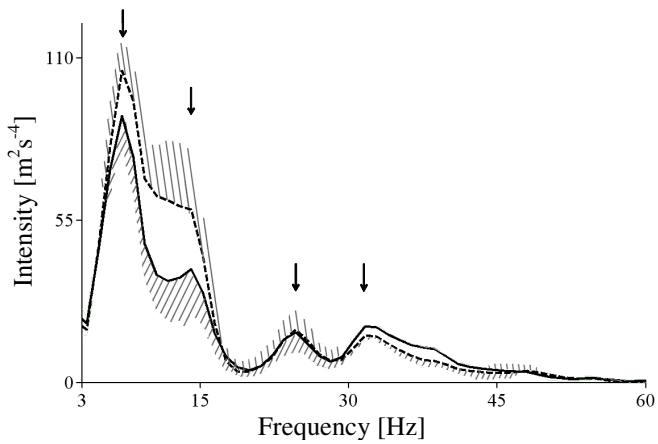

Figure 1: Example for a power spectrum from vibration data in axial direction. The solid line represents NF (mean - STD), the dashed line condition F (mean + STD). The arrows are pointing at local maxima.

DISCUSSION AND CONCLUSIONS

A possible mechanism for the intensity increases, which mainly occurred in axial and M-L direction and a later appearance of the maximum intensities might be a disturbance of *muscle tuning* with fatigue. Thus a fatigued muscle might not be able to control the damping mechanisms as well as a non-fatigued muscle. The protecting mechanism appears to be negatively influenced by fatigue. The effect of sports induced vibrations to human skeletal muscle needs further studies to determine if the increased vibration intensities actually represent potential harm to an athlete's body.

REFERENCES

[1] Bongiovanni, L.G. et al. (1990). Prolonged muscle vibration reducing motor unit output in maximal voluntary contractions in man. *J. of Applied Physiology* 423; p. 15-26.
[2] Dupuis, H. and Jansen, G. Immediate effects of vibration transmitted to the hand. In: *Man Under Vibration – Suffering and Protection*, Elsevier, 1981.
[3] Nigg, B. M. (1997). Impact forces in running. *Current Opinion in Orthopaedics* 8; p. 43-47.

Table 1: Summation of significant changes of vibration intensity in fatigued state for each subject and direction

Subject 1-10	Direction	Intensity increase in F	Intensity decrease in F
Total	Axial	24	8
	M-L	21	9
	A-P	22	22

THE IMPACT OF MINI-BANDS ON FRONTAL PLANE KNEE KINEMATICS DURING SQUAT TRAINING

Chad E. Gooyers, Tyson A.C. Beach, David M. Frost & Jack P. Callaghan
Department of Kinesiology, University of Waterloo, Waterloo, ON, CA
Email: cgooyers@uwaterloo.ca

INTRODUCTION

One commonly observed movement pattern in athletic competition that is associated with the development of knee dysfunction is excessive knee motion in the frontal plane [1]. Large amounts of mediolaeral motion of the knee joint has been linked to the development of patellofemoral pain syndrome [2], as well as anterior cruciate ligament rupture [3]. As such, it has become increasingly popular for strength and conditioning coaches to counter these aberrant movement patterns using elastic "mini-bands" (Mini-Bands, Perform Better, Cranston, RI) as an aid to cue proper technique in various closed-chain lower body exercises; however there is limited scientific evidence to support the use of this aid in athletes with normal knee mechanics. The purpose of this investigation was to compare the frontal plane knee kinematics in recreational athletes when performing both a body-weight squat (BWS) and squat jump (SJ) with and without the elastic exercise bands placed around the thighs (Figure 1).

Figure 1. Sample body-weight squat with mini-bands.

METHODS

All data used for this investigation were collected in a biomechanics laboratory during one testing session. A convenience sample of 12 recreationally trained athletes participated in this investigation (4 males, 8 females; mean/S.D. height = 1.70/0.07 cm, mass = 68.0/13.5 kg). The testing protocol consisted of participants completing a total of three repetitions of both the BWS and SJ in each of the following experimental conditions: (1) control condition with no mini-band, (2) BWS/SJ squat with a 'light' tension (yellow) mini-band placed 10 cm proximal to the knees and (3) BWS/SJ with a 'medium' tension (green) mini-band placed 10 cm proximal to the knees. The SJ was perfomed with no counter-movement prior to take-off. The order in which each of the 6 conditions were performed was completely randomized across all subjects. In addition, prior to participating, all subjects were provided an opportunity to familiarize themselves with wearing the bands and performing the two exercises.

For this study motion data were captured at 60 Hz using ten VICON MX40 cameras (Vicon Motion Systems, Oxford, UK). Three-dimensional kinematics of the left and right lower limbs were tracked using five-marker rigid bodies placed on the thighs, shanks and feet; seven virtual markers collected during a standing calibration trial were used to define the position of relevant anatomical landmarks with respect to the rigid bodies. Using Visual3D (C-Motion, Germantown, MD, USA), these data were used to calculate joint motion in the frontal plane of both the left and right knees for all trials. From these data the peak abduction angle was calculated and compared across all three experimental conditions. For SJ activity only the take-off portion of the movement was considered. A two-factor (side and condition) repeated measures ANOVA ($p < .05$) was used for statistical analyses.

RESULTS

For both the BWS ans SJ, there were no significant differences in the peak abduction angle measured across any of the experimental conditions ($p > .05$). In addition, there were no differences found in the peak abduction angle measured between the left and right sides ($p > .05$).

DISCUSSION AND CONCLUSIONS

Based on the results of the present work it would appear that attempts to exaggerate the frontal plane collapse of the knees do not alter the frontal plane knee kinematics during a squat motion in healthy recreational athletes. Despite these findings, future work examining knee joint kinetic responses to mini-band use are warranted, especially if insight is to be gained regarding the possibility for mini-bands to alter knee injury potential during training. The potential influence of the mini-bands on individuals exhibiting mediolateral knee motion during exercise needs to be assessed. When used on healthy athletes, mini-bands do not adversely impact the knee joint during squatting motions.

REFERENCES

[1] Kritz et al., 2009. *Strength & Conditioning Journal.* 31(1) – 76-85
[2] Levinger et al. 2007. *Physical Therapy in Sport.* 8: 163-168
[3] Quatman, CE and Hewett, TE. 2009. *Br J Sports Med.* 43(5): 328-335

PREDICTORS OF LOWER EXTREMITY INJURIES IN VARSITY ATHLETES

Timothy A. Burkhart[1,2], Alison Schinkel-Ivy[1], David M. Andrews[1,2]
[1]Department of Kinesiology, University of Windsor, Windsor, ON, Canada
[2]Department of Industrial and Manufacturing Systems Engineering, University of Windsor

INTRODUCTION

The magnitude of tibial shock has been shown to affect the risk of injury in athletes [1]. The mass of shank tissues (muscle, fat, bone) have also been shown to have a significant effect on properties of the shock after traveling through the leg [2]. However, the effect that the tissue masses have on lower extremity injuries and whether they have any interacting effects with other previously determined risk factors such as race, physical activity level and sport, has not been considered to date. Therefore, the purpose of this study was to determine the significant predictors of lower extremity injury in varsity athletes with emphasis on leg tissue masses and tissue mass ratios.

METHODS

Male and female basketball (BB) (M=18, F=9), volleyball (VB) (F=10), soccer (S) (M=29 F=7) and cross-country (CC) (M=18, F=13) varsity athletes participated in this study. Data were collected on 86 variables, including demographics, physical activity history, medication use, footwear (categorized as wearing different footwear in games and practices), playing surface and injury history, over the course of their respective seasons. Tissue mass prediction equations [3] were used to calculate the lean mass (LM), fat mass (FM), wobbling mass (WM) and bone mineral content (BMC) of the lower extremities. Injuries were reported by athletes and confirmed by two certified athletic therapists. Stress fractures were also confirmed by an orthopedic surgeon. Injuries were first categorized generally (left and right leg separately) and then divided into bone and soft tissue injuries. Logistic regression analysis was used to determine the multivariate predictors of lower extremity bone and soft tissue injuries.

RESULTS

Overall, 36% of the athletes reported an injury, of which, 15% were considered bone injuries. In general, sport and playing surface were significant injury predictors, with BB athletes (OR=0.11) and athletes who play on hardwood (OR=0.13) at a lower risk of sustaining any type of injury (Table 1). With respect to tissue mass ratios, left leg LM:BMC (OR=0.028) was the best predictor, suggesting that as the ratio of LM to BMC increased, the risk of injury decreased. The best predictors of injuries to bone were leg FM:BMC (OR=1.80) and left foot LM:FM (OR=0.63). Interestingly, athletes who reported wearing different footwear in games and practices were 4 times more likely to sustain an injury to the bone (OR=4.02).

DISCUSSION

The influence of sport on lower extremity injuries could be indicative of the different loading patterns across sports. For example, BB players are subjected to impacts from both running and jumping whereas S players and CC athletes are subjected to forces strictly from running. This suggests that variation in loading patterns may be beneficial to athletes. However, the type of playing surface may also explain why BB and VB players are at a decrease risk of injury as they compete and practice exclusively on the more compliant hardwood surfaces. The results also suggest that inconsistent use of footwear may have implications for the leg in terms of how it can adequately adapt its protective muscle tuning effects [4]. This may lead to increases in the magnitude of shock that travels through the leg, which has been implicated in lower extremity injuries [1]. Finally, it appears that an optimal level of BMC exists and that a leg with more muscle than fat surrounding the bone is better suited to increasing the attenuation of shock waves as they progress proximally through the leg after impact.

REFERENCES

[1] Milner, C.E. et al. (2006). Med. Sci. Sport Exer., 38, 323-328.
[2] Schinkel, A. et al. (2009). Proceedings of the 22nd ISB Congress, Cape Town, South Africa.
[3] Holmes, J. et al. (2005). J. Appl. Biomech., 21, 371-382.
[4] Wakeling J. M. et al. (2002). Med. Sci. Sport Exer. 34, 1529-1532.

ACKNOWLEDGEMENT

Thanks to NSERC for funding this project.

Table 1: Summary of lower extremity injury predictors (OR=Odds ratio; CI=Confidence interval) (* $X^2<0.05$; $^{\dagger}p<0.05$).

Variable	Category	n	Uninjured	Injured		95% CI
Sport*	BB /CC	31/27	85.1%/41.9%	14.2%/ 58.1%	0.1	0.1-0.7
Different Footwear*	No/Yes	52/51	73.1% / 49.0%	26.9% / 51.0%	2.0	0.5-9.0
Playing surface*	Hardwood/Mondo	39/25	82.1% / 40.0%	17.9 % / 60.0%	0.13	0.0-0.8
Left leg LM:BMC†		106	11.9	12.0	0.03	0.0-0.8
Left leg FM:BMC		106	2.0	2.7	1.9	1.1-3.1
Left foot LM:BMC		106	3.9	3.7	0.9	0.8-0.9

Dynamic Tracking of Myotendinous Junction: Effect of Immediate Exercise on Tendon Property using Ultrasound Imaging

Mahta Karimpoor, Richard Twycross-Lewis, Hazel Screen, Dylan Morrissey
School of Engineering and Material Science, Queen Mary University of London, London, E1 4NS, UK
ex07322@qmul.ac.uk, richard.twycross-lewis@thpct.nhs.uk, h.r.c.screen@qmul.ac.uk, dylan.morrissey@thpct.nhs.uk

INTRODUCTION

In vivo measurements of tendon mechanics is important to understand tendon properties. This is mainly determined by plotting force against elongation [1]. Tendon elongation is achieved by looking at the changing position of Myotendinous Junction (MTJ) using Ultrasound (US) [2]. The aim is to develop an automatic method to track MTJ movement dynamically in a sequence of Ultrasound images [3] which is then used to compare tendon properties before and after exercise in this study.

METHODS

Isokinetic Measurements: 12 male subjects (mean age 26 (± 7.50) years old) were recruited from the student body of Queen Mary, University of London. Each subject lay prone on an Isokinetic dynamometer (Biodex Series 2) and was then asked to push against the footplate for 5 seconds with as much force as he could with his test foot. The foot was strapped into the footpad so as to ensure isometric contraction was performed. During this period an ultrasound probe (12L-RS 5.0-13.0 MHz wideband linear array probe) was placed on their Achilles tendon at the MTJ to record MTJ movements at 25 frames per second. During isometric contraction, force was recorded by the dynamometer. Details of Isokinetic measurements are the same as described in [2].

Exercise protocol: Each subject was asked to stand on a step and perform a series of single leg heel drops. This was performed for a total of 3 sets of 15 repetitions with 1 minute rest intervals between each set. The knee of their test leg was kept in a full extension; the contralateral knee was kept at 45° flexion during the test. After the eccentric exercise test, the isokinetic measurements were repeated a further 3 times.

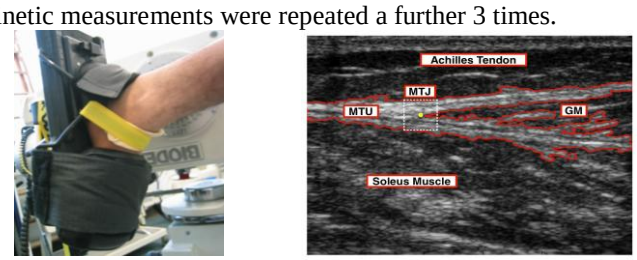

(a) (b)

Figure 1: a- strapping ankle, b- position of the Achilles tendon, gastrocenemius muscle (GM), the soleus muscle and MTJ at resting state in the body.

Proposed dynamic method for MTJ tracking:
US data was exported in the form of AVI movie in to an external computer for further analysis. Each image was enhanced using an isotropic diffusion method [4], which links nearby image components together and smoothes the image. It should be noted that two white visible lines coming into MTJ is referred to as MTU in this study. The images were then binarized and segmented to extract the related MTJ component MTU. A rectangular template from previous images was then defined to cross-correlate with the extracted MTU of the next frame. The point at which maximum cross correlation occurs was considered as the new position of MTJ. This process was repeated iteratively for the remaining sequence of images to find new location of MTJ. The force-Elongation curve was plotted in MATLAB after calculating the MTJ position [3].

RESULTS

Force-elongation curves before and after eccentric exercise display a curvi-linear relationship. A significant decrease in the slope of normalized force to normalized tendon elongation can be observed in the results.

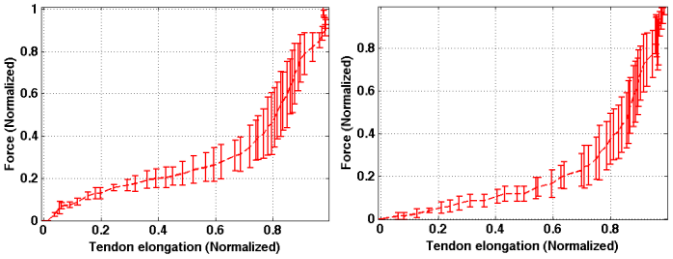

(a) (b)

Figure 2: Force-Elongation curve with standard deviation recruited on 12 individuals: a) Before exercise; b) After exercise

CONCLUSION

Force-Elongation curve shows more compliant profile at low loads in post-exercise condition. Our results indicate that exercise might result in improved flexibility of tendon. Image analysis by cross-correlation was found to be an effective tool for tracking of the dynamic response of the MTJ during isometric contractions.

REFERENCES

[1] Joza, L. G., Kannus, P., and Josza, L., "*Human Tendons: Anathomy*, Physiology and Pathology" (1997).
[2] Maganaris, C. N. and Paul, J. P., "Tensile properties of the in vivo human gastrocnemius tendon," *Journal of Biomechanics* 35(12), 1639–1646 (2002).
[3] Karimpoor, M., Screen, H., and Morrissey, D., "Dynamic Tracking of Tendon Elongation In Ultrasound Imaging," in Proc. of SPIE Medical Imaging, February 13-18, San Diego CA, 2010.
[4] Perona, P. and Malik, J., "Scale-space and edge detection using anisotropic diffusion," *Pattern Analysis and Machine Intelligence, IEEE Transactions on* 12, 629–639 (Jul 1990).

3-DIMENSIONAL KINETIC ANALYSIS OF OLYMPIC SNATCH LIFT

David John Saxby[1] and D. Gordon E. Robertson[2],
School of Human Kinetics, University of Ottawa, Ottawa, Canada
[1]davidsaxby@gmail.com, [2]dger@uottawa.ca, http://www.health.uottawa.ca/biomech

INTRODUCTION

Olympic Weightlifting (OL) is a sport requiring tremendous muscular effort in addition to excellent coordination and timing [1]. The components of Olympic Weightlifting, the snatch and the clean & jerk, involve all large muscle groups and are performed with emphasis on speed of movement and technical mastery [1]. Limited 3-dimensional kinetic research has been conducted on OL movements [2]. This study will examine selected kinetic and kinematic differences in lift mechanics as barbell load varied between 80-90% of maximal.

METHODS

The selection method was opportunistic to ensure competent lifting performances. The five male participants (4 adult, 1 junior) were National or International caliber weightlifters. A 14-segment rigid-link model represented the musculoskeletal system. Participants executed 3 snatch lifts at predetermined relative capacities. Trial order was balanced to limit order effects. A five-camera Vicon MX system, sampling at 200 Hz, captured lift kinematics. Trajectories were low-pass filtered using Butterworth filters with 6 Hz cut-offs. Ground reaction forces of both feet were recorded from two Kistler force platforms and digitally filtered (10 Hz cut-offs). Net moments and powers were computed using Visual3D.

RESULTS

Figure 1 shows the results of one subject's successful and unsuccessful attempt at a 95% capacity lift. Peak moments of force and powers about the joints of the lower extremity in the sagittal plane across both trials are presented in Table 1 below.

DISCUSSION AND CONCLUSIONS

Inspection of Figure 1 shows sagittal plane angular velocities, moment of force and power about the joints of the lower extremity are similar. Ankle net moment of force was plantiflexor from lift-off through to explosion its power production was punctuated with two distinct periods of positive work occurring during barbell lift-off (A1) and explosion (A2) with a small burst of negative between.

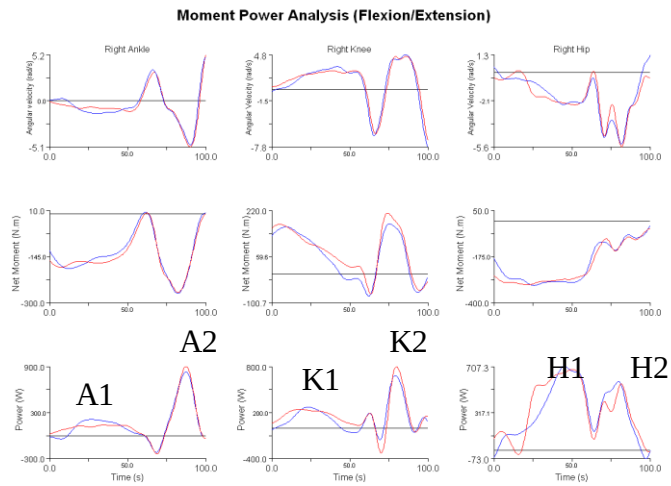

Figure 1: The angular velocities (rad/s), moments of force (N.m) and powers (W) about the ankle (left), knee (middle) and hip (right) about the flexion/extension axis. Successful trial variables are blue, and missed lift is red.

The knee moment of force produced two bursts of extensor positive work (K1 and K2) separated by short bursts of positive work by the flexors and of negative work by the extensors. These correspond to the initial knee extension during liftoff, rapid flexion during transition (due to double knee bend technique), and a prestretch before the final extension during the explosion phase (K2). The hip moment was extensor throughout the lift producing two peaks of positive work, first during liftoff (H1) and a second during the explosion (H2). These patterns of activity are similar to those of vertical jumping where all three joints also produce extensor moments nearly simultaneously.

REFERENCES

[1] Garhammer J (1980). Power production by Olympic weightlifters. *Med Sci Sports Exercise* Vol 12(1); p.54-60.
[2] Baumann W et al (1985). The Snatch Technique of World Class Weightlifters at the 1985 World Championships. *Int J Sport Biomech* Vol 4; p. 68-89.

ACKNOWLEDGEMENTS

Kind regards to PM for assisting with participants.

Table 1: Summary of peak moments of force and powers across successful and an unsuccessful 95% snatch lift

	Ankle Moment (N.m)	Ankle Power (W)	Knee Moment (N.m)	Knee Power (W)	Hip Moment (N.m)	Hip Power (W)
Successful	-268.52	832.76	174.4	685.96	-315.28	707.26
Unsuccessful	-265.13	909.5	211.7	802.14	-311.73	802.14

THE INFLUENCE OF SHOE CONSTRUCTION ON WALKING AND BALANCE PERFORMANCE

Ann-Kathrin Hömme[1], Ewald M. Hennig[1], Seungbum Park[2]
[1] Biomechanics Laboratory, University Duisburg-Essen, Essen, Germany, Ann-Kathrin.hoemme@uni-due.de
[2] Busan Footwear Promotion Center, Busan, South Korea

INTRODUCTION

Masai Barefoot Technology (MBT) shoes have become increasingly popular in recent years. Nowadays, many other shoe companies produce shoe design of similar shape and construction features. These shoes are marketed by claiming a number of benefits for the human body: a better posture during standing and walking, reducing loads in the joints, strengthening and shaping muscles, and increasing metabolic energy consumption. Many of these claims are not proven, although there is clinical evidence that these shoe constructions can have a beneficial effect on pain in osteoarthritis patients [1]. Our study compared gait and balance characteristics for an MBT shoe with a conventional leather shoe, a running shoe, and barefoot.

METHODS

13 male and 6 female subjects between 20 and 30 years participated in this study. They walked with three different pair of shoes at a speed of 1.6 m/s across a "Kistler" force platform: a conventional running shoe (RS) (ASICS™ GT 2140), a leather business shoe (LS) and a MBT shoe (MBT) (MBT™ Chapa Caviar). Moreover, tibial shock was measured with a miniature accelerometer (Entran™ EGAX-25). Pronation angle and pronation velocity were collected by an electro-goniometer. In-shoe pressures were recorded by miniature piezoceramic force transducers.

The subjects also participated in a balance control experiment. They stood on a force platform during two different tasks for a duration of 10 seconds. They were instructed to stand as quiet as possible during both leg support with closed eyes and during one-leg standing with open eyes. Each task was performed in all shoe models as well as barefoot (BAR) on a "Kistler" force plate. The order of shoe and task assignment was randomized. During the balancing tasks the path of the Centre of Gravity (CoG) was measured. Simultaneously, muscle activity of the m. vastus lateralis (VL), m. biceps femoris (BF), m. tibialis anterior (TA) and m. gastrocnemius (GA) were recorded by four bipolar EMG electrodes (Delsys Inc., Boston, MA, USA). For statistical evaluation a dependent measures ANOVA was used.

RESULTS

The MBT shoe (622 ms) showed significantly ($p<0.01$) lower ground contact times during stance against RS (644 ms) and LS (653 ms). Against both other shoe conditions peak tibial acceleration was significantly higher ($p<0.01$) in the leather shoe (4,4 g), followed by the MBT (3,1 g) and RS (2.8 g). Subtalar range of motion was significantly higher ($p<0.01$) in the leather shoe (15.7 °) against both the MBT (13.2 °) and RS (12.1 °). Similarly, maximum pronation velocity was highest in LS (583 °/s) against MBT (397 °/s) and RS (371 °/s). Peak plantar pressures were highest in LS (heel = 478 kPa; forefoot = 405 kPa) as compared to the MBT (heel = 310 kPa; forefoot = 227 kPa) and RS (heel = 206 kPa; forefoot = 197 kPa).

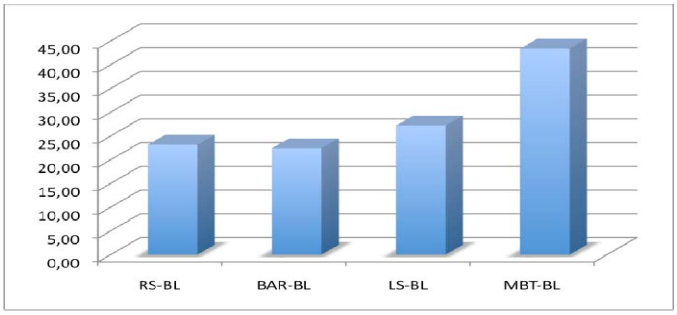

Figure 1: CoG path length during 10 sec both leg standing with closed eyes

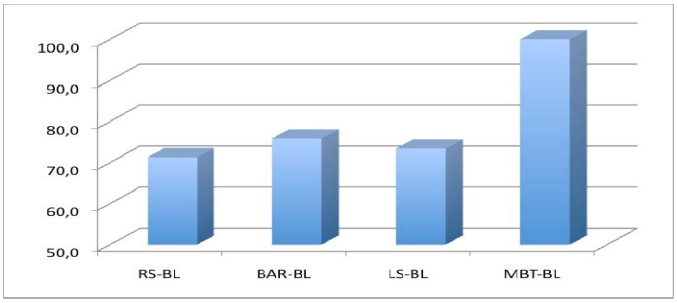

Figure 2: Normalized IEMG (%) of the biceps femoris during 10 sec of both leg standing with closed eyes

The length of the CoG during both leg standing with closed eyes (figure 1) and one leg standing with open eyes was significantly ($p<0.01$) increased for the MBT against all other conditions. Similarly, the IEMG with MBT shoe was also increased ($p<0.01$) against all other conditions in both standing situations for the three muscles VL, BF (figure 2) and TA. For GA no significant EMG differences were found.

DISCUSSION AND CONCLUSIONS

The running shoe shows lowest shock, pronation and plantar pressure values during gait. In the MBT shoe all of these values are moderately higher. However, the leather shoe shows by far the highest values for these variables. The CoG length during standing and the EMG activity is considerably increased for the MBT shoe. Therefore, the MBT shoe is less stable and requires more muscle activity for balance control.

REFERENCES

[1] Nigg, B. M. et al. (2006): Unstable Shoe Construction and Reduction of Pain in Osteoarthritis Patients, MSSE, 38 (10), p. 1701–1708

ACKNOWLEDGEMENTS

This research was supported by the Busan Footwear Promotion Center, South Korea.

Quantification of inertial sensor-based 3D knee joint angle measurement accuracy using an instrumented gimbal

A. Brennan, K. Deluzio and Q. Li
Department of Mechanical and Materials Engineering, Queen's University, Kingston ON, Canada
Human Mobility Research Centre, Queen's University and Kingston General Hospital, Kingston ON, Canada

INTRODUCTION

Quantification of knee joint kinematics is important in the diagnosis of knee joint disorders, in the evaluation of functional ability following rehabilitation, and in the control of wearable robotic devices. To bring the analysis out of the laboratory and make it portable, recent efforts have focused on estimating knee joint kinematics using accelerometers and gyroscopes [1, 2]. For example, Favre et al. (2009) proposed a novel IMU alignment procedure to estimate knee joint angle according to the International Society of Biomechanics (ISB) recommendation [2].

To determine the feasibility of using inertial sensor to estimate 3D knee angle, it is necessary to quantify the performance of an IMU system by comparing the anatomical knee joint angle estimates with those directly measured from a mechanical device with a higher accuracy, which is the objective of this study.

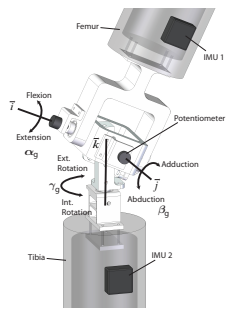

Figure 1: Schematic of instrumented gimbal.

METHODS

Two IMUs (Ineria-Link, Microstrain Inc., VT.), one attached to the femur and one attached to tibia limb segment of the instrumented gimbal (Figure 1), were used to estimate 3D joint angles through a series of transformations between measurements in different coordinate frames (Figure 2).

The IMU sensor attachment transformations T_{TATM} and T_{FAFM}, and the orientation estimates M_F and M_T, both contributed to the angle estimation error. To separate these two error sources, we calculated 3D joint angles using two methods. The visual sensor alignment method used the nominal sensor attachment transformations —arrived by a careful visual alignment of the sensors with the segment anatomical frames—to estimate joint angles. The optimized sensor alignment method used the adjusted sensor attachment transformations—obtained from minimizing the sum of squared errors between the gimbal measured angles and the inertial system—to compute joint angles. We computed the root mean square error (RSME) between the reference gimbal and the two inertial methods. We also presented the results using the Bland-Altman limits of agreement.

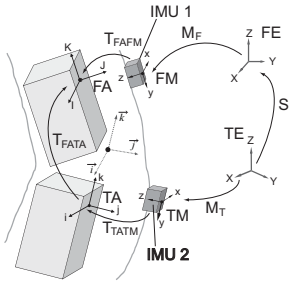

Figure 2: Individual frames and the sequence of transformation for knee anatomical angle estimation.

Table 1: Results from Bland-Altman.

Method	Anatomical angle	RMSE	Bland-Altman Mean	Limit of agreement
Visual	Flexion/Extension	6.30	5.92 (1.61)	(2.69, 9.14)
sensor	Adduction/Abduction	3.74	2.65(1.61)	(-0.56, 5.87)
alignment	Internal/External Rotation	8.79	2.85(2.34)	(-1.83, 7.53)
Optimized	Flexion/Extension	1.54	0.00 (1.54)	(-3.09, 3.09)
sensor	Adduction/Abduction	0.81	-0.01(0.81)	(-1.62, 1.62)
alignment	Internal/External Rotation	1.81	0.00(1.81)	(-3.61, 3.61)

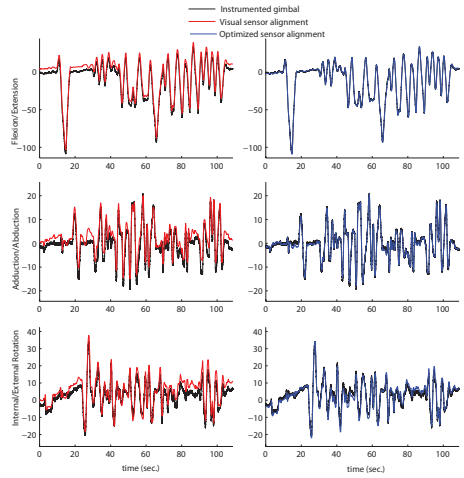

Figure 3: Anatomical knee joint angle estimation using visual sensor alignment and optimized sensor alignment

RESULTS

As expected, angle estimation errors in visual sensor alignment were higher than those of optimized sensor alignment. With a careful visual sensor alignment, the limits of agreement (Table 1) for flexion/extension, adduction/abduction and internal/external rotations are $(2.69, 9.14), (-0.56, 5.87)$, and $(-1.83, 7.53)$ respectively. The optimized sensor alignment method reduced the limits of agreement to $(-3.09, 3.09), (-1.62, 1.62)$, and $(-3.61, 3.61)$ respectively and the RMS errors decreased by 75%. As shown in Figure 3, the optimization procedure increased the joint angle estimation accuracy mainly by eliminating the biases. This implies that any misrepresentation of the sensor attachment matrix would introduce kinematic cross-talk, resulting a systematic error in the angle estimate.

DISCUSSION AND CONCLUSIONS

Instead of the IMU sensor itself, the sensor misalignment (*i.e.*, the error in the transformation matrix from sensor measurement frame to anatomical frame) is one major contributor to the anatomical knee joint angle estimation error. Due to a complex geometry of leg segments, it is reasonable to expect that the contribution of sensor misalignment error would be even larger when estimating human knee joint angles. Inertial motion tracking suffers from an inability to locate the anatomical landmarks for determining the transformation matrix between measurement and anatomical frame. In conclusion, an accurate calibration procedure for identifying the sensor attachment matrix needs to be developed in order to use IMU for ambulatory joint angle measurement.

References

[1] G. Cooper, Y. Sheret, L. McMillian, K. Siliverdis, N. Sha, D. Hodgins, L. Kenney, and D. Howard, "Inertial sensor-based knee flexion/extension angle estimation," *Journal of Biomechanics*, vol. 42, pp. 2678–2685, 2009.

[2] J. Favre, R. Aissaoui, B. Jolles, J. de Guise, and K. Aminian, "Functional calibration procedure for 3d knee joint angle description using inertial sensors," *Journal of Biomechanics*, vol. 41, pp. 2330–2335, 2009.

A NEW APPROACH TO POSTURAL STABILITY RESEARCH USING THE INVERTED PENDULUM MODEL

Nicholas Ali[1]; Gordon Robertson[1]; Gholamreza Rouhi[2]
[1]School of Human Kinetics, University of Ottawa, nali065@uottawa.ca
[2]Department of Mechanical Engineering, University of Ottawa, grouhi@uottawa.ca

INTRODUCTION

The ability to maintain the centre of mass (COM) in relation to the base of support (BOS) is termed postural stability (PS). For PS studies, the human body is often modeled as a single-segment inverted pendulum rotating about the ankle joint. Winter's model [1] utilized such an inverted pendulum to predict PS during quiet standing yielding the following equation:

$$\text{COP} - \text{COM} = k\,\ddot{x} \qquad (1)$$

where $k = I / Wh$. Here $\ddot{x}$ is the horizontal acceleration of the body's COM, I is the body's moment of inertia, W is the body's weight, and h is the height from COM to the ankle. A challenge with this model is that it requires motion capture data from very precise optical systems such as Optotrak [1]. The purpose of this paper is to present a more economical approach that requires only force platform and electrogoniometry data and thus might be more suitable for use in clinical applications.

PROPOSED APPROACH

The proposed approach is based on inverse dynamics analysis (IDA) and also work-energy theorem. This approach uses a two-segment inverted pendulum model (see Figure 1).

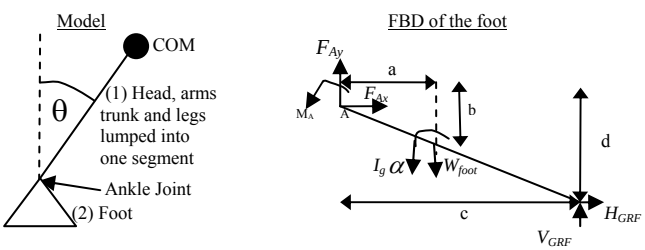

Figure 1: Two-segment inverted pendulum model

In Fig. 1, H_{GRF} and F_{Ax} are the horizontal forces at the ground and ankle; V_{GRF} and F_{Ay} are the vertical forces at the ground and ankle. M_A is the moment about the ankle, θ is the sway angle with respect to a fixed vertical axis, W_{foot} the foot weight, and I_g the foot's moment of inertia about its centre of mass and around the axis perpendicular to this plane. W_{foot}, a, b, c, and d can be measured or determined from Dempster's data [2].

Applying IDA equations of motion to segment 2:

$$\sum F_x = ma_x = H_{GRF} + F_{Ax} \qquad (2)$$

$$\sum F_y = ma_y = V_{GRF} + F_{Ay} - W_{foot} \qquad (3)$$

$$\sum M_A = I_g\alpha + ma_x b + ma_y a \qquad (4)$$

$$M_A - W_{foot}a + V_{GRF}c + H_{GRF}d = I_g\alpha + ma_x b + ma_y a \qquad (4a)$$

Since the foot is not accelerating during quiet standing α, a_x, and a_y can be approximated as 0. Therefore equation (4a) becomes:

$$M_A = W_{foot}a - V_{GRF}c - H_{GRF}d \qquad (5)$$

Values on the right-hand side of Eq.5 can be obtained using a force platform and anthropometrics. Thus, the work required to displace the COP to maintain the COM within the BOS is:

$$W = M_A\theta \qquad (6)$$

To validate this approach, θ was measured electronically and compared with data measured by motion capture. The findings from Winter's approach (Eq.1) are then compared to the present study's approach (Eq.6).

METHODS

A five-camera Vicon MX motion capture system sampling at 100 Hz recorded the three-dimensional marker trajectories of a male subject. Simultaneously an electrogoniometer measured θ and an AMTI force platform quantified the ground reaction forces and moments. The subject was requested to stand as still as possible, barefoot on a block that reduced the A/P BOS, chin parallel to the ground, and arms resting to the side. The postural sway in the A/P direction was recorded over a 60-s period for two conditions namely: normal quiet standing, eyes open (EO) and normal quiet standing, eyes closed (EC). A trial was recorded for each condition.

RESULTS

To improve the quality of the graphics only part of the trial is shown in Fig. 2. Fig. 2-A reveals that the COP—with higher amplitudes—moves on either side of the COM to maintain balance. Fig. 2-B demonstrates that COP-COM predicted using Eq.1 is highly correlated to $\ddot{x}$. Fig. 2-C shows that the work predicted by Eq.6 negatively correlates to $\ddot{x}$. Fig. 2-D shows that as body sway increases the work required increases linearly. Although not evident from Fig. 2, when $\ddot{x}$ is approximately zero, θ is typically a maximum and subsequently work is a maximum.

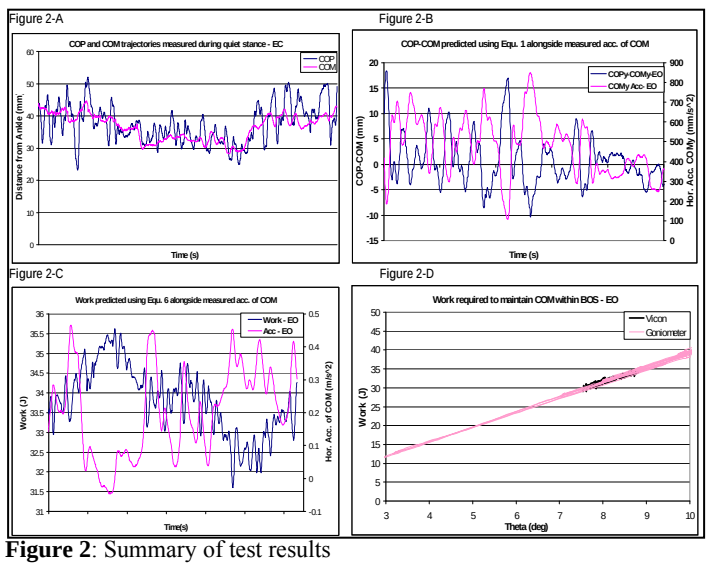

Figure 2: Summary of test results

SUMMARY AND DISCUSSION

Equations 1 and 6 yield similar results (Fig. 2-C & 2-D), so one can conclude that postural stability may very well be related to the work required to maintain balance. Compared to Eq.1's approach, the simplistic method proposed in this study reduces the amount of data to be processed and analyzed, as well as, the complexity of the computations required. More trials and varied subject population are required to illuminate and further validate the proposed approach.

REFERENCES

1. Winter DA. *Human balance and posture control during standing and walking.* Gait Posture **3**(4): p. 193-214, 1995.
2. Dempster WT. WADC-TR-55-159 1955, Wright-Patterson Air Force Base: Dayton, OH.

RUNNING SPEED ESTIMATION USING A LEG-MOUNTED INERTIAL MEASUREMENT UNIT

Chris Mohr, Shuozhi Yang and Qingguo Li
Department of Mechanical and Materials Engineering, Queen's University, Kingston, Canada

INTRODUCTION

There is growing interest in portable, real-time methods for studying human gait behaviour. Techniques have been developed to analyze walking gait [1, 2] using acceleration and angular velocity data from inertial measurement units (IMU). However, few attempts have been made to use similar approaches for running gait. The purpose of this study was to develop an algorithm capable of estimating running speed using a single IMU and to determine the optimum location of that sensor.

METHODS

Inertial measurements were taken at a rate of 100Hz from an Inertia-Link® IMU (MicroStrain Inc. Vermont, USA) attached at various locations along the leg in the sagittal plane. The orientation of the sensor, and the sensor axes, are shown in Figure 1. A Butterworth low-pass filter with cut-off frequency of 7Hz was used to remove electrical and vibrational noise from the signals. To estimate running speed from the IMU data, the angle of the leg segment was found by integrating the filtered angular velocity signal. The integration interval was determined using peaks in the recorded signals corresponding to key gait events. Using the segment's orientation, the acceleration data (tangential and normal to the rotating leg) was converted into horizontal and vertical components. Gravity was compensated by subtracting it from the vertical component. A double integral was applied to the horizontal acceleration to calculate the stride length. The average speed of each stride was then calculated by dividing the calculated stride length by the duration of each step.

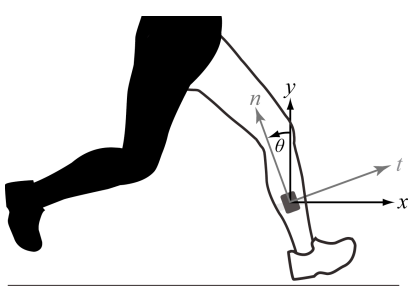

Figure 1: Location and orientation of IMU sensors.

Treadmill running experiments were conducted to evaluate the performance of this method. During the experiment, the IMU was attached to the midpoint of the subjects' shank on the lateral side. The subject was instructed to run at five different speeds: 2.5m/s, 3.0m/s, 3.25m/s, 3.5m/s and 3.75m/s. Each trial lasted for 90 seconds, and the data from the stable part of the trial was chosen for processing. The data was processed in MATLAB (The MathWorks, Natick, MA, USA).

RESULTS

The results of the algorithm at various treadmill speeds are shown in Figure 2. The estimation results give a root mean square error of 0.23 m/s.

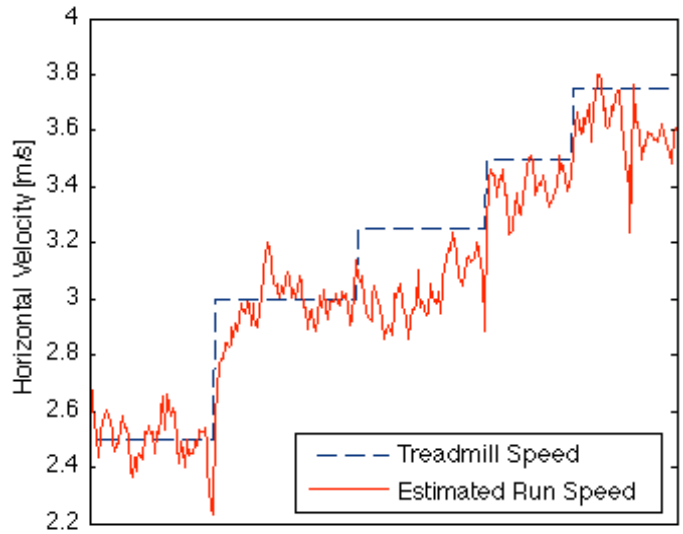

Figure 2: Preliminary results of running speed estimation.

DISCUSSION AND CONCLUSIONS

The preliminary results show that the algorithm produced values that agreed relatively well with the reported treadmill speeds. Error appeared to increase at higher running speeds. This is likely related to the initial velocity of the leg segment not being zero at the beginning of the integration interval, instead having a small amount of rotational motion. Further investigation will be concentrated on the improvement of the data processing and the algorithm, including signal filtering and estimation method optimization. Testing will be expanded to include approximately 15 student volunteer subjects, running at speeds between 2.5 and 3.5 m/s. Sensor placement will be experimented with to potentially increase the algorithm's accuracy. Finally, the sources and extent of error in the method's results will be investigated.

REFERENCES

[1] Li Q et al. (2009). Walking speed estimation using shank-mounted IMU. in ICORR 2009, IEEE International, pp. 839-844, 2009.

[2] Liu T et al. (2009) Development of a Wearable Sensor System for Quantitative Gait Analysis. *Measurement.* Vol **42**; p. 978-988

REORGANIZATION OF FRONTAL PLANE BIOMECHANICS AT THE HIP WHEN WALKING WITH A LOAD ON THE AFFECTED OR NON-AFFECTED LEG IN INDIVIDUALS WITH HEMIPARESIS

Carole Miéville[1], Cyril Duclos[1,2], Sylvie Nadeau[1,2]
[1]Laboratoire de pathokinésiologie, Centre de Recherche Interdisciplinaire en Réadaptation, Institut de Réadaptation Gingras-Lindsay-de-Montréal et École de réadaptation, Université de Montréal, Montréal, Canada, carmiel76@yahoo.fr
[2]Équipe multidisciplinaire en réadaptation locomotrice

INTRODUCTION

Improving gait is one of the main rehabilitation goals for patients with lower-limb motor deficits and their therapists. Individuals with hemiparesis due to stroke show muscle weakness and slower gait speed in comparison with healthy people [1]. There is scarce evidence that adding a load to the lower leg could help strengthen weak muscles that are important for faster gait [2]. However, no study has shown the effects of such loading on the kinematics and kinetics of gait in persons with hemiparesis, in particular at the hip where weakness of the abductors will prevent proper control of pelvis stability and thus impair foot clearance during the swing phase of the opposite foot. The aim of this pilot study, therefore, was to determine the kinematic and kinetic changes in the affected hip in the frontal plane when walking with a load on the affected or non-affected lower leg.

METHODS

Five chronic hemiparetic participants (4 men, 1 right stroke, 58 ± 17 years) with severe to moderate motor impairments at the affected lower limb and five healthy individuals paired for age, gender, height and weight were recruited. The gait pattern was assessed with an Optotrak 3020 system that recorded (at 60 Hz) the 3-D coordinates of infrared markers placed on the trunk pelvis and lower limbs. For the kinetic data, AMTI force platforms allowed quantification of the ground reaction forces (GRF) at a frequency of 600 Hz. Participants walked at their self-selected gait speed under three conditions: 1) without load (WL), the control condition; 2) with a load on the affected/non-dominant leg (AL); 3) with a load on the non-affected/dominant leg (NAL). Healthy controls also performed at an average cadence of 72 step/min (slow speed) to match the self-selected cadence of the stroke participants. The load, placed at the distal part of the leg, was equivalent to 20% of the thigh mass (~3% of the total body mass). Hip kinematics (angles) and kinetics (moments) computed in the frontal plane (average values from 10% to 60% of the gait cycle) on the affected or non-dominant hip along with GRF were compared between the conditions with a load (AL, NAL) and the condition without load (WL) at similar cadences using non-parametric statistical tests.

RESULTS

The gait speed, cadence and step length were not significantly affected by the load in either group. The mean gait speed was 0.58 ± 0.09m/s in the stroke group. The load on the affected side (AL) increased the single stance asymmetry whereas the load on the non-affected side (NAL) reduced it. For the swing phase proportion, it increased towards the loaded leg in patients whereas it increased with the load on the opposite side in healthy subjects. At the hip, the frontal kinematics and kinetics did not differ from the WL condition when the load was on the affected/non-dominant leg. For healthy subjects, when the dominant leg was loaded, the increase in the non-dominant hip abductor average moments (0.70 to 0.77 Nm/kg) did not reach a threshold of significance (p=0.080). On the contrary, the affected hip abductor average moments decreased from 0.44 to 0.37 Nm/kg (p=0.043) in the stroke group (Figure 1). Although not significant, the medial component of the GRF showed an increase in the NAL compared to WL in both groups. No changes were observed in the frontal hip angles.

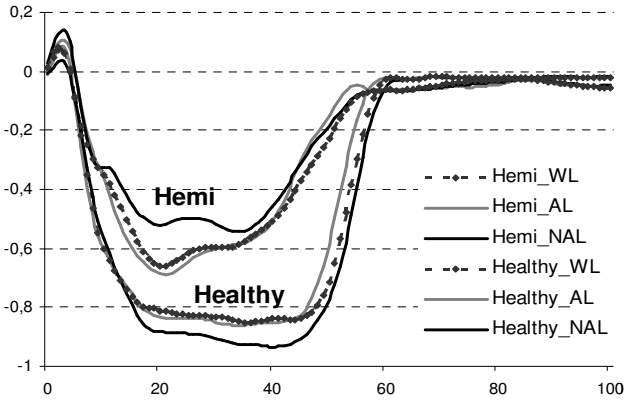

Figure 1: Hip moments (Nm/kg) in the three conditions in both groups. Negative values refer to an abductor moment.

DISCUSSION AND CONCLUSIONS

Our results show that loading the non-affected leg during gait unexpectedly reduces the effort on the affected hip abductor muscles during the stance phase in chronic stroke people. This reorganization in the hip motor pattern response to loading is opposite to that of the healthy subjects. Some hemiparetic patients might reduce their effort by using greater acceleration at the trunk towards the swing limb since the medial GRF showed an increase at that time. Future studies are required to better understand the motor reorganization of patients in response to leg loading. Mainly, the affected hip and pelvis movements in the horizontal plane of motion as well as the trunk linear and angular accelerations will need to be considered.

REFERENCES

[1] Milot MH, Nadeau S. et al. (2007) JEK, 17:184-193
[2] Noble JW, Prentice SD (2006) Exp Brain Res, 169:482-95.

ACKNOWLEDGMENTS

Réseau provincial de recherche en adaptation-réadaptation (REPAR/FRSQ) and Équipe multidisciplinaire en réadaptation locomotrice (IRSC). S. Nadeau is a senior researcher supported by FRSQ. C. Miéville is supported by a scholarship from Université de Montréal.

CUMULATIVE LOADING IS SUPERIOR TO THE PEAK KNEE ADDUCTION MOMENT WHEN DISTINGUISHING BETWEEN HEALTHY ADULTS AND ADULTS WITH KNEE OSTEOARTHRITIS

Monica R. Maly[1,2] and Shawn M.K. Robbins[2]
[1]School of Rehabilitation Science, McMaster University, Hamilton Ontario, Canada, mmaly@mcmaster.ca
[2]School of Physical Therapy, University of Western Ontario, London, Canada, smrobbin@uwo.ca

INTRODUCTION

The peak knee adduction moment (PKAM) is the primary measure used to identify the pathomechanics of knee osteoarthritis (OA). Yet, the PKAM does not consistently distinguish between healthy and osteoarthritic knees [1]. The PKAM reflects only one instant, rather than exposures to knee loading that occur daily. A dose-response relationship exists between loading repetition and risk for knee OA [2]. Cumulative knee adductor load (CKAL) reflects repetitive exposure to medial knee loading encountered during daily activity [3]. The purpose of this study was to investigate whether CKAL was superior to PKAM in distinguishing between adults with and without knee OA.

METHODS

Thirty-one adults with radiographic knee OA (53.2 ± 6.1 years, BMI 30.6 ± 4.2 kg/m^2) and 30 healthy adults (33.5 ± 8.0 years, BMI 25.0 ± 4.2 kg/m^2) participated. This younger comparison group was selected to avoid subclinical knee OA frequently found in asymptomatic knees of 50 year olds on magnetic resonance images [4]. Gait data were collected from an 8 camera system (Motion Analysis Corp., Santa Rosa, USA) at a sample rate of 60 Hz and a synchronized floor-mounted force plate (AMTI, Watertown, USA) at 1200 Hz.

To calculate PKAM, the knee adduction moment waveform was normalized to body mass. CKAL was calculated as the product of the knee adduction moment impulse during stance and the mean number of steps taken per day for the test limb. The knee adduction moment waveform was presented in absolute values for magnitude and time to represent the total load through the medial compartment. From this waveform, the stance phase was integrated using the trapezoidal rule in a custom Matlab program (Mathworks Inc., Natick, USA). The mean number of steps taken daily was measured with a uni-dimensional accelerometer (Actigraph, Fort Walton Beach, USA). Participants wore the accelerometer for at least 12 waking hours over 7 consecutive days.

T-tests compared independent sample means. To determine whether CKAL was better than PKAM at discriminating between people with and without knee OA, 1000 bootstrap *t*-tests were applied. The between measure differences in pair-wise *p*-values for the 1000 bootstrap estimates were rank ordered and the percentile associated with the first positive difference defined the level of significance. Analyses were performed using STATA V10.1 (StataCorp, Texas, USA).

RESULTS

Table 1 shows that both CKAL and PKAM were greater in the OA compared to healthy group. CKAL was nearly two times larger in the knee OA compared to the healthy group (df=51, p=0.001). PKAM was larger in adults with knee OA than the healthy adults (df=59, p=0.003). However, the bootstrap analysis revealed that CKAL was better than PKAM at discriminating between groups (p = 0.04).

A secondary analysis examined the components of CKAL. The impulse was over two times greater (df=41, p=0.001) in the OA compared to the healthy sample. Those with knee OA were less active than the healthy group (df=59, p=0.03).

DISCUSSION AND CONCLUSIONS

CKAL was superior to PKAM in distinguishing between adults with and without knee OA. Cumulative exposures to medial knee loading may be more important to consider than maximal loads because cumulative loading accounts for loading repetition. Perhaps even more important, non-normalization of the adduction moment impulse in the CKAL calculation emphasized the importance of actual loads borne through the medial knee compartment during each step.

Among the knee OA group, reductions in physical activity did not appear adequate to compensate for increased absolute loading, reflected by impulse, during each step. This work provides a foundation for future studies aiming to identify cumulative load thresholds for knee OA progression.

REFERENCES

[1] Foroughi N et al. (2009) *Knee* **16**: pp 303-309.
[2] Vignon E et al. (2006) *Joint Bone Spine* **73**: pp 442-455.
[3] Robbins S et al. (2009) *Gait Posture* **30**: pp 497-501.
[4] Reichenbach et al. (2010) *Ann Rheum Dis* **69**: pp143-149.

ACKNOWLEDGEMENTS: NSERC Discovery #353715. The authors gratefully acknowledge T. Birmingham for use of equipment and P. Stratford for assistance in analysis.

Table 1: Features that distinguish between adults with and without knee OA.

	Knee OA (n=31)	Healthy (n=30)
Peak Knee Adduction Moment (Nm/kg)	0.51 ± 0.13	0.42 ± 0.13
Cumulative Knee Adductor Load (kNms)	80.80 ± 44.54	42.79 ± 28.10
• Knee Adduction Moment Impulse (Nms)	22.3 ± 10.7	9.5 ± 4.7
• Steps per day	7390.9 ± 2674.6	8762.3 ± 2716.0

QUADRICEPS IMPAIRMENT AFFECTS LOWER EXTREMITY JOINT MOMENTS DURING GAIT IN YOUNG ADULTS

Gillian Hatfield[1], Cheryl Hubley-Kozey[1], William Stanish[1,2]
[1]School of Biomedical Engineering, Dalhousie University, Halifax, Canada, GHatfield@dal.ca
[2]Department of Surgery, School of Biomedical Engineering, Dalhousie University, Halifax, Canada

INTRODUCTION

Adults with knee osteoarthritis have alterations in gait biomechanics that reflect a negative mechanical loading environment at the joint [1]. Impairment in the ability of the quadriceps muscle to generate a torque has been hypothesized to be one cause for this negative loading environment [2]. Fatigue models in young adults are one way of isolating quadriceps impairment without the confounding effects of joint pathology including pain and swelling. The purpose of this study was to mimic quadriceps impairment using a fatigue model in young adults to determine if this produced a negative mechanical loading environment at the knee.

METHODS

18 young sedentary adults (mean age 25 ± 3 years) underwent three-dimensional gait analysis, walking at their self-selected walking speed, before and after completing a quadriceps fatigue protocol. The fatigue protocol was based on a previously described endurance test and consisted of 50 maximum effort knee extensions against a Cybex™ isokinetic dynamometer (Cybex International Inc, MA) [3]. Knee extensor torque and median power frequencies from three quadriceps muscle sites verified local muscle fatigue.

Ground reaction forces during gait were measured using an AMTI™ force platform (Advanced Mechanical Technology Inc, Watertown MA) sampled at 2000 Hz. Segment motion was recorded at 100 Hz using an Optotrak™ motion capture system (Northern Digital Inc, Waterloo ON) synchronized with the force platform. Motion and force data were used to calculate three-dimensional moments at the hip, knee and ankle using inverse dynamics [1].

Three-dimensional knee moment waveforms were analyzed using Principal Component Analysis (PCA) [1]. *Scores* for each principal component (PC) for each moment were used in the statistical analysis. Paired t-tests (α=0.05) were used to determine the effect of fatigue-induced quadriceps impairment on the PC *scores*. A repeated measures ANOVA (α=0.05) was used to detect significant changes in the knee extensor torque and median power frequencies of the three quadriceps at the beginning and end of the fatigue protocol and following the post-fatigue walking trials.

RESULTS

Fatigue-induced quadriceps impairment resulted in decreased maximum knee extensor torque and decreased quadriceps median power frequencies ($p<0.05$). Walking velocity did not change between the pre and post-fatigue walking trials (1.26 m/s pre and 1.23 m/s post-fatigue). Post-fatigue, significant changes were seen in PC *scores* for the knee moments in all three planes ($p<0.05$). PC2, capturing the difference between the first peak and mid stance knee adduction moment, increased post-fatigue indicating an increase in the first peak in the knee adduction moment. PC2 for the knee flexion moment, capturing the difference between the early stance knee flexion moment and the late stance knee extension moment, decreased post-fatigue. This decrease was due a drop in the early stance knee flexion moment. PC2 for the knee rotation moment, capturing the external rotation moment in early stance, decreased post-fatigue.

DISCUSSION AND CONCLUSIONS

Induced quadriceps impairment (via a fatigue model) resulted in biomechanical gait changes that indicated a decreased ability to dissipate impact loads, higher medial compartment loading in early stance, and changes in the shear moments around the joint. These changes would result in a negative mechanical loading environment at the knee. The observed changes are also consistent with gait characteristics observed in patients with knee OA. This study indicates that endurance as well as strength of the quadriceps muscle is important in protecting the knee from harmful loads.

REFERENCES

[1] Landry S et al. (2007). Knee Biomechanics of Moderate OA Patients Measured During Gait at a Self-Selected and Fast Walking Speed. *Journal of Biomechanics* **40**(8); p. 1754-61.
[2] Syed IY and Davis BL (2000). Obesity and osteoarthritis of the knee: hypotheses concerning the relationship between ground reaction forces and quadriceps fatigue in long-duration walking. *Medical Hypotheses* **54**(2); p. 182-5.
[3] Larsson B et al. (2003) Test-retest reliability of EMG and peak torque during repetitive maximum concentric knee extensions. *Journal of Electromyography and Kinesiology* **13**(3):p.281-7.

ACKNOWLEDGEMENTS

NSERC and CIHR for funding.

MODEL-BASED RADIOSTEREOMETRIC ANALYSIS OF AN UNCEMENTED MOBILE-BEARING TOTAL ANKLE ARTHROPLASTY SYSTEM

Jason Fong[1], David Wilson[1,2], Allan Hennigar[2], Michael Dunbar[1,2], Mark Glazebrook[1,2]
[1]School of Biomedical Engineering, Dalhousie University, Halifax, Canada, jason.fong@dal.ca, http://bme.medicine.dal.ca
[2]Department of Surgery, Division of Orthopaedics, Dalhousie University, Halifax, Canada

INTRODUCTION

Recently, classical marker-based radiostereometric analysis (RSA) has been used to assess the precise 3D migration of total ankle arthroplasty (TAA) implants. To date, implants that have been studied are the the Scandinavian Total Ankle Replacement® (STAR) (W. Link and Co., Hamburg, Germany) tibial and talar implants, and the Buechel-Pappas™ (BP) (Endotec, New Jersey, USA) total ankle prosthesis tibial implant [1,2]. Generally, the results of these studies have shown that all the implants migrate initially then stabilize in 6wk for the STAR [1], and 6mth for the BP [2]. This study examines the biomechanical fixation of the Mobility™ Total Ankle System (DePuy, Indiana, USA) tibial and talar implants using novel model-based RSA (MBRSA) technology.

METHODS

Twenty patients (10M and 10F) undergoing TAA surgery were enrolled consecutively for this study. Exclusion criteria restricted patients that could be considered for TAA surgery. All patients participating in this study and undergoing TAA were provided with informed consent.

During surgery seven 0.8mm diameter tantalum markers were implanted in the tibia above the tibial implant and 8 markers were implanted in the talus below the talar implant per the protocol developed at our institution. These markers formed the tibial and talar rigid bodies that acted as the references for the respective implant migrations. Uniplanar RSA X-rays were taken post-op and at 6wk, 3mth, 6mth, 1yr and 2yr follow-ups.

Implant migrations were assessed using MBRSA (MEDIS, Leiden, The Netherlands). Both the tibial and talar migrations were determined using model-based pose estimation [3,6]. The Elementary Geometric Shapes (EGS) module was used to assess the migration of the spherical tip of the tibial implant [5]. Marker models were identified from bone rigid bodies and used in cases where there were marker obstructions and/or independent marker migrations [4]. Implant migrations were compared with the results for the STAR and BP prosthesis.

RESULTS

The talar and tibial implants mean longitudinal migration showed initial subsidence (migration into the bone) followed by stabilization patterns at 1yr (Figure 1). Subsidence in the inferior/superior direction was the main direction of movement. The mean maximum total point motion (MTPM) for the implants at 2yr were 1.29±0.62mm for the talar implant and 1.15±0.57mm for the tip of the tibia implant (Table 1). Subjects 11 and 19 were omitted due to missed post-op exams. Subject 10 was omitted due to substantial independent bone marker migrations. Subjects 2 and 6 had revision surgery and incomplete follow-up. Subjects 7, 9, 13, 14 and 20 had surgical complications but had complete follow-up.

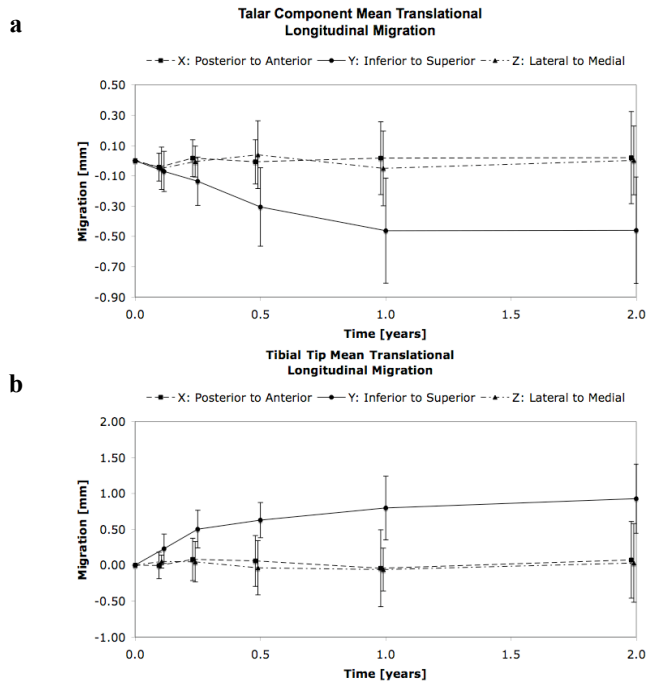

Figure 1: Mean translational migrations for the Mobility™: (a) talar implants and (b) tibial implants. Error bars are SD.

Table 1: Mean 2yr longitudinal migrations for talar implant and tibial implant spherical tip. Values are mean and SD.

	x, PA [mm]	y, IS [mm]	z, LM [mm]	R_x [°]	R_y [°]	R_z [°]	MTPM [mm]
talar	0.02±0.30	0.46±0.35	0.00±0.23	-0.2±1.5	0.0±1.1	-0.6±1.8	1.29±0.62
tibial	0.07±0.53	0.93±48	0.03±0.55				1.15±0.57

DISCUSSION AND CONCLUSIONS

Mean subsidence and stabilization patterns in the superior/inferior direction were similar to those seen in previous TAA RSA publications [1,2]. Stabilization occurred at 6wk in the STAR, at 6mth in the BP, and did not occur until 1yr for the Mobility™. The high variability in the subject-specific implant position shown by the error bars suggests there are also differences in the implant in vivo mechanics. TAA prostheses need to adapt to the broad range of strenuous mechanical conditions due to inter-patient variability. MBRSA has been successfully used for the first-time to assess the biomechanical fixation of a TAA prosthesis.

REFERENCES

[1] Carlsson A et al. (2005). *SORT* Vol **76**(4); p. 573-79.
[2] Nelissen RGHH et al. (2006). *CORR* Vol **448**; p. 146-51.
[3] Kaptein B et al. (2003). *J Biomech* Vol **36**; p. 873-82.
[4] Kaptein B et al. (2005). *J Biomech* Vol **38**; p. 2330-4.
[5] Kaptein B et al. (2006). *CORR* Vol **448**; p. 92-7.
[6] Seehaus F et al. (2009). *J Biomech* Vol **131**; p. 0410041-10.

UNCEMENTED FEMORAL STEM LENGTH EFFECT ON ITS PRIMARY STABILITY

Michael Reimeringer[1], Christian Desmarais-Trépanier[1], Natalia Nuño[1], Martin Lavigne[2], Pascal-André Vendittoli[2]
[1]Imaging & Orthopaedic Research Lab., École de technologie supérieure, Montréal, Canada, mickareim@gmail.com
[2]Hôpital Maisonneuve-Rosemont, Montréal, Canada

INTRODUCTION

One of the crucial features for long-term clinical success of Total Hip Arthroplasty's (THA) uncemented implants is primary stability. Presence of motion may prevent bone ingrowth and eventually lead to loosening of the implant. Indeed, it has been shown that interfacial micromotion around 40 µm gives partial ingrowth while micromotion exeeding 150 µm inhibits bone ingrowth completly [1]. The aim of this study is to investigate the effect of stem length on primary stability of a cementless tapered femoral prosthesis.

METHODS

Finite Element Analysis (FEA) was performed on a new prosthetic design implanted into Sawbones® 4th generation (Pacific Research Labs., Inc., Vashon Island, WA, USA). The implant orientation was validated by experienced surgeons. Four stem lengths were defined: 105mm, 86mm, 70mm and 54mm (Figure 1). FEA was carried out for the loading conditions simulating Walking Fastly (WF) and Stair Climbing (SC) as defined by [2]. Micromotion was extracted on 24 points: 18 on the posterior and anterior faces (9 on each face) and 6 on the medial and lateral faces (3 on each face).

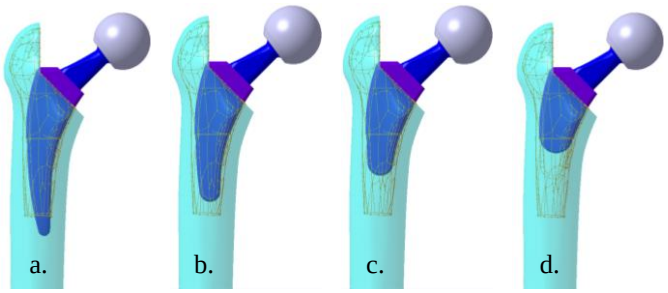

Figure 1: Length of the stem - a) 105mm b) 86mm c) 70mm d) 54mm

RESULTS

Table 1 presents results of mean and peak micromotion and Table 2 shows the range of micromotion predicted for each length of the prosthesis for walking fastly and stair climbing.

Table 1: Mean and peak micromotions predicted for each stem length for walking fastly and stair climbing

	Walking fastly (µm)		Stair climbing (µm)	
Length (mm)	Mean	Peak	Mean	Peak
105	10	34	13	54
86	13	44	14	60
70	18	65	20	86
54	29	101	30	122

Table 2: Range of micromotion predicted for each stem lengthfor walking fastly and stair climbing

Length (mm)	Range walking fastly (µm)	Range stair climbing (µm)
105	0→37	1→54
86	0→44	1→60
70	0→65	1→86
54	1→101	1→122

DISCUSSION AND CONCLUSIONS

Overall, the results show a direct relation between stem length and micromotion. The shorter the implant is, the higher the micromotion is. However for all stem lengths, none of the values predicted are over the bone loss threshold, namely 150 µm. Comparing micromotion progressions between each size, there seems to be a broader difference between length 86mm→70mm and also 70mm→54mm, as well as on mean and peak micromotions, than for the 105→86mm as it can be seen on Table 3. For all stem lengths, the mean and peak micromotions for stair climbing were higher than for walking fastly. However, the difference between mean micromotion is weak (average of 1.7 µm) compared to the difference between the peak micromotion (average of 19.5 µm). The peak micromotions are in agreement with those found by [3]. In the present study, the peak micromotions are predicted on the anterior medial and posterior lateral area of the stem. These predictions are in agreement with those found by [4].

Table 3: Difference between mean and peak micromotions for walking fastly and stair climbing between lengths

		Walking fastly		Stair climbing	
Length (mm)	Length	Mean	Peak	Mean	Peak
105 →86	-18%	+30%	+29%	+8%	+11%
86 →70	-18%	+38%	+48%	+42%	+43%
70→54	-22%	+61%	+55%	+50%	+42%

To conclude, this study indicates that the length of this cementless tapered stem could be reduced to 86mm without compromising the primary stability of the stem.

REFERENCES

[1] Pilliar et al., 1986, Clin. Orthop Rel. Res. 208, 108-113
[2] Bergmann et al., 2001, J. Biomechanics, 34, 859-871
[3] Pancanti et al., 2003, J. Biomechanics, 36, 777-785
[4] Abdul Kadir et al., 2007, Jurnal Mekanical, 23, 50-61

PROBABILISTIC COMPARISION OF SHOULDER KINEMATIC DESCRIPTIONS FOR ROTATOR CUFF TEAR PATIENTS PRE- AND POST-SUBACROMIAL INJECTION

Joseph E. Langenderfer[1], Jason Scibek[2]
[1]School of Engineering and Technology, Central Michigan University, Mount Pleasant, MI, USA, j.langend@cmich.edu
[2]Department of Athletic Training, Duquesne University, Pittsburgh, PA, USA

INTRODUCTION

Algorithms for calculating joint kinematics from defined joint centers and anatomically-based coordinate systems are affected by the accuracy in locating anatomical landmarks (ALs) [1]. Such algorithms are developed and verified with data from healthy normal subjects [2] and then used to calculate kinematics for normal subjects and patients with joint pathologies. Subsequently, analyses are performed comparing the described kinematics for the two groups. However, when the joint morphology is altered relative to ALs (e.g. arthritis and arthroplasty) joint center locations may also be affected. Consequently, the algorithms may also yield remarkably different descriptions for patients with pathological joint conditions compared to normal subjects.

Probabilistic modeling has been applied to evaluate sensitivities of kinematic descriptions to ALs for the knee [3] and shoulder [4]. The purpose of this study was to use probabilistic analysis to compare the sensitivities of humeral and scapular kinematic descriptions to ALs for a group of rotator cuff tear patients whose kinematics were altered following a sub-acromial injection of lidocaine [5]. The hypothesis was that the analysis would yield the same sensitivities of Euler angles to ALs both pre- and post-injection.

METHODS

The previously described experiment [5] is summarized here. Data were collected from fifteen patients with chronic full thickness rotator cuff tear and consisted of thirteen digitized ALs and position and orientation of electromagnetic sensors attached to the sternum, forearm, humerus and a scapular tracker while the patients performed humeral elevation in the scapular plane before and after a subacromial injection of lidocaine. Data were processed to calculate Euler angles describing humero-thoracic and scapulo-thoracic kinematics. Sensitivities of Euler angles to ALs were calculated throughout the elevation motion via the Advanced Mean Value (AMV) method [6]. AMV was implemented with a probabilistic model in NESSUS (Southwest Research Institute, San Antonio, TX) which was linked to custom code for calculating kinematics. In the model, Normal distributions were assigned to the AL digitization data. Absolute sensitivities of each Euler angle to each AL were averaged over the elevation motion for each subject. The probabilistic model was applied to the pre- and post-injection data. Sensitivities were analyzed with 3-way ANOVAs to detect differences attributable to ALs, subjects and pre- and post-injection conditions.

RESULTS

Significant differences in sensitivities of Euler angles to ALs ($p<<0.05$) were found. Sensitivities were not significantly different between subjects or between the pre- and post injection conditions for the humeral (Figure 1) and scapular (Figure 2) angles.

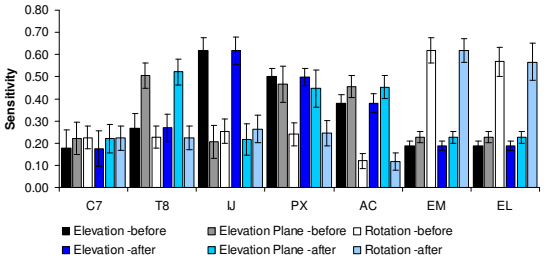

Figure 1: Mean (S.D.) sensitivities of Humeral Euler angles to anatomical landmarks.

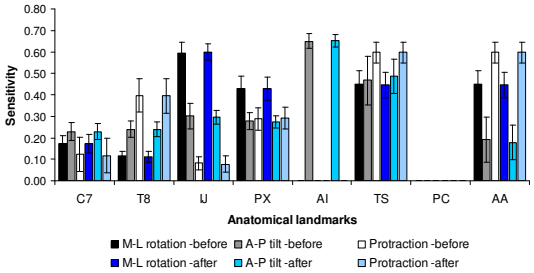

Figure 2: Mean (S.D.) sensitivities of Scapular Euler angles to anatomical landmarks.

DISCUSSION AND CONCLUSIONS

The novel approach of using the AMV to analyze kinematic data for a unique data set under different kinematic conditions yielded consistent results in sensitivities to ALs across multiple patients with rotator cuff tears. A similar analysis could be used to understand how ALs may contribute to kinematic descriptions differently for patients with arthritis or following shoulder arthoplasty. Future use of this approach might involve validating the ALs identified by computer-assisted joint replacement systems, and thereby aid in reproducing normal shoulder kinematics.

REFERENCES

[1] Besier, et al. (2003) *J Biomech* 36, 1159-1168.
[2] Meskers et al. (1998) *J Biomech* 31, 93-96.
[3] Morton et al. (2007) *J Orthop Res* 25 1221-1230.
[4] Langenderfer, et al. (2009) *CMBBE* 12, 211-216.
[5] Scibek et al. (2008) *J.S.E.S.* 17, 172-181.
[6] Wu and Millwater (1990) *A.I.A.A.J.* 28, 1663-1669.

FEA OF MECHANICAL STIMULI TRANSFER BETWEEN ORTHOPAEDIC SCREWS AND SURROUNDING BONE: A POSSIBLE METHOD FOR PREDICTING STRESS SHIELDING

Kristina Haase, Gholamreza Rouhi
Department of Mechanical Engineering, University of Ottawa, Ottawa, Canada, khaas028@uottawa.ca

INTRODUCTION

The holding power of screws is affected by the trauma of insertion, the reaction of bone to the implant, and bone remodeling as a result of healing [1]. Experimental evidence reveals the importance of host material density and screw geometry in relation to pullout strengths [2], but little information regarding the long term effects of bone-screw interactions exists [1, 3]. There are still reports of screw loosening post-implantation, particularly when screws remain *in vivo*. The question as to why the screw loosening occurs, after decades of research still remains unanswered. It is possible that stress shielding plays a role in screw loosening, particularly if insufficient mechanical stimuli is transfered from the screw to the bone via micromotion following healing at the bone-screw interface. In order to shed some light on this open question, a new model of an implanted bone-screw is developed to gauge which screw parameters are more likely to promote bone remodeling through transfer of mechanical stimuli. Moreover, a comparison between two possible stimuli, i.e. stress versus strain energy density (SED), is made, as both are commonly proposed as bone remodeling stimuli [4, 5].

METHODS

ANSYS v.11.0 is used to develop a 2D finite element (FE) model that includes a homogeneous cortical bone layer (E=20GPa, v=0.35), and a trabecular region (E=1GPa, v=0.35) interposed with a screw (Ti-6Al-4V, E=105GPa, and a treated Ti alloy E=40GPa, v=0.35) of interchangeable parameters, including: thread profile shape; shaft length; and outer and inner thread diameter. The model is used to test the relative biocompatibility of a given set of screw parameters; wherein biocompatibility is a measure of the ratio of mechanical stimuli between the screw and adjacent bone. Time-independent compressive and tensile loads (80N) are applied to the head of the screw. Data is collected along adjacent path points (Figure 1) descending the mid-plane of the outer screw diameter to the root diameter, and is compared using two sets of parameters: previously defined stress transfer parameters: STP$\alpha = \sigma_b/\sigma_t$, STP$\beta = \sum(\sigma_b / \sigma_t)$ [3], and newly defined SED transfer parameters: SEDTP$\alpha = \sigma_t \cdot \varepsilon_b / \sigma_t \cdot \varepsilon_t$, and SEDTP$\beta = \sum(\sigma_b \cdot \varepsilon_b / \sigma_t \cdot \varepsilon_t)$ [6], where σ_b, σ_t, ε_b, and ε_t are the stresses and strains in bone and in threads, respectively.

RESULTS

An example of a typical distribution of stress (Figure 1) demonstrates that equivalent stresses are highest at the peaks of triangular screw threads, and that high stresses occur in the distal region. Distributions are identical for both tensile and compressive loading conditions, showing that mechanical stimuli distribution is independent of loading direction (with constant boundary conditions).

It is also found that the level of mechanical stimuli transferred to the bone is highly dependent on outer profile shape and material properties of the screw, and differs somewhat between stress and SED.

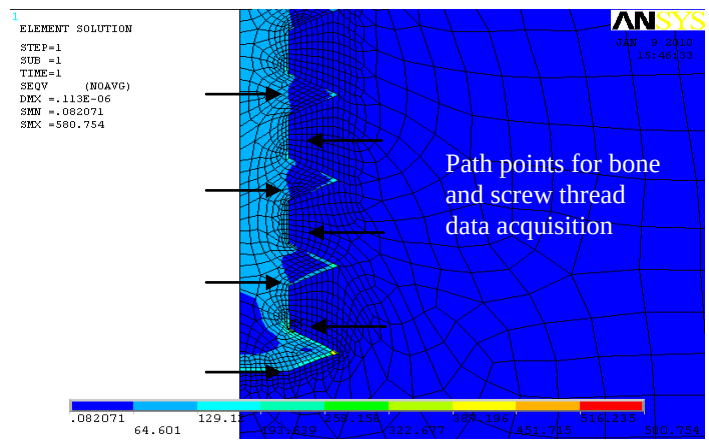

Figure 1: Stress along screw-bone interface during tensile loading.

DISCUSSION AND CONCLUSION

Most of our results, are in good agreement with others [3, 7], and suggest a highly interdependent interactions between the varied screw parameters. However, our results show that a reduced elastic modulus for the screw; and also triangular/trapezoidal profile shaped threads result in increased biocompatibility. It is also found in this study that the choice of outer thread diameter should be based on the pullout strength required and the density of bone. Moreover, our investigation shows that the root diameter of the screw should be limited in order to decrease stress shielding, yet should be large enough to maintain an appropriate torsional strength. Finally, it is found that increasing the depth of penetration by decreasing pitch or shaft length will balance the load distribution. Although we have used simplified geometry and material properties, our results compare well with similar stress distributions from a 3D model [7]. A more complex model including an adaptive bone remodeling algorithm is the ultimate goal of this work, in order to gain a better understanding of this inherently time-dependent problem.

REFERENCES

[1] Schatzker J et al. (1975). *Clinical Ortho & Rel Research* Vol **108**; p. 115-126.
[2] Asnis SE et al. (1996). *OrthoTrauma* Vol **10**; p. 462-469.
[3] Gefen A. (2002). *J. Medical Eng.& Physics*; Vol**24**; p. 337-347.
[4] Rouhi G et al. (2006). *Int. J. Eng. Science*; Vol**44**; p. 456-469.
[5] Vahdati A and Rouhi G (2009). *Mech. Res. Comm;* Vol**36**(3); p. 284-293.
[6] Haase K. MASc thesis, University of Ottawa, Dec. 2009.
[7] Inceoglua S et al. (2006). *Med. Eng. & Physics*; Vol**28**; p.888-893.

FORCE VARIABILITY DURING FATIGUING MAXIMAL ISOMETRIC ELBOW FLEXION EXERTIONS

Tara Kajaks[1], Erik Paerels[2], Jim Potvin[1]
[1]Department of Kinesiology, McMaster University, Hamilton, ON, Canada, kajakst@mcmaster.ca
[2]Faculty of Human Movement Science, Vrie University, Amsterdam, Netherlands

INTRODUCTION

Understanding the patterns in force variability throughout the time-history of a fatiguing contraction may be useful in predicting instantaneous relative effort levels associated with an absolute known force demand, providing a ration that could indicate fatigue level. To date, those exploring force variability in fatiguing contractions have shown that the standard deviation (SD) and coefficient of variation (CV) of the force output increases with fatigue [1], although few researchers have sought to use this measure, or any other, to predict relative effort. Although unsuccessful, Robinson et al. (1994) did attempt to classify submaximal and maximal isometric efforts using torque CV. Their findings show good classification of maximal isometric efforts using CV, but poor classification of submaximal isometric efforts due to highly variable CVs under submaximal conditions. Thus, the purpose of this study was to quantify the changes in force variability during a fatiguing maximal effort isometric exertion of the elbow flexors using different filtering techniques in order to identify a method least sensitive to fatigue, and therefore useful in predicting relative effort.

METHODS

Sixteen healthy subjects volunteered for this study. Subjects sat in a chair alongside a height-adjustable table such that their right elbow rested comfortably, flexed 90 degrees and supinated, on a foam pad with their shoulder abducted 90 degrees. One end of a cuff was fixed to a force transducer while the other end was wrapped around the subject's distal forearm. Subjects performed three isometric elbow flexion exertions trials. The first trial was used to determine the maximal voluntary contraction (MVC) force in this posture. Subjects then traced a pattern on a computer monitor that consisted of 11 randomly selected 7-second plateaus at target force levels ranging from 10-95% MVC. This served as a rested force variability calibration trial. Next, subjects maintained a 100% isometric elbow flexion effort until there was a 75% decrease in the force generating capacity.

Data were collected with LabVIEW software (National Instruments, Austin Tx.) using a PC compatible computer and converted by a 12-bit A/D card (National Instruments, Austin Tx.). The force transducer (MLP-300-C0, A-Tech Instruments, Scarborough, Canada) data were sampled at 1000 Hz. Post-processing of the force signal was performed using a custom-made LabView program. For the calibration trial, 3-second windows of data were extracted from each of the plateaus. The fatigue trial was divided equally into fifty 3-second windows to represent the time-history of the trial. Each window was linearly detrended, then both highpass (HP) filtered and lowpass (LP) filtered with a 6th order Butterworth filter (cutoff = 6 Hz for both). The standard deviations (SD) from each of the filtered, non-filtered detrended, and raw windows were calculated. For each subject, a regression analysis was performed to determine the linearity and slope of the relationship between the SD, from each processing technique, and the mean force for each window. The consistency of the observed trends across subjects was determined using one-sample t-tests.

RESULTS

For the rested calibration trials, there was a positive relationship between SD and force for both LP (slope = 0.0168, r = 0.987) and HP force filtering (slope = 0.0052, r = 0.881). The fatigued and rested trends were similar for the HP filter technique (slope = 0.0034, r = 0.542), indicating that force variability was tracking the absolute force and not the relative effort (which was always 100%). However, as demonstrated in Figure 1, with the LP filter technique (slope = 0.00672, r = 0.12245), the SD started higher and did not appear to be dependent on absolute force.

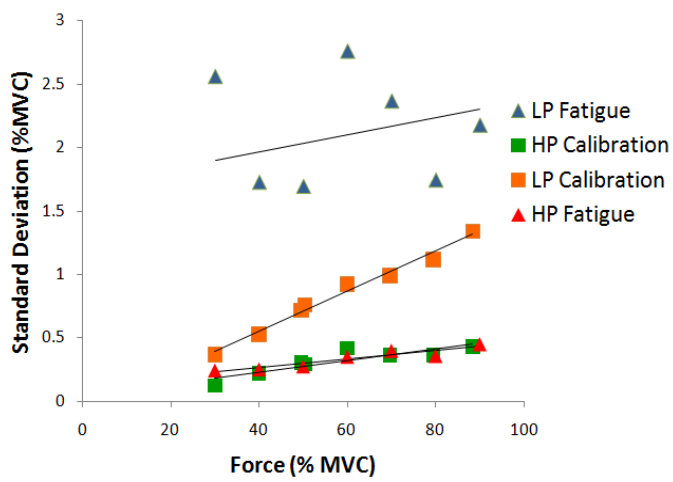

Figure 1: Ensemble average of the force standard deviations of the calibration and fatiguing trials at each % MVC interval for the HP and LP filtering techniques.

DISCUSSION AND CONCLUSIONS

The results demonstrate a potential use of the LP filtering technique to track relative effort for a given known force level so that instantaneous fatigue level can be estimated. However, other filtering techniques will be tested to see if they are even more robust for this purpose.

REFERENCES

[1] Svendsen JH and Madeleine P (2009) Amount and structure of force variability during short, ramp, and sustained contractions in males and females. *Human Movement Science*, **29**, 35-47.

[2] Robinson ME et al. (1994) Variability of isometric and isotonic leg exercise: utility for detection of submaximal effort. *Journal of Occupational Rehabilitation*, **4**(3) 163-169.

COMPREHENSIVE ANALYTICAL DESCRIPTION OF KINEMATIC CROSSTALK

A. Brennan, Q. Li, K. Deluzio
Department of Mechanical and Materials Engineering, Queen's University, Kingston ON, Canada
Human Mobility Research Centre, Queen's University and Kingston General Hospital, Kingston ON, Canada

INTRODUCTION

Accurate quantification of three-dimensional joint motion is a fundamental concern in kinematic studies related to orthopaedics and rehabilitative medicine. In biomechanics, joint motion between two bodies is quantified by comparing the relative orientation between Cartesian coordinate systems established in each body segment. Axes from these coordinate systems are often used to represent the rotational axes of the joint and when these axes are not aligned with the true rotational axes of the joint, kinematic crosstalk is introduced.

Crosstalk has been previously studied experimentally. Kadaba et al. [1] used a numerical model and gait data to perform a sensitivity analysis on the choice of flexion axis, showing that the errors in abduction/adduction and internal/external rotations were dependent both on the degree of axis misalignment and amount of true flexion. Piazza and Cavanagh [2] used two mechanical models to show that the screw-home mechanism in the knee may be a manifestation of kinematic crosstalk.

The aim of the present study was to develop a comprehensive analytical description of kinematic crosstalk and validate it with numerical simulation.

METHODS

The approach considered true anatomical coordinate frames F and T, which were perturbed slightly to make alternate frames, $\widetilde{F}$ and $\widetilde{T}$, shown in Figure 1. The difference between the corresponding component angles is the error due to the alternate frame definitions.

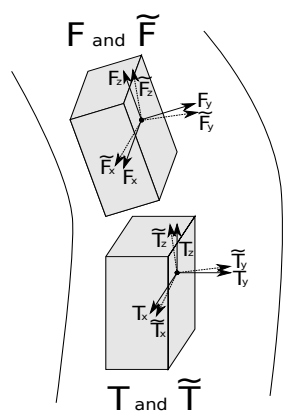

Figure 1: Definitions of the four coordinate frames: F and $\widetilde{F}$ for the femur; T and $\widetilde{T}$ for the tibia.

Understanding crosstalk can be done by separately considering each of the six basis misalignments: the $\widetilde{F}$ frame rotated about the F_x, F_y, or F_z axis; or the $\widetilde{T}$ frame rotated about the T_x, T_y, or T_z axis. Since the analysis made a first-order approximation that holds for small perturbations, the overall component error is the superposition of the errors due to each basis misalignment.

Table 1: Analytical descriptions of component error due to alternate coordinate frame definitions. (α, β, γ) are flexion/extension (F/E), abduction/adduction (A/A), and internal/external rotation (I/E), respectively. δ_{Ab} is the magnitude of perturbation about the b axis of the A frame, in radians.

Segment	Axis	F/E	A/A	I/E
	x	$-\delta_{Fx}$	0	0
Femur	y	$-\delta_{Fy}\frac{\sin\beta\sin\alpha}{\cos\beta}$	$-\delta_{Fy}\cos\alpha$	$\delta_{Fy}\frac{\sin\alpha}{\cos\beta}$
	z	$\delta_{Fz}\frac{\sin\beta\cos\alpha}{\cos\beta}$	$-\delta_{Fz}\sin\alpha$	$-\delta_{Fz}\frac{\cos\alpha}{\cos\beta}$
	x	$\delta_{Tx}\frac{\cos\gamma}{\cos\beta}$	$\delta_{Tx}\sin\gamma$	$-\delta_{Tx}\frac{\sin\beta\cos\gamma}{\cos\beta}$
Tibia	y	$-\delta_{Ty}\frac{\sin\gamma}{\cos\beta}$	$\delta_{Ty}\cos\gamma$	$\delta_{Ty}\frac{\sin\beta\sin\gamma}{\cos\beta}$
	z	0	0	δ_{Tz}

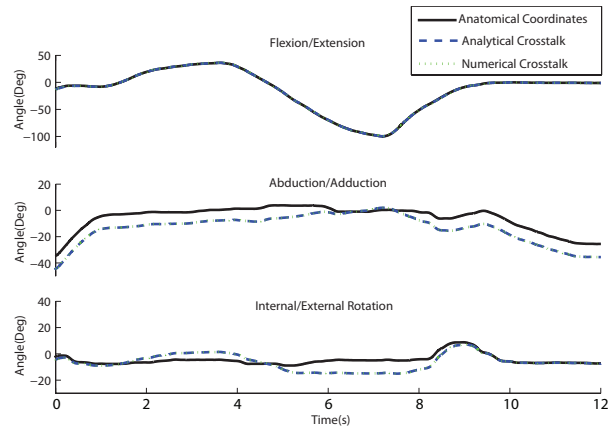

Figure 2: Crosstalk from a ten degree frame discrepancy about the F_y axis

The analytical results were validated with numerical simulations using generated data, with frame perturbations on the order of ten degrees.

RESULTS

Table 1 shows the error at each component for the six basis misalignments. The characteristic of crosstalk is that the error is a function of both the magnitude of the coordinate frame misalignment and the true values of the component angles, causing features from one waveform appear as anomalies in other waveforms. For example, the error in rotation increases with the magnitude of frame misalignment about the F_y axis and the sine of the flexion angle, as seen in Figure 2.

DISCUSSION AND CONCLUSIONS

The sinusoidal behaviour pervading the analytical expressions agrees with the experimental results from Piazza [2]. Furthermore, the equations agree very well with the numerical simulations when perturbations are under ten degrees.

This study extends previous results in two ways. The first is that it examines all possible frame misalignments, instead of limiting the scope to the flexion axis. The second is that it describes the mathematical foundation for experimental phenomenon of crosstalk, allowing it to be better understood.

References

[1] M. Kadaba, H. Ramakrishnan, and M. Wootten, "Measurement of lower extremity kinematics during level walking," *Journal of Orthopaedic Research*, vol. 8, no. 3, pp. 383–392, 1990.

[2] S. Piazza and P. Cavanagh, "Measurement of the screw-home motion of the knee is sensitive to errors in axis alignment," *Journal of biomechanics*, vol. 33, no. 8, pp. 1029–1034, 2000.

SINGLE-PLANE FLUOROSCOPY ACCURACY FOR DETERMINING THE RELATIVE POSE BETWEEN TOTAL KNEE REPLACEMENT COMPONENTS

Stacey Acker[*1,2], Heather Murray[1], Paul St. John[2], Scott Banks[3], Shang Mu[3], Urs Wyss[1], Kevin Deluzio[1,2]
[1]Mechanical and Materials Engineering, Queen's University, Kingston, ON, Canada
[2]Human Mobility Research Centre, Kingston General Hospital, Kingston, ON, Canada
[3]Mechanical and Aerospace Engineering; and Orthopaedics and Rehabilitation, University of Florida, Gainesville, FL, USA

INTRODUCTION

In this study, the accuracy of a fluoroscopic shape matching approach is investigated. The objective was to determine the accuracy of knee joint kinematics calculated using the fluoroscopic shape matching approach in comparison to an optoelectronic system. The accuracy of fluoroscopic methods involving the registration of three-dimensional total knee replacement models to two-dimensional fluoroscopic images has been investigated previously [1,2]. However, limitations of some of the previous studies include: acquiring fluoroscopic images while the implant components are static, small ranges of motion between components, or reporting the accuracy of the method without extrapolating the results to the effect on measuring the joint angle, which would be the most clinically relevant measure.

METHODS

The kinematics of total knee replacement components implanted in Sawbones were tracked simultaneously while in motion using an Optotrak Certus optoelectronic motion capture system (Northern Digital Inc., Waterloo, Ontario, Canada) and fluoroscopic imaging (GE OEC Medical Systems, Salt Lake City, Utah, USA). The resulting images were processed by a single operator using JointTrack radiographic shape-matching software (University of Florida, Gainesville, FL, USA). Since fluoroscopy overcomes errors associated with skin motion, it is expected that the accuracy of the fluoroscopic approach will be significantly better than what has been reported for skin marker motion tracking systems. The differences between the two methods were calculated as a measure of the accuracy of the fluoroscopy approach.

RESULTS

All average angle differences during dynamic trials were under 1.0°, while all average translation differences were within 1 mm (bold values, Table 1.) The limits of agreement (in brackets, Table 1) are the bounds between which 95% of the differences between the two methods can be expected to fall [3].

DISCUSSION AND CONCLUSIONS

The results of this study are limited in that this study focused on only one joint, the knee, and used only one total knee replacement design. Other designs (or models of natural knee bones) may be easier or harder to manually match. In addition, this study was performed on Sawbones. In the study of human subjects, the contrast between the implant, cement, bone and surrounding soft tissue may not be as clear. For this reason, the results in Table 1 can be considered a "best case scenario" and provide bounds on the accuracy that is achievable. In the study of human subjects, the contrast between the implant and surrounding soft tissue may not be as clear. When considering the values in Table 1, the accuracy of the optoelectronic system to which the fluoroscopic approach was compared must also be considered.

The objective of this study was to determine the accuracy of fluoroscopic shape matching using JointTrack software. Zuffi et al. [2] defined the expected fluoroscopic accuracy threshold for relative position and orientation between components as "a few millimeters and a few degrees." In this study, the authors defined this threshold numerically as a difference of 2˚ and 3 mm or less between the optoelectronic and fluoroscopic methods. The difference between the two methods in this study was always significantly different from zero. However, the mean accuracy values (Table 1) are significantly lower than the errors measured using skin marker systems, and are below the acceptable mean accuracy threshold of 2˚ and 3 mm for fluoroscopically-determined knee angles and translations [2]. This means that although the differences between the two methods are statistically significant, the differences are likely too small to be clinically significant.

Table 1: Mean differences between methods during dynamic trials. (Limits of agreement [3] in brackets.)

Mean Difference Between Methods	Manual Shape-Matching
Flexion [deg]	**1.0** *(-1.9, 4.1)*
Abduction [deg]	**0.3** *(-0.5, 1.2)*
External Rotation [deg]	**-0.5** *(-2.0, 1.1)*
Anterior-Posterior [mm]	**0.8** *(-1.6, 3.2)*
Distal-Proximal [mm]	**-1.0** *(-2.0, 0.0)*
Medial-Lateral [mm]	**0.5** *(-5.3, 6.3)*

REFERENCES

[1] Banks, SA, Hodge, WA (1996) IEEE Transactions on Bio-Medical Engineering 43(6), 638-649.
[2] Zuffi, S, et al (1999) IEEE Transactions on Medical Imaging 18(10):981-991
[3] Altman, DG, Bland, JM (1983) The Statistician 32(3), 307-317.

ACKNOWLEDGEMENTS

Maarten Beek, for programming synchronization software.
Financial support from NSERC and Zimmer Inc., Warsaw, IN

The Biomechanics of Articular Cartilage Chondrocytes *In Vivo*

Ziad Abusara and Walter Herzog
Human Performance Laboratory, University of Calgary, Calgary, Alberta, Canada
Email: zabusara@kin.ucalgary.ca

INTRODUCTION

Mechanical loading of joints deforms articular cartilage, which in turn causes deformation of the matrix embedded cells, the chondrocytes[1]. Chondrocyte deformation has been associated with biosynthetic responses aimed at maintaining the tissue healthy and strong[2]. However, excessive loading of cartilage and cells is thought to lead to cartilage degeneration and osteoarthritis[3]. Much of the work relating mechanical states of cells and their biosynthetic response is based on isolated cells, or cells embedded in explant samples removed from their natural *in situ* environment. Neither the mechanics nor the associated biological responses of chondrocytes have been studied in intact cartilage attached to its native bone or in the intact joint. The purpose of this study was to design and apply methods to study the mechanics of chondrocytes in the intact knee in live animals while loaded physiologically through muscular contraction.

METHODS

In order to achieve the purpose of this study, we developed a novel *in vivo* testing system that allows for quantification of the mechano-biology of chondrocytes in the intact knee of live mice (Figure 1). Mice are fixed in a custom-built jig on the stage of a dual photon microscope. Controlled forces of the knee extensor muscles is produced through direct muscle stimulation.. Imaging of the chondrocytes is performed using a Zeiss 40× 0.95 NA water-immersion objective coupled with a Coherent Chameleon IR laser tuned at 780 nm for two-photon excitation. Characterization of cell shapes was performed in six animals and eighty cells. Controlled muscular loading and associated cell deformation and recovery measurements have been made in two animals and seven cells.

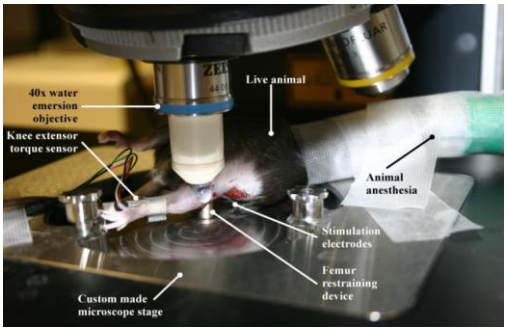

Figure 1: In vivo mouse knee preparation for imaging of dynamic chondrocyte deformation.

RESULTS

Chondrocytes and their nuclei deform on average 25-30% for sub-maximal muscular loading in the intact mouse knee. Deformation occurs "instantaneously" upon loading, but requires minutes for full cell shape recovery (Figure 2).

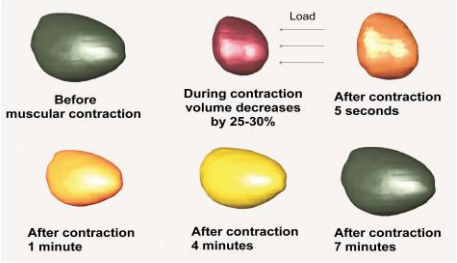

Figure 2: Cell deformation in the knee of a live mouse before, during and after muscular contraction.

Application of muscle forces below a certain threshold did not cause cell deformation, while increasing the loading beyond that threshold was associated with a nearly linear decrease in cell volume (Figure 3).

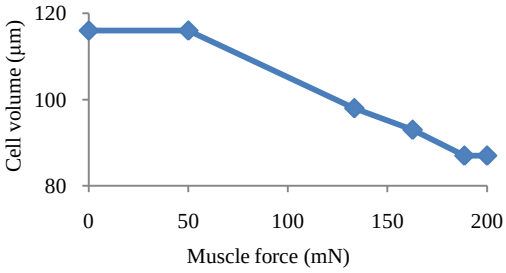

Figure 3: Cell volume as a function of muscle force.

DISCUSSION AND CONCLUSIONS

We developed an accurate and reliable method to measure dynamic cell deformations in the intact knee of live mice. Our results indicate that cell deformations occur "instantaneously upon muscular loading of the joint but require minutes to recover their original shape upon unloading. The quick deformation and volume loss during loading is probably a mechanism aimed at limiting pressure build up inside chondrocytes that might be fatal. The loss of volume, the associated cell strains, and the loss of ions during volume regulation upon loading all provide possible pathways for chondrocyte signalling that may result in adaptive or degenerative responses of the tissue to joint loading. These pathways will need careful exploration in future studies.

REFERENCES

[1] Guilak, F., J. Biomech. 28**,** 1529-1541, 1995.
[2] Sah, R.L., Kim, at al. J. Orthop Res 7, 619-636, 1989.
[3] Moskowitz R. Experimental models of OA. 213-232, 1984.

ACKNOWLEDGEMENTS

AHFMR Team grant on Osteoarthritis, CIHR, CFI, Canada Research Chair Program.

Bilateral Frequency Content Differences in Isokinetic Knee Extension Curves of Osteoarthritis Patients

Patrick A. Costigan[1,2], Sivan Almosnino[1], Elizabeth A. Sled [2],Alison Chalmers [2], Joan M. Stevenson[1,2]
[1]School of Kinesiology and Health Studies, Queen's University, Kingston, ON, CA
[2]School of Rehabilitation Therapy, Queen's University, Kingston, ON, CA
pat.costigan@queensu.ca

INTRODUCTION

Assessment of the knee extensor strength in individuals suffering from knee osteoarthritis (KOA) is of interest to researchers and clinicians, since knee pathogenesis might be, in part, a result of muscular dysfunction [1]. In this regard, quantification of knee extensors function in KOA patients has been achieved using mainly isokinetic dynamometers and, to our knowledge, all studies using this technology report time-domain based outcome measures. However, anecdotal observations of isokinetic knee extension curves obtained from KOA patients show not only differences in amplitude compared to curves obtained from either the uninvolved knee or age-matched, healthy control groups, but also diverse shape irregularities that may be characterized by rapidly changing oscillations producing a "jagged" curve. The purpose of this investigation was to assess whether quantification of these torque-curve irregularity differences between the involved and contra-lateral knee can be done based on examination of the frequency content of the isokinetic curve.

METHODS

Thirty-two participants with physician-diagnosed tibiofemoral OA were recruited through newspaper advertisements and from a list of patients waiting for total knee joint replacement. Participants met the following inclusion criteria: age $\geq$ 40 years; self-reported pain in the knee(s) for most days of the month; and one of the following applied: a) radiographic evidence of knee OA as indicated by definite osteophytes in the medial and/or lateral tibiofemoral compartment in one or both knees; b) documented evidence of cartilage loss in the knee by arthroscopy or magnetic resonance imaging (MRI).
After a short warm-up, each participant performed 5 maximal concentric knee extensions bilaterally at 60°/sec using a Biodex system 3 isokinetic dynamometer (Biodex Medical Systems., Shirley, NY, USA). Following, the power spectrum for each time-domain extension curve was calculated using a fast Fourier transform and the value of the maximum frequency content contained within 99% of the total signal power was extracted [2]. For each limb, the mean of repetitions 2 through 5 served as the representative score.

RESULTS

Data inspection revealed that all data were positively skewed. As such, the data were log-transformed to adhere to normality assumptions. Of the 32 participants, 26 exhibited higher frequency contents in the isokinetic curves obtained from their involved knee. The results of a paired t-test support this general trend, where the mean frequency content of the involved knee was significantly greater than the that of contra-lateral knee, $t(31)=3.13$, one-tail $p = 0.002$. In addition, the effect size (ES) value for this comparison was found to be 0.49, representing a moderate to large effect.

DISCUSSION AND CONCLUSIONS

Optimal muscle function is inferred, in part, from the smoothness of torque production exhibited throughout the range of motion tested. In the assessment of knee extensor function in KOA patients, spectral analysis of isokinetic curves provides quantitative information that may be in addition to the traditional time-domain based outcome measures. However, additional investigations are needed to understand the causes responsible for the increased frequency content observed in knee extensor torque curves obtained from KOA patients.

REFERENCES

[1] Segal N et al. (2009).Effect of thigh strength on incident radiographic and symptomatic knee osteoarthritis in a longitudinal cohort. *Arthritis Care & Research* Vol **61**(9); p. 1210-1217.

[2] Tsepis E et al. (2004).Frequency content asymmetry of the isokinetic curve between ACL deficient and healthy knee. *J Biomech* Vol **37** (6); p. 857-864.

Table 1: Differences in isokinetic knee extension torque curve frequency content between the involved and contra lateral knees of KOA patients (mean ± SD).

	Frequency > involved	Frequency Content (Hz)	Log-transformed Frequency content*
Involved Knee	26/32 participants	8.9 ± 7.3	1.9 ± 0.8
Contra lateral Knee		5.4 ± 2.8	1.5 ± 0.6

*difference between knees; paired $t(31) = 3.13$, $p = 0.002$, Effect size = 0.49.

VERTICAL JUMP FORCE PREDICTS UNILATERAL PLANTAR FLEXOR DEFICITS IN ARTHRITIC CHILDREN

Matthew J Kennedy[1], M.Sc.; Mario Lamontagne[1,2], Ph.D.; Johannes Roth, MD.[3]
[1]School of Human Kinetics, University of Ottawa, Canada,
[2]Department of Mechanical Engineering, University of Ottawa, Canada,
[3]Pediatric Rheumatology, Children's Hospital of Eastern Ontario, Canada. Contact: mkenned4@uottawa.ca

INTRODUCTION

Jump mechanography is a non-invasive method frequently used as a measure of muscle force and power [1]. One type of jump mechanography uses the vertical ground reaction force (vGRF) from repetitive one-legged vertical jumps (1LJs) which has the potential to predict unilateral musculo-tendenous deficiencies. However, 1LJ mechanography has not previously been validated as a measure of muscle function. The purpose of this study was to determine whether unilateral deficits in maximal vGRF generated during repetitive 1LJs correspond with unilateral deficits in maximal ankle plantar flexor isokinetic torque and power.

METHODS

Seventeen children (4 males) aged 11.6 (± 3.1) years of age with juvenile idiopathic arthritis (JIA) participated in this study. All participants had been in remission for at least one year. After a warm-up, participants performed two sets of three maximal isokinetic (90°/s) concentric and eccentric ankle plantar flexion contractions with each leg using a dynamometer (System 4, Biodex Medical Systems, NY, USA). After a rest period, a series of ten maximal 1LJs were performed on a force plate (Bertec Corp., OH, USA) using each leg. For the jumps participants were asked to maintain a rigid upper body, keep their arms at their sides, keep the hip and knee joint of the jumping leg rigid and extended, and bounce maximally on the ball of their foot without touching their heel to the force.

The variables analysed from the maximal isokinetic contractions on the dynamometer were peak concentric and eccentric torque and power for each leg. The variables analysed from the 1LJs were the peak vGRF for each leg. Left leg: right leg ratios (LR-R) were then calculated for each of the variables to determine any unilateral deficits, with ratios of > 1 indicating a right leg deficit, and ratios of < 1 indicating a left leg deficit. The relationship between the vGRF LR-R and the plantar flexion torque and power LR-Rs were then determined using one-tailed Pearson correlations ($\alpha = 0.05$).

RESULTS

There were significant Pearson correlations found between the LR-Rs of weight normalized vGRF and each of the mass normalized maximal concentric torque ($R = .650$, $p = .002$), eccentric torque ($R = .687$, $p = .001$), concentric power ($R = .636$, $p = .003$) and eccentric power ($R = .716$, $p = .001$). The LR-Rs of eccentric torque and power were most strongly correlated with the LR-R of vGRF with R^2 values of .472 and .513 respectively (Figure 1).

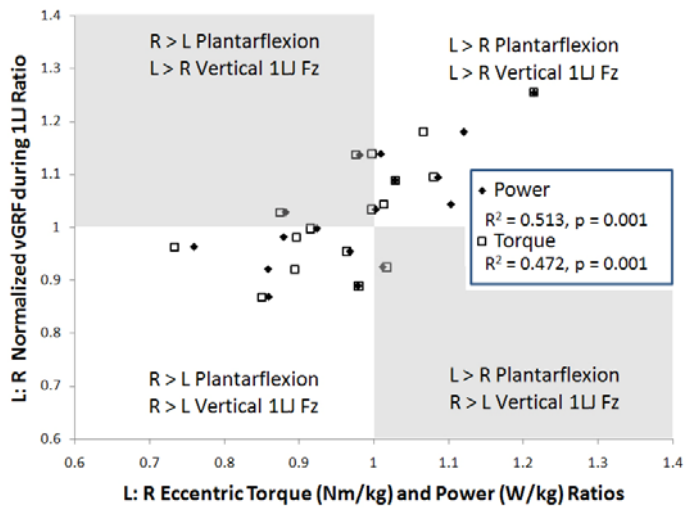

Figure 1. LR-R of maximal mass normalized eccentric torque (□) and power (♦) (X-axis) relative to the LR-R of weight normalized vGRF (Y-axis) during maximal 1LJs. Data points in the white quadrants depict unilateral strength discrepancies found by the vGRF which correspond with those measured by dynamometry.

DISCUSSION AND CONCLUSION

One LJ mechanography is quick and easy to perform, and requires only a measure of vGRF, and minimal processing. Moreover, it holds the potential to differentiate unilateral musculo-tendenous deficiencies using a single force plate. This is ideal for clinical settings where time and expense are limiting factors.

Unilateral strength discrepancies can cause adverse joint loading, and can lead to or accelerate joint degeneration [2]. This is of particular concern in populations with pre-existing degenerative diseases, such as children with JIA.

The moderate R values show that unilateral deficits in vGRF correspond with unilateral concentric and eccentric torque and power deficits in the plantar flexors. R^2 values of .513 and .472 for eccentric power and torque respectively, indicate that the eccentric capacity of the plantar flexors explain approximately 50% of the vGRF, slightly higher than concentric capacity.

The results from this study indicate that vGRF from 1LJs can be used to identify unilateral musculo-tendenous discrepancies in children with JIA.

REFERENCES

[1] Fricke, O., et al., Mechanography-a new device for the assessment of muscle function in pediatrics. *Pediatr Res*, 2006. Vol **59**(1): p. 46-9.

[2] Herzog, W., D. Longino, and A. Clark, The role of muscles in joint adaptation and degeneration. *Langenbecks Arch Surg*, 2003. Vol **388**(5): p. 305-1

Author Index

Mohammad abdoli-Eramaki 17, 19, 58
Ziad Abusara 198
Stacey Acker 197
Rachid Aissaoui 121
Ameet Aiyangar 48
Wayne Albert 68, 99, 103, 113, 114, 115
Fahad Algarni 159
Nicholas Ali 186
Paul Allard 85
Sivan Almosnino 80, 178, 199
Katharina Althoff 51
Matthias Amrein 166
Paul Anderson 48
David Andrews 16, 57, 65, 66, 181
Jan Andrysek 164
Kory Arsenault 69
Janie Astephen Wilson 1, 69, 76, 77, 78, 79, 171, 172
Ali Ataei 145
Ryan Atkison 149
Anthony Au 48
Daniel Avrahami 155
Nadia Azar 50, 134
Lauren Bailey 128, 129
Scott Banks 197
Simon Batz 51
Tyson Beach 133, 180
Erica Beaucage-Gauvreau 15
Paul E. Beaule 142
Daniel Bechard 144
Mickaël Begon 32, 33, 85
Alicia Belbeck 18
Petra Bendova 35
Daniel Benoit 170
Jessica Berrigan 29
Hu Bin 122
Rebecca Birkhofer 93
Trevor Birmingham 23, 144
Jacinte Bleau 85
Malika Bongué Boma 41
Tomas Bouda 138
Yan Bourgeois 83
Jonathan W. Bourne 86
Lara Boyd 169
Steven K Boyd 14
Chris Boyle 81
Scott Brandon 72, 80
Andrew Brennan 185, 196
Rebecca Brookham 12
Brenda Brouwer 25, 173
Martin Brummund 122
Tim Bryant 71
Valérie Burdin 84
Martin N. Bureau 82
Timothy Burkhart 57, 181
Heather Butler 47, 160
David Bürgel 51
Kristina Calder 3
Graham Caldwell 98
Matthew Calhoun 27
Jack Callaghan 6, 7, 36, 39, 64, 65, 103, 113, 132, 133, 157, 180
John Callaghan 61
Rachel Campbell 92
Christiane Caouette 82
Robert Caryn 38
Joshua Cashaback 131
Alison Chalmers 80, 199
Justin Chee 74
Vicky Chester 27
Lisa Chisholm 147
Amy Chow 18
John Christenson 58
Michael Cinelli 28, 175
Emílio Cipolli 40
Allison Clouthier 72
Matt Cochran 68
Leanne Conrad 116
Hélène Corriveau 25
Patrick Costigan 22, 199
Rachel Cotton 33, 85
Marc-André Cyr 151
François D.Beaulieu 54
Heather Daley 62
Mohsen Damavandi 30, 91
Caroline Damecour 17, 19, 58
Michel Danakas 136
Diana De Carvalho 39

Author Index

Kevin Deluzio 72, 185, 196, 197
Marc Denninger 90
Marc DeRochie 26
Ariane Desharnais 4
Pierre Desjardins 25, 31, 136
Christian Desmarais-Trépanier 192
Clark Dickerson . 2, 10, 12, 18, 34, 100, 177
James Dickey 38, 101, 116, 140, 150
Tara Diesbourg 50
Philippe Dixon 91
Jon Doan 112
Cynthia Doré 90
Maryline Doyon 85
Andrew Dragunas 150
Janessa Drake 50, 56
Cyril Duclos 25, 136, 188
Geneviève Dumas 15, 108
Michael Dunbar .. 1, 75, 76, 77, 78, 79, 191
Carolyn Duncan 99, 114
Mike DuVall 166
Block Ed 122
Tammy Eger 101, 116, 117, 118
Janice Eng 161, 169
Andrew Engbretson 108
Kevin Englehart 62, 123
Marcelo Epstein 41
Mansour Eslami 30
Donald Everson 103, 115
Salvatore Federico 41, 42, 105
Peter Federolf 94, 119, 179
Reed Ferber 30
Abdolhosein Fereidoon 110
Krysia Fiedler 65, 66
Stephan Fischer 87
Steven Fischer 34, 100, 113
David FitzPatrick 130
Teresa Flaxman 170
Jason Flindall 112
Jason Fong 69, 191
Ali Forghani 163
Rafael Fortuna 168
Patricia Francis 69
Ryan Frayne 140
Benoît Frenette 176
Bernd Friesenbichler 179
David Frost 55, 133, 180
William Gage 74, 137
Dany Gagnon 4, 136
Marine Gaihlard 33
Victoria Galea 3
Kaitlin M. Gallagher 113
Christian Gasser 105
Stephen Gausman 112
Ahmad Ghasempoor 17, 19
Rouhi Gholamreza 194
J. Robert Giffin 23
Jessica Gifford 166
Guillaume Giraudet 176
Cheryl Glazebrook 164
Mark Glazebrook 69, 191
Alison Godwin 67, 117, 118
Sara Gombatto 49
Chad Gooyers 36, 180
Karen Gordon 5, 8, 107
Philippe Gourdou 121
Ryan B Graham 11, 13
Diane Gregory 7
Sylvain Grenier 118
Jacques Gresset 176
Tej-jaskirat Grewal 12, 34
Alfio Grillo 42
Michael Gross 76
Ke Gu 44
Amr Guaily 42, 105
Kristina Haase 194
Amy Hackney 28
Jeffery Haddad 174
Marlee Hahn 97
Laurie Hall 10
Robin Hampton 68
Edwin Hanada 47, 159
Ashley Hannon 53
Graeme Harding 171, 172
Levi Hargrove 123
Gillian Hatfield 75, 190
Tom Hazell 38

Author Index

Blair Healy 88
Aaron Hefferman 61
Behnam Heidari 130
Nicole Helle 61
Ewald Hennig 51, 52, 87, 184
Allan Hennigar 76, 191
Walter Herzog .. 59, 97, 143, 165, 166, 167, 168, 198
Gordon Higgins 139
Tamotsu Hirata 40, 127
Joanne Hodder 104, 135
Michael Holmes 6
Ron House 117
Samuel Howarth 6, 113, 157
Cheryl Hubley-Kozey 1, 47, 75, 79, 159, 160, 171, 172, 190
Tom Hubrecht 55
Nicolas Huppé 152
Mark Hurtig 5, 107
Ann-Kathrin Hömme 184
Paul Ivancic 46, 153
Robert J. Jack 116
Nima Jamilpour 110
Thomas Jenkyn 144
Doan Jon 122
Ian Jones 23, 144
Tara Kajaks 195
Thomas Karakolis 7
mahta karimpoor 182
April Karlinsky 54
Amanda Kay 24
Peter Keir 6, 60, 102, 104
Matthew Kennedy 142, 200
Tina Khazaei 145
Andrew Kim 164
Il Yong Kim 81, 141
David Kobylak 88
Kristen Kokotilo 169
David Konadu 76
Svatava Konvickova 138
John Kozey 160
Mark Kroll 49
Manuela Kunz 107
Usha Kuruganti 62, 68, 103
Elise Laende 76
Yves Laflamme 83
Andrew Laing 70
Ashkan Lakzadeh 145
Mario Lamontagne 142, 200
Scott Landry 146, 147
Eve Langelier 90, 151, 152
Joseph Langenderfer 193

Joel Lanovaz 71, 88
Martin Lavigne 82, 192
Mohamed Lawani 15
Marie-Pierre Leblanc-Lebeau 151
Julien Leboucher 84
Julie Lecours 176
Mallorie Leduc 117

Soul Lee 124
Jennifer Lembke 66
Peter Lemon 38
Mathieu Lempereur 84
Tim Leonard 143, 165
Brown Lesley 122
Jean-Luc Lessard 151, 152
Ryan Lewinson 63
Jing Xian Li 124
Leping Li 44
Qingguo Li 37, 185, 187, 196
Xianjie Li 45
Heather Linley 135
David Longino 168
Mark Lowerison 107
Joy MacDermid 3
Kristen MacDonell 92
Norma MacIntyre 3
Sasho MacKenzie 148
Scott MacKinnon 99, 114
Forough Madeh Khaksar 130
Brian Maki 73
Monica Maly 135, 189
Sarah L Manske 14
Stéphane Martel 152
Alyson Martin 164
Kara McCallum 49
Alison McDonald 18
Stuart McGill 55, 133, 156

Author Index

William McIlroy 24, 73, 74, 162
Phillip McKeen 134
Audree McKenzie 59
John J McPhee 96
Wissal Mesfar 158
Anna Michalski 164
Yannick Michaud-Paquette 53
Erin Middlebrook 10, 12
Ross Miller 98
Theodore Milner 154, 163
Carole Miéville 188
Kodjo Moglo 158
Chris Mohr 187
Samantha Molenaar 2
Tony Monnet 32
Janice Moreside 156
Zachary Morison 139
Gary Morphy 140
Dylan Morrissey 182
Rebecca Moyer 23
Shang Mu 197
Brittney Muir 174
Mark Munro 20, 21, 111
Krista Munroe-Chandler 134
Heather Murray 197
Sylvie Nadeau . 4, 25, 31, 121, 136, 176, 188
Brian Nairn 56
Erika Nelson-Wong 64, 132
K.C. Geoffrey Ng 142
Benno Nigg 94, 179
Jeremy Noble 26, 95, 161, 169
Sarah Nolte 61
Volker Nolte 149, 150

Katherine Norrish 92
Alison Novak 173
Marilee Nugent 154
Natalia Nuño 82, 109, 192

Kathleen O'Reilly 92
Donatus Oguamanam 106
Danielle Oliveira 127
João Oliveira 120, 127
Michele Oliver 8, 20, 21, 101, 111, 116, 128, 129
Michael Olsen 139
Ryan Ouckama 89
Erik Paerels 195
Matt Pain 32
Jan Pajerski 105
Appaji Panchangam 59, 167
Marcello Papini 106
Seungbum Park 184
Kimberly Patton 93
David Pearsall 53, 89, 91
Lucie Pelland 178
Ruth Pelleg-Kallevag 47
Stephen Perry 24, 29
Yvan Petit 83
Bryan Picco 18, 100
Michael Pierrynowski 135
André Plamondon 31
Tova Plashkes 135
Katherine Plewa 101
Heidi-Lynn Ploeg 48
James Potvin 131, 155, 195
Stephen Prentice 26, 162
Sheida Rabipour 163
Michelle Rae 103, 115
Denis Rancourt 90, 151, 152
Debbie Rand 161
Aliaa Rehan Youssef 143
Samantha Reid 22
Susan Reid 67
Michael Reimeringer 109, 192
Glen Richardson 77, 78
Shirley Rietdyk 174
Shawn Robbins 189
Gordon Robertson ... 54, 63, 125, 126, 183, 186
Richard Roda 77, 78
Dan Rogers 123
Johannes Roth 200
Gholamreza Rouhi ... 45, 63, 110, 125, 142, 186
John Rudan 72
Pavel Ruzicka 35, 138
Olivier Rémy-Néris 84
Erin M Sadler 11, 13
Nancy Salbach 164

Alan Salmoni 38

Author Index

Kia Sanei 60
David John Saxby 183
Emil Schemitsch 139
Alison Schinkel-Ivy 57, 181
Marvin Schwartz 140
Jason Scibek 193
Hazel Screen 182
Jessica Seaman 174
Roxanne Seaman 147
Radek Sedlacek 138
Alireza Seifzadeh 106
James Sexsmith 20, 21, 111
Mohammad Sharif Shourijeh 96
Melissa Shiffer 49
Glauce Silva 120
Ann Simon 123
Jonathan Singer 26, 162
Bhupinder Singh 61, 93
Megan Sinnott 93
Elizabeth Sled 80, 199
Cécile Smeesters 90, 151, 152
Jacob Smith 146
Mike Smith 88
Michael Sonne 16
Andrew Speirs 170
Paul St. John 197
William Stanish 190
Paul Stapley 163
Justin Steeds 5
Bryan Steinnagel 164
Joan Stevenson . 11, 13, 17, 19, 58, 67, 178, 199
Lisa Stirling 179
Chad Sutherland 56
Conrad Tang 9
Karelia E. Tecante G. 94
Connor Telles 46
Patricia Teran-Yengle 93
Aaron Thompson 117
Arsène Thouzé 32, 33
Mostafa Toloui 43
Ricardo Torres-Moreno 164
Peter A. Torzilli 86
Nikolas Trutiak 107
James Tung 73, 74
Rene Turcotte 53
Richard Twycross-Lewis 182
Marco Aurelio Vaz 168
Pascal-André Vendittoli 82, 192
Dmitry Verniba 137
Dino Villalta 16
Nina Völkel 52
Micha Wallace 20, 21, 111
Coren Walters-Stewart 125
William Warren 175
Joanna Weber 8
Patricia Weir 65, 66
Valérie Wellens 71
Richard Wells 34, 96, 100
Justin Weresch 102
Jean Wessel 3
Kristen Whitney 92
Rebecca Wightman 147
Ryan Willing 141
David Wilson 1, 191
William Wong 164
Alexander Wright 70
Urs Wyss 197
Ming Xiao 153
John H Yack 61, 93

Shuozhi Yang 37, 187
Megan Yaraskavitch 97
Aliaa Rehan Youssef 168
Karl F Zabjek 92
Karl Zabjek 74, 164
Ronald F Zernicke 14
Li Zhang 126

Reviewers

Alice Aiken
David Andrews
Janie Astephen Wilson
Trevor Birmingham
Steven Boyd
Brenda Brouwer
Tim Bryant
Jack P. Callaghan
Peter Cripton
Elsie Culham
Kevin Deluzio
Nandini Deshpande
Clark Dickerson
Jim Dickey
Jon Doan
Genevieve Dumas
Mansour Eslami
Dany Gagnon
Paul Ivancic
Joel Lanovaz
Qingguo Li
Monica Maly
Linda McLean
Sylvie M. Nadeau
Kathleen Norman
David Pearsall
Lucie Pelland
André Plamondon
Gordon Robertson
Cécile Smeesters
Les Sudak
James Tung
Stephen Waldman
R. Wells
Karl Zabjek